

博士論文

Development of Photoredox- and Transition Metal-Catalyzed Alkylation of Alkynes with 4-Alkyl-1,4-dihydropyridines

(光誘起電子移動触媒と遷移金属触媒による
4-アルキル-1,4-ジヒドロピリジンを用いた
アルキン誘導体のアルキル化反応の開発)

Yulin Zhang
張 煜林

Development of Photoredox- and
Transition Metal-Catalyzed Alkylation of Alkynes
with 4-Alkyl-1,4-dihydropyridines

(光誘起電子移動触媒と遷移金属触媒による
4-アルキル-1,4-ジヒドロピリジンを用いた
アルキン誘導体のアルキル化反応の開発)

2022 年

Yulin Zhang
張 煜林

List of Abbreviations

Ac	Acetyl
acac	Acetylacetonate
aq	Aqueous solution
Ar	Aryl
BINAP	2,2'-Bis(diphenylphosphino)-1,1'-binaphthyl
Bn	Benzyl
Boc	<i>tert</i> -Butoxycarbonyl
ⁿ Bu	<i>n</i> -Butyl
^t Bu	2,2'-Bis(diphenylphosphino)-1,1'-binaphthyl
bpy	2,2'-Bipyridine
Cbz	Benzyloxycarbonyl
(CF ₃)ppy	2-(Pyrid-2-yl)-4-(trifluoromethyl)phenyl
Cod	1,5-Cyclooctadiene
Cp	Cyclopentadienyl; η^5 -C ₅ H ₅
Cp*	1,2,3,4,5-Pentamethylcyclopentadienyl; η^5 -C ₅ Me ₅
Cy	Cyclohexyl
δ	Chemical shift
dba	Dibenzylideneacetone
DBU	1,8-Diazabicyclo[5.4.0]undec-7-ene
DEMS	Diethoxymethylsilane
dF(CF ₃)ppy	3,5-Difluoro-2-(5-trifluoromethyl-2-pyridyl)phenyl
DFT	Density Functional Theory
diglyme	Diethylene glycol dimethyl ether; Bis(2-methoxyethyl) ether
DIPEA	<i>N,N</i> -Diisopropylethylamine
DMA	<i>N,N</i> -Dimethylacetamide
DMDC	Dimethyl decarbonate
DME	Dimethoxyethane
dMe bpy	4,4'-Dimethyl-2,2'-bipyridine
dMeObpy	4,4'-Dimethoxyl-2,2'-bipyridine
DMF	<i>N,N</i> -Dimethylformamide
DMMS	Dimethoxymethylsilane
DMSO	Dimethylsulfoxide
dr	Diastereomeric ratio
dtbbpy	4,4'-Di- <i>tert</i> -butyl-2,2'-bipyridine
dppe	1,2-Bis(diphenylphosphino)ethane
ee	Enantiomeric excess
Et	Ethyl
<i>fac</i>	Facial
Fc	1-Ferrocenyl
Fppy	3,5-Difluoro-2-(2-pyridyl)phenyl
η	Description for hapticity
ⁿ hex	<i>n</i> -Hexyl
HFIP	Hexafluoroisopropanol
HPLC	High Performance Liquid Chromatography

HRMS	High Resolution Mass Spectrometry
L	Ligand
LED	Light-emitting diode
LG	Leaving group
μ	Description for bridging
M	Metal
Me	Methyl
MeO	Methoxy
Mes	Mesityl
NHPI	<i>N</i> -Hydroxyphthalimide
NMR	Nuclear magnetic resonance
NuH	Nucleophile
OTf	Trifluoromethanesulfonate
PC	Photoredox catalysis
Ph	Phenyl
ⁿ Pr	<i>n</i> -Propyl
ⁱ Pr	Isopropyl
Piv	Pivaloyl
ppy	2-(2-Pyridyl)phenyl
R	Substituent
rac	Racemic
rt	Room temperature
SET	Single electron transfer
TBHP	<i>tert</i> -Butyl hydroperoxide
TEMPO	2,2,6,6-Tetramethylpiperidin-1-yl)oxyl
TIPS	Triisopropylsilyl
TMHD	2,2,6,6-Tetramethyl-3,5-heptanedione
TMS	Trimethylsilyl
Tf	Trifluoromethanesulfonyl
THF	Tetrahydrofuran
Ts	Tosyl

Contents

1. General Introduction	1
1.1 Organometallic Reagents	2
1.2 Photoredox Catalysis	4
1.3 Photoredox-catalyzed Alkylation Reactions with 4-Alkyl-1,4-dihydropyridines	7
1.3.1 Photoredox-catalyzed Free Radical Alkylation Reactions with 4-Alkyl-1,4-dihydropyridines	7
1.3.2 Dual Photoredox/Nickel-catalyzed Alkylation Reactions with 4-Alkyl-1,4-dihydropyridines	18
1.3.3 Dual Photoredox/Palladium-catalyzed Alkylation Reactions with 4-Alkyl-1,4-dihydropyridines	26
1.3.4 Dual Photoredox/Chromium-catalyzed Alkylation Reactions with 4-Alkyl-1,4-dihydropyridines	29
1.4 Transition Metal-catalyzed Propargylic Substitution Reactions	32
1.4.1 Transition Metal-catalyzed Non-enantioselective Propargylic Substitution Reactions	32
1.4.2 Transition Metal-catalyzed Enantioselective Propargylic Substitution Reactions	37
1.4.2.1 Ruthenium-catalyzed Enantioselective Propargylic Substitution Reactions	37
1.4.2.2 Copper-catalyzed Enantioselective Propargylic Substitution Reactions.....	45
1.4.2.2.1 Copper-catalyzed Enantioselective Propargylic Substitution Reactions with Carbon- centered Nucleophiles	45
1.4.2.2.2 Copper-catalyzed Enantioselective Propargylic Substitution Reactions with Nitrogen, Oxygen- and Sulfur-centered Nucleophiles	55
1.4.2.3 Nickel-catalyzed Enantioselective Propargylic Substitution Reactions.....	59
1.4.2.3.1 Nickel-catalyzed Enantioselective Propargylic Substitution Reactions with Carbon- centered Nucleophiles	59
1.4.2.3.2 Nickel-catalyzed Enantioselective Propargylic Substitution Reactions with Nitrogen. and Oxygen-centered Nucleophiles.....	66
1.4.2.4 Palladium-catalyzed Enantioselective Propargylic Substitution Reactions	68
1.4.2.5 Dual Photoredox/Copper-catalyzed Enantioselective Propargylic Substitution Reactions 	69
1.4.2.6 Summary on Enantioselective Propargylic Substitution Reactions.....	70
1.5 Catalytic Hydroalkylation Reactions of Alkynes to Afford Alkenes	73

1.5.1	Transition Metal-catalyzed Hydroalkylation Reactions of Alkynes	73
1.5.2	Nickel-catalyzed Hydroalkylation Reactions of Alkynes	79
1.5.3	Photoredox-catalyzed Hydroalkylation Reactions of Alkynes	84
1.5.4	Dual Photoredox/Nickel-catalyzed Hydroalkylation Reactions of Alkynes	87
1.6	Perspective for Following Chapters in This Thesis	96
1.7	References.....	98
 2. Photoredox- and Ruthenium-Catalyzed Enantioselective Propargylic Alkylation of Propargylic Alcohols with 4-Alkyl-1,4-dihydropyridines.....		105
2.1	Introduction.....	106
2.2	Results and Discussion	109
2.3	Conclusion for Chapter 2	129
2.4	Experimental Section	130
2.5	References.....	169
 3. Photoredox- and Nickel-Catalyzed Hydroalkylation of Alkynes with 4-Alkyl-1,4-dihydropyridines: Ligand-Controlled Regioselectivity		174
3.1	Introduction.....	175
3.2	Results and Discussion	177
3.3	Conclusion for Chapter 3	190
3.4	Experimental Section	191
3.5	References.....	220
 4. Cooperative Photoredox- and Nickel-Catalyzed Alkylative Cyclization Reactions of Alkynes with 4-Alkyl-1,4-dihydropyridines		226
4.1	Introduction.....	227
4.2	Results and Discussion	228
4.3	Conclusion for Chapter 4.....	242
4.4	Experimental Section	243
4.5	References.....	269
 5. Summary and Perspective.....		273
 List of Publications.....		277
Acknowledgement.....		278

Chapter 1

General Introduction

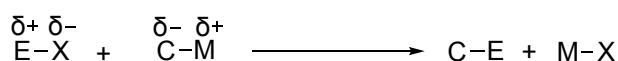
In Chapter 1, the author introduces the research backgrounds and an outline of the author's doctoral thesis entitled "Development of Photoredox- and Transition Metal-Catalyzed Alkylation of Alkynes with 4-Alkyl-1,4-dihydropyridines" First, the author introduces some basic concepts including alkylation reactions by using organometallic compounds as alkylation reagents. Then, the author introduces principles of photoredox catalysis, and the photoredox-catalyzed alkylation strategies without using organometallic alkylation reagents but using 4-alkyl-1,4-dihydropyridines. The author next introduces 4-alkyl-1,4-dihydropyridines as the alkylation reagents under photoredox catalytic conditions more in detail, and summarizes recent advances in photoredox-catalyzed alkylation reactions and dual photoredox/transition metal-catalyzed alkylation reactions using 4-alkyl-1,4-dihydropyridines as the alkylation reagents. Subsequently, the author introduces transition metal-catalyzed propargylic substitution reactions including propargylic alkylation reactions, and summarizes especially transition metal-catalyzed enantioselective propargylic substitution reactions. Next, the author describes photoredox-catalyzed hydroalkylation reactions of alkynes with alkylation reagents other than 4-alkyl-1,4-dihydropyridines, and further summarizes applications of dual catalytic systems to hydroalkylation reactions of alkynes under photoredox conditions. Finally, the author introduces the outline of the author's doctoral thesis studies on dual photoredox and transition metal-catalyzed alkylation reactions of alkyne derivatives with 4-alkyl-1,4-dihydropyridines.

1.1. Organometallic Reagents

Organometallic reagents are compounds which contain carbon–metal bonds, where most notable metals can be alkali metals (Li, Na, K), alkaline earth metals (Mg, Ca), or metalloids (Cu, Zn, B). As these metals or metalloids have less electronegativity compared to that of carbon, the carbon–metal bonds are polarized toward the effective formation of carbanion that can work as nucleophiles in organic synthesis (Scheme 1-1). Here, organometallic reagents can be utilized toward either nucleophilic substitution reactions (Scheme 1-1a) or nucleophilic addition reactions (Scheme 1-1b), which have been developed as fundamental synthetic methods for more than a century. And these reagents have been applied to synthesize high-value-added pharmaceuticals and chemical products in industrial.

Scheme 1-1. Organometallic Reagents Applied to Nucleophilic Substitution and Addition Reactions

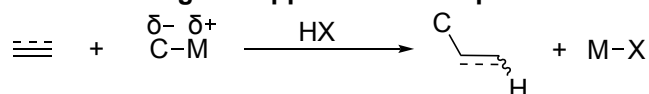
a) Organometallic reagents applied to nucleophilic substitution reactions



nucleophilic substitution

M = Mg, Zn, Li, B etc.

b) Organometallic reagents applied to nucleophilic addition reactions



nucleophilic addition

M = Mg, Zn, Li, B etc.

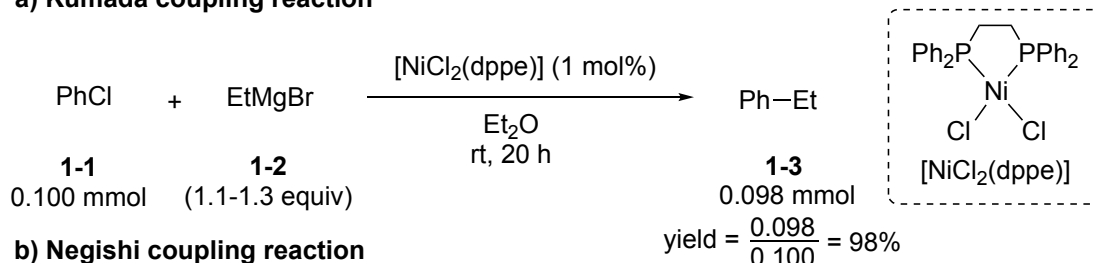
Among several nucleophilic substitution and addition reactions, the author focused upon the alkylation reactions using alkylation reagents, which have been well known as ones of the most convenient methods to introduce a new C–C bond between two specific carbon atoms. For this purpose, several organometallic alkylation reagents have been prepared to react with electrophiles. In general, the organometallic reagents such as alkyl-magnesium,¹ alkyl-zinc,² alkyl-lithium,³ and alkyl-boron⁴ reagents have been developed so far and these reagents have been playing a central role in a variety of direct alkylation reactions.

As the typical examples, alkyl-magnesium reagents, which are known as Grignard reagents, have been applied in the nickel-catalyzed Kumada coupling reactions of alkyl chlorides to obtain new products with new C–C bonds formed between these two reagents (Scheme 1-2a).⁵ Here, “yield” in percent is defined as the percent ratio of the amount of a product divided by the theoretical amount of the product based on the amount of a raw material. The amount of the raw material is 0.100 mmol, and the amount of the product is 0.098 mmol, thus, the yield of this reaction is given as 98%. In addition, alkyl-zinc reagents have been applied in the Negishi coupling reactions in the presence of palladium catalysts to afford the corresponding products with new C–C bonds (Scheme 1-2b).⁶ On the other hand, alkyl-lithium reagents have been applied

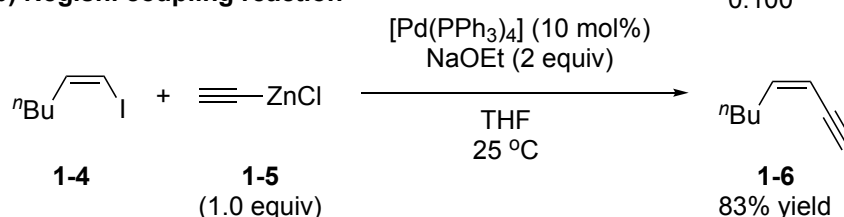
in the Murahashi coupling reactions (Scheme 1-2c),⁷ as well as organoboron reagents in the Suzuki coupling reactions, both catalyzed by palladium compounds to obtain new compounds with the formation of new C–C bonds (Scheme 1-2d).⁸

Scheme 1-2. Selected Examples of the Usage of Organometallic Reagents toward the Formation of New C–C Bonds via Coupling Reactions

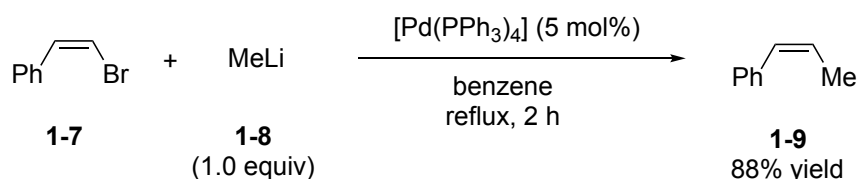
a) Kumada coupling reaction



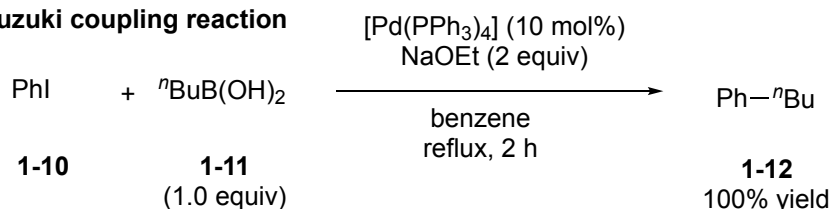
b) Negishi coupling reaction



c) Murahashi coupling reaction



d) Suzuki coupling reaction



Accordingly, the alkylation reactions by using organometallic alkylation reagents as nucleophiles to react with electrophiles have been widely applied to obtain new alkylated products with new C–C bonds, providing one of the most important synthetic tools to date. However, the nature of nucleophiles is predominantly dependent on the nature of metal species. And there are lots of problems with these organometallic reagents. For example, stoichiometric amounts of metal wastes are always formed. Secondary, most of these organometallic reagents are air-sensitive, thus they must be treated carefully, for example, under inert gas or under lower temperatures. In addition, these reagents are too reactive, that several functional groups must be protected before starting reactions.

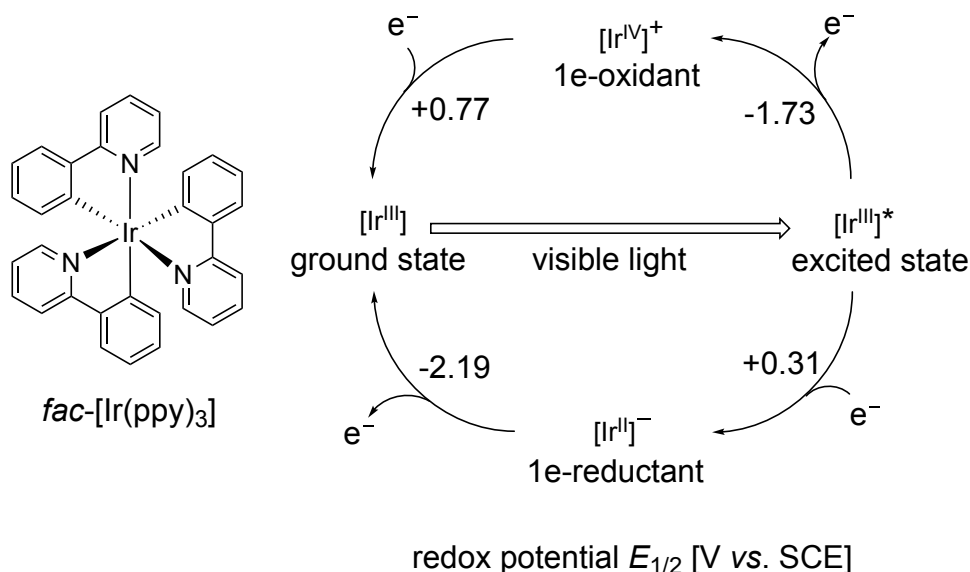
Thus, it is necessary to develop new alkylation reagents which may replace the metal resources to nonmetal organic molecules.

1.2. Photoredox Catalysis

Photoredox catalysis is a class of photochemical catalytic reactions, where a single-electron-transfer (SET) process between a photoinduced photosensitizing compound (*i.e.* photoredox catalyst) and a substrate participates to initiate subsequent conversions of the substrate.⁹ Although the history of photoredox catalysis goes back to the 1980's, the organic molecule transformations based on photoredox catalysis especially under visible light irradiation have received much attention for these two decades, as visible light irradiation usually reduces side reactions that can occur under high energy UV light irradiation.¹⁰ Both transition metal complexes and organic dyes are powerful in the ability to mediate SET processes under mild conditions and visible light irradiation. Besides many different kinds of the photoredox catalysis, polypyridyl complexes of ruthenium and iridium are most commonly and widely used in organic transformations.

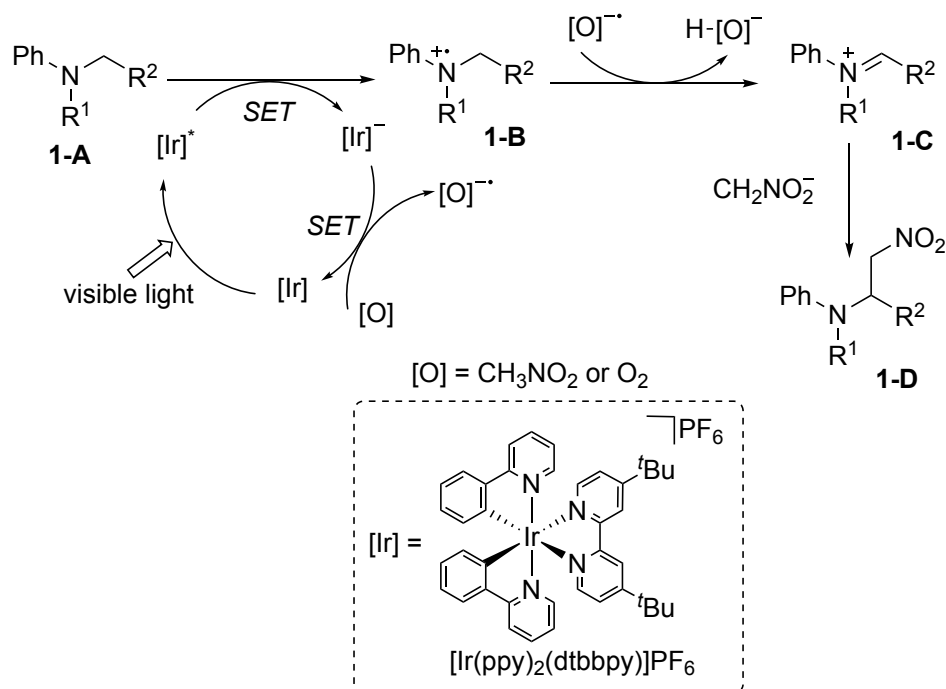
Typically, a photoredox catalytic cycle is completed by two SET processes: single electron reduction or oxidation of a substrate by a photoinduced photoredox catalyst, and subsequent single electron oxidation or reduction of a converted substrate to recover the original ground state of the photoredox catalyst. For example, *fac*-[Ir(ppy)₃] (ppy = 2-phenylpyridine) is a well-known iridium(III)-based photoredox catalyst having a maximum absorption band at 375 nm and emission band at 494 nm, corresponding to a triplet energy of 2.50 eV, with a long-lived photoexcited triplet state (1900 ns). The energy gap at 2.50 eV is relatively high, where the reduction and oxidation potentials at -2.19 V and +0.77 eV versus SCE, respectively, in the ground state shift to +0.31 V and -1.73 V versus SCE, respectively, in the excited state as shown in [Scheme 1-3](#).^{10e} Thus, photoexcited species can act as much more powerful oxidizing as well as reducing reagent than the ground state species. Here, a single electron transfer between the photoexcited species with a substrate occurs either via a single electron reduction or oxidation of the photoredox catalyst and single electron oxidation or reduction of the substrate, respectively. The formed anionic iridium(II) or cationic iridium(IV) species at ground state then works as a reductant (-2.19 V) or an oxidant (+0.77 V), respectively, to complete photoredox catalytic cycles.

Scheme 1-3. Redox Potentials of *fac*-[Ir(ppy)₃] in Ground and Excited States



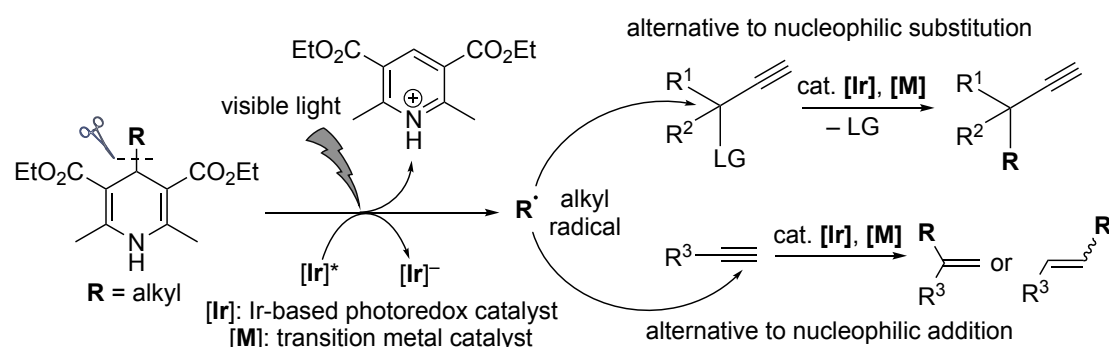
By using *fac*-[Ir(ppy)₃] or related compound as a photoredox catalyst, many photochemical organic conversions have been reported so far. For example in the visible-light-induced oxidative aza-Henry reactions of aniline derivatives **1-A**, where the ammonium radical cations **1-B** and the powerful reducing Ir(II) reagent are formed by the reductive quenching of the photoexcited state of the iridium photoredox catalyst and the substrate, followed by reduction of nitromethane to its radical anions and/or adventitious oxygen mediated by Ir(II) reagent. The radical anion originated from nitromethane or oxygen abstract a hydrogen atom from the ammonium radical cations to afford the iminium ions **1-C**, where further addition of secondary substrate gives the desired products **1-D**, (Scheme 1-4).¹¹

Scheme 1-4. Visible-light-induced Oxidative Aza-Henry Reaction of Aniline Derivatives



In order to overcome the defect of organometallic alkylation reagents, the author has focused on the usage of 4-alkyl-1,4-dihydropyridines, which has attracted much attention as versatile alkyl radical reservoirs under photoredox reaction conditions, where alkyl radicals formed in situ act as formal nucleophilic alkylation reagents to furnish radical alkylation alternative to both nucleophilic substitution and addition reactions (Scheme 1-5).¹² This strategy is accomplished by aromatization-induced C(sp³)–C(sp³) bond cleavage of 4-alkyl-1,4-dihydropyridines to afford the corresponding alkyl radicals via a SET with a photoredox catalyst under photoirradiation of visible light, and the generated alkyl radicals are captured by reaction counterparts to afford formal nucleophilic alkyl substitution or addition products, where enantioselectivity or regioselectivity of the products can be controlled by the additional transition metal catalysts. Here, use of alkyl radicals has an advantage over classical nucleophilic alkylation reagents retaining inadequate scope limitations due to side reactions such as rearrangements and eliminations.¹³

Scheme 1-5. Strategy of this Thesis: Utilization of 4-Alkyl-1,4-dihydropyridines as Versatile Alkyl Radical Reservoirs under Photoredox Reaction Conditions



In order to achieve this synthetic strategy, the author has engaged in the research to expand the utility of alkyl radicals derived from 4-alkyl-1,4-dihydropyridines as alkylation reagents to formal nucleophilic substitution and addition reactions of alkynes, and has succeeded in the development of enantioselective or regioselective alkylation of alkynes including photoredox- and ruthenium-catalyzed enantioselective propargylic alkylation of propargylic alcohols accomplished by the substitution of a hydroxyl group (Chapter 2), Markovnikov- and anti-Markovnikov-type photoredox- and nickel-catalyzed hydroalkylation of alkynes accomplished by the formation of alkylated alkenes via the addition of alkyl radicals and a proton (Chapter 3), and alkylative cyclization reactions of iodoalkynes accomplished by the substitution of an iodine (Chapter 4). For the historical background, principles, and reactivity of 4-alkyl-1,4-dihydropyridines, the author will introduce in details in Section 1.3. Then, the author will introduce the historical background, principles, and recent advances in the propargylic substitution reactions catalyzed by transition metal complexes in Section 1.4 (in connection with Chapter 2), and catalytic hydroalkylation reaction of alkynes to afford alkenes in Section 1.5 (in connection with Chapters 3 and 4). Finally, the perspective of this thesis is summarized in Section 1.6.

1.3. Photoredox-catalyzed Alkylation Reactions with 4-Alkyl-1,4-dihydropyridines

1,4-Dihydropyridine derivatives, also known as Hantzsch esters, were first prepared in 1881,¹⁴ and were usually used as reductants for transfer hydrogenation processes, working as hydride donors.¹⁵ In addition, reducing ability of 1,4-dihydropyridines has been recently applied in photochemistry.^{12,16}

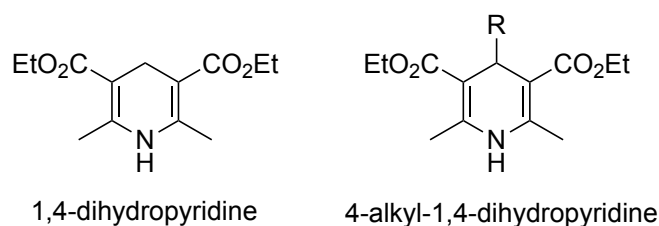
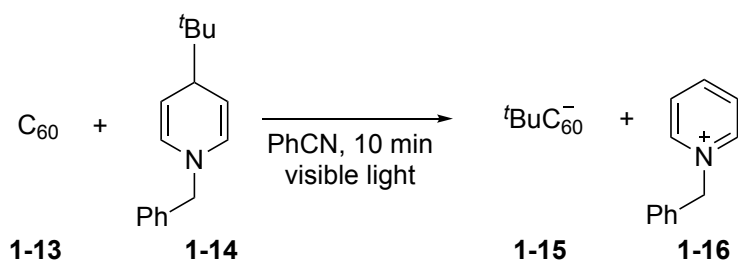


Figure 1-1. 1,4-Dihydropyridine and its derivatives.

1.3.1. Photoredox-catalyzed Free Radical Alkylation Reactions with 4-Alkyl-1,4-dihydropyridines

The first example of the application of 4-alkyl-1,4-dihydropyridine derivatives toward alkylation reactions under photochemical conditions was reported by Fukuzumi and Ito et al. in 1998,¹⁷ where the reaction of C₆₀ (Fullerene) **1-13** with 4-*tert*-butyl-1-benzyl-1,4-dihydropyridine **1-14** in PhCN under visible light irradiation for 10 min afforded *tert*-butylated C₆₀ anion **1-15** and pyridinium cation **1-16** (Scheme 1-6).

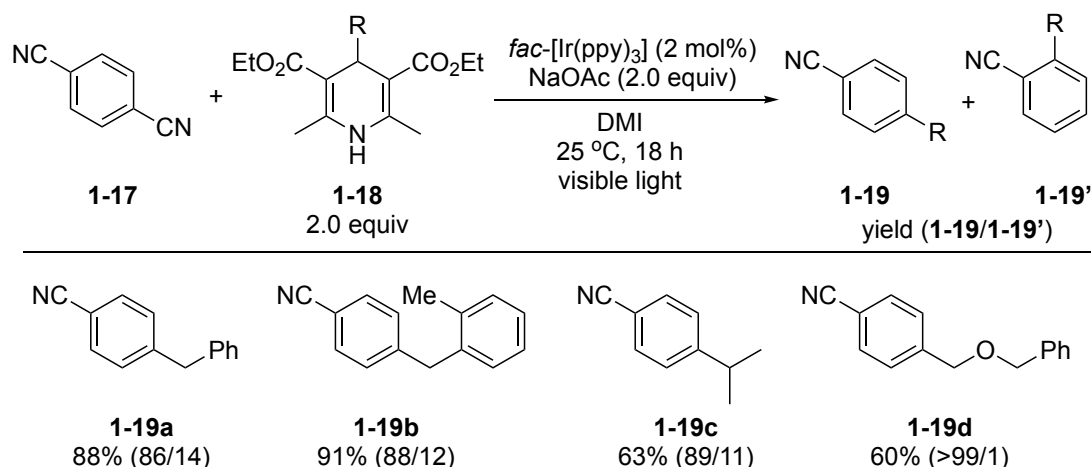
Scheme 1-6. First Application of a 4-Alkyl-1,4-dihydropyridine Derivative toward Alkylation of a Substrate under Photochemical Conditions Reported by Fukuzumi and Ito et al.



Further investigation on the application of 4-alkyl-1,4-dihydropyridines as alkylation reagents under photochemical conditions was left unexplored, but it was since 2016 that a great number of researches for the utilization of 4-alkyl-1,4-dihydropyridines as alkylation reagents have been reported.¹² One of the pioneering work in this field is done by the author's group (the former members of Nishibayashi lab), who reported photoredox-catalyzed alkylation reactions of cyanoarenes **1-17** with 4-alkyl-1,4-dihydropyridines **1-18** in the presence of *fac*-[Ir(ppy)₃] as a photoredox catalyst and NaOAc as a base in THF under visible light irradiation (12 W white LED)

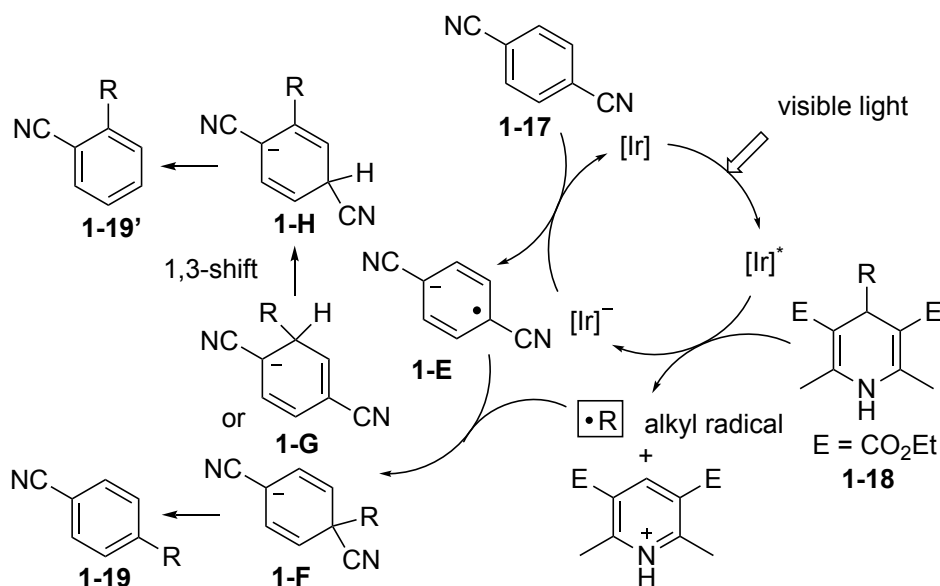
at 25 °C for 18 h to afford the alkylated products as a mixture of 1-alkyl-4-cyanobenzene **1-19a-d** and 1-alkyl-2-cyanobenzene **1-19'a-d** in good to high yields (Scheme 1-7).¹⁸

Scheme 1-7. Photoredox-catalyzed Alkylation Reactions of Cyanoarenes with 4-Alkyl-1,4-dihydropyridines Reported by the Author's Group



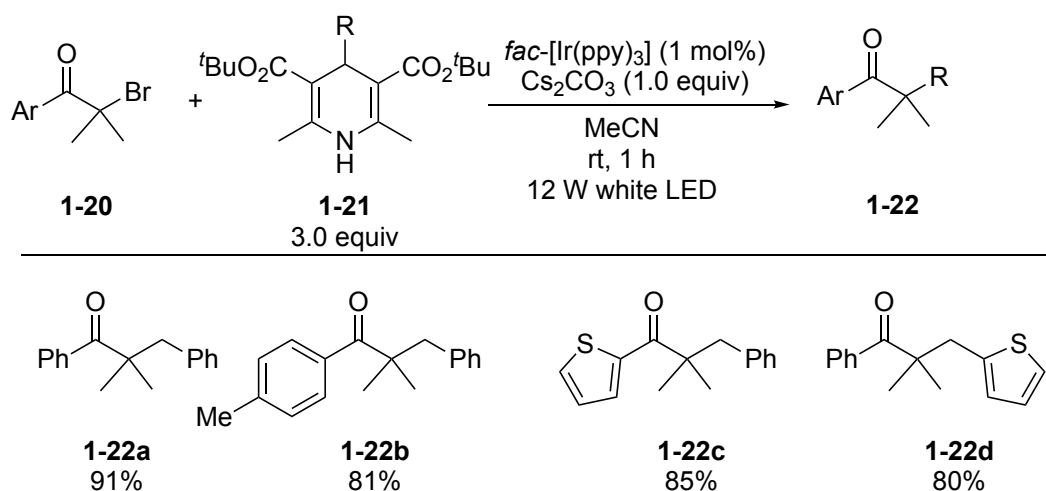
In this report, a plausible reaction pathway was proposed as shown in Scheme 1-8. First, single electron oxidation of 4-alkyl-1,4-dihydropyridine **1-18** by the excited catalyst $[\text{Ir}]^*$ occurs, which gives an alkyl radical and an aromatized pyridine derivative via C–C bond cleavage. Then, subsequent reduction of cyanoarene **1-17** by the reduced catalyst $[\text{Ir}]^-$ occurs to give a radical anion **1-E**. Then, radical coupling between alkyl radical and **1-E** gives **1-F** or **1-G**. Then, decyanation from **1-F** affords 4-substituted arene **1-19** as the major product. However, decyanation from **1-G** after 1,3-shift can also occur to give 2-substituted arene **1-19'** as a minor product. This result has clearly demonstrated that 4-alkyl-1,4-dihydropyridines can work as versatile and mild alkylation reagents under photoredox reaction conditions.

Scheme 1-8. Proposed Mechanism for Photoredox-catalyzed Alkylation Reactions of Cyanoarenes with 4-Alkyl-1,4-dihydropyridines Reported by the Author's Group



Also in 2016, Cheng et al. independently reported alkylation reactions of α -bromo-ketones with 4-alkyl-1,4-dihydropyridines as alkylation reagents. Reactions of α -bromo-ketones **1-20** with 4-alkyl-1,4-dihydropyridines **1-21** in the presence of *fac*-[Ir(ppy)₃] as a photoredox catalyst and Cs₂CO₃ as a base in MeCN under 12 W white LED (light source is dependent on the instrument in lab) irradiation at room temperature for 1 h yielded the products **1-22a-d** in high yields (Scheme 1-9).¹⁹ This research has clearly demonstrated that 4-alkyl-1,4-dihydropyridines can be applied in the formation of quaternary carbon centers.

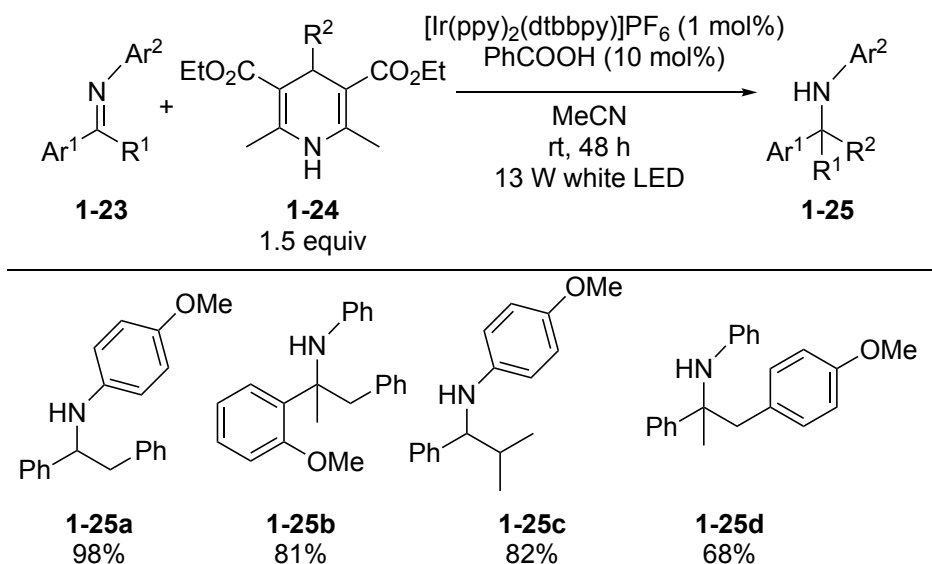
Scheme 1-9. Photoredox-catalyzed Alkylation Reactions of α -Bromo-ketones with 4-Alkyl-1,4-dihydropyridines Reported by Cheng et al.



In 2017, Yu et al. reported reactions of imines with 4-alkyl-1,4-dihydropyridines. Reactions of imines **1-23** with 4-alkyl-1,4-dihydropyridines **1-24** in the presence of

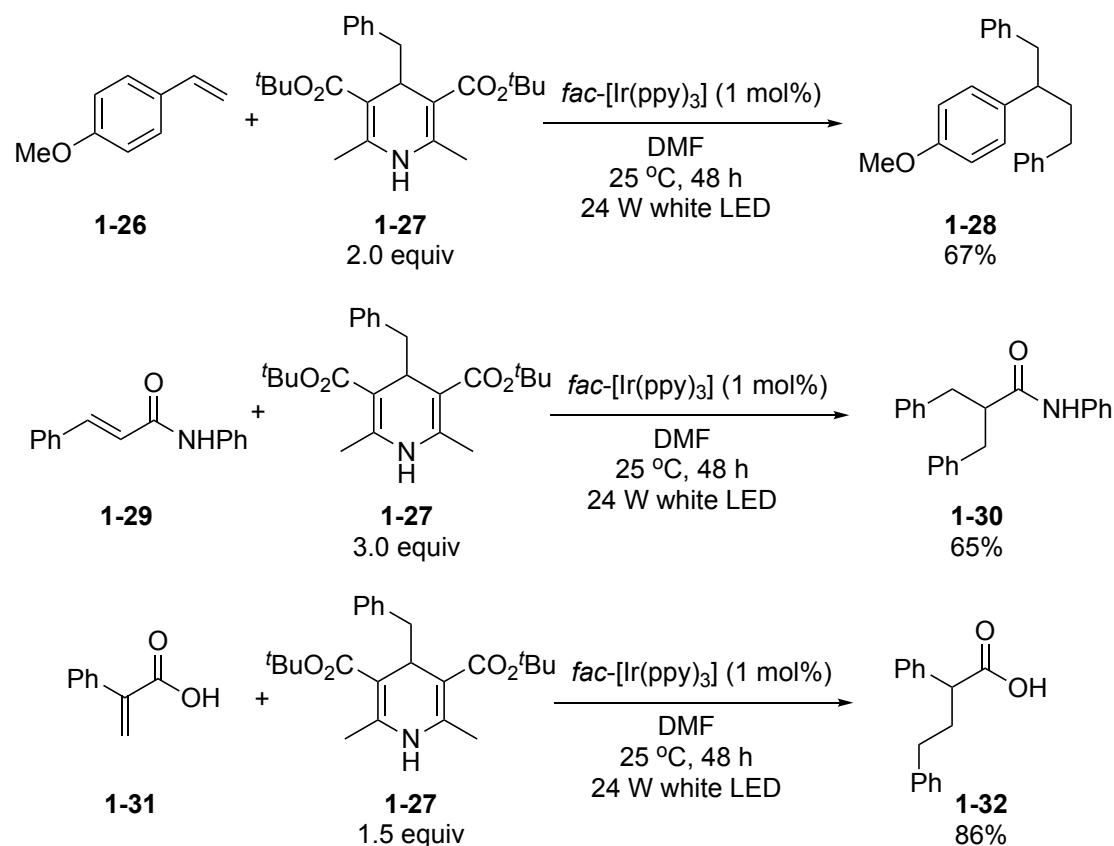
[Ir(ppy)₂(dtbbpy)]PF₆ as a photoredox catalyst and PhCOOH as an acid in MeCN under 13 W white LED irradiation at room temperature for 48 h gave the α -branched C-alkylated amines **1-25a-d** in good to high yields (Scheme 1-10).²⁰ This result has clearly shown that 4-alkyl-1,4-dihydropyridines can be applied in nucleophilic addition reactions to imines.

Scheme 1-10. Photoredox-catalyzed Alkylation Reactions of Imines with 4-Alkyl-1,4-Dihydropyridines Reported by Yu et al.



Also in 2017, Cheng et al. reported reactions of alkenes with 4-alkyl-1,4-dihydropyridines. Reactions of different alkenes **1-26**, **1-29** and **1-31** with 4-alkyl-1,4-dihydropyridines **1-27** in the presence of *fac*-[Ir(ppy)₃] as a photoredox catalyst in DMF under 24 W white LED irradiation at room temperature for 48 h afforded the bis(hydroalkylated) and mono(hydroalkylated) products **1-28**, **1-30** and **1-32** in good yields (Scheme 1-11).²¹ This result has demonstrated that 4-alkyl-1,4-dihydropyridines can be applied in hydroalkylation reactions of alkenes, where 4-alkyl-1,4-dihydropyridines also work as proton sources as well as alkylation reagents.

Scheme 1-11. Photoredox-catalyzed Alkylation Reactions of Alkenes with 4-Alkyl-1,4-dihydropyridines Reported by Cheng et al.



In 2018, Meggers et al. reported reactions of imidazoles with 4-alkyl-1,4-dihydropyridines. Reactions of 2-acyl-imidazoles **1-33** with 4-alkyl-1,4-dihydropyridines **1-34** in the presence of Λ -RhS as a photoredox catalyst in CH_2Cl_2 under 21 W white LED irradiation at room temperature for 13-18 h afforded the products **1-35a-d** in high yields with a high enantioselectivity. (Scheme 1-12).²² This result has demonstrated that enantioselective alkylation of alkenes with 4-alkyl-1,4-dihydropyridines can be achieved by using a transition metal photosensitizer with an optically active ligand as a photoredox catalyst.

Here, “ee” is the abbreviation for “enantiomeric excess” to quantify the purity of chiral substrates, which can be calculated by the subtraction of the percentage of a minor enantiomer in moles from that of a major enantiomer in moles. For example, the enantiomeric excess of **1-35a** at 93% ee means that two enantiomers, (*R*)-**1-35a** and (*S*)-**1-35a**, were obtained as a mixture containing 96.5 mol% of (*R*)-**1-35a** and 3.5 mol% of (*S*)-**1-35a**, respectively. The enantiomeric excess at 93% ee can be given by subtracting 3.5% from 96.5% (Figure 1-2).

Scheme 1-12. Photoredox-catalyzed Alkylation Reactions of Imidazoles with 4-Alkyl-1,4-dihydropyridines Reported by Meggers et al.

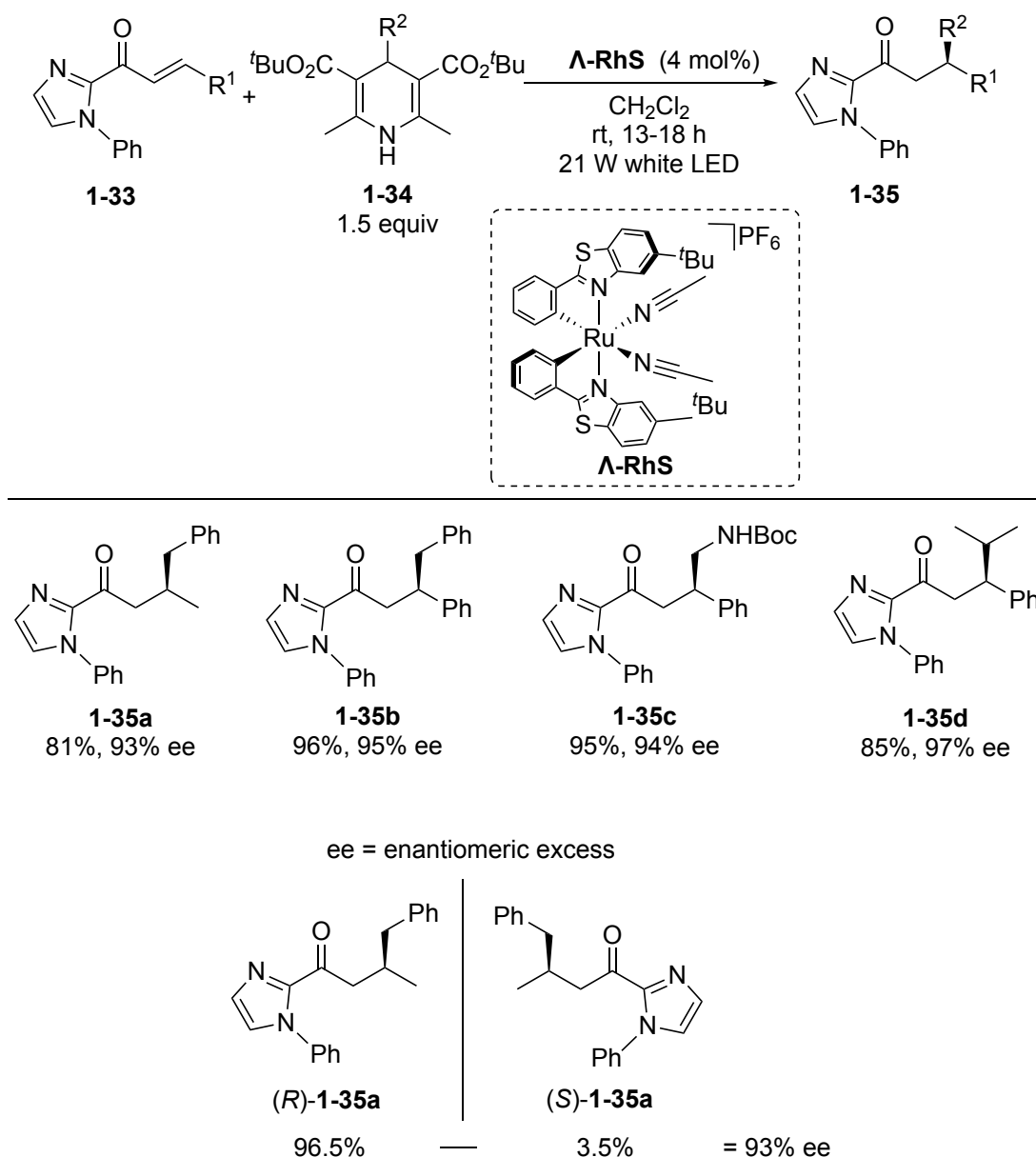
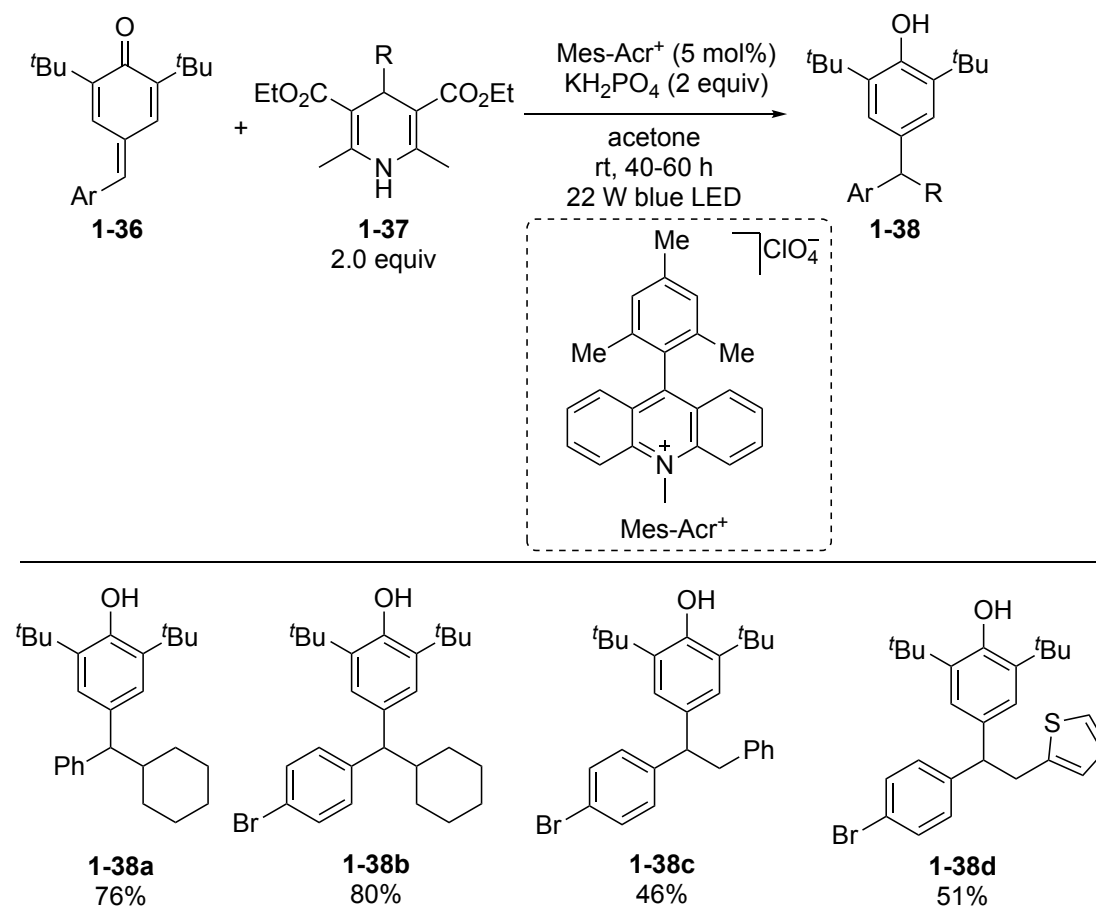


Figure 1-2. How to calculate enantiomeric excess (ee).

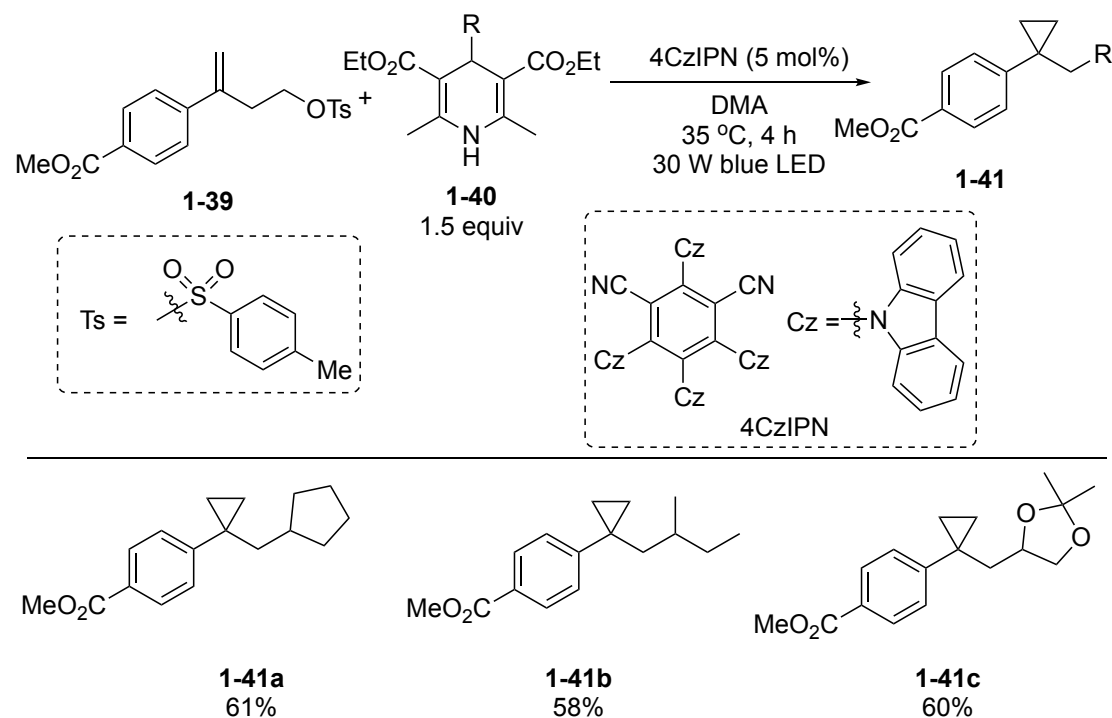
Also in 2018, Liu et al. reported reactions of *para*-quinone methides with 4-alkyl-1,4-dihydropyridines. Reactions of *para*-quinone methides **1-36** with 4-alkyl-1,4-dihydropyridines **1-37** in the presence of Mes-Acr⁺ as a photoredox catalyst and KH_2PO_4 as an additive in acetone under 22 W blue LED irradiation at room temperature for 40-60 h afforded the alkylated phenols **1-38a-d** in moderate to good yields (Scheme 1-13).²³ This research has shown that organophotoredox catalysts can be also applied to alkylation reactions with 4-alkyl-1,4-dihydropyridines instead of well-known transition metal photoredox catalysts.

Scheme 1-13. Photoredox-catalyzed Alkylation Reactions of *para*-Quinone methides with 4-Alkyl-1,4-dihydropyridines Reported by Liu et al.



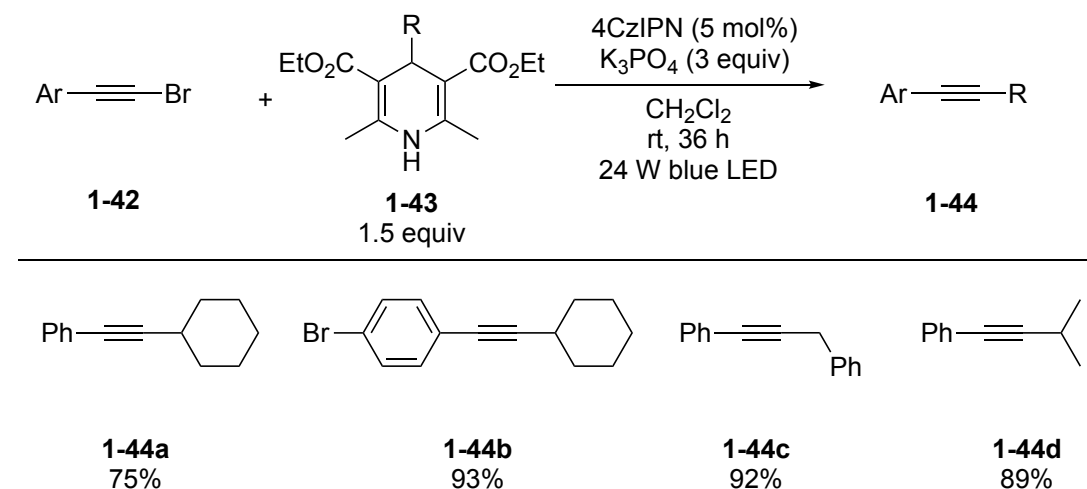
Also in 2018, Molander et al. reported cyclopropanation reactions of an alkene with 4-alkyl-1,4-dihydropyridines. Reactions of an alkene **1-39** with 4-alkyl-1,4-dihydropyridines **1-40** in the presence of 4CzIPN as a photoredox catalyst in DMA under 30 W blue LED irradiation at room temperature for 4 h led to the formation of 1,1-disubstituted cyclopropanes **1-41a-c** in moderate yields (Scheme 1-14).²⁴ This result has clarified that 4-alkyl-1,4-dihydropyridines can be applied in radical/polar annulation reactions.

Scheme 1-14. Photoredox-catalyzed Cyclopropanation Reactions of an Alkene with 4-Alkyl-1,4-dihydropyridines Reported by Molander et al.



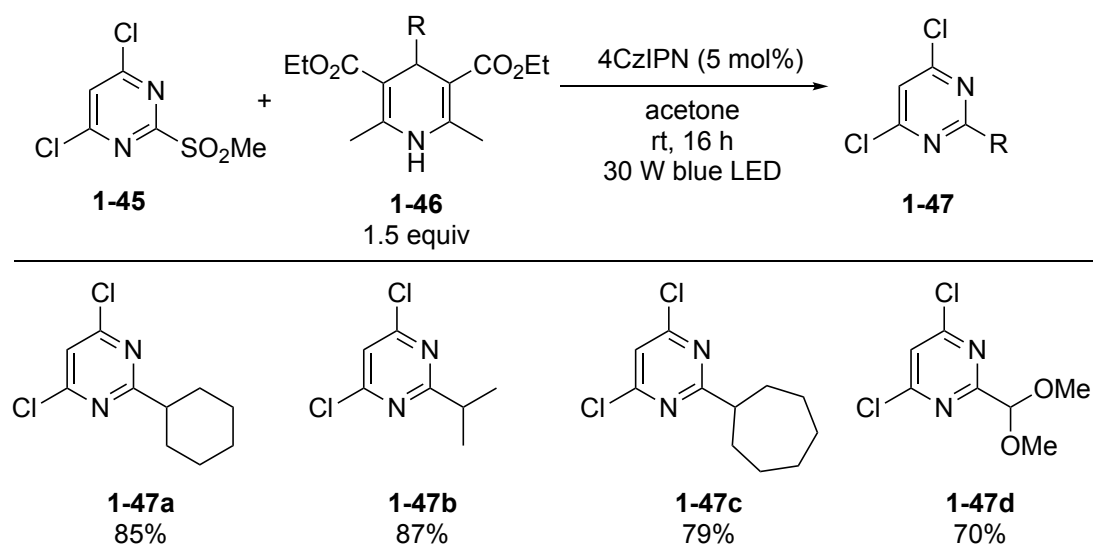
Then in 2019, Ye et al. reported substitution reactions of alkynes with 4-alkyl-1,4-dihydropyridines. Reactions of alkyne bromides **1-42** with 4-alkyl-1,4-dihydropyridines **1-43** in the presence of 4CzIPN as a photoredox catalyst and K_3PO_4 as a base in CH_2Cl_2 under 24 W blue LED irradiation at room temperature for 36 h afforded the alkylated alkynes **1-44a-d** in good to high yields (Scheme 1-15).²⁵ This research has demonstrated that 4-alkyl-1,4-dihydropyridines can be applied in the formation of $\text{C}(\text{sp}^3)\text{--C}(\text{sp})$ bonds by the substitution reaction of haloalkynes.

Scheme 1-15. Photoredox-catalyzed Substitution Reactions of Alkynes with 4-Alkyl-1,4-dihydropyridines Reported by Ye et al.



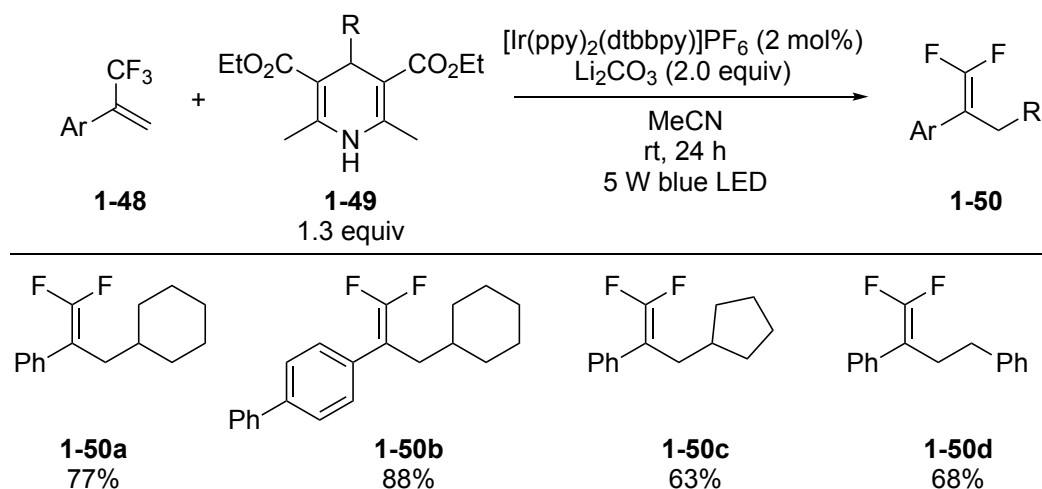
Also in 2019, Molander et al. reported substitution reactions of a *N*-heteroaryl sulfone with 4-alkyl-1,4-dihydropyridines. Reactions of a *N*-heteroaryl sulfone **1-45** with 4-alkyl-1,4-dihydropyridines **1-46** in the presence of 4CzIPN as a photoredox catalyst in acetone under 30 W blue LED irradiation at room temperature for 4 h afforded the alkylated products **1-47a-d** in good yields (Scheme 1-16).²⁶ This research has shown that 4-alkyl-1,4-dihydropyridines can be applied to the preparation of medicinally valuable heteroaromatic compounds.

Scheme 1-16. Photoredox-catalyzed Substitution Reactions of a *N*-Heteroaryl Sulfone with 4-Alkyl-1,4-dihydropyridines Reported by Molander et al.



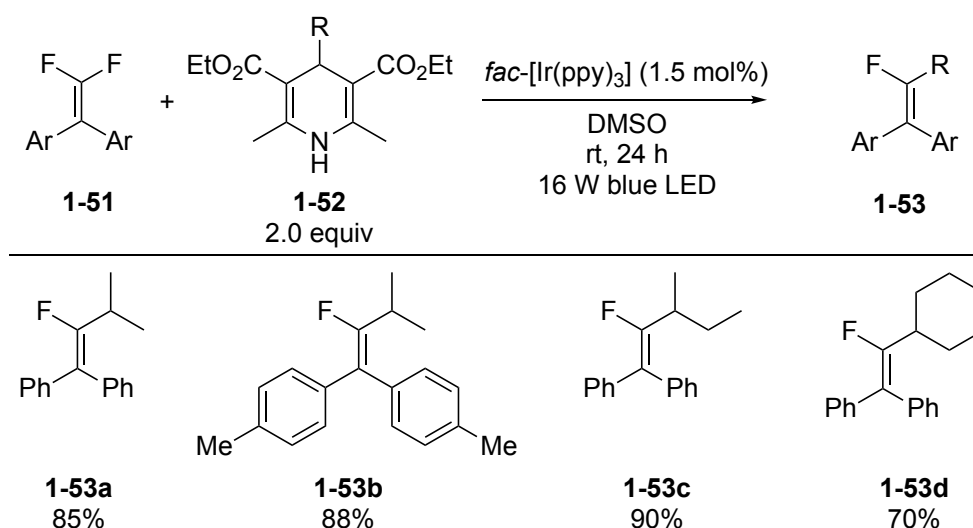
And in 2019, Zhou et al. reported defluorinative alkylation reactions of 1-trifluoromethyl alkenes with 4-alkyl-1,4-dihydropyridines. Reactions of 1-trifluoromethyl alkenes **1-48** with 4-alkyl-1,4-dihydropyridines **1-49** in the presence of $[\text{Ir}(\text{ppy})_2(\text{dtbbpy})]\text{PF}_6$ as a photoredox catalyst and Li_2CO_3 as a base in MeCN under 5 W blue LED irradiation at room temperature for 24 h gave 1,1-difluoroalkenes **1-50a-d** in good yields (Scheme 1-17).²⁷ This research has revealed that 4-alkyl-1,4-dihydropyridines can be applied in the synthesis of *gem*-difluoroalkenes, with one of fluorine atoms of trifluoromethyl moiety of 1-trifluoromethyl alkenes working as a leaving group.

Scheme 1-17. Photoredox-catalyzed Defluorinative Alkylation Reactions of 1-Trifluoromethyl Alkenes with 4-Alkyl-1,4-dihydropyridines Reported by Zhou et al.



Then, in 2020, another Zhou's group reported further defluorinative alkylation reactions of *gem*-difluoroalkenes with 4-alkyl-1,4-dihydropyridines. Reactions of *gem*-difluoroalkenes **1-51** with 4-alkyl-1,4-dihydropyridines **1-52** in the presence of *fac*- $[\text{Ir}(\text{ppy})_3]$ as a photoredox catalyst in DMSO under 16 W blue LED irradiation at room temperature for 24 h gave the monofluoroalkenes **1-53a-d** in good yields (Scheme 1-18).²⁸ This research has shown that the 4-alkyl-1,4-dihydropyridines can be applied in the preparation of monofluoroalkenes via defluorinative alkylation of *gem*-difluoroalkenes.

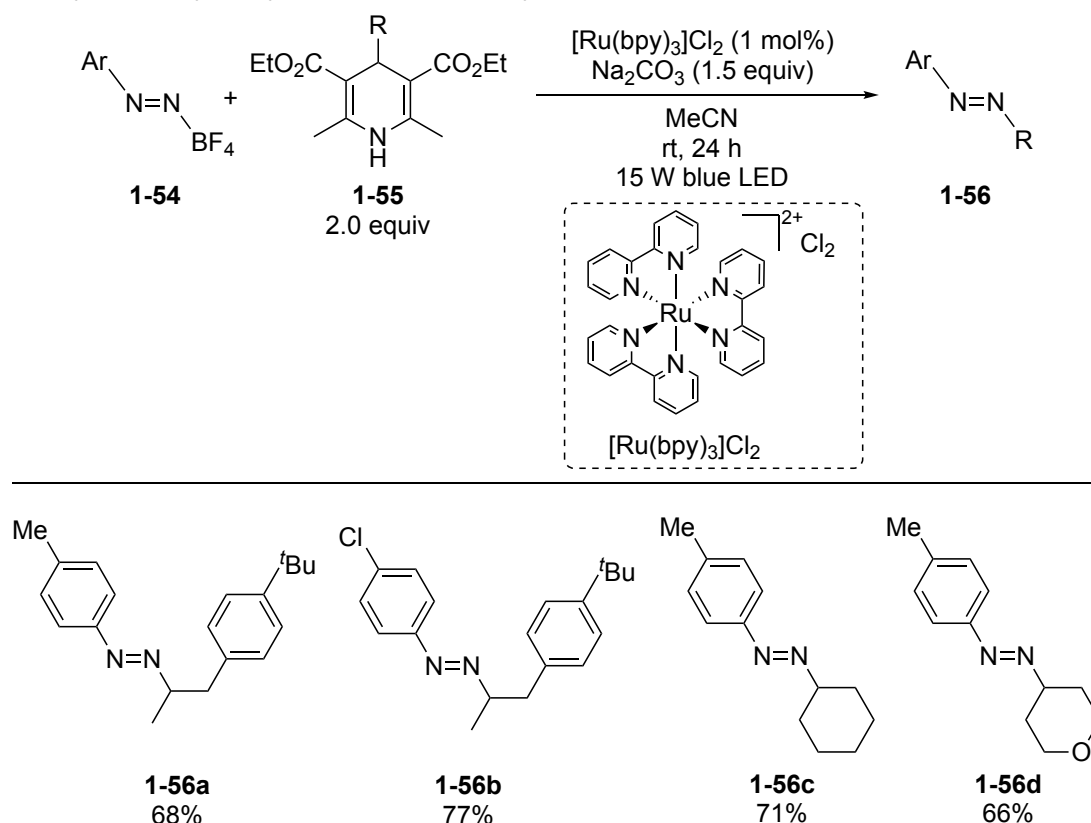
Scheme 1-18. Photoredox-catalyzed Defluorinative Alkylation Reactions of *gem*-Difluoroalkenes with 4-Alkyl-1,4-dihydropyridines Reported by Zhou et al.



Also in 2020, Hammond et al. reported substitution reactions of diazonium salts with 4-alkyl-1,4-dihydropyridines. Reactions of diazonium salts **1-54** with 4-alkyl-1,4-dihydropyridines **1-55** in the presence of $[\text{Ru}(\text{bpy})_3]\text{Cl}_2$ as a photoredox catalyst in MeCN under 15 W blue LED irradiation at room temperature for 24 h afforded *N*-

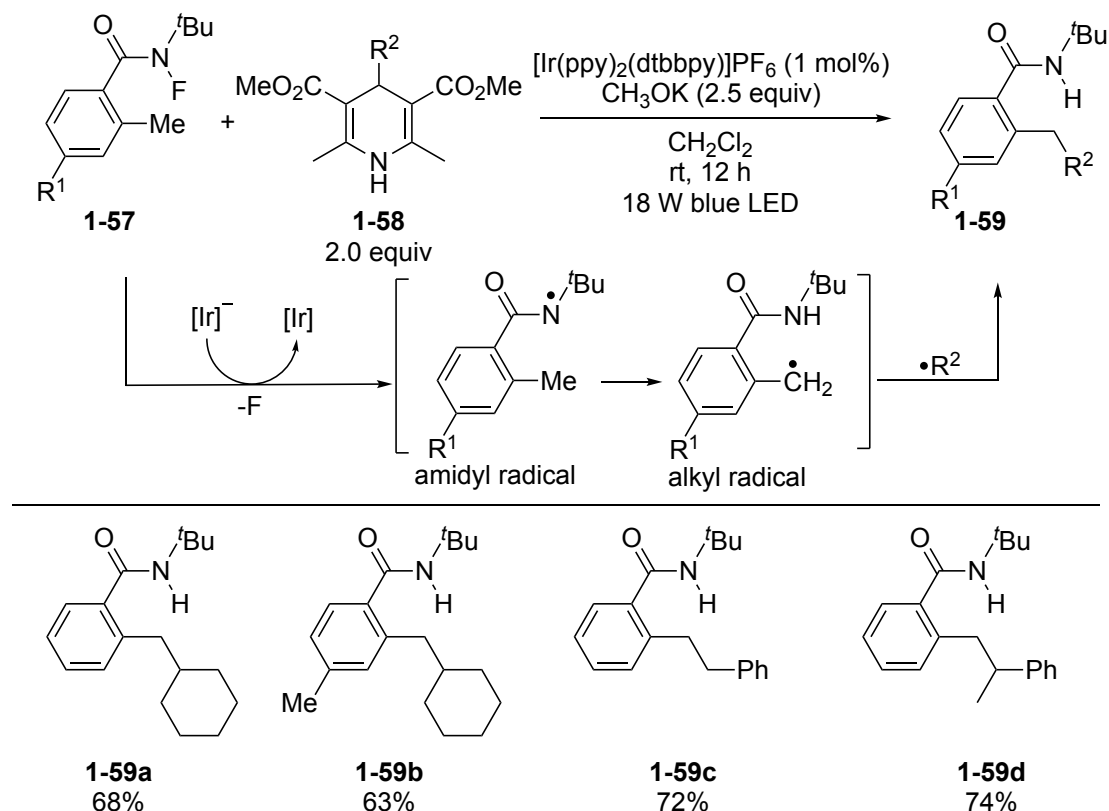
alkylated alkylaryldiazenes **1-56a-d** in good yields (Scheme 1-19).²⁹ This result has revealed that 4-alkyl-1,4-dihydropyridines can be applied in the formation of C-N bonds via alkylation at nitrogen atoms under photochemical conditions.

Scheme 1-19. Photoredox-catalyzed Substitution Reactions of Diazonium Salts with 4-Alkyl-1,4-dihydropyridines Reported by Hammond et al.



And in 2020, Xu et al. reported $\text{C}(\text{sp}^3)\text{--C}(\text{sp}^3)$ coupling reactions of carboxylamides with 4-alkyl-1,4-dihydropyridines. Treatment of carboxylamides **1-57** with 4-alkyl-1,4-dihydropyridines **1-58** in the presence of $[\text{Ir}(\text{ppy})_2(\text{dtbbpy})]\text{PF}_6$ as a photoredox catalyst and CH_3OK as a base in CH_2Cl_2 under 18 W blue LED irradiation at room temperature for 12 h afforded the products **1-59a-d** in good yields (Scheme 1-20).³⁰ Here, the reduced iridium photoredox catalyst works as a reductant to react with **1-57** to generate amidyl radicals, where 1,5-hydrogen atom transfer occurs to afford alkyl radicals, which further react with the other alkyl radicals generated from **1-58** to afford the $\text{C}(\text{sp}^3)\text{--C}(\text{sp}^3)$ coupled products. This research has shown that 4-alkyl-1,4-dihydropyridines can be applied in the alkylation reactions of remote $\text{C}(\text{sp}^3)\text{--H}$ bonds of methyl groups.

Scheme 1-20. Photoredox-catalyzed C(sp³)-C(sp³) Coupling Reactions of Carboxylamides with 4-Alkyl-1,4-dihydropyridines Reported by Xu et al.



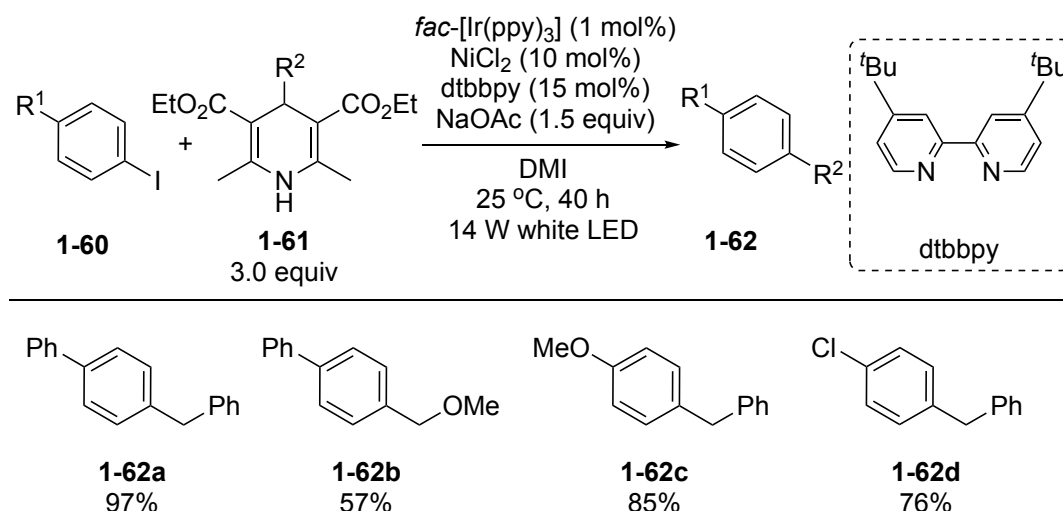
As summarized above, a variety of alkylation reactions using the combination of several photoredox catalysts and 4-alkyl-1,4-dihydropyridines under visible light irradiation have been developed since 2016. In these reaction systems, SET processes between photoredox catalysts and 4-alkyl-1,4-dihydropyridines lead to the formation of alkyl radicals, which act as alternatives to nucleophiles to react with electrophiles or radicals to afford the alkylated products either via substitution or addition reactions.

The scope of the application of the combination of photoredox catalysts and 4-alkyl-1,4-dihydropyridines was drastically expanded by using dual catalytic systems, which will be discussed below.

1.3.2. Dual Photoredox/Nickel-catalyzed Alkylation Reactions with 4-Alkyl-1,4-dihydropyridines

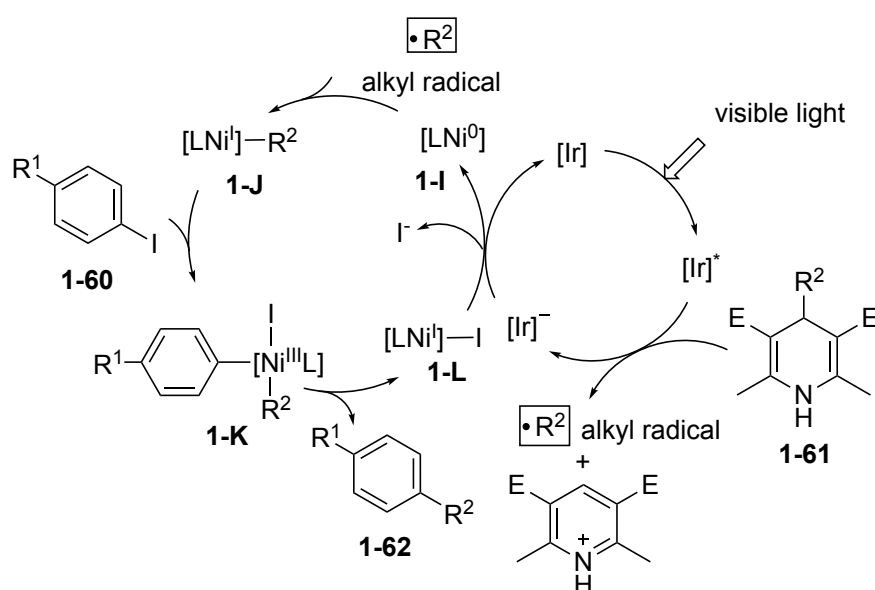
The first dual photoredox/nickel-catalyzed alkylation reactions with 4-alkyl-1,4-dihydropyridines were reported by the author's group in 2016. Reactions of aryl iodides **1-60** with 4-alkyl-1,4-dihydropyridines **1-61** in the presence of *fac*-[Ir(ppy)₃] as a photoredox catalyst, NiCl₂ as a cross-coupling nickel catalyst, dtbbpy as a ligand, and NaOAc as a base in DMI under 14 W white LED irradiation at 25 °C for 40 h afforded the alkylated products **1-62a-d** in good to high yields (Scheme 1-21).³¹

Scheme 1-21. First Dual Photoredox/Nickel-catalyzed Alkylation Reactions of Aryl Iodides with 4-Alkyl-1,4-dihydropyridines Reported by the Author's Group



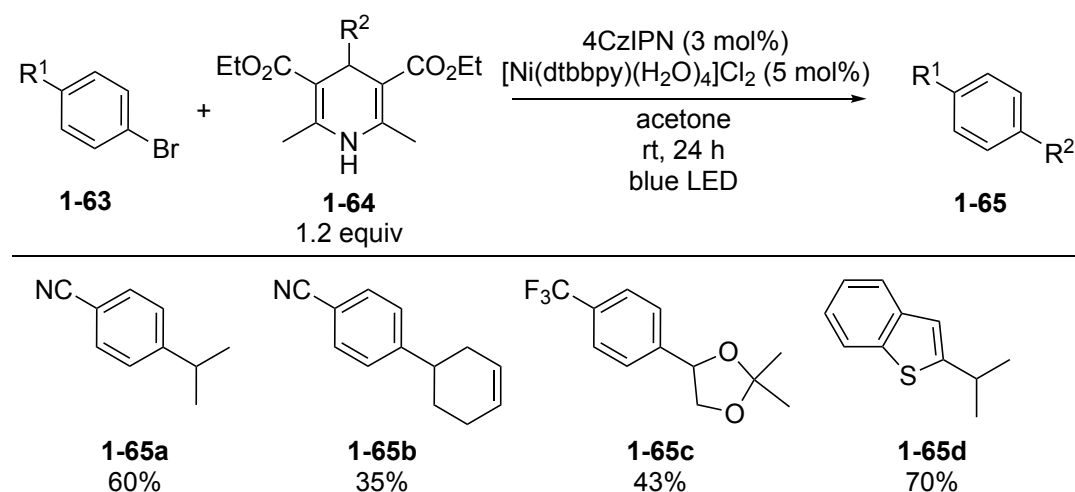
In this report, a plausible reaction pathway was proposed as shown in [Scheme 1-22](#). First, single electron oxidation of 4-alkyl-1,4-dihydropyridine **1-61** by the excited catalyst $[Ir]^*$ occurs, which gives an alkyl radical and an aromatized pyridine derivative via C–C bond cleavage. Then, radical capture by a $Ni(0)$ complex **1-I** occurs to give an alkyl-Ni complex **1-J**. Then, oxidative addition of aryl iodide **1-60** to **1-J** occurs to give a $Ni(III)$ complex **1-K**. Then, reductive elimination takes place to give the cross-coupling product **1-62**. Finally, the catalytic cycle is completed by a single-electron transfer between the resulting $Ni(I)$ halide complex **1-L** and reduced $[Ir]^-$ complex. This result has clearly demonstrated that 4-alkyl-1,4-dihydropyridines can work as versatile and mild alkylation reagents in nickel-catalyzed cross-coupling reactions.

Scheme 1-22. Proposed Mechanism for Dual Photoredox/Nickel-catalyzed Alkylation Reactions of Aryl Iodides with 4-Alkyl-1,4-dihydropyridines Reported by the Author's Group



At the same time, Molander et al. reported dual photoredox/nickel-catalyzed alkylation reactions of aryl halides with 4-alkyl-1,4-dihydropyridines. Reactions of aryl bromides **1-63** with 4-alkyl-1,4-dihydropyridines **1-64** in the presence of 4CzIPN as a photoredox catalyst and $[\text{Ni}(\text{dtbbpy})(\text{H}_2\text{O})_4]\text{Cl}_2$ as a nickel catalyst in acetone under blue LED irradiation at room temperature for 24 h afforded the products **1-65a-d** in moderate to good yields (Scheme 1-23).³² Here, secondary alkyl groups were successfully introduced to the aryl moieties by using 4-alkyl-1,4-dihydropyridines with secondary alkyl groups as the alkylation reagents, in contrast to the result previously reported by the author's group.³¹

Scheme 1-23. Dual Photoredox/Nickel-catalyzed Alkylation Reactions of Aryl Bromides with 4-Alkyl-1,4-dihydropyridines Reported by Molander et al.



Then in 2018, Molander et al. reported dual photoredox/nickel-catalyzed alkylation reactions of carboxylic acids with complicated 4-alkyl-1,4-dihydropyridines containing glycoside structures to prepare C-acyl glycosides. Reactions of carboxylic acids **1-66** with 4-alkyl-1,4-dihydropyridines **1-67** in the presence of 4CzIPN as a photoredox catalyst, $[\text{Ni}(\text{dtbbpy})(\text{H}_2\text{O})_4]\text{Cl}_2$ as a nickel catalyst, and dimethyl decarbonate (DMDC) as an additive to capture free hydroxy groups in acetone/ i PrOAc under blue LED irradiation at room temperature for 24 h afforded the products **1-68a-c** in good yields with a moderate diastereoselectivity (Scheme 1-24).³³ Here, “dr” is the abbreviation for “diastereomeric ratio”, the ratio of two diastereomers, while “diastereomers” are defined as the stereoisomers which are not mirror images nor superposable to each other, that is, stereoisomers excluding enantiomers are diastereomers. For example, as the amount of **1-68a** is 4.3 times as much as that of **1-68a'**, diastereomeric ratio of **1-68a** and **1-68a'** can be given as 4.3/1 (Figure 1-3; note that absolute configuration of **1-68a** or **1-68a'** was not determined in the article). Consequently, C–C bond formation between acyl and alkyl groups was successfully achieved by the cross-coupling reactions between carboxylic acids and 4-alkyl-1,4-dihydropyridines acting as alternatives to electrophilic acylation and nucleophilic alkylation reagents, respectively.

Scheme 1-24. Dual Photoredox/Nickel-catalyzed Alkylation Reactions of Carboxylic Acids with 4-Alkyl-1,4-dihydropyridines Reported by Molander et al.

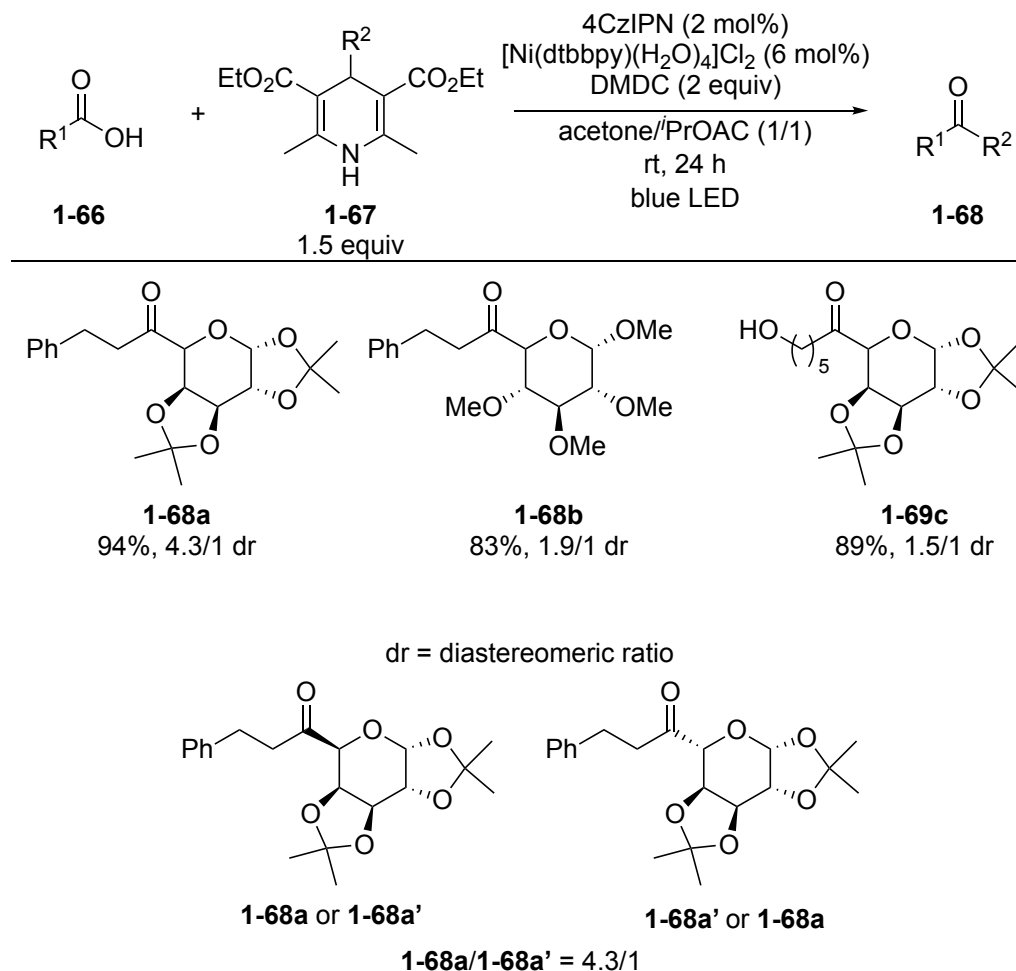
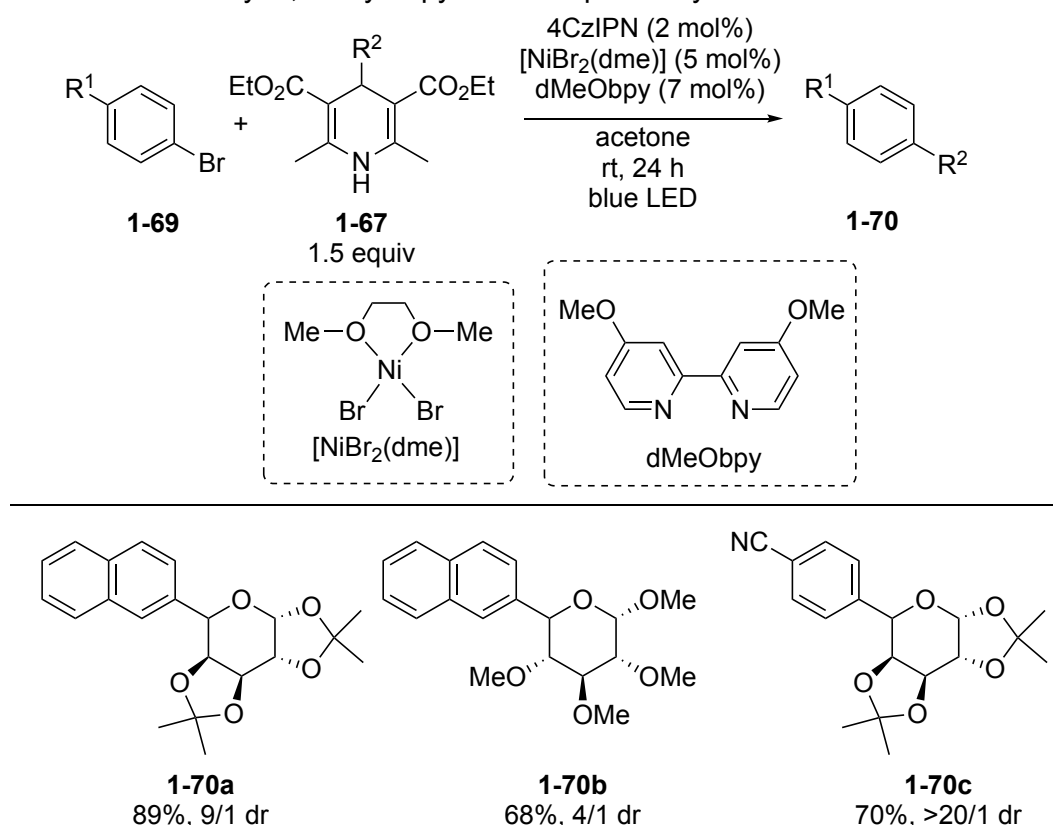


Figure 1-3. Diastereomeric ratio

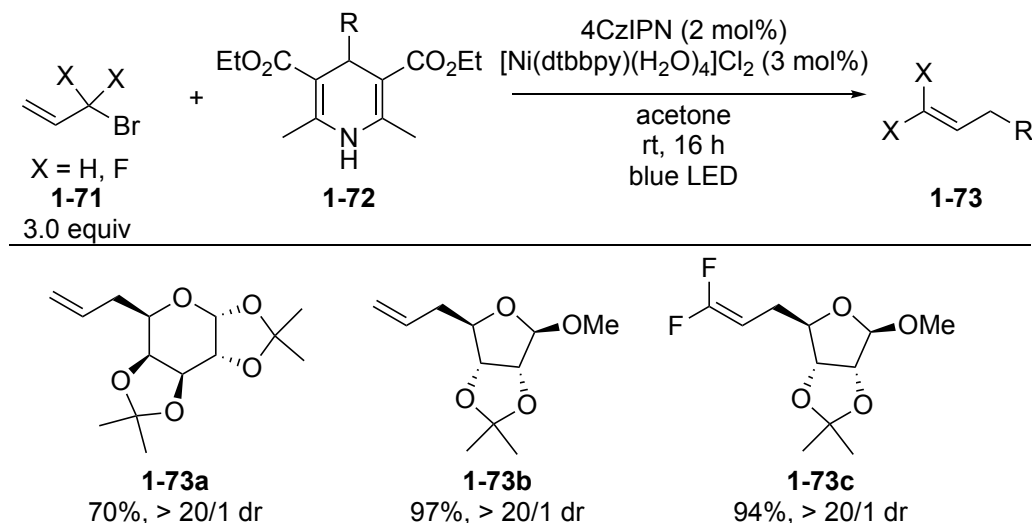
They also reported dual photoredox/nickel-catalyzed alkylation reactions of aryl halides with complicated 4-alkyl-1,4-dihydropyridines containing glycoside structures to prepare C-aryl glycosides. Reactions of aryl bromides **1-69** with 4-alkyl-1,4-dihydropyridines **1-67** in the presence of 4CzIPN photoredox catalyst, $[\text{NiBr}_2(\text{dme})]$ and dMeObpy as the ligand in acetone under blue LED irradiation at room temperature for 24 h afforded the products **1-70a-c** in good yields (Scheme 1-25).³⁴ Here, C–C bond formation between aryl and alkyl groups was successfully achieved by the cross-coupling reactions between aryl halides and 4-alkyl-1,4-dihydropyridines acting as alternatives to electrophilic arylation and nucleophilic alkylation reagents, respectively.

Scheme 1-25. Dual Photoredox/Nickel-catalyzed Alkylation Reactions of Aryl Bromides with 4-Alkyl-1,4-dihydropyridines Reported by Molander et al



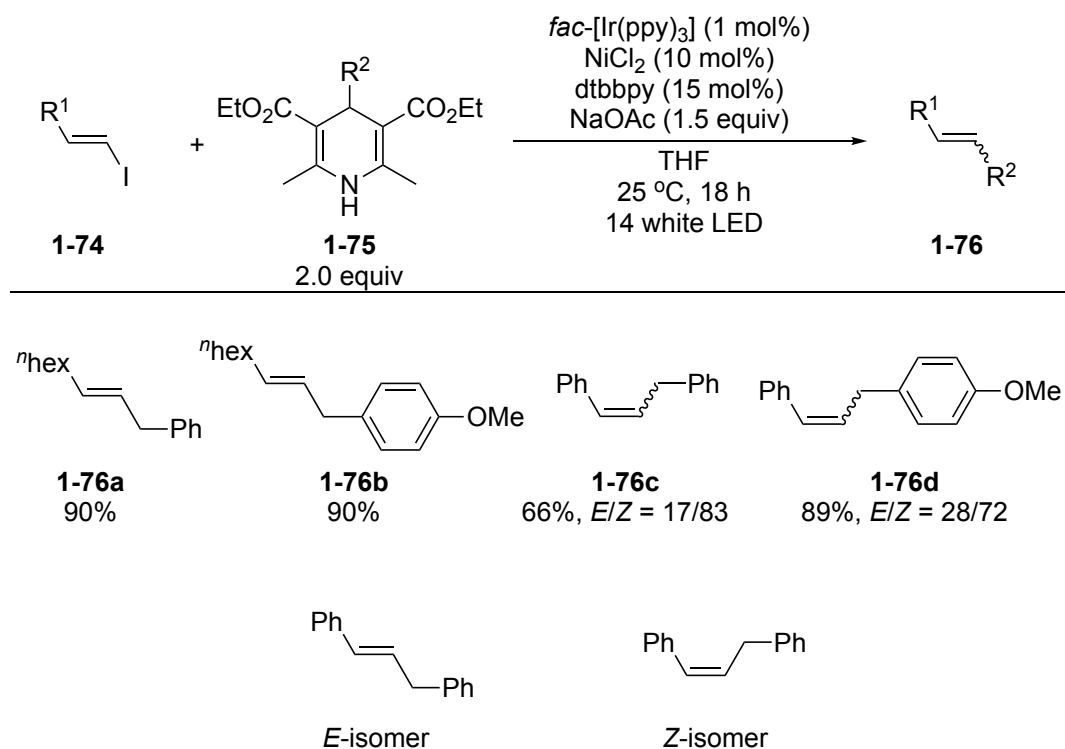
Also in the same year, Molander et al. reported dual photoredox/nickel-catalyzed alkylation reactions of allyl halides with complicated 4-alkyl-1,4-dihydropyridines. Reactions of allyl bromides **1-71** with 4-alkyl-1,4-dihydropyridines **1-72** in the presence of 4CzIPN as a photoredox catalyst and [Ni(dtbbpy)(H₂O)₄]Cl₂ as a nickel catalyst in acetone under blue LED irradiation at room temperature for 16 h afforded the products **1-73a-c** in good yields (Scheme 1-26).^{35a} This research has demonstrated that 4-alkyl-1,4-dihydropyridines can be applied in the Tsuji–Trost reactions.^{35b,c}

Scheme 1-26. Dual Photoredox/Nickel-catalyzed Alkylation Reactions of Allyl Bromides with 4-Alkyl-1,4-dihydropyridines Reported by Molander et al.



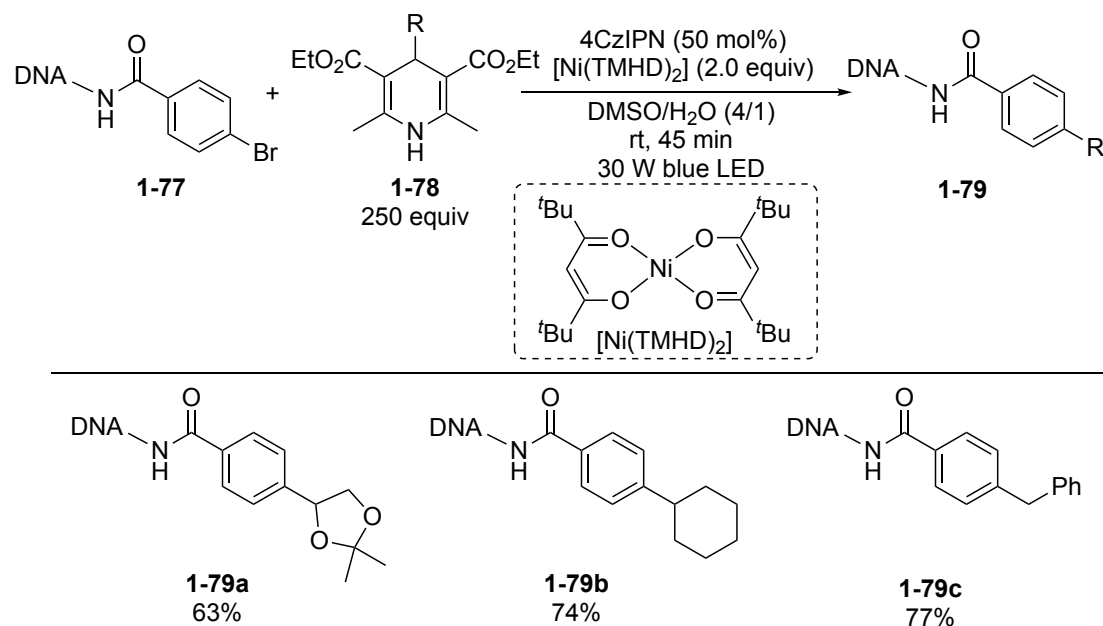
In 2018, the author's group reported dual photoredox/nickel-catalyzed alkylation reactions of alkenyl halides with 4-alkyl-1,4-dihydropyridines. Reactions of alkenyl iodides **1-74** with 4-alkyl-1,4-dihydropyridines **1-75** in the presence of *fac*-[Ir(ppy)₃] as a photoredox catalyst, NiCl₂ as a nickel catalyst, dtbbpy as a ligand, and NaOAc as a base in THF under 14 W white LED irradiation at 25 °C for 18 h afforded the products **1-76a-d** in good to high yields (Scheme 1-27). Here, “*E*-isomer” of an alkene is defined as the compound with two substituents attached on opposite sides of the double bond, while “*Z*-isomer” as those with two substituents on the same sides of the double bond. It must be noteworthy that *E*-isomers were obtained as sole products when alkyl-substituted alkenyl iodides were used as the substrates to react with 4-alkyl-1,4-dihydropyridines, whereas mixtures of *E*- and *Z*-isomers were obtained when aryl-substituted alkenyl iodides were used as the substrates. In general, *E*-isomers are thermodynamically more stable than *Z*-isomers. Thus, *E*-isomers are obtained as major products. However, aryl-substituted alkenyl iodides are susceptible to *E*-to-*Z* isomerization process mediated by energy transfer from the excited photoredox catalyst.³⁶ Accordingly, alkenyl iodides were shown to react with 4-alkyl-1,4-dihydropyridines to afford alkylated alkenes.

Scheme 1-27. Dual Photoredox/Nickel-catalyzed Alkylation Reactions of Alkenyl Iodides with 4-Alkyl-1,4-dihydropyridines Reported by the Author's Group



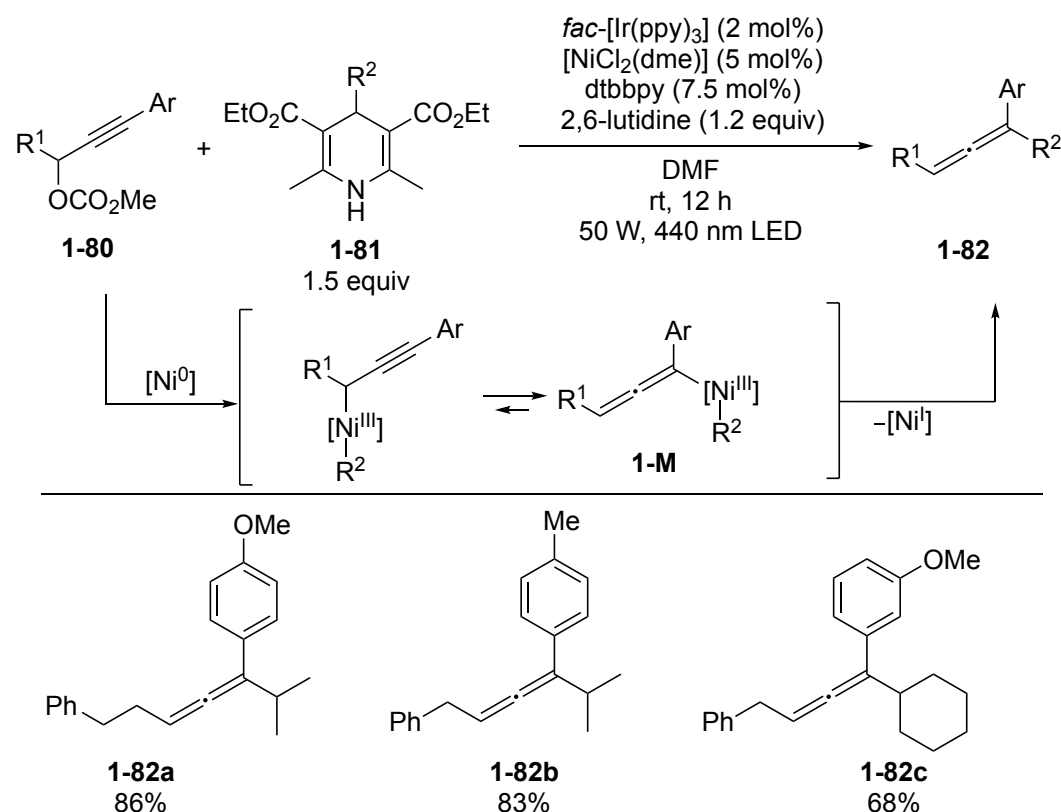
In 2019, Molander et al. applied the dual photoredox/nickel-catalyzed alkylation reactions of aryl bromides with 4-alkyl-1,4-dihydropyridines toward the DNA-encoded library synthesis. Reactions of 14 base-containing DNA fragment-linked aryl bromides **1-77** with 4-alkyl-1,4-dihydropyridines **1-78** in the presence of 4CzIPN as a photoredox catalyst and $[Ni(TMHD)_2]$ as a nickel catalyst in DMSO/H₂O under 30 W blue LED irradiation at room temperature for 24 h afforded the products **1-79a-c** in good yields (Scheme 1-28).³⁷ Thus, dual photoredox/nickel-catalyzed alkylation reaction with 4-alkyl-1,4-dihydropyridines was shown to be applicable for the modification of bioactive oligomeric molecules with molecular weights more than 5,000.

Scheme 1-28. Dual Photoredox/Nickel-catalyzed Alkylation Reactions of DNA-linked Aryl Halides with 4-Alkyl-1,4-dihydropyridines Reported by Molander et al



In 2021, Liang et al. reported dual photoredox/nickel-catalyzed regioselective alkylation of propargylic carbonates with 4-alkyl-1,4-dihydropyridines for synthesis of trisubstituted allenes. Reactions of propargylic carbonates **1-80** with 4-alkyl-1,4-dihydropyridines **1-81** in the presence of *fac*-[Ir(ppy)₃] as a photoredox catalyst, [NiCl₂(dme)] as a nickel catalyst, dtbbpy as a ligand, and 2,6-lutidine as a base in DMF under 50 W, 440nm LED irradiation at room temperature for 12 h afforded the alkylated allenes **1-82a-c** in good to high yields. (Scheme 1-29).³⁸ In this reaction, the iridium photoredox catalyst works as a reductant against nickel catalyst to afford Ni(0) species, where oxidative addition of propargylic carbonates **1-80** and trap of alkyl radicals generated from **1-81** undergo to afford the alkyl allenyl nickel intermediates **1-M**, which control the regioselectivity of the alkylated products **1-82**. This research has demonstrated that 4-alkyl-1,4-dihydropyridines can be applied in the alkylation of propargylic carbonates toward the formation of alkylated allenes.

Scheme 1-29. Dual Photoredox/Nickel-catalyzed Regioselective Alkylation of Propargylic Carbonates with 4-Alkyl-1,4-dihydropyridines Reported by Liang et al.

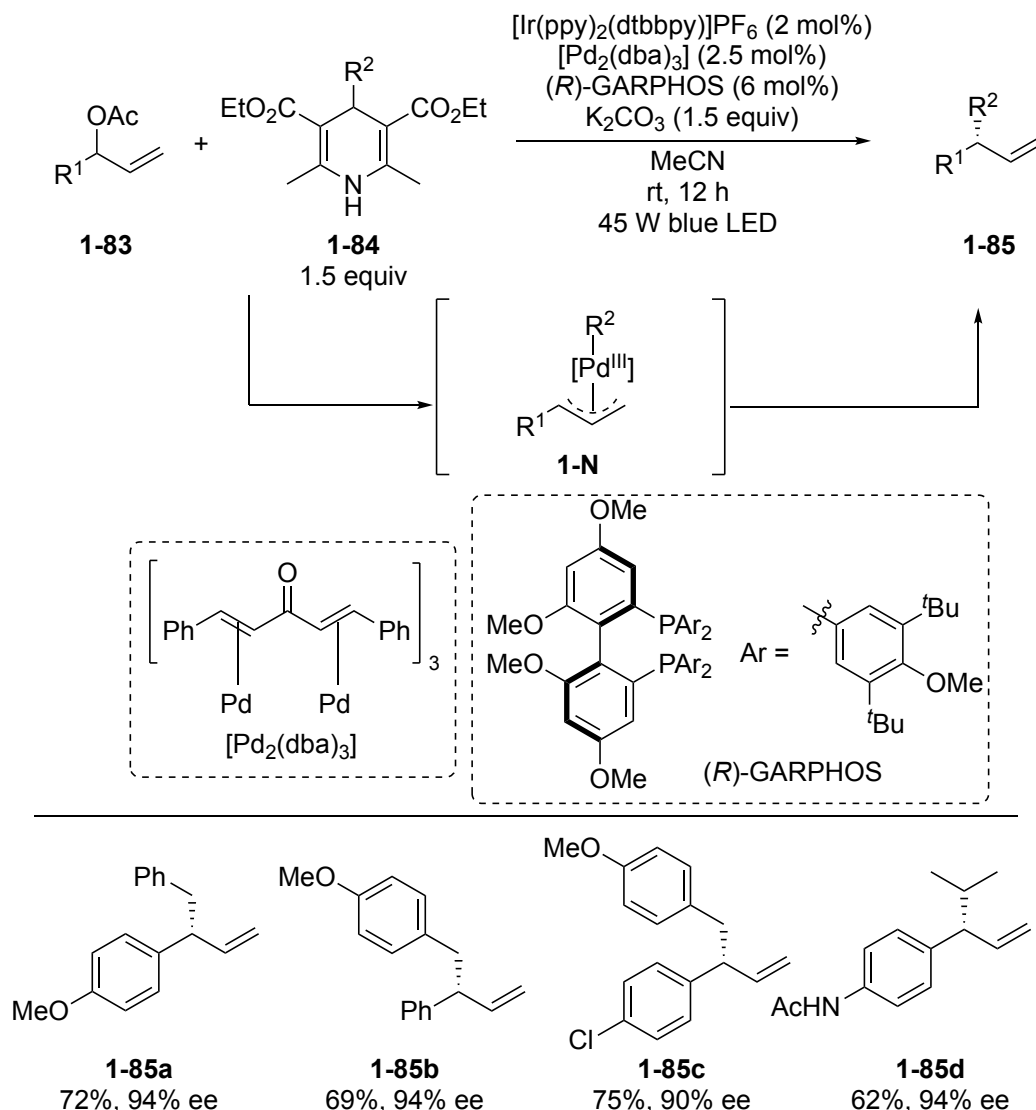


1.3.3. Dual Photoredox/Palladium-catalyzed Alkylation Reactions with 4-Alkyl-1,4-dihydropyridines

Although palladium compounds have been known to work as more effective catalysts toward cross-coupling reactions compared to those for nickel compounds, examples of dual photoredox/palladium-catalyzed alkylation reactions with 4-alkyl-1,4-dihydropyridines have been rather limited in number, probably because nickel compounds have been rather known to stabilize alkyl radicals.

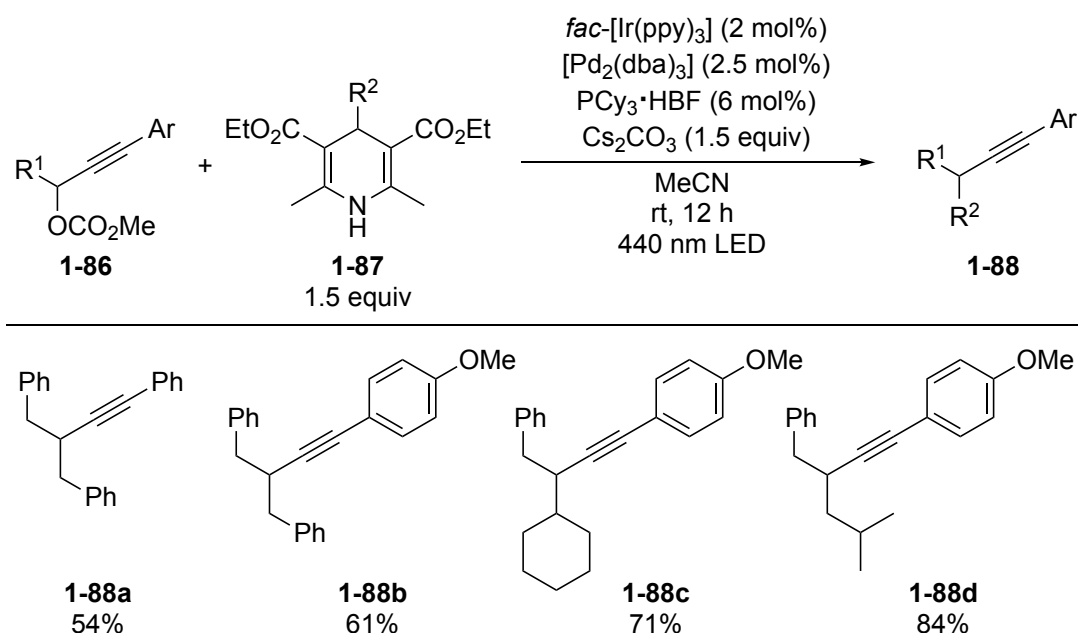
In 2018, Yu et al. reported dual photoredox/palladium-catalyzed enantioselective alkylation reactions of allylic acetates with 4-alkyl-1,4-dihydropyridines, which are based on the traditional asymmetric allylic alkylation reactions.^{39a} Reactions of allylic acetates **1-83** with 4-alkyl-1,4-dihydropyridines **1-84** in the presence of $[\text{Ir(ppy)}_2(\text{dtbbpy})]\text{PF}_6$ as a photoredox catalyst, $[\text{Pd}_2(\text{dba})_3]$ as a palladium catalyst, (*R*)-GARP₂PHOS as a ligand, and K_2CO_3 as a base in MeCN under 45 W blue LED irradiation at room temperature for 12 h afforded the alkylated allylic compounds **1-85a-d** in good yields with a high enantioselectivity via key intermediates **1-N**. (Scheme 1-30).^{39b} This research is the first dual photoredox/palladium-catalyzed enantioselective coupling of allyl esters with 4-alkyl-1,4-dihydropyridines.

Scheme 1-30. Dual Photoredox/Palladium-catalyzed Enantioselective Alkylation Reactions of Allylic Acetates with 4-Alkyl-1,4-dihydropyridines Reported by Yu et al.



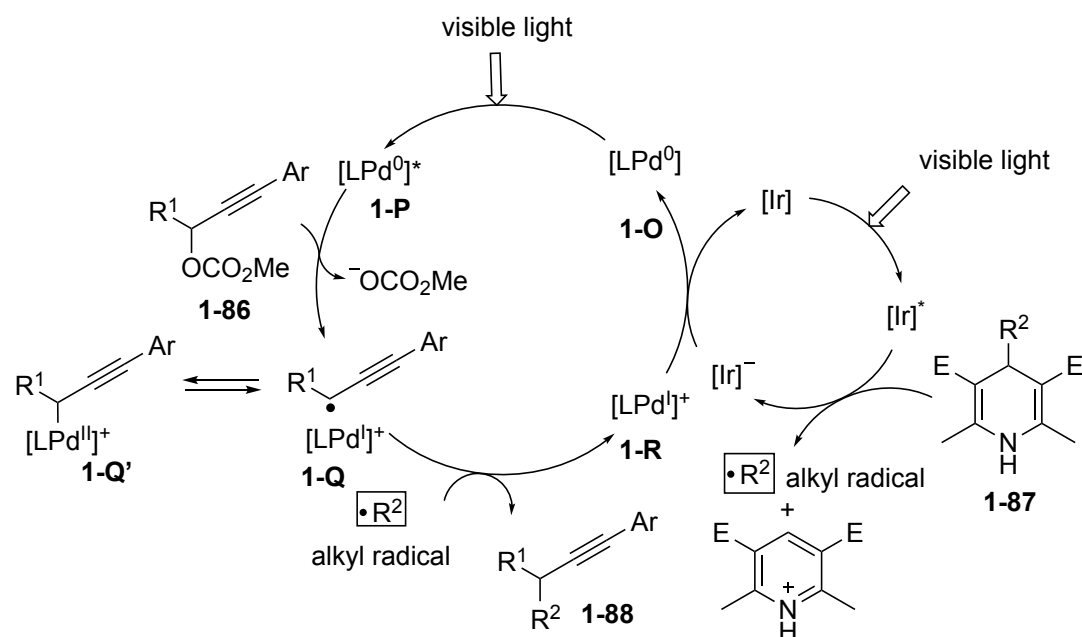
Then, in 2020, Liang et al. reported dual photoredox/palladium-catalyzed propargylic alkylation reactions of internal propargylic carbonates with 4-alkyl-1,4-dihydropyridines. Reactions of internal propargylic carbonates **1-86** with 4-alkyl-1,4-dihydropyridines **1-87** in the presence of *fac*- $[\text{Ir}(\text{ppy})_3]$ as a photoredox catalyst, $[\text{Pd}_2(\text{dba})_3]$ as a palladium catalyst, $\text{PCy}_3 \cdot \text{HBF}_4$ as a ligand, and Cs_2CO_3 as a base in MeCN under 50 W, 440 nm LED irradiation at room temperature for 12 h afforded the propargylic alkylated products **1-88a-d** in good yields (Scheme 1-31).⁴⁰

Scheme 1-31. Dual Photoredox/Palladium-catalyzed Propargylic Alkylation Reactions of Internal Propargylic Carbonates with 4-Alkyl-1,4-dihydropyridines Reported by Liang et al.



In this report, a hypothetical reaction mechanism containing iridium and palladium catalytic cycles, in both of which photoexcitation by visible light participates, was proposed as shown in [Scheme 1-32](#). In the iridium catalytic cycle, single electron oxidation of 4-alkyl-1,4-dihydropyridine **1-87** by the photoexcited catalyst [Ir]^{*} occurs to give an alkyl radical and an aromatized pyridine derivative via C–C bond cleavage. Likewise in the palladium catalytic cycle, an *in situ* generated Pd(0) complex **1-O** also absorbs visible light to become an excited Pd(0) complex **1-P**, which further promotes decarboxylation of propargylic carbonate **1-86** to generate a propargylic radical and a Pd(I) species **1-Q**, in equilibrium with propargylic Pd(II) complex **1-Q'**. Then, **1-Q** traps the alkyl radical to generate the propargylic alkylated product **1-88**. Finally, the catalytic cycle is completed by a single-electron transfer between the resulting Pd(I) complex **1-R** and reduced [Ir][–] complex. Here, formation of both propargylic and alkyl radicals *in situ* was confirmed by the radical trap experiment and detection of alkyl dimers, respectively. To the best of the author's knowledge, this is the only example, where propargylic substitution reactions are induced by photoredox catalysts.

Scheme 1-32. Proposed Mechanism for Dual Photoredox/Palladium-catalyzed Propargylic Alkylation Reactions of Internal Propargylic Carbonates with 4-Alkyl-1,4-dihydropyridines Reported by Liang et al.

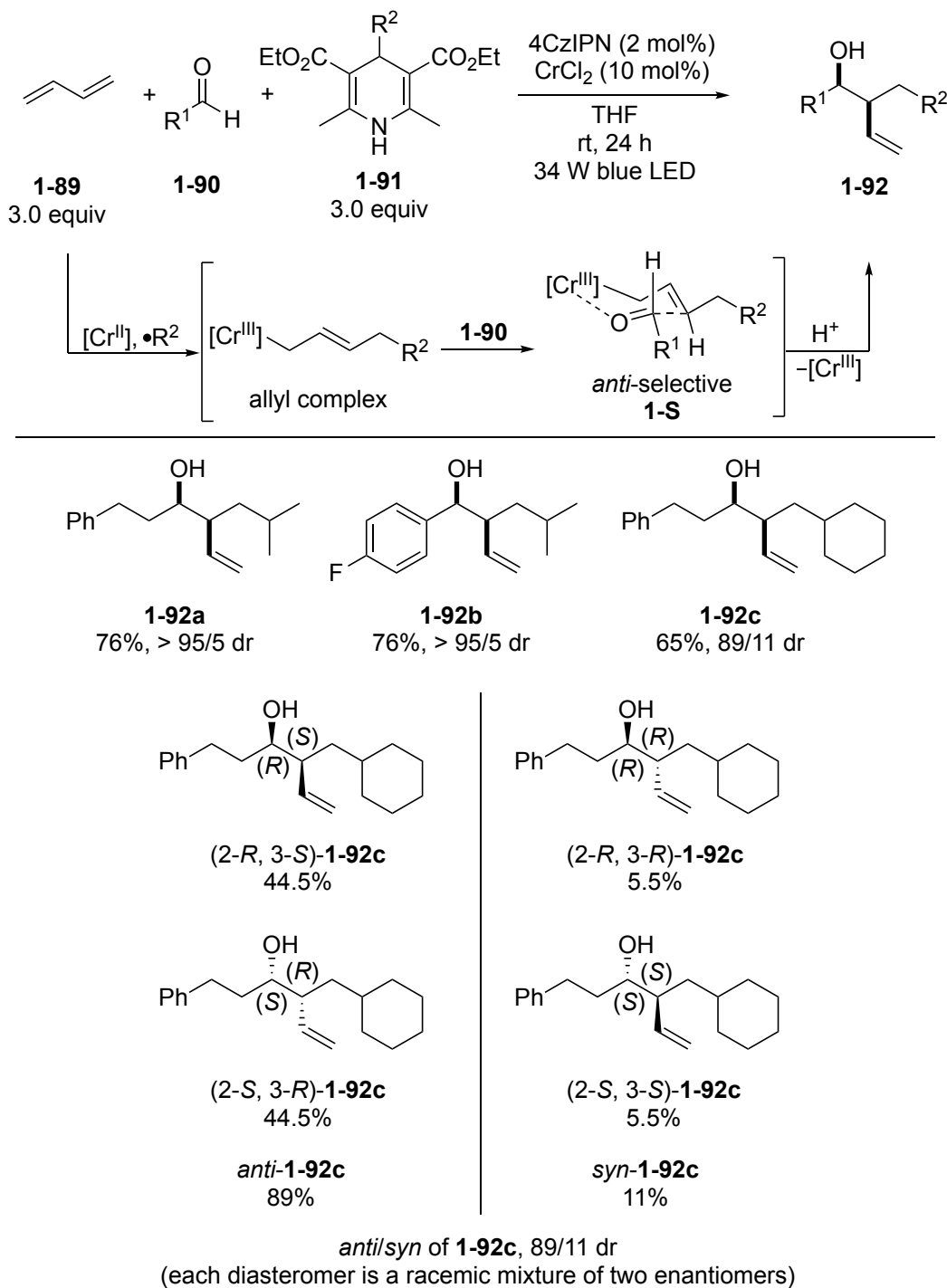


1.3.4. Dual Photoredox/Chromium-catalyzed Alkylation Reactions with 4-Alkyl-1,4-dihydropyridines

Compared to those reported for dual photoredox/nickel or photoredox/palladium catalytic mode, dual photoredox/chromium catalytic mode is less explored in synthetic chemistry, while chromium(II) species have been known to trap and stabilize alkyl radicals. In 2020, Glorius et al. who engaged in the development of CrCl_2 -catalyzed Nozaki-Hiyama-Kishi-type three-component allylic functionalization reactions of dienes with aldehydes and alkylation reagents to obtain acylated and alkylated products,^{41a} focused upon the usage of dual photoredox/chromium-catalyzed alkylation reactions of 1,3-dienes with aldehydes and 4-alkyl-1,4-dihydropyridines. Reactions of buta-1,3-diene **1-89** with aldehydes **1-90** and 4-alkyl-1,4-dihydropyridines **1-91** in the presence of 4CzIPN as a photoredox catalyst and CrCl_2 as a chromium catalyst in THF under 34 W blue LED irradiation at room temperature for 24 h afforded the acylated and alkylated products **1-92a-c** in good yields with a high diastereoselectivity, where *anti*-selectivity was proposed to be preferred by the formation of six-membered transition states **1-S** by the reaction of alkylated allyl complex with **1-90** to afford *anti*-**1-90** as a major product (Scheme 1-33).^{41b} Here, “*syn*”-isomers correspond to those where two substituents are introduced at the same sides or faces, whereas “*anti*”-isomers correspond to those where two substituents are introduced at the opposite sides or faces. In case of **1-92c**, *syn*-**1-92c** and *anti*-**1-92c** are diastereomers obtained in a ratio of 89:11, where both *syn*-**1-92c** and *anti*-**1-92c** are racemates. Thus, the *syn/anti* ratio is given as 89/11 dr. Accordingly, dual photoredox/chromium catalytic system has

become another reaction pattern where alkylation with 4-alkyl-1,4-dihydropyridines can take place.

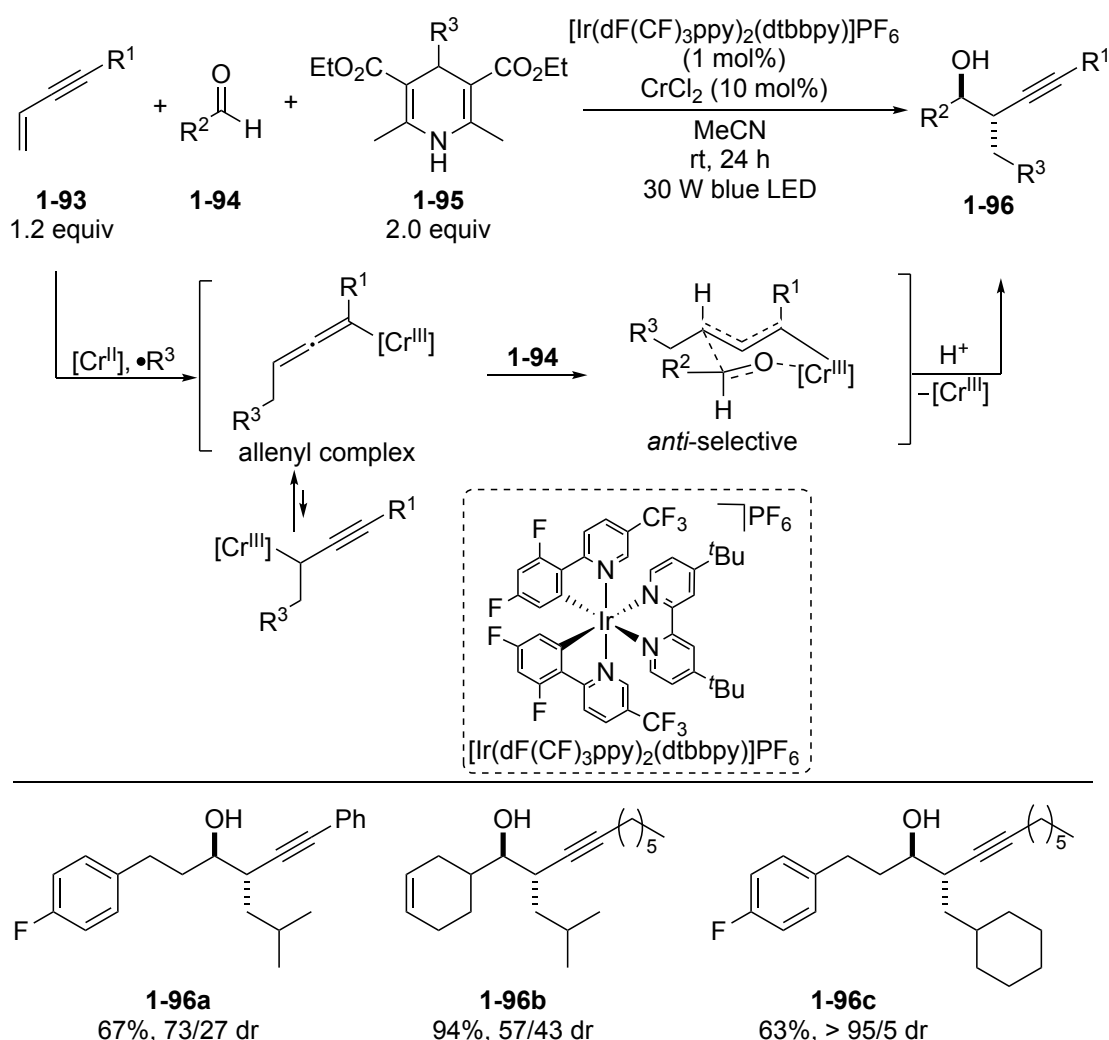
Scheme 1-33. Dual Photoredox/Chromium-catalyzed Acylation and Alkylation Reactions of Buta-1,3-diene with Aldehydes with 4-Alkyl-1,4-dihydropyridines Reported by Glorius et al.



Then, in 2021, Glorius et al. reported dual photoredox/chromium-catalyzed alkylation reactions of enynes with aldehydes and 4-alkyl-1,4-dihydropyridines.

Reactions of enynes **1-93** with aldehydes **1-94** and 4-alkyl-1,4-dihydropyridines **1-95** in the presence of $[\text{Ir}(\text{dF}(\text{CF}_3)\text{ppy})_2(\text{dtbbpy})]\text{PF}_6$ as a photoredox catalyst and CrCl_2 as a chromium catalyst in MeCN under 30 W blue LED irradiation at room temperature for 24 h gave the propargylic acylated and homopropargylic alkylated products **1-96a-c** in good yields with a good to high diastereoselectivity. (Scheme 1-34).⁴² Here, allenyl compounds are supposed to be formed as intermediates via the alkylation reactions of **1-93** with **1-95**, where insertion of **1-94** occurs in an *anti* fashion to afford the propargylic acylated products **1-96a**. Thus, dual photoredox/chromium-catalyzed reactions with 4-alkyl-1,4-dihydropyridines have shown potential ability for alkylation reactions comparable to those by dual photoredox/nickel catalytic systems, although reported examples are very limited in number.

Scheme 1-34. Dual Photoredox/Chromium-catalyzed Propargylic Acylation and Homopropargylic Alkylation Reactions of Enyne with Aldehyde and 4-Alkyl-1,4-dihydropyridine Reported by Glorius et al.

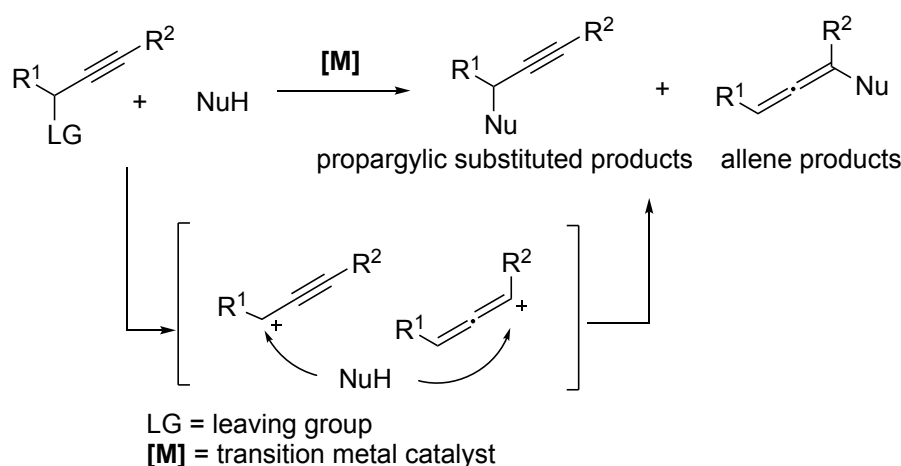


1.4. Transition Metal-catalyzed Propargylic Substitution Reactions

1.4.1 Transition Metal-catalyzed Non-enantioselective Propargylic Substitution Reactions

Propargylic substitution reactions, where nucleophiles react with the carbon adjacent to the carbon-carbon triple bond to introduce themselves as new substituents, have drawn much attention in the last two decades (Scheme 1-35).⁴³ In these reaction systems, formation of propargylic cations as reactive intermediates *in situ* with the liberation of leaving groups is the key, although free propargylic cations are perfectly in resonance with free allenyl cations, leading to the formation of propargylic substituted products or allene products, respectively, on further reactions with nucleophiles. Thus, it is very difficult to control the selectivity of the products.

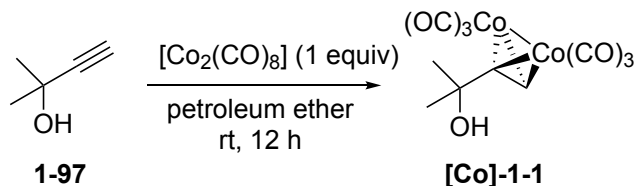
Scheme 1-35. Propargylic Substitution Reactions



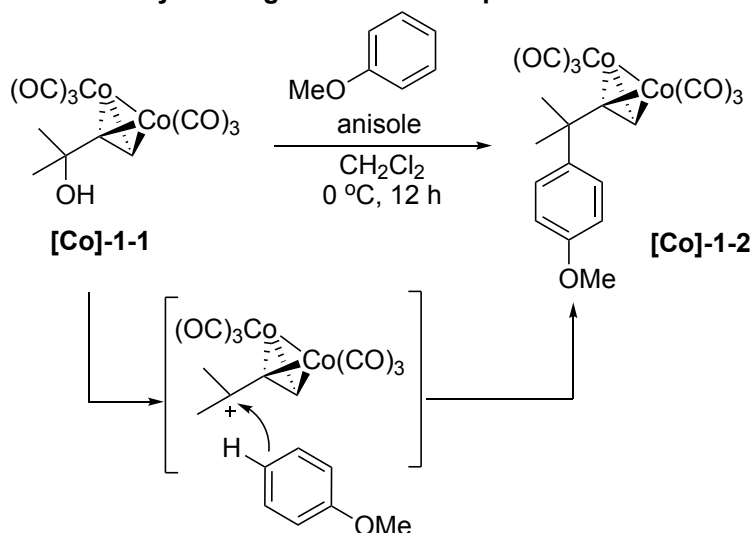
In 1977, Nicholas reported the first stoichiometric propargylic substitution reaction of a propargylic alcohol with anisole in the presence of a stoichiometric amount of $[\text{Co}_2(\text{CO})_8]$. Here, the reaction of propargylic alcohol **1-97** with $[\text{Co}_2(\text{CO})_8]$ occurs to afford an alkyne-bridged dicobalt complex **[Co]-1-1** (Scheme 1-36a). Then, nucleophilic attack of anisole to the cationic carbon of the complex **[Co]-1-1** occurs to form the propargylic substituted complex **[Co]-1-2** (Scheme 1-36b). Further treatment of **[Co]-1-2** with $\text{Fe}(\text{NO}_3)_3$ as an oxidant impels the cobalt species to dissociate the desired propargylic substituted product **1-98** (Scheme 1-36c).⁴⁴

Scheme 1-36. Nicholas Reaction

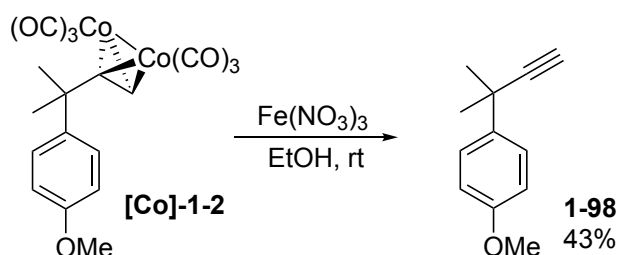
a) Reaction of propargylic alcohol with $[\text{Co}_2(\text{CO})_8]$



b) Reaction of alkyne-bridged dicobalt complex with anisole



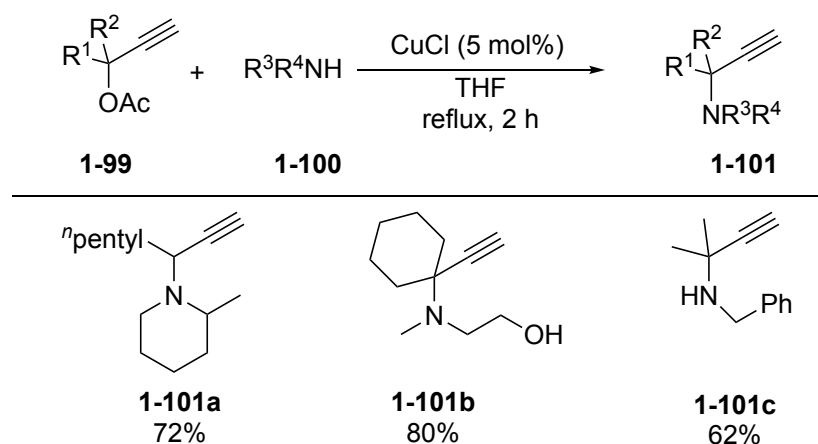
c) Reaction of propargylic substituted complex with $\text{Fe}(\text{NO})_3$



The Nicholas reaction has provided a novel method to prepare propargylic substituted products solely by avoiding the generation of allene-type side products. However, the use of a stoichiometric amount of $\text{Co}_2(\text{CO})_8$ restricts its further application in organic synthesis. Thus, catalytic propargylic substitution reactions are necessary to be developed.

In 1994, Murahashi et al. reported copper-catalyzed propargylic amination of propargylic esters with amines. When propargylic esters **1-99** were treated with a variety of amine nucleophiles **1-100** in the presence of 5 mol% of CuCl as a catalyst in THF at reflux for 2 h, the propargylic aminated products **1-101a-c** were obtained in high yields (Scheme 1-37).⁴⁵ This is the first example where propargylic substituted products were obtained catalytically.

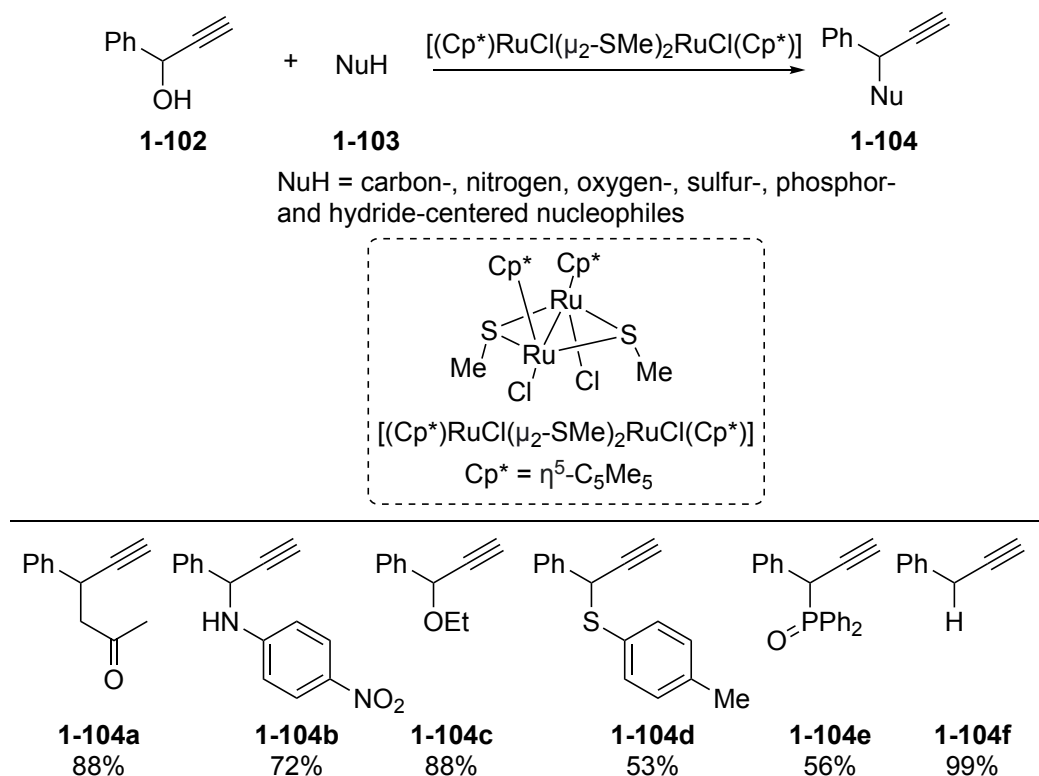
Scheme 1-37. First Copper-catalyzed Propargylic Amination of Propargylic Esters with Amines Reported by Murahashi et al.



Although after this first discovery of the catalytic propargylic substitution reactions, some other copper-catalyzed propargylic substitution reactions have been reported.⁴⁶ However, the choice of nucleophiles has been limited.

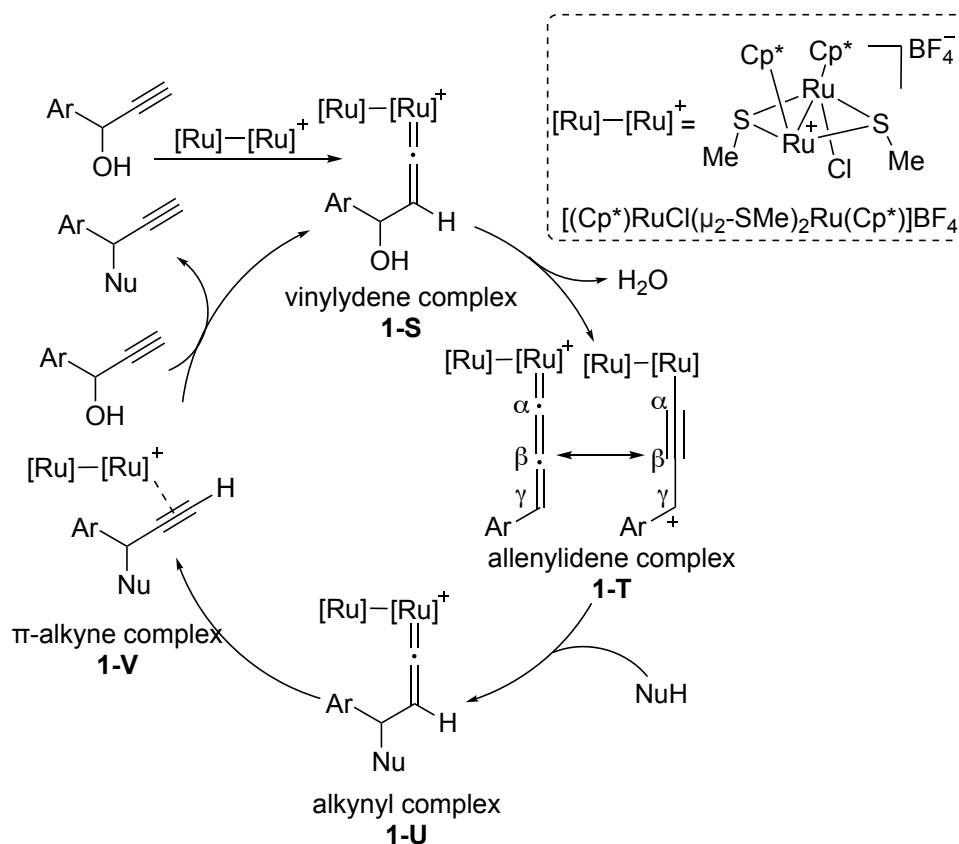
As a breakthrough on the transition metal-catalyzed propargylic substitution reactions, ruthenium-catalyzed propargylic substitution reactions have been achieved by the author's group in 2000.⁴⁷ In this reaction systems, thiolate-bridged binuclear ruthenium complex $[(\text{Cp}^*)\text{RuCl}(\mu_2\text{-SMe})_2\text{RuCl}(\text{Cp}^*)]$ ($\text{Cp}^* = 1,2,3,4,5\text{-pentamethylcyclopentadienyl}$) was used as a catalyst toward catalytic propargylic substitution reactions of a propargylic alcohol **1-102** with carbon-,⁴⁸ nitrogen,⁴⁹ oxygen-,⁴⁹ sulfur-,⁴⁹ phosphor-⁴⁹ and hydride-centered⁵⁰ nucleophiles to afford the corresponding propargylic substituted products (**1-104a** to **1-104f**, for example) in good to high yields (Scheme 1-38).

Scheme 1-38. Thiolate-bridged Binuclear Ruthenium-Catalyzed Propargylic Substitution Reactions of Propargylic Alcohols with a Variety of Nucleophiles



Based on the mechanism in these reports, a reaction pathway is proposed via the formation of ruthenium-allenylidene intermediates. As shown in [Scheme 1-39](#). First, coordination of the propargylic alcohol occurs, where a proton transfer of the acetylenic hydrogen occurs to the β -position to give the vinylidene complex (**1-S**). Then, dehydration takes place to give the allenylidene complex (**1-T**). Then nucleophilic attack at the γ position of the allenylidene complex (**1-T**) gives rise to the formation of the alkynyl complex (**1-U**), followed by a proton transfer to afford the π -alkyne complex (**1-V**). Ligand exchange with a propargylic alcohol gives the product and regenerates the starting vinylidene complex (**1-S**).

Scheme 1-39. Proposed Mechanism for Ruthenium-catalyzed Propargylic Substitution Reactions



The success in the catalytic activity mediated by these thiolate-bridged diruthenium complexes compared to those found for mononuclear ruthenium ones can be attributable to two factors: One is the higher stability of the coordinatively unsaturated complexes found in binuclear systems, which provides smooth catalyst turnover. The other is the weaker back-donation, which makes the reaction steps easy by decreasing the reaction barriers in the reaction pathway. Both features are due to the synergistic effect of the binuclear core, where the counter ruthenium atom works as an electron acceptor for the ruthenium atom where the conversion of substrates occurs.⁵¹

1.4.2 Transition Metal-catalyzed Enantioselective Propargylic Substitution Reactions

Optically active compounds in a single enantiomeric form (>99% ee) are widely existing in nature.⁵² Indeed, each enantiomer of biologically active compounds has a different biological effect. For example, the Efavirenz is widely used as a drug for treating and preventing HIV/AIDS. However, only its *S*-enantiomer is effective as a drug (Figure 1-4).⁵³ Therefore, synthesizing pure enantiomers is one of the most important targets in synthetic, medicinal, and industrial chemistry.

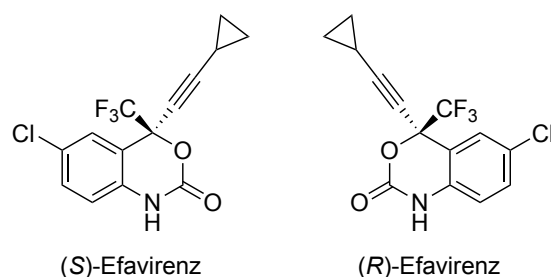
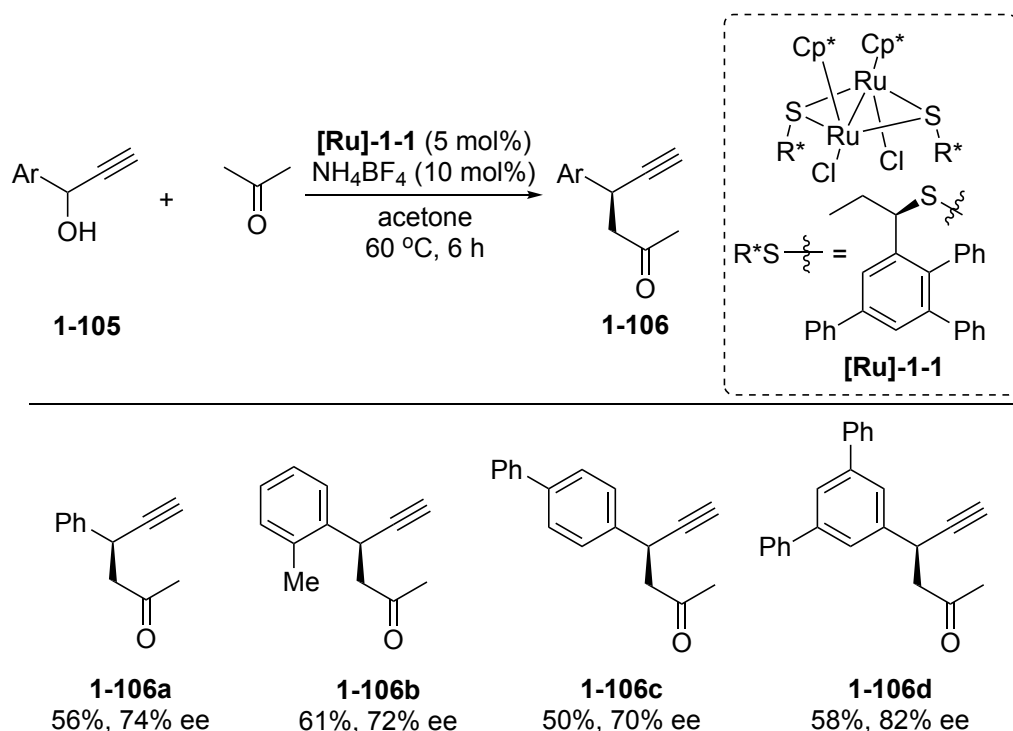


Figure 1-4. Efavirenz

1.4.2.1 Ruthenium-catalyzed Enantioselective Propargylic Substitution Reactions

Although a variety of transition metal-catalyzed propargylic substitution reactions have been developed since 1994, transition metal-catalyzed enantioselective propargylic substitution reactions have not been realized until 2005. In 2005, the author's group reported a novel thiolate-bridged dinuclear ruthenium complex bearing an optically active ligand, which works as an efficient catalyst in the enantioselective propargylic substitution reactions of propargylic alcohols with acetone. Reactions of propargylic alcohols **1-105** in the presence of **[Ru]-1-1** bearing an optically active ligand with three phenyl substituents introduced to the phenyl group as a ruthenium catalyst and NH_4BF_4 as an additive in acetone at 60 °C for 6 h gave the propargylic alkylated products **1-106a-d** in moderate yields with a high enantioselectivity (Scheme 1-40).⁵⁴

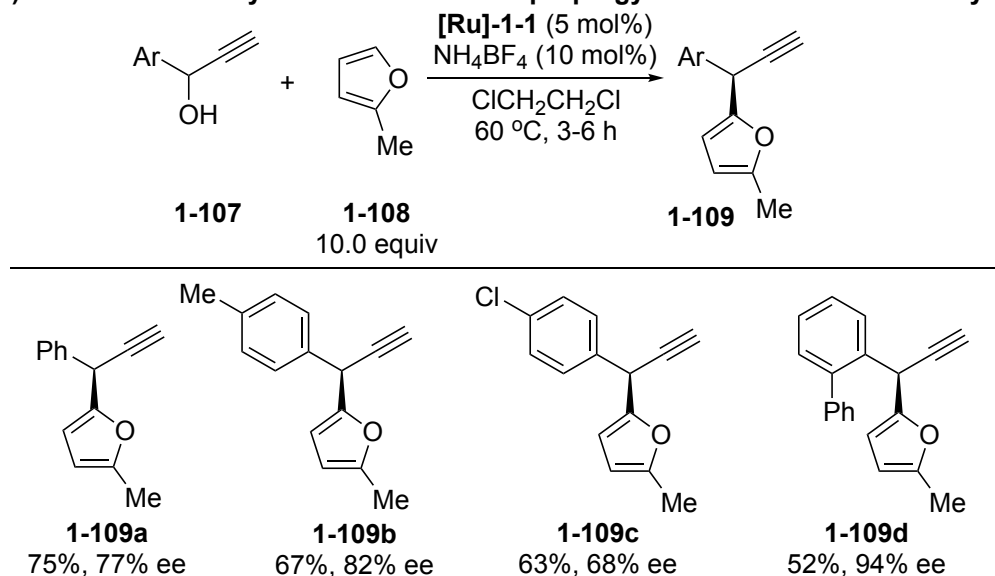
Scheme 1-40. Ruthenium-catalyzed Enantioselective Propargylic Substitution Reactions of Propargylic Alcohols with Acetone



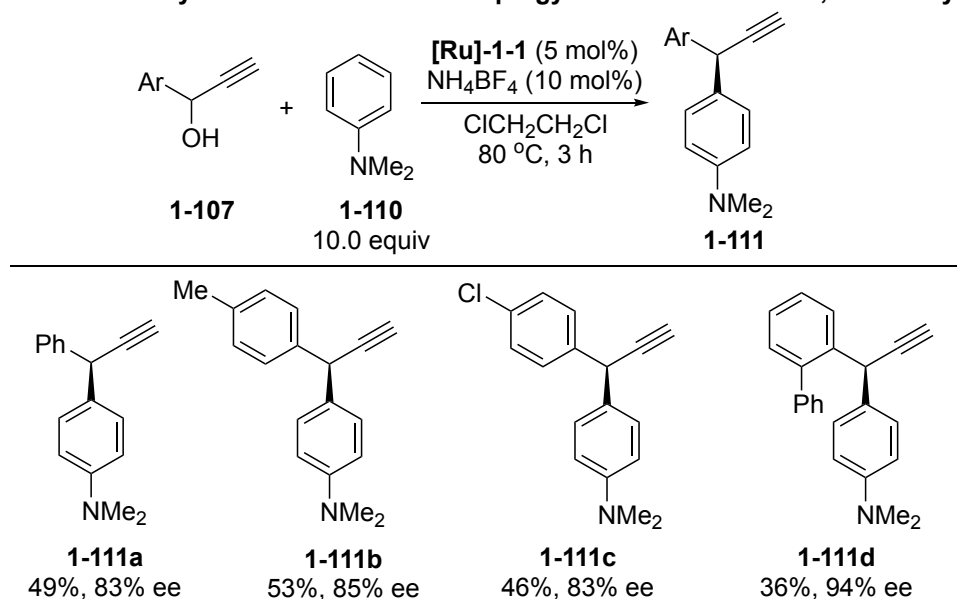
Furthermore in 2007, the author's group reported the enantioselective propargylation reactions of aromatic compounds with propargylic alcohols. Reactions of propargylic alcohols **1-107** with 2-methylfuran **1-108** in the presence of **[Ru]-1-1** as a ruthenium catalyst and NH_4BF_4 as an additive in $\text{ClCH}_2\text{CH}_2\text{Cl}$ at 60 °C for 3-6 h afforded the propargylation products **1-109a-d** in moderate yields with a high enantioselectivity (Scheme 1-41a). Reactions of propargylic alcohols **1-107** with *N,N*-dimethylaniline **1-110** in the presence of **[Ru]-1-1** as an optically active ruthenium catalyst and NH_4BF_4 as an additive in $\text{ClCH}_2\text{CH}_2\text{Cl}$ at 80 °C for 3 h also gave the products **1-111a-d** in moderate yields with a good with a high enantioselectivity (Scheme 1-41b).⁵⁵

Scheme 1-41. Ruthenium-catalyzed Enantioselective Propargylation Reactions of 2-Methylfuran or *N,N*-Dimethylaniline with Propargylic Alcohols

a) Ruthenium-catalyzed enantioselective propargylation reactions of 2-methylfuran

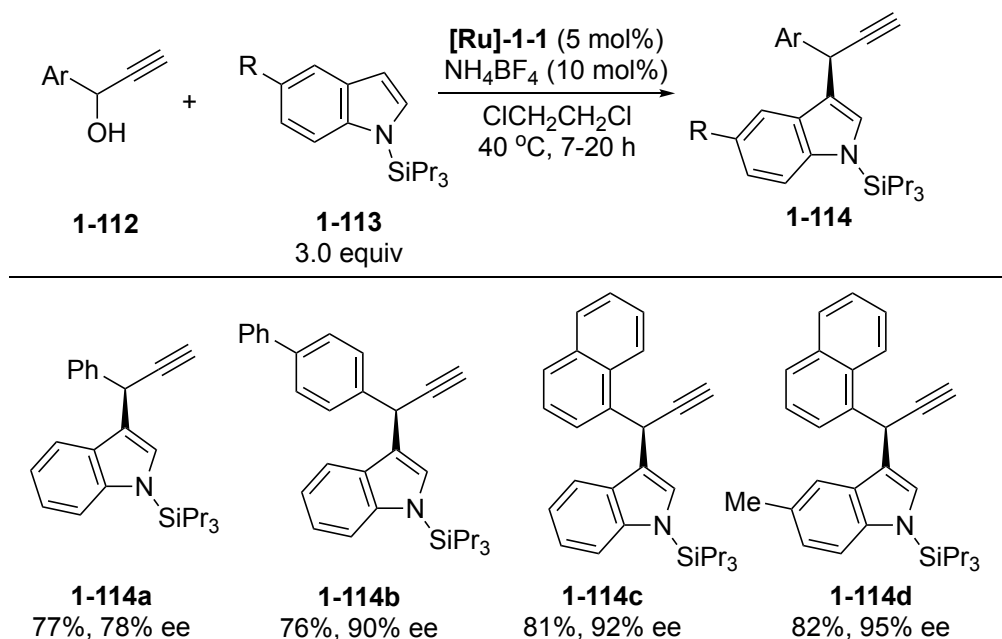


b) Ruthenium-catalyzed Enantioselective Propargylation Reactions of *N,N*-Dimethylaniline



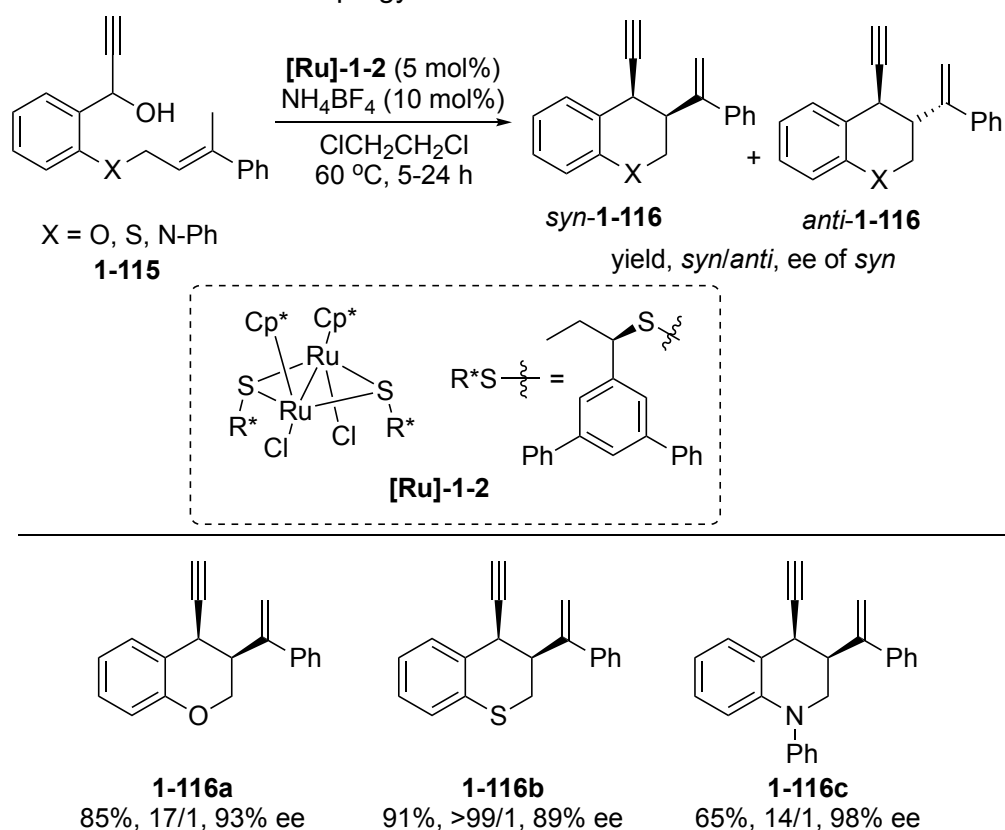
Also in 2007, the author's group reported the enantioselective propargylation reactions of indoles with propargylic alcohols. Reactions of propargylic alcohols **1-112** with indoles **1-113** in the presence of [Ru]-1-1 as an optically active ruthenium catalyst and NH₄BF₄ as an additive in ClCH₂CH₂Cl at 40 °C for 7-20 h gave the propargylation products **1-114a-d** in good yields with a high enantioselectivity (Scheme 1-42).⁵⁶

Scheme 1-42. Ruthenium-Catalyzed Enantioselective Propargylation Reactions of Indoles with Propargylic Alcohols



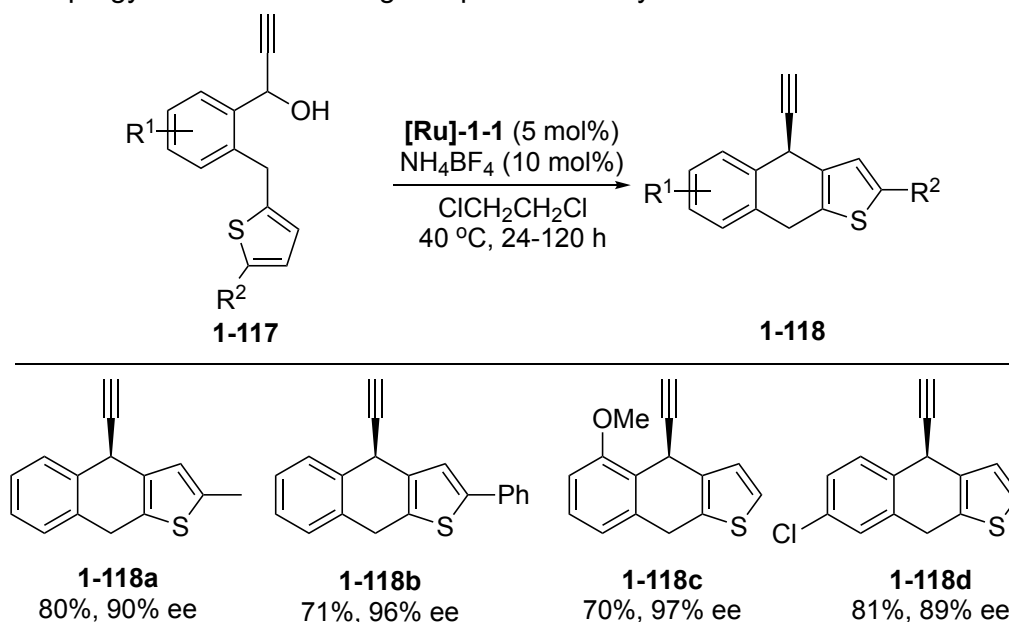
In 2009, the author's group reported the ruthenium-catalyzed enantioselective intramolecular propargylic substitution reactions of propargylic alcohols to afford the chiral heterocycles such as chromane, thiochromane, and 1,2,3,4-tetrahydroquinoline derivatives. Reactions of propargylic alcohols bearing (*E*)-alkene moiety **1-115** in the presence of [Ru]-1-2 bearing another optically active ligand as a ruthenium catalyst and NH_4BF_4 as an additive in $\text{ClCH}_2\text{CH}_2\text{Cl}$ at 60 °C for 5-24 h afforded the propargylic substituted products **1-116a-c** in good yields with high diastereo- and enantioselectivities (Scheme 1-43).⁵⁷

Scheme 1-43. Ruthenium-catalyzed Enantioselective Intramolecular Propargylic Substitution Reactions of Propargylic Alcohols



In 2009, the author's group reported the ruthenium-catalyzed enantioselective intramolecular propargylation reactions of thiophenes with propargylic alcohols. Reactions of propargylic alcohols bearing a thiophene moiety **1-117** in the presence of **[Ru]-1-1** as an optically active ruthenium catalyst and NH_4BF_4 as an additive in $\text{ClCH}_2\text{CH}_2\text{Cl}$ at 40 °C for 24-120 h yielded the propargylation products **1-118a-d** in good yields with a high enantioselectivity (Scheme 1-44).⁵⁸

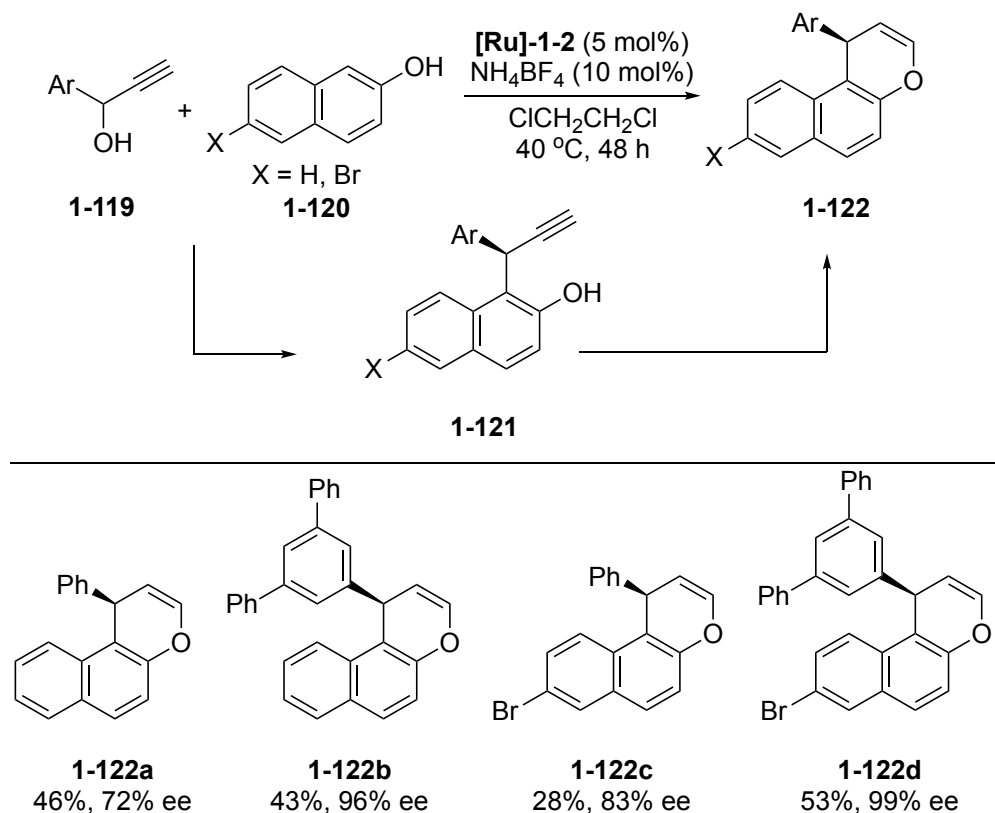
Scheme 1-44. Ruthenium-Catalyzed Enantioselective Intramolecular Propargylation with Propargylic Alcohols Bearing Thiophenes Moiety



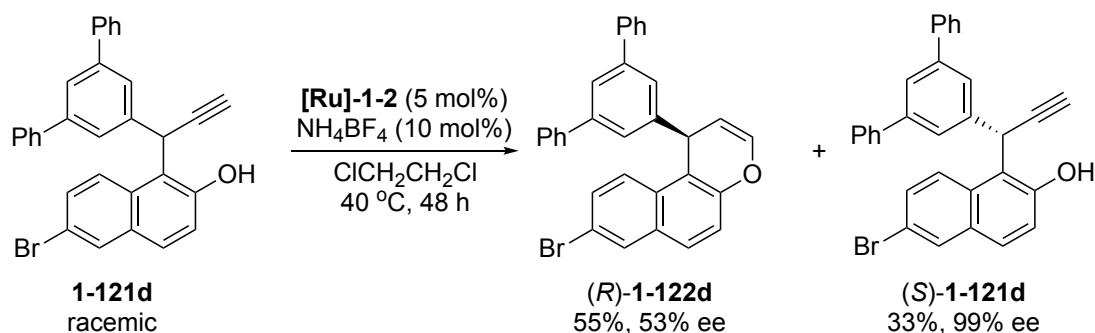
In 2010, the author's group reported the ruthenium-catalyzed enantioselective [3+3] cycloaddition of propargylic alcohols with 2-naphthols. Reactions of propargylic alcohols **1-119** with 2-naphthols **1-120** in the presence of **[Ru]-1-2** as an optically active ruthenium catalyst and NH_4BF_4 as an additive in $\text{ClCH}_2\text{CH}_2\text{Cl}$ at 40 °C for 48 h afforded the propargylation products **1-121** as reactive intermediates, which were further transformed into cycloaddition products **1-122** in moderate yields with a high enantioselectivity (Scheme 1-45a).⁵⁹ In the latter cyclization step of **1-121** to afford **1-122**, kinetic resolution occurred efficiently: *i.e.* ruthenium-catalyzed cyclization of (*R*)-**1-121** occurs more smoothly to afford (*R*)-**1-122** via an intramolecular attack of the hydroxyl group compared to that for the cyclization of (*S*)-**1-121** to afford (*S*)-**1-122**. Indeed, transformation of racemic **1-121d** to **1-122d** in $\text{ClCH}_2\text{CH}_2\text{Cl}$ in the presence of **[Ru]-1-2** at 40 °C for 48 h afforded the cycloaddition product (*R*)-**1-122d** (53% ee) in 55% yield together with the recovery of (*S*)-**1-121d** (99% ee) in 33% yield (Scheme 1-45b).

Scheme 1-45. Ruthenium-catalyzed Enantioselective Intramolecular Propargylation of 2-Naphthols with Propargylic Alcohols

a) Ruthenium-catalyzed Enantioselective Intramolecular Propargylation of 2-Naphthols



b) Reactoin of Racemic 1-121d



Among these reaction systems catalyzed by optically active ruthenium complexes, the C–H/ π interaction between the two phenyl groups in the optically active thiolate and allenylidene ligands of the intermediary allenylidene complexes plays an important role in the achievement of the high enantioselectivity (Figure 1-5). This structure has been confirmed by an X-ray analysis of the isolated allenylidene complexes. Here, NuH (carbon-centered nucleophiles) can attack at the cationic γ -carbon atom of the allenylidene ligand only from the *Si* face.⁶⁰

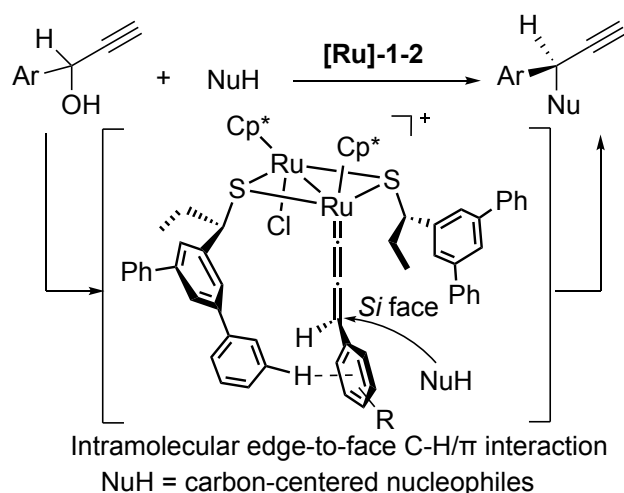
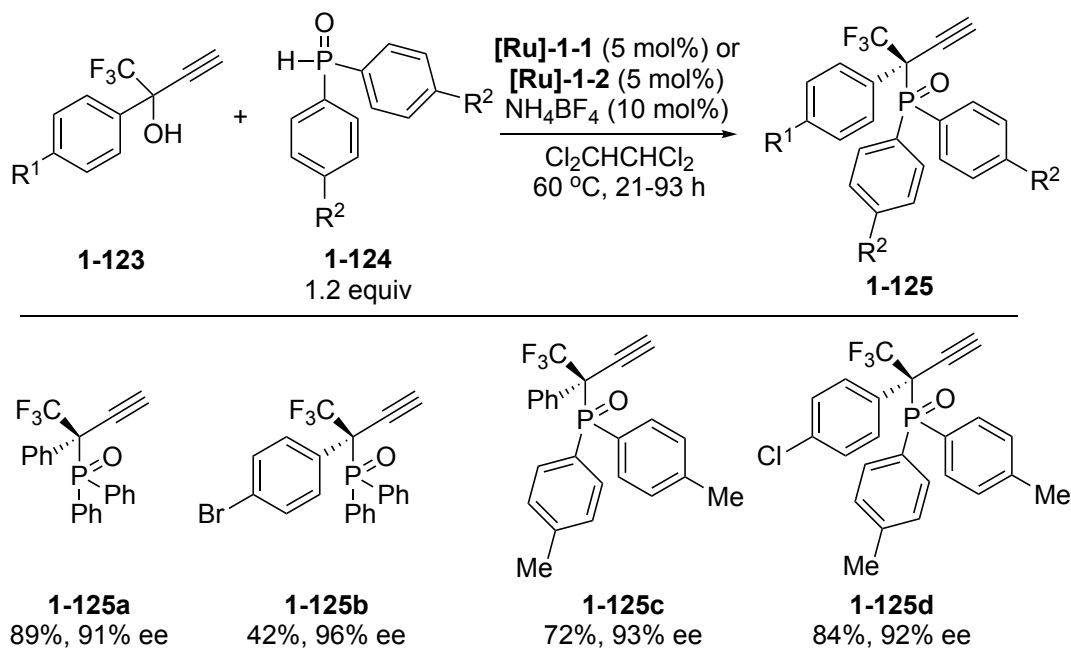


Figure 1-5. C-H/π interaction between the allenyldiene moiety and a phenyl ring of one of the optically active ligands

In 2021, the author's group reported the ruthenium-catalyzed enantioselective propargylic substitution reactions of propargylic alcohols with phosphorus-centered nucleophiles. Reactions of propargylic alcohols **1-123** with phosphine oxides **1-124** in the presence of **[Ru]-1-1** or **[Ru]-1-2** as an optically active ruthenium complex and NH_4BF_4 as an additive in $\text{Cl}_2\text{CHCHCl}_2$ at 60 °C for 21 to 93 h yielded the propargylic substituted products **1-125a-d** in good to high yields with a high enantioselectivity (Scheme 1-46).⁶¹

Scheme 1-46. Ruthenium-catalyzed Enantioselective Phosphinylation of Propargylic Alcohols with Phosphine Oxides



Here, the C-F/π interaction between the phenyl group in the optically active thiolate ligand and CF_3 group in the allenylidene ligand of the intermediary allenylidene

complexes plays an important role in the achievement of high enantioselectivity (Figure 1-6). Here, diarylphosphinous acids (HOPAr'_2), in tautomeric equilibrium with diarylphosphine oxides ($\text{HP(O)Ar}'_2$), should attack at the cationic γ -carbon atom of the allenylidene ligand only from the *Re* face.

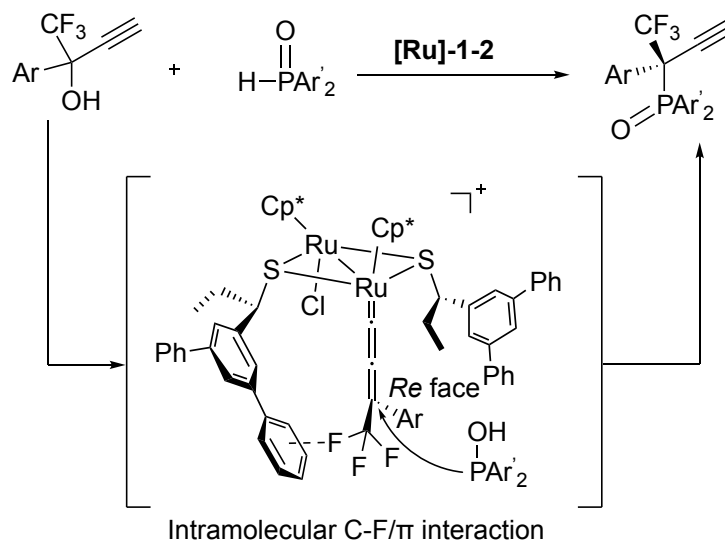


Figure 1-6. C–F/ π interaction between CF_3 group of the allenylidene moiety and a phenyl ring of one of the optically active ligands

In summary, the author's group has developed many ruthenium-catalyzed propargylic substitution reactions and propargylation reactions by using thiolate-bridged diruthenium complexes as catalysts. Furthermore, ruthenium-catalyzed enantioselective propargylic substitution reactions and propargylation reactions have been achieved by using optically active ruthenium complexes as catalysts.

1.4.2.2 Copper-catalyzed Enantioselective Propargylic Substitution Reactions

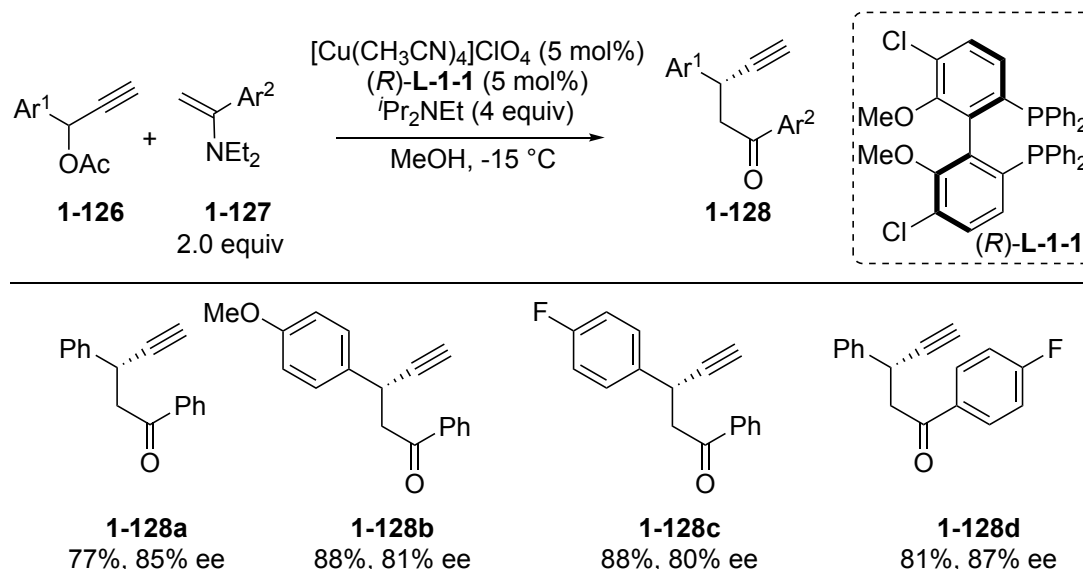
The first copper-catalyzed enantioselective propargylic substitution reactions were independently reported by the author's group and Maarseveen's group in 2008, where the amines were used as nitrogen-centered nucleophiles.⁶² Since then, a variety of copper-catalyzed enantioselective propargylic substitution reactions have been reported.⁶³ In this part, propargylic alkylation reaction with carbon-centered nucleophiles will be first introduced.

1.4.2.2.1 Copper-catalyzed Enantioselective Propargylic Substitution Reactions with Carbon-centered Nucleophiles

Copper-catalyzed enantioselective propargylic substitution reactions with carbon-centered nucleophiles were first reported in 2009 by Hou et al., who conducted

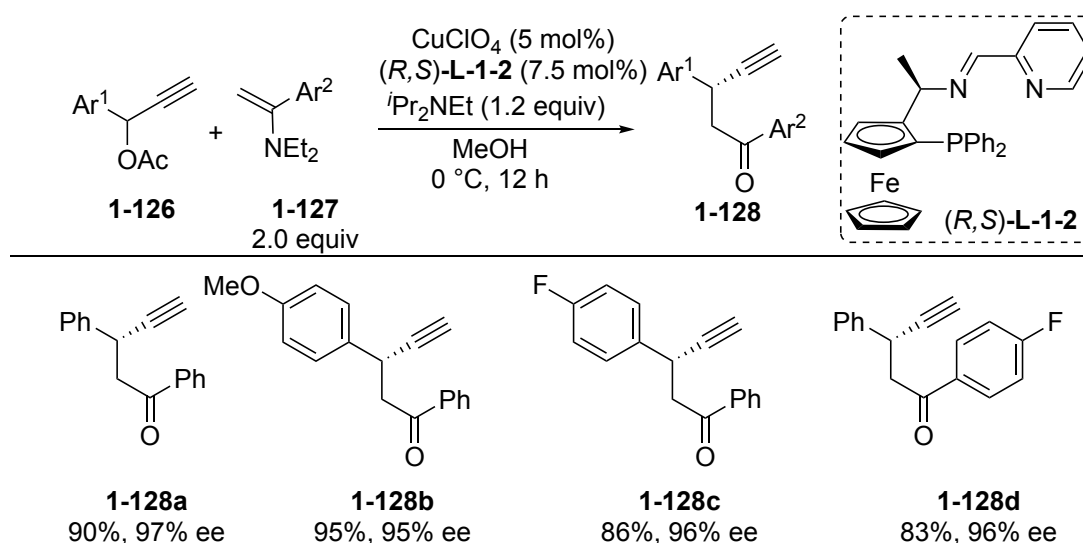
propargylic alkylation reactions of propargylic esters **1-126** with enamines **1-127** in the presence of $[\text{Cu}(\text{CH}_3\text{CN})_4]\text{ClO}_4$ as a copper catalyst, **L-1-1** as an optically active ligand, and $i\text{Pr}_2\text{NEt}$ as a base in MeOH at $-15\text{ }^\circ\text{C}$ to obtain the propargylic alkylated products **1-128a-d** in high yields with a high enantioselectivity (Scheme 1-47).⁶⁴

Scheme 1-47. First Copper-catalyzed Enantioselective Propargylic Alkylation Reactions of Propargylic Esters with Enamines Reported by Huo et al.



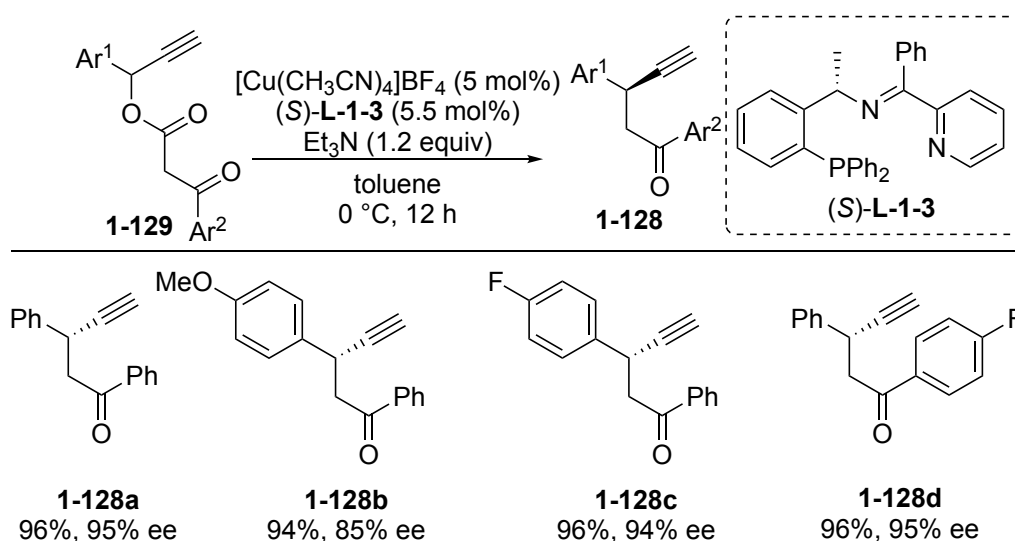
Later in 2014, a similar combination of reaction substrates to obtain the alkylated products similar to Scheme 1-47 but with higher enantioselectivity was reported by Guo et al. who treated propargylic esters **1-126** with enamines **1-127** in the presence of CuClO_4 as a copper catalyst, $(R,S)\text{-L-1-2}$ as an optically active P,N,N-type ligand, and $i\text{Pr}_2\text{NEt}$ as a base in MeOH at $0\text{ }^\circ\text{C}$ for 12 h to afford the propargylic alkylated products **1-128a-d** in high yields with a high enantioselectivity (Scheme 1-48).⁶⁵

Scheme 1-48. Copper-catalyzed Enantioselective Propargylic Alkylation Reactions of Propargylic Esters with Enamines Reported by Guo et al.



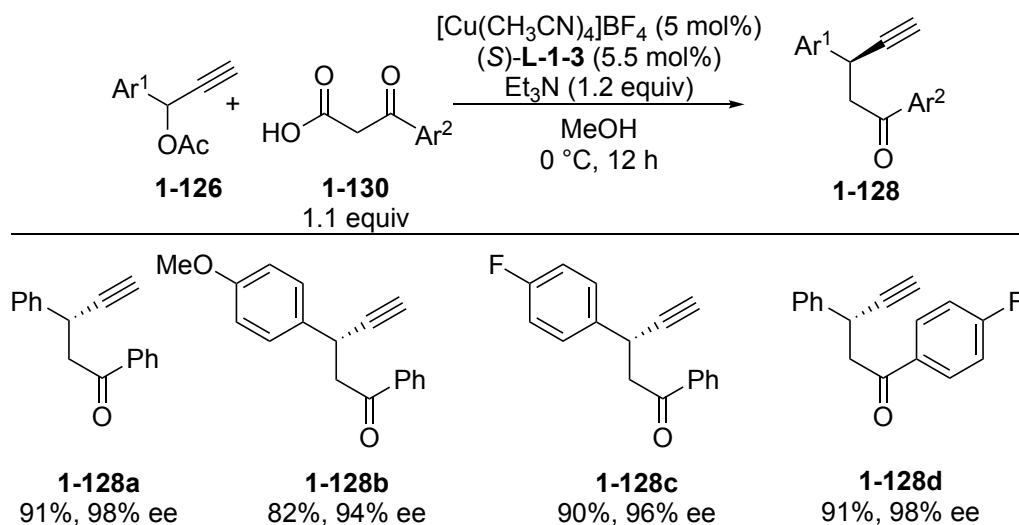
Copper-catalyzed enantioselective intramolecular propargylic alkylation of propargylic esters via decarboxylation was reported in 2014 by Hu et al., who reacted propargylic esters **1-129** in the presence of $[\text{Cu}(\text{CH}_3\text{CN})_4]\text{BF}_4$ as a copper catalyst, (*S*)-**L-1-3** as an optically active P,N,N-type ligand, and Et_3N as a base in toluene at 0 °C for 12 h to obtain the propargylic products **1-128a-d** in high yields with a high enantioselectivity (Scheme 1-49).⁶⁶

Scheme 1-49. Copper-catalyzed Enantioselective Intramolecular Propargylic Alkylation of Propargylic Esters Reported by Hu et al.



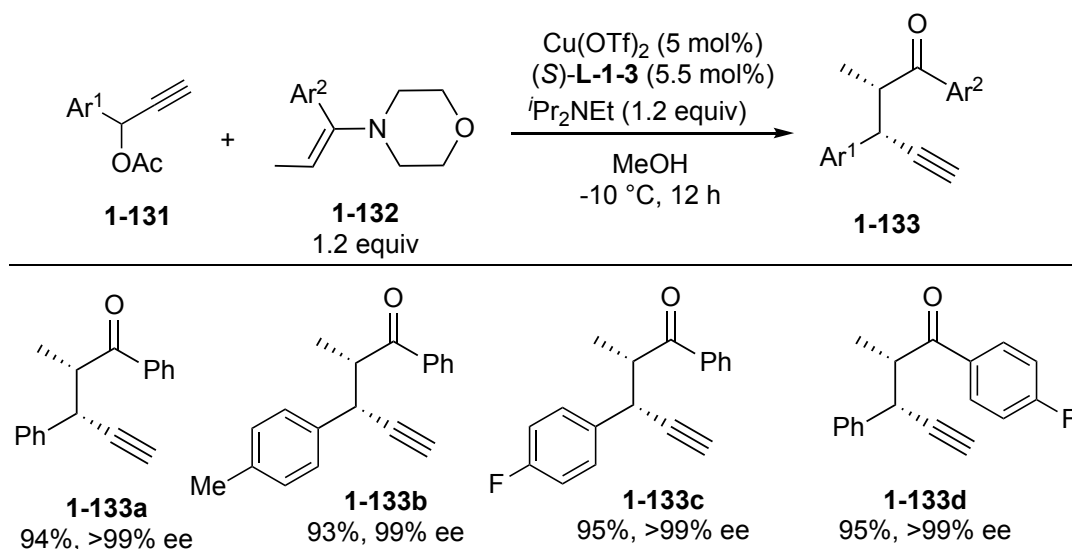
Furthermore, Hu et al. also examined copper-catalyzed enantioselective decarboxylative intermolecular propargylic alkylation of propargylic esters **1-126** with β -keto acids **1-130** in the presence of $[\text{Cu}(\text{CH}_3\text{CN})_4]\text{BF}_4$ as a copper catalyst, (*S*)-**L-1-3** as an optically active P,N,N-type ligand, and Et_3N as a base in MeCN at 0 °C for 12 h to afford the propargylic alkylated products **1-128a-d** in high yields with a high enantioselectivity (Scheme 1-50).⁶⁷

Scheme 1-50. Copper-catalyzed Enantioselective Intermolecular Propargylic Alkylation of Propargylic Esters Reported by Hu et al.



Copper-catalyzed enantioselective propargylic alkylation of propargylic esters with acyclic enamines was also reported in 2014 by Hu et al., who conducted reactions of propargylic esters **1-131** with acyclic enamines **1-132** in the presence of $\text{Cu}(\text{OTf})_2$ as a copper catalyst, (S)-L-1-3 as an optically active P,N,N-type ligand, and $i\text{Pr}_2\text{NEt}$ as a base in MeOH at -10 °C for 12 h to give the propargylic alkylated products **1-133a-d** in high yields with a high enantioselectivity (Scheme 1-51).⁶⁸

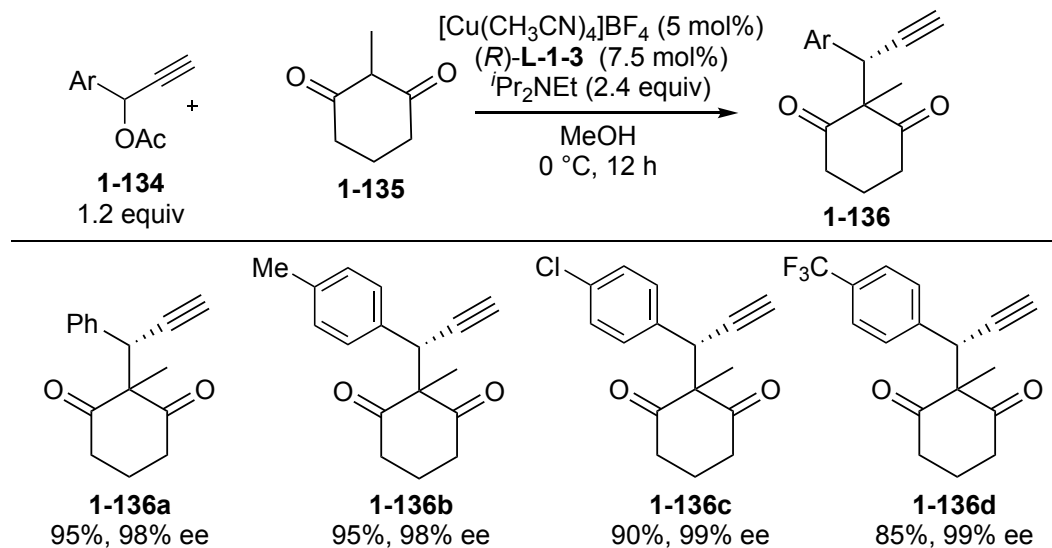
Scheme 1-51. Copper-catalyzed Enantioselective Propargylic Alkylation of Propargylic Esters with Acyclic Enamines Reported by Hu et al.



Hu et al. also reported copper-catalyzed enantioselective propargylic alkylation of propargylic esters with a 1,3-dicarbonyl compound. Treatment of propargylic esters **1-134** with a 1,3-dicarbonyl compound **1-135** in the presence of $[\text{Cu}(\text{CH}_3\text{CN})_4]\text{BF}_4$ as a copper catalyst, (R)-L-1-3 as an optically active P,N,N-type ligand, and $i\text{Pr}_2\text{NEt}$ as a

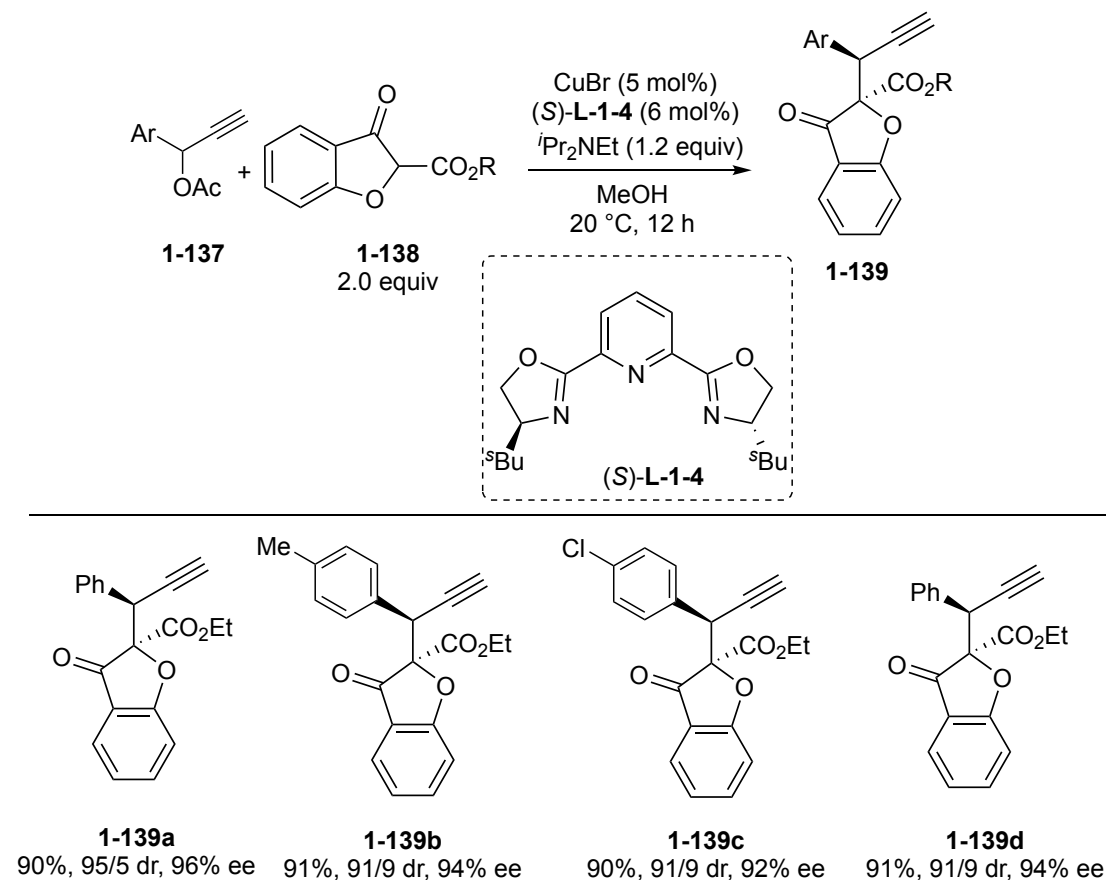
base in MeOH at 0 °C for 12 h led to the formation of the propargylic alkylated products **1-136a-d** in high yields with a high enantioselectivity (Scheme 1-52).⁶⁹

Scheme 1-52. Copper-catalyzed Enantioselective Propargylic Alkylation of Propargylic Esters with a 1,3-Dicarbonyl Compound Reported by Hu et al.



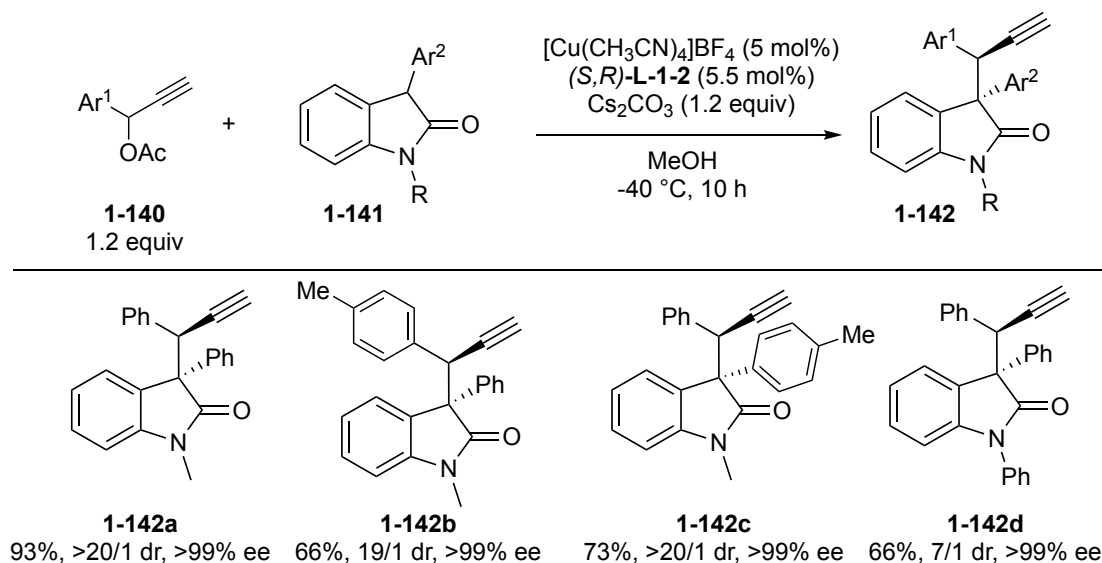
Also in 2014, copper-catalyzed diastereo- and enantio-selective propargylic alkylation reactions of propargylic esters with benzofuranones were reported by Wu et al., who conducted treatment of propargylic esters **1-137** with benzofuranones **1-138** in the presence of CuBr as a copper catalyst, $(S)\text{-L-1-4}$ as an optically active ligand, and $i\text{Pr}_2\text{NEt}$ as a base in MeOH at 20 °C for 12 h to obtain the propargylic alkylated products **1-139a-d** in high yields with high diastereo- and enantio-selectivities (Scheme 1-53).⁷⁰

Scheme 1-53. Copper-catalyzed Diastereo- and Enantio-selective Propargylic Alkylation of Propargylic Esters with Benzofuranones Reported by Wu et al.



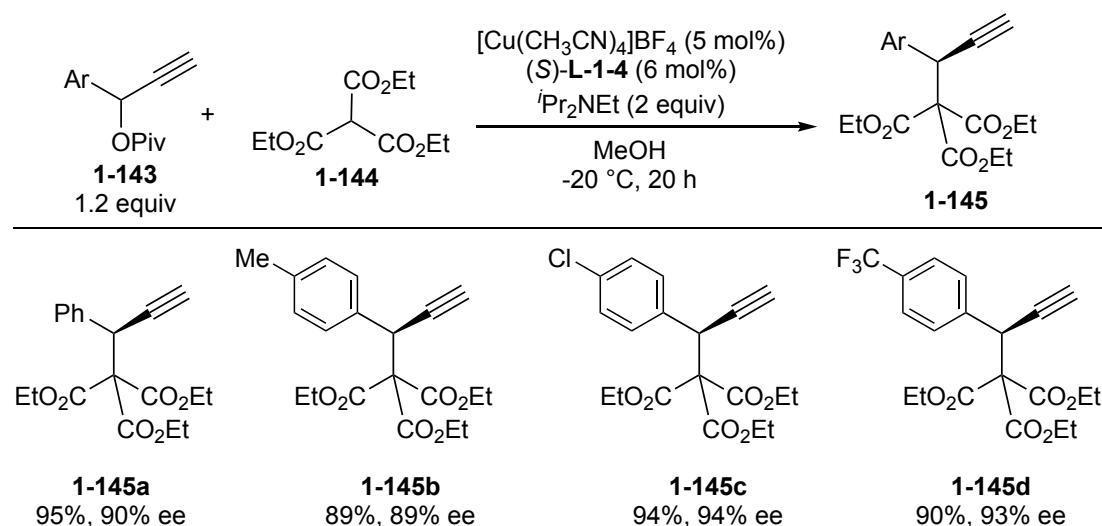
Copper-catalyzed diastereo- and enantio-selective propargylic alkylation of propargylic esters with oxindoles was also reported in 2014 by Hu et al. who treated propargylic esters **1-140** with **1-141** in the presence of $[\text{Cu}(\text{CH}_3\text{CN})_4]\text{BF}_4$ as a copper catalyst, $(S,R)\text{-L-1-2}$ as an optically active P,N,N-type ligand, and Cs_2CO_3 as a base in MeOH at -40 °C for 10 h to obtain the propargylic alkylated products **1-142a-d** in high yields with high diastereo- and enantio-selectivities (Scheme 1-54).⁷¹

Scheme 1-54. Copper-catalyzed Diastereo- and Enantio-selective Propargylic Alkylation of Propargylic Esters with Oxindoles Reported by Hu et al.



In 2015, Wu et al. reported the copper-catalyzed enantioselective propargylic alkylation reactions of propargylic esters with trialkyl methanetricarboxylates. When propargylic esters **1-143** were reacted with trialkyl methanetricarboxylates **1-144** in the presence of $[\text{Cu}(\text{CH}_3\text{CN})_4]\text{BF}_4$ as a copper catalyst, (S)-L-1-4 as an optically active ligand, and $i\text{Pr}_2\text{NEt}$ as a base in MeOH at $-20\text{ }^\circ\text{C}$ for 20 h, the propargylic alkylated products **1-145a-d** were obtained in high yields with a high enantioselectivity (Scheme 1-55).⁷²

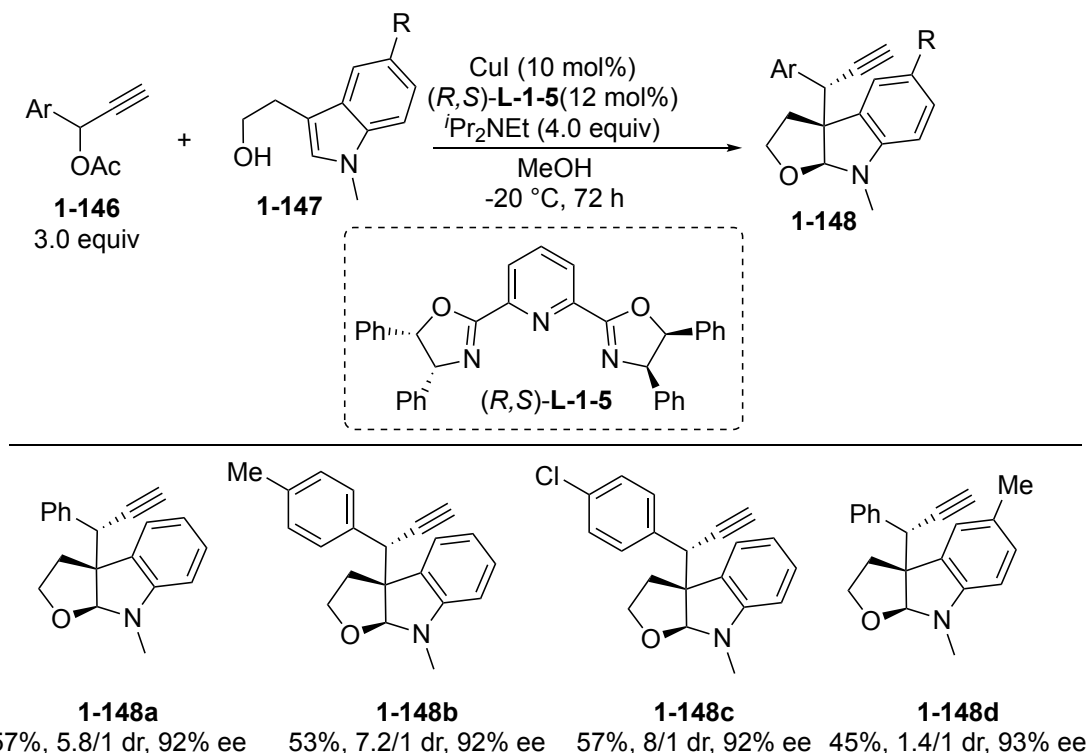
Scheme 1-55. Copper-catalyzed Enantioselective Propargylic Alkylation of Propargylic esters with Trialkyl methanetricarboxylates Reported by Wu et al.



Copper-catalyzed enantioselective dearomative propargylation of indoles was reported in 2015 by You et al. who conducted dearomative propargylation of indoles **1-146** with **1-147** in the presence of CuI as a copper catalyst, (R,S)-L-1-5 as an optically

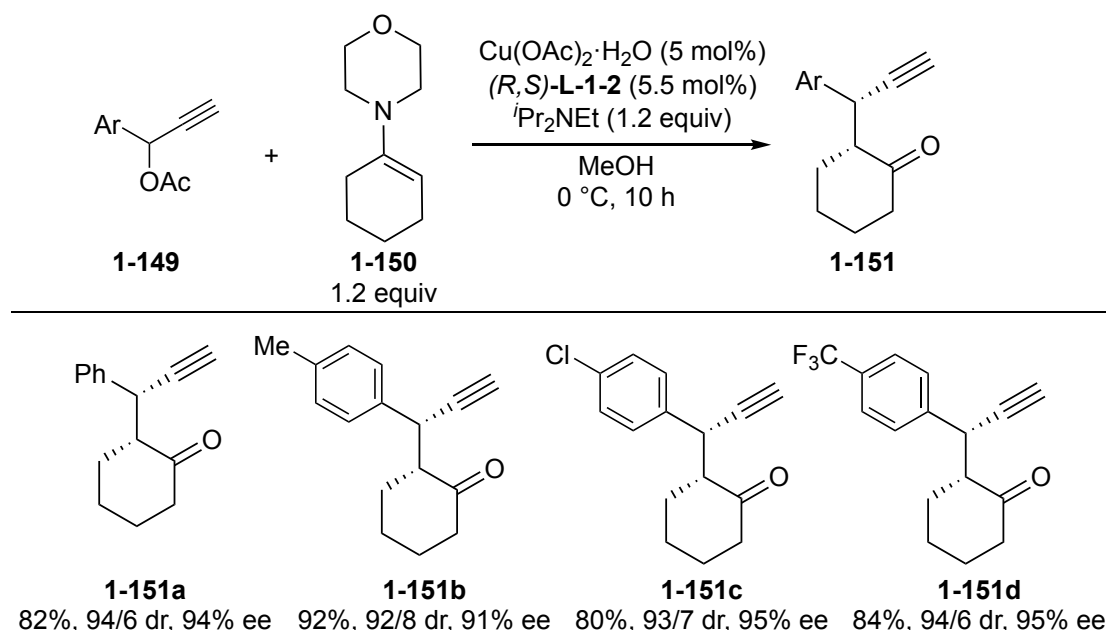
active ligand, and $i\text{Pr}_2\text{NEt}$ as a base in MeOH at $-20\text{ }^\circ\text{C}$ for 72 h to afford the corresponding dearomatized propargylation products **1-148a-d** in high yields with high diastereo- and enantio-selectivities ([Scheme 1-56](#)).⁷³

Scheme 1-56. Copper-catalyzed Enantioselective Dearomative Propargylation of Indoles Reported by You et al.



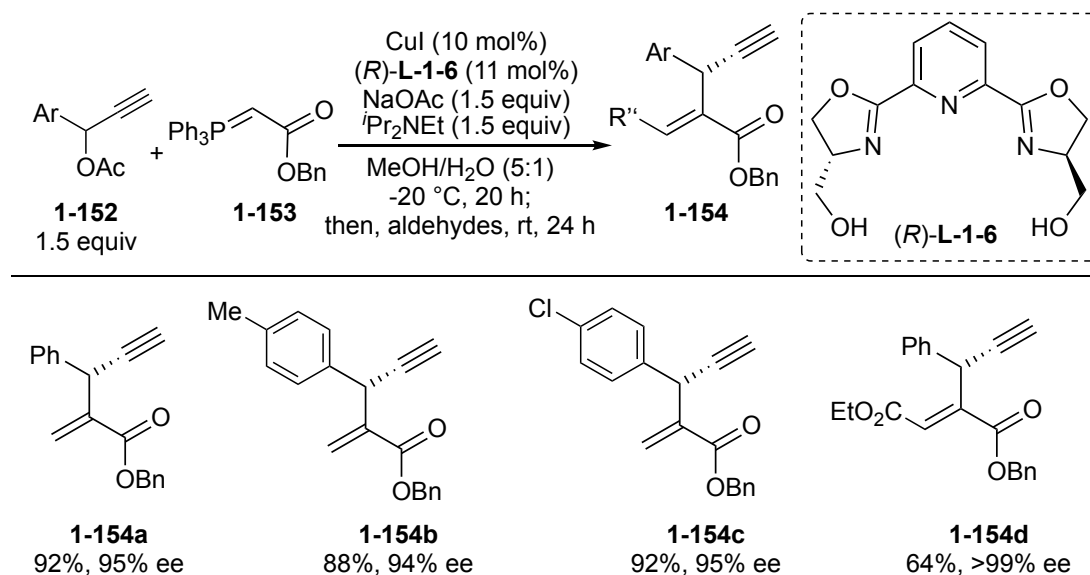
In 2016, Hu et al. reported copper-catalyzed diastereo- and enantio-selective propargylic alkylation of propargylic esters with a cyclic enamine. Treatment of propargylic esters **1-149** with a cyclic enamine **1-150** in the presence of $\text{Cu}(\text{OAc})_2\cdot\text{H}_2\text{O}$ as a copper catalyst, $(R,S)\text{-L-1-2}$ as an optically active ligand, and $i\text{Pr}_2\text{NEt}$ as a base in MeOH at $0\text{ }^\circ\text{C}$ for 10 h gave the propargylic alkylated products **1-151a-d** in high yields with high diastereo- and enantio-selectivities ([Scheme 1-57](#)).⁷⁴

Scheme 1-57. Copper-catalyzed Diastereo- and Enantio-selective Propargylic Alkylation of Propargylic Esters with a Cyclic Enamine Reported by Hu et al.



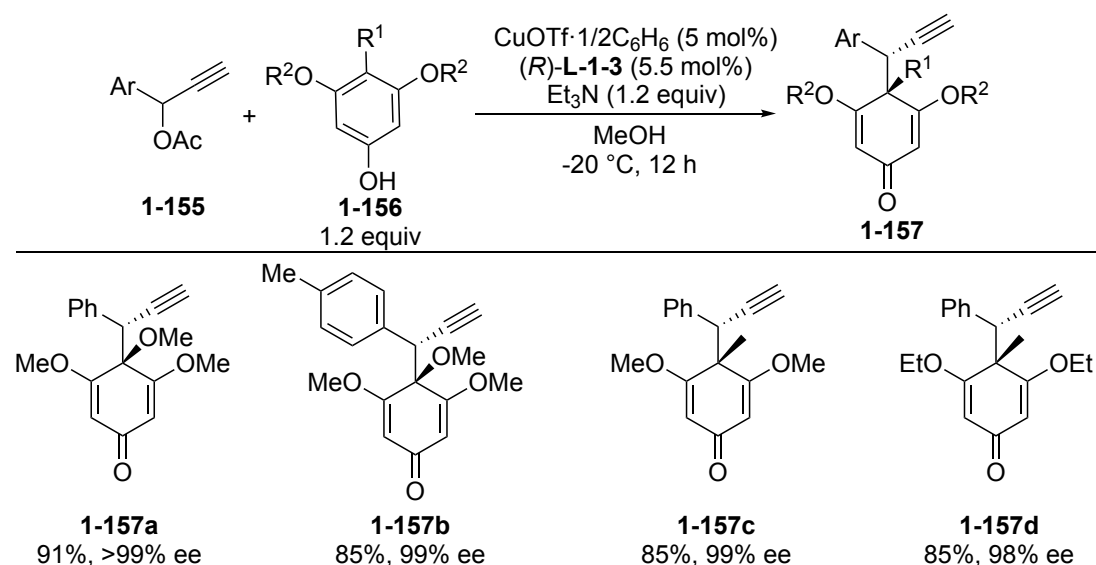
Then, in 2017, Xiao et al. reported copper-catalyzed enantioselective propargylic alkylation reactions of propargylic esters with a phosphorus ylide. In this reaction, propargylic esters **1-152** were first treated with a phosphorus ylide **1-153** in the presence of CuI as a copper catalyst, $(R)\text{-L-1-6}$ as an optically active ligand, and NaOAc and $i\text{Pr}_2\text{NEt}$ as bases in MeOH/H₂O at –20 °C for 20 h. Then, an aldehyde was added into the solution at room temperature with further stirring for 24 h to afford the propargylic acrylate products **1-154a-d** in high yields with a high enantioselectivity (Scheme 1-58).⁷⁵

Scheme 1-58. Copper-catalyzed Enantioselective Propargylic Alkylation of Propargylic Esters with a Phosphorus Ylide Reported by Xiao et al.



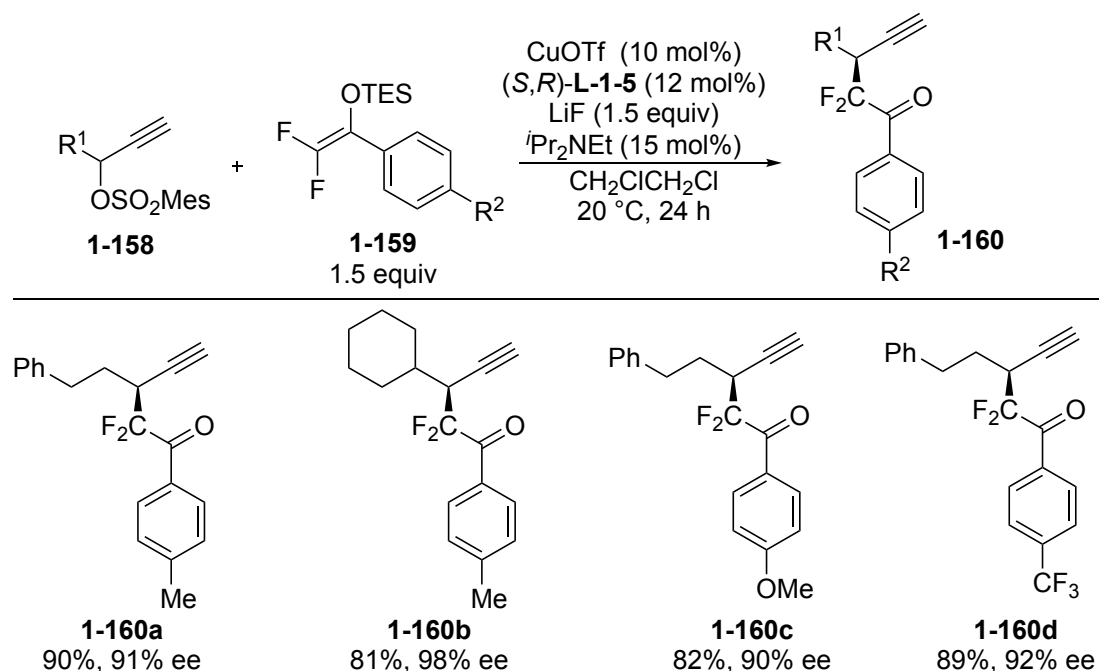
Copper-catalyzed enantioselective dearomative propargylation of phenol derivatives was reported in 2017 by Hu et al. who reacted phenol derivatives **1-155** with propargylic esters **1-156** in the presence of CuOTf·1/2C₆H₆ as a copper catalyst, (*R*)-**L-1-3** as an optically active chiral ligand, and Et₃N as a base in MeOH at -20 °C for 12 h to obtain the propargylic dearomatized product **1-157** in high yields with a high enantioselectivity (Scheme 1-59).⁷⁶

Scheme 1-59. Copper-catalyzed Enantioselective Dearomative Propargylation of Phenol Derivatives Reported by Hu et al.



In 2019, Zhang et al. reported the first copper-catalyzed enantioselective propargylic difluoroalkylation. Treatment of propargylic sulfonates **1-158** with difluoroenoxytriethylsilanes **1-159** in the presence of CuOTf as a copper catalyst, (*S,R*)-**L-1-5** as an optically active ligand, and LiF and ⁱPr₂NEt as bases in CH₂ClCH₂Cl at 20 °C for 24 h gave rise to the formation of propargylic difluoroalkylated products **1-160a-d** in high yields with a high enantioselectivity (Scheme 1-60).⁷⁷

Scheme 1-60. First Copper-catalyzed Enantioselective Propargylic Difluoroalkylation Reported by Zhang et al.



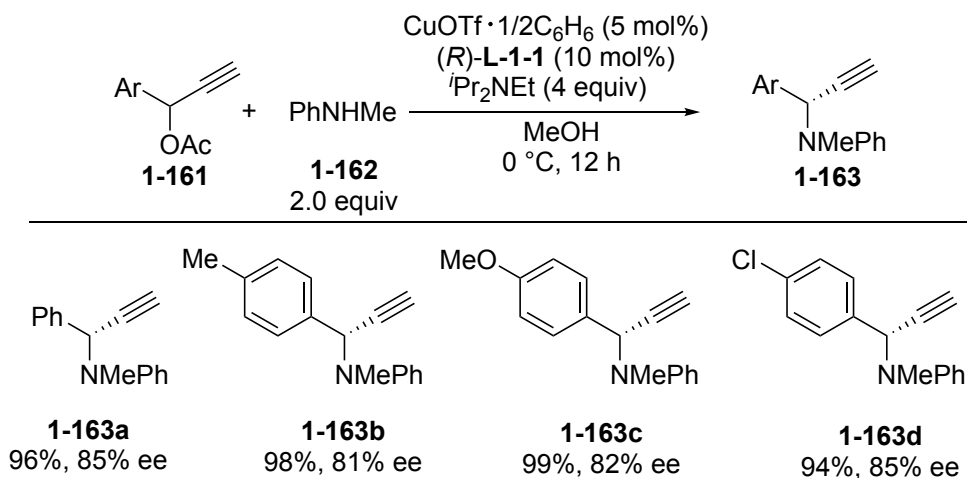
In addition, there are a variety of copper-catalyzed enantioselective propargylation reactions of aromatic compounds with propargylic alcohols.⁷⁸ Copper-catalyzed enantioselective propargylic cycloaddition reactions have been also achieved in the last decade.⁷⁹

1.4.2.2.2 Copper-catalyzed Enantioselective Propargylic Substitution Reactions with Nitrogen, Oxygen- and Sulfur-centered Nucleophiles

The first copper-catalyzed enantioselective propargylic substitution reactions were achieved with nitrogen-centered nucleophiles in 2008 by the author's group and Maarseveen's group independently, who reported the first copper-catalyzed enantioselective propargylic amination of propargylic esters with amines.

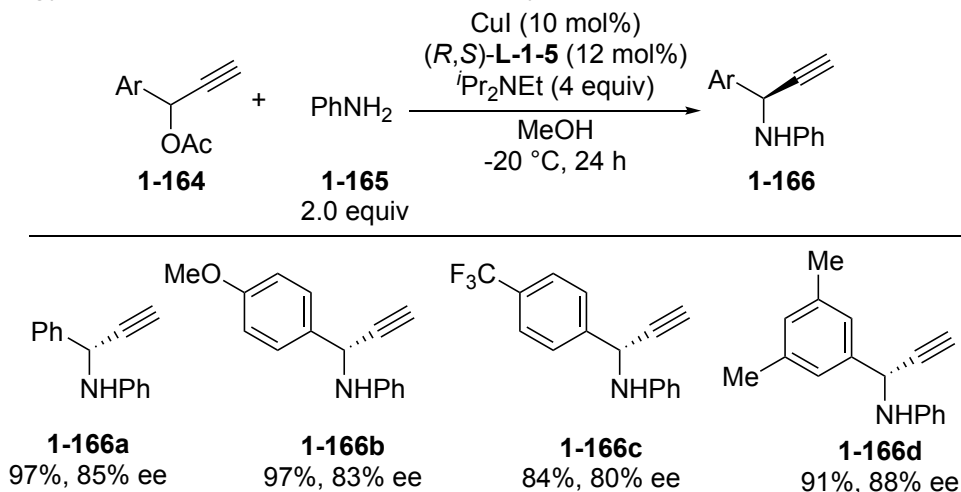
In the author's group reaction system, treatment of propargylic esters **1-161** with a secondary amine *N*-methylaniline **1-162** in the presence of CuOTf·1/2C₆H₆ as a copper catalyst, (*R*)-**L-1-1** as an optically active ligand, and *i*Pr₂NEt as a base in MeOH at 0 °C for 12 h gave the tertiary propargylic amination products **1-163a-d** in high yields with a high enantioselectivity (Scheme 1-61).^{62a}

Scheme 1-61. First Copper-catalyzed Enantioselective Propargylic Amination of Propargylic Esters with an Amine Reported by the Author's Group



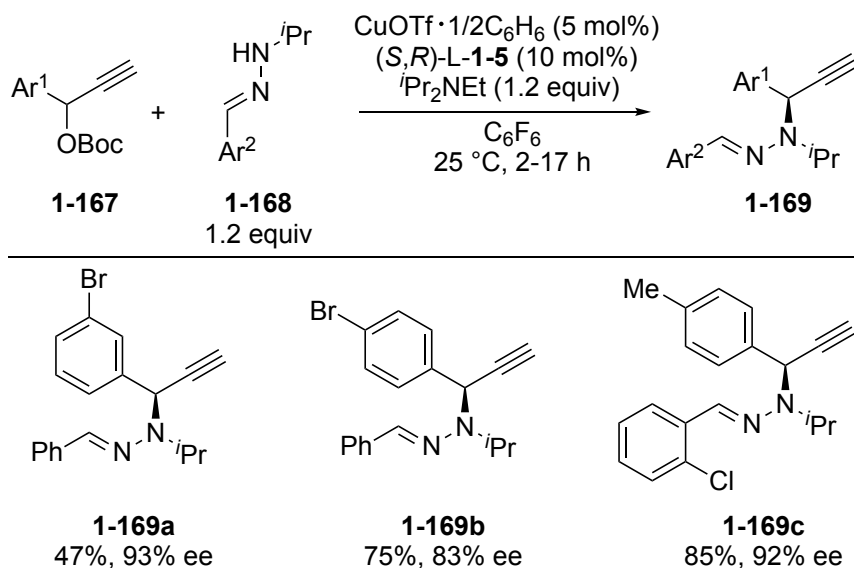
On the other hand, in Maarseveen's reaction system, a similar result was obtained as that of the author's group. Treatment of propargylic esters **1-164** with a primary amine aniline **1-165** in the presence of CuI, ligand $(R,S)\text{-L-1-5}$, and $i\text{Pr}_2\text{NEt}$ in MeOH at -20 °C for 24 h gave the propargylic amination products **1-166a-d** in high yields with a high enantioselectivity (Scheme 1-62).^{62b}

Scheme 1-62. First Copper-catalyzed Enantioselective Propargylic Amination of Propargylic Esters with an Amine Reported by Maarseveen et al.



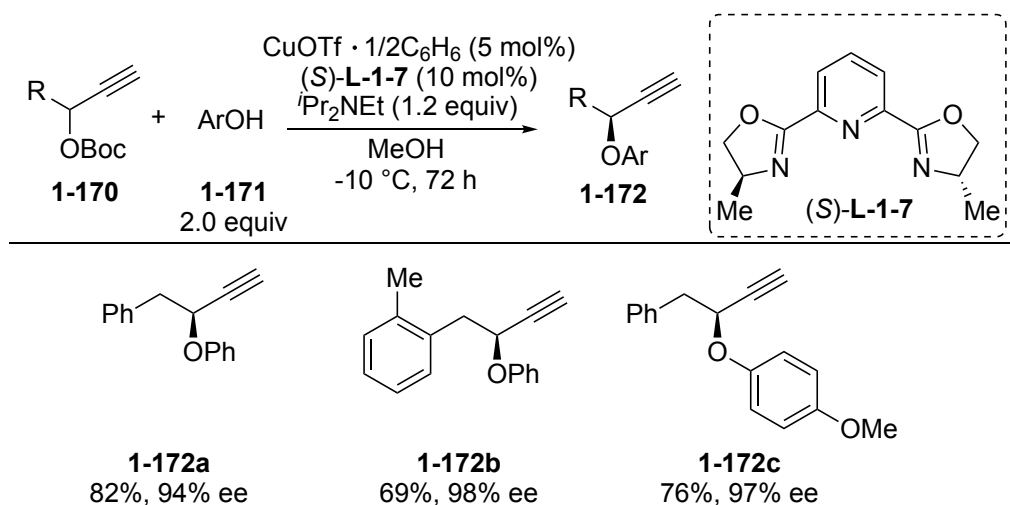
Since then, a great number of enantioselective propargylic amination of propargylic esters catalyzed by copper complexes have been reported.⁸⁰ Especially in 2021, the author's group reported copper-catalyzed propargylic substitution reactions of propargylic alcohol derivatives with *N*-monosubstituted hydrazones. Reactions of propargylic esters **1-167** with *N*-monosubstituted hydrazones **1-168** in the presence of $\text{CuOTf} \cdot 1/2\text{C}_6\text{H}_6$ as a copper catalyst, $(S,R)\text{-L-1-5}$ as an optically active ligand, and $i\text{Pr}_2\text{NEt}$ as a base in C_6F_6 at 25 °C for 2 to 17 h afforded the propargylic amination products **1-169a-d** in good to high yield with a high enantioselectivity (Scheme 1-63).⁸¹

Scheme 1-63. Copper-catalyzed Enantioselective Propargylic Amination of Propargylic Esters with *N*-Monosubstituted Hydrazones



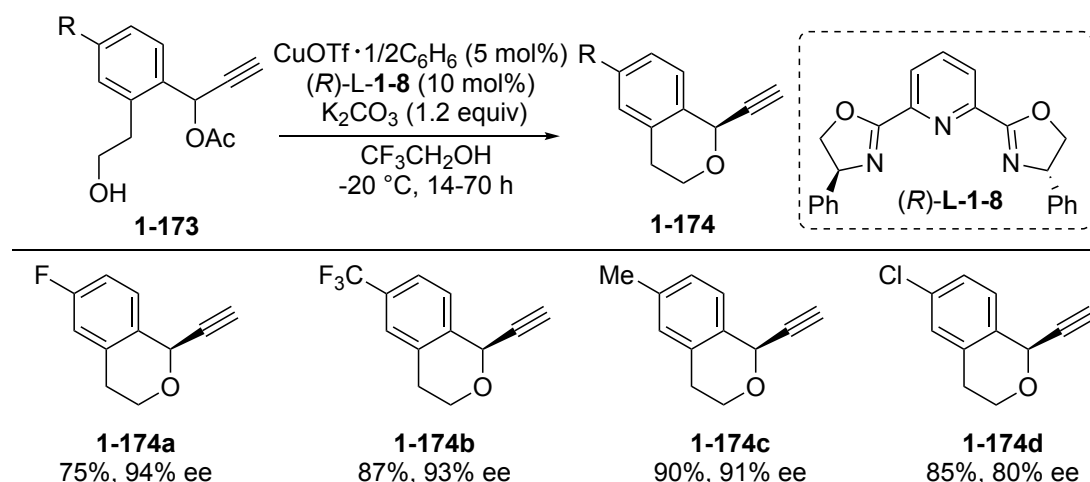
As for the copper-catalyzed enantioselective propargylic substitution reactions with oxygen-centered nucleophiles, the author's group reported the first copper-catalyzed enantioselective propargylic etherification of propargylic esters with alcohols in 2015. Treatment of propargylic esters **1-170** with alcohols **1-171** in the presence of $\text{CuOTf} \cdot 1/2\text{C}_6\text{H}_6$ as a copper catalyst, (*S*)-**L-1-7** as an optically active ligand, and $i\text{Pr}_2\text{NEt}$ as a base in MeOH at $-10\text{ }^\circ\text{C}$ for 72 h led to the formation of the propargylic etherification products **1-172a-d** in high yields with a high enantioselectivity (Scheme 1-64).⁸²

Scheme 1-64. First Copper-catalyzed Enantioselective Propargylic Etherification of Propargylic Esters with Alcohols



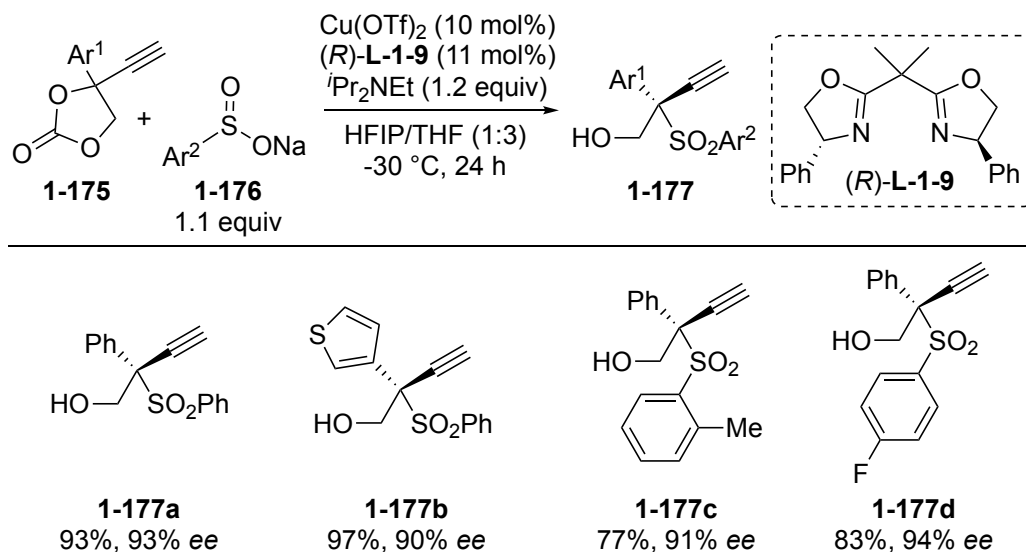
Since then, a great number of copper-catalyzed enantioselective propargylic etherification reactions of propargylic esters have been reported.⁸³ In 2019, the author's group reported copper-catalyzed enantioselective propargylic intramolecular etherification of propargylic esters. Reactions of propargylic esters bearing a hydroxyl group **1-173** in the presence of $\text{CuOTf} \cdot 1/2\text{C}_6\text{H}_6$ as a copper catalyst, (*R*)-**L-1-8** as an optically active ligand, and K_2CO_3 as a base in $\text{CF}_3\text{CH}_2\text{OH}$ at $-20\text{ }^\circ\text{C}$ for 14 to 70 h afforded the propargylic cyclic ether products **1-174a-d** in high yields with a high enantioselectivity (Scheme 1-65).⁸⁴

Scheme 1-65. Copper-catalyzed Enantioselective Propargylic Intramolecular Etherification of Propargylic Esters



Several examples exist for the copper-catalyzed enantioselective propargylic substitution reactions with sulfur-centered nucleophiles.⁸⁵ As a typical example, in 2019, Kleij et al. reported the first copper-catalyzed enantioselective propargylic sulfonylation of propargylic cyclic carbonates with sulfinates as sulfur-centered nucleophiles. When propargylic cyclic carbonates **1-175** were treated with sodium benzenesulfonates **1-176** in the presence of $\text{Cu}(\text{OTf})_2$ as a copper catalyst, (*R*)-**L-1-9** as an optically active ligand, and $i\text{Pr}_2\text{NEt}$ as a base in hexafluoroisopropanol (HFIP)/THF at $-30\text{ }^\circ\text{C}$ for 24 h, the propargylic sulfone products **1-177a-d** were obtained in high yields with a high enantioselectivity (Scheme 1-66).^{85a}

Scheme 1-66. First Copper-catalyzed Enantioselective Propargylic Sulfonylation of Propargylic Cyclic Carbonates with Sulfinate Salts Reported by Kleij et al.



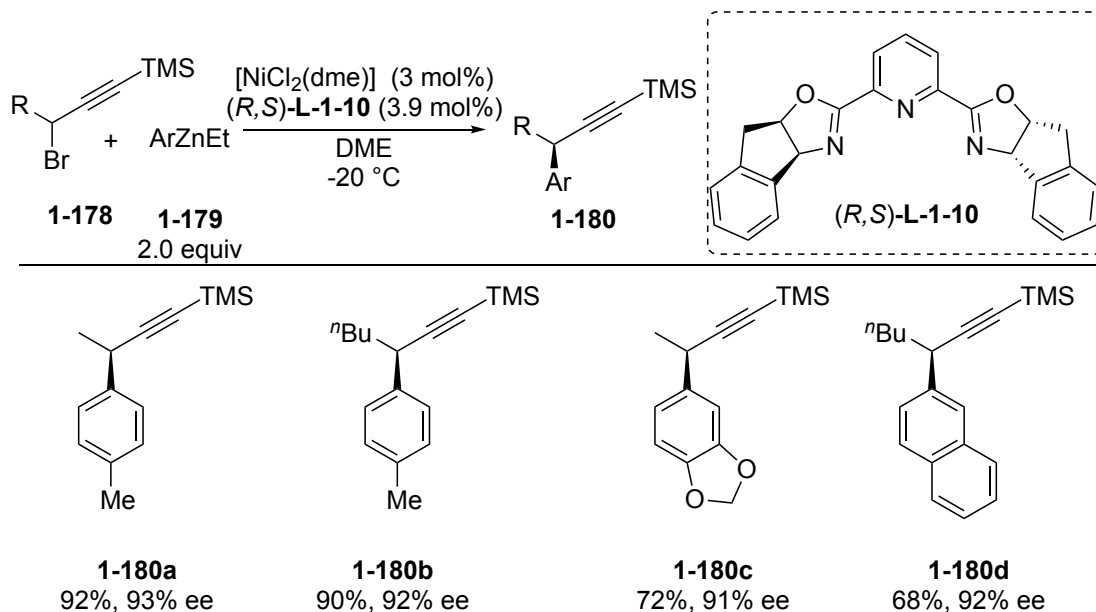
1.4.2.3 Nickel-catalyzed Enantioselective Propargylic Substitution Reactions

Compared with a vast number of reports on the ruthenium- and copper-catalyzed enantioselective propargylic substitution reactions, examples of nickel-catalyzed enantioselective propargylic substitution reactions are still rather limited in number, although some important works have been reported very recently. In this part, propargylic alkylation reactions with carbon-centered nucleophiles will be first introduced.

1.4.2.3.1 Nickel-catalyzed Enantioselective Propargylic Substitution Reactions with Carbon-centered Nucleophiles

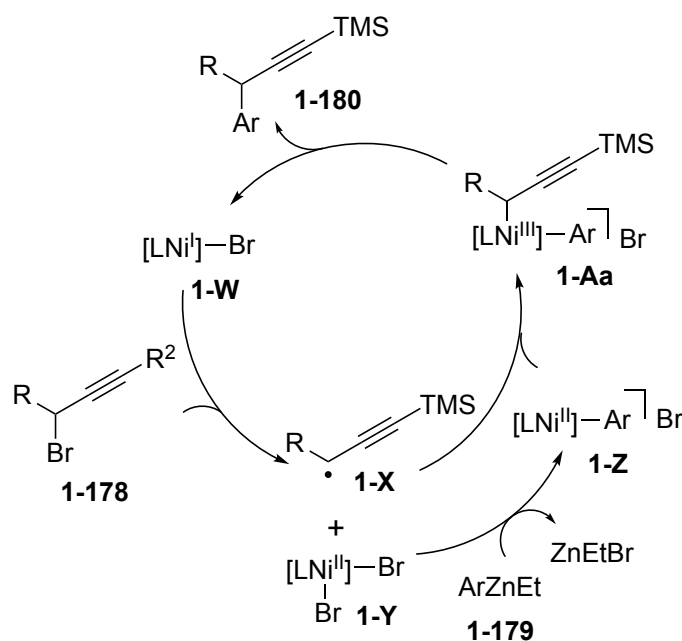
In 2008, Fu et al. reported the first nickel-catalyzed enantioselective cross-coupling reactions of propargylic halides with arylzinc reagents. Reactions of propargylic halides **1-178** with arylzinc reagents **1-179** in the presence of $[\text{NiCl}_2(\text{dme})]$ as a nickel catalyst and $(R,S)\text{-L-1-10}$ as an optically active ligand in DME at $-20\text{ }^\circ\text{C}$ afforded the cross-coupling products **1-180a-d** in high yields with a high enantioselectivity (Scheme 1-67).^{86a}

Scheme 1-67. Frist Nickel-catalyzed Enantioselective Cross-coupling Reactions of Propargylic Bromides with Arylzinc Reagents Reported by Fu et al.



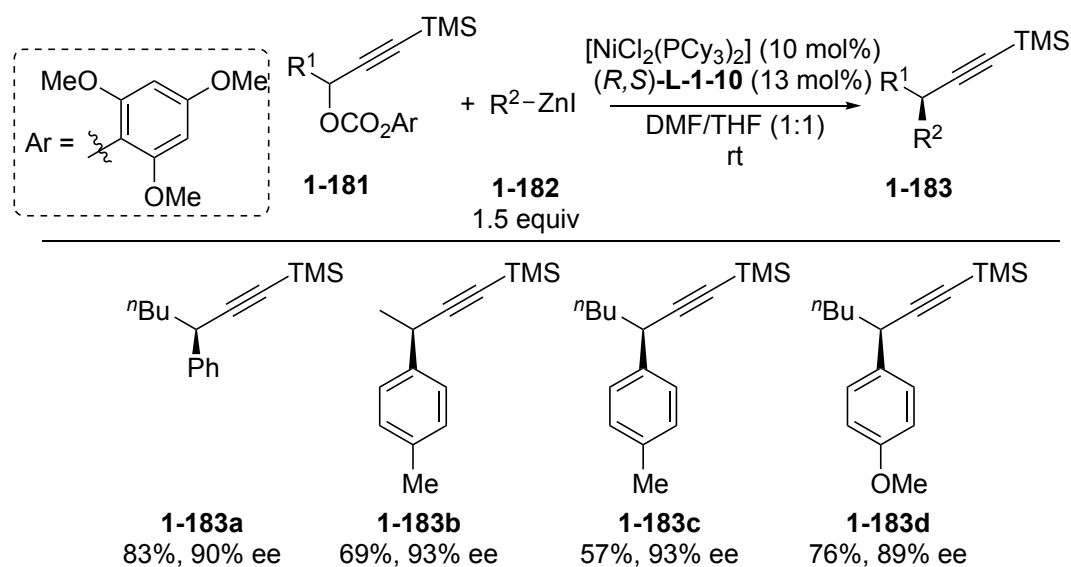
In this reaction system (Scheme 1-67), a radical process has been reported (Scheme 1-68).^{86b} First, an *in situ* generated Ni(I) complex **1-W** reacts with propargylic halide and generates a propargylic radical **1-X** with a Ni(II) complex **1-Y**. Then, transmetalation occurs between Ni(II) complex **1-Y** and an arylzinc reagent **1-179**, which generates an arylnickel complex **1-Z**. Further reaction of **1-Z** with the propargylic radical **1-X** generates propargylic nickel complex **1-Aa**. Finally, reductive elimination occurs to afford the product **1-180** and Ni(I) complex **1-W**.

Scheme 1-68. Proposed Mechanism for Nickel-catalyzed Enantioselective Cross-coupling Reactions of Propargylic Bromides with Arylzinc Reagents Reported by Fu et al.



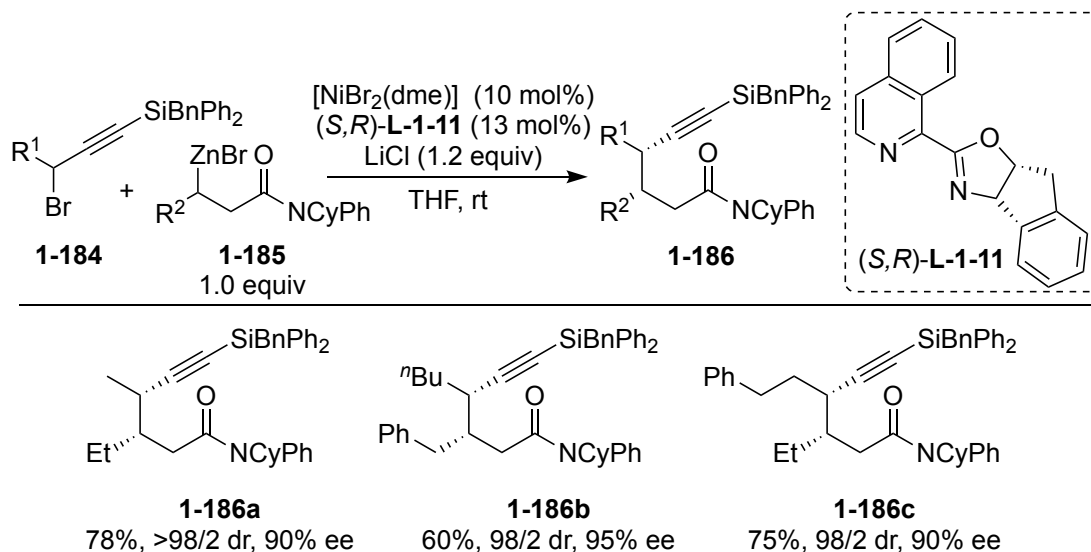
In 2012, Fu et al. reported nickel-catalyzed enantioselective cross-coupling reactions of propargylic esters with arylzinc reagents. Reactions of propargylic esters **1-181** with arylzinc reagents **1-182** in the presence of $[\text{NiCl}_2(\text{PCy}_3)_2]$ as a nickel catalyst and *(R,S)*-**L-1-10** as an optically active ligand in DMF/THF at room temperature afforded the cross-coupling products **1-183a-d** in high yields with a high enantioselectivity (Scheme 1-69).⁸⁷

Scheme 1-69. Nickel-catalyzed Enantioselective Cross-coupling Reactions of Propargylic Esters with Arylzinc Reagents Reported by Fu et al.



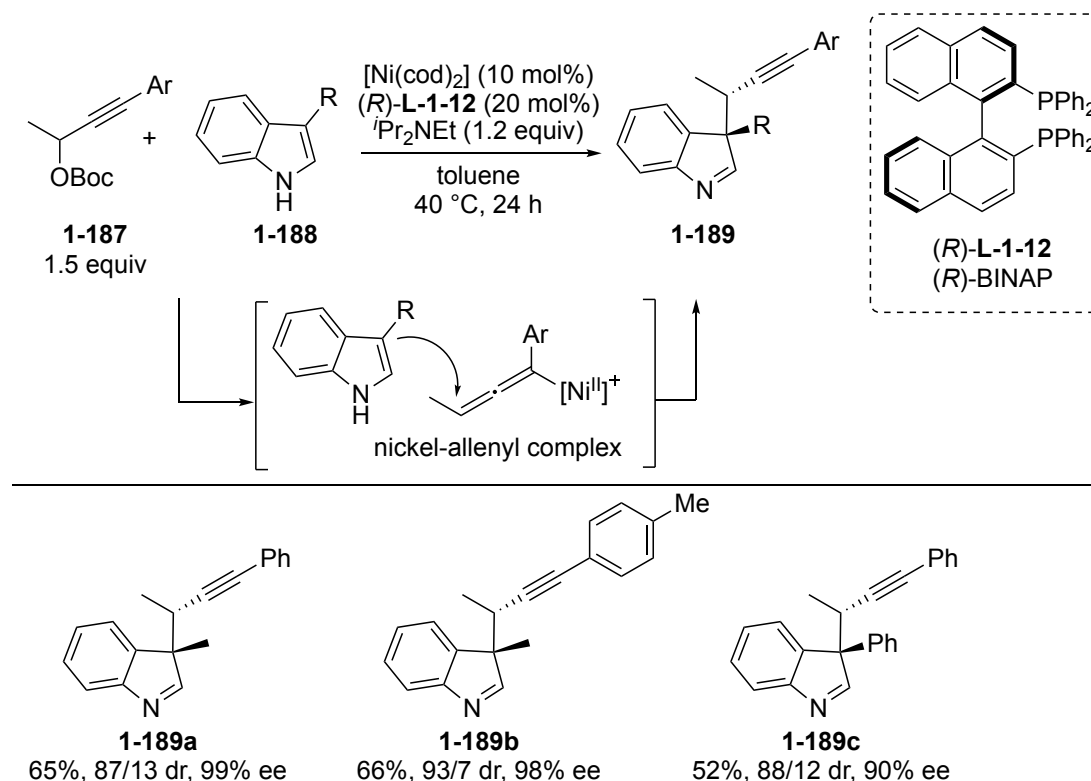
Later in 2020, Fu et al. reported nickel-catalyzed diastereo- and enantio-selective cross-coupling reactions of propargylic halides with secondary alkylzinc reagents. Reactions of propargylic halides **1-184** with alkylzinc reagents **1-185** in the presence of $[\text{NiBr}_2(\text{dme})]$ as a nickel catalyst, *(S,R)*-**L-1-11** as an optically active ligand, LiCl as a base in THF at room temperature afforded the coupling products **1-186a-c** in high yields with high diastereo- and enantio-selectivities (Scheme 1-70).⁸⁸

Scheme 1-70. Nickel-catalyzed Diastereo- and Enantio-selective Cross-coupling Reactions of Propargylic Bromides with Alkylzinc Reagents Reported by Fu et al.



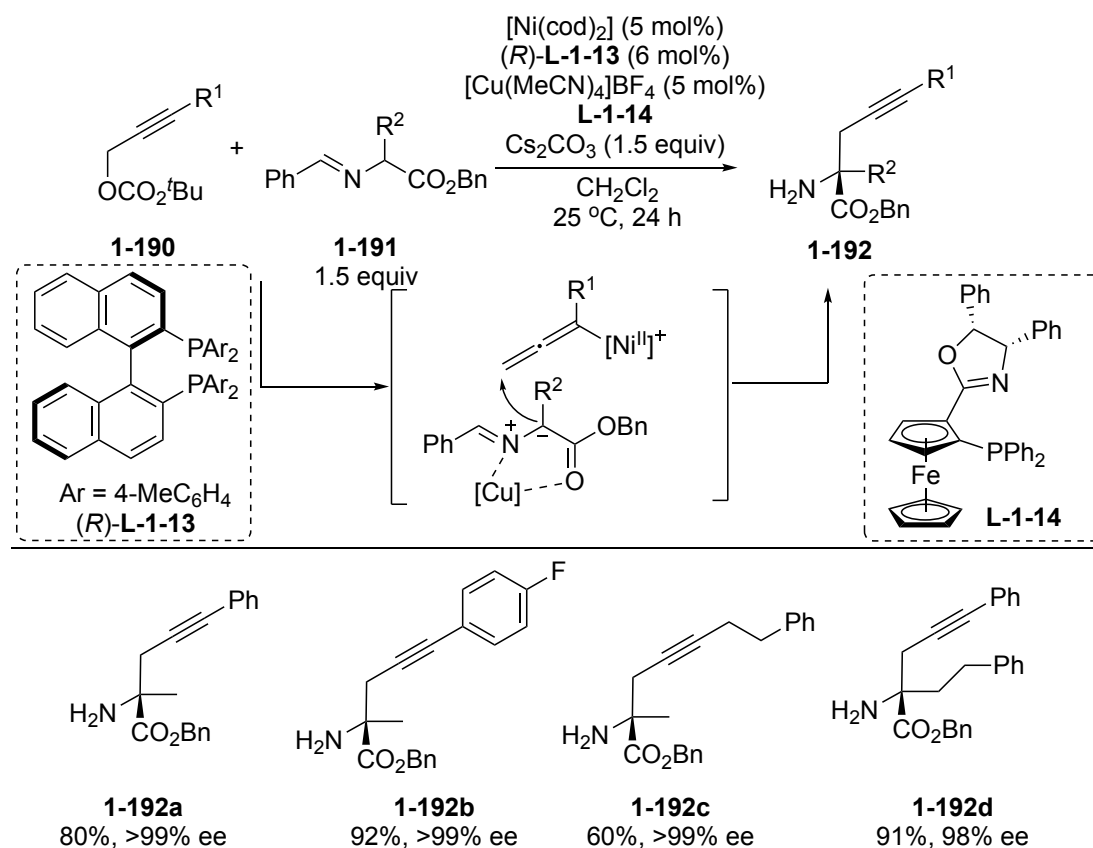
Also in 2020, Kawatsura et al. reported nickel-catalyzed enantioselective Friedel-Crafts propargylation of indoles with propargylic esters. Treatment of propargylic esters **1-187** with indoles **1-188** in the presence of $[\text{Ni}(\text{cod})_2]$ (cod = 1,5-cyclooctadiene), $(R)\text{-L-1-12}$ ((R) -BINAP) as an optically active ligand, and $i\text{Pr}_2\text{NEt}$ as a base in toluene at 40 °C for 24 h afforded the Friedel–Crafts propargylation products **1-189a-c** in high yields with high diastereo- and enantio-selectivities (Scheme 1-71).^{89a} In this reaction system, formation of nickel-allenyl complexes as reactive intermediates was proposed.

Scheme 1-71. Nickel-catalyzed Diastereo- and Enantio-selective Friedel–Crafts Propargylation Reactions of Indoles with Propargylic Esters Reported by Kawatsura et al.



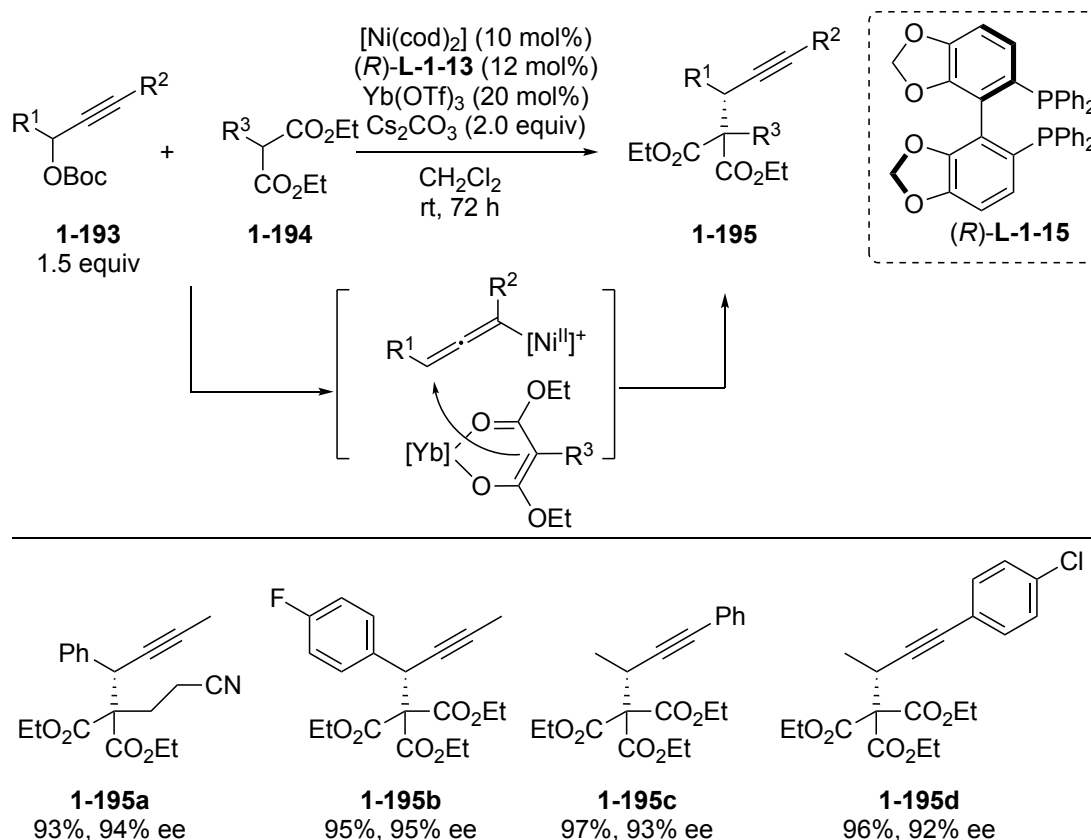
In 2020, Guo et al. reported cooperative nickel/copper-catalyzed enantioselective propargylic alkylation reactions of propargylic esters with aldimine esters. Reactions of propargylic esters **1-190** with aldimine esters **1-191** in the presence of $[\text{Ni}(\text{cod})_2]$ as a nickel catalyst, $(R)\text{-L-1-13}$ as an optically active ligand for nickel catalyst, $[\text{Cu}(\text{MeCN})_4]\text{BF}_4$ as a copper catalyst, **L-1-14** as an optically active ligand for copper catalyst, and Cs_2CO_3 as a base in CH_2Cl_2 at 25 °C for 24 h afforded the propargylic alkylated products **1-192a-d** in high yields with a high enantioselectivity (Scheme 1-72).⁹⁰ In this reaction system, the nickel catalyst activates propargylic esters toward the formation of electrophilic allenyl intermediates, whereas copper catalyst activates aldimine esters toward the formation of nucleophilic azomethane ylides, leading to the nucleophilic substitution reactions to afford the propargylic alkylated products.

Scheme 1-72. Nickel/Copper-catalyzed Enantioselective Propargylic Alkylation Reactions of Propargylic Esters with Aldimine Esters Reported by Guo et al.



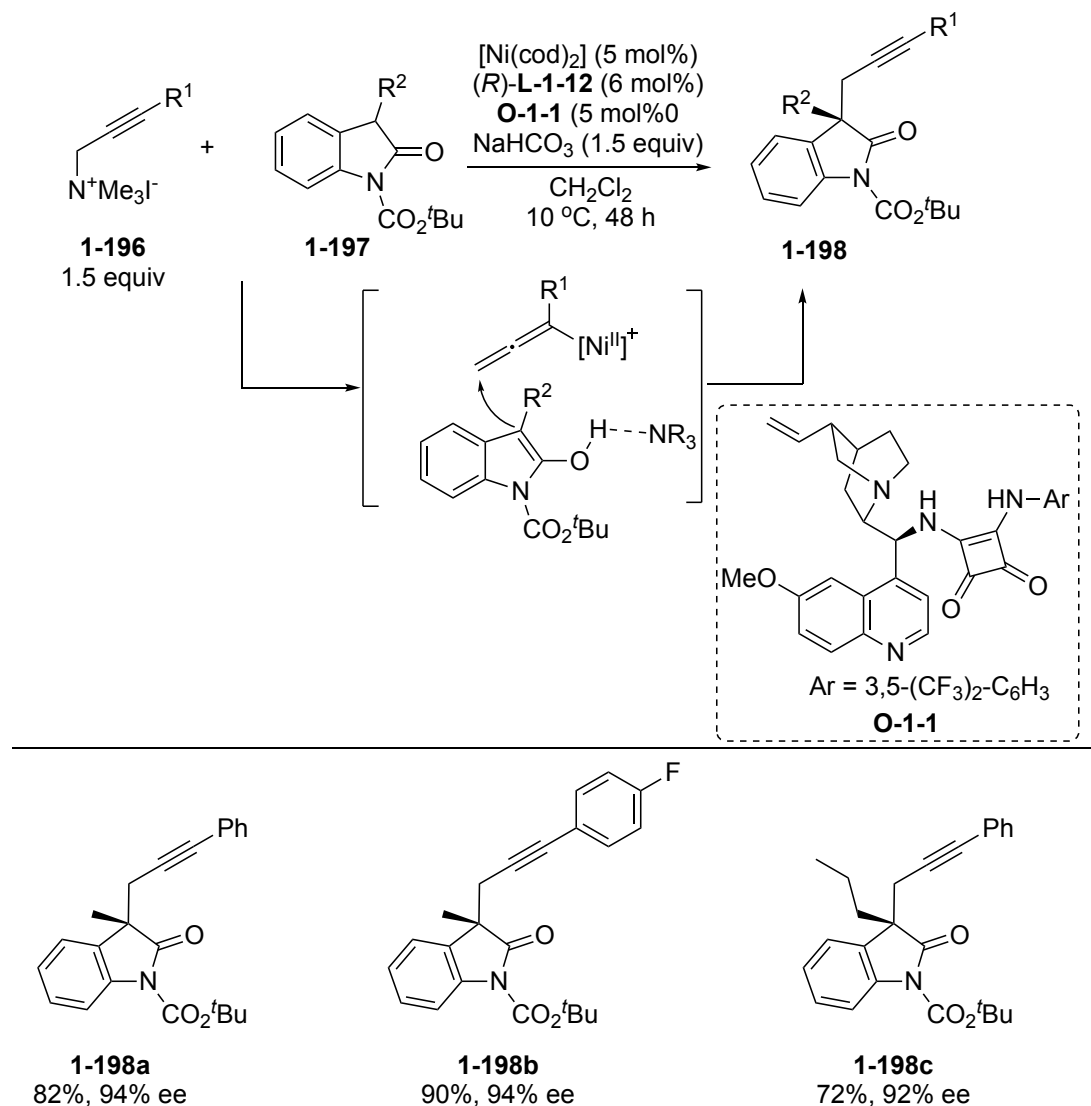
In 2021, Guo et al. reported dual nickel/Lewis acid-catalyzed enantioselective propargylic alkylation reactions of propargylic esters with alkyl malonates. Reactions of propargylic esters **1-193** with alkyl malonates **1-194** in the presence of $[\text{Ni}(\text{cod})_2]$ as a nickel catalyst, $(R)\text{-L-1-15}$ as an optically active ligand, $\text{Yb}(\text{OTf})_3$ as a Lewis acid, and Cs_2CO_3 as a base in CH_2Cl_2 at room temperature for 72 h afforded propargylic alkylated products **1-195a-d** in high yields with a high enantioselectivity (Scheme 1-73).⁹¹

Scheme 1-73. Dual Nickel/Lewis Acid-catalyzed Enantioselective Propargylic Alkylation Reactions of Propargylic Esters with Alkyl Malonates Reported by Guo et al.



In 2022, Guo et al. reported nickel/organocatalyst-catalyzed enantioselective propargylation reactions of oxindoles with propargylic esters. Reactions of propargylic esters **1-196** with oxindoles **1-197** in the presence of $[\text{Ni}(\text{cod})_2]$ as a nickel catalyst, $(R)\text{-L-1-12}$ ((R) -BINAP) as an optically active ligand, **O-1-1** as an organocatalyst, and NaHCO_3 as a base in CH_2Cl_2 at 10 °C for 48 h afforded propargylation products **1-198a-d** in high yields with a high enantioselectivity (Scheme 1-74).⁹²

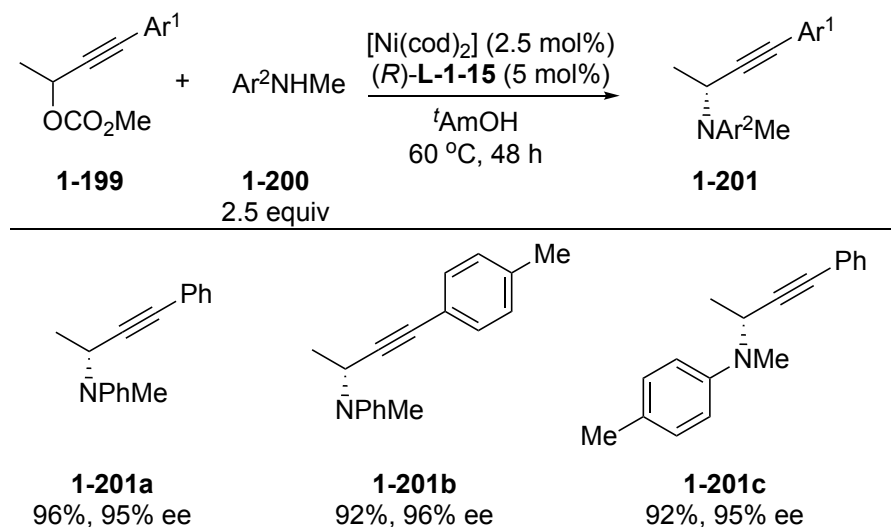
Scheme 1-74. Dual Nickel/Organocatalyst-catalyzed Enantioselective Propagation Reactions of Oxindoles with Propargylic Esters Reported by Guo et al.



1.4.2.3.2 Nickel-catalyzed Enantioselective Propargylic Substitution Reactions with Nitrogen and Oxygen-centered Nucleophiles

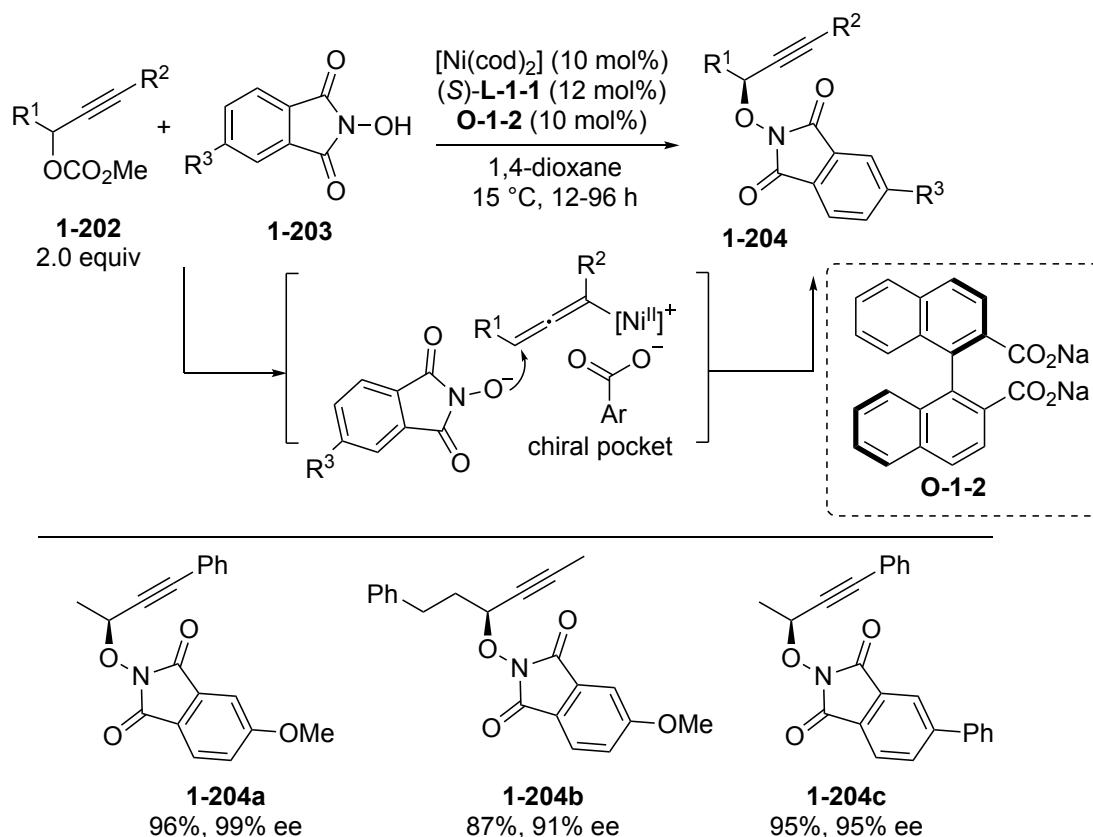
Nickel-catalyzed enantioselective propargylic amination reactions of propargylic esters with nitrogen-centered nucleophiles were first reported in 2018 by Kawatsura et al. Reactions of propargylic esters **1-199** with amines **1-200** in the presence of $[\text{Ni}(\text{cod})_2]$ as a nickel catalyst and $(R)\text{-L-1-15}$ as an optically active ligand in *t*-AmOH (*tert*-amyl alcohol) at $60\text{ }^\circ\text{C}$ for 48 h afforded propargylic aminated products **1-201a-c** in high yields with a high enantioselectivity (Scheme 1-75).⁹³

Scheme 1-75. Nickel-catalyzed Enantioselective Propargylic Amination Reactions of Propargylic Esters with Amines Reported by Kawatsura et al.



Nickel-catalyzed enantioselective O-propargylation reactions of propargylic esters with oxygen-centered nucleophiles were first reported in 2021 by Guo et al. Reactions of propargylic esters **1-202** with *N*-hydroxyphthalimides **1-203** in the presence of $[\text{Ni}(\text{cod})_2]$ as a nickel catalyst, $(S)\text{-L-1-1}$ as an optically active ligand, and the chiral sodium carboxylate **O-1-2** as a co-catalyst in 1,4-dioxane at 15 °C for 12 to 96 h afforded O-propargylation products **1-204a-c** in high yields with a high enantioselectivity (Scheme 1-76).⁹⁴ In this reaction system, the chiral sodium carboxylate **O-1-2** may serve as the ancillary ligand that fine-tunes the chiral pocket surrounding the nickel center in the catalytic systems to modulate the degree of enantioselectivity.

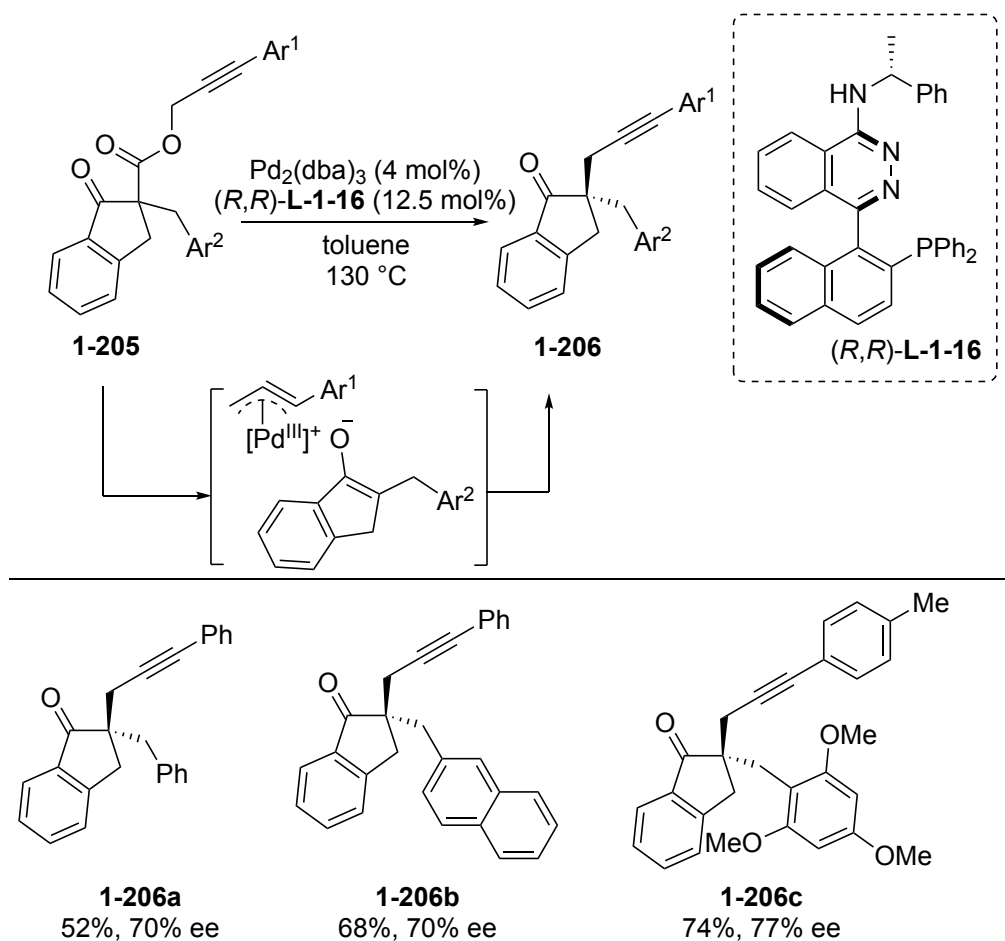
Scheme 1-76. Dual Nickel/Chiral Sodium Carboxylate-catalyzed Enantioselective Propargylation Reactions of *N*-hydroxyphthalimides with Propargylic Esters Reported by Guo et al.



1.4.2.4 Palladium-catalyzed Enantioselective Propargylic Substitution Reactions

In 2019, Guiry et al. reported the first palladium-catalyzed enantioselective intramolecular propargylic alkylation of propargylic esters via decarboxylation. Treatment of propargylic esters **1-205** in the presence of $[\text{Pd}_2(\text{dba})_3]$ and (*R,R*)-L-1-16 as an optically active ligand in toluene at 130 °C afforded the propargylic alkylated products **1-206a-c** in high yields with a good enantioselectivity (Scheme 1-77).⁹⁵

Scheme 1-77. First Palladium-catalyzed Enantioselective Decarboxylative Propargylation Reactions of Propargylic Esters Reported by Guiry et al.



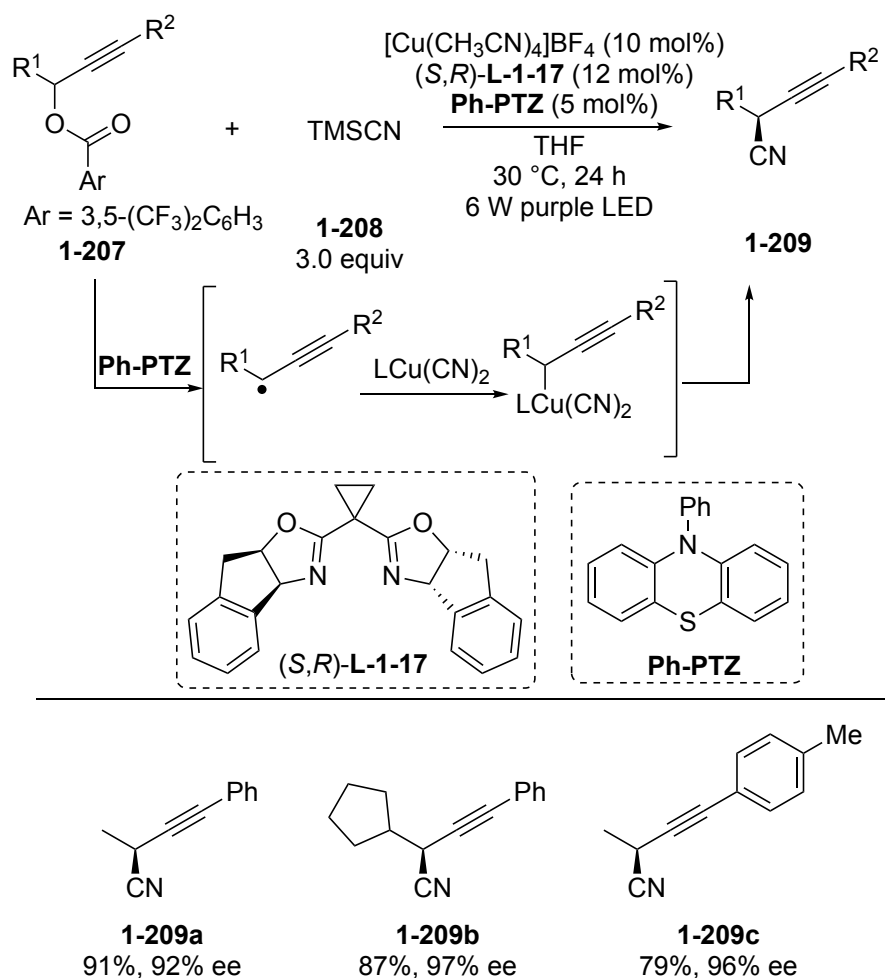
To the best of the author's knowledge, this is the only example, where palladium-catalyzed enantioselective propargylic substitution reactions were achieved.

1.4.2.5 Dual Photoredox/Copper-catalyzed Enantioselective Propargylic Substitution Reactions

In 2019, Xiao et al. reported the first dual photoredox/copper-catalyzed enantioselective cyanation of propargylic esters with trimethylsilyl cyanide. Reactions of propargylic esters **1-207** with trimethylsilyl cyanide **1-208** in the presence of $[\text{Cu}(\text{CH}_3\text{CN})_4]\text{BF}_4$ as a copper catalyst, $(S,R)\text{-L-1-17}$ as an optically active ligand, and **Ph-PTZ** as an organic photocatalyst in THF at $30\text{ }^\circ\text{C}$ for 24 h afforded the propargylic cyanation products **1-209a-c** in high yields with a high enantioselectivity (Scheme 1-78).⁹⁶ In this reaction system, a SET process between the photoexcited **Ph-PTZ** and **1-207** occurs to afford the propargylic radicals containing prochiral centers at the propargylic position. On the other hand, cyanide anion is transferred onto the chiral copper catalyst, which also captures the propargylic radicals in a stereoselective manner, where reduction elimination affords the propargylic cyanation products

enantioselectively. This is the only example of the enantioselective propargylic substitution reactions with carbon-centered nucleophiles under photoredox catalyzed conditions.

Scheme 1-78. First Dual Photoredox and Copper-catalyzed Enantioselective Cyanation of Propargylic Esters with Trimethylsilyl Cyanide Reported by Xiao et al.



1.4.2.6 Summary on Enantioselective Propargylic Substitution Reactions

As described above, the author summarized recent advances of catalytic enantioselective propargylic substitution reactions from the first example reported in 2005 to the latest articles published very recently. Over the past 17 years, enantioselective propargylic substitution reactions have been developed to obtain the corresponding propargylic substituted products with a high enantioselectivity.

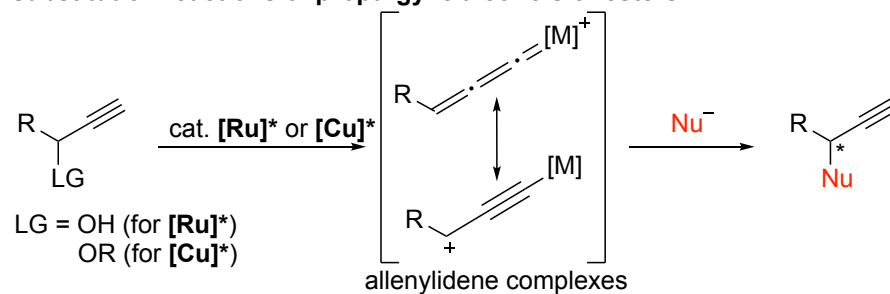
In view of synthetic chemistry, not only carbon-centered nucleophiles but also heteroatom (nitrogen, oxygen, sulfur, phosphorus, etc.)-centered nucleophiles have been applicable to introduce new carbon–carbon or carbon–heteroatom bonds at the propargylic position of propargylic alcohol derivatives. In addition, there are some other

examples of enantioselective propargylic substitution reactions catalyzed by cooperative catalytic combinations^{97,98} or organocatalysts.^{99,100}

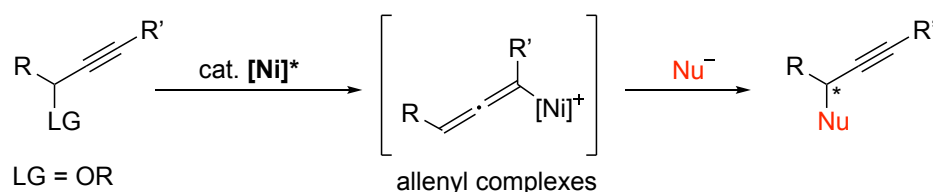
In view of reaction mechanism, most of the propargylic substitution reactions proceed via ruthenium- or copper-allenylidene complexes as key intermediates (Scheme 1-79a),⁴³ whereas nickel catalysis provides allenyl complexes as key intermediates (Scheme 1-79b).^{89b} Furthermore, transition metal-catalyzed enantioselective propargylic cyanation reactions of propargylic radicals have been reported (Scheme 1-79c).⁹⁶ Formation of propargylic radicals and further participation of propargylic substitution reactions have been also proposed for some nickel-catalyzed enantioselective propargylic substitution reactions.^{86c} However, until now, no successful example in the transition metal-catalyzed enantioselective propargylic alkylation reactions with carbon-centered alkyl radicals has been reported. Hence, if alkyl radicals formed in photoredox catalyses are shown to work as alternatives to nucleophilic alkylation reagents to react with propargylic alcohols or esters to afford enantioselective propargylic alkylation products in the presence of additional chiral transition metal catalysts (Scheme 1-79d), it can be claimed that a new method for enantioselective propargylic alkylation reactions is successfully developed. By the importation of photoredox catalytic system using alkyl radicals as alternatives to nucleophilic alkylation reagents, deduction of several functional group protections from previous methods and drastic expansion of scope of substrates to react with propargylic alcohols or esters can be expected.

Scheme 1-79. Enantioselective Propargylic Substitution Reactions

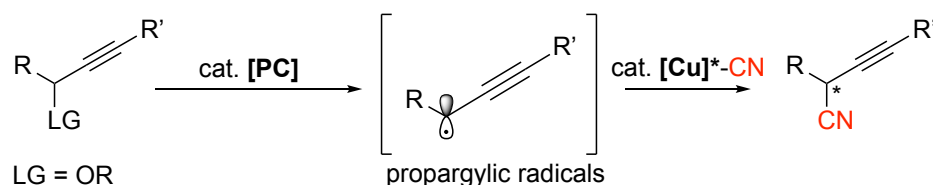
a) Ruthenium- or copper-catalyzed enantioselective propargylic substitution reactions of propargylic alcohols or esters



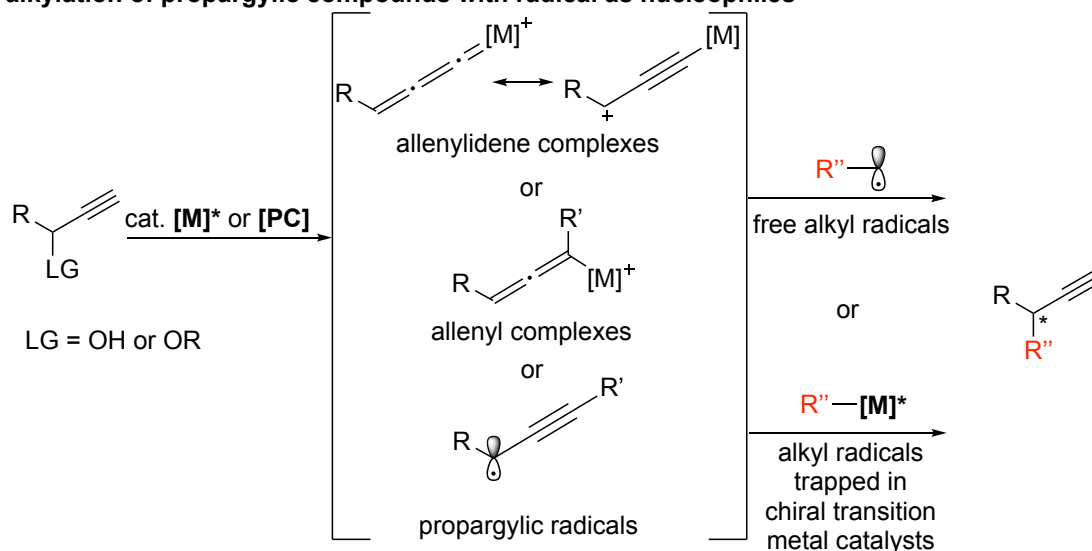
b) Nickel-catalyzed enantioselective propargylic substitution reaction of propargylic halides or propargylic esters



c) Dual photoredox/copper-catalyzed enantioselective propargylic cyanation of propargylic esters reported by Xiao et al.



d) This work and perspectives: transition metal-catalyzed enantioselective propargylic alkylation of propargylic compounds with radical as nucleophiles

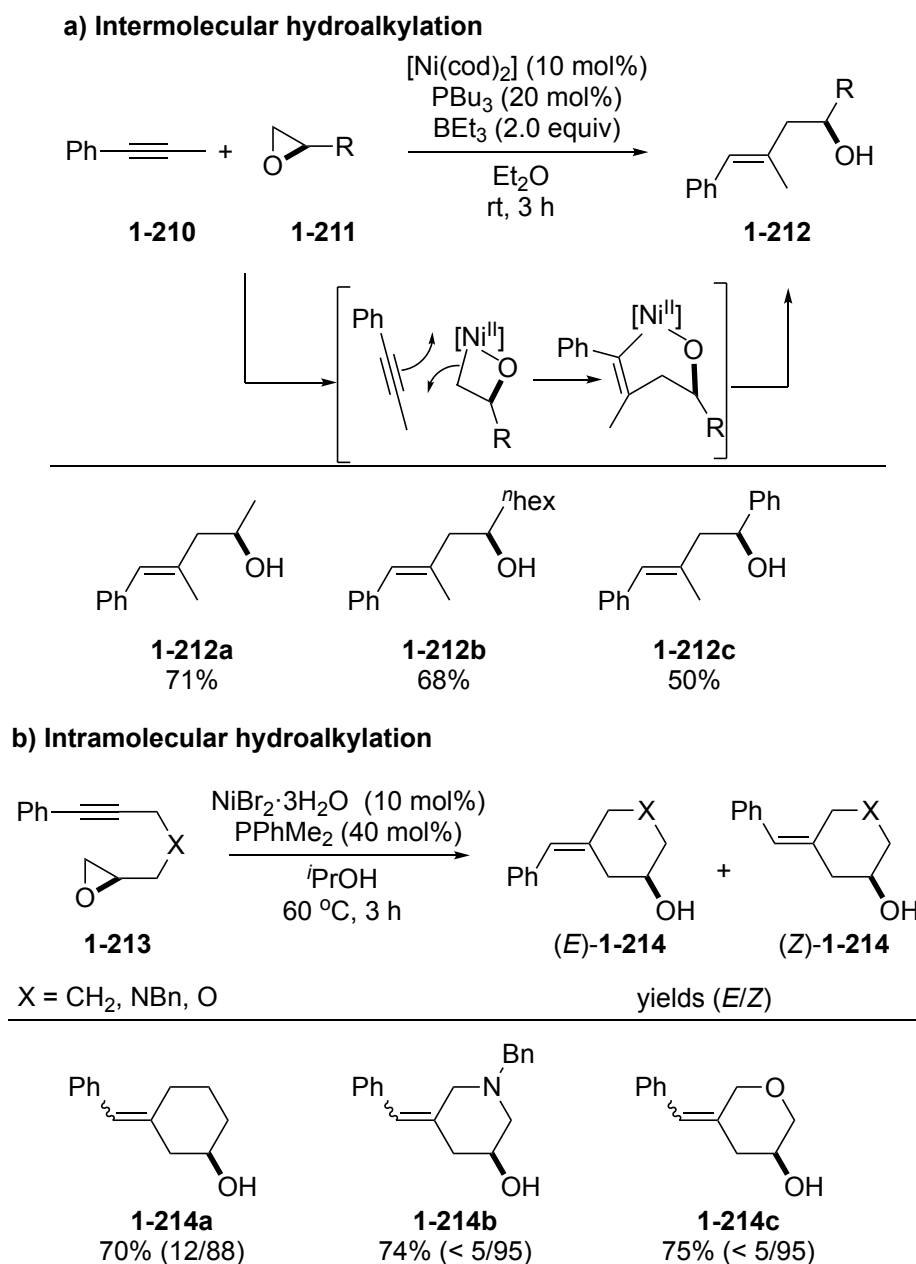


1.5. Catalytic Hydroalkylation Reactions of Alkynes to Afford Alkenes

1.5.1. Transition Metal-catalyzed Hydroalkylation Reactions of Alkynes

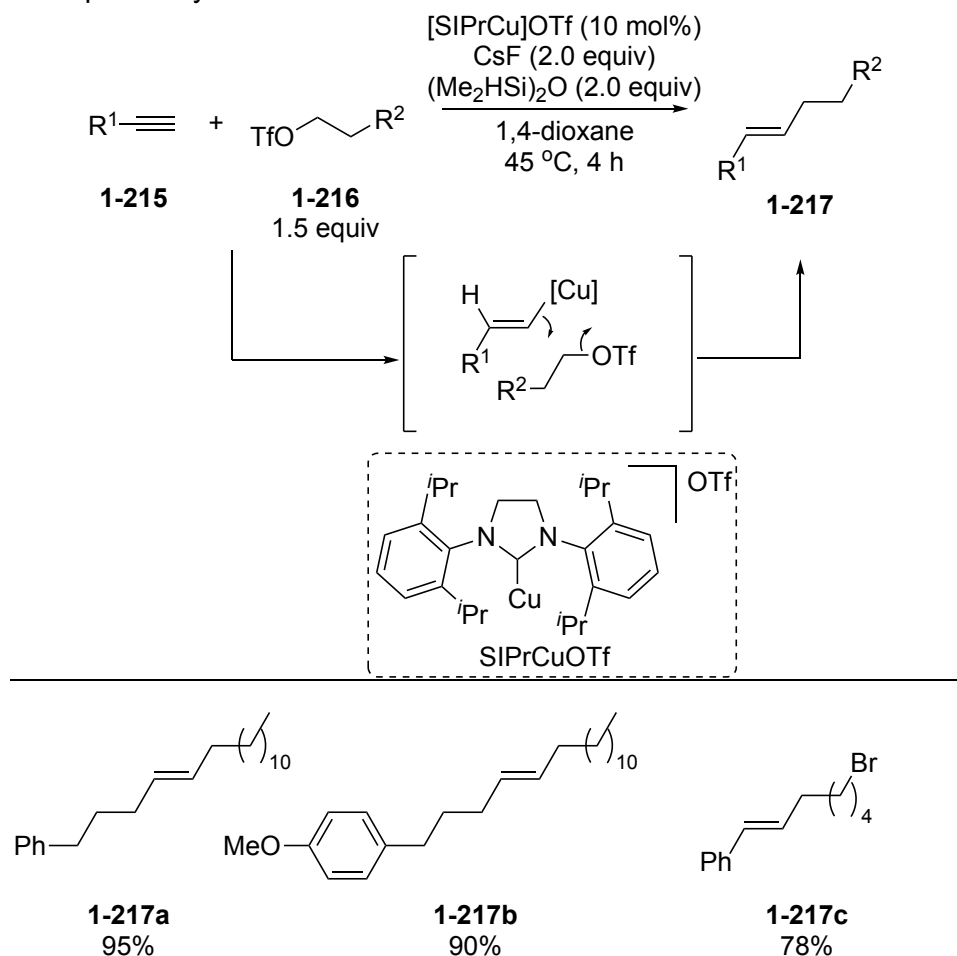
Although there have been several methods for the cross-coupling reactions of alkynes with π -electrophiles such as aldehydes,¹⁰¹ ketones,¹⁰² enones,¹⁰³ formamides,¹⁰⁴ and imines,¹⁰⁵ examples of hydroalkylation cross-coupling reactions of alkynes with alkyl σ -electrophiles have been rather limited in number. As an early example of nickel-catalyzed hydroalkylation of alkynes, Jamison and co-workers reported nickel-catalyzed reductive coupling reactions of an internal alkyne **1-210** with epoxides **1-211** in the presence of [Ni(cod)₂] as a nickel catalyst, PBu₃ as a ligand, and BEt₃ as a base in Et₂O at room temperature for 3 h to afford the ring-opening products **1-212** in good yields (Scheme 1-80a).^{106a} Intramolecular hydroalkylation of alkynes **1-213** containing an epoxide moiety was also reported to occur in the presence of NiBr₃·3H₂O as a nickel catalyst and PPhMe₂ as a ligand in *i*PrOH at 60 °C for 3 h to afford the cyclic products **1-214** in good yields with a good *E/Z*-selectivity (Scheme 1-80b).^{106b}

Scheme 1-80. Nickel-catalyzed Hydroalkylation Reactions of an Internal Alkyne with Epoxides Reported by Jamison et al.



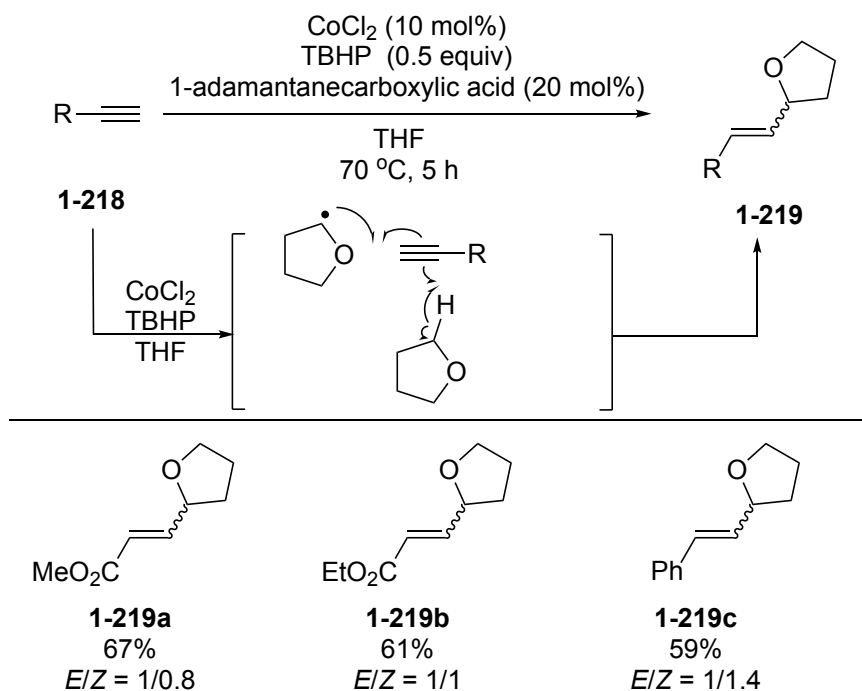
Other transition metal-catalyzed hydroalkylation of alkynes was also examined. For example, copper catalysis was applied into hydroalkylation reactions of alkynes.¹⁰⁷ As a typical example, Lalic et al. reported the copper-catalyzed hydroalkylation reactions of alkynes with alkyl triflates. Reactions of terminal alkynes **1-215** with alkyl triflates **1-216** in the presence of [SIPrCu]OTf (*N*-heterocyclic carbene copper complex) as a copper catalyst, CsF as a base, and (Me₂HSi)₂O as a hydride source in 1,4-dioxane at 45 °C for 4 h afforded the hydroalkylation products **1-217a-c** in good yields (Scheme 1-81).^{107b}

Scheme 1-81. Copper-catalyzed Hydroalkylation Reactions of Alkynes with Alkyl Triflates Reported by Lalic et al.



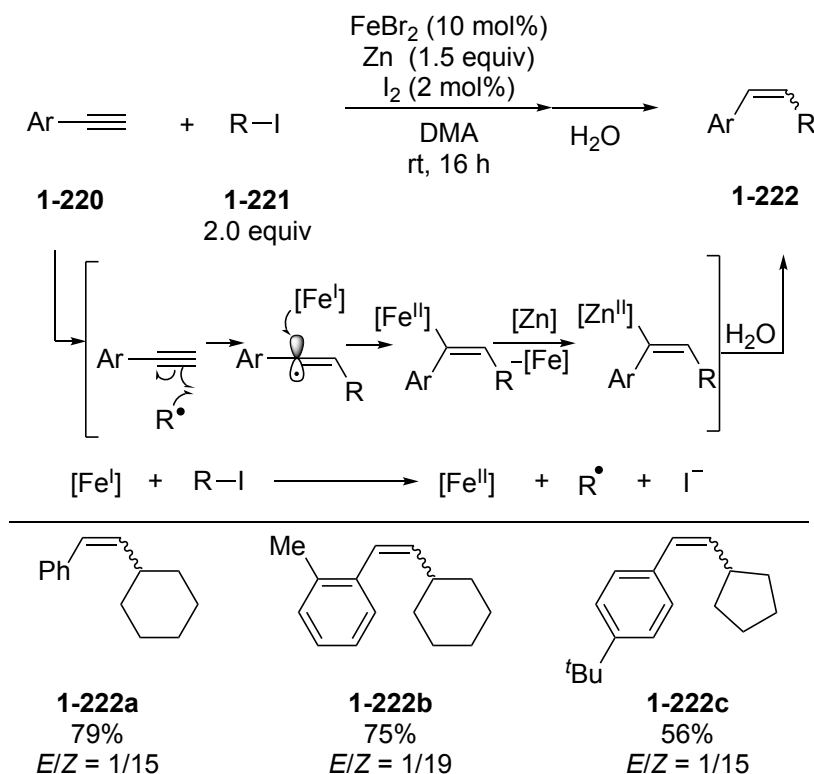
In 2014, Kang et al. reported cobalt catalyzed hydroalkylation reactions of alkynes with THF. Reactions of terminal alkynes **1-218** in the presence of CoCl_2 as a cobalt catalyst, *tert*-butyl hydroperoxide (TBHP) as a radical initiator, and 1-adamantanecarboxylic acid as a proton source in THF at 70 °C for 5 h afforded the hydroalkylation products **1-219a-c** in good yields (Scheme 1-82).^{108a} Later, their subsequent research has clarified that the reaction proceeds through radical pathway, where CoCl_2 catalyzes the formation of tetrahydrofuran-2-yl radical by abstracting hydrogen atom with the aid of TBHP.^{108b}

Scheme 1-82. Cobalt-catalyzed Hydroalkylation Reactions of Alkynes with THF Reported by Kang et al.



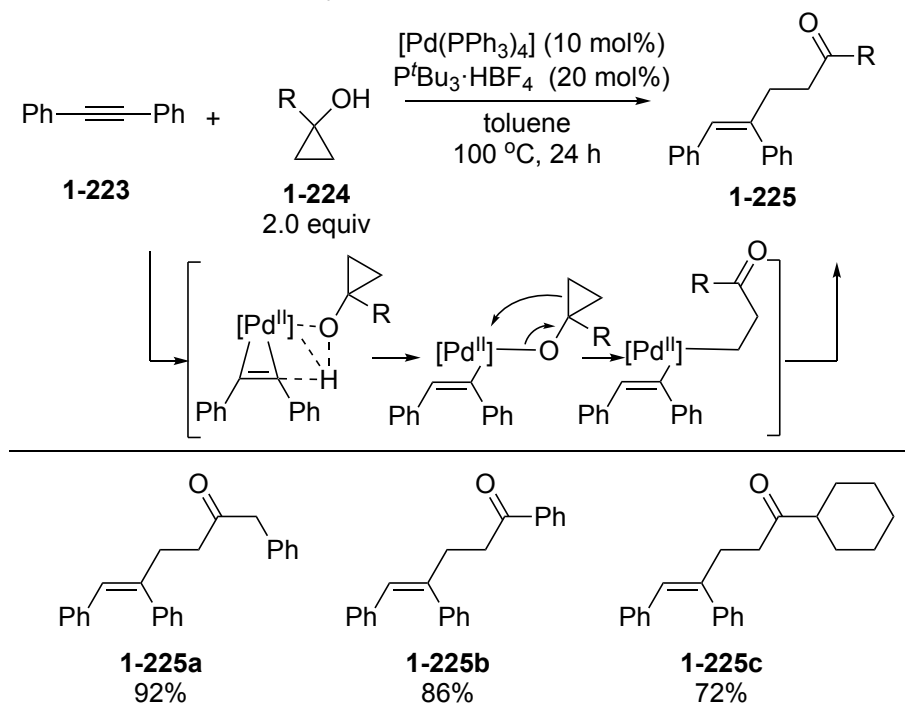
In 2015, Hu et al. reported the iron-catalyzed reductive hydroalkylation reactions of alkynes with alkyl iodide. Reactions of terminal alkynes **1-220** with alkyl iodides **1-221** in the presence of FeBr_2 as an iron catalyst, Zn as a reductant, and I_2 as a Zn-activating reagent in DMA at room temperature for 16 h afforded the hydroalkylation products **1-222a-c** in good yields with a good *E/Z*-selectivity, after quenching with H_2O (Scheme 1-83).¹⁰⁹ In this reaction system, the iron bromide not only catalyzes the formation of alkyl radicals which react with terminal alkynes but also controls *Z*-selectivity as shown below to afford alkenyl iron complexes as key intermediates.

Scheme 1-83. Iron-catalyzed Hydroalkylation Reactions of Alkynes with Alkyl Iodide Reported by Hu et al.



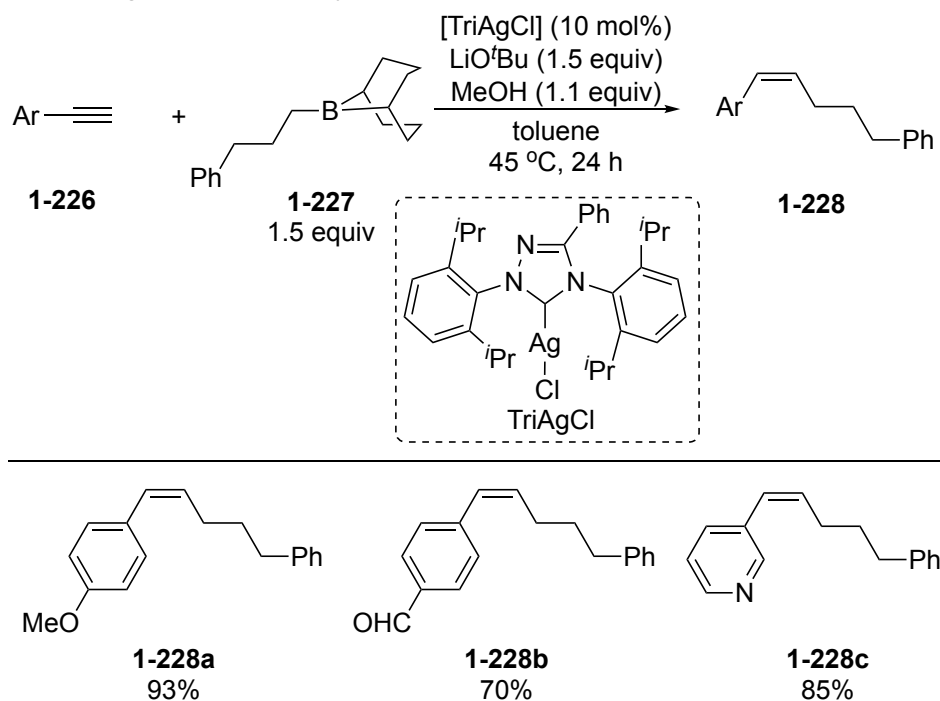
Palladium catalysis can be also applied into hydroalkylation reactions of alkynes.¹¹⁰ As a typical example, Yao et al. reported the palladium-catalyzed hydroalkylation reactions of an internal alkyne with cyclopropanols. Reactions of an internal alkyne **1-223** with cyclopropanols **1-224** in the presence of $[\text{Pd}(\text{PPh}_3)_4]$ as a palladium catalyst and $\text{P}^t\text{Bu}_3 \cdot \text{HBF}_4$ as a ligand in toluene at 100 °C for 24 h afforded the ring-opening product **1-225** in good yields (Scheme 1-84).^{110a} In this reaction system, hydrogen transfer between the two substrates occurs, followed by β -carbon elimination and further reductive elimination to give the alkylated products.

Scheme 1-84. Palladium-catalyzed Hydroalkylation Reactions of an Internal Alkyne with Cyclopropanols Reported by Yao et al



In addition, there are some examples with silver catalysis.¹¹¹ As a typical example, Lalic et al. reported the first silver-catalyzed hydroalkylation reactions of alkynes with alkylboron reagent. Reactions of terminal alkynes **1-226** with an alkylboron reagent **1-227** in the presence of $[\text{TriAgCl}]$ (Tri = 1,4-bis(2,6-diisopropylphenyl)-3-phenyl-1,2,4-triazole-based *N*-heterocyclic carbene) as a silver catalyst, LiO^tBu as a base, and MeOH as a proton source in toluene at 45°C for 24 h afforded the hydroalkylation products **1-228a-c** in good yields (Scheme 1-85).^{111a}

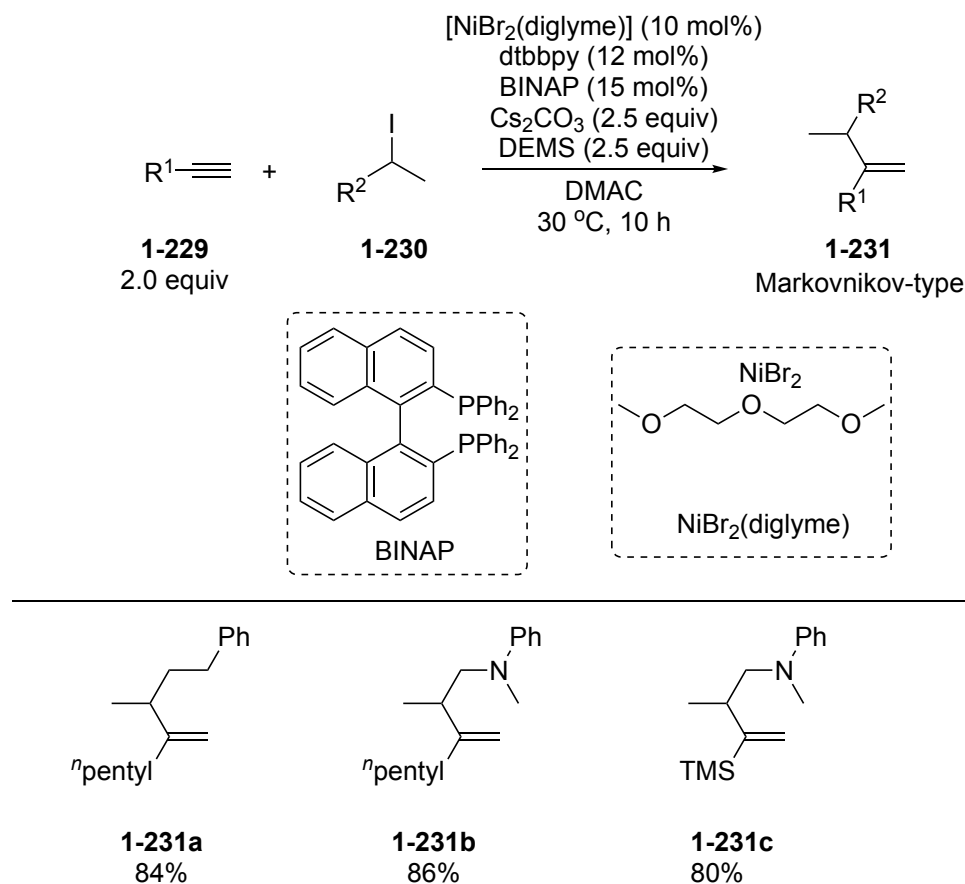
Scheme 1-85. Silver-catalyzed Hydroalkylation Reactions of Alkynes with an Alkylboron Reagent Reported by Lalic et al



1.5.2. Nickel-catalyzed Hydroalkylation Reactions of Alkynes

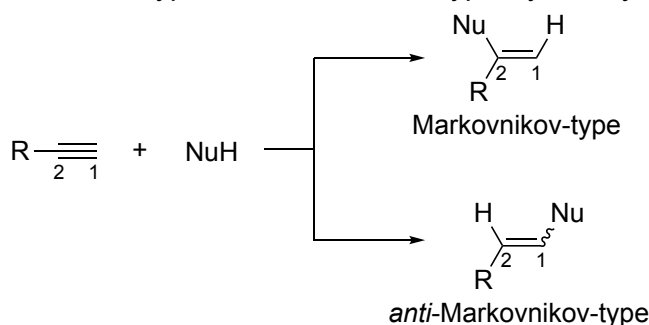
In 2016, Fu et al. reported nickel-catalyzed hydroalkylation reactions of alkynes with alkyl halides. Reactions of terminal alkynes **1-229** with alkyl iodides **1-230** in the presence of [NiBr₂(diglyme)] (diglyme = bis(2-methoxyethyl) ether) as a nickel catalyst, dtbbpy and BINAP as ligands to coordinate with the nickel catalyst, Cs₂CO₃ as a base, and diethoxymethylsilane (DEMS) as a hydride donor in *N,N*-dimethylacetamide (DMAC) at 30 °C for 10 h afforded the Markovnikov-type alkylated alkenes **1-231a-c** in good yields (Scheme 1-86).¹¹²

Scheme 1-86. Nickel-Catalyzed Hydroalkylation Reactions of Terminal Alkynes with Alkyl iodides Reported by Fu et al.



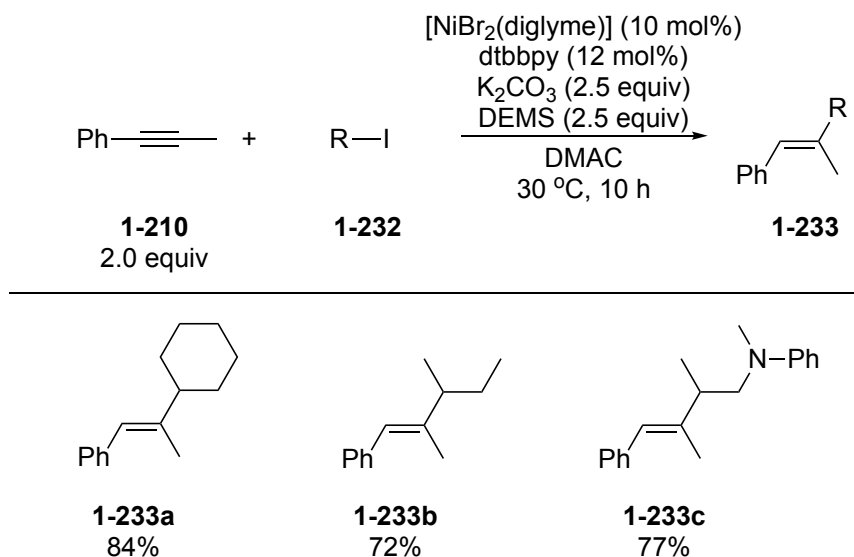
An explanation for Markovnikov-type/*anti*-Markovnikov-type hydroalkylation of terminal alkynes is shown in [Scheme 1-87](#). When nucleophiles NuH adds to terminal alkynes in typical organic reactions, the proton first adds to the carbon containing more hydrogen atoms (1-C in case of terminal alkynes) to form stable carbocations at the neighboring more branched carbon centers (2-C in case of terminal alkynes), where the nucleophilic anions Nu[−] add to give the Markovnikov-type products. The reverse products, where Nu add to the less branched carbons (1-C) and the hydrogen atom adds to the more branched carbons (2-C), are the *anti*-Markovnikov-type ones. The latter products are obtained especially for nucleophilic radicals, whereas use of transition metal catalysts also controls the selectivity for Markovnikov-type and *anti*-Markovnikov-type products.

Scheme 1-87. Markovnikov-type/anti-Markovnikov-type Hydroalkylation



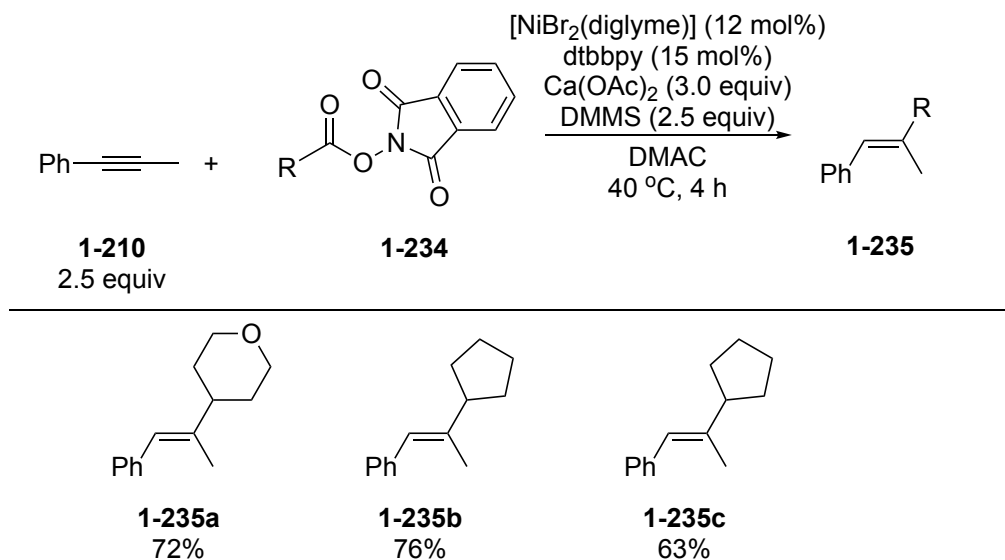
Later, in 2018, Lu et al. reported nickel-catalyzed hydroalkylation reactions of an internal alkyne. Reactions of an internal alkyne **1-210** with alkyl iodides **1-232** in the presence of $NiBr_2(diglyme)$ as a nickel catalyst, dtbbpy as a ligand, K_2CO_3 as a base, and DEMS as a hydride donor in DMAC at 30 °C for 10 h afforded the alkylated alkenes **1-233a-c** in good yields (Scheme 1-88).¹¹³ Here, alkyl groups are introduced to the alkyne carbon atoms attached to alkyl group rather than those attached to aryl groups, for secondary carbocations containing alkyl groups are more planar and stable than those containing aryl groups.

Scheme 1-88. Nickel-Catalyzed Hydroalkylation Reactions of an Internal Alkyne with Alkyl iodides Reported by Lu et al.



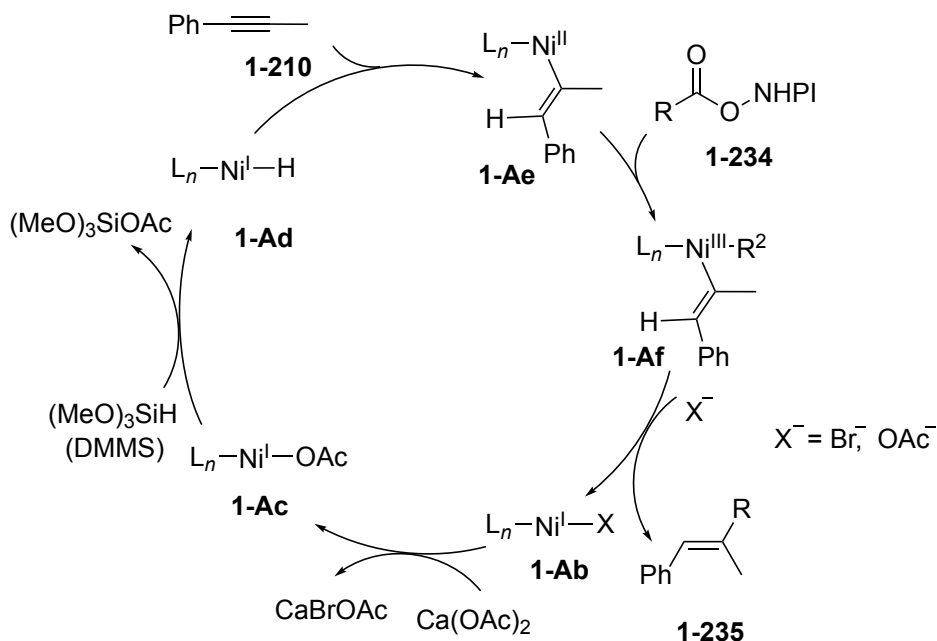
In the same year, Lu et al. also reported similar hydroalkylation reactions of an internal alkyne with NHPI (N-hydroxyphthalimide) esters. Reactions of an internal alkyne **1-210** with NHPI esters **1-234** in the presence of $[NiBr_2(diglyme)]$ as a nickel catalyst, dtbbpy as a ligand, $Ca(OAc)_2$ as a base, and dimethoxymethylsilane (DMMS) as a hydride donor in DMAC at 40 °C for 4 h afforded the alkylated alkenes **1-235a-c** in good yields (Scheme 1-89).¹¹⁴

Scheme 1-89. Nickel-Catalyzed Hydroalkylation Reactions of an Internal Alkyne with NHPI Esters Reported by Lu et al.



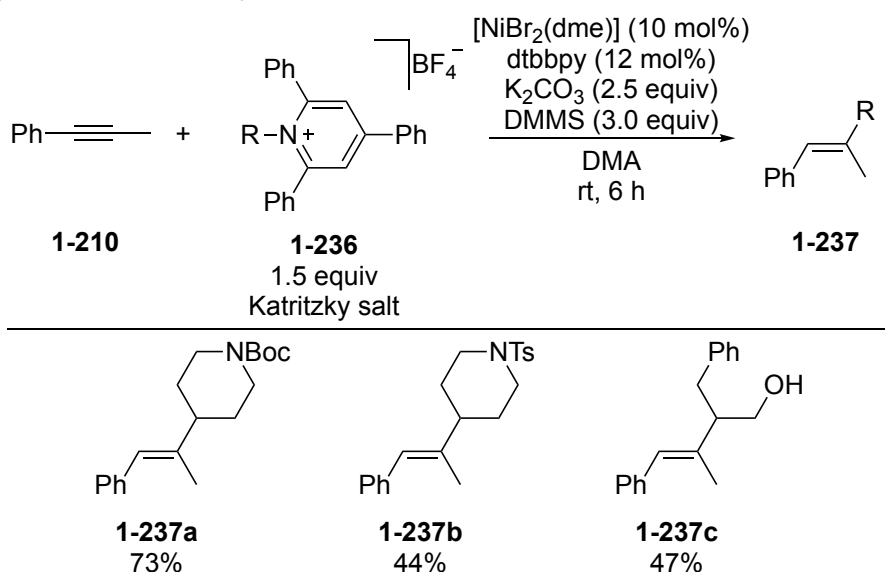
A typical proposed catalytic reaction pathway of the nickel-catalyzed hydroalkylation reactions of alkynes is shown in [Schemes 1-90](#) based on the Lu's proposals ([Scheme 1-89](#)).¹¹⁴ In this case, ligand exchange of Ni(I) species **1-Ab** between halide and acetate occurs to afford another Ni(I) complex **1-Ac**, which reacts with DMMS as a hydride donor to afford the Ni(I)–H complex **1-Ad**. Then, insertion of alkyne occurs to afford alkenyl complex **1-Ae**, which reacts with the alkyl radical generated via the decarboxylation of **1-234** to afford the Ni(III) alkenyl alkyl complex **1-Af**. Then, the insertion of alkenyl moiety into the Ni(III)–alkyl bond occurs, followed by coordination of bromide or acetate, and reductive elimination to afford the alkylated alkenes **1-235** and to recover Ni(I) species **1-Ab**.

Scheme 1-90. Proposed Mechanism for Nickel-catalyzed Hydroalkylation Reactions of Internal Alkynes with NHPI Esters Reported by Lu et al.



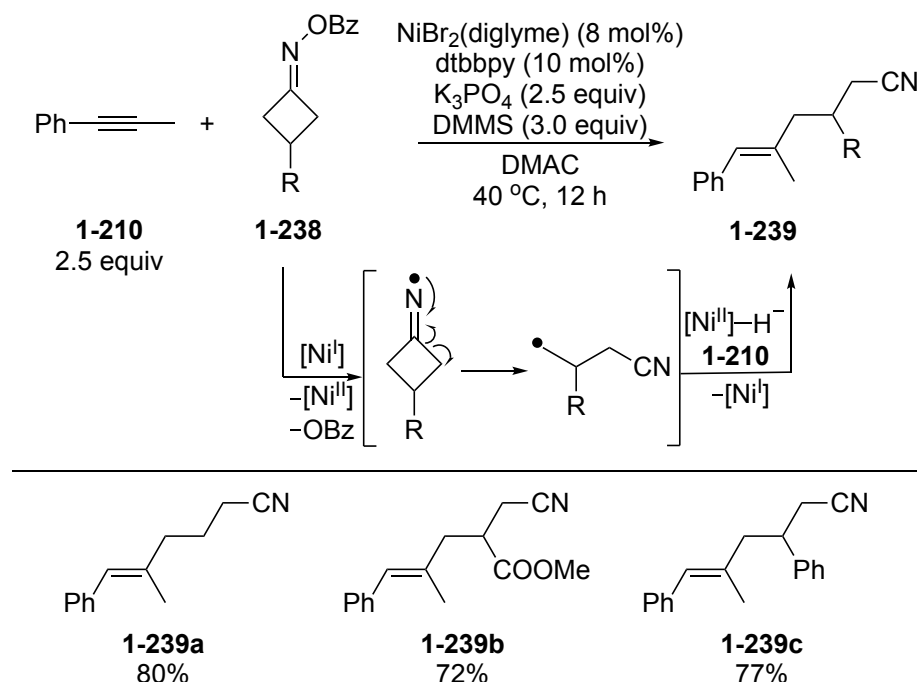
In 2019, Liu et al. reported the nickel-catalyzed hydroalkylation reactions of an internal alkyne with Katritzky salts. Reactions of an internal alkyne **1-210** with Katritzky salts **1-236** in the presence of $[NiBr_2(dme)]$ as a nickel catalyst, dtbbpy as a ligand, K_2CO_3 as a base, and DMMS as a hydride donor in *N,N*-dimethylacetamide (DMA) at room temperature for 6 h afforded the alkylated alkenes **1-237a-c** in good yields (Scheme 1-91).¹¹⁵

Scheme 1-91. Nickel-catalyzed Hydroalkylation Reactions of an Internal Alkyne with Katritzky Salts Reported by Liu et al.



In 2020, Lu et al. reported nickel-catalyzed hydroalkylation reactions of an internal alkyne with cycloketone oxime esters. Reactions of an internal alkyne **1-210** with cycloketone oxime esters **1-238** in the presence of $[\text{NiBr}_2(\text{diglyme})]$ as a nickel catalyst, dtbbpy as a ligand, K_2CO_3 as a base, and DMMS as a hydride source in DMAC at 40 °C for 12 h afforded the ring-opening products **1-239a-c** in good yields (Scheme 1-92).¹¹⁶ In this reaction system, a SET process occurs between the cycloketone oxime esters and the nickel catalyst to afford the iminyl radicals, which undergo β -C-C bond scission to generate cyanoalkyl radicals, which react with the internal alkyne catalyzed by the nickel complex to afford the alkylated alkenes

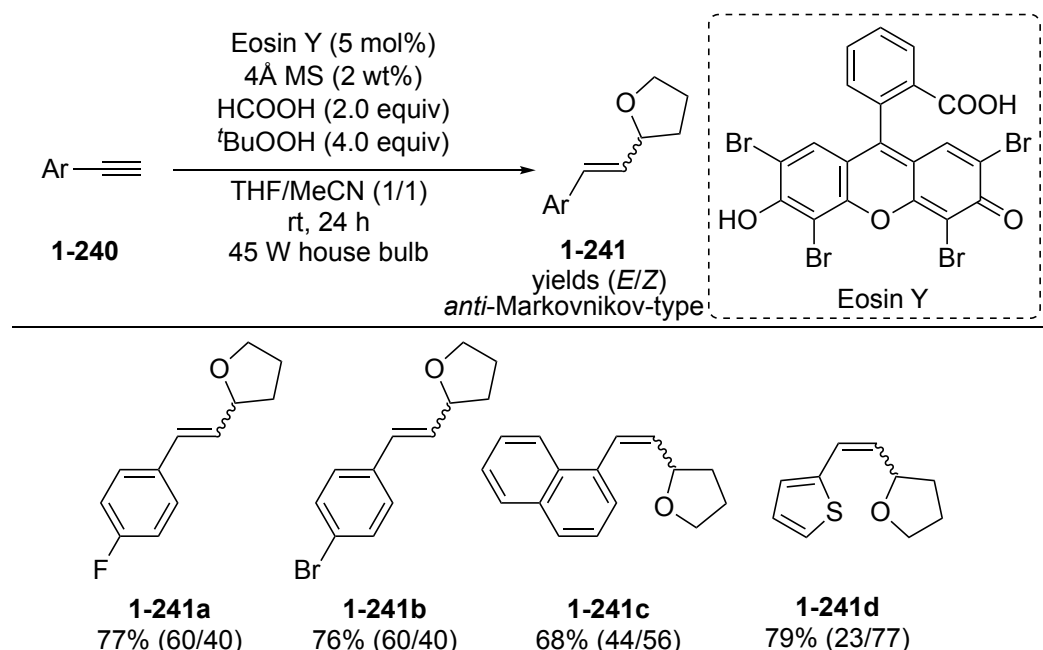
Scheme 1-92. Nickel-catalyzed Hydroalkylation Reactions of an Internal Alkyne with Cycloketone Oxime Esters Reported by Lu et al.



1.5.3. Photoredox-catalyzed Hydroalkylation Reactions of Alkynes

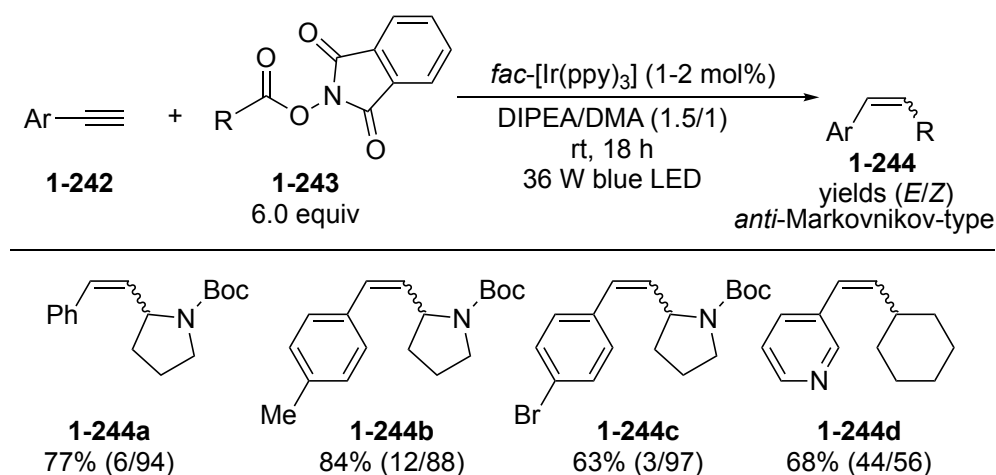
It was as late as in 2015 that the photoredox catalysis was first applied for hydroalkylation reactions of alkynes as reported by the Wang's group. Reactions of terminal alkynes **1-240** with THF in the presence of Eosin Y as a photoredox catalyst with 4 Å molecular sieves as a drying reagent, HCOOH as a proton source, and $t\text{-BuOOH}$ as an oxidant in THF/MeCN under 45 W house bulb irradiation at room temperature for 24 h afforded the *anti*-Markovnikov-type products as an *E/Z* mixture **1-241a-d** in good yields (Scheme 1-93).¹¹⁷

Scheme 1-93. First Photoredox-catalyzed Hydroalkylation Reactions of Terminal Alkynes Reported by Wang et al.



Then, in 2019, Tang et al. reported *anti*-Markovnikov-type *Z*-selective decarboxylative hydroalkylation reactions of alkynes with *N*-hydroxyphthalimide esters. Reactions of terminal alkynes **1-242** with *N*-hydroxyphthalimide esters **1-243** in the presence of *fac*-[Ir(ppy)₃] as a photoredox catalyst in DIPEA/DMA (DIPEA = *N,N*-diisopropylethylamine) as a solvent under 36 W blue LED irradiation at room temperature for 18 h yielded the alkylated alkenes **1-244a-d** in good yields, where *Z*-isomers were major products (Scheme 1-94).¹¹⁸

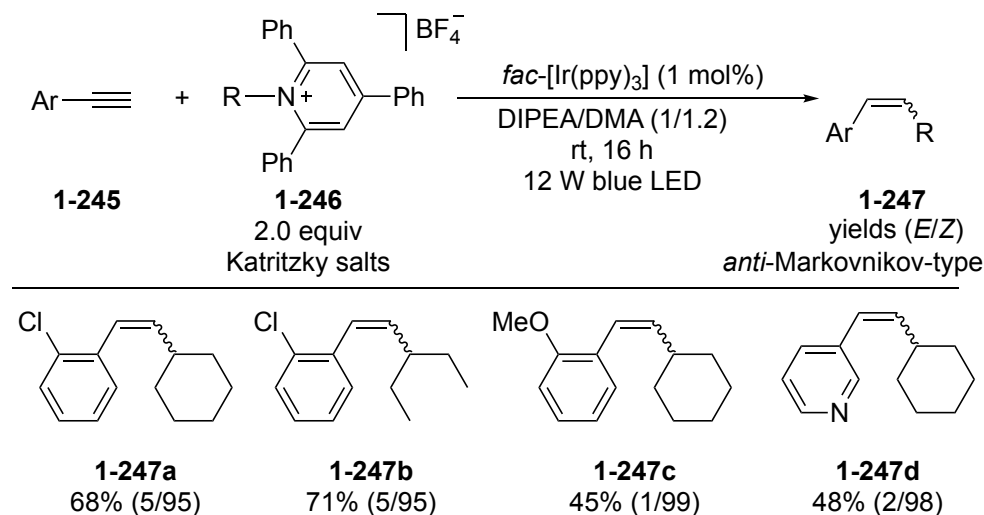
Scheme 1-94. Photoredox-catalyzed *Z*-Selective Hydroalkylation Reactions of Terminal Alkynes with *N*-Hydroxyphthalimide Esters Reported by Tang et al.



In 2020, Luo et al. also reported *anti*-Markovnikov-type *Z*-selective hydroalkylation reactions of terminal alkynes with Katritzky salts. Reactions of

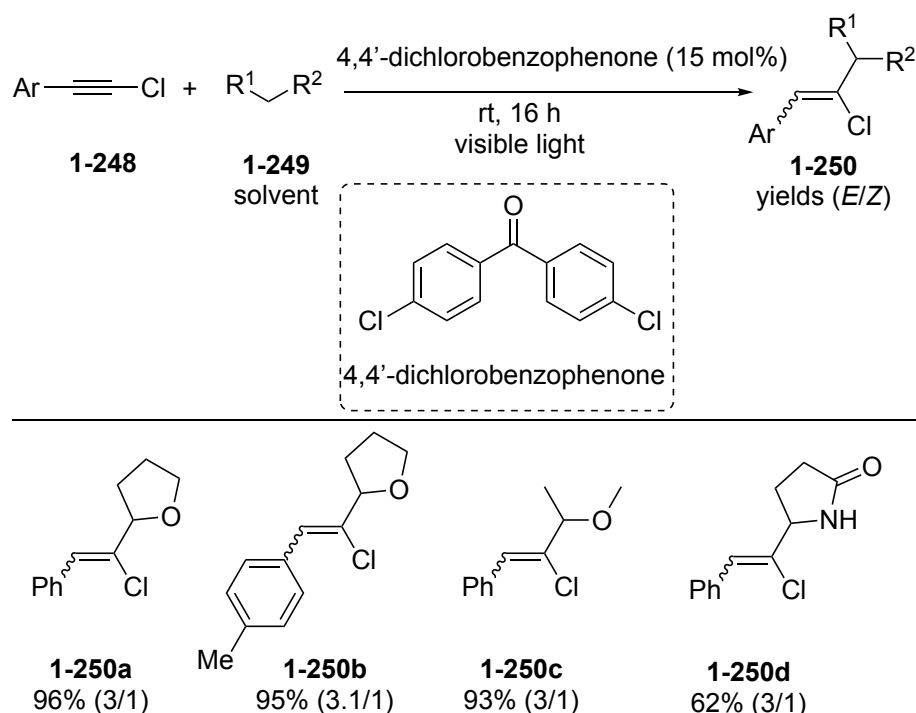
terminal alkynes **1-245** with Katritzky salts **1-246** in the presence of *fac*-[Ir(ppy)₃] as a photoredox catalyst in DIPEA/DMA as a solvent under 12 W blue LED irradiation at room temperature for 16 h afforded the alkylated alkenes **1-247a-d** in moderate to good yields, where *Z*-isomers were major products (Scheme 1-95).¹¹⁹

Scheme 1-95. Photoredox-catalyzed *Z*-selective Hydroalkylation Reactions of Terminal Alkynes with Katritzky Salts Reported by Luo et al.



In 2020, Hashmi et al. reported hydroalkylation reactions of chloroalkynes with ethers or amides. Reactions of chloroalkynes **1-248** with ethers (such as THF, EtOMe) or amides (such as 2-pyrrolidone) **1-249**, which also served as solvents, in the presence of 4,4'-dichlorobenzophenone as an organophotoredox catalyst under visible light irradiation at room temperature for 16 h afforded the alkylated vinyl chlorides **1-250a-d** in high yields (Scheme 1-96).¹²⁰ Here, *E*-isomers were obtained as major products.

Scheme 1-96. Photoredox-catalyzed Hydroalkylation Reactions of Chloroalkynes with Ethers or Amides Reported by Hashmi et al.

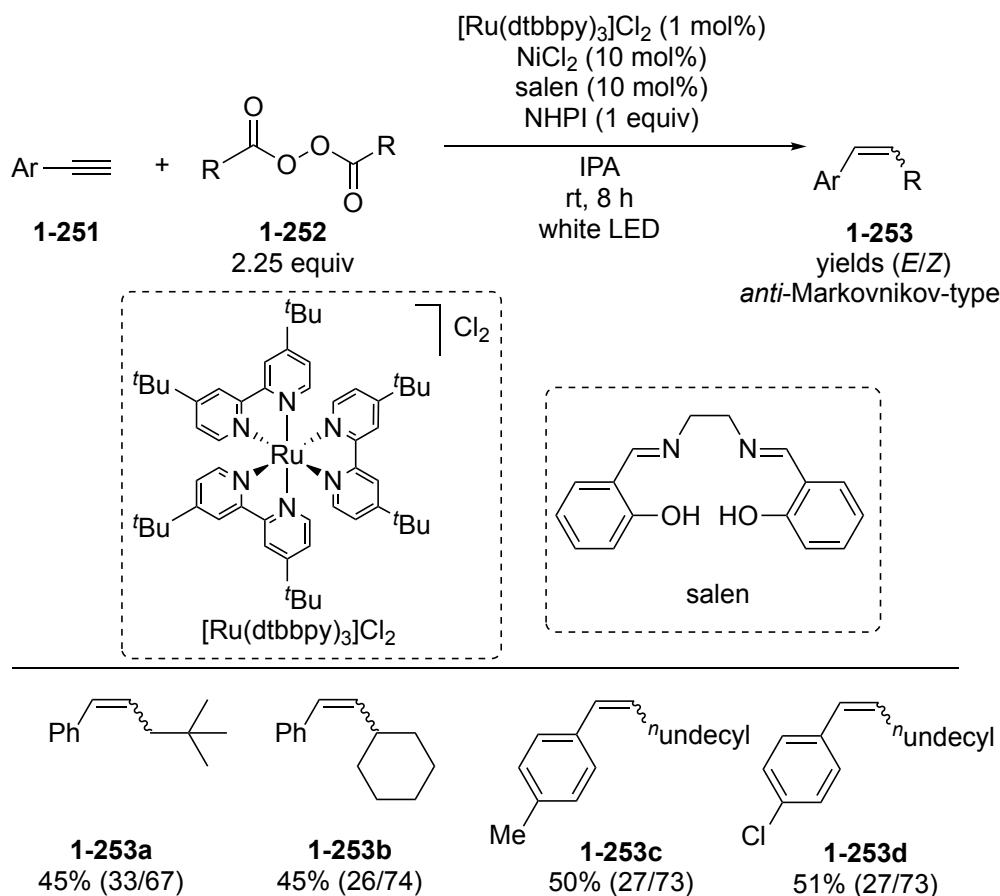


As shown above, several photoredox-catalyzed hydroalkylation reactions of alkynes have been developed under visible light irradiation, although alkylation reagents available for such hydroalkylation reactions are limited to decarboxylative alkylation reagents, Katritzky salt, or those in solvent amounts (such as THF). To expand the availability of alkylation reagents, dual catalytic systems have been developed.

1.5.4. Dual Photoredox/Nickel-catalyzed Hydroalkylation Reactions of Alkynes

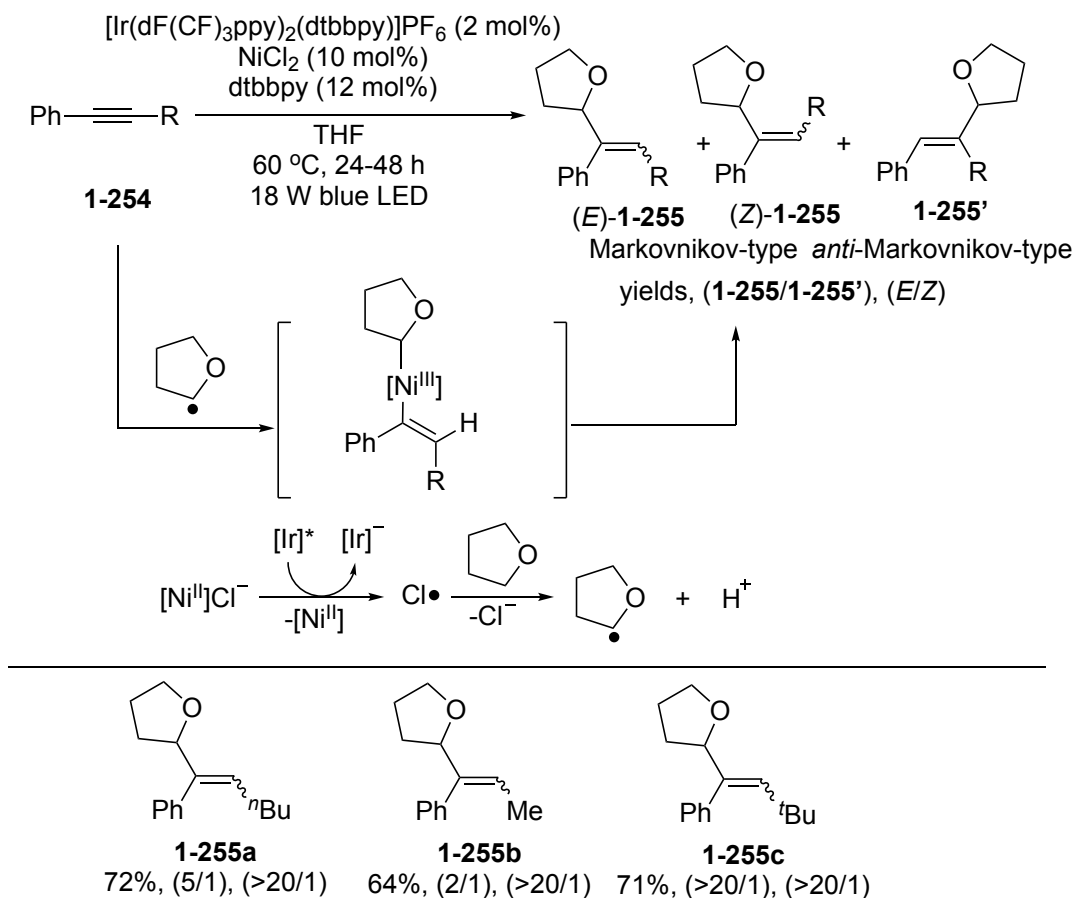
In 2016, Bao et al reported the first example of the dual photoredox/nickel-catalyzed hydroalkylation reactions of terminal alkynes. Reactions of terminal alkynes **1-251** with alkyl diacyl peroxides **1-252** in the presence of $[\text{Ru}(\text{dtbbpy})_3]\text{Cl}_2$ as a photoredox catalyst, NiCl_2 as a nickel catalyst, salen as a ligand, and *N*-hydroxyphthalimide (NHPI) as a reductant in 2-propanol (IPA) under white LED irradiation at room temperature for 8 h afforded the *anti*-Markovnikov-type alkylated alkenes **1-253a-d** in moderate yields (Scheme 1-97).¹²¹ Here, *Z*-isomers were obtained as major products.

Scheme 1-97. First Dual Photoredox/Nickel-catalyzed Hydroalkylation Reactions of Terminal Alkynes with Alkyl Diacyl Peroxides Reported by Bao et al.



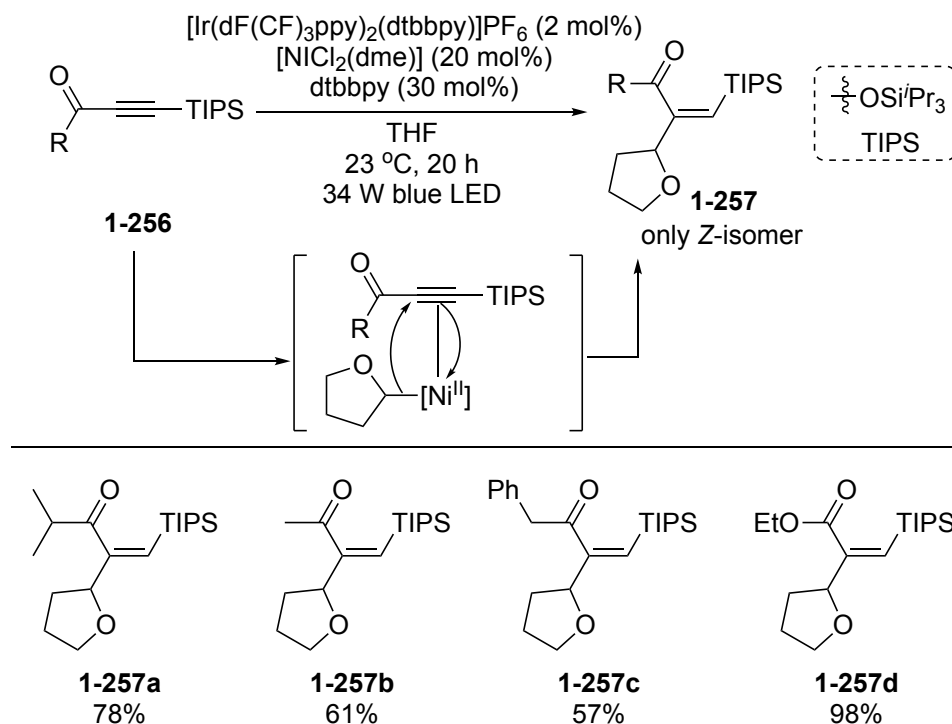
In 2017, Wu et al reported dual photoredox/nickel-catalyzed hydroalkylation reactions of alkynes. Reactions of internal alkynes **1-254** with THF in the presence of $[\text{Ir}(\text{dF}(\text{CF}_3)_3\text{ppy})_2(\text{dtbbpy})]\text{PF}_6$ as a photoredox catalyst, NiCl_2 as a nickel catalyst, and dtbbpy as a ligand in THF under 18 W blue LED irradiation at 60 °C for 24-48 h gave mixtures of alkylated products (*E*)-**1-255a-c**, (*Z*)-**1-255a-c**, where alkylation occurred to the carbon atoms attached to aryl groups, and **1-255'a-c**, where alkylation occurred to the carbon atoms attached to alkyl groups, in good yields (Scheme 1-98).¹²² In this reaction system, the nickel catalyst excited by the iridium photoredox catalyst is proposed to afford chlorine radical (Cl^\bullet), which reacts with a THF molecule to afford the tetrahydrofuran-2-yl radical and a proton, while the observed regioselectivity is complementary to conventional radical addition processes probably because hydrogen transfer to the internal alkynes catalyzed by the nickel complex precedes the addition of tetrahydrofuran-2-yl radical.

Scheme 1-98. Dual Photoredox/Nickel-catalyzed Hydroalkylation Reactions of Internal Alkynes with THF Reported by Wu et al.



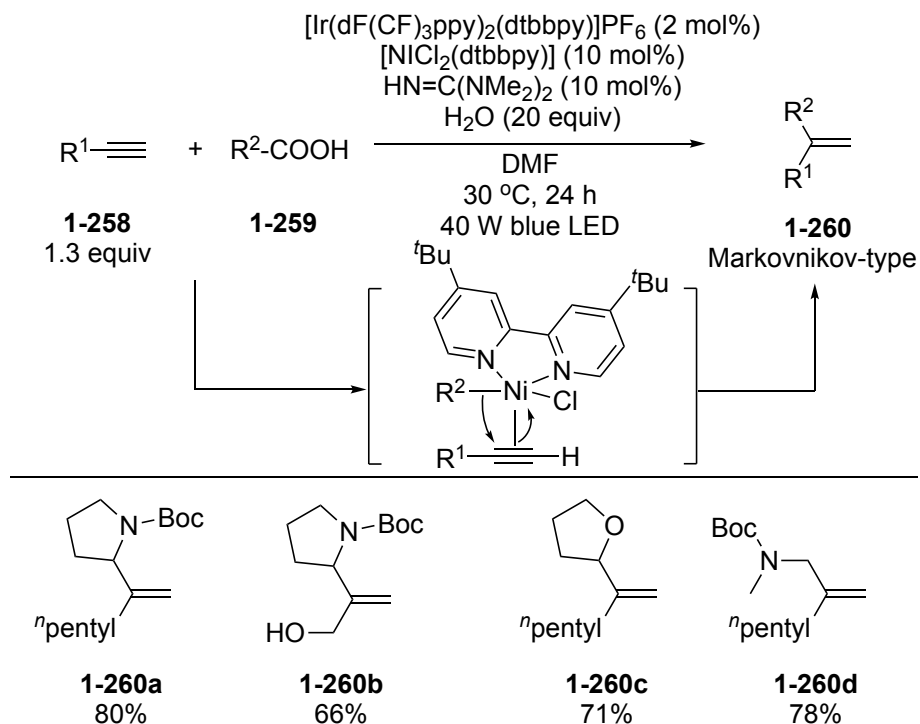
Then, in 2018, Hong et al. reported highly regioselective and *E/Z*-selective hydroalkylation reactions of alkynes. Reactions of internal alkynes **1-256** in the presence of $[\text{Ir}(\text{dF}(\text{CF}_3)\text{ppy})_2(\text{dtbbpy})]\text{PF}_6$ as a photoredox catalyst, $[\text{NiCl}_2(\text{dme})]$ as a nickel catalyst, and dtbbpy as a ligand in THF under 34 W blue LED irradiation at 23 °C for 20 h selectively afforded the *Z*-alkylated alkenes **1-257a-d** in good to high yields (Scheme 1-99).¹²³ In this reaction system, the tetrahydrofuran-2-yl radical is also generated by the dual iridium and nickel-catalyzed system, while the alkylated products are proposed to be formed via the insertion of internal alkynes to the tetrahydrofuran-2-yl–nickel bond.

Scheme 1-99. Dual Photoredox/Nickel-catalyzed Hydroalkylation Reactions of Internal Alkynes with THF Reported by Hong *et al.*



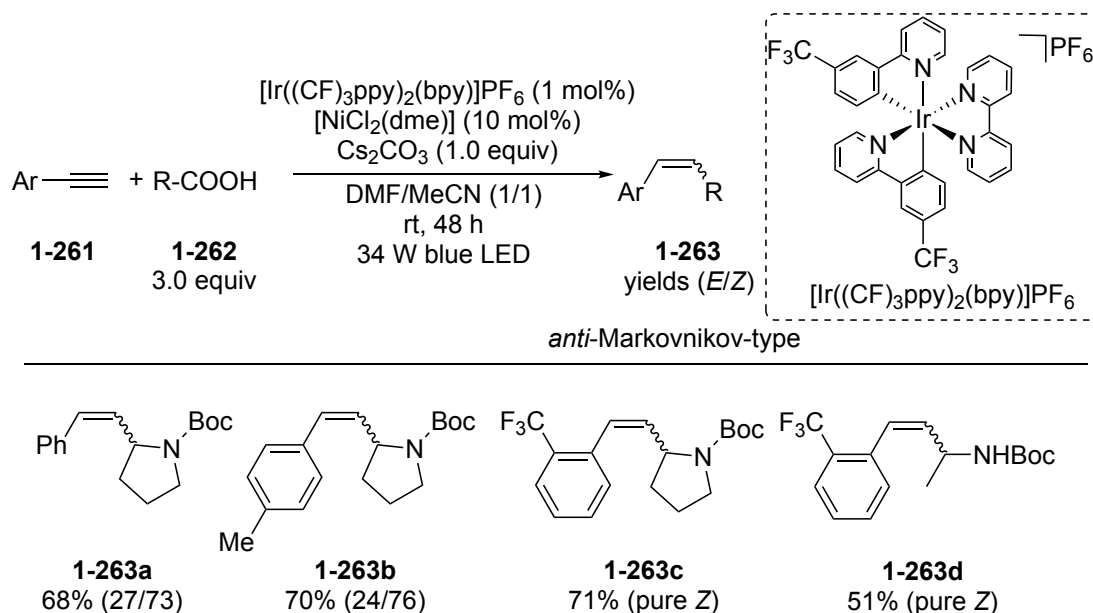
In 2018, MacMillan *et al.* reported Markovnikov-type hydroalkylation reactions of alkynes with alkanecarboxylic acids. Reactions of alkynes **1-258** with alkanecarboxylic acids **1-259** in the presence of $[\text{Ir}(\text{dF}(\text{CF}_3)\text{ppy})_2(\text{dtbbpy})]\text{PF}_6$ as a photoredox catalyst, $[\text{NiCl}_2(\text{dtbbpy})]$ as a nickel catalyst, $\text{HN}=\text{C}(\text{NMe}_2)_2$ (1,1,3,3-tetramethylguanidine) as a base, and H_2O as a proton source in DMF under 40 W blue LED irradiation at $30\text{ }^\circ\text{C}$ for 24 h gave the Markovnikov-type alkylated alkenes **1-260a-d** in good yields (Scheme 1-100).¹²⁴ Here, regioselectivity of the products is likely controlled by the bulkiness of the ligand coordinated to the nickel catalyst.

Scheme 1-100. Dual Photoredox/Nickel-catalyzed Markovnikov-type Hydroalkylation Reactions of Terminal Alkynes with Alkyl carboxylic acids Reported by MacMillan et al.



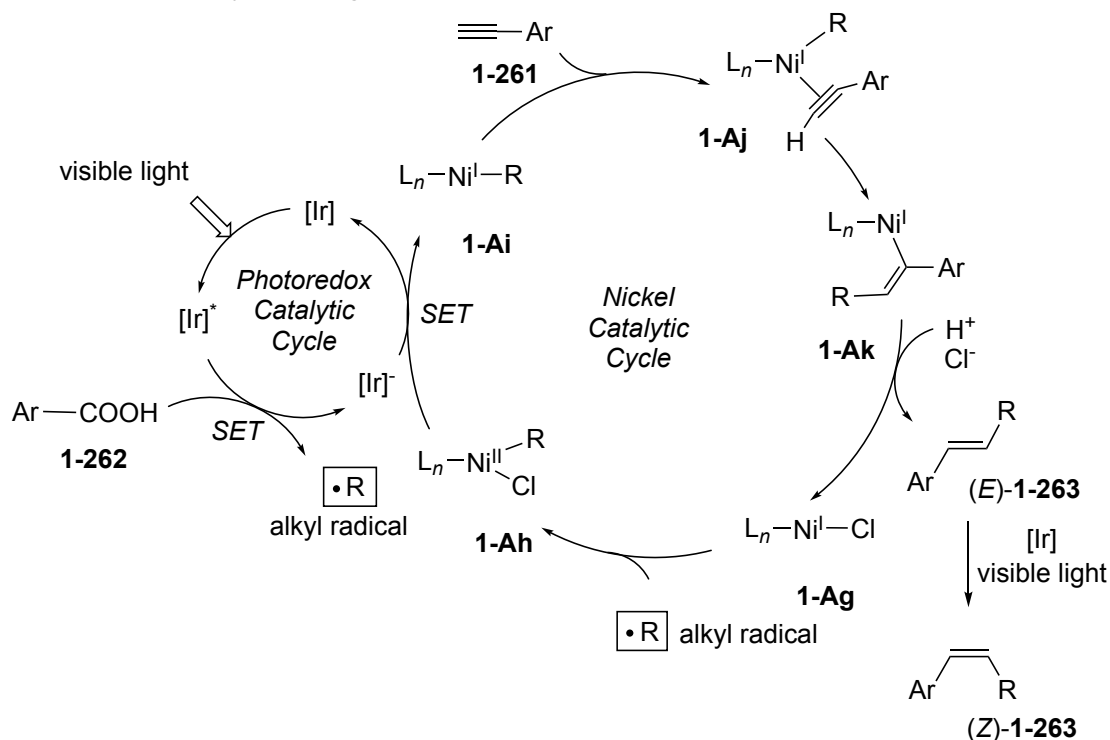
In contrast to MacMillan's result, Rueping et al. reported *anti*-Markovnikov-type hydroalkylation reactions of alkynes with alkanecarboxylic acids in 2020. Reactions of alkynes **1-261** with alkanecarboxylic acids **1-262** in the presence of $[\text{Ir}((\text{CF}_3)\text{ppy})_2(\text{bpy})]\text{PF}_6$ as a photoredox catalyst, $[\text{NiCl}_2(\text{dme})]$ as a nickel catalyst, and Cs_2CO_3 as a base in DMF/MeCN under 34 W blue LED irradiation at room temperature for 48 h gave the *anti*-Markovnikov-type alkylated alkenes **1-263a-d** in good yields, where *Z*-isomers were major products (Scheme 1-101).¹²⁵ Here, regioselectivity of the products is likely controlled by the bulkiness of the ligand coordinated to the nickel catalyst.

Scheme 1-101. Dual Photoredox/Nickel-catalyzed *anti*-Markovnikov-type Hydroalkylation Reactions of Terminal Alkynes with Alkyl Carboxylic Acids Reported by Rueping et al.



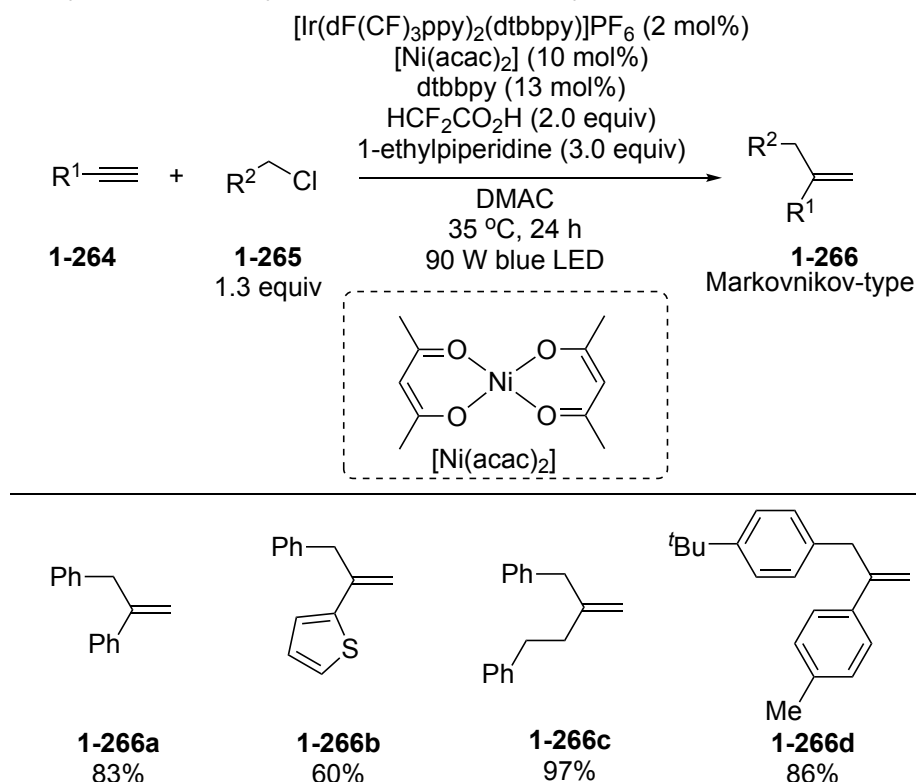
Proposed catalytic reaction pathways of hydroalkylation reactions of alkynes are shown in Schemes 1-102 based on the Rueping's results (Scheme 1-101).¹²⁵ In this case, a single electron transfer (SET) process between the excited photoredox catalyst $[\text{Ir}]^*$ and the alkylation reagent **1-262** affords the reducing Ir(II) species and the alkyl radical. In the nickel catalytic cycle, reaction of Ni(I) halide complex **1-Ag** with the alkyl radical occurs to afford the Ni(II) alkyl complex **1-Ah**, which is reduced by Ir(II) species to afford Ni(I) alkyl complex **1-Ai**. Then coordination of alkyne **1-261** occurs to afford π -alkyne complex **1-Aj**, where insertion of alkyne further occurs to afford *anti*-Markovnikov-type alkylated alkenyl complex **1-Ak**. Further protonation and liberation of the product (*E*)-**1-263** recover Ni(I) halide complex **1-Ag**. Here, *E*-isomers are rather obtained as major products. However, if the alkenes contain aryl groups as substituents, further *E* to *Z* isomerization is known to occur via energy transfer process with visible light.¹²⁶ This can be one of the main reasons why the products in Schemes 1-93, 1-94, 1-95, 1-96, 1-97, 1-98, and 1-101 become mixtures of *E/Z* isomers.

Scheme 1-102. Proposed Mechanism for Dual Photoredox/Nickel-catalyzed *anti*-Markovnikov-type Hydroalkylation Reactions of Terminal Alkynes with Alkyl Carboxylic Acids Reported by Rueping et al.



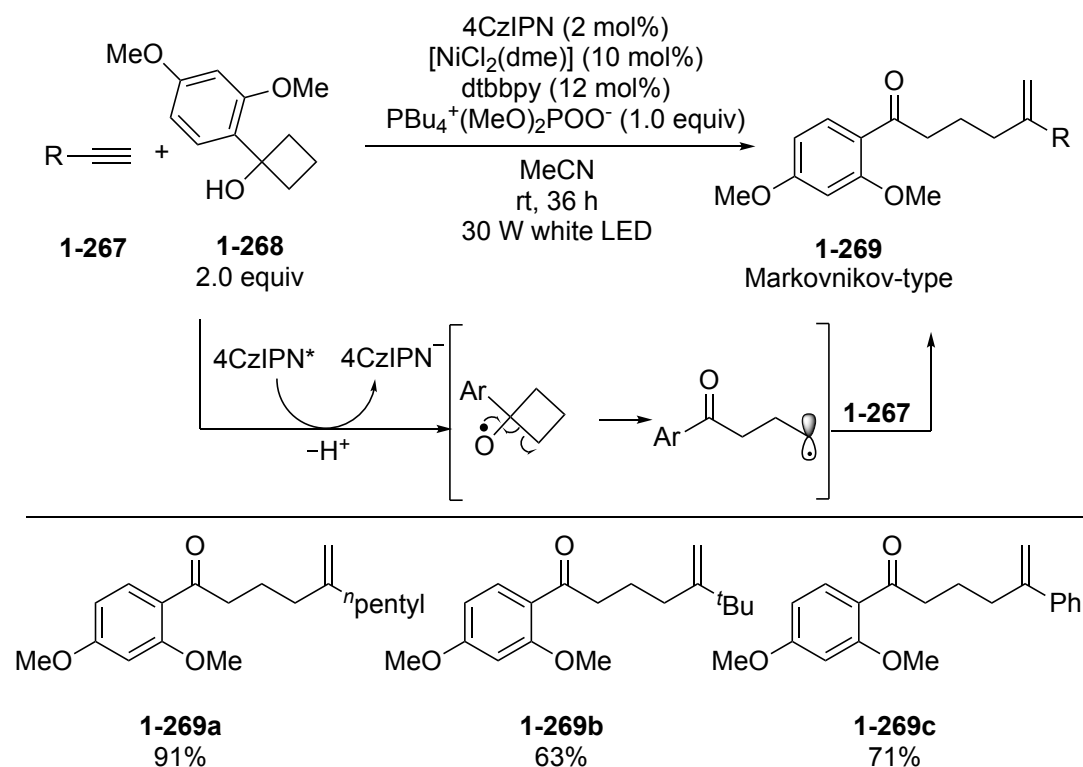
Then, in 2021, Chu et al. reported Markovnikov-type hydroalkylation reactions of alkynes with benzyl chlorides. Reactions of alkynes **1-264** with benzyl chlorides **1-265** in the presence of 2 [Ir(dF(CF)₃ppy)₂(dtbbpy)]PF₆ as a photoredox catalyst, [Ni(acac)₂] as a nickel catalyst, dtbbpy as a ligand, HCF₂CO₂H as a proton source, and 1-ethylpiperidine as a reductant in DMAC under 90 W blue LED irradiation at 35 °C for 24 h gave the Markovnikov-type alkylated alkenes **1-266a-d** in good to high yields (Scheme 1-103).¹²⁷

Scheme 1-103. Dual Photoredox/Nickel-catalyzed Hydroalkylation Reactions of Terminal Alkynes with Benzyl Chlorides Reported by Chu et al.



Also in 2020, Xu, et al. reported Markovnikov-type hydroalkylation reactions of alkynes with 1-(2,4-dimethoxyphenyl)cyclobutan-1-ol via C-C bond cleavage. Reactions of alkynes **1-267** with 1-(2,4-dimethoxyphenyl)cyclobutan-1-ol **1-268** in the presence of 4CzIPN as a photoredox catalyst, $[\text{NiCl}_2(\text{dme})]$ as a nickel catalyst, dtbbpy as a ligand, and $\text{PBu}_4^+(\text{MeO})_2\text{POO}^-$ as a base in MeCN under 30 W white LED irradiation at room temperature for 36 h afforded the Markovnikov-type alkylated alkenes **1-269a-c** in good to high yields (Scheme 1-104).¹²⁸ In this reaction system, the photoexcited 4CzIPN* oxidizes alkynols **1-268** to generate alkoxy radicals, followed by the $\beta\text{-C—C}$ bond scission to produce ring-opened alkyl radicals, which participate in the alkylation of alkynes catalyzed by the nickel complex.

Scheme 1-104. Dual Photoredox/Nickel-catalyzed Hydroalkylation Reactions of Terminal Alkynes with 1-(2,4-Dimethoxyphenyl)cyclobutan-1-ol Reported by Xu et al.



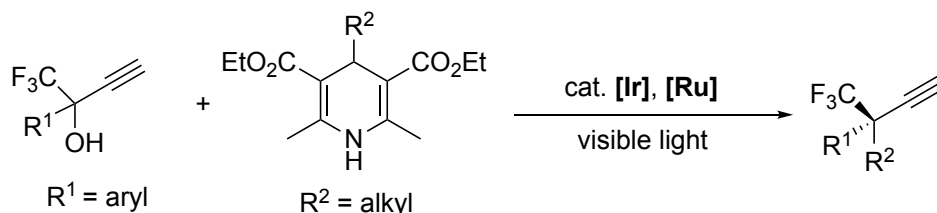
As summarized above, the regioselectivity between Markovnikov-type and *anti*-Markovnikov-type hydroalkylation of terminal alkynes was shown to be quite controllable, especially by using nickel catalyst in combination with bulkiness of the ligands. Use of photoredox and nickel catalysts could also slightly expand the availability of alkylation reagents.

1.6. Perspective for Following Chapters in This Thesis

In order to expand the scope of the previous investigations on the transition metal-catalyzed enantioselective propargylic substitution reactions and photoredox-catalyzed alkylation reactions with 4-alkyl-1,4-dihydropyridines, the author of this thesis has investigated the dual photoredox- and transition metal-catalyzed alkylation of alkynes with 4-alkyl-1,4-dihydropyridines. In the subsequent Chapters, the author describes the following research topics: (1) photoredox- and ruthenium-catalyzed enantioselective propargylic alkylation of propargylic alcohols with 4-alkyl-1,4-dihydropyridines; (2) photoredox- and nickel-catalyzed hydroalkylation of alkynes with 4-alkyl-1,4-dihydropyridines: ligand-controlled regioselectivity; (3) photoredox- and nickel-catalyzed alkylative cyclization reactions of 6-iodohexynes with 4-alkyl-1,4-dihydropyridines.

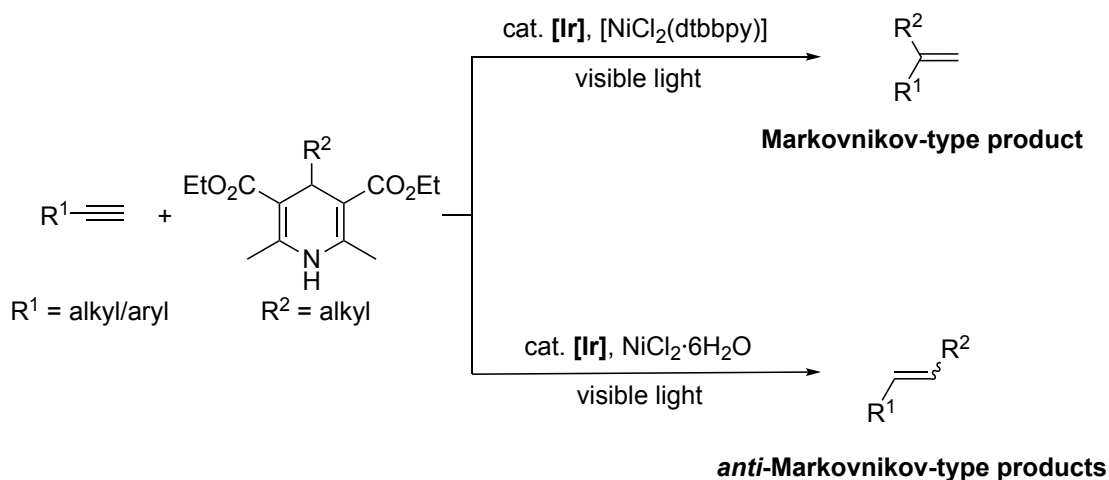
In Chapter 2, the author established the enantioselective photoredox- and ruthenium-catalyzed propargylic alkylation of propargylic alcohols with 4-alkyl-1,4-dihydropyridines ([Scheme 1-105](#)). This is the first successful example of photoredox- and ruthenium-catalyzed enantioselective propargylic alkylation reactions, where alkyl radicals as alkylation reagents are generated from 4-alkyl-1,4-dihydropyridines under photoredox reaction conditions, providing a new strategy to the chemistry of enantioselective propargylic substitution reactions.

Scheme 1-105. Photoredox- and Ruthenium-catalyzed Enantioselective Propargylic Alkylation of Propargylic Alcohols with 4-Alkyl-1,4-dihydropyridines



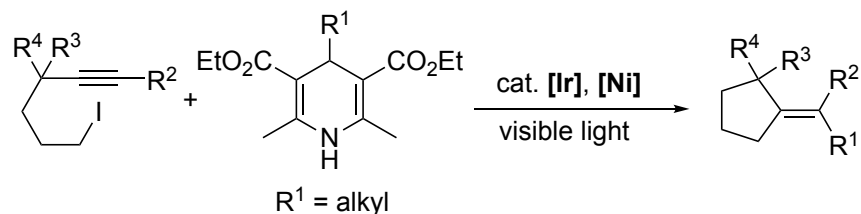
In Chapter 3, the author has developed the cooperative photoredox- and nickel-catalyzed hydroalkylation of alkylacetylenes or arylacetylenes with 4-alkyl-1,4-dihydropyridines to afford Markovnikov- or *anti*-Markovnikov-type alkylated alkenes, where the regioselectivity is controlled by the difference in coordination ligands for nickel complexes ([Scheme 1-106](#)). In all cases, the regioselectivity was simply controlled by the choice of coordination ligands bound to nickel species, providing a new strategy in the preparation of regioselective functionalized alkenes from alkynes.

Scheme 1-106. Photoredox- and Nickel-catalyzed Hydroalkylation of Alkynes with 4-Alkyl-1,4-dihydropyridines



In Chapter 4, the author has developed the alkylative cyclization reactions of 6-iodohex-1-yne with 4-alkyl-1,4-dihydropyridines in the presence of photoredox and nickel dual catalysts ([Scheme 1-107](#)). The reaction system provides a novel synthetic method for alkylative cyclization reactions of both terminal and internal alkynes with cooperative photoredox and nickel catalysis.

Scheme 1-107. Photoredox- and Nickel-catalyzed Alkylative Cyclization Reactions of 6-Iodohex-1-yne with 4-Alkyl-1,4-dihydropyridines



Overall in this thesis, a series of dual photoredox- and transition metal-catalyzed alkylation of alkynes with 4-alkyl-1,4-dihydropyridines has been successfully developed, and has clarified that alkyl radicals generated from 4-alkyl-1,4-dihydropyridines act as alkylation reagents that can be treated with various alkyne substrates under rather mild reaction conditions.

1.7. References

- (1) Smith, M. B.; March, J. *Advanced Organic Chemistry: Reactions, Mechanisms, and Structure* (6th ed.), **2007**, New York: Wiley-Interscience,
- (2) Rappoport, E. Z.; Marek, I. *The Chemistry of Organozinc Compounds* (Patai Series: The Chemistry of Functional Groups), **2006**, John Wiley & Sons: Chichester, UK.
- (3) Zabicky, J. "Analytical aspects of organolithium compounds". *PATAI'S Chemistry of Functional Groups*. **2009**, John Wiley & Sons, Ltd.
- (4) Grimes, R. N. *Carboranes*, (3rd ed.), **2016**, New York: Academic Press.
- (5) Kiso, Y.; Yamamoto, K.; Tamao, K. Kumada. M. *J. Am. Chem. Soc.* **1972**, *94*, 4374–4376.
- (6) King, A. O.; Okukado, N.; Negishi, E. *J. Chem. Soc., Chem. Commun.* **1977**, 683–684.
- (7) Murahashi, S. Yamamura, M.; Yanagisawa, K.; Mita, N.; Kondo, K. *J. Org. Chem.* **1979**, *44*, 2408–2417.
- (8) Miyaura, N.; Suzuki, A. *J. Chem. Soc., Chem. Commun.* **1979**, 866–867.
- (9) Shaw, M. H.; Twilton, J.; MacMillan, D. W. C. *J. Org. Chem.* **2016**, *81*, 6898–6926.
- (10) (a) Narayanam, J. M. R.; Stephenson, C. R. *J. Chem. Soc. Rev.* **2011**, *40*, 102–113. (b) Ischay, M. A.; Yoon, T. P. *Eur. J. Org. Chem.* **2012**, *2012*, 3359–3372. (c) Xuan, J.; Xiao, W.-J. *Angew. Chem., Int. Ed.* **2012**, *51*, 6828–6838. (d) Prier, C. K.; Rankic, D. A.; MacMillan, D. W. C. *Chem. Rev.* **2013**, *113*, 5322–5363. (e) Xi, Y.; Yi, H.; Lei, A. *Org. Biomol. Chem.* **2013**, *11*, 2387–2403. (f) Koike, T.; Akita, M. *Inorg. Chem. Front.* **2014**, *1*, 562–576. (g) Romero, N. A.; Nicewicz, D. A. *Chem. Rev.* **2016**, *116*, 10075–10166.
- (11) Condie, A.; Gonzalez-Gomez, J. C.; Stephenson, C. R. *J. Am. Chem. Soc.* **2010**, *132*, 1464–1465.
- (12) Wang, P.-Z.; Chen, J.-R.; Xiao, W.-J. *Org. Biomol. Chem.* **2019**, *17*, 6936–6951.
- (13) Fu, G. C. *ACS Cent. Sci.* **2017**, *3*, 692–700.
- (14) Hantzsch, A. *Ber. Dtsch. Chem. Ges.* **1881**, *14*, 1637–1638.
- (15) (a) Stout, D. M.; Meyers, A. I. *Chem. Rev.* **1982**, *82*, 223–243. (b) Lavilla, R. *J. Chem. Soc., Perkin Trans. I.* **2002**, 1141–1156.; (c) Zheng, C.; You, S. L. *Chem. Soc. Rev.* **2012**, *41*, 2498–2518.
- (16) Prier, C. K.; Rankic, D. A.; MacMillan, D. W. C. *Chem. Rev.* **2013**, *113*, 5322–5363.
- (17) Fukuzumi, S.; Suenobu, T.; Patz, M.; Hirasaka, T.; Itoh, S.; Fujitsuka, M.; Ito, O. *J. Am. Chem. Soc.* **1998**, *120*, 8060–8068.
- (18) Nakajima, K.; Nojima, S.; Sakata K.; Nishibayashi, Y. *ChemCatChem* **2016**, *8*, 1028–1032.
- (19) Chen, W.; Liu, Z.; Tian, J.; Li, J.; Ma, J.; Cheng, X.; Li, G. *J. Am. Chem. Soc.* **2016**, *138*, 12312–12315.
- (20) Zhang, H.-H.; Yu, S. *J. Org. Chem.* **2017**, *82*, 9995–10006.
- (21) Gu, F.; Huang, W.; Liu, X.; Chen, W.; Cheng, X. *Adv. Synth. Catal.* **2018**, *360*, 925–931.
- (22) de Assis, F. F.; Huang, X.; Akiyama, M.; Pilli, R. A.; Meggers, E. *J. Org. Chem.* **2018**, *83*, 10922–10932.

- (23) Wu, Q.-Y.; Min, Q.-Q.; Ao, G.-Z.; Liu, F. *Org. Biomol. Chem.* **2018**, *16*, 6391–6394.
- (24) Milligan, J. A.; Phelan, J. P.; Polites, V. C.; Kelly, C. B.; Molander, G. A. *Org. Lett.* **2018**, *20*, 6840–6844.
- (25) Song, Z. Y.; Zhang, C. L.; Ye, S. *Org. Biomol. Chem.* **2019**, *17*, 181–185.
- (26) Wang, Z.-J.; Zheng, S.; Matsui, J. K.; Lu Z.; Molander, G. A. *Chem. Sci.* **2019**, *10*, 4389–4393.
- (27) Chen, H.; Anand, D.; Zhou, L. *Asian J. Org. Chem.* **2019**, *8*, 661–664.
- (28) Du, H.-W.; Sun, J.; Gao, Q.-S.; Wang, J.-Y.; Wang, H.; Xu, Z.; Zhou, M.-D. *Org. Lett.* **2020**, *22*, 1542–1546.
- (29) Angnes, R. A.; Potnis, C.; Liang, S.; Correia, C. R. D.; Hammond, G. B. *J. Org. Chem.* **2020**, *85*, 4153–4164.
- (30) Guo, Q.; Peng, Q.; Chai, H.; Huo, Y.; Wang, S.; Xu, Z. *Nat. Commun.* **2020**, *11*, 1463.
- (31) Nakajima, K.; Nojima, S.; Nishibayashi, Y. *Angew. Chem. Int. Ed.* **2016**, *55*, 14106–14110.
- (32) Gutiérrez-Bonet, Á.; Tellis, J. C.; Matsui, J. K.; Vara, B. A.; Molander, G. A. *ACS Catal.* **2016**, *6*, 8004–8008.
- (33) Badir, S. O.; Dumoulin, A.; Matsui, J. K.; Molander, G. A. *Angew. Chem. Int. Ed.* **2018**, *57*, 6610–6613.
- (34) Dumoulin, A.; Matsui, J. K.; Gutiérrez-Bonet, Á.; Molander, G. A. *Angew. Chem. Int. Ed.* **2018**, *57*, 6614–6618.
- (35) (a) Matsui, J. K.; Gutiérrez-Bonet, Á.; Rotella, M.; Alam, R.; Gutierrez, O.; Molander, G. A. *Angew. Chem. Int. Ed.* **2018**, *57*, 15847–15851. (b) Tsuji, J.; Takahashi, H.; Morikawa, M. *Tetrahedron Lett.* **1965**, *6*, 4387–4388. (c) Trost, B. M.; Fullerton, T. *J. J. Am. Chem. Soc.* **1973**, *95*, 292–294.
- (36) Nakajima, K.; Guo, X.; Nishibayashi, Y. *Chem. Asian J.* **2018**, *13*, 3653–3657.
- (37) Phelan, J. P.; Lang, S. B.; Sim, J.; Berritt, S.; Peat, A. J.; Billings, K.; Fan, L.; Molander, G. A. *J. Am. Chem. Soc.* **2019**, *141*, 3723–3732.
- (38) Zhou, Z.-Z.; Song, X.-R.; Du, Sha.; Xia, K.-J.; Tian, W.-F.; Xiao, Q.; Liang, Y.-M. *Chem. Commun.* **2021**, *57*, 9390–9393.
- (39) (a) Trost, B. M.; Dietsch, T. J. New Synthetic Reactions. Asymmetric Induction in Allylic Alkylations. *J. Am. Chem. Soc.* **1973**, *95*, 8200–8201. (b) Zhang, H.-H.; Zhao, J.-J.; Yu, S. *J. Am. Chem. Soc.* **2018**, *140*, 16914–16919.
- (40) Zhou, Z.-Z.; Jiao, R.-Q.; Yang, K.; Chen, X.-M.; Liang, Y.-M. *Chem. Commun.* **2020**, *56*, 12957–12960.
- (41) (a) Schwarz, J. L.; Huang, H.-M.; Paulisch, T. O.; Glorius, F. *ACS Catal.* **2020**, *10*, 1621–1627. (b) Huang, H.-M.; Bellotti, P.; Glorius, F. *Chem. Soc. Rev.* **2020**, *49*, 6186–6197.
- (42) Huang, H.-M.; Bellotti, P.; Daniliuc, C. G.; Glorius, F. *Angew. Chem., Int. Ed.* **2021**, *60*, 2464–2471.
- (43) (a) Miyake, Y.; Uemura, S.; Nishibayashi, Y. *ChemCatChem* **2009**, *1*, 342–356. (b) Ding, C.-H.; Hou, X.-L. *Chem. Rev.* **2011**, *111*, 1914–1937. (c) Nishibayashi, Y. *Synthesis* **2012**, *44*, 489–503. (d) Zhang, D.-Y.; Hu, X.-P. *Tetrahedron Lett.* **2015**, *56*,

- 283–295. (e) Sakata, K.; Nishibayashi, Y. *Catal. Sci. Technol.* **2018**, *8*, 12–25. (f) Roh, S. W.; Choi, K.; Lee, C. *Chem. Rev.* **2019**, *119*, 4293–4356. (g) Tsuji, H.; Kawatsura, M. *Asian J. Org. Chem.* **2020**, *9*, 1924 – 1941. (h) Nishibayashi, Y. *Chem. Lett.* **2021**, *50*, 1282–1288.
- (44) Nicholas, K. M. *Acc. Chem. Res.* **1987**, *20*, 207–214.
- (45) Imada, Y.; Yuasa, M.; Nakamura, I.; Murahashi, S.-I. *J. Org. Chem.* **1994**, *59*, 2282–2284.
- (46) Godfrey, J. D., Jr.; Mueller, R. H.; Sedergran, T. C.; Soundararajan, N.; Colandrea, V. J. *Tetrahedron Lett.* **1994**, *35*, 6405–6408.
- (47) Nishibayashi, Y.; Wakiji, I.; Hidai, M. *J. Am. Chem. Soc.* **2000**, *122*, 11019–11020.
- (48) (a) Nishibayashi, Y.; Wakiji, I.; Ishii, Y.; Uemura, S.; Hidai, M. *J. Am. Chem. Soc.* **2001**, *123*, 3393–3394. (b) Nishibayashi, Y.; Yoshikawa, M.; Inada, Y.; Hidai, M.; Uemura, S. *J. Am. Chem. Soc.* **2002**, *124*, 11846–11847. (c) Nishibayashi, Y.; Onodera, G.; Inada, Y.; Hidai, M.; Uemura, S. *Organometallics* **2003**, *22*, 873–876. (d) Nishibayashi, Y.; Yoshikawa, M.; Inada, Y.; Milton, M. D.; Hidai, M.; Uemura, S. *Angew. Chem. Int. Ed.* **2003**, *42*, 2681–2684. (e) Nishibayashi, Y.; Inada, Y.; Hidai, M.; Uemura, S. *J. Am. Chem. Soc.* **2003**, *125*, 6060–6061. (f) Nishibayashi, Y.; Imajima, H.; Onodera, G.; Hidai, M.; Uemura, S. *Organometallics* **2004**, *23*, 26–30. (g) Nishibayashi, Y.; Yoshikawa, M.; Inada, Y.; Hidai, M.; Uemura, S. *J. Org. Chem.* **2004**, *69*, 3408–3412. (h) Nishibayashi, Y.; Imajima, H.; Onodera, G.; Inada, Y.; Hidai, M.; Uemura, S. *Organometallics* **2004**, *23*, 5100–5103.
- (49) (a) Inada, Y.; Nishibayashi, Y.; Hidai, M.; Uemura, S. *J. Am. Chem. Soc.* **2002**, *124*, 15172–15173. (b) Nishibayashi, Y.; Milton, M. D.; Inada, Y.; Yoshikawa, M.; Wakiji, I.; Hidai, M.; Uemura, S. *Chem. Eur. J.* **2005**, *11*, 1433–1451.
- (50) Ding, H.; Sakata, K.; Kuriyama, S.; Nishibayashi, Y. *Organometallics* **2020**, *39*, 2130–2134.
- (51) Ammal, S. C.; Yoshikai, N.; Inada, Y.; Nishibayashi, Y.; Nakamura, E. *J. Am. Chem. Soc.* **2005**, *127*, 9428–9438.
- (52) Gawley, R. E.; Aube, J. *Principles of Asymmetric Synthesis*; Elsevier Science: Oxford, 1996.
- (53) Efavirenz: FDA-Approved Drugs. U.S. Food and Drug Administration (FDA). Retrieved 25 April 2020.
- (54) Inada, Y.; Nishibayashi, Y.; Uemura, S. *Angew. Chem., Int. Ed.* **2005**, *44*, 7715–7717.
- (55) Matsuzawa, H.; Miyake, Y.; Nishibayashi, Y. *Angew. Chem., Int. Ed.* **2007**, *46*, 6488–6491.
- (56) Matsuzawa, H.; Kanao, K.; Miyake, Y.; Nishibayashi, Y. *Org. Lett.* **2007**, *9*, 5561–5564.
- (57) Fukamizu, K.; Miyake, Y.; Nishibayashi, Y. *J. Am. Chem. Soc.* **2008**, *130*, 10498–10499.
- (58) Kanao, K.; Miyake, Y.; Nishibayashi, Y. *Organometallics* **2009**, *28*, 2920–2926.
- (59) Kanao, K.; Miyake, Y.; Nishibayashi, Y. *Organometallics* **2010**, *29*, 2126–2131.
- (60) (a) Kanao, K.; Tanabe, Y.; Miyake, Y.; Nishibayashi, Y. *Organometallics* **2010**, *29*, 2381–2384. (b) Sakata, K.; Goto, Y.; Nishibayashi, Y. *Chem. Asian J.* **2021**, *16*, 3760–

3766.

- (61) Liu, S.; Tanabe, Y.; Kuriyama, S.; Sakata, K.; Nishibayashi, Y. *Angew. Chem. Int. Ed.* **2021**, *60*, 11231–11236.
- (62) (a) Hattori, G.; Matsuzawa, H.; Miyake, Y.; Nishibayashi, Y. *Angew. Chem. Int. Ed.* **2008**, *47*, 3781–3783. (b) Detz, R. J.; Delville, M. M. E.; Hiemstra, H.; van Maarseveen, J. H. *Angew. Chem. Int. Ed.* **2008**, *47*, 3777–3780.
- (63) (a) Zhang, D.-Y.; Hu, X.-P. *Tetrahedron Lett.* **2015**, *56*, 283–295. (b) Roh, S. W.; Choi, K.; Lee, C. *Chem. Rev.* **2019**, *119*, 4293–4356.
- (64) Fang, P.; Hou, X.-L. *Org. Lett.* **2009**, *11*, 4612–4615.
- (65) Wang, B.; Liu, C.; Guo, H. *RSC Adv.* **2014**, *4*, 53216–53219.
- (66) Zhu, F.-L.; Zou, Y.; Zhang, D.-Y.; Wang, Y.-H.; Hu, X.-H.; Chen, S.; Xu, J.; Hu, X.-P. *Angew. Chem. Int. Ed.* **2014**, *53*, 1410–1414.
- (67) Zhu, F.-L.; Wang, Y.-H.; Zhang, D.-Y.; Hu, X.-H.; Chen, S.; Hou, C.-J.; Xu, J.; Hu, X.-P. *Adv. Synth. Catal.* **2014**, *356*, 3231–3236.
- (68) Zhang, D.-Y.; Zhu, F.-L.; Wang, Y.-H.; Hu, X.-H.; Chen, S.; Hou, C.-J.; Hu, X.-P. *Chem. Commun.* **2014**, *50*, 14459–14462.
- (69) Han, F.-Z.; Zhu, F.-L.; Wang, Y.-H.; Zou, Y.; Hu, X.-H.; Chen, S.; Hu, X.-P. *Org. Lett.* **2014**, *16*, 588–591.
- (70) Zhao, L.; Huang, G.; Guo, B.; Xu, L.; Chen, J.; Cao, W.; Zhao, G.; Wu, X. *Org. Lett.* **2014**, *16*, 5584–5587.
- (71) Xia, J.-T.; Hu, X.-P. *Org. Lett.* **2020**, *22*, 1102–1107.
- (72) Huang, G.; Cheng, C.; Ge, L.; Guo, B.; Zhao, L.; Wu, X. *Org. Lett.* **2015**, *17*, 4894–4897.
- (73) Shao, W.; Li, H.; Liu, C.; Liu, C.-J.; You, S.-L. *Angew. Chem. Int. Ed.* **2015**, *54*, 7684–7687.
- (74) Zhang, C.; Hui, Y.-Z.; Zhang, D.-Y.; Hu, X.-P. *RSC Adv.* **2016**, *6*, 14763–14767.
- (75) Zhang, K.; Lu, L.-Q.; Yao, S.; Chen, J.-R.; Shi, D.-Q.; Xiao, W.-J. *J. Am. Chem. Soc.* **2017**, *139*, 12847–12854.
- (76) Shao, L.; Hu, X.-P. *Chem. Commun.* **2017**, *53*, 8192–8195.
- (77) Gao, X.; Cheng, R.; Xiao, Y.-L.; Wan, X.-L.; Zhang, X. *Chem* **2019**, *5*, 2987–2999.
- (78) (a) Detz, R. J.; Abiri, Z.; le Griel, R.; Hiemstra, H.; van Maarseveen, J. H. *Chem.–Eur. J.* **2011**, *17*, 5921–5930. (b) Tsuchida, K.; Senda, Y.; Nakajima, K.; Nishibayashi, Y. *Angew. Chem. Int. Ed.* **2016**, *55*, 9728–9732. (c) Yang, L.; Pu, X.; Niu, D.; Fu, Z.; Zhang, X. *Org. Lett.* **2019**, *21*, 8553–8557. (d) Shao, L.; Hu, X.-P. *Org. Biomol. Chem.* **2017**, *15*, 9837–9844.
- (79) (a) Wang, Q.; Li, T.-R.; Lu, L.-Q.; Li, M.-M.; Zhang, K.; Xiao, W.-J. *J. Am. Chem. Soc.* **2016**, *138*, 8360–8363. (b) Song, J.; Zhang, Z.-J.; Gong, L.-Z. *Angew. Chem. Int. Ed.* **2017**, *56*, 5212–5216. (c) Shao, W.; You, S.-L. *Chem. Eur. J.* **2017**, *23*, 12489–12493. (d) Xu, Y.-W.; Hu, X.-P. *Org. Lett.* **2019**, *21*, 8091–8096. (e) Zhang, J.; Ni, T.; Yang, W.-L.; Deng, W.-P. *Org. Lett.* **2020**, *22*, 4547–4552.
- (80) (a) Hattori, G.; Yoshida, A.; Miyake, Y.; Nishibayashi, Y. *J. Org. Chem.* **2009**, *74*, 7603–7607. (b) Gomez, J. E.; Guo, W.; Gaspa, S.; Kleij, A. W. *Angew. Chem. Int. Ed.* **2017**, *56*, 15035–15038. (c) Yoshida, A.; Hattori, G.; Miyake, Y.; Nishibayashi, Y. *Org. Lett.* **2011**, *13*, 2460–2463. (d) Zhang, C.; Wang, Y.-H.; Hu, X.-H.; Zheng, Z.; Xu, J.;

- Hu, X.-P. *Adv. Synth. Catal.* **2012**, *354*, 2854–2858. (e) Shibata, M.; Nakajima, K.; Nishibayashi, Y. *Chem. Commun.* **2014**, *50*, 7874–7877. (f) Cheng, L.-J.; Brown, A. P. N.; Cordier, C. J. *Chem. Sci.* **2017**, *8*, 4299–4305. (g) Ji, D.; Wang, C.; Sun, J. *Org. Lett.* **2018**, *20*, 3710–3713. (h) Li, S.-J.; Huang, J.; He, J.-Y.; Zhang, R.-J.; Qian, H.-D.; Dai, X.-L.; Kong, H.-H.; Xu, H. *RSC Adv.* **2020**, *10*, 38478–38483. (i) Huang, J.; Kong, H.-H.; Li, S.-J.; Zhang, R.-J.; Qian, H.-D.; Li, D.-R.; He, J.-Y.; Zheng, Y.-N.; Xu, H. *Chem. Commun.* **2021**, *57*, 4674–4677.
- (81) Liu, S.; Tanabe, Y.; Kuriyama, S.; Sakata, K.; Nishibayashi, Y. *Chem. Eur. J.* **2021**, *27*, 15650–15659.
- (82) Nakajima, K.; Shibata, M.; Nishibayashi, Y. *J. Am. Chem. Soc.* **2015**, *137*, 2472–2475.
- (83) (a) Shao, L.; Zhang, D.-Y.; Wang, Y.-H.; Hu, X.-P. *Adv. Synth. Catal.* **2016**, *358*, 2558–2563. (b) Li, R.-Z.; Tang, H.; Yang, K. R.; Wan, L.-Q.; Zhang, X.; Liu, J.; Fu, Z.; Niu, D. *Angew. Chem. Int. Ed.* **2017**, *56*, 7213–7217. (c) Li, R.-Z.; Tang, H.; Wan, L.; Zhang, X.; Fu, Z.; Liu, J.; Yang, S.; Jia, D.; Niu, D. *Chem* **2017**, *3*, 834–845. (d) Tsuchida, K.; Yuki, M.; Nakajima, K.; Nishibayashi, Y. *Chem. Lett.* **2018**, *47*, 671–673. (e) Wei, D.-Q.; Liu, Z.-T.; Wang, X.-M.; Hou, C.-J.; Hu, X.-P. *Tetrahedron Lett.* **2019**, *60*, 151305. (f) Li, R.-Z.; Liu, D.-Q.; Niu, D. *Nat. Catal.* **2020**, *3*, 672–680.
- (84) Liu, S.; Nakajima, K.; Nishibayashi, Y. *RSC Adv.* **2019**, *9*, 18918–18922.
- (85) (a) Gomez, J. E; Cristòfol, À.; Kleij, A. W. *Angew. Chem. Int. Ed.* **2019**, *58*, 3903–3907. (b) Gao, X.; Xiao, Y.-L.; Zhang, S.; Wu, J.; Zhang, X. *CCS Chem.* **2020**, *2*, 1463–1471.
- (86) (a) Smith, S. W.; Fu, G. C. *J. Am. Chem. Soc.* **2008**, *130*, 12645–12647. (b) Schley, N. D.; Fu, G. C. *J. Am. Chem. Soc.* **2014**, *136*, 16588–16593. (c) Fu, G. C. *ACS Cent. Sci.* **2017**, *3*, 692–700.
- (87) Oelke, A. J.; Sun, J.; Fu, G. C. *J. Am. Chem. Soc.* **2012**, *134*, 2966–2969.
- (88) Huo, H.; Gorsline, B. J.; Fu, G. C. *Science* **2020**, *367*, 559–564.
- (89) (a) Miyazaki, Y.; Zhou, B.; Tsuji, H.; Kawatsura, M. *Org. Lett.* **2020**, *22*, 2049–2053. (b) Tsuji, H.; Kawatsura, M. *Asian J. Org. Chem.* **2020**, *9*, 1924–1941.
- (90) Peng, L.; He, Z.; Xu, X.; Guo, C. *Angew. Chem. Int. Ed.* **2020**, *59*, 14270–14274.
- (91) Chang, X.; Zhang, J.; Peng, L.; Guo, C. *Nat. Commun.* **2021**, *12*, 299.
- (92) Hu, Q.; He, Z.; Peng, L.; Guo, C. *Nat. Synth.* **2022**, *1*, 322–331.
- (93) Watanabe, K.; Miyazaki, Y.; Okubo, M.; Zhou, B.; Tsuji, H.; Kawatsura, M. *Org. Lett.* **2018**, *20*, 5448–5451.
- (94) Xu, X.; Peng, L.; Chang, X.; Guo, C. *J. Am. Chem. Soc.* **2021**, *143*, 21048–21055.
- (95) O’Broin, C. Q.; Guiry, P. J. *Org. Lett.* **2019**, *21*, 5402–5406.
- (96) Lu, F.-D.; Liu, D.; Zhu, L.; Lu, L.-Q.; Yang, Q.; Zhou, Q.-Q.; Wei, Y.; Lan, Y.; Xiao, W.-J. *J. Am. Chem. Soc.* **2019**, *141*, 6167–6172.
- (97) (a) Allen, A. E.; MacMillan, D. W. C. *Chem. Sci.* **2012**, *3*, 633–658. (b) Du, Z.; Shao, Z. *Chem. Soc. Rev.* **2013**, *42*, 1337–1378. (c) Inamdar, S. M.; Shinde, V. S.; Patil, N. T. *Org. Biomol. Chem.* **2015**, *13*, 8116–8162. (d) Kim, U. B.; Jung, D. J.; Jeon, H. J.; Rathwell, K.; Lee, S. *Chem. Rev.* **2020**, *120*, 13382–13433.
- (98) (a) Ikeda, M.; Miyake, Y.; Nishibayashi, Y. *Angew. Chem. Int. Ed.* **2010**, *49*, 7289–7293. (b) Yoshida, A.; Ikeda, M.; Hattori, G.; Miyake, Y.; Nishibayashi, Y. *Org. Lett.*

2011, 13, 592–595. (c) Zhang, Y.-C.; Zhang, B.-W.; Geng, R.-L.; Song, J. *Org. Lett.* **2018**, 20, 7907–7911. (d) Motoyama, K.; Ikeda, M.; Miyake, Y.; Nishibayashi, Y. *Eur. J. Org. Chem.* **2011**, 2239–2246. (e) Sinisi, R.; Vita, M. V.; Gualandi, A.; Emer, E.; Cozzi, P. G. *Chem. Eur. J.* **2011**, 17, 7404–7408. (f) Ikeda, M.; Miyake, Y.; Nishibayashi, Y. *Chem. Eur. J.* **2012**, 18, 3321–3328. (g) Motoyama, K.; Ikeda, M.; Miyake, Y.; Nishibayashi, Y. *Organometallics* **2012**, 31, 3426–3430. (h) Fu, Z.; Deng, N.; Su, S.-N.; Li, H.; Li, R.-Z.; Zhang, X.; Liu, J.; Niu, D. *Angew. Chem. Int. Ed.* **2018**, 57, 15217–15221. (i) Peng, L.; He, Z.; Xu, X.; Guo, C. *Angew. Chem. Int. Ed.* **2020**, 59, 14270–14274. (j) Chang, X.; Zhang, J.; Peng, L.; Guo, C. *Nat. Commun.* **2021**, 12, 299.

(99) (a) MacMillan, D. W. C. *Nature* **2008**, 455, 304–308. (b) Bertelsen, S.; Jørgensen, K. A. *Chem. Soc. Rev.* **2009**, 38, 2178–2189. (c) Akiyama, T. *Chem. Rev.* **2007**, 107, 5744–5758. (d) Xia, Z.-L.; Xu-Xu, Q.-F.; Zheng, C.; You, S.-L. *Chem. Soc. Rev.* **2020**, 49, 286–300.

(100) (a) Saha, S.; Schneider, C. *Org. Lett.* **2015**, 17, 648–651. (b) Chen, M.; Sun, J. *Angew. Chem. Int. Ed.* **2017**, 56, 11966–11970. (c) Bai, J.-F.; Yasumoto, K.; Kano, T.; Maruoka, K. *Angew. Chem. Int. Ed.* **2019**, 58, 8898–8901. (d) Li, F.; Chen, X.; Liang, S.; Shi, Z.; Li, P.; Li, W. *Org. Chem. Front.* **2020**, 7, 3446–3451. (e) Ma, Y.; Liu, X.; Mao, Y.; Huang, J.; Ma, S.; Liu, L. *Org. Chem. Front.* **2020**, 7, 2526–2530.

(101) (a) Oblinger, E.; Montgomery, J. *J. Am. Chem. Soc.* **1997**, 119, 9065–9066. (b) Miller, K. M.; Huang, W.-S.; Jamison, T. F. *J. Am. Chem. Soc.* **2003**, 125, 3442–3443. (c) Mahandru, G. M.; Liu, G.; Montgomery, J. *J. Am. Chem. Soc.* **2004**, 126, 3698–3699. (d) Herath, A.; Thompson, B. B.; Montgomery, J. *J. Am. Chem. Soc.* **2007**, 129, 8712–8713. (e) Patman, R. L.; Chaulagain, M. R.; Williams, V. M.; Krische, M. J. *J. Am. Chem. Soc.* **2009**, 131, 2066–2067. (f) Malik, H. A.; Sormunen, G. J.; Montgomery, J. *J. Am. Chem. Soc.* **2010**, 132, 6304–6305. (g) Leung, J. C.; Patman, R. L.; Sam, B.; Krische, M. J. *Chem. Eur. J.* **2011**, 17, 12437–12443. (h) McInturff, E. L.; Nguyen, K. D.; Krische, M. J. *Angew. Chem., Int. Ed.* **2014**, 53, 3232–3235. (i) Nakai, K.; Yoshida, Y.; Kurahashi, T.; Matsubara, S. *J. Am. Chem. Soc.* **2014**, 136, 7797–7800.

(102) Ngai, M.-Y.; Barchuk, A.; Krische, M. J. *J. Am. Chem. Soc.* **2007**, 129, 280–281.

(103) (a) Wang, C.-C.; Lin, P.-S.; Cheng, C.-H. *J. Am. Chem. Soc.* **2002**, 124, 9696–9697. (b) Li, W.; Herath, A.; Montgomery, J. *J. Am. Chem. Soc.* **2009**, 131, 17024–17029. (c) Wei, C.-H.; Mannathan, S.; Cheng, C.-H. *J. Am. Chem. Soc.* **2011**, 133, 6942–6944.

(104) Nakao, Y.; Idei, H.; Kanyiva, K. S.; Hiyama, T. *J. Am. Chem. Soc.* **2009**, 131, 5070–5071.

(105) Zhou, C.-Y.; Zhu, S.-F.; Wang, L.-X.; Zhou, Q.-L. *J. Am. Chem. Soc.* **2010**, 132, 10955–10957.

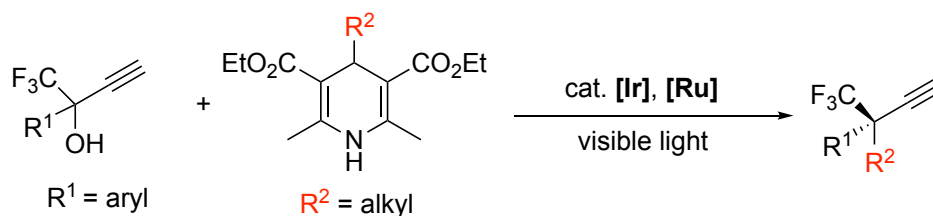
(106) (a) Molinaro, C.; Jamison, T. F. *J. Am. Chem. Soc.* **2003**, 125, 8076–8077. (b) Beaver, M. G.; Jamison, T. F. *Org. Lett.* **2011**, 13, 4140–4143.

(107) (a) Huang, L.; Cheng, K.; Yao, B.; Zhao, J.; Zhang, Y. *Synthesis* **2009**, 20, 3504–3510. (b) Uehling, M. R.; Suess, A. M.; Lalic, G. *J. Am. Chem. Soc.* **2015**, 137, 1424–1427. (c) Suess, A. M.; Uehling, M. R.; Kaminsky, W.; Lalic, G. *J. Am. Chem. Soc.* **2015**, 137, 7747–7753. (d) Wakamatsu, T.; Nagao, K.; Ohmiya, H.; Sawamura, M. *Beilstein J. Org. Chem.* **2015**, 11, 2444–2450. (e) Suess, A. M.; Lalic, G. *Synlett* **2016**,

- 27, 1165–1174. (f) Mailing, M.; Hazra, A.; Armstrong, M. K.; Lalic, G. *J. Am. Chem. Soc.* **2017**, *139*, 6969–6977. (g) Nakamura, K.; Nishikata, T. *ACS Catal.* **2017**, *7*, 1049–1052. (h) Hazra, A.; Kephart, J. A.; Velian, A.; Lalic, G. *J. Am. Chem. Soc.* **2021**, *143*, 7903–7908.
- (108) (a) Chen, L.; Yang, J.; Li, L.; Weng, Z.; Kang, Q. *Tetrahedron Lett.* **2014**, *55*, 6096–6100. (b) Zhang, M.; Zhao, Y.; Chen, W. *Synthesis* **2017**, *49*, 1342–1348.
- (109) Cheung, C. W.; Zhurkin, F. E.; Hu, X. *J. Am. Chem. Soc.* **2015**, *137*, 4932–4935.
- (110) (a) Liu, H.; Fu, Z.; Gao, S.; Huang, Y.; Lin, A.; Yao, H. *Adv. Synth. Catal.* **2018**, *360*, 3171–3175. (b) Yu, L.; Lv, L.; Qiu, Z.; Chen, Z.; Tan, Z.; Liang, Y.-F.; Li, C.-J. *Angew. Chem. Int. Ed.* **2020**, *59*, 14009–14013.
- (111) (a) Lee, M. T.; Goodstein, M. B.; Lalic, G. *J. Am. Chem. Soc.* **2019**, *141*, 17086–17091. (b) Hu, L.; Gao, H.; Hu, Y.; Lv, X.; Wu, Y.-B.; Lu, G. *Chem. Commun.* **2021**, *57*, 6412–6415. (c) Lee, M. T.; Lalic, G. *J. Am. Chem. Soc.* **2021**, *143*, 16663–16672.
- (112) (a) Lu, X.-Y.; Liu, J.-H.; Lu, X.; Zhang, Z.-Q.; Gong, T.-J.; Xiao, B.; Fu, Y. *Chem. Commun.* **2016**, *52*, 5324–5327.
- (113) Lu, X.-Y.; Hong, M.-L.; Zhou, H.-P.; Wang, Y.; Wang, J.-Y.; Ge, X.-T. *Chem. Commun.* **2018**, *54*, 4417–4420.
- (114) Lu, X.-Y.; Li, J.-S.; Hong, M.-L.; Wang, J.-Y.; Ma, W.-J. *Tetrahedron* **2018**, *74*, 6979–6984.
- (115) Zhu, Z.-F.; Tu, J.-L.; Liu, F. *Chem. Commun.* **2019**, *55*, 11478–11481.
- (116) Lu, X.-Y.; Liu, C.-C.; Jiang, R.-C.; Yan, L.-Y.; Liu, Q.-L.; Wang, Q.-Q.; Li, J.-M. *Chem. Commun.* **2020**, *56*, 14191–14194.
- (117) Li, J.; Zhang, J.; Tan, H.; Wang, D. Z. *Org. Lett.* **2015**, *17*, 2522–2525.
- (118) Dai, G.-L.; Lai, S.-Z.; Luo, Z.; Tang, Z.-Y. *Org. Lett.* **2019**, *21*, 2269–2272.
- (119) Lai, S.-Z.; Yang, Y.-M.; Xu, H.; Tang, Z.-Y.; Luo, Z. *J. Org. Chem.* **2020**, *85*, 15638–15644.
- (120) Adak, T.; Hoffmann, M.; Witzel, S.; Rudolph, M.; Dreuw, A.; Hashmi, A. S. K. *Chem. Eur. J.* **2020**, *26*, 15573–15580.
- (121) Li, Y.; Ge, L.; Qian, B.; Babu, K. R.; Bao, H. *Tetrahedron Lett.* **2016**, *57*, 5677–5680.
- (122) Ding, H.-P.; Fan, X.-Z.; Chen, Z.-H.; Xu, Q.-H.; Wu, J. *J. Am. Chem. Soc.* **2017**, *139*, 13579–13584.
- (123) Go, S. Y.; Lee, G. S.; Hong, S. H. *Org. Lett.* **2018**, *20*, 4691–4694.
- (124) Till, N. A.; Smith, R. T.; MacMillan, D. W. C. *J. Am. Chem. Soc.* **2018**, *140*, 5701–5705.
- (125) Yue, H.; Zhu, C.; Kancharla, R.; Liu, F.; Rueping, M. *Angew. Chem. Int. Ed.* **2020**, *59*, 5738–5746.
- (126) Nevesely, T.; Wienhold, M.; Molloy, J. J.; Gilmour, R. *Chem. Rev.* **2022**, *122*, 2650–2694.
- (127) Zhao, X.; Zhu, S.; Qing, F.; Chu, L. *Chem. Commun.* **2021**, *57*, 9414–9417.
- (128) Zhao, T.-T.; Yu, W.-L.; Feng, Z.-T.; Qin, H.-N.; Zheng, H.; Xu, P.-F. *Chem. Commun.* **2022**, *58*, 1171–1174.

Chapter 2

Photoredox- and Ruthenium-Catalyzed Enantioselective Propargylic Alkylation of Propargylic Alcohols with 4-Alkyl-1,4-dihydropyridines



In Chapter 2, the author has developed the first successful example of photoredox- and ruthenium-catalyzed enantioselective propargylic substitution reactions of propargylic alcohols with alkyl radicals, which are generated from 4-alkyl-1,4-dihydropyridines under photoredox reaction conditions, providing a new strategy to the chemistry of enantioselective propargylic substitution reactions.

2.1. Introduction

Nucleophilic substitution reactions at the allylic or propargylic position of unsaturated compounds containing alkene or alkyne moieties have attracted attentions as convenient methods to introduce substituents to the starting materials by retaining the unsaturated moieties. Here, transition metal-catalyzed allylic substitution reactions have been widely investigated since the 1960s.^{1,2} However, examples of catalytic propargylic substitution reactions have been rather limited in number until 2000, when the author's group reported the catalytic propargylic substitution reactions by using thiolate-bridged diruthenium complexes as catalysts.³ Furthermore in 2005, the author's group reported the first enantioselective propargylic substitution reactions catalyzed by the thiolate-bridged diruthenium complexes by introducing chiral moiety onto the thiolate ligands.⁴ Since then, enantioselective propargylic substitution reactions of propargylic alcohols or esters with several carbon- and heteroatom-centered nucleophiles to afford the corresponding propargylic substitution products have been achieved by using ruthenium, copper, and nickel complexes as catalysts.^{5,6,7,8}

In these reaction systems, the key reaction intermediates are the allenylidene complexes in case of ruthenium and copper-catalyzed systems (Scheme 2-1a),^{5d} or the allenyl complexes in case of nickel catalyzed systems (Scheme 2-1b), respectively.⁸ In both cases, enantioselectivity is controlled by the steric effect of chiral ligands bound to ruthenium, copper, or nickel centers, leading to the determination of the faces for the reactive intermediate to capture nucleophiles. On the other hand, enantioselective propargylic substitution reactions via propargylic radicals have been also reported for nickel⁹ and copper-catalyzed systems.¹⁰ Among them, Lu, Lan, Xiao, and co-workers reported the enantioselective propargylic cyanation by using dual organophotoredox- and copper catalysts. Here, a single electron transfer (SET) between the propargylic esters with a photoinduced organophotoredox catalyst occurs to afford the propargylic radicals, which react with the nucleophilic copper cyanate complex, formed via the reaction of a chiral copper catalyst and CN^- in situ, to afford the corresponding propargylic cyanated products (Scheme 2-1c), demonstrating that photoredox catalysis can be applied to enantioselective propargylation process.^{10a} However, to the best of the author's knowledge, catalytic enantioselective propargylic substitution reactions with a simple alkyl group (not activated by functional groups such as methyl derivatives attached with ketone, aldehyde, or ether groups) introduced at the propargylic position to afford the propargylic alkylated products have not been yet achieved.

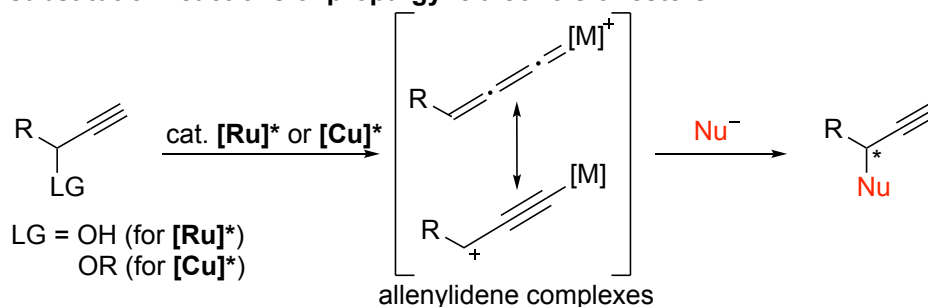
On the other hand, the author's group and others have shown that 4-alkyl-1,4-dihydropyridines can supply alkyl radicals under photoredox reaction conditions, where several alkylated products can be obtained by reactions of these alkyl radicals with various substrates,¹¹ clarifying that 4-alkyl-1,4-dihydropyridines provide a new platform of alkylation reagents designed for the use under milder reaction conditions, which can be substituted for considerably reactive organometallic alkylation reagents by reducing functional groups protections.¹²⁻²⁶ Until now, the alkyl radicals generated via the SET processes between visible light-excited photoredox catalysts and 4-alkyl-1,4-dihydropyridines have enabled simple alkylation reactions,¹³⁻¹⁶ alkylative

reactions,^{17–24} and enantioselective alkylation reactions.²⁵ Indeed, the author's group has already reported the aromatic substitution reactions of cyanoarenes with 4-alkyl-1,4-dihydropyridines catalyzed by photoredox catalysts¹³ and the cross-coupling reactions of aryl,¹⁷ alkenyl,¹⁸ alkynyl halides,¹⁹ and alkynes²⁶ with 4-alkyl-1,4-dihydropyridines catalyzed by dual photoredox- and nickel catalysts

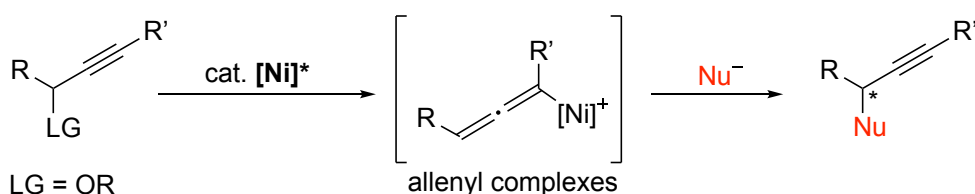
It must be noted that Chen and co-workers have recently shown that 4-alkyl-1,4-dihydropyridines are applicable as alkylation reagents in the dual photoredox- and palladium-catalyzed propargylic substitution reactions of propargylic esters to afford the propargylic alkylated products.^{21d} However, no enantioselectivity was introduced in this reaction system. In order to achieve enantioselective propargylic alkylation reactions, the author has planned to apply 4-alkyl-1,4-dihydropyridines as alkylation reagents. Herein, the author wishes to report the dual photoredox- and ruthenium-catalyzed enantioselective propargylic alkylation reactions of propargylic alcohols (Scheme 2-1d). This is the first successful example, where propargylic alkylated products with nonactivated, simple alkyl group introduced at the propargylic position are obtained enantioselectively, demonstrating that alkyl radicals generated by the photoredox catalysis can act as the alternatives to nucleophiles for propargylic substitution reactions.

Scheme 2-1. Enantioselective Propargylic Substitution Reactions

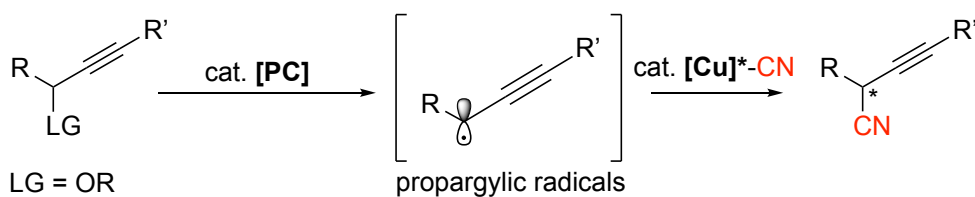
a) Ruthenium- or copper-catalyzed enantioselective propargylic substitution reactions of propargylic alcohols or esters



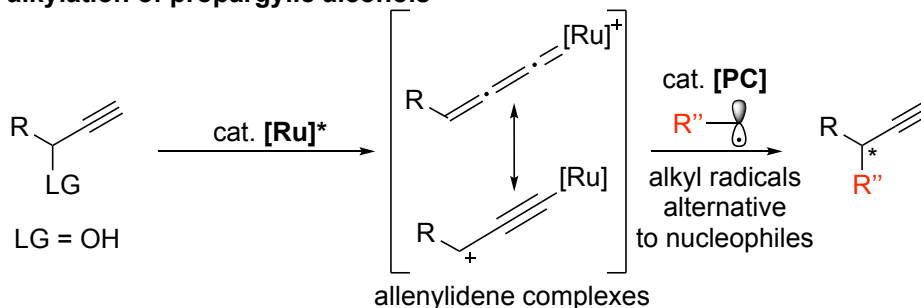
b) Nickel-catalyzed enantioselective propargylic substitution reaction of propargylic halides or propargylic esters



c) Dual photoredox/copper-catalyzed enantioselective propargylic cyanation of propargylic esters



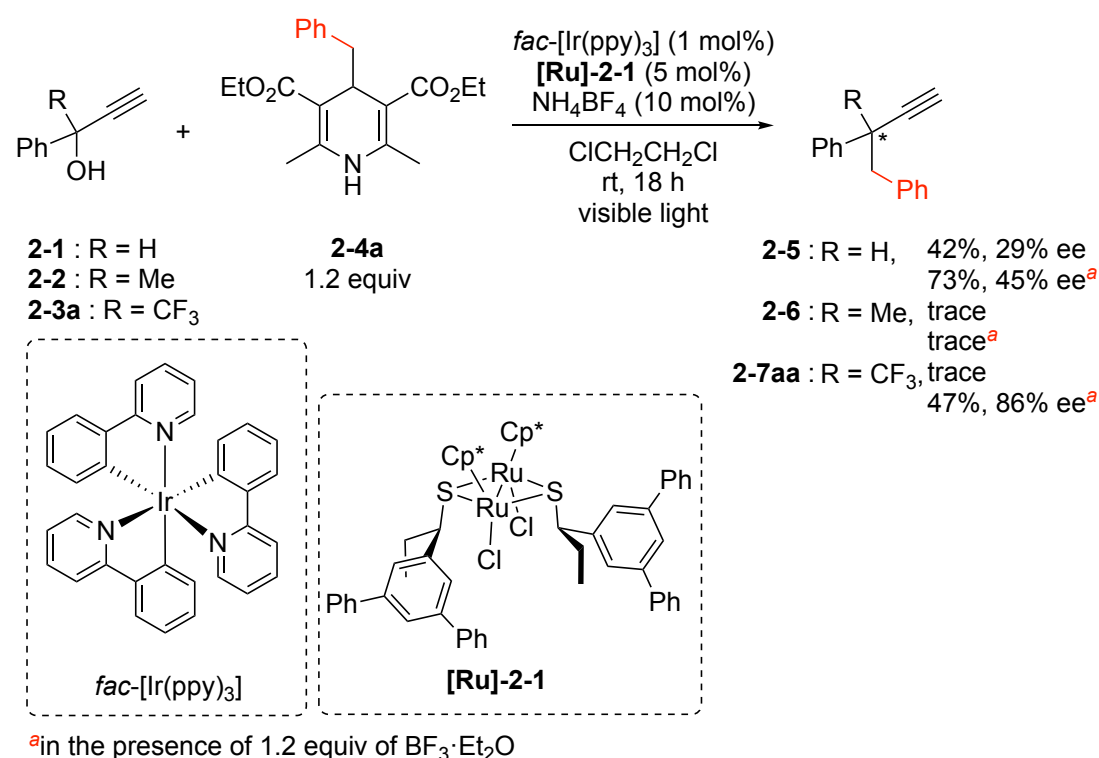
d) This work: Dual photoredox/ruthenium-catalyzed enantioselective propargylic alkylation of propargylic alcohols



2.2. Results and Discussions

As the beginning, the author carried out reactions of 1-phenyl-prop-2-ynes with substituents introduced at the propargylic position ($\text{HC}\equiv\text{CC}(\text{OH})(\text{R})\text{Ph}$, $\text{R} = \text{H}$ (**2-1**), Me (**2-2**), or CF_3 (**2-3a**)) with 1.2 equiv of 4-benzyl-1,4-dihydropyridine (**2-4a**) in the presence of 5 mol% of an optically active thiolate-bridged diruthenium complex $[\{\text{Cp}^*\text{RuCl}(\text{SR}^*)\}_2]$ ($\text{Cp}^* = \eta^5\text{-C}_5\text{Me}_5$, $\text{SR}^* = (R)\text{-SCH}(\text{Et})\text{C}_6\text{H}_3\text{Ph}_2$: **[Ru]-2-1**), 1 mol% of *fac*- $[\text{Ir}(\text{ppy})_3]$ ($\text{ppy} = 2\text{-(2-pyridyl)phenyl}$), and 10 mol% of NH_4BF_4 in 1,2-dichloroethane ($\text{ClCH}_2\text{CH}_2\text{Cl}$) at 25 °C under visible light irradiation (Scheme 2-2). The reaction of **2-1** with 1.2 equiv of **2-4a** afforded the corresponding propargylic alkylated product (**2-5**) in 42% yield with 29% ee. Interestingly, addition of 1.2 equiv of $\text{BF}_3\cdot\text{Et}_2\text{O}$ increased both the yield and enantioselectivity of **2-5** up to 73% and 45% ee, respectively. In contrast, the reaction of **2-2**, a tertiary propargylic alcohol, with 1.2 equiv of **2-4a** gave only a trace amount of the desired alkylated product (**2-6**) under similar reaction conditions even in the presence of 1.2 equiv of $\text{BF}_3\cdot\text{Et}_2\text{O}$. The reaction of **2-3a**, another tertiary propargylic alcohol bearing a trifluoromethyl group at the propargylic position, with 1.2 equiv of **2-4a** in the presence of 5 mol% of **[Ru]-2-1**, 1 mol% *fac*- $[\text{Ir}(\text{ppy})_3]$ and 10 mol% of NH_4BF_4 in $\text{ClCH}_2\text{CH}_2\text{Cl}$ at 25 °C under visible light irradiation for 18 h gave only a trace amount of the desired alkylated product (**2-7aa**). However, addition of 1.2 equiv of $\text{BF}_3\cdot\text{Et}_2\text{O}$ fairly increased the yield of **2-7aa** up to 47% with a high enantioselectivity such as 86% ee. These experimental results indicate that introduction of a trifluoromethyl group at the propargylic position is an essential factor to achieve the high enantioselectivity of the propargylic alkylated products.

Scheme 2-2. Screening of Propargylic Alcohols as Substrates

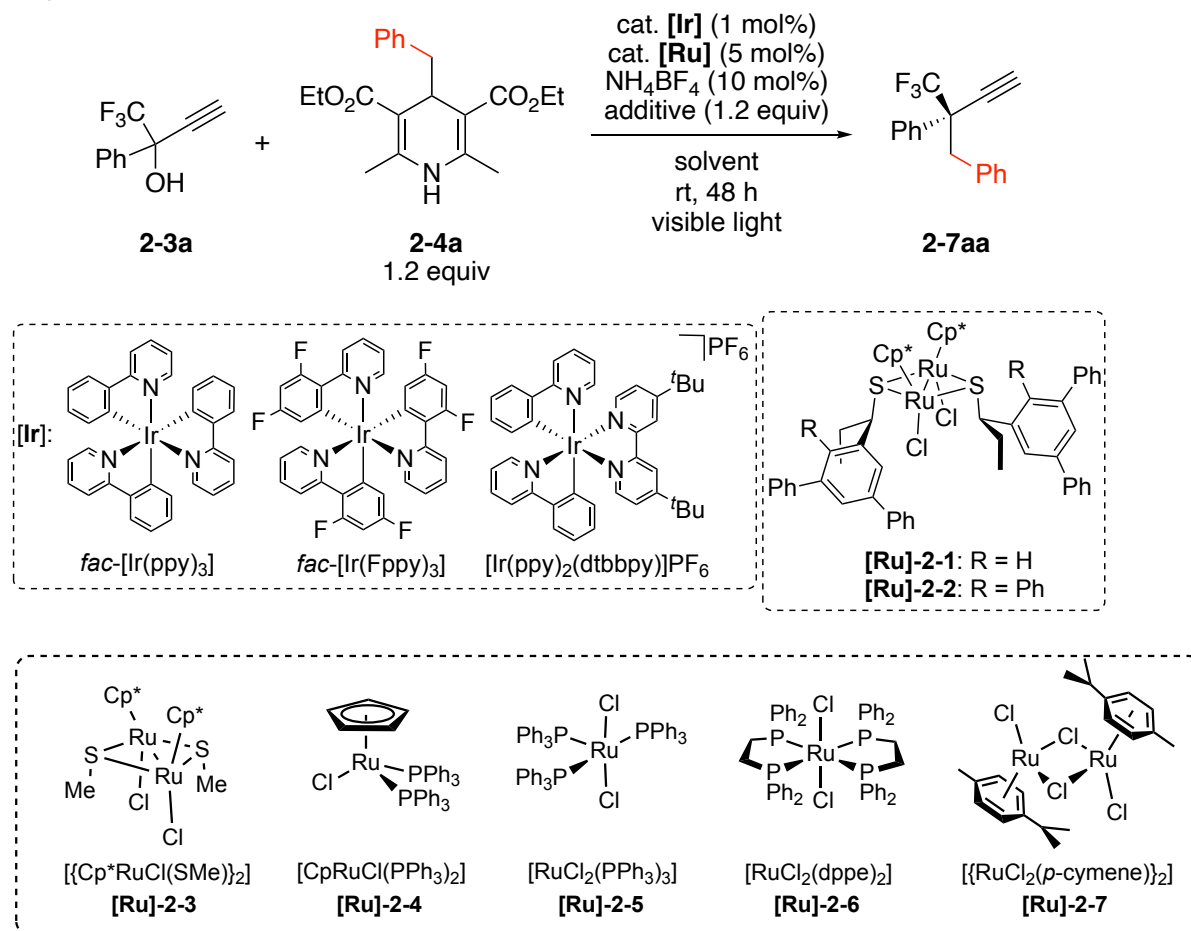


Next, the author examined optimization of the reaction conditions (Table 2-1). When the reaction of **2-3a** with 1.2 equiv of **2-4a** was carried out in the presence of 5 mol% of **[Ru]-2-2**, 1 mol% *fac*-[Ir(ppy)₃], 10 mol% of NH₄BF₄, and 1.2 equiv of BF₃·Et₂O in ClCH₂CH₂Cl at 25 °C under visible light irradiation for 18 h, *i.e.* under the reaction conditions similar to Scheme 2-1 (Table 2-1, entry 1) but employing **[Ru]-2-2** instead of **[Ru]-2-1** as the catalyst, the isolated yield of **2-7aa** was decreased to 35%, but the enantioselectivity was fairly increased to 93% ee (Table 2-1, entry 2). Interestingly, yield of **2-7aa**, obtained as a mixture of racemates, increased up to 84% when [$\{\text{Cp}^*\text{RuCl}(\mu\text{-SMe})\}_2$] (**[Ru]-2-3**), another thiolate-bridged diruthenium complex with non-chiral centers, was used as the ruthenium catalyst instead of **[Ru]-2-1** or **[Ru]-2-2** (Table 2-1, entry 3). In addition, several mononuclear and binuclear ruthenium complexes such as [CpRuCl(PPh₃)₂] (Cp = $\eta^5\text{-C}_5\text{H}_5$) (**[Ru]-2-4**), [RuCl₂(PPh₃)₃] (**[Ru]-2-5**), [RuCl₂(dppe)₂] (**[Ru]-2-6**), and [$\{(p\text{-cymene})\text{RuCl}(\mu\text{-Cl})\}_2$] (**[Ru]-2-7**) were further examined as catalysts. However, only a trace amount of **7aa** was obtained when **[Ru]-2-4** was used as a catalyst (Table 2-1, entry 4), or **7aa** was not obtained at all when **[Ru]-2-5**, **[Ru]-2-6**, or **[Ru]-2-7** was used as a catalyst (Table 2-1, entries 5–7), demonstrating that thiolate-bridged diruthenium core containing ruthenium–ruthenium bond, where electron transfers between the two ruthenium atoms easily occur to stabilize reactive intermediates including coordinatively unsaturated species during redox reactions, is necessary for catalytic propargylic substitution reactions with alkyl radicals.^{5e,27}

It should be cautioned that in both cases (Table 2-1, entries 1 and 2), starting materials (both **2-3a** and **2-4a**) were recovered. Furthermore, examination on the elongation of the reaction time up to 48 h also increased the yield of **2-7aa** up to 81% with 94% ee (Table 2-1, entry 8). Use of other iridium-based photoredox catalysts such as *fac*-[Ir(Fppy)₃] (Fppy = 3,5-difluoro-2-(2-pyridyl)phenyl) and [Ir(ppy)₂(dtbbpy)]PF₆ (dtbbpy = 4,4'-di-*tert*-butyl-2,2'-bipyridine) instead of *fac*-[Ir(ppy)₃] was also examined, where yields of **2-7aa** became slightly lower with a lower enantioselectivity (Table 2-1, entries 9 and 10). Reactions were also carried out in other solvents such as CH₂Cl₂ and Cl(CH₂)₃Cl, but the yields of **2-7aa** also got lower with a lower enantioselectivity (Table 2-1, entries 11 and 12) compared to those in ClCH₂CH₂Cl. Next, reactions using some other Lewis acids such as B(OH)₃, Sc(OTf)₃, and BCl₃ instead of BF₃·Et₂O were examined, but trace amounts of **2-7aa** detectable only by GC-MS were formed in all cases (Table 2-1, entries 13–15). In addition, reducing the amount of BF₃·Et₂O down to 10 mol% did not change the enantioselectivity of **2-7aa** with 93% ee but decreased the isolated yield of **2-7aa** to 13% (Table 2-1, entry 16), demonstrating that the addition of almost a stoichiometric amount of BF₃·Et₂O is necessary to enhance the reaction. It must be noted that the present substitution reaction is also the dehydration process, giving a stoichiometric amount of H₂O as a byproduct. Indeed, addition of 1.2 equiv of H₂O was shown to inhibit the reaction (Table 2-1, entry 17). However, addition of 2.0 equiv of anhydrous MgSO₄ in the absence of BF₃·Et₂O did not give the desired product (Table 2-1, entry 18), while the addition of both 2.0 equiv of anhydrous MgSO₄ and 10 mol% of BF₃·Et₂O gave **2-7aa** in 15% yield with 92% ee (Table 2-1, entry 19), demonstrating that main roles of BF₃·Et₂O may be not only to work as a drying reagent

to trap H₂O, but also to work as an accelerator for the dehydration process more efficiently than other Lewis acids (B(OH)₃, Sc(OTf)₃, and BCl₃) and MgSO₄. Finally, additional control experiments were investigated. In the absence of photoredox catalyst but under visible light irradiation (Table 2-1, entry 20) or in the presence of photoredox catalyst but under dark (Table 2-1, entry 21), only trace amounts of **2-7aa** were obtained, while formation of **2-7aa** was perfectly not observed in the absence of ruthenium catalyst (Table 2-1, entry 22), clarifying that the photoredox catalyst, light, and ruthenium catalyst are all necessary to carry out reactions.

Table 2-1. Photoredox- and Ruthenium-catalyzed Enantioselective Propargylic Alkylation of **2-3a** with **2-4a**^a



entry	cat. [Ir]	cat. [Ru]	solvent	additive	yield (%) ^b	ee (%)
1 ^c	<i>fac</i> -[Ir(ppy) ₃]	[Ru]-2-1	ClCH ₂ CH ₂ Cl	BF ₃ ·Et ₂ O	47	86
2 ^c	<i>fac</i> -[Ir(ppy) ₃]	[Ru]-2-2	ClCH ₂ CH ₂ Cl	BF ₃ ·Et ₂ O	35	93
3 ^c	<i>fac</i> -[Ir(ppy) ₃]	[Ru]-2-3	ClCH ₂ CH ₂ Cl	BF ₃ ·Et ₂ O	84	-
4 ^c	<i>fac</i> -[Ir(ppy) ₃]	[Ru]-2-4	ClCH ₂ CH ₂ Cl	BF ₃ ·Et ₂ O	<5	-
5 ^c	<i>fac</i> -[Ir(ppy) ₃]	[Ru]-2-5	ClCH ₂ CH ₂ Cl	BF ₃ ·Et ₂ O	n.d. ^d	-
6 ^c	<i>fac</i> -[Ir(ppy) ₃]	[Ru]-2-6	ClCH ₂ CH ₂ Cl	BF ₃ ·Et ₂ O	n.d	-
7 ^c	<i>fac</i> -[Ir(ppy) ₃]	[Ru]-2-7	ClCH ₂ CH ₂ Cl	BF ₃ ·Et ₂ O	n.d	-
8	<i>fac</i> -[Ir(ppy) ₃]	[Ru]-2-2	ClCH ₂ CH ₂ Cl	BF ₃ ·Et ₂ O	81	94
9	<i>fac</i> -[Ir(Fppy) ₃]	[Ru]-2-2	ClCH ₂ CH ₂ Cl	BF ₃ ·Et ₂ O	54	51

10	[Ir(ppy) ₂ -(dtbbpy)]PF ₆	[Ru]-2-2	ClCH ₂ CH ₂ Cl	BF ₃ ·Et ₂ O	39	73
11	<i>fac</i> -[Ir(ppy) ₃]	[Ru]-2-2	CH ₂ Cl ₂	BF ₃ ·Et ₂ O	<5	—
12	<i>fac</i> -[Ir(ppy) ₃]	[Ru]-2-2	Cl(CH ₂) ₃ Cl	BF ₃ ·Et ₂ O	32	83
13	<i>fac</i> -[Ir(ppy) ₃]	[Ru]-2-2	ClCH ₂ CH ₂ Cl	B(OH) ₃	Trace ^e	—
14	<i>fac</i> -[Ir(ppy) ₃]	[Ru]-2-2	ClCH ₂ CH ₂ Cl	Sc(OTf) ₃	trace	—
15	<i>fac</i> -[Ir(ppy) ₃]	[Ru]-2-2	ClCH ₂ CH ₂ Cl	BCl ₃	trace	—
16 ^f	<i>fac</i> -[Ir(ppy) ₃]	[Ru]-2-2	ClCH ₂ CH ₂ Cl	BF ₃ ·Et ₂ O	13	93
17 ^g	<i>fac</i> -[Ir(ppy) ₃]	[Ru]-2-2	ClCH ₂ CH ₂ Cl	BF ₃ ·Et ₂ O	trace	—
18 ^h	<i>fac</i> -[Ir(ppy) ₃]	[Ru]-2-2	ClCH ₂ CH ₂ Cl	none	trace	—
19 ^{f,h}	<i>fac</i> -[Ir(ppy) ₃]	[Ru]-2-2	ClCH ₂ CH ₂ Cl	BF ₃ ·Et ₂ O	15	92
20	none	[Ru]-2-2	ClCH ₂ CH ₂ Cl	BF ₃ ·Et ₂ O	trace	—
21 ⁱ	<i>fac</i> -[Ir(ppy) ₃]	[Ru]-2-2	ClCH ₂ CH ₂ Cl	BF ₃ ·Et ₂ O	trace	—
22	<i>fac</i> -[Ir(ppy) ₃]	none	ClCH ₂ CH ₂ Cl	BF ₃ ·Et ₂ O	n.d.	—

^aReactions of **2-3a** (0.10 mmol) with **2-4a** (0.12 mmol) were carried out in the presence of cat. **[Ir]** (0.001 mmol), cat. **[Ru]** (0.005 mmol), NH₄BF₄ (0.01 mmol), and an additive (0.12 mmol) in solvent (2.0 mL) with 12 W white LED illumination at 25 °C for 48 h. ^bIsolated yield. ^c18 h instead of 48 h. ^dNot detected by GC-MS. ^eDetected by GC-MS for crude mixture but not isolable. ^f10 mol% of BF₃·Et₂O. ^gIn the presence of 1.2 equiv of H₂O. ^hIn the presence of 2.0 equiv of anhydrous MgSO₄. ⁱIn the absence of visible light.

Taking the reaction conditions of entry 8 in Table 2-1 as optimized, reactions of **2-3a** with several 4-alkyl-1,4-dihydropyridines (**2-4**) to obtain the corresponding propargylic alkylated products were next examined (Scheme 2-3). The use of 4-benzyl-1,4-dihydropyridine derivatives, where either electron-donating (**2-4b**, Me; **2-4c**, MeO; **2-4d**, OH) or electron-withdrawing substituents (**2-4e**, F, **2-4f**, Cl; **2-4g**, Br; **2-4h**, CF₃; **2-4i**, MeOCO) were imported at the 4-position of the benzene ring, afforded the corresponding propargylic alkylated products in good to high yields with a high enantioselectivity (**2-7ab**, 78% yield, 94% ee; **2-7ac**, 79% yield, 92% ee; **2-7ad**, 72% yield, 92% ee; **2-7ae**, 80% yield, 92% ee; **2-7af**, 70% yield, 90% ee; **2-7ag**, 68% yield, 94% ee; **2-7ah**, 74% yield, 91% ee; **2-7ai**, 75% yield, 96% ee), demonstrating that even phenolic OH group is tolerant (**2-7ad**), while the highest enantioselectivity at 96% ee was achieved for that containing benzoate ester (**2-7ai**). On the other hand, the use of the 4-benzyl-1,4-dihydropyridine derivatives, where bulky substituents were imported at the 4-position of the benzene ring (**2-4j**, ^tBu; **2-4k**, Ph), afforded the corresponding propargylic alkylated products in good yields with a little lower enantioselectivity (**2-7aj**, 70% yield, 84% ee; **2-7ak**, 71% yield, 83% ee). 4-Benzyl-1,4-dihydropyridine derivatives with either electron-donating substituents imported at the 3-position (**2-4l**, Me; **2-4m**, 2-F; **2-4n**, Cl; **2-4o**, Br) or the 2-position (**2-4p**, Me; **2-4q**, F) of the benzene ring were also applicable to afford the corresponding propargylic alkylated products in good yields with a high enantioselectivity (**2-7al**, 73% yield, 90% ee; **2-7am**, 75% yield, 90% ee; **2-7an**, 77% yield, 91% ee; **2-7ao**, 72% yield, 93% ee; **2-7ap**, 74% yield, 90% ee; **2-7aq**, 78% yield, 93% ee).

Scope of alkyl radicals is not limited to substituted benzyl radicals. Indeed, 1,4-dihydropyridine derivatives with arylmethyl groups such as 1-naphthylmethyl (**2-4r**), 2-naphthylmethyl (**2-4s**), piperonyl (**2-4t**), 2-furylmethyl (**2-4u**), and 2-thienylmethyl (**2-4v**) substituents imported at the 4-position of the dihydropyridine skeleton could be successfully converted into the corresponding propargylic alkylated products in good to high yields with a high enantioselectivity (**2-7ar**, 69% yield, 90% ee; **2-7as**, 71% yield, 95% ee; **2-7at**, 66% yield, 91% ee; **2-7au**, 80% yield, 90% ee; **2-7av**, 75% yield, 94% ee), providing a new syntetic tool to construct heterocycle-containing alkynes. On the other hand, the use of 1,4-dihydropyridine derivatives with a pyridine-, ether, or amine-containing methyl group, a secondary alkyl group, or a long chain primary alkyl groups (R² = 3-pyridylmethyl, benzyloxymethyl, *N,N*-dibenzylaminomethyl-, 3-pentyl, or *n*-nonyl) imported at the 4-position of the dihydropyridine skeleton gave only trace amounts of desired products, leading to failure of their isolation, which might be due to either their steric bulkiness or instability of the corresponding alkyl radicals²⁸ generated under photoredox conditions.

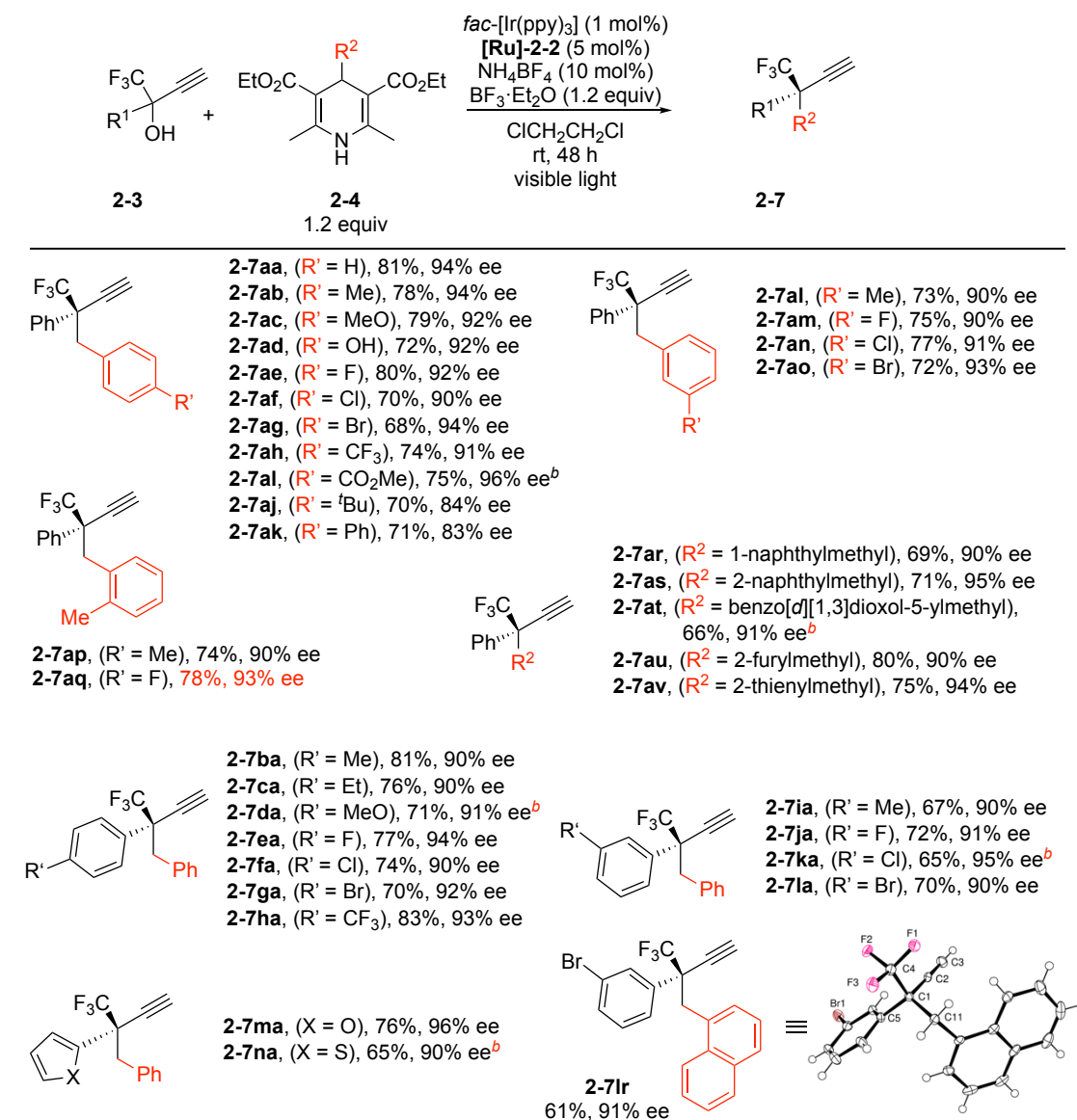
Subsequently, propargylic alkylation reactions of various propargylic alcohols (**2-3**) with **2-4a** were investigated. 1,1,1-Trifluoro-2-phenyl-but-3-yn-2-ol derivatives with either electron-donating (**2-3b**, Me; **2-3c**, Et; **2-3d**, MeO) or electron-withdrawing substituents (**2-3e**, F; **2-3f**, Cl; **2-3g**, Br; **2-3h**, CF₃) imported at the 4-position of the benzene ring were successfully alkylated to afford the desired products in good to high yields with a high enantioselectivity (**2-7ba**, 81% yield, 90% ee; **2-7ca**, 76% yield, 90% ee; **2-7da**, 71% yield, 91% ee; **2-7ea**, 77% yield, 94% ee; **2-7fa**, 74% yield, 90% ee; **2-**

7ga, 70% yield, 92% ee; **2-7ha**, 83% yield, 93% ee). 1,1,1-Trifluoro-2-phenyl-but-3-yn-2-ol derivatives, where either electron-donating or electron-withdrawing substituents were imported at the 3-position of the benzene ring (**2-3i**, Me; **2-3j**, F; **2-3k**, Cl; **2-3l**, Br), were also applicable to afford the corresponding propargylic alkylated products in good yields with a high enantioselectivity (**2-7ia**, 67% yield, 90% ee; **2-7ja**, 72% yield, 91% ee; **2-7ka**, 65% yield, 95% ee; **2-7la**, 70% yield, 90% ee).

Interestingly, not only propargylic alcohols containing phenyl derivatives (**2-3a–2-3l**) but also those containing heterocycles such as 2-furyl and 2-thienyl groups (**2-3m** and **2-3n**) were shown to be converted into the corresponding propargylic alkylated products in good yields with a high enantioselectivity (**2-7ma**, 67% yield, 90% ee; **2-7na**, 72% yield, 91% ee). However, the reaction of 1,1,1-trifluoro-2-phenyl-but-3-yn-2-ol derivatives ($\text{HC}^\circ\text{CC}(\text{OH})(\text{CF}_3)\text{R}^1$) with substituents (Me or F) at the 2-position of the benzene ring ($\text{R}^1 = 2\text{-tolyl}$ or 2-fluorophenyl) or 2-([1,1'-biphenyl]-4-yl)-1,1,1-trifluorobut-3-yn-2-ol ($\text{R}^1 = 2\text{-naphthyl}$) with **2-4a** gave only trace amounts of the desired products, presumably due to their steric hindrance. In addition, formation of the corresponding alkylated products was not observed at all by GC-MS for the reactions of 3-(trifluoromethyl)pent-1-yn-3-ol ($\text{HC}^\circ\text{CC}(\text{OH})(\text{CF}_3)\text{Et}$) with **2-4a**, or of 1,1,1-trifluoro-2-phenylpent-3-yn-2-ol ($\text{MeC}^\circ\text{CC}(\text{OH})(\text{CF}_3)\text{Ph}$) with **2-4a**. Namely, introduction of an aromatic moiety (such as substituted phenyl, 2-furyl, or 2-thienyl group) at the propargylic position of propargylic alcohols are necessary for the propargylic alkylation reaction with 4-alkyl-1,4-dihydropyridines under photoredox conditions, while the propargylic moiety of the propargylic alcohols must contain terminal ethynyl group to form ruthenium–allenylide intermediates.

Reaction of **2-3l** with **2-4r** was further examined to obtain the corresponding propargylic alkylated product (**2-7lr**) in 61% yield with a high enantioselectivity at 91% ee. The molecular structure of **2-7lr** has been determined by a single-crystal X-ray diffraction study, which has clarified that the absolute configuration of **2-7lr** is (*R*), the chirality of which is same with those obtained for the ruthenium-catalyzed enantioselective propargylic phosphinylation of propargylic alcohols similarly bearing both CF_3 and aromatic groups at the propargylic position.^{6f,29}

Scheme 2-3. Scope of Propargylic Alkylation Reactions^a



Reaction conditions: **2-3** (0.10 mmol), **2-4** (0.12 mmol), [Ru]-**2-2** (0.005 mmol), *fac*-[Ir(ppy)₃] (0.001 mmol), NH₄BF₄ (0.01 mmol), BF₃·Et₂O (0.12 mmol), and ClCH₂CH₂Cl (2.0 mL) at 25 °C for 48 h under visible light irradiation with a 12 W white LED. Isolated yield given for each.

^aFormation of trace amounts of the desired products observed by GC-MS but not isolable for the reactions of **2-3a** with **2-4** (R² = 3-pyCH₂, PhCH₂OCH₂, (PhCH₂)₂NCH₂, (CH₃CH₂)₂CH, or CH₃(CH₂)₆). ^b72 h instead of 48 h.

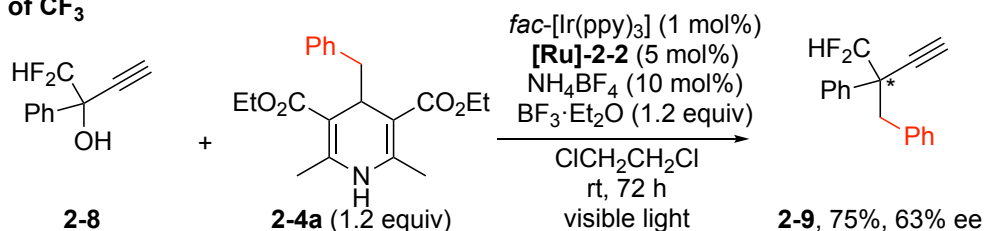
^cFormation of trace amounts of the desired products observed by GC-MS but not isolable for the reactions of **2-3** (R¹ = 2-MeC₆H₄, 2-FC₆H₄, or 2-naphthyl) with **2-4a**. Formation of the desired products not detected by GC-MS for the reaction of **3** (R¹ = Et) or MeCCC(OH)(CF₃)Ph with **4a**.

Interestingly, 1,1-difluoro-2-phenyl-but-3-yn-2-ol (**2-8**), where CF₂H group was introduced at the propargylic position instead of CF₃ group, was found to react with **2-4a** to afford the corresponding propargylic alkylated product (**2-9**) in 75% yield, although the enantioselectivity at 63% ee was significantly lower than that obtained for **2-7aa** at 94% ee (Scheme 2-4a), demonstrating that the existence of trifluoromethyl group at the propargylic position plays an important role for the enantioselective propargylic alkylation as has been previously found for the enantioselective propargylic phosphinylation reaction.^{6f,29}

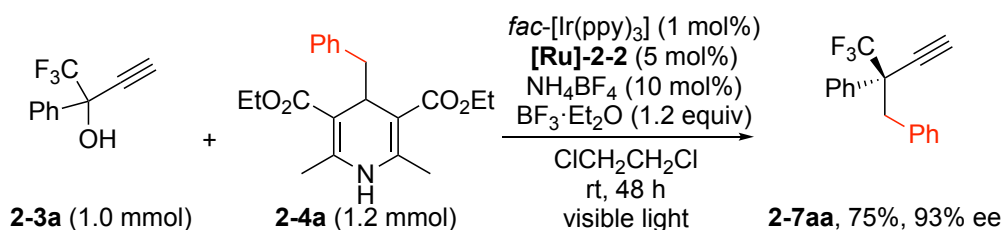
The practicality and synthetic potential of the enantioselective propargylic alkylation reactions was then investigated. The author first performed a larger-scale reaction of **2-3a** (1.0 mmol) with **2-4a** (1.2 mmol) under the optimized reaction conditions to obtain the propargylic alkylated product **2-7aa** in 75% isolated yield (0.75 mmol) with keeping a high enantioselectivity at 93% ee (Scheme 2-4b). Further transformations of **2-7aa** using a batch with an enantioenrichment at 93% ee was then examined, because terminal alkyne moieties have a wide range of synthetic utility.³⁰ Indeed, AgNO₃-catalyzed electrophilic bromination³¹ of **2-7aa** with NBS (N-bromosuccinimide) afforded the corresponding bromoalkyne (**2-9**) (Scheme 2-4c(i)), while the Sonogashira coupling³² of **2-7aa** with PhI afforded the corresponding internal alkyne (**2-10**) (Scheme 2-4c(ii)), both in high yields without any loss of the optical purity of **2-7aa**, providing a new synthetic tool for the enantioselective preparation of internal alkynes with propargylic alkyl substituents. Furthermore, Pd/C-catalyzed hydrogenation³³ of **2-7aa** gave the corresponding diphenylalkane (**2-11**) in 96% yield (Scheme 2-4c(iv)), while the photoredox- and NiCl₂·6H₂O-catalyzed hydroalkylation of **2-7aa** with **2-4a**, the synthetic method very recently reported by our group,²⁶ afforded anti-Markovnikov-type alkylated alkene (**2-12**) in 70% yield as a mixture of (*E*)- and (*Z*)-isomers (*E/Z* = 89/11) (Scheme 2-4c(iv)), both almost without a loss of the optical purity of **2-7aa**.

Scheme 2-4. Additional scope and application for enantioselective propargylic alkylation reactions.

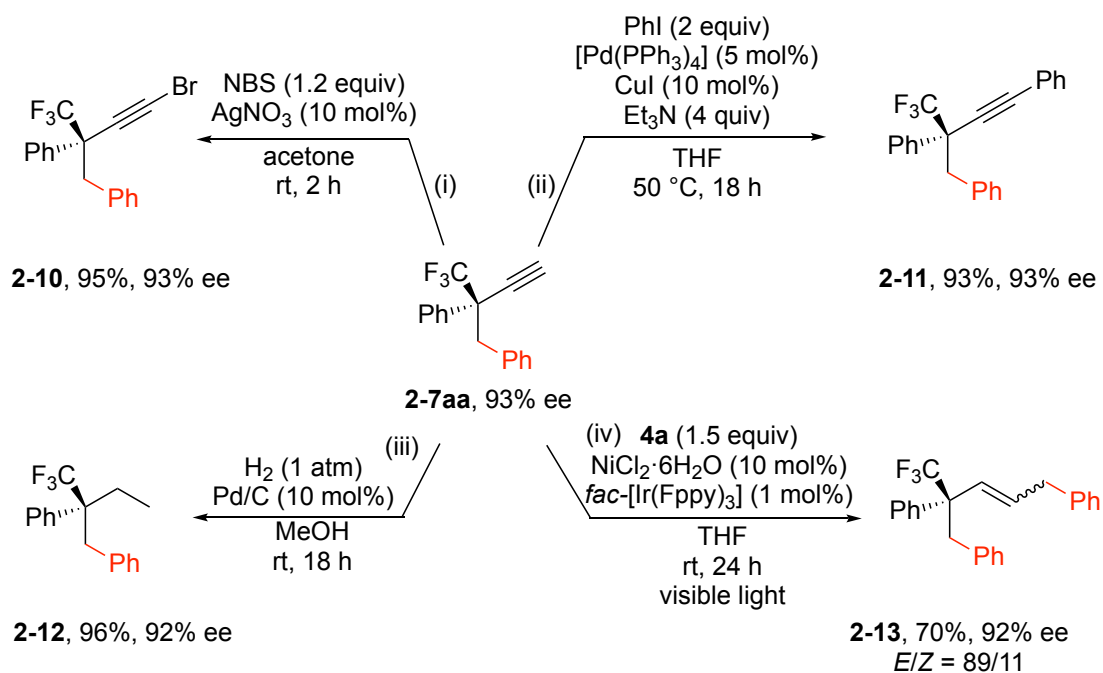
a. Enantioselective propargylic alkylation reaction of a propargylic alcohol bearing CF₂H instead of CF₃



b. Large-scale preparation of a chiral propargylic alkylated terminal alkyne



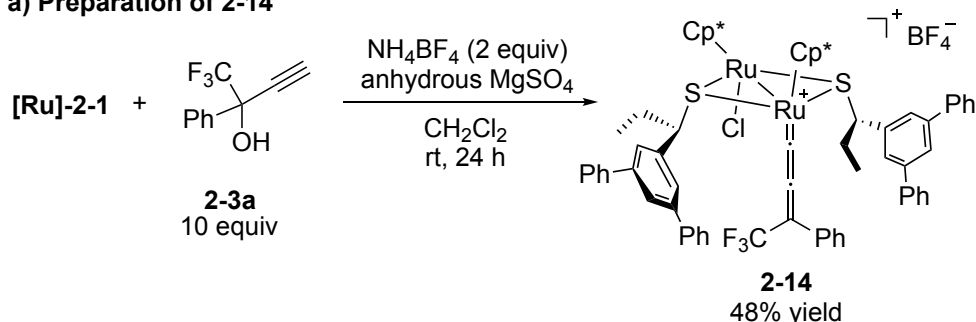
c. Transformations of a chiral propargylic alkylated terminal alkyne



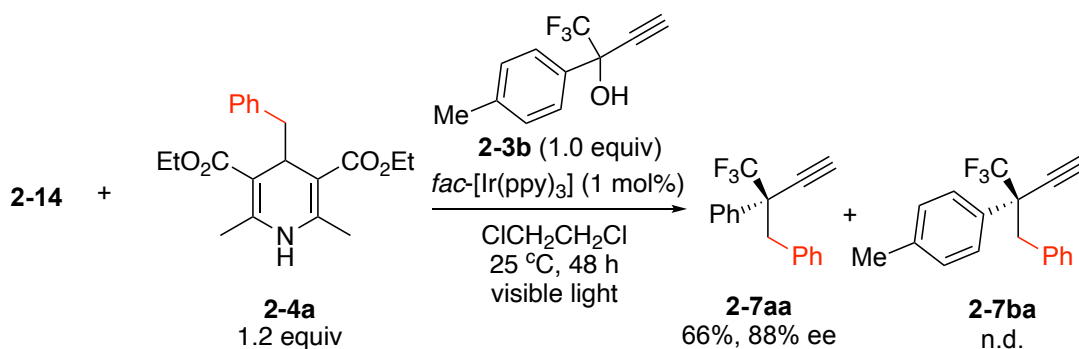
To obtain more information on the enantioselective induction, the corresponding ruthenium–allenylidene complex (**2-14**) was prepared in 48% yield from the reaction of **[Ru]-2-1** with 10 equiv of propargylic alcohol **2-3a** in the presence of 2 equiv of NH_4BF_4 and an excess amount of anhydrous MgSO_4 in CH_2Cl_2 at room temperature for 24 h (Scheme 2-5a).^{6f} When the reaction of **2-14** with 1.2 equiv of **2-4a** was carried out in the presence of 1 mol% of *fac*- $[\text{Ir}(\text{ppy})_3]$ and 1.0 equiv of **2-3b** but in the absence of $\text{BF}_3 \cdot \text{Et}_2\text{O}$ in $\text{ClCH}_2\text{CH}_2\text{Cl}$ at 25 °C for 48 h under visible light irradiation, the propargylic alkylated product **2-7aa** was obtained in 66% yield with 88% ee (Scheme 2-5b). Here, the corresponding propargylic alkylated product **2-7ba**, supposed to be produced by the reaction of **2-3b** with **2-4a**, was not obtained at all. Namely, **2-3b** only worked to promote the liberation of **2-7aa** from the ruthenium complex by ligand exchange, but further transformation did not take place for **2-3b** coordinated to the ruthenium catalyst **[Ru]-2-1**, when $\text{BF}_3 \cdot \text{Et}_2\text{O}$ was not present. These results clearly indicate that $\text{BF}_3 \cdot \text{Et}_2\text{O}$ does not participate in the alkylation of the allenylidene complex, but is necessary for the formation of allenylidene complex by accelerating the dehydration process from propargylic alcohols. Separately, the reaction of **2-3a** with 1.2 equiv of **2-4a** in the presence of 5 mol% of **2-14**, 1 mol% of *fac*- $[\text{Ir}(\text{ppy})_3]$, and 1.2 equiv of $\text{BF}_3 \cdot \text{Et}_2\text{O}$ in $\text{ClCH}_2\text{CH}_2\text{Cl}$ at 25 °C for 48 h was examined to afford **2-7aa** in 85% yield with 85% ee (Scheme 2-5c), clarifying that ruthenium–allenylidene complexes such as **2-14** worked as key reactive intermediates for the propargylic alkylation reactions.

Scheme 2-5. Preparation, Stoichiometric Conversion, and Catalytic Activity of Ru-Allenylidene Benzyl Complex

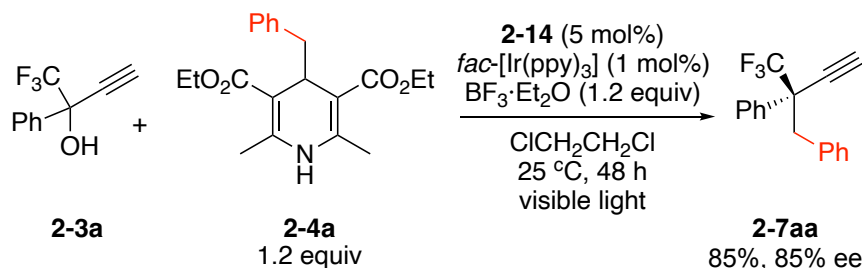
a) Preparation of 2-14



b) Stoichiometric reaction of 2-14 to afford 2-7aa



c) Reaction of 2-4a with 2-5a in the presence of 2-14 as catalyst



In order to get more mechanistic information of the reaction pathway, the author next investigated the propargylic alkylation reaction of **2-3a** with **2-4a** in the presence of 1.2 equiv of (2,2,6,6-tetramethylpiperidin-1-yl)oxyl (TEMPO) to capture radicals under the optimized reaction conditions. As a result, formation of propargylic alkylation product **2-7aa** was perfectly inhibited, while 1-(benzyloxy)-2,2,6,6-tetramethylpiperidine (**2-15**),³⁴ the TEMPO-trapped benzyl adduct, was obtained in 34% yield (Figure 2-1a). In contrast, formation of other TEMPO-trapped compounds was not observed, demonstrating that the formation of benzyl radicals preferentially occurred under photoredox catalytic conditions,^{13,15,17,19-21,35} whereas formation of propargylic radicals did not take place. This experimental result is in contrast to that obtained for palladium- and photoredox-catalyzed alkylation of a propargylic ester with **2-4a**, where TEMPO did not trap a benzyl radical but trapped a propargylic radical, which was proposed to be generated via a SET process between an excited palladium species and a propargylic ester in the presence of a base under visible light irradiation.^{21d}

Next, the propargylic alkylation reaction of **2-3a** with 1-deuterated 4-benzyl-1,4-dihydropyridine (**2-4a-D**) under the optimized reaction conditions was carried out to obtain the desired product **2-7aa** in 77% yield with 93% ee, where 30% of the acetylenic hydrogen atom of the product was found to be deuterium-labeled (Figure 2-1b), suggesting that a proton transfer occurs for the presumable intermediary alkynyl complex with the deuterated pyridinium cation obtained via the cleavage of **2-4a-D** to afford alkyl radical. Here, the lower D content of the acetylenic proton of **2-7aa** may be due to the presumable H–D isotope scrambling among the deuterated pyridinium cation derived from **2-4a-D**, NH_4BF_4 , and H_2O formed by the dehydration process from **2-3a**.

Next, Stern–Volmer analysis for emission quenching of *fac*-[Ir(ppy)₃] by **2-16** (allenylidene complex prepared by the reaction of $[\text{Cp}^*\text{RuCl}(\text{SMe})]_2$ with **2-3a** in the presence of NH_4BF_4 and anhydrous MgSO_4),^{3a} **2-3a** or **2-4a** was performed in $\text{ClCH}_2\text{CH}_2\text{Cl}$. As a result, the quenching rate constants were calculated to be $k_{2-16} = 1.7 \times 10^7 \text{ M}^{-1} \text{ s}^{-1}$, $k_{2-3a} = 5.3 \times 10^7 \text{ M}^{-1} \text{ s}^{-1}$ and $k_{2-4a} = 1.1 \times 10^8 \text{ M}^{-1} \text{ s}^{-1}$, respectively, by using the Stern–Volmer linear correlation relationships³⁶ and the lifetime of excited *fac*-[Ir(ppy)₃] at $\tau = 1.9 \text{ } \mu\text{s}$.³⁷ This result revealed that the quenching of photoexcited *fac*-[Ir(ppy)₃] by **2-4a** can occur twice as fast as that by **2-3a**, and 6.5 times as fast as that by **2-10** (Figure 2-1c). Here, cyclic voltammetric study of *fac*-[Ir(ppy)₃] revealed that the 1st oxidation wave of *fac*-[Ir(ppy)₃] in $\text{ClCH}_2\text{CH}_2\text{Cl}$ appeared at +0.25 V vs $\text{FeCp}_2^{+/0}$ ($\text{Cp} = \eta^5\text{-C}_5\text{H}_5$) as a reversible process, whereas the 1st reduction wave appeared at –1.60 V vs $\text{FeCp}_2^{+/0}$ as an irreversible process (Figure 2-4a). These correspond to the estimated redox potentials of *fac*-[Ir(ppy)₃][•]/*fac*-[Ir(ppy)₃][–] at +0.90 V vs $\text{FeCp}_2^{+/0}$ and *fac*-[Ir(ppy)₃]⁺/*fac*-[Ir(ppy)₃][•] at –2.25 V vs $\text{FeCp}_2^{+/0}$ by using the reported optical gap of *fac*-[Ir(ppy)₃] at 2.50 eV.³⁸ On the other hand, cyclic voltammogram of **2-4a** exhibited an irreversible oxidation wave at +0.53 vs $\text{FeCp}_2^{+/0}$ (Figure 2-4b), clarifying that photoexcited *fac*-[Ir(ppy)₃] can oxidize **2-4a** to afford the radical cation **2-4a**^{•+} via a SET process, where the C–C bond scission further occurs to give the benzyl radical and a pyridinium cation. As for the propargylic moiety, oxidation of **2-3a** was found to be difficult to occur, but an irreversible reduction wave was observed at –1.36 V vs $\text{FeCp}_2^{+/0}$ of **2-3a** in $\text{ClCH}_2\text{CH}_2\text{Cl}$ (Figure 2-4c). Thus, the possibility that the reduction of **2-3a** by the photoexcited *fac*-[Ir(ppy)₃] proceeds to afford the radical anion **2-3a**^{•–} via a SET process, as has been proposed for the formation of propargylic radicals via a SET process of propargylic esters with an excited palladium species,^{21d} cannot be excluded based on the Stern–Volmer and cyclic voltammetric studies. However, radical capture experiment by TEMPO has clearly clarified that such a SET process to generate the corresponding propargylic radical almost did not occur, but quenching of photoexcited *fac*-[Ir(ppy)₃] by **2-3a** occurred rather via triple state energy transfer. Similarly, the possibility of the redox of diruthenium complexes by the photoexcited *fac*-[Ir(ppy)₃] cannot be excluded based on the previous CV measurements,³⁹ whereas quenching experiments have clarified that such a SET process occurs by one order of magnitude less frequently than the SET process between *fac*-[Ir(ppy)₃] and **2-4a**.

Additionally, a light on/off experiment was performed for propargylic alkylation

reaction of **2-3a** with **2-4a** to afford **2-7aa**, under the typical catalytic reaction conditions. As shown in Figure 2-2a, the reaction proceeded smoothly under visible light irradiation, but did not proceed in dark, which evinced the requirement of continuous visible light irradiation is necessary, but less possibility of chain propagation participating in the main reaction pathway. By using Hg lamp filtered at 440 nm instead of LED light, the quantum yield of alkylation reactions of **2-3a** with **2-4a** under typical reaction conditions was determined at $\Phi = 0.05$ by chemical actinometry⁴⁰ (Figure 2-2a). Both the light on/off experiment and the quantum yield measurement have clarified that the rate-determining step of the catalytic formation of **2-7aa** proceeds rather via sequential redox pathways, but not via a radical chain process.⁴¹ Thus, the alkyl radicals *in situ* are mainly formed by the SET process between an excited-state photoredox catalyst and 4-alkyl-1,4-dihydropyridines.^{13,17–19,3513,17–19,42}

Finally, the time course study for propargylic alkylation reaction of **2-3a** with **2-4a** to afford **2-7aa** under the typical catalytic reaction conditions was investigated (Figure 2-2b). As a result, the present dual photoredox- and ruthenium-catalyzed reaction was shown to follow the zeroth order kinetics, typical for photochemical reactions under saturation of catalysts with reactants, in the optimized reaction conditions.

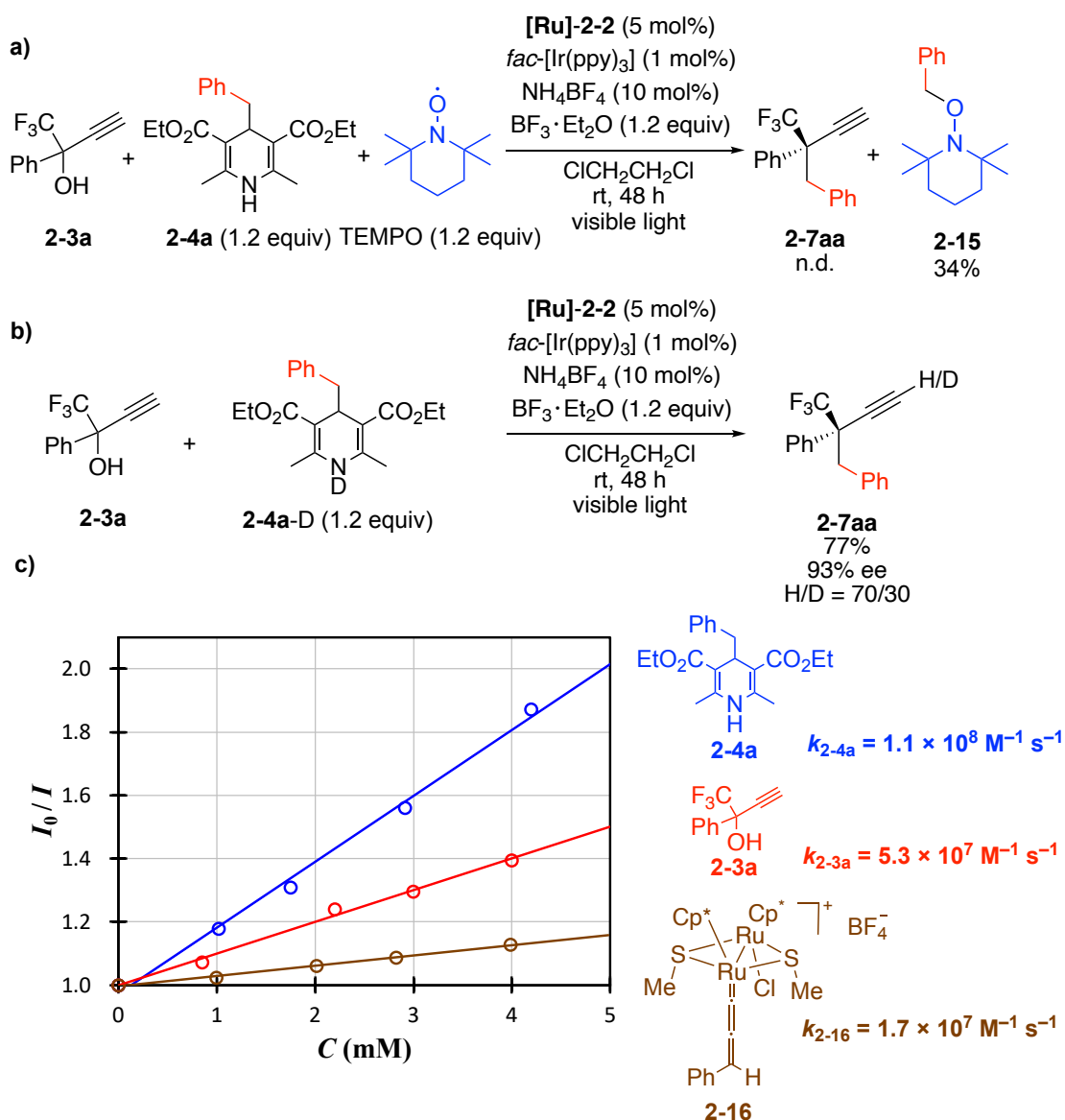


Figure 2-1. Mechanistic studies on the propargylic alkylation reactions of **2-3a** with **2-4a**. (a) Reactions in the presence of TEMPO. (b) Deuterium labeled reaction. (c) Determination of quenching constants by Stern–Volmer plot.

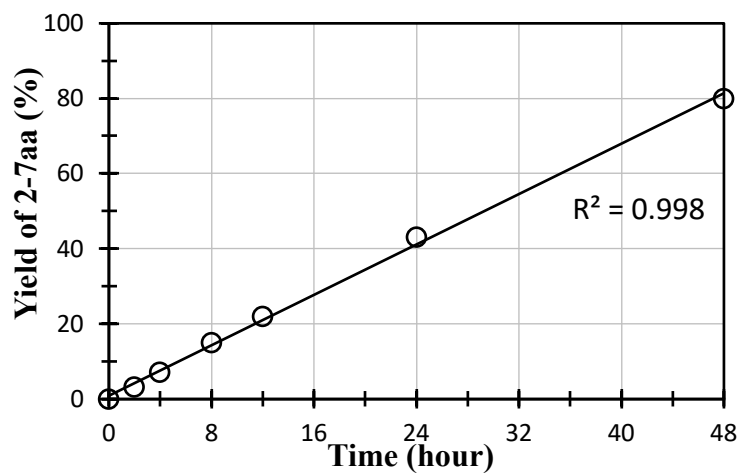
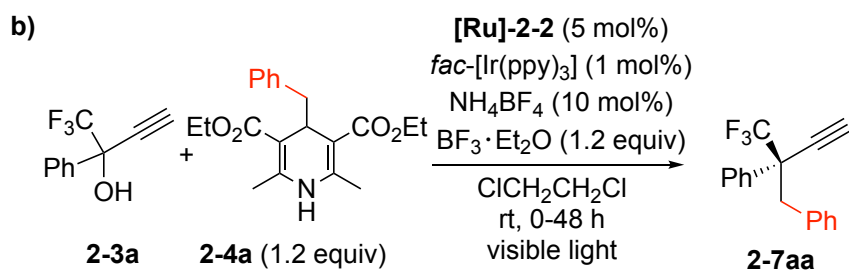
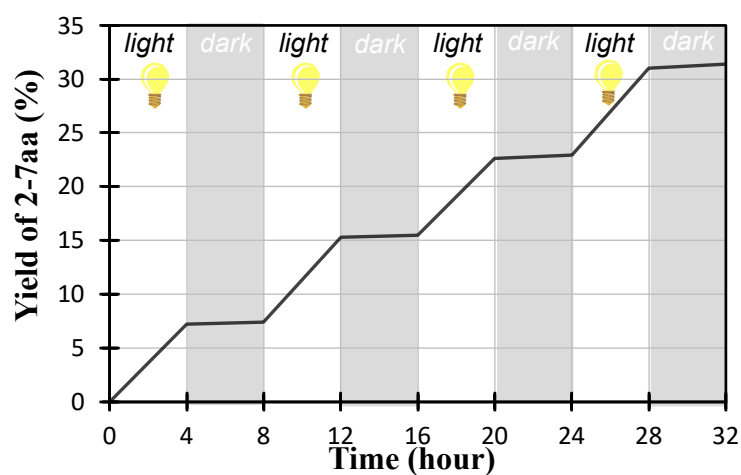
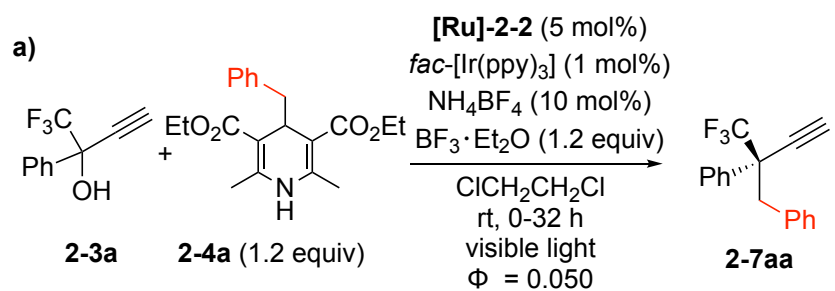


Figure 2-2. Mechanistic studies on the propargylic alkylation reactions of **2-3a** with **2-4a**. (a) Reaction profiles during the light-on and -off sequences. (b) Reaction profile for the time course study.

To obtain more information on the radical reactions mediated by ruthenium–allenylidene complexes, DFT calculations have been performed for the reaction of the achiral diruthenium–allenylidene complex **2-17**⁺ with the benzyl radical (Bn•) and the pyridinium cation (PyH⁺) (pKa = 2.96 in H₂O)⁴³ generated via the scission of 4-benzyl-1,4-dihydropyridine **2-4a**, and the reduced iridium(II) species *fac*-[Ir(ppy)₃][−] (²[Ir(ppy)₃][−]) in ClCH₂CH₂Cl to afford a vinylidene complex, aromatized pyridine (Py), and the regenerated iridium(III) catalyst *fac*-[Ir(ppy)₃] (¹[Ir(ppy)₃]) (Figure 2-3a). Here, the attack of the benzyl radical (Bn•) to the γ-carbon (C^γ) atom in the monocationic diruthenium–allenylidene complex **I** (= **2-17**⁺) gives the monocationic diruthenium–alkynyl radical complex **III** via the formation of the reactant complex **II** and the transition state **TSII-III**. The Gibbs free energies (Δ*G*^{298K}) of **II**, **TSII-III**, and **III** relative to the initial state (**I** + Bn•) are 4.0, 7.5 and −24.8 kcal/mol, respectively (Figure 2-3a and Fig. S4 for energy diagram and structures, respectively), indicating that these reaction steps smoothly proceed. The results of IRC calculations for **TSII-III** are shown Fig. S5. The change in the Mulliken spin density of atoms (Fig. S5b) shows that the radical center moves from the carbon atom of the benzyl radical to the allenylidene region along the reaction coordinate (ruthenium and C^β atoms). The SOMO, which has in-phase overlapping between the C^γ atom in the allenylidene complex and the carbon atom in benzyl radical, is gradually stabilized along the reaction coordinate, and the MO becomes doubly occupied (Fig. S6). The spin density surface of **III** (Fig. S6) also demonstrates delocalization of spin density, indicating the importance of the diruthenium system.

The monocationic diruthenium–alkynyl radical complex **III** is then exergonically reduced by ²[Ir(ppy)₃][−] to form the neutral diruthenium–alkynyl complex **IV** (**III** + ²[Ir(ppy)₃][−] (Δ*G*^{298K} = −24.8 kcal/mol) → **IV** + ¹[Ir(ppy)₃] (Δ*G*^{298K} = −92.8 kcal/mol)), while **III** is endergonically protonated by protonated pyridine to afford the dicationic diruthenium–vinylidene complex **VI** (**III** + PyH (Δ*G*^{298K} = −24.8 kcal/mol) → **VI** + Py (Δ*G*^{298K} = −9.5 kcal/mol)). Thus, it is more likely that **III** is first reduced to afford **IV**, and then **IV** is protonated to afford the diruthenium–vinylidene complex **V** (Δ*G*^{298K} = −98.5 kcal/mol). The protonation of **IV** was calculated to be endergonic by 5.7 kcal/mol. The present DFT calculations indicate that the attack of benzyl radical to the C^γ atom in the ruthenium–allenylidene complex followed by the reduction and protonation easily gives the ruthenium–vinylidene complex.

It should be carefully paid attention that two reaction pathways can be possible for the formation of the vinylidene complex **V** from the allenylidene complex **I** (or **2-17**⁺): one is the attack of Bn• to the allenylidene complex **2-17**⁺ to form the monocationic alkynyl radical complex **III** at first, followed by the one-electron reduction by ²[Ir(ppy)₃][−] to generate the vinylidene complex **V** (Figure 2-3b(i)) as has been shown by the DFT calculations in Figure 2-3a; the other is one-electron reduction of the allenylidene complex **2-17**⁺ by ²[Ir(ppy)₃][−] to form the neutral alkynyl radical complex **III'** (or **2-17**•) at first, followed by the attack of Bn• (Figure 2-3b(ii)). Indeed, mononuclear ruthenium allenylidene complexes were known to be reduced by strong reducing reagents such as cobaltocene to afford the radical species,⁴⁴ which were known to react with radical reagents.⁴⁵ However, the author's group previously found that the

thiolate-bridged diruthenium complex [$\{\text{Cp}^*\text{RuCl}(\mu\text{-SMe})\}_2$] underwent reductive coupling of propargylic alcohols including **2-1** to afford 1,5-hexadiynes under reductive conditions.⁴⁶ Here, a neutral alkynyl radical complex (**2-17•**) was generated in situ by the reaction of **2-17**⁺BF₄ with a trace amount of oxygen, which reacted with another radical species in the presence of a proton source to afford the corresponding propargylic homo-coupled product (Figure 2-3b). However, such compounds were not obtained at all, both for the reaction of **2-3a** with **2-4a** (Table 1, entry 8) or for the reaction of **2-3a** with **2-4a** in the present reaction conditions except for using [$\{\text{Cp}^*\text{RuCl}(\mu\text{-SMe})\}_2$] as a ruthenium catalyst instead of **[Ru]-2-1** or **[Ru]-2-2**. The corresponding propargylic radicals were also not trapped by TEMPO (Figure 2-1a), ruling out the possibility of the formation of ruthenium(II) radical species before the attack of benzyl radical.

For the enantioselective induction, similar enantioselectivity was already observed for the ruthenium-catalyzed enantioselective propargylic phosphinylation of propargylic alcohols,⁴ where the mechanism of enantioselective induction has been recently revised by DFT calculations for the reaction of the ruthenium–allenylidene complex **2-14**⁺,²⁹ which can be prepared by the reaction of **[Ru]-2-1** with **2-3a**, with a nucleophile.⁴ Here, enantioselectivity has been indicated to be induced by intramolecular C–H/F and π/π interactions among the allenylidene, the optically active thiolate, and pentamethylcyclopentadienyl ligands in the ruthenium–allenylidene complex, where a nucleophile attacks from the *Re* face (Figure 2-3c).²⁹

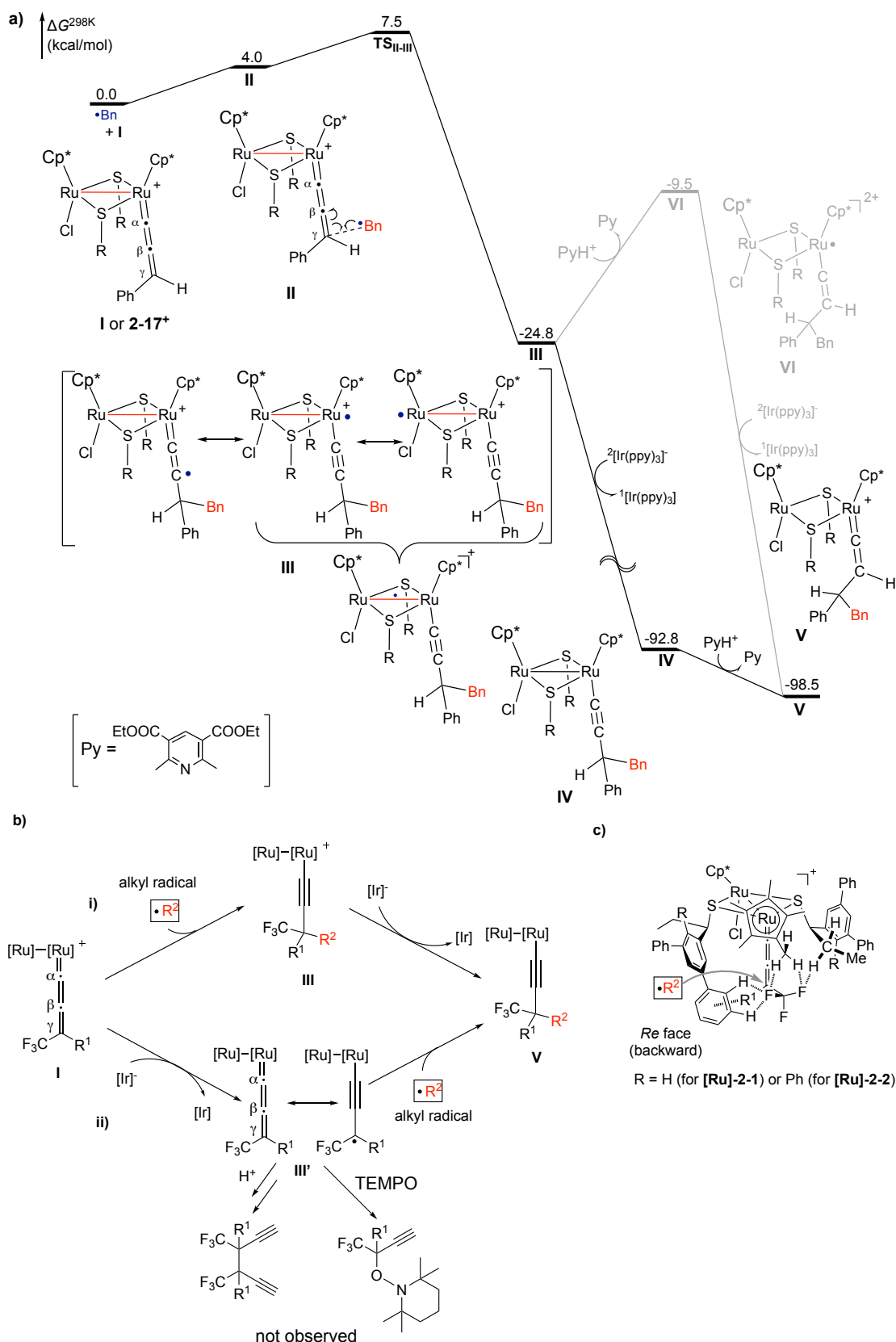
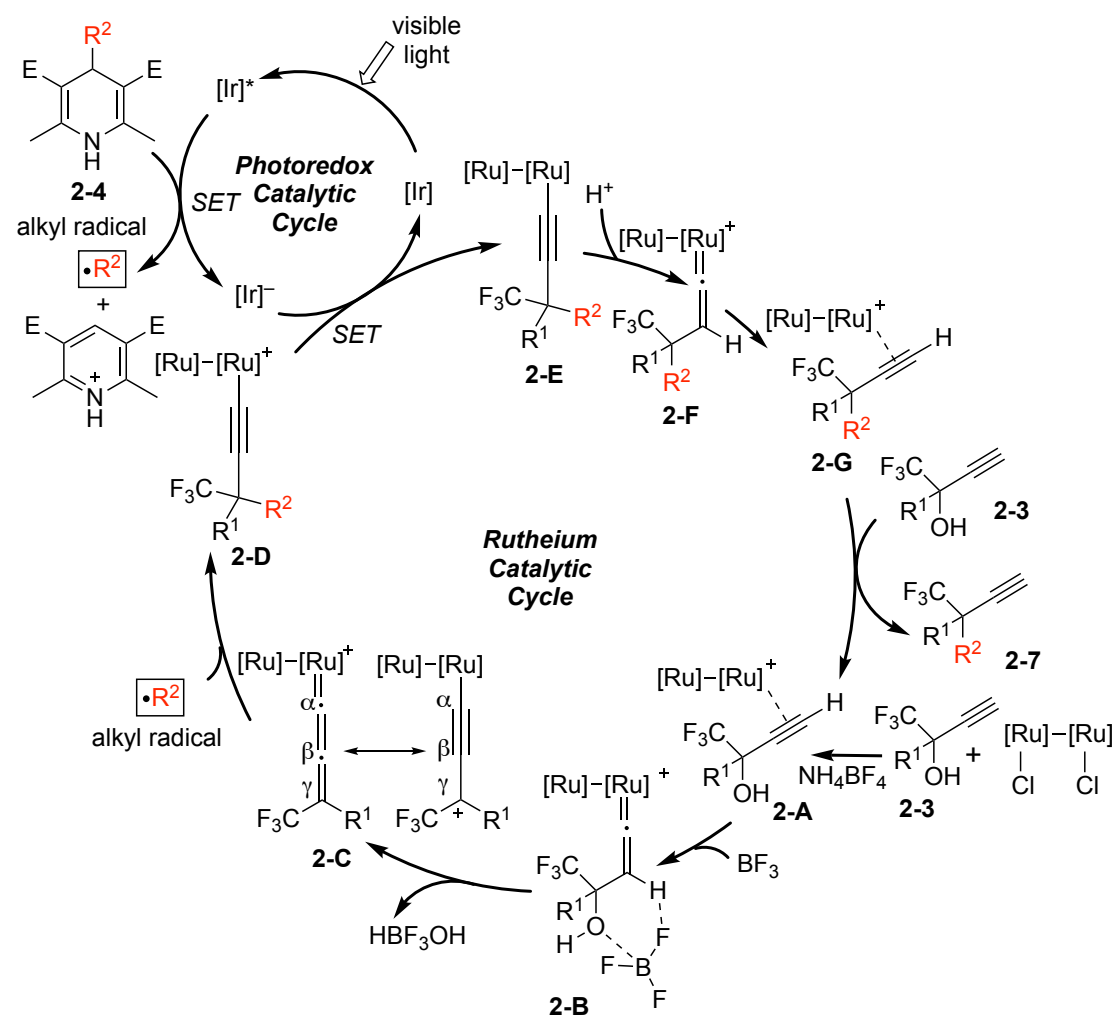


Figure 2-3. DFT calculations for reactions of allenylidene complexes. (a) Energy diagram for the reaction of a ruthenium–allenyldiene complex with benzyl radical, a reduced Ir(II) species, and a pyridinium cation. (b) Two possible reaction pathways. (c)

Intramolecular π/π and C–H/F interactions for the reaction of a ruthenium–allenylidene complex with a nucleophile (NuH) proposed by the DFT calculations.⁸⁶

Based on the mechanistic studies, a plausible catalytic reaction pathway can be drawn as depicted in [Scheme 2-6](#), containing two catalytic cycles: the photoredox catalytic cycle and the ruthenium catalytic cycle. In the photoredox cycle, the iridium catalyst [Ir] is excited under visible light irradiation to afford a photoexcited iridium catalyst [Ir]*. Then, a SET process between [Ir]* and 4-alkyl-1,4-dihydropyridine (**2-4**) occurs to give the reduced iridium catalyst [Ir][–], an alkyl radical, and a pyridinium cation via C–C bond scission. On the other hand, in the ruthenium cycle, coordination of the propargylic alcohol first occurs to afford π -alkyne complex (**2-A**), leading to the formation of the vinylidene complex (**2-B**) via 1,2-proton transfer. Then, dehydration accelerated by BF₃·Et₂O occurs to give the allenylidene complex (**2-C**). Then, alkyl radical attacks at the γ -position of the allenylidene ligand of (**2-C**) from *Re* face to afford the alkynyl radical complex ((**2-D**)), where the enantioselectivity is inducted by intramolecular C–H/ π and π/π interactions among the allenylidene, the optically active thiolate, and pentamethylcyclopentadienyl ligands in the ruthenium–allenylidene complex. The alkynyl complex (**2-D**) is then reduced by the iridium(II) species [Ir][–] through single electron transfer to afford the allenylidene complex (**2-E**), then protonation at the β -position occurs, presumably by the pyridinium cation ($pK_a = 2.96$ in H₂O)³⁶ formed via the scission of 4-alkyl-1,4-dihydropyridines to afford the vinylidene complex (**2-F**), followed by the proton transfer to afford the π -alkyne complex (**2-G**). Finally, ligand exchange with propargylic alcohol gives the product (**2-7**) and regenerates the starting π -alkyne complex (**2-A**).

Scheme 2-6. Plausible Catalytic Reaction Pathways



2.3. Conclusion for Chapter 2

The author has succeeded in the photoredox- and ruthenium-catalyzed enantioselective propargylic alkylation of propargylic alcohols with 4-alkyl-1,4-dihydropyridines under ambient conditions under visible light irradiation. Especially, the author has succeeded in the construction of a quaternary stereogenic carbon center at the propargylic position. This is the first successful example of photoredox- and ruthenium-catalyzed enantioselective propargylic substitution reactions, where propargylic alkylated products with nonactivated, simple alkyl group introduced at the propargylic position are obtained enantioselectively, demonstrating that alkyl radicals generated by the photoredox catalysis can act as the alternatives to nucleophiles for propargylic substitution reactions. Here, the key reaction step is the attack of alkyl radical to the γ -carbon of the ruthenium-allenylidene complex, where enantioselectivity of the product is determined by the optically active thiolate ligands. This present work has newly developed dual photoredox- and ruthenium-catalytic systems, and has successfully expanded the usage of 4-alkyl-1,4-dihydropyridine skeletons as milder alkylation reagents toward the enantioselective propargylic substitution reactions. The author believes this work provides a new fundamental method for organic syntheses under mild reaction conditions.

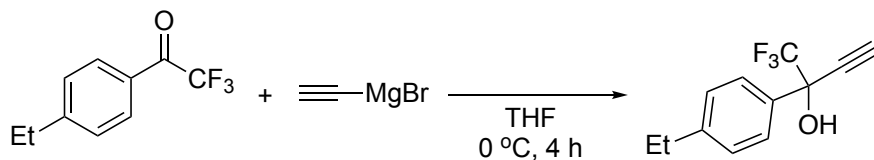
2.4. Experimental Section

2.4.1. General Methods

All reactions were carried out under a dry nitrogen atmosphere by using standard Schlenk techniques. **2-1**,⁴⁷ **2-2**,⁴⁸ **2-3a**,⁴⁹ **2-3b**,⁵⁰ **2-3d**,^{6f} **2-3e**,⁵¹ **2-3f**,⁵¹ **2-3g**,⁵² **2-3i**,^{7q} **2-3j**,⁵¹ **2-3n**,⁵¹ **2-4a**,⁵³ **2-4b**,⁵³ **2-4c**,⁵³ **2-4e**,⁵⁴ **2-4f**,⁵³ **2-4g**,²² **2-4j**,¹³ **2-4k**,¹⁸ **2-4d**,⁵³ **2-4l**,¹³ **2-4m**,⁵⁴ **2-4n**,^{25b} **2-4p**,¹³ **2-4q**,⁵³ **2-4r**,¹⁷ **2-4t**,⁵⁵ **2-4u**,¹⁹ **2-4v**,²² **[Ru]-2-1**,⁴ and **[Ru]-2-2**⁴ were prepared according to the literature procedures. Other reagents include starting materials for the preparation of **2-3a–t**, **2-4a–y**, *fac*-[Ir(ppy)₃], *fac*-[Ir(Fppy)₃], [Ir(ppy)₂(dtbbpy)]PF₆, NH₄BF₄, Lewis acids, TEMPO, and solvents were obtained from commercial sources. Solvents were dried by general methods and degassed before use. Flash column chromatography was carried out on a Yamazen YFLC-AI-580 system. Gas chromatography–mass spectroscopy (GC–MS) was performed on a Shimadzu GCMS-QP2010 PLUS instrument. HPLC analyses were performed on Hitachi L-7100 and GL-7410 apparatuses equipped with a UV detector using 25 cm x 4.6 mm DAICEL Chiralpak columns. Specific rotations were measured on a JASCO DIP-1000 polarimeter. X-ray analysis was performed by a Rigaku XtaLAB Synergy-S diffractometer. Photoluminescence spectra were measured on a Shimadzu RF-5300PC spectrophotometer. Melting points were measured by using a Stanford Research Systems OptiMelt MPA100. High-resolution FAB mass spectra were measured on a JEOL JMS-700 mass spectrometer. Specific rotations were measured on a JASCO DIP-1000 polarimeter. ¹H NMR (400 MHz), ¹³C {¹H} NMR (100 MHz), and ¹⁹F NMR (376 MHz, referenced to CF₃C₆H₅ in CDCl₃ at δ –64.0) spectra were measured in CDCl₃, (CD₃)₂CO or CD₃CN on a JEOL ECS-400 spectrometer with δ values in ¹H and ¹³C {¹H} NMR calibrated by using residual peaks of CHCl₃ (¹H: 7.26; ¹³C: 77.0), (CD₂H)₂CO (¹H, 2.09; ¹³C: 206.0), CD₂HCN (¹H, 1.93; ¹³C: 117.7) respectively.

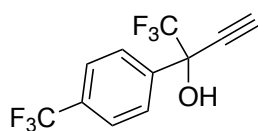
2.4.2. General Procedure for the Preparation of Propargylic Alcohol Substrates (2-3 and 2-8) (Taking 1,1,1-Trifluoro-2-(4-ethylphenyl)but-3-yn-2-ol (2-3c) as an Example)

Scheme 2-7. Preparation of Propargylic Alcohol Substrates 2-3c



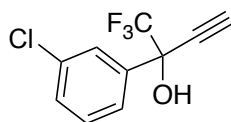
To a solution of 2,2,2-trifluoro-1-(4-ethylphenyl)ethan-1-one (3.00 mmol, 607 mg) in anhydrous THF (15 mL) was added ethynylmagnesium bromide (0.5 M in THF, 9.0 mL, 4.5 mmol) at 0 °C. After stirring for 4 h, the mixture was quenched by saturated NH₄Cl aq. (4 mL), and the solution was extracted with Et₂O (10 mL x 2). The combined organic layers were dried over anhydrous Na₂SO₄ and concentrated under reduced pressure. The residue was purified by column chromatography with hexane/EtOAc

(95:5-90:10) to give 1,1,1-trifluoro-2-(4-ethylphenyl)but-3-yn-2-ol (**2-3c**) as a pale yellow oil (588.8 mg, 2.58 mmol, 86% isolated yield), (**Scheme 2-7**). ^1H NMR ($(\text{CD}_3)_2\text{CO}$, 400 MHz): δ 7.76 (d, J = 8.0 Hz, 2H, *m*-H of C_6H_4), 7.33 (d, J = 8.8 Hz, 2H, *o*-H of C_6H_4), 6.67 (s, 1H, H of OH), 3.49 (s, 1H, $\text{HC}\equiv$), 2.71 (q, J = 7.6 Hz, 2H, CH_2), 1.27 (t, J = 7.6 Hz, 3H, CH_3). $^{13}\text{C}\{^1\text{H}\}$ NMR ($(\text{CD}_3)_2\text{CO}$, 100 MHz): δ 145.7 (*ipso*-C of C_6H_4), 133.8 (*p*-CH of C_6H_4), 127.7 (*m*-CH of C_6H_4), 127.4 (*o*-CH of C_6H_4), 124.1 (q, $^1J_{\text{C-F}}$ = 284 Hz, CF_3 of C_6H_4), 80.3 ($\text{C}\equiv$), 77.1 ($\text{HC}\equiv$), 71.4 (q, $^2J_{\text{C-F}}$ = 31.7 Hz, $\text{CC}\equiv$), 28.4 (CH_2), 15.2 (CH_3). ^{19}F NMR ($(\text{CD}_3)_2\text{CO}$): δ -82.4. HRMS (FAB+) Calcd. for $\text{C}_{12}\text{H}_{11}\text{F}_3\text{O}$ $[\text{M}]^+$: 228.0762. Found: 228.0763.



2-3h

1,1,1-Trifluoro-2-(4-(trifluoromethyl)phenyl)but-3-yn-2-ol (2-3h). ^1H NMR (CDCl_3 , 400 MHz): δ 7.88 (d, J = 8.8 Hz, 2H, *m*-H of C_6H_4), 7.69 (t, J = 8.0 Hz, 2H, *o*-H of C_6H_4), 3.37 (s, 1H, $\text{HC}\equiv$), 2.87 (s, 1H, H of OH). ^{13}C NMR spectrum of this compound was measured in acetone- d_6 because some peaks of this compound overlapped with those of CDCl_3 . $^{13}\text{C}\{^1\text{H}\}$ NMR ($(\text{CD}_3)_2\text{CO}$, 100 MHz): δ 141.3 (*ipso*-C of C_6H_4), 131.7 (q, $^1J_{\text{C-F}}$ = 31.7 Hz, *p*-CH of C_6H_4), 128.8 (*m*-CH of C_6H_4), 125.9 (q, $^2J_{\text{C-F}}$ = 3.9 Hz, *o*-CH of C_6H_4), 124.9 (q, $^3J_{\text{C-F}}$ = 270 Hz, CF_3 of C_6H_4), 124.2 (q, $^4J_{\text{C-F}}$ = 284 Hz, CF_3), 79.7 ($\text{C}\equiv$), 78.7 ($\text{HC}\equiv$), 72.6 (q, $^5J_{\text{C-F}}$ = 32.6 Hz, $\text{CC}\equiv$). ^{19}F NMR (CDCl_3): δ -62.9, -80.4. HRMS (FAB+) Calcd. for $\text{C}_{11}\text{H}_7\text{F}_6\text{O}$ $[\text{M}+\text{H}]^+$: 269.0401. Found: 269.0401.



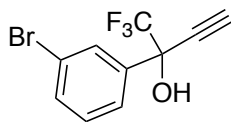
2-3k

1,1,1-Trifluoro-2-(3-chlorophenyl)but-3-yn-2-ol (2-3k). A pale yellow oil (667.1 mg, 2.49 mmol, 83% isolated yield).

^1H NMR ($(\text{CD}_3)_2\text{CO}$, 400 MHz): δ 7.75 (s, 1H, *o*-H of C_6H_4), 7.63 (d, J = 7.6 Hz, 1H, *p*-H of C_6H_4), 7.42-7.40 (m, 1H, *m*-H of C_6H_4), 7.36 (t, J = 7.8 Hz, 1H, *o*-H of C_6H_4), 3.26 (s, 1H, $\text{HC}\equiv$), 2.85 (s, 1H, H of OH).

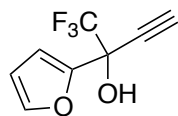
$^{13}\text{C}\{^1\text{H}\}$ NMR ($(\text{CD}_3)_2\text{CO}$, 100 MHz): δ 136.4 (*ipso*-C of C_6H_4), 134.3 (*m*-CH of C_6H_4), 129.9 (*m*-CH of C_6H_4), 129.5 (*o*-CH of C_6H_4), 127.4 (*p*-CH of C_6H_4), 125.3 (*o*-CH of C_6H_4), 122.8 (q, $^1J_{\text{C-F}}$ = 284 Hz, CF_3), 78.8 ($\text{C}\equiv$), 77.2 ($\text{HC}\equiv$), 72.3 (q, $^2J_{\text{C-F}}$ = 32.5 Hz, $\text{CC}\equiv$).

^{19}F NMR ($(\text{CD}_3)_2\text{CO}$): δ -82.0. HRMS (FAB+) Calcd. for $\text{C}_{10}\text{H}_6\text{ClF}_3\text{O}$ $[\text{M}]^+$: 234.0059. Found: 234.0068.



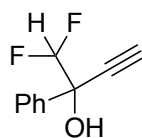
2-3l

1,1,1-Trifluoro-2-(3-bromophenyl)but-3-yn-2-ol (2-3h). A pale yellow oil (667.1 mg, 2.40 mmol, 80% isolated yield). ^1H NMR ($(\text{CD}_3)_2\text{CO}$, 400 MHz): δ 8.09 (s, 1H, *o*-H of C_6H_4), 7.92 (d, $J = 8.0$ Hz, 1H, *p*-H of C_6H_4), 7.77-7.75 (m, 1H, *m*-H of C_6H_4), 7.54 (t, $J = 8.0$ Hz, 1H, *o*-H of C_6H_4), 7.09 (s, 1H, H of OH), 3.68 (s, 1H, $\text{HC}\equiv$). $^{13}\text{C}\{^1\text{H}\}$ NMR ($(\text{CD}_3)_2\text{CO}$, 100 MHz): δ 138.6 (*ipso*-C of C_6H_4), 132.3 (*o*-CH of C_6H_4), 130.0 (*o*-CH of C_6H_4), 129.9 (*m*-CH of C_6H_4), 126.1 (*m*-CH of C_6H_4), 123.4 (q, $^1J_{\text{C-F}} = 284$ Hz, CF_3), 121.6 (*p*-CH of C_6H_4), 79.0 ($\text{C}\equiv$), 77.6 ($\text{HC}\equiv$), 71.5 (q, $^2J_{\text{C-F}} = 31.9$ Hz, $\text{CC}\equiv$). ^{19}F NMR ($(\text{CD}_3)_2\text{CO}$): δ -82.3. HRMS (FAB+) Calcd. for $\text{C}_{10}\text{H}_6\text{BrF}_3\text{O}$ $[\text{M}]^+$: 277.9554. Found: 277.9565.



2-3m

1,1,1-Trifluoro-2-(furan-2-yl)but-3-yn-2-ol (2-3m). A pale yellow oil (427.7 mg, 2.25 mmol, 75% isolated yield). ^1H NMR (CDCl_3 , 400 MHz): δ 7.48 (d, $J = 1.2$ Hz, 1H, 5-H of $\text{C}_4\text{H}_3\text{O}$), 6.69 (d, $J = 3.6$ Hz, 1H, 3-H of $\text{C}_4\text{H}_3\text{O}$), 6.42 (q, $J = 1.7$ Hz, 1H, 4-H of $\text{C}_4\text{H}_3\text{O}$), 3.52 (brs, 1H, H of OH), 2.77 (s, 1H, $\text{HC}\equiv$). $^{13}\text{C}\{^1\text{H}\}$ NMR (CDCl_3 , 100 MHz): δ 146.8 (*ipso*-C of $\text{C}_4\text{H}_3\text{O}$), 144.2 (5-C of $\text{C}_4\text{H}_3\text{O}$), 122.4 (q, $^1J_{\text{C-F}} = 285$ Hz, CF_3), 111.1 (4-C of $\text{C}_4\text{H}_3\text{O}$), 110.8 (3-C of $\text{C}_4\text{H}_3\text{O}$), 76.7 ($\text{C}\equiv$), 76.3 ($\text{HC}\equiv$), 69.0 (q, $^2J_{\text{C-F}} = 34.5$ Hz, $\text{CC}\equiv$). ^{19}F NMR ($(\text{CD}_3)_2\text{CO}$): δ -81.5. HRMS (FAB+) Calcd. for $\text{C}_8\text{H}_6\text{F}_3\text{O}_2$ $[\text{M}+\text{H}]^+$: 191.0320. Found: 191.0318.

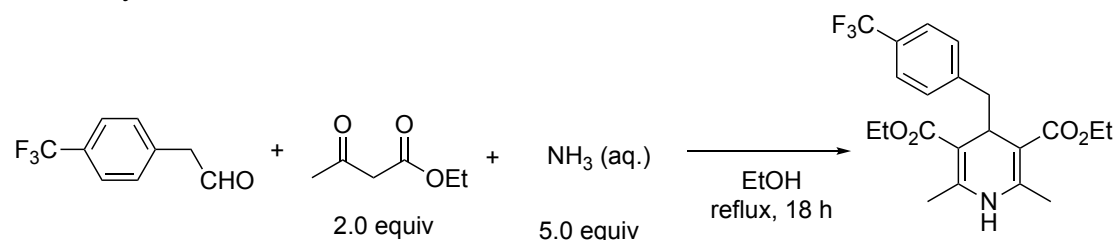


2-8

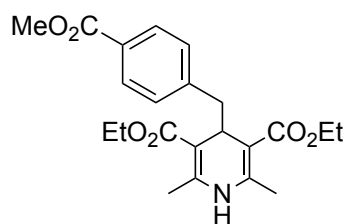
1,1-Difluoro-2-phenylbut-3-yn-2-ol (2-8). A pale yellow oil (477.3 mg, 2.61 mmol, 87% isolated yield). ^1H NMR ($(\text{CD}_3)_2\text{CO}$, 400 MHz): δ 7.70-7.68 (m, 2H, *m*-H of Ph), 7.47-7.39 (m, 3H, *o*-H and *p*-H of Ph), 5.72 (t, $J_{\text{H-F}} = 56.0$ Hz, 1H, CF_2H), 3.02 (s, 1H, $\text{HC}\equiv$), 2.80 (s, 1H, H of OH). ^{13}C NMR spectrum of this compound was measured in acetone- d_6 because some peaks of this compound overlapped with those of CDCl_3 . $^{13}\text{C}\{^1\text{H}\}$ NMR ($(\text{CD}_3)_2\text{CO}$, 100 MHz): δ 137.8 (*ipso*-C of Ph), 128.8 (*m*-CH of Ph), 128.1 (*p*-CH of Ph), 127.0 (*o*-CH of Ph), 115.4 (t, $^1J_{\text{C-F}} = 250$ Hz, CF_2H), 81.2 ($\text{C}\equiv$), 76.9 ($\text{HC}\equiv$), 72.3 (t, $^2J_{\text{C-F}} = 23.5$ Hz, $\text{CC}\equiv$). ^{19}F NMR ($(\text{CD}_3)_2\text{CO}$): δ -129.2 (dd, $J = 276, 56.9$ Hz), -129.3 (dd, $J = 276, 59.7$ Hz). HRMS (FAB+) Calcd. for $\text{C}_{10}\text{H}_8\text{F}_2\text{O}$ $[\text{M}]^+$: 182.0543. Found: 182.0548.

2.4.3. General Procedure for the Preparation of 4-Alkyl-1,4-dihydropyridine Derivatives (2-4) (Taking Diethyl 2,6-dimethyl-4-(4-(trifluoromethyl)benzyl)-1,4-dihydropyridine-3,5-dicarboxylate (2-4h) as an Example)

Scheme 2-8. Preparation of Diethyl 4-Alkyl-2,6-dimethyl-1,4-dihydropyridine-3,5-dicarboxylate Derivatives **2-4h**



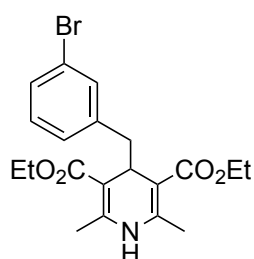
In a 50 mL Schlenk flask were placed 2-(4-(trifluoromethyl)phenyl)acetaldehyde (940.8 mg, 5.00 mmol), ethyl acetoacetate (1301.4 mg, 10.00 mmol), and ethanol (20 mL) at room temperature under N₂, where an aqueous solution of 28 wt % NH₃ (1.5 mL, *ca.* 25 mmol) was added. The reaction mixture was stirred and refluxed for 18 h by using an oil bath, then was dried in vacuo. The residue was further purified by column chromatography (SiO₂) with a mixture of *n*-hexane/ethyl acetate (7:3) as an eluent to afford diethyl 2,6-dimethyl-4-(4-(trifluoromethyl)benzyl)-1,4-dihydropyridine-3,5-dicarboxylate (**2-4h**) as a white solid (1070.1 mg, 2.60 mmol, 52% yield based on the amount of 2-(4-(trifluoromethyl)phenyl)acetaldehyde) m.p.= 129.0-130.2 °C. ¹H NMR (400 MHz, CDCl₃, δ): 7.40 (d, *J* = 8.0 Hz, 2H, *m*-H of C₆H₄), 7.11 (d, *J* = 7.6 Hz, 2H, *o*-H of C₆H₄), 6.02 (s, 1H, NH), 4.18 (t, *J* = 5.8 Hz, 1H, 4-CH of 1,4-dihydropyridine), 4.08–3.92 (m, 4H, CH₃CH₂), 2.60 (d, *J* = 5.6 Hz, 2H, CH₂ of 4-(trifluoromethyl)phenylmethyl), 2.16 (s, 6H, 2-CCH₃ of 1,4-dihydropyridine) 1.17 (t, *J* = 7.2 Hz, 6H, CH₃CH₂). ¹³C {¹H} NMR (100 MHz, CDCl₃, δ): 167.6 (CO₂), 145.9 (2-C of 1,4-dihydropyridine), 143.6 (1-C of C₆H₄), 130.1 (*o*-CH of C₆H₄), 127.8 (q, ²*J*_{C-F} = 31.6 Hz, *ipso*-C of C₆H₄), 124.4 (q, ¹*J*_{C-F} = 270 Hz, CF₃), 124.0, (*m*-CH of C₆H₄), 101.2 (3-C of 1,4-dihydropyridine), 59.6 (CH₃CH₂), 42.1, 35.3 (4-CHCH₂ of 1,4-dihydropyridine), 18.9 (2-CCH₃ of 1,4-dihydropyridine), 14.1 (CH₃CH₂). ¹⁹F NMR (CDCl₃): δ -63.7. HRMS (FAB⁺) Calcd. for C₂₁H₂₄F₃NO₄ [M]⁺: 411.1657. Found: 411.1653.



2-4i

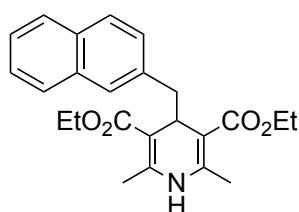
Diethyl 4-(4-(methoxycarbonyl)benzyl)-2,6-dimethyl-1,4-dihydropyridine-3,5-

dicarboxylate (2-4i). A white solid (762.2 mg, 1.90 mmol, 38% isolated yield, based on the amount of methyl 4-(2-oxoethyl)benzoate). m.p.= 86.5-88.0 °C. ¹H NMR (400 MHz, CDCl₃): δ 7.84 (d, *J* = 8.4 Hz, 2H, *m*-H of C₆H₄), 7.08 (d, *J* = 8.4 Hz, 1H, *o*-H of C₆H₄), 5.20 (s, 1H, NH), 4.24 (t, *J* = 5.4 Hz, 1H, 4-CH of 1,4-dihydropyridine), 4.13-4.04 (m, 4H, CH₃CH₂), 3.89 (s, 3H, CH₃), 2.65 (d, *J* = 5.6 Hz, 2H, CH₂), 2.15 (s, 6H, 2-CCH₃ of 1,4-dihydropyridine), 1.24 (t, *J* = 7.4 Hz, 6H, CH₃CH₂). ¹³C{¹H} NMR (100 MHz, CDCl₃, δ): 167.6 (CO₂), 167.4 (CO₂), 145.5 (2-C of 1,4-dihydropyridine), 145.2 (1-C of C₆H₄), 130.1 (*o*-CH of C₆H₄), 128.5 (*ipso*-C of C₆H₄), 127.6 (*m*-CH of C₆H₄), 101.4 (3-C of 1,4-dihydropyridine), 59.7 (CH₃CH₂), 51.9 (CH₃), 42.2, 35.4 (4-CHCH₂ of 1,4-dihydropyridine), 19.2 (2-CCH₃ of 1,4-dihydropyridine), 14.3 (CH₃CH₂). HRMS (FAB⁺) Calcd. for C₂₂H₂₈NO₆ [M+H]⁺: 402.1917. Found: 402.1936.



2-4o

Diethyl 4-(3-bromobenzyl)-2,6-dimethyl-1,4-dihydropyridine-3,5-dicarboxylate (2-4o). A white solid (971.3 mg, 2.30 mmol, 46% isolated yield, based on the amount of 2-(3-bromobenzyl)acetaldehyde). m.p.= 88.3-89.5 °C. ¹H NMR (400 MHz, CDCl₃): δ 7.28-7.26 (m, 1H, *m*-H of C₆H₄), 7.20 (t, *J* = 2.0 Hz, 1H, *o*-H of C₆H₄), 7.03 (t, *J* = 7.8 Hz, 1H, *p*-H of C₆H₄), 6.91 (d, *J* = 8.0 Hz, 1H, *o*-H of C₆H₄), 5.36 (s, 1H, NH), 4.19 (t, *J* = 5.6 Hz, 1H, 4-CH of 1,4-dihydropyridine), 4.13-4.04 (m, 4H, CH₃CH₂), 2.54 (d, *J* = 5.6 Hz, 2H, CH₂), 2.18 (s, 6H, 2-CCH₃ of 1,4-dihydropyridine), 1.26 (t, *J* = 7.2 Hz, 6H, CH₃CH₂). ¹³C{¹H} NMR (100 MHz, CDCl₃, δ): 167.6 (CO₂), 145.7 (2-C of 1,4-dihydropyridine), 141.7 (*ipso*-C of C₆H₄), 133.0 (*m*-CH of C₆H₄), 128.8 (C-Br of C₆H₄), 128.7 (*p*-CH of C₆H₄), 128.6 (*o*-CH of C₆H₄), 121.3 (*m*-CH of C₆H₄), 101.4 (3-C of 1,4-dihydropyridine), 59.7 (CH₃CH₂), 41.9, 35.4 (4-CHCH₂ of 1,4-dihydropyridine), 19.2 (2-CCH₃ of 1,4-dihydropyridine), 14.3 (CH₃CH₂). HRMS (FAB⁺) Calcd. for C₂₀H₂₅BrNO₄ [M+H]⁺: 422.0967. Found: 422.0946.



2-4s

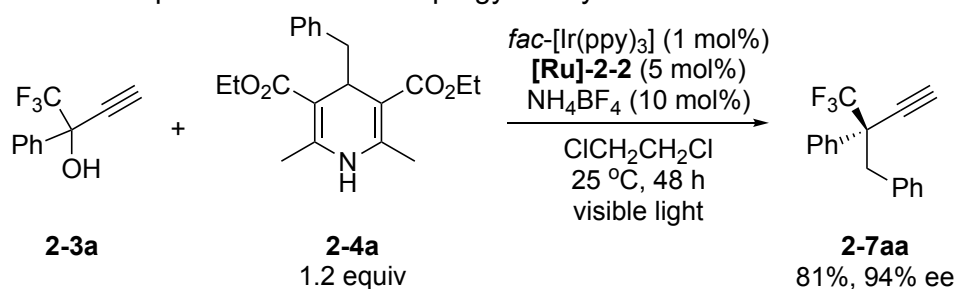
Diethyl 2,6-dimethyl-4-(naphthalen-2-ylmethyl)-1,4-dihydropyridine-3,5-dicarboxylate (2-4s). A white solid (846.0 mg, 2.15 mmol, 43% isolated yield, based

on the amount of 2-(4-(naphthalen-2-ylmethyl))acetaldehyde). m.p.= 119.0-120.6 °C. ¹H NMR (400 MHz, CDCl₃): δ 7.78-7.71 (m, 2H, aromatic H), 7.65 (d, *J* = 8.8 Hz, 1H), 7.43 (s, 1H, aromatic H), 7.41-7.36 (m, 2H, aromatic H), 7.20 (dd, *J* = 8.0 Hz, 1.2Hz, 1H, aromatic H), 5.09 (s, 1H, NH), 4.28 (t, *J* = 5.4 Hz, 1H, 4-CH of 1,4-dihydropyridine), 4.10-3.95 (m, 4H, CH₃CH₂), 2.75 (d, *J* = 5.2 Hz, 2H, CH₂), 2.12 (s, 6H, 2-CCH₃ of 1,4-dihydropyridine), 1.19 (t, *J* = 7.2 Hz, 6H, CH₃CH₂).

¹³C{¹H} NMR (100 MHz, CDCl₃, δ): 167.8 (CO₂), 145.4 (2-C of 1,4-dihydropyridine), 137.0, 133.2, 131.9 (2-, 4a- and 8a-C of naphthyl), 129.1, 128.2, 127.4, 126.3, 125.5, 124.9 (C of naphthyl), 101.8(3-C of 1,4-dihydropyridine), 59.6 (CH₃CH₂), 42.4, 35.6 (4-CHCH₂ of 1,4-dihydropyridine), 19.2 (2-CCH₃ of 1,4-dihydropyridine), 14.3 (CH₃CH₂). HRMS (FAB⁺) Calcd. for C₂₄H₂₇NO₄ [M]⁺: 393.1940. Found: 393.1951.

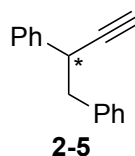
2.4.4. General Procedure for the Preparation of Chiral Propargylic Alkylation Products (Taking (*R*)-(2-(trifluoromethyl)but-3-yne-1,2-diyl)dibenzene (2-7aa) as an Example)

Scheme 2-9. Preparation of Chiral Propargylic Alkylation Products **2-7aa**

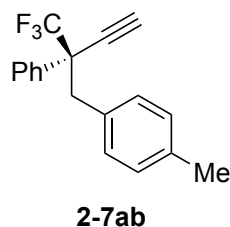


In an oven dried 20 mL Schlenk flask were placed **[Ru]-2-2** (6.3 mg, 0.0050 mmol) and NH₄BF₄ (1.1 mg, 0.010 mmol) under N₂. Anhydrous ClCH₂CCH₂Cl (2.0 mL) was added, and then the mixture was magnetically stirred at room temperature for 30 min. Then, 1,1,1-trifluoro-2-phenylbut-3-yn-2-ol (**2-3a**) (20.0 mg, 0.10 mmol), diethyl 4-benzyl-2,6-dimethyl-1,4-dihydropyridine-3,5-dicarboxylate (**2-4a**) (41.2 mg, 0.12 mmol), *fac*-[Ir(ppy)₃] (0.7 mg, 0.0011 mmol) were added under N₂ at room temperature. The reaction flask was placed in an As One LTB-125 constant low temperature water bath set at 25 °C, and was illuminated from the bottom of the bath with an Aitech System TMN100×120–22WD 12 W white LED lamp (400 nm to 750 nm) at a distance of approximately 2 cm from the light source for 48 h. The volatiles were removed *in vacuo*, and the residue was purified by column chromatography (SiO₂) with *n*-hexane as an eluent to afford (*R*)-(2-(trifluoromethyl)but-3-yne-1,2-diyl)dibenzene (**2-7aa**) as a colorless oil (22.2 mg, 0.081 mmol, 81% yield based on the amount of **2-3a**). [α]_D²⁰ = -12.2 (*c* = 0.5 in CHCl₃). ¹H NMR (CDCl₃, 400 MHz) δ 7.67-7.65 (m, 2H, *o*-H of Ph), 7.39-7.33 (m, 3H, *m*-H and *p*-H of Ph), 7.18-7.10 (m, 3H, *m*-H and *p*-H of Ph), 6.99-6.98 (m, 2H, *o*-H of Ph), 3.52 (d, *J* = 13.2 Hz, 1H, CH₂), 3.42 (d, *J* = 13.2 Hz, 1H, CH₂), 2.66 (s, 1H, HC≡). ¹³C{¹H} NMR (CDCl₃, 100 MHz) δ 134.4 (*ipso*-C of Ph), 133.3 (*ipso*-C of Ph), 130.8 (*o*-CH of Ph), 128.5 (*m*-CH of Ph), 128.5 (*m*-CH of Ph), 127.6

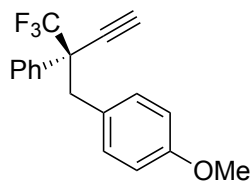
(*p*-CH of Ph), 127.0 (*p*-CH of Ph), 125.7 (q, $^1J_{C-F}$ = 283 Hz, CF₃), 79.0 (C≡), 78.1 (HC≡), 53.0 (q, $^2J_{C-F}$ = 26.5 Hz, CC≡), 40.7 (CH₂). ¹⁹F NMR (CDCl₃): δ -73.5. HRMS (FAB+) Calcd. for C₁₇H₁₃F₃ [M]⁺: 274.0969. Found: 274.0964. The enantiomeric excess of **2-7aa** was determined by HPLC analysis; DAICEL Chiralpak OJ-H, hexane/*i*PrOH = 99/1, flow rate = 0.5 mL/min, λ = 220 nm, retention time: 14.6 min (major) and 19.9 min (minor), 94% ee.



But-3-yn-1,2-diylidibenzene (2-5). A colorless oil (15.1 mg, 0.073 mmol, 73% yield based on the amount of **2-1**). $[\alpha]_D^{20}$ = -14.8 (c = 0.5 in CHCl₃). ¹H NMR (CDCl₃, 400 MHz) δ 7.31-7.30 (m, 4H, *o*-H and *m*-H of Ph), 7.28-7.20 (m, 4H, *o*-H and *m*-H of Ph), 7.14-7.12 (m, 2H, *p*-H of Ph), 3.90-3.86 (m, 1H, CH), 3.10-3.00 (m, 2H, CH₂), 2.28 (s, 1H, HC≡). ¹³C{¹H} NMR (CDCl₃, 100 MHz) δ 140.7 (*ipso*-C of Ph), 138.6 (*ipso*-C of Ph), 131.2 (*ipso*-C of C₆H₄), 129.4 (*m*-CH of Ph), 128.4 (*m*-CH of Ph), 128.1 (*o*-CH of Ph), 127.6 (*o*-CH of Ph), 126.9 (*p*-CH of Ph), 126.4 (*p*-CH of Ph), 85.3 (C≡), 71.9 (HC≡), 44.7 (CH₂), 39.8 (CH). HRMS (FAB+) Calcd. for C₁₆H₁₅ [M+H]⁺: 207.1174. Found: 207.1173. The enantiomeric excess of **2-5** was determined by HPLC analysis; DAICEL Chiralpak OJ-H, hexane/*i*PrOH = 99/1, flow rate = 0.5 mL/min, λ = 220 nm, retention time: 21.8 min (minor) and 44.7 min (major), 45% ee.

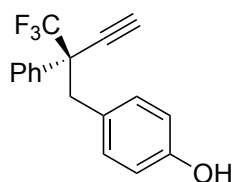


(*R*)-1-Methyl-4-(2-phenyl-2-(trifluoromethyl)but-3-yn-1-yl)benzene (2-7ab). A colorless oil (22.5 mg, 0.078 mmol, 78% yield based on the amount of **2-3a**). $[\alpha]_D^{20}$ = +21.9 (c = 0.5 in CHCl₃). ¹H NMR (CDCl₃, 400 MHz) δ 7.67-7.65 (m, 2H, *o*-H of Ph), 7.39-7.33 (m, 3H, *m*-H and *p*-H of Ph), 6.93-6.91 (m, 2H, *m*-H of C₆H₄), 6.87-6.85 (m, 2H, *o*-H of C₆H₄), 3.48 (d, *J* = 13.6 Hz, 1H, CH₂), 3.38 (d, *J* = 13.6 Hz, 1H, CH₂), 2.65 (s, 1H, HC≡), 2.24 (s, 3H, CH₃). ¹³C{¹H} NMR (CDCl₃, 100 MHz) δ 136.5 (*ipso*-C of Ph), 133.4 (*p*-C of C₆H₄), 131.2 (*ipso*-C of C₆H₄), 130.6 (*m*-CH of C₆H₄), 128.5 (*m*-CH of Ph), 128.3 (*o*-CH of C₆H₄), 128.2 (*o*-CH and *p*-CH of Ph), 125.7 (q, $^1J_{C-F}$ = 283 Hz, CF₃), 79.1 (C≡), 78.0 (HC≡), 53.0 (q, $^2J_{C-F}$ = 25.9 Hz, CC≡), 40.3 (CH₂), 21.0 (CH₃). ¹⁹F NMR (CDCl₃): δ -73.4. HRMS (FAB+) Calcd. for C₁₈H₁₅F₃ [M]⁺: 288.1126. Found: 288.1128. The enantiomeric excess of **2-7ab** was determined by HPLC analysis; DAICEL Chiralpak OJ-H, hexane/*i*PrOH = 99/1, flow rate = 0.5 mL/min, λ = 220 nm, retention time: 13.7 min (major) and 18.9 min (minor), 94% ee.



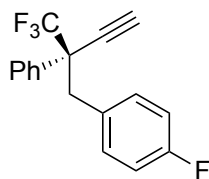
2-7ac

(*R*)-1-Methyl-4-(2-phenyl-2-(trifluoromethyl)but-3-yn-1-yl)benzene (2-7ac). A colorless oil (24.0 mg, 0.079 mmol, 79% yield based on the amount of **2-3a**). $[\alpha]_D^{20} = +66.9$ ($c = 0.5$ in CHCl_3). ^1H NMR (CDCl_3 , 400 MHz) δ 7.67-7.65 (m, 2H, *o*-H of Ph), 7.39-7.34 (m, 3H, *m*-H and *p*-H of Ph), 6.91-6.88 (m, 2H, *o*-H of C_6H_4), 6.67-6.64 (m, 2H, *m*-H of C_6H_4), 3.72 (s, 3H, CH_3), 3.46 (d, $J = 13.6$ Hz, 1H, CH_2), 3.37 (d, $J = 13.6$ Hz, 1H, CH_2), 2.65 (s, 1H, $\text{HC}\equiv$). $^{13}\text{C}\{^1\text{H}\}$ NMR (CDCl_3 , 100 MHz) δ 158.5 (*p*-C of C_6H_4), 133.4 (*ipso*-C of Ph), 131.7 (*ipso*-C of C_6H_4), 128.5 (*o*-CH of C_6H_4), 128.3 (*m*-CH of Ph), 126.3 (*o*-CH and *p*-CH of Ph), 125.7 (q, $^1J_{\text{C-F}} = 283$ Hz, CF_3), 113.0 (*m*-CH of C_6H_4), 79.1 ($\text{C}\equiv$), 78.0 ($\text{HC}\equiv$), 55.0 (CH_3), 53.1 (q, $^2J_{\text{C-F}} = 25.9$ Hz, $\text{CC}\equiv$), 40.0 (CH_2). ^{19}F NMR (CDCl_3): δ -73.3. HRMS (FAB+) Calcd. for $\text{C}_{18}\text{H}_{15}\text{F}_3\text{O}$ $[\text{M}]^+$: 304.1075. Found: 304.1088. The enantiomeric excess of **2-7ac** was determined by HPLC analysis; DAICEL Chiralpak OJ-H, hexane/*i*PrOH = 90/10, flow rate = 0.5 mL/min, $\lambda = 220$ nm, retention time: 20.1 min (major) and 23.7 min (minor), 92% ee.



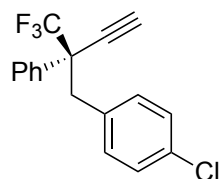
2-7ad

(*R*)-4-(2-Phenyl-2-(trifluoromethyl)but-3-yn-1-yl)phenol (2-7ad). A colorless oil (20.3 mg, 0.070 mmol, 70% yield based on the amount of **2-3a**). $[\alpha]_D^{20} = -40.9$ ($c = 0.5$ in CHCl_3). ^1H NMR (CDCl_3 , 400 MHz) δ 7.65-7.62 (m, 2H, *o*-H of Ph), 7.38-7.33 (m, 3H, *m*-H and *p*-H of Ph), 6.86-6.82 (m, 2H, *o*-H of C_6H_4), 6.59-6.56 (m, 2H, *m*-H of C_6H_4), 3.44 (d, $J = 13.6$ Hz, 1H, CH_2), 3.35 (d, $J = 14.0$ Hz, 1H, CH_2), 2.65 (s, 1H, $\text{HC}\equiv$), 1.70 (brs, 1H, OH). $^{13}\text{C}\{^1\text{H}\}$ NMR (CDCl_3 , 100 MHz) δ 154.5 (*p*-C of C_6H_4), 133.4 (*ipso*-C of Ph), 131.9 (*ipso*-C of C_6H_4), 128.5 (*o*-CH of C_6H_4), 128.3 (*m*-CH of Ph), 126.6 (*o*-CH and *p*-CH of Ph), 125.7 (q, $^1J_{\text{C-F}} = 283$ Hz, CF_3), 114.5 (*m*-CH of C_6H_4), 79.1 ($\text{C}\equiv$), 78.0 ($\text{HC}\equiv$), 53.2 (q, $^2J_{\text{C-F}} = 25.9$ Hz, $\text{CC}\equiv$), 40.0 (CH_2). ^{19}F NMR (CDCl_3): δ -73.3. HRMS (FAB+) Calcd. for $\text{C}_{17}\text{H}_{13}\text{F}_3\text{O}$ $[\text{M}]^+$: 290.0918. Found: 290.0912. The enantiomeric excess of **2-7d** was determined by HPLC analysis; DAICEL Chiralpak OJ-H, hexane/*i*PrOH = 80/20, flow rate = 0.5 mL/min, $\lambda = 220$ nm, retention time: 19.8 min (major) and 31.3 min (minor), 92% ee.



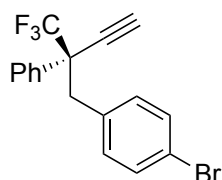
2-7ae

(*R*)-1-Fluoro-4-(2-phenyl-2-(trifluoromethyl)but-3-yn-1-yl)benzene (2-7ae). A colorless oil (23.4 mg, 0.080 mmol, 80% yield based on the amount of **2-3a**). $[\alpha]_D^{20} = -17.1$ ($c = 0.5$ in CHCl_3). ^1H NMR (CDCl_3 , 400 MHz) δ 7.64-7.62 (m, 2H, *m*-H of Ph), 7.38-7.34 (m, 3H, *o*-H and *p*-H of Ph), 6.95-6.91 (m, 2H, *m*-H of C_6H_4), 6.82-6.78 (m, 2H, *o*-H of C_6H_4), 3.47 (d, $J = 13.2$ Hz, 1H, CH_2), 3.39 (d, $J = 13.2$ Hz, 1H, CH_2), 2.66 (s, 1H, $\text{HC}\equiv$). $^{13}\text{C}\{^1\text{H}\}$ NMR (CDCl_3 , 100 MHz) δ 162.0 (d, $^1J_{\text{C-F}} = 244$ Hz, CF), 133.2 (*ipso*-C of Ph), 132.2 (d, $^3J_{\text{C-F}} = 7.6$ Hz, *o*-CH of C_6H_4), 130.0 (*ipso*-C of C_6H_4), 128.7 (*m*-CH of Ph), 128.4 (*o*-CH and *p*-CH of Ph), 125.6 (q, $^1J_{\text{C-F}} = 282$ Hz, CF_3), 114.5 (d, $^2J_{\text{C-F}} = 21$ Hz, *m*-CH of C_6H_4), 78.8 ($\text{C}\equiv$), 78.2 ($\text{HC}\equiv$), 53.0 (q, $^2J_{\text{C-F}} = 26.9$ Hz, $\text{CC}\equiv$), 40.0 (CH_2). ^{19}F NMR (CDCl_3): δ -73.4, -117.3. HRMS (FAB+) Calcd. for $\text{C}_{17}\text{H}_{13}\text{F}_4$ $[\text{M}+\text{H}]^+$: 293.0953. Found: 293.0962. The enantiomeric excess of **2-7ae** was determined by HPLC analysis; DAICEL Chiralpak OJ-H, hexane/*i*PrOH = 99/1, flow rate = 0.3 mL/min, $\lambda = 220$ nm, retention time: 32.2 min (major) and 35.0 min (minor), 92% ee.



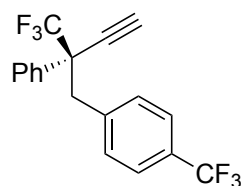
2-7af

(*R*)-1-Chloro-4-(2-phenyl-2-(trifluoromethyl)but-3-yn-1-yl)benzene (2-7af). A colorless oil (22.8 mg, 0.074 mmol, 74% yield based on the amount of **2-3a**). $[\alpha]_D^{20} = -19.5$ ($c = 0.5$ in CHCl_3). ^1H NMR (CDCl_3 , 400 MHz) δ 7.64-7.62 (m, 2H, *m*-H of C_6H_4), 7.44-7.33 (m, 3H, *o*-H of C_6H_4 and *p*-H of Ph), 7.10-7.07 (m, 2H, *m*-H of Ph), 6.91-6.88 (m, 2H, *o*-H of Ph), 3.47 (d, $J = 13.6$ Hz, 1H, CH_2), 3.38 (d, $J = 13.6$ Hz, 1H, CH_2), 2.67 (s, 1H, $\text{HC}\equiv$). $^{13}\text{C}\{^1\text{H}\}$ NMR (CDCl_3 , 100 MHz) δ 133.0 (*ipso*-C of C_6H_4), 132.8 (*ipso*-C of Ph), 132.0 (CCl of C_6H_4), 128.8 (*m*-CH of Ph), 128.7 (*m*-CH of C_6H_4), 128.6 (*o*-CH of Ph), 128.4 (*o*-CH of C_6H_4), 127.8 (*p*-CH of Ph), 125.6 (q, $^1J_{\text{C-F}} = 283$ Hz, CF_3), 78.7 ($\text{C}\equiv$), 78.3 ($\text{HC}\equiv$), 52.9 (q, $^2J_{\text{C-F}} = 26.8$ Hz, $\text{CC}\equiv$), 40.1 (CH_2). ^{19}F NMR (CDCl_3): δ -73.5. HRMS (FAB+) Calcd. for $\text{C}_{17}\text{H}_{12}\text{ClF}_3$ $[\text{M}]^+$: 308.0580. Found: 308.0570. The enantiomeric excess of **2-7af** was determined by HPLC analysis; DAICEL Chiralpak OJ-H, hexane/*i*PrOH = 99/1, flow rate = 0.5 mL/min, $\lambda = 220$ nm, retention time: 17.3 min (major) and 25.4 min (minor), 90% ee.



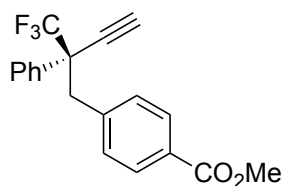
2-7ag

(*R*)-1-Bromo-4-(2-phenyl-2-(trifluoromethyl)but-3-yn-1-yl)benzene (2-7ag). A colorless oil (24.0 mg, 0.068 mmol, 68% yield based on the amount of **2-3a**). $[\alpha]_{\text{D}}^{20} = -49.5$ ($c = 0.5$ in CHCl_3). ^1H NMR (CDCl_3 , 400 MHz) δ 7.64-7.63 (m, 2H, *m*-H of C_6H_4), 7.38-7.35 (m, 3H, *o*-H of C_6H_4 and *p*-H of Ph), 7.25-7.22 (m, 2H, *m*-H of Ph), 6.86-6.83 (m, 2H, *o*-H of Ph), 3.46 (d, $J = 13.6$ Hz, 1H, CH_2), 3.38 (d, $J = 13.6$ Hz, 1H, CH_2), 2.67 (s, 1H, $\text{HC}\equiv$). $^{13}\text{C}\{^1\text{H}\}$ NMR (CDCl_3 , 100 MHz) δ 133.3 (*ipso*-C of Ph), 133.0 (*ipso*-C of C_6H_4), 132.4 (*o*-CH of C_6H_4), 130.7 (*m*-CH of C_6H_4), 128.7 (*m*-CH of Ph), 128.4 (*o*-CH and *p*-CH of Ph), 125.6 (q, $^1J_{\text{C-F}} = 283$ Hz, CF_3), 121.2 (CBr of C_6H_4), 78.7 ($\text{C}\equiv$), 78.4 ($\text{HC}\equiv$), 52.8 (q, $^2J_{\text{C-F}} = 26.8$ Hz, $\text{CC}\equiv$), 40.2 (CH_2). ^{19}F NMR (CDCl_3): δ -73.5. HRMS (FAB+) Calcd. for $\text{C}_{17}\text{H}_{12}\text{BrF}_3$ $[\text{M}]^+$: 352.0074. Found: 352.0083. The enantiomeric excess of **2-7ag** was determined by HPLC analysis; DAICEL Chiralpak OJ-H, hexane/*i*PrOH = 99/1, flow rate = 0.5 mL/min, $\lambda = 220$ nm, retention time: 15.4 min (major) and 23.7 min (minor), 94% ee.



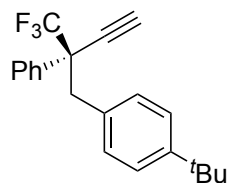
2-7ah

(*R*)-1-(2-Phenyl-2-(trifluoromethyl)but-3-yn-1-yl)-4-(trifluoromethyl)benzene (2-7ah). A colorless oil (25.3 mg, 0.074 mmol, 74% yield based on the amount of **2-3a**). $[\alpha]_{\text{D}}^{20} = -49.1$ ($c = 0.5$ in CHCl_3). ^1H NMR (CDCl_3 , 400 MHz) δ 7.65-7.63 (m, 2H, *m*-H of C_6H_4), 7.39-7.35 (m, 5H, Ph), 7.06 (d, 2H, $J = 8.4$ Hz, *o*-H of C_6H_4), 3.56 (d, $J = 13.6$ Hz, 1H, CH_2), 3.46 (d, $J = 13.2$ Hz, 1H, CH_2), 2.68 (s, 1H, $\text{HC}\equiv$). ^{13}C NMR spectrum of this compound was measured in acetone- d_6 because some peaks of this compound overlapped with those of CDCl_3 . $^{13}\text{C}\{^1\text{H}\}$ NMR ($(\text{CD}_3)_2\text{CO}$, 100 MHz) δ 140.1 (*ipso*-C of Ph), 133.6 (*ipso*-C of C_6H_4), 132.3 (*m*-CH of Ph), 129.8 (*o*-CH of C_6H_4), 129.4 (*o*-CH of Ph), 129.3 (q, $^2J_{\text{C-F}} = 31.6$ Hz, CCF_3), 128.9 (*m*-CH of C_6H_4), 126.6 (q, $^1J_{\text{C-F}} = 282$ Hz, CF_3 of C_6H_4), 125.2 (q, $^1J_{\text{C-F}} = 269$ Hz, CF_3), 125.0 (*p*-CH of Ph), 80.8 ($\text{C}\equiv$), 79.1 ($\text{HC}\equiv$), 53.4 (q, $^2J_{\text{C-F}} = 25.9$ Hz, $\text{CC}\equiv$), 40.2 (CH_2). ^{19}F NMR (CDCl_3): δ -64.1, -73.6. HRMS (FAB+) Calcd. for $\text{C}_{18}\text{H}_{12}\text{F}_6$ $[\text{M}]^+$: 342.0843. Found: 342.0856. The enantiomeric excess of **2-7ah** was determined by HPLC analysis; DAICEL Chiralpak OJ-H, hexane/*i*PrOH = 99/1, flow rate = 0.5 mL/min, $\lambda = 220$ nm, retention time: 11.4 min (major) and 15.6 min (minor), 91% ee.



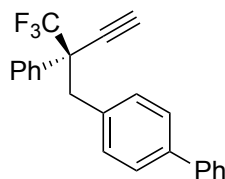
2-7ai

Methyl (*R*)-4-(2-phenyl-2-(trifluoromethyl)but-3-yn-1-yl)benzoate (2-7ai). A pale yellow solid (24.9 mg, 0.075 mmol, 75% yield based on the amount of **2-3a**). m.p.= 74.0-75.5 °C [α]_D²⁰ = -45.6 (*c* = 0.5 in CHCl₃). ¹H NMR (CDCl₃, 400 MHz) δ 7.79 (d, *J* = 8.0 Hz, 2H, *m*-H of C₆H₄), 7.65-7.62 (m, 2H, *o*-H of Ph), 7.38-7.34 (m, 3H, *m*-H and *p*-H of Ph), 7.05 (d, *J* = 8.8 Hz, 2H, *o*-H of C₆H₄), 3.86 (s, 3H, CH₃), 3.56 (d, *J* = 14.0 Hz, 1H, CH₂), 3.47 (d, *J* = 14.0 Hz, 1H, CH₂), 2.67 (s, 1H, HC \equiv). ¹³C{¹H} NMR (CDCl₃, 100 MHz) δ 166.9 (CO₂), 139.7 (*ipso*-C of Ph), 133.0 (*ipso*-C of C₆H₄), 130.8 (*m*-CH of C₆H₄), 128.9 (*m*-CH of Ph), 128.8 (*o*-CH of C₆H₄), 128.7 (*o*-CH and *p*-CH of Ph), 128.4 (*p*-CH of C₆H₄), 125.6 (q, ¹*J*_{C-F} = 283 Hz, CF₃), 78.6 (C \equiv), 78.4 (HC \equiv), 52.8 (q, ²*J*_{C-F} = 26.9 Hz, CC \equiv), 52.0 (CH₃), 40.7 (CH₂). ¹⁹F NMR (CDCl₃): δ -73.5. HRMS (FAB+) Calcd. for C₁₉H₁₆F₃O₂ [M+H]⁺: 333.1102. Found: 333.1107. The enantiomeric excess of **2-7ai** was determined by HPLC analysis; DAICEL Chiralpak OJ-H, hexane/*i*PrOH = 90/10, flow rate = 0.5 mL/min, λ = 220 nm, retention time: 18.9 min (major) and 31.1 min (minor), 96% ee.



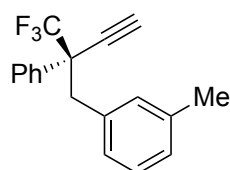
2-7aj

(*R*)-1-(*tert*-Butyl)-4-(2-phenyl-2-(trifluoromethyl)but-3-yn-1-yl)benzene (2-7aj). A white solid (23.1 mg, 0.070 mmol, 70% yield based on the amount of **2-3a**). m.p.= 88.7-89.9 °C. [α]_D²⁰ = -13.2 (*c* = 0.5 in CHCl₃). ¹H NMR (CDCl₃, 400 MHz) δ 7.69-7.67 (m, 2H, *o*-H of Ph), 7.39-7.33 (m, 3H, *m*-H and *p*-H of Ph), 7.15-7.12 (m, 2H, *m*-H of C₆H₄), 6.93-6.91 (m, 2H, *o*-H of C₆H₄), 3.50 (d, *J* = 13.6 Hz, 1H, CH₂), 3.39 (d, *J* = 13.6 Hz, 1H, CH₂), 2.65 (s, 1H, HC \equiv), 1.24 (s, 9H, *t*Bu). ¹³C{¹H} NMR (CDCl₃, 100 MHz) δ 149.6 (*ipso*-C of Ph), 133.4 (*p*-C of C₆H₄), 131.3 (*ipso*-C of C₆H₄), 130.3 (*m*-CH of C₆H₄), 128.6 (*m*-CH of Ph), 128.5 (*o*-CH of C₆H₄), 128.2 (*o*-CH of Ph), 125.7 (q, ¹*J*_{C-F} = 284 Hz, CF₃), 124.5 (*p*-CH of Ph), 79.2 (C \equiv), 77.8 (HC \equiv), 52.9 (q, ²*J*_{C-F} = 26.8 Hz, CC \equiv), 40.0 (CH₂), 34.3 (C(CH₃)₃), 21.0 (CH₃). ¹⁹F NMR (CDCl₃): δ -73.6. HRMS (FAB+) Calcd. for C₂₁H₂₁F₃ [M]⁺: 330.1595. Found: 330.1594. The enantiomeric excess of **2-7aj** was determined by HPLC analysis; DAICEL Chiralpak OJ-H, hexane/*i*PrOH = 99/1, flow rate = 0.5 mL/min, λ = 220 nm, retention time: 9.9 min (major) and 17.9 min (minor), 84% ee.



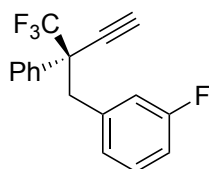
2-7ak

(R)-4-(2-Phenyl-2-(trifluoromethyl)but-3-yn-1-yl)-1,1'-biphenyl (2-7ak). A white solid (24.9 mg, 0.071 mmol, 71% yield based on the amount of **2-3a**). m.p.= 102.6-103.7 °C. $[\alpha]_D^{20} = -46.4$ ($c = 0.5$ in CHCl_3). ^1H NMR (CDCl_3 , 400 MHz) δ 7.70-7.68 (m, 2H, 2',6'-CH of biphenyl), 7.53-7.51 (m, 2H, *m*-H of C_6H_4), 7.41-7.35 (m, 7H, 3',4',5'-CH of biphenyl, *o*-H of C_6H_4 and *o*-H of Ph), 7.33-7.29 (m, 1H, *p*-H of Ph), 7.06-7.04 (m, 2H, *m*-H of Ph), 3.56 (d, $J = 13.2$ Hz, 1H, CH_2), 3.47 (d, $J = 13.2$ Hz, 1H, CH_2), 2.69 (s, 1H, $\text{HC}\equiv$). $^{13}\text{C}\{^1\text{H}\}$ NMR (CDCl_3 , 100 MHz) δ 140.6 (*ipso*-C of Ph), 139.7 (1'-C of biphenyl), 133.4 (1-C of C_6H_4), 133.3 (*ipso*-C of C_6H_4), 131.1 (*o*-CH of C_6H_4), 128.7 (3',5'-C of biphenyl), 128.6 (*m*-CH of Ph), 128.5 (*m*-CH of C_6H_4), 128.3 (*o*-CH of Ph), 127.2 (2',6'-C of biphenyl), 126.9 (4'-C of biphenyl), 126.2 (*p*-CH of Ph), 125.7 (q, $^1J_{\text{C-F}} = 284$ Hz, CF_3), 79.0 ($\text{C}\equiv$), 78.1 ($\text{HC}\equiv$), 53.0 (q, $^2J_{\text{C-F}} = 25.9$ Hz, $\text{CC}\equiv$), 40.3 (CH_2). ^{19}F NMR (CDCl_3): δ -73.5. HRMS (FAB+) Calcd. for $\text{C}_{23}\text{H}_{17}\text{F}_3$ $[\text{M}]^+$: 350.1282. Found: 350.1270. The enantiomeric excess of **2-7ak** was determined by HPLC analysis; DAICEL Chiralpak OD, hexane/ i PrOH = 99/1, flow rate = 0.5 mL/min, $\lambda = 220$ nm, retention time: 11.4 min (minor) and 12.4 min (major), 83% ee.



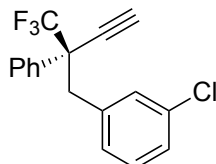
2-7al

(R)-1-Methyl-3-(2-phenyl-2-(trifluoromethyl)but-3-yn-1-yl)benzene (2-7al). A colorless oil (21.0 mg, 0.073 mmol, 73% yield based on the amount of **2-3a**). $[\alpha]_D^{20} = -14.9$ ($c = 0.5$ in CHCl_3). ^1H NMR (CDCl_3 , 400 MHz) δ 7.67-7.65 (m, 2H, *o*-H of Ph), 7.39-7.33 (m, 3H, *m*-H and *p*-H of Ph), 7.02-6.91 (m, 2H, *m*-H of C_6H_4), 6.79-6.75 (m, 2H, *o*-H and *p*-H of C_6H_4), 3.47 (d, $J = 13.6$ Hz, 1H, CH_2), 3.38 (d, $J = 13.6$ Hz, 1H, CH_2), 2.65 (s, 1H, $\text{HC}\equiv$), 2.19 (s, 3H, CH_3). $^{13}\text{C}\{^1\text{H}\}$ NMR (CDCl_3 , 100 MHz) δ 137.0 (*ipso*-C of Ph), 134.2 (*m*-C of C_6H_4), 133.4 (*ipso*-C of C_6H_4), 131.7 (*m*-CH of C_6H_4), 128.4 (*m*-CH of Ph), 128.2 (*o*-CH of C_6H_4), 127.0, 127.0 (*o*-CH and *p*-CH of Ph), 127.4 (*p*-CH of C_6H_4), 125.7 (q, $^1J_{\text{C-F}} = 283$ Hz, CF_3), 79.0 ($\text{C}\equiv$), 78.0 ($\text{HC}\equiv$), 53.0 (q, $^2J_{\text{C-F}} = 26.9$ Hz, $\text{CC}\equiv$), 40.7 (CH_2), 21.3 (CH_3). ^{19}F NMR (CDCl_3): δ -73.4. HRMS (FAB+) Calcd. for $\text{C}_{18}\text{H}_{15}\text{F}_3$ $[\text{M}]^+$: 288.1126. Found: 288.1137. The enantiomeric excess of **2-7al** was determined by HPLC analysis; DAICEL Chiralpak OJ-H, hexane/ i PrOH = 99/1, flow rate = 0.5 mL/min, $\lambda = 220$ nm, retention time: 13.6 min (major) and 17.7 min (minor), 90% ee.



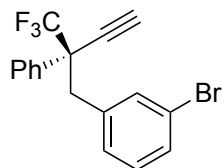
2-7am

(*R*)-1-Fluoro-3-(2-phenyl-2-(trifluoromethyl)but-3-yn-1-yl)benzene (2-7am). A colorless oil (23.4 mg, 0.080 mmol, 80% yield based on the amount of **2-3a**). $[\alpha]_D^{20} = -48.0$ ($c = 0.5$ in CHCl_3). ^1H NMR (CDCl_3 , 400 MHz) δ 7.66-7.62 (m, 2H, *o*-H of Ph), 7.40-7.35 (m, 3H, *m*-H of Ph and *m*-H of C_6H_4), 7.10-7.04 (m, 1H, *p*-H of Ph), 6.88-6.82 (m, 1H, *p*-H of C_6H_4), 6.75-6.70 (m, 2H, *o*-H of C_6H_4), 3.50 (d, $J = 13.2$ Hz, 1H, CH_2), 3.41 (d, $J = 13.2$ Hz, 1H, CH_2), 2.69 (s, 1H, $\text{HC}\equiv$). $^{13}\text{C}\{^1\text{H}\}$ NMR (CDCl_3 , 100 MHz) δ 162.1 (d, $^1J_{\text{C-F}} = 243$ Hz, CF), 136.8 (d, $^3J_{\text{C-F}} = 7.7$ Hz, *ipso*-C of C_6H_4), 133.0 (*ipso*-C of Ph), 128.9 (*o*-CH and *m*-CH of Ph), 128.7 (*o*-CH of C_6H_4), 128.4 (*p*-CH of Ph), 126.5 (d, $^3J_{\text{C-F}} = 1.9$ Hz, *m*-CH of C_6H_4), 125.5 (q, $^1J_{\text{C-F}} = 284$ Hz, CF_3), 117.6 (d, $^2J_{\text{C-F}} = 22$ Hz, *o*-CH of C_6H_4), 114.0 (d, $^2J_{\text{C-F}} = 20.1$ Hz, *p*-CH of C_6H_4), 78.7 ($\text{C}\equiv$), 78.3 ($\text{HC}\equiv$), 52.8 (q, $^2J_{\text{C-F}} = 26.9$ Hz, $\text{CC}\equiv$), 40.4 (CH_2). ^{19}F NMR (CDCl_3): δ -73.6, -115.7. HRMS (FAB+) Calcd. for $\text{C}_{17}\text{H}_{12}\text{F}_4$ $[\text{M}]^+$: 292.0875. Found: 292.0872. The enantiomeric excess of **2-7am** was determined by HPLC analysis; DAICEL Chiralpak OJ-H, hexane/*i*PrOH = 99/1, flow rate = 0.5 mL/min, $\lambda = 220$ nm, retention time: 11.9 min (major) and 16.0 min (minor), 90% ee.



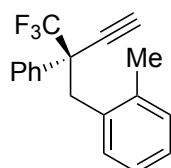
2-7an

(*R*)-1-Chloro-3-(2-phenyl-2-(trifluoromethyl)but-3-yn-1-yl)benzene (2-7an). A colorless oil (23.8 mg, 0.077 mmol, 77% yield based on the amount of **2-3a**). $[\alpha]_D^{20} = -13.5$ ($c = 0.5$ in CHCl_3). ^1H NMR (CDCl_3 , 400 MHz) δ 7.65-7.62 (m, 2H, *o*-H of Ph), 7.39-7.35 (m, 3H, *m*-H of Ph and *o*-H of C_6H_4), 7.15-7.12 (m, 1H, *p*-H of Ph), 7.05-7.00 (m, 2H, *m*-H and *p*-H of C_6H_4), 6.82 (d, $J = 8.0$ Hz, 1H, *o*-H of C_6H_4), 3.47 (d, $J = 14.0$ Hz, 1H, CH_2), 3.38 (d, $J = 13.6$ Hz, 1H, CH_2), 2.70 (s, 1H, $\text{HC}\equiv$). $^{13}\text{C}\{^1\text{H}\}$ NMR (CDCl_3 , 100 MHz) δ 136.3 (*ipso*-C of Ph), 133.3 (*ipso*-C of C_6H_4), 133.0 (CCl), 130.9 (*m*-CH of C_6H_4), 128.8 (*o*-CH of C_6H_4), 128.8 (*m*-CH of Ph), 128.6 (*o*-CH of C_6H_4), 128.4 (*p*-CH of C_6H_4), 127.2 (*o*-CH and *p*-CH of Ph), 125.5 (q, $^1J_{\text{C-F}} = 283$ Hz, CF_3), 78.6 ($\text{C}\equiv$), 78.4 ($\text{HC}\equiv$), 52.8 (q, $^2J_{\text{C-F}} = 26.8$ Hz, $\text{CC}\equiv$), 40.4 (CH_2). ^{19}F NMR (CDCl_3): δ -73.5. HRMS (FAB+) Calcd. for $\text{C}_{17}\text{H}_{12}\text{ClF}_3$ $[\text{M}]^+$: 308.0580. Found: 308.0578. The enantiomeric excess of **2-7an** was determined by HPLC analysis; DAICEL Chiralpak OJ-H, hexane/*i*PrOH = 99/1, flow rate = 0.5 mL/min, $\lambda = 220$ nm, retention time: 22.4 min (major) and 33.0 min (minor), 91% ee.



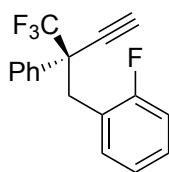
2-7ao

(*R*)-1-Bromo-3-(2-phenyl-2-(trifluoromethyl)but-3-yn-1-yl)benzene (2-7ao). A colorless oil (25.4 mg, 0.072 mmol, 72% yield based on the amount of **2-3a**). $[\alpha]_{\text{D}}^{20} = -44.5$ ($c = 0.5$ in CHCl_3). ^1H NMR (CDCl_3 , 400 MHz) δ 7.63 (t, $J = 3.6$ Hz, 2H, *o*-H of Ph), 7.39-7.35 (m, 3H, *m*-H of Ph and *o*-H of C_6H_4), 7.30-7.27 (m, 1H, *p*-H of Ph), 7.16 (t, $J = 4.0$ Hz, 1H, *p*-H of C_6H_4), 6.97 (t, $J = 15.6$ Hz, 1H, *m*-H of C_6H_4), 6.86 (d, $J = 8.0$ Hz, 1H, *o*-H of C_6H_4), 3.46 (d, $J = 13.6$ Hz, 1H, CH_2), 3.37 (d, $J = 13.6$ Hz, 1H, CH_2), 2.70 (s, 1H, $\text{HC}\equiv$). $^{13}\text{C}\{^1\text{H}\}$ NMR (CDCl_3 , 100 MHz) δ 136.6 (*ipso*-C of Ph), 133.8 (*ipso*-C of C_6H_4), 133.0 (CBr), 130.1 (*o*-CH of C_6H_4), 129.3 (*p*-CH of C_6H_4), 129.1 (*m*-CH of Ph), 128.8 (*o*-CH of C_6H_4), 128.6 (*o*-CH of Ph), 128.4 (*p*-CH of Ph), 125.5 (q, $^1J_{\text{C-F}} = 283$ Hz, CF_3), 121.5 (*m*-CH of C_6H_4), 78.6 ($\text{C}\equiv$), 78.5 ($\text{HC}\equiv$), 52.9 (q, $^2J_{\text{C-F}} = 26.9$ Hz, $\text{CC}\equiv$), 40.4 (CH_2). ^{19}F NMR (CDCl_3): δ -73.4. HRMS (FAB+) Calcd. for $\text{C}_{17}\text{H}_{12}\text{BrF}_3$ $[\text{M}]^+$: 352.0074. Found: 352.0073. The enantiomeric excess of **2-7ao** was determined by HPLC analysis; DAICEL Chiralpak OJ-H, hexane/*i*PrOH = 99/1, flow rate = 0.5 mL/min, $\lambda = 220$ nm, retention time: 19.5 min (major) and 27.8 min (minor), 93% ee.



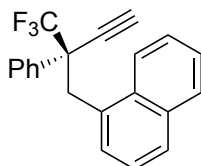
2-7ap

(*R*)-1-Methyl-2-(2-phenyl-2-(trifluoromethyl)but-3-yn-1-yl)benzene (2-7ap). A colorless oil (21.3 mg, 0.074 mmol, 74% yield based on the amount of **2-3a**). $[\alpha]_{\text{D}}^{20} = -50.8$ ($c = 0.5$ in CHCl_3). ^1H NMR (CDCl_3 , 400 MHz) δ 7.67-7.64 (m, 2H, *o*-H of Ph), 7.39-7.35 (m, 3H, *m*-H and *p*-H of Ph), 7.11-7.05 (m, 2H, *m*-H of C_6H_4), 6.90-6.86 (m, 1H, *o*-H of C_6H_4), 6.69-6.67 (m, 1H, *p*-H of C_6H_4), 3.61 (d, $J = 14.4$ Hz, 1H, CH_2), 3.44 (d, $J = 14.4$ Hz, 1H, CH_2), 2.55 (s, 1H, $\text{HC}\equiv$), 2.25 (s, 3H, CH_3). ^{13}C NMR spectrum of this compound was measured in acetone- d_6 because some peaks of this compound overlapped with those of CDCl_3 . $^{13}\text{C}\{^1\text{H}\}$ NMR ($(\text{CD}_3)_2\text{CO}$, 100 MHz) δ 138.3 (*ipso*-C of Ph), 134.6 (*o*-C of C_6H_4), 133.6 (*ipso*-C of C_6H_4), 130.7 (*m*-CH of C_6H_4), 130.6 (*m*-CH of Ph), 129.2 (*o*-CH of C_6H_4), 129.1, 128.9 (*o*-CH and *p*-CH of Ph), 127.3 (*m*-CH of C_6H_4), 126.7 (q, $^1J_{\text{C-F}} = 282$ Hz, CF_3), 125.4 (*m*-CH of C_6H_4), 79.4 ($\text{C}\equiv$), 79.2 ($\text{HC}\equiv$), 52.9 (q, $^2J_{\text{C-F}} = 26.9$ Hz, $\text{CC}\equiv$), 36.7 (CH_2), 19.9 (CH_3). ^{19}F NMR (CDCl_3): δ -73.5. HRMS (FAB+) Calcd. for $\text{C}_{18}\text{H}_{15}\text{F}_3$ $[\text{M}]^+$: 288.1126. Found: 288.1112. The enantiomeric excess of **2-7ap** was determined by HPLC analysis; DAICEL Chiralpak OJ-H, hexane/*i*PrOH = 99/1, flow rate = 0.5 mL/min, $\lambda = 220$ nm, retention time: 14.4 min (major) and 20.0 min (minor), 90% ee.



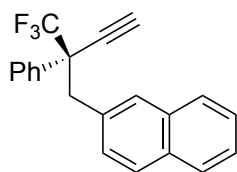
2-7aq

(*R*)-1-Fluoro-2-(2-phenyl-2-(trifluoromethyl)but-3-yn-1-yl)benzene (2-7aq). A colorless oil (22.8 mg, 0.078 mmol, 78% yield based on the amount of **2-3a**). $[\alpha]_{\text{D}}^{20} = -47.0$ ($c = 0.5$ in CHCl_3). ^1H NMR (CDCl_3 , 400 MHz) δ 7.70-7.68 (m, 2H, *m*-H and *p*-H of C_6H_4), 7.37-7.34 (m, 3H, *o*-H and *p*-H of Ph), 7.17-7.12 (m, 1H, *o*-H of C_6H_4), 7.02-6.86 (m, 3H, *m*-H of Ph and *m*-H of C_6H_4), 3.62 (d, $J = 13.6$ Hz, 1H, CH_2), 3.51 (d, $J = 13.6$ Hz, 1H, CH_2), 2.64 (s, 1H, $\text{HC}\equiv$). $^{13}\text{C}\{^1\text{H}\}$ NMR (CDCl_3 , 100 MHz) δ 161.4 (d, $^1J_{\text{C-F}} = 245$ Hz, CF), 133.4 (*ipso*-C of Ph), 132.0 (d, $^3J_{\text{C-F}} = 3.8$ Hz, *o*-CH of C_6H_4), 128.8 (d, $^2J_{\text{C-F}} = 8.6$ Hz, *m*-CH of C_6H_4), 128.6 (*m*-CH of Ph), 128.4 (*o*-CH of Ph), 128.2 (*p*-CH of Ph), 125.6 (q, $^1J_{\text{C-F}} = 283$ Hz, CF_3), 123.2 (d, $^3J_{\text{C-F}} = 3.8$ Hz, *p*-CH of C_6H_4), 121.8 (d, $^2J_{\text{C-F}} = 14.4$ Hz, *ipso*-C of C_6H_4), 78.8 ($\text{C}\equiv$), 77.6 ($\text{HC}\equiv$), 52.3 (q, $^2J_{\text{C-F}} = 26.8$ Hz, $\text{CC}\equiv$), 33.1 (CH_2). ^{19}F NMR (CDCl_3): δ -73.4, -116.8. HRMS (FAB+) Calcd. for $\text{C}_{17}\text{H}_{12}\text{F}_4$ $[\text{M}]^+$: 292.0875. Found: 292.0865. The enantiomeric excess of **2-7aq** was determined by HPLC analysis; DAICEL Chiralpak OJ-H, hexane/*i*-PrOH = 99/1, flow rate = 0.5 mL/min, $\lambda = 220$ nm, retention time: 15.6 min (major) and 18.7 min (minor), 93% ee.



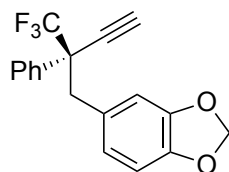
2-7ar

(*R*)-1-(2-Phenyl-2-(trifluoromethyl)but-3-yn-1-yl)naphthalene (2-7ar). A white solid (22.4 mg, 0.069 mmol, 69% yield based on the amount of **2-3a**). m.p. = 83.6-84.2 °C. $[\alpha]_{\text{D}}^{20} = +26.9$ ($c = 0.5$ in CHCl_3). ^1H NMR (CDCl_3 , 400 MHz) δ 8.10-8.07 (m, 1H, aromatic H), 7.82-7.77 (m, 1H, aromatic H), 7.69-7.67 (m, 3H, aromatic H), 7.47-7.42 (m, 2H, *o*-H of Ph), 7.37-7.33 (m, 2H, *m*-H and *p*-H of Ph), 7.19-7.15 (m, 1H, aromatic H), 6.95-6.93 (m, 1H, aromatic H), 4.16 (d, $J = 14.4$ Hz, 1H, CH_2), 3.89 (d, $J = 14.4$ Hz, 1H, CH_2), 2.41 (s, 1H, $\text{HC}\equiv$). $^{13}\text{C}\{^1\text{H}\}$ NMR (CDCl_3 , 100 MHz) δ 134.0 (*ipso*-C of Ph), 134.2, 133.0, 130.5 (1-, 4a- and 8a-C of naphthyl), 128.5 (CH of naphthyl), 128.5 (*m*-CH of Ph), 128.4 (*o*-CH of Ph), 128.3, 127.6 (CH of naphthyl), 125.9 (q, $^1J_{\text{C-F}} = 283$ Hz, CF_3), 125.5 (*p*-CH of Ph), 125.3, 124.7, 124.2 (CH of naphthyl), 79.2 ($\text{C}\equiv$), 78.0 ($\text{HC}\equiv$), 52.4 (q, $^2J_{\text{C-F}} = 25.8$ Hz, $\text{CC}\equiv$), 36.1 (CH_2). ^{19}F NMR (CDCl_3): δ -73.5. HRMS (FAB+) Calcd. for $\text{C}_{21}\text{H}_{15}\text{F}_3$ $[\text{M}]^+$: 324.1126. Found: 324.1132. The enantiomeric excess of **2-7ar** was determined by HPLC analysis; DAICEL Chiralpak OD, hexane/*i*-PrOH = 99/1, flow rate = 0.5 mL/min, $\lambda = 220$ nm, retention time: 10.4 min (minor) and 12.9 min (major), 90% ee.



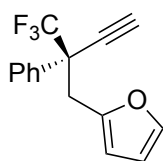
2-7as

(*R*)-2-(2-Phenyl-2-(trifluoromethyl)but-3-yn-1-yl)naphthalene (2-7as). A colorless oil (23.0 mg, 0.071 mmol, 71% yield based on the amount of **2-3a**). $[\alpha]_{\text{D}}^{20} = +37.9$ ($c = 0.5$ in CHCl_3). ^1H NMR (CDCl_3 , 400 MHz) δ 7.75-7.72 (m, 1H, aromatic H), 7.70-7.68 (m, 1H, aromatic H), 7.66-7.63 (m, 3H, aromatic H), 7.58 (d, $J = 8.2$ Hz, 1H, aromatic H), 7.47 (s, 1H, aromatic H), 7.43-7.39 (m, 2H, *o*-H of Ph), 7.38-7.34 (m, 3H, *m*-H and *p*-H of Ph), 7.07 (dd, $J = 8.0$ Hz, 2.0 Hz, 1H, aromatic H), 3.69 (d, $J = 13.6$ Hz, 1H, CH_2), 3.60 (d, $J = 13.2$ Hz, 1H, CH_2), 2.66 (s, 1H, $\text{HC}\equiv$). $^{13}\text{C}\{^1\text{H}\}$ NMR (CDCl_3 , 100 MHz) δ 133.4 (*ipso*-C of Ph), 132.9, 132.4, 131.9 (2-, 4a- and 8a-C of naphthyl), 129.9 (*m*-CH of Ph), 128.7, 128.6, 128.5, 128.3, 127.7, 127.4, 126.9 (CH of naphthyl), 125.7 (*o*-CH of Ph), 125.7 (*p*-CH of Ph), 125.7 (q, $^1J_{\text{C-F}} = 283$ Hz, CF_3), 79.0 ($\text{C}\equiv$), 78.2 ($\text{HC}\equiv$), 53.1 (q, $^2J_{\text{C-F}} = 25.9$ Hz, $\text{CC}\equiv$), 40.9 (CH_2). ^{19}F NMR (CDCl_3): δ -73.4. HRMS (FAB+) Calcd. for $\text{C}_{21}\text{H}_{15}\text{F}_3$ $[\text{M}]^+$: 324.1126. Found: 324.1115. The enantiomeric excess of **2-7as** was determined by HPLC analysis; DAICEL Chiralpak OJ-H, hexane/*i*PrOH = 99/1, flow rate = 0.5 mL/min, $\lambda = 220$ nm, retention time: 22.3 min (minor) and 26.3 min (major), 95% ee.



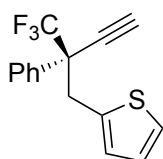
2-7at

(*R*)-5-(2-Phenyl-2-(trifluoromethyl)but-3-yn-1-yl)benzo[d][1,3]dioxole (2-7at). A colorless oil (21.0 mg, 0.066 mmol, 66% yield based on the amount of **2-3a**). $[\alpha]_{\text{D}}^{20} = +52.5$ ($c = 0.5$ in CHCl_3). ^1H NMR (CDCl_3 , 400 MHz) δ 7.67-7.64 (m, 2H, *o*-H of Ph), 7.38-7.35 (m, 3H, *m*-H and *p*-H of Ph), 6.57 (d, $J = 8.4$ Hz, 1H, *m*-H of C_6H_3), 6.49 (d, $J = 1.2$ Hz, 1H, *o*-H of C_6H_3), 6.44 (dd, $J = 7.6$ Hz, 1.6 Hz, 1H, *o*-H of C_6H_3), 5.86 (q, $J = 1.3$ Hz, 2H, CH_2), 3.43 (d, $J = 14.0$ Hz, 1H, CH_2), 3.34 (d, $J = 13.2$ Hz, 1H, CH_2), 2.68 (s, 1H, $\text{HC}\equiv$). $^{13}\text{C}\{^1\text{H}\}$ NMR (CDCl_3 , 100 MHz) δ 146.8 (*m*-C of C_6H_3), 146.5 (*p*-C of C_6H_3), 133.3 (*ipso*-C of Ph), 128.6 (*ipso*-C of C_6H_3), 128.4 (*m*-CH of Ph), 128.3 (*o*-CH of Ph), 127.9 (*p*-CH of Ph), 125.6 (q, $^1J_{\text{C-F}} = 284$ Hz, CF_3), 124.2 (*o*-CH of C_6H_3), 111.0 (*o*-CH of C_6H_3), 107.5 (*m*-CH of C_6H_3), 100.8 (CH_2), 79.0 ($\text{C}\equiv$), 78.1 ($\text{HC}\equiv$), 53.1 (q, $^2J_{\text{C-F}} = 25.9$ Hz), 40.5 (CH_2). ^{19}F NMR (CDCl_3): δ -73.4. HRMS (FAB+) Calcd. for $\text{C}_{18}\text{H}_{13}\text{F}_3\text{O}_2$ $[\text{M}]^+$: 318.0868. Found: 318.0865. The enantiomeric excess of **2-7at** was determined by HPLC analysis; DAICEL Chiralpak OJ-H, hexane/*i*PrOH = 90/10, flow rate = 1.0 mL/min, $\lambda = 220$ nm, retention time: 22.7 min (minor) and 48.1 min (major), 91% ee.



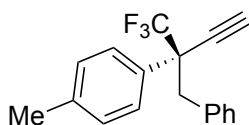
2-7au

(R)-2-(2-Phenyl-2-(trifluoromethyl)but-3-yn-1-yl)furan (2-7au). A colorless oil (19.7 mg, 0.080 mmol, 80% yield based on the amount of **2-3a**). $[\alpha]_D^{20} = -16.2$ ($c = 0.5$ in CHCl_3). ^1H NMR (CDCl_3 , 400 MHz) δ 7.63-7.61 (m, 2H, *o*-H of Ph), 7.44-7.36 (m, 3H, *m*-H and *p*-H of Ph), 6.42 (d, $J = 3.2$ Hz, 1H, 5-H of $\text{C}_4\text{H}_3\text{O}$), 6.00-5.99 (m, 1H, 4-H of $\text{C}_4\text{H}_3\text{O}$), 6.73-6.72 (m, 1H, 3-H of $\text{C}_4\text{H}_3\text{O}$), 2.74 (s, 1H, $\text{HC}\equiv$), 2.90 (d, $J = 0.8$ Hz, 2H, CH_2). $^{13}\text{C}\{^1\text{H}\}$ NMR (CDCl_3 , 100 MHz) δ 153.3 (2-C of $\text{C}_4\text{H}_3\text{O}$), 146.0 (5-CH of $\text{C}_4\text{H}_3\text{O}$), 134.2 (*ipso*-C of Ph), 128.8 (*m*-CH of Ph), 128.5 (*o*-CH of Ph), 128.3 (*p*-CH of Ph), 124.1 (q, $^1J_{\text{C-F}} = 284$ Hz, CF_3), 111.0 (4-CH of $\text{C}_4\text{H}_3\text{O}$), 106.4 (3-CH of $\text{C}_4\text{H}_3\text{O}$), 78.2 ($\text{C}\equiv$), 75.7 ($\text{HC}\equiv$), 52.3 (q, $^2J_{\text{C-F}} = 29.7$ Hz, $\text{CC}\equiv$), 13.6 (CH_2). ^{19}F NMR (CDCl_3): δ -72.2. HRMS (FAB+) Calcd. for $\text{C}_{15}\text{H}_{11}\text{F}_3\text{O}$ $[\text{M}]^+$: 264.0762. Found: 264.0752. The enantiomeric excess of **2-7au** was determined by HPLC analysis; DAICEL Chiralpak OJ-H, hexane/*i*PrOH = 99/1, flow rate = 0.5 mL/min, $\lambda = 220$ nm, retention time: 21.0 min (major) and 27.2 min (minor), 90% ee.



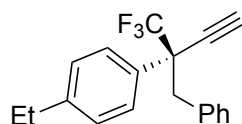
2-7av

(R)-2-(2-Phenyl-2-(trifluoromethyl)but-3-yn-1-yl)thiophene (2-7av). A colorless oil (21.0 mg, 0.075 mmol, 75% yield based on the amount of **2-3a**). $[\alpha]_D^{20} = -12.5$ ($c = 0.5$ in CHCl_3). ^1H NMR (CDCl_3 , 400 MHz) δ 7.70-7.68 (m, 2H, *o*-H of Ph), 7.42-7.36 (m, 3H, *m*-H and *p*-H of Ph), 7.04-7.02 (m, 1H, 5-H of $\text{C}_4\text{H}_3\text{S}$), 6.81-6.79 (m, 1H, 4-H of $\text{C}_4\text{H}_3\text{S}$), 6.73-6.72 (m, 1H, 3-H of $\text{C}_4\text{H}_3\text{S}$), 3.80 (d, $J = 14.8$ Hz, 1H, CH_2), 3.68 (d, $J = 14.8$ Hz, 1H, CH_2), 2.67 (s, 1H, $\text{HC}\equiv$). $^{13}\text{C}\{^1\text{H}\}$ NMR (CDCl_3 , 100 MHz) δ 135.8 (*ipso*-C of Ph), 132.8 (2-C of $\text{C}_4\text{H}_3\text{S}$), 128.8 (*m*-CH of Ph), 128.6 (5-C of $\text{C}_4\text{H}_3\text{S}$), 128.4 (4-C of $\text{C}_4\text{H}_3\text{S}$), 128.3 (3-C of $\text{C}_4\text{H}_3\text{S}$), 126.0 (*o*-CH of Ph), 125.3 (q, $^1J_{\text{C-F}} = 283$ Hz, CF_3), 124.9 (*o*-CH of Ph), 78.9 ($\text{C}\equiv$), 77.7 ($\text{HC}\equiv$), 52.9 (q, $^2J_{\text{C-F}} = 25.8$ Hz, $\text{CC}\equiv$), 35.4 (CH_2), 21.0 (CH_3). ^{19}F NMR (CDCl_3): δ -74.1. HRMS (FAB+) Calcd. for $\text{C}_{15}\text{H}_{11}\text{F}_3\text{S}$ $[\text{M}]^+$: 280.0534. Found: 280.0522. The enantiomeric excess of **2-7av** was determined by HPLC analysis; DAICEL Chiralpak OJ-H, hexane/*i*PrOH = 99/1, flow rate = 0.5 mL/min, $\lambda = 220$ nm, retention time: 15.4 min (major) and 22.9 min (minor), 94% ee.



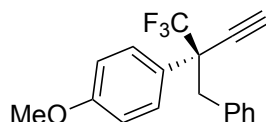
2-7ba

(R)-1-(2-Benzyl-1,1,1-trifluorobut-3-yn-2-yl)-4-methylbenzene (2-7ba). A colorless oil (23.4 mg, 0.081 mmol, 81% yield based on the amount of **2-3b**). $[\alpha]_D^{20} = -44.6$ ($c = 0.5$ in CHCl_3). ^1H NMR (CDCl_3 , 400 MHz) δ 7.54-7.52 (m, 2H, *o*-H of C_6H_4), 7.18-7.10 (m, 5H, H of Ph), 7.02-6.95 (m, 2H, *m*-H of C_6H_4), 3.50 (d, $J = 13.2$ Hz, 1H, CH_2), 3.40 (d, $J = 13.2$ Hz, 1H, CH_2), 2.63 (s, 1H, $\text{HC}\equiv$), 2.35 (s, 3H, CH_3). $^{13}\text{C}\{^1\text{H}\}$ NMR (CDCl_3 , 100 MHz) δ 138.4 (*ipso*-C of C_6H_4), 134.5 (*ipso*-C of Ph), 130.7 (*p*-C of C_6H_4), 130.3 (*m*-CH of Ph), 129.0 (*m*-CH of C_6H_4), 128.3 (*o*-CH of Ph), 127.5 (*o*-CH of C_6H_4), 126.9 (*o*-CH of Ph), 125.7 (q, $^2J_{\text{C-F}} = 283$ Hz, CF_3), 79.1 ($\text{C}\equiv$), 77.8 ($\text{HC}\equiv$), 52.6 (q, $^3J_{\text{C-F}} = 25.9$ Hz, $\text{CC}\equiv$), 40.6 (CH_2), 21.0 (CH_3). ^{19}F NMR (CDCl_3): δ -73.8. HRMS (FAB+) Calcd. for $\text{C}_{18}\text{H}_{15}\text{F}_3$ $[\text{M}]^+$: 288.1126. Found: 288.1123. The enantiomeric excess of **2-7ba** was determined by HPLC analysis; DAICEL Chiralpak OJ-H, hexane/*i*PrOH = 99/1, flow rate = 0.5 mL/min, $\lambda = 220$ nm, retention time: 15.1 min (major) and 22.2 min (minor), 90% ee.



2-7ca

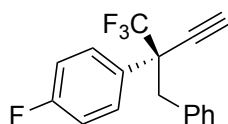
(R)-1-(2-Benzyl-1,1,1-trifluorobut-3-yn-2-yl)-4-ethylbenzene (2-7ca). A colorless oil (23.0 mg, 0.076 mmol, 76% yield based on the amount of **2-3c**). $[\alpha]_D^{20} = -47.4$ ($c = 0.5$ in CHCl_3). ^1H NMR (CDCl_3 , 400 MHz) δ 7.56 (d, $J = 7.6$ Hz, 2H, *o*-H of C_6H_4), 7.20-7.11 (m, 5H, H of Ph), 7.03-7.00 (m, 2H, *m*-H of C_6H_4), 3.51 (d, $J = 13.2$ Hz, 1H, CH_2), 3.41 (d, $J = 13.2$ Hz, 1H, CH_2), 2.66 (q, $J = 7.7$ Hz, 2H, CH_2CH_3), 2.63 (s, 1H, $\text{HC}\equiv$), 1.25 (t, $J = 7.6$ Hz, 3H, CH_3). $^{13}\text{C}\{^1\text{H}\}$ NMR (CDCl_3 , 100 MHz) δ 144.6 (*ipso*-C of C_6H_4), 134.6 (*ipso*-C of Ph), 130.8 (*p*-C of C_6H_4), 130.6 (*m*-CH of Ph), 128.4 (*m*-CH of C_6H_4), 127.7 (*o*-CH of Ph), 127.5 (*o*-CH of C_6H_4), 126.9 (*o*-CH of Ph), 125.7 (q, $^2J_{\text{C-F}} = 283$ Hz, CF_3), 79.2 ($\text{C}\equiv$), 77.8 ($\text{HC}\equiv$), 52.6 (q, $^3J_{\text{C-F}} = 25.9$ Hz, $\text{CC}\equiv$), 40.7 (CH_2), 28.3 (CH_2CH_3), 15.2 (CH_3). ^{19}F NMR (CDCl_3): δ -73.6. HRMS (FAB+) Calcd. for $\text{C}_{19}\text{H}_{17}\text{F}_3$ $[\text{M}]^+$: 302.1282. Found: 302.1280. The enantiomeric excess of **2-7ca** was determined by HPLC analysis; DAICEL Chiralpak OJ-H, hexane/*i*PrOH = 99/1, flow rate = 0.5 mL/min, $\lambda = 220$ nm, retention time: 11.7 min (major) and 14.6 min (minor), 90% ee.



2-7da

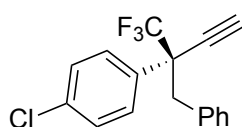
(R)-1-(2-Benzyl-1,1,1-trifluorobut-3-yn-2-yl)-4-methylbenzene (2-7da). A colorless oil (21.6 mg, 0.071 mmol, 71% yield based on the amount of **2-3d**). $[\alpha]_D^{20} = -43.6$ ($c = 0.5$ in CHCl_3). ^1H NMR (CDCl_3 , 400 MHz) δ 7.59-7.56 (m, 2H, *o*-H of C_6H_4), 7.18-7.12 (m, 3H, *m*-H and *p*-H of Ph), 7.03-7.00 (m, 3H, *o*-H of Ph), 6.91-6.87 (m, 2H, *m*-H of C_6H_4), 3.82 (s, 3H, CH_3), 3.50 (d, $J = 13.2$ Hz, 1H, CH_2), 3.40 (d, $J = 13.2$ Hz, 1H,

CH₂), 2.63 (s, 1H, HC≡). ¹³C{¹H} NMR (CDCl₃, 100 MHz) δ 159.5 (*p*-C of C₆H₄), 134.5 (*ipso*-C of Ph), 130.8 (*ipso*-C of C₆H₄), 129.7 (*o*-CH of C₆H₄), 127.6 (*m*-CH of Ph), 126.9 (*o*-CH of Ph), 125.7 (q, ¹J_{C-F} = 283 Hz, CF₃), 125.2 (*p*-CH of Ph), 113.5 (*m*-CH of C₆H₄), 79.2 (C≡), 77.8 (HC≡), 55.2 (CH₃), 52.3 (q, ²J_{C-F} = 25.8 Hz, CC≡), 40.6 (CH₂). ¹⁹F NMR (CDCl₃): δ -74.0. HRMS (FAB+) Calcd. for C₁₈H₁₆F₃O [M+H]⁺: 304.1153. Found: 305.1140. The enantiomeric excess of **2-7da** was determined by HPLC analysis; DAICEL Chiralpak OJ-H, hexane/ⁱPrOH = 90/10, flow rate = 0.5 mL/min, λ = 220 nm, retention time: 23.2 min (major) and 34.6 min (minor), 91% ee.



2-7ea

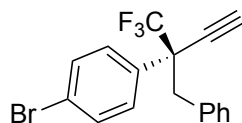
(R)-1-(2-Benzyl-1,1,1-trifluorobut-3-yn-2-yl)-4-fluorobenzene (2-7ea). A colorless oil (22.5 mg, 0.077 mmol, 77% yield based on the amount of **2-3e**). [α]_D²⁰ = -58.8 (c = 0.5 in CHCl₃). ¹H NMR (CDCl₃, 400 MHz) δ 7.64-7.60 (m, 2H, *o*-H of C₆H₄), 7.19-7.11 (m, 3H, *m*-H and *p*-H of Ph), 7.07-7.01 (m, 2H, *o*-H of Ph), 7.00-6.96 (m, 2H, *m*-H of C₆H₄), 3.46 (d, *J* = 13.2 Hz, 1H, CH₂), 3.41 (d, *J* = 13.2 Hz, 1H, CH₂), 2.67 (s, 1H, HC≡). ¹³C{¹H} NMR (CDCl₃, 100 MHz) δ 162.7 (d, ¹J_{C-F} = 247 Hz, CF of C₆H₄), 134.1 (*ipso*-C of C₆H₄), 130.7 (*ipso*-C of Ph), 130.4 (*o*-CH of Ph), 130.3 (*m*-CH of Ph), 129.1 (*o*-CH of C₆H₄), 129.1 (*m*-CH of Ph), 125.6 (q, ¹J_{C-F} = 283 Hz, CF₃), 115.3 (*p*-CH of Ph), 115.1 (*m*-CH of C₆H₄), 78.8 (C≡), 78.2 (HC≡), 52.5 (q, ²J_{C-F} = 26.8 Hz, CC≡), 40.8 (CH₂). ¹⁹F NMR (CDCl₃): δ -73.8, -115.1. HRMS (FAB+) Calcd. for C₁₇H₁₃F₄ [M+H]⁺: 293.0953. Found: 293.0945. The enantiomeric excess of **2-7ea** was determined by HPLC analysis; DAICEL Chiralpak OD, hexane/ⁱPrOH = 99/1, flow rate = 0.5 mL/min, λ = 220 nm, retention time: 9.0 min (major) and 10.0 min (minor), 94% ee.



2-7fa

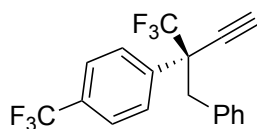
(R)-1-(2-Benzyl-1,1,1-trifluorobut-3-yn-2-yl)-4-chlorobenzene (2-7fa). A colorless oil (22.8 mg, 0.074 mmol, 74% yield based on the amount of **2-3f**). [α]_D²⁰ = -54.2 (c = 0.5 in CHCl₃). ¹H NMR (CDCl₃, 400 MHz) δ 7.59-7.57 (m, 2H, *m*-H of C₆H₄), 7.34-7.30 (m, 2H, *o*-H of C₆H₄), 7.18-7.10 (m, 3H, *m*-H and *p*-H of Ph), 7.00-6.98 (m, 2H, *o*-H of Ph), 3.47 (d, *J* = 13.2 Hz, 1H, CH₂), 3.42 (d, *J* = 13.2 Hz, 1H, CH₂), 2.68 (s, 1H, HC≡). ¹³C{¹H} NMR (CDCl₃, 100 MHz) δ 134.7 (*ipso*-C of C₆H₄), 134.0 (*ipso*-C of Ph), 131.9 (CCl of C₆H₄), 130.7 (*m*-CH of Ph), 129.9 (*m*-CH of C₆H₄), 128.5 (*o*-CH of Ph), 127.7 (*o*-CH of C₆H₄), 127.1 (*p*-CH of Ph), 125.5 (q, ²J_{C-F} = 283 Hz, CF₃), 78.6 (C≡), 78.4 (HC≡), 52.6 (q, ³J_{C-F} = 26.8 Hz, CC≡), 40.6 (CH₂). ¹⁹F NMR (CDCl₃): δ -73.7. HRMS (FAB+) Calcd. for C₁₇H₁₂ClF₃ [M]⁺: 308.0580. Found: 308.0590. The enantiomeric excess of **2-7fa** was determined by HPLC analysis; DAICEL Chiralpak

OJ-H, hexane/*i*PrOH = 99/1, flow rate = 0.5 mL/min, λ = 220 nm, retention time: 15.2 min (major) and 16.6 min (minor), 90% ee.



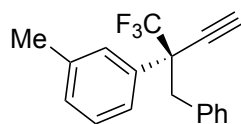
2-7ga

(*R*)-1-(2-Benzyl-1,1,1-trifluorobut-3-yn-2-yl)-4-bromobenzene (2-7ga). A white solid (24.7 mg, 0.070 mmol, 70% yield based on the amount of **2-3g**). m.p.= 49.2-59.3 °C. $[\alpha]_D^{20}$ = -20.3 (c = 0.5 in CHCl₃). ¹H NMR (CDCl₃, 400 MHz) δ 7.53-7.46 (m, 4H, *o*-H and *m*-H of C₆H₄), 7.20-7.12 (m, 3H, *m*-H and *p*-H of Ph), 7.01-6.98 (m, 2H, *o*-H of Ph), 3.46 (d, J = 14.0 Hz, 1H, CH₂), 3.41 (d, J = 14.0 Hz, 1H, CH₂), 2.67 (s, 1H, HC \equiv). ¹³C{¹H} NMR (CDCl₃, 100 MHz) δ 133.9 (*ipso*-C of C₆H₄), 132.5 (*ipso*-C of Ph), 131.4 (*m*-CH of Ph), 130.7 (*m*-CH of C₆H₄), 130.3 (*o*-CH of Ph), 127.7 (*o*-CH of C₆H₄), 127.2 (*p*-CH of Ph), 125.4 (q, ² J_{C-F} = 284 Hz, CF₃), 123.0 (CBr of C₆H₄), 78.5 (C \equiv), 78.4 (HC \equiv), 52.7 (q, ³ J_{C-F} = 26.8 Hz, CC \equiv), 40.6 (CH₂). ¹⁹F NMR (CDCl₃): δ -73.7. HRMS (FAB+) Calcd. for C₁₇H₁₂BrF₃ [M]⁺: 352.0074. Found: 352.0083. The enantiomeric excess of **2-7ga** was determined by HPLC analysis; DAICEL Chiralpak OD, hexane/*i*PrOH = 99/1, flow rate = 0.5 mL/min, λ = 220 nm, retention time: 8.8 min (major) and 9.8 min (minor), 92% ee.



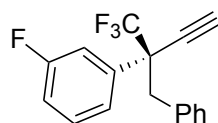
2-7ha

(*R*)-1-(2-Benzyl-1,1,1-trifluorobut-3-yn-2-yl)-4-(trifluoromethyl)benzene (2-7ha). A colorless oil (28.4 mg, 0.083 mmol, 83% yield based on the amount of **2-3h**). $[\alpha]_D^{20}$ = -50.2 (c = 0.5 in CHCl₃). ¹H NMR (CDCl₃, 400 MHz) δ 7.78 (d, 2H, J = 8.0 Hz, *m*-H of C₆H₄), 7.61 (d, 2H, J = 8.0 Hz, *o*-H of C₆H₄), 7.19-7.11 (m, 3H, *m*-H and *p*-H of Ph), 6.99-6.96 (m, 2H, *o*-H of Ph), 3.50 (d, J = 13.6 Hz, 1H, CH₂), 3.46 (d, J = 13.2 Hz, 1H, CH₂), 2.72 (s, 1H, HC \equiv). ¹³C{¹H} NMR (CDCl₃, 100 MHz) δ 137.5 (*ipso*-C of C₆H₄), 133.7 (*ipso*-C of Ph), 130.7 (*m*-CH of Ph), 129.0 (*o*-CH of Ph), 128.4 (q, ² J_{C-F} = 31.6 Hz, *p*-C of C₆H₄), 127.8 (*o*-CH of C₆H₄), 125.4 (q, ¹ J_{C-F} = 283 Hz, CF₃ of C₆H₄), 125.2 (q, ³ J_{C-F} = 3.8 Hz, *m*-CH of C₆H₄), 124.2 (q, ¹ J_{C-F} = 270 Hz, CF₃), 78.8 (C \equiv), 78.3 (HC \equiv), 53.0 (q, ² J_{C-F} = 26.8 Hz, CC \equiv), 40.7 (CH₂). ¹⁹F NMR (CDCl₃): δ -64.3, -73.3. HRMS (FAB+) Calcd. for C₁₈H₁₂F₆ [M]⁺: 342.0843. Found: 342.0847. The enantiomeric excess of **2-7ha** was determined by HPLC analysis; DAICEL Chiralpak OD, hexane/*i*PrOH = 99/1, flow rate = 0.5 mL/min, λ = 220 nm, retention time: 9.7 min (major) and 10.7 min (minor), 93% ee.



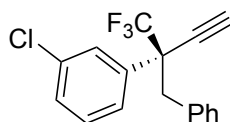
2-7ia

(*R*)-1-(2-Benzyl-1,1,1-trifluorobut-3-yn-2-yl)-3-methylbenzene (2-7ia). A colorless oil (19.3 mg, 0.067 mmol, 67% yield based on the amount of **2-3i**). $[\alpha]_{\text{D}}^{20} = -49.4$ ($c = 0.5$ in CHCl_3). ^1H NMR (CDCl_3 , 400 MHz) δ 7.45 (s, 2H, *m*-H of Ph), 7.27-7.22 (m, 1H, *m*-H of C_6H_4), 7.18-7.10 (m, 4H, *o*-H and *o*-H of C_6H_4 and *p*-H of Ph), 7.01-6.98 (m, 2H, *o*-H Ph), 3.51 (d, $J = 14.0$ Hz, 1H, CH_2), 3.40 (d, $J = 13.2$ Hz, 1H, CH_2), 2.64 (s, 1H, $\text{HC}\equiv$), 2.36 (s, 3H, CH_3). $^{13}\text{C}\{^1\text{H}\}$ NMR (CDCl_3 , 100 MHz) δ 137.9 (*ipso*-C of Ph), 134.5 (*m*-C of C_6H_4), 133.2 (*ipso*-C of C_6H_4), 130.8 (*m*-CH of C_6H_4), 129.3 (*m*-CH of Ph), 129.2 (*o*-CH of C_6H_4), 128.1, 127.5 (*o*-CH and *p*-CH of Ph), 126.9 (*p*-CH of C_6H_4), 125.7 (q, $^1J_{\text{C-F}} = 283$ Hz, CF_3), 125.4 (*o*-CH of C_6H_4), 79.1 ($\text{C}\equiv$), 78.0 ($\text{HC}\equiv$), 52.9 (q, $^2J_{\text{C-F}} = 26.8$ Hz, $\text{CC}\equiv$), 40.7 (CH_2), 21.6 (CH_3). ^{19}F NMR (CDCl_3): δ -73.4. HRMS (FAB+) Calcd. for $\text{C}_{18}\text{H}_{16}\text{F}_3$ $[\text{M}+\text{H}]^+$: 289.1204. Found: 289.1203. The enantiomeric excess of **2-7ia** was determined by HPLC analysis; DAICEL Chiralpak OJ-H, hexane/*i*PrOH = 99/1, flow rate = 0.5 mL/min, $\lambda = 220$ nm, retention time: 13.9 min (major) and 15.4 min (minor), 90% ee.



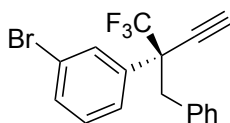
2-7ja

(*R*)-1-(2-Benzyl-1,1,1-trifluorobut-3-yn-2-yl)-3-fluorobenzene (2-7ja). A colorless oil (21.0 mg, 0.072 mmol, 72% yield based on the amount of **2-3j**). $[\alpha]_{\text{D}}^{20} = -18.5$ ($c = 0.5$ in CHCl_3). ^1H NMR (CDCl_3 , 400 MHz) δ 7.48-7.43 (m, 1H, *m*-H of C_6H_4), 7.39-7.36 (m, 1H, *o*-H of C_6H_4), 7.34-7.30 (m, 1H, *p*-H of C_6H_4), 7.20-7.11 (m, 3H, *m*-H and *p*-H of Ph), 7.07-7.02 (m, 1H, *o*-H of C_6H_4), 7.00-6.97 (m, 2H, *o*-H of Ph), 3.47 (d, $J = 13.6$ Hz, 1H, CH_2), 3.42 (d, $J = 13.2$ Hz, 1H, CH_2), 2.68 (s, 1H, $\text{HC}\equiv$). $^{13}\text{C}\{^1\text{H}\}$ NMR (CDCl_3 , 100 MHz) δ 163.2 (d, $^1J_{\text{C-F}} = 243$ Hz, CF), 136.8 (d, $^3J_{\text{C-F}} = 7.6$ Hz, *ipso*-C of C_6H_4), 135.0 (*ipso*-C of Ph), 131.5 (*m*-CH of Ph), 130.9 (d, $^3J_{\text{C-F}} = 8.6$ Hz, *m*-C of C_6H_4), 128.3 (*o*-CH of Ph), 127.8 (*p*-CH of Ph), 126.5 (q, $^1J_{\text{C-F}} = 283$ Hz, CF_3), 116.6 (d, $^2J_{\text{C-F}} = 24.0$ Hz, *o*-CH of C_6H_4), 116.3 (d, $^2J_{\text{C-F}} = 21.1$ Hz, *p*-CH of C_6H_4), 80.7 ($\text{C}\equiv$), 79.0 ($\text{HC}\equiv$), 53.6 (q, $^2J_{\text{C-F}} = 27.8$ Hz, $\text{CC}\equiv$), 40.5 (CH_2). ^{19}F NMR (CDCl_3): δ -73.4, -113.8. HRMS (FAB+) Calcd. for $\text{C}_{17}\text{H}_{12}\text{F}_4$ $[\text{M}]^+$: 292.0875. Found: 292.0878. The enantiomeric excess of **2-7ja** was determined by HPLC analysis; DAICEL Chiralpak OJ-H, hexane/*i*PrOH = 99/1, flow rate = 0.5 mL/min, $\lambda = 220$ nm, retention time: 11.9 min (major) and 16.0 min (minor), 90% ee.



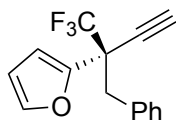
2-7ka

(*R*)-1-(2-Benzyl-1,1,1-trifluorobut-3-yn-2-yl)-3-chlorobenzene (2-7ka). A colorless oil (20.1 mg, 0.065 mmol, 65% yield based on the amount of **2-3k**). $[\alpha]_D^{20} = -50.0$ ($c = 0.5$ in CHCl_3). ^1H NMR (CDCl_3 , 400 MHz) δ 7.64 (s, 1H, *o*-H of C_6H_4), 7.54 (d, $J = 7.2$ Hz, 1H, *p*-H of C_6H_4), 7.34-7.27 (m, 2H, *m*-H and *p*-H of C_6H_4), 7.18-7.12 (m, 3H, *m*-H and *p*-H of Ph), 7.01-6.98 (m, 2H, *o*-H of Ph), 3.47 (d, $J = 13.6$ Hz, 1H, CH_2), 3.42 (d, $J = 13.6$ Hz, 1H, CH_2), 2.69 (s, 1H, $\text{HC}\equiv$). $^{13}\text{C}\{^1\text{H}\}$ NMR (CDCl_3 , 100 MHz) δ 135.5 (*ipso*-C of C_6H_4), 134.3 (*ipso*-C of Ph), 133.9 (CCl), 130.7 (*m*-C of C_6H_4), 129.4 (*o*-CH of Ph), 128.9 (*m*-CH of Ph), 128.8, (*p*-CH of Ph), 127.7 (*p*-CH of C_6H_4), 127.2 (*o*-CH of C_6H_4), 126.6 (*o*-CH of C_6H_4), 125.4 (q, $^1J_{\text{C-F}} = 284$ Hz, CF_3), 78.6 ($\text{C}\equiv$), 78.4 ($\text{HC}\equiv$), 52.9 (q, $^2J_{\text{C-F}} = 26.9$ Hz, $\text{CC}\equiv$), 40.7 (CH_2). ^{19}F NMR (CDCl_3): δ -73.4. HRMS (FAB+) Calcd. for $\text{C}_{17}\text{H}_{12}\text{ClF}_3$ $[\text{M}]^+$: 308.0580. Found: 308.0576. The enantiomeric excess of **2-7ka** was determined by HPLC analysis; DAICEL Chiralpak OJ-H, hexane/ i PrOH = 99/1, flow rate = 0.5 mL/min, $\lambda = 220$ nm, retention time: 27.9 min (major) and 35.2 min (minor), 95% ee.



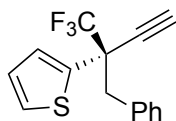
2-7la

(*R*)-1-(2-Benzyl-1,1,1-trifluorobut-3-yn-2-yl)-3-bromobenzene (2-7la). A colorless oil (24.7 mg, 0.070 mmol, 70% yield based on the amount of **2-3l**). $[\alpha]_D^{20} = -45.9$ ($c = 0.5$ in CHCl_3). ^1H NMR (CDCl_3 , 400 MHz) δ 7.79 (s, 1H, *o*-H of C_6H_4), 7.60-7.57 (m, 1H, *p*-H of C_6H_4), 7.50-7.47 (m, 1H, *m*-H of C_6H_4), 7.25-7.12 (m, 1H, *o*-H of C_6H_4), 7.17-7.12 (m, 3H, *o*-H and *p*-H of C_6H_4), 7.01-6.98 (m, 1H, *m*-H of Ph), 3.46 (d, $J = 13.6$ Hz, 1H, CH_2), 3.41 (d, $J = 13.6$ Hz, 1H, CH_2), 2.69 (s, 1H, $\text{HC}\equiv$). $^{13}\text{C}\{^1\text{H}\}$ NMR (CDCl_3 , 100 MHz) δ 135.7 (*ipso*-C of C_6H_4), 133.8 (*ipso*-C of C_6H_4), 131.8, (*o*-CH of C_6H_4), 131.7 (*m*-CH of C_6H_4), 130.7 (*p*-CH of C_6H_4), 127.7 (*m*-CH of Ph), 127.2 (*o*-CH of Ph), 127.1 (*p*-CH of Ph), 125.4 (q, $^1J_{\text{C-F}} = 284$ Hz, CF_3), 122.5 (CBr of Ph), 78.7 ($\text{C}\equiv$), 78.3 ($\text{HC}\equiv$), 52.8 (q, $^2J_{\text{C-F}} = 25.9$ Hz, $\text{CC}\equiv$), 40.7 (CH_2). ^{19}F NMR (CDCl_3): δ -73.4. HRMS (FAB+) Calcd. for $\text{C}_{17}\text{H}_{12}\text{BrF}_3$ $[\text{M}]^+$: 352.0074. Found: 352.0070. The enantiomeric excess of **2-7la** was determined by HPLC analysis; DAICEL Chiralpak OJ-H, hexane/ i PrOH = 99/1, flow rate = 0.5 mL/min, $\lambda = 220$ nm, retention time: 14.1 min (minor) and 18.4 min (major), 90% ee.



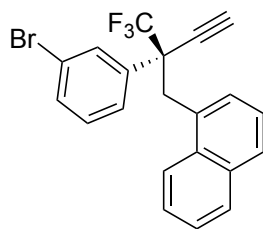
2-7ma

(R)-2-(2-Benzyl-1,1,1-trifluorobut-3-yn-2-yl)furan (2-7ma). A colorless oil (20.1 mg, 0.076 mmol, 76% yield based on the amount of **2-3m**). $[\alpha]_D^{20} = -11.0$ ($c = 0.5$ in CHCl_3). ^1H NMR (CDCl_3 , 400 MHz) δ 7.50 (q, $J = 0.9$ Hz, 1H, 5-H of $\text{C}_4\text{H}_3\text{O}$), 7.21-7.15 (m, 3H, *m*-H and *p*-H of Ph), 7.00-6.96 (m, 2H, *o*-H of Ph), 6.40-6.39 (m, 1H, 4-H of $\text{C}_4\text{H}_3\text{O}$), 6.32 (dd, $J = 3.2$ Hz, 1.2 Hz, 1H, 3-H of $\text{C}_4\text{H}_3\text{O}$), 3.61 (d, $J = 12.8$ Hz, 1H, CH_2), 3.22 (d, $J = 12.8$ Hz, 1H, CH_2), 2.47 (s, 1H, $\text{HC}\equiv$). $^{13}\text{C}\{^1\text{H}\}$ NMR (CD_3CN , 100 MHz) δ 147.2 (*ipso*-C of $\text{C}_4\text{H}_3\text{O}$), 144.4 (5-CH of $\text{C}_4\text{H}_3\text{O}$), 134.6 (*ipso*-C of Ph), 130.9 (*m*-CH of Ph), 128.2 (*o*-CH of Ph), 127.7 (*p*-CH of Ph), 125.2 (q, $^1J_{\text{C-F}} = 283$ Hz, CF_3), 112.8 (4-CH of $\text{C}_4\text{H}_3\text{O}$), 111.2 (3-CH of $\text{C}_4\text{H}_3\text{O}$), 77.5 ($\text{C}\equiv$), 76.9 ($\text{HC}\equiv$), 49.7 (q, $^2J_{\text{C-F}} = 27.8$ Hz, $\text{CC}\equiv$), 38.7 (CH_2). ^{19}F NMR (CDCl_3): δ -74.7. HRMS (FAB+) Calcd. for $\text{C}_{15}\text{H}_{11}\text{F}_3\text{O}$ $[\text{M}]^+$: 264.0762. Found: 264.0758. The enantiomeric excess of **2-7ma** was determined by HPLC analysis; DAICEL Chiralpak OJ-H, hexane/*i*PrOH = 99/1, flow rate = 0.5 mL/min, $\lambda = 220$ nm, retention time: 13.2 min (minor) and 16.0 min (major), 96% ee.



2-7na

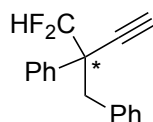
(S)-2-(2-Benzyl-1,1,1-trifluorobut-3-yn-2-yl)thiophene (2-7na). A colorless oil (18.2 mg, 0.065 mmol, 65% yield based on the amount of **2-3n**). $[\alpha]_D^{20} = -51.6$ ($c = 0.5$ in CHCl_3). ^1H NMR (CDCl_3 , 400 MHz) δ 7.30 (dd, $J = 5.2$ Hz, 3.6 Hz, 1H, 5-H of $\text{C}_4\text{H}_3\text{S}$), 7.21-7.15 (m, 4H, *m*-H and *p*-H of Ph, 4-H of $\text{C}_4\text{H}_3\text{S}$), 7.05-7.02 (m, 2H, *o*-H of Ph), 6.98 (dd, $J = 4.8$ Hz, 1.2 Hz, 1H, 3-H of $\text{C}_4\text{H}_3\text{S}$), 3.41 (d, $J = 12.8$ Hz, 1H, CH_2), 3.36 (d, $J = 12.8$ Hz, 1H, CH_2), 2.60 (s, 1H, $\text{HC}\equiv$). $^{13}\text{C}\{^1\text{H}\}$ NMR (CD_3CN , 100 MHz) δ 137.3 (*ipso*-C of $\text{C}_4\text{H}_3\text{S}$), 134.0 (*ipso*-C of Ph), 130.6 (*m*-CH of Ph), 128.3 (*o*-CH of Ph), 127.6 (4-CH of $\text{C}_4\text{H}_3\text{O}$), 127.2 (3-CH of $\text{C}_4\text{H}_3\text{O}$), 126.8 (*p*-CH of Ph), 126.3 (5-CH of $\text{C}_4\text{H}_3\text{O}$), 125.1 (q, $^1J_{\text{C-F}} = 282$ Hz, CF_3), 78.5 ($\text{C}\equiv$), 76.8 ($\text{HC}\equiv$), 50.5 (q, $^2J_{\text{C-F}} = 27.8$ Hz), 42.6 (CH_2). ^{19}F NMR (CDCl_3): δ -75.1. HRMS (FAB+) Calcd. for $\text{C}_{15}\text{H}_{11}\text{F}_3\text{S}$ $[\text{M}]^+$: 280.0534. Found: 280.0527. The enantiomeric excess of **2-7na** was determined by HPLC analysis; DAICEL Chiralpak OJ-H, hexane/*i*PrOH = 99/1, flow rate = 0.5 mL/min, $\lambda = 220$ nm, retention time: 18.4 min (minor) and 23.6 min (major), 90% ee.



2-7lr

(*R*)-1-(2-(3-Bromophenyl)-2-(trifluoromethyl)but-3-yn-1-yl)naphthalene (2-7lr).

A white solid (24.6 mg, 0.061 mmol, 61% yield based on the amount of **2-3l**). m.p.= 95.2-96.4 °C. $[\alpha]_D^{20} = +36.9$ ($c = 0.5$ in CHCl_3). ^1H NMR (CDCl_3 , 400 MHz) δ 8.07-8.03 (m, 1H, aromatic H), 7.84-7.79 (m, 2H, aromatic H), 7.72-7.70 (m, 1H, aromatic H), 7.60-7.58 (m, 1H, aromatic H), 7.50-7.45 (m, 3H, *o*-H and *p*-H of C_6H_4), 7.24-7.18 (m, 1H, *m*-H of Ph), 6.98-6.97 (m, 1H, aromatic H), 4.14 (d, $J = 14.4$ Hz, 1H, CH_2), 3.85 (d, $J = 14.4$ Hz, 1H, CH_2), 2.45 (s, 1H, $\text{HC}\equiv$). $^{13}\text{C}\{^1\text{H}\}$ NMR (CDCl_3 , 100 MHz) δ 136.3 (*ipso*-C of Ph), 133.6, 132.9, (1- and 4a-C of naphthyl), 131.8 (*o*-CH of C_6H_4), 131.6 (8a-C of naphthyl), 130.0 (CH of naphthyl), 129.8 (*m*-CH of Ph), 128.6 (*o*-CH of Ph), 128.4 (CH of naphthyl), 127.9 (*p*-CH of Ph), 126.9 (CH of naphthyl), 125.6 (q, $^1J_{\text{C-F}} = 284$ Hz, CF_3), 125.5, 124.7 (CH of naphthyl), 122.6 (CBr of Ph), 78.7 ($\text{C}\equiv$), 78.5 ($\text{HC}\equiv$), 52.3 (q, $^2J_{\text{C-F}} = 26.9$ Hz, $\text{CC}\equiv$), 36.2 (CH_2). ^{19}F NMR (CDCl_3): δ -73.3. HRMS (FAB+) Calcd. for $\text{C}_{21}\text{H}_{14}\text{BrF}_3$ $[\text{M}]^+$: 402.0231. Found: 402.0240. The enantiomeric excess of **2-7lr** was determined by HPLC analysis; DAICEL Chiralpak OD, hexane/*i*PrOH = 99/1, flow rate = 0.5 mL/min, $\lambda = 220$ nm, retention time: 13.6 min (minor) and 18.9 min (major), 91% ee.



2-9

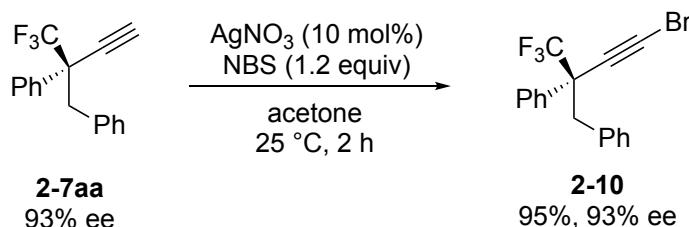
(*R*)-2-(2-(Difluoromethyl)but-3-yn-1,2-diyl)dibenzene (2-9). A colorless oil (19.2 mg, 0.075 mmol, 75% yield based on the amount of **2-8**). $[\alpha]_D^{20} = -32.7$ ($c = 0.5$ in CHCl_3). ^1H NMR (CDCl_3 , 400 MHz) δ 7.62-7.59 (m, 2H, *o*-H of Ph), 7.40-7.34 (m, 3H, *m*-H and *p*-H of Ph), 7.21-7.16 (m, 3H, *m*-H and *p*-H of Ph), 7.09-7.06 (m, 2H, *o*-H of Ph), 6.00 (t, $J_{\text{H-F}} = 56.0$ Hz, 1H, CF_2H), 3.39 (d, $J = 13.2$ Hz, 1H, CH_2), 3.31 (d, $J = 13.2$ Hz, 1H, CH_2), 2.62 (s, 1H, $\text{HC}\equiv$). $^{13}\text{C}\{^1\text{H}\}$ NMR (CDCl_3 , 100 MHz) δ 135.2 (*ipso*-C of Ph), 134.9 (*ipso*-C of Ph), 130.7 (*o*-CH of Ph), 128.3 (*m*-CH of Ph), 128.2 (*m*-CH of Ph), 128.1 (*p*-CH of Ph), 126.9 (*p*-CH of Ph), 116.5 (t, $^1J_{\text{C-F}} = 250$ Hz, CF_2H), 80.8 (dd, $^3J_{\text{C-F}} = 5.7, 3.8$ Hz, $\text{C}\equiv$), 78.1 ($\text{HC}\equiv$), 51.1 (t, $^2J_{\text{C-F}} = 20.1$ Hz, $\text{CC}\equiv$), 41.2 (CH_2). ^{19}F NMR (CDCl_3): δ -123.2 (dd, $J = 274, 59.4$ Hz), -126.4 (dd, $J = 274, 59.4$ Hz). HRMS (FAB+) Calcd. for $\text{C}_{17}\text{H}_{15}\text{F}_2$ $[\text{M}+\text{H}]^+$: 257.1142. Found: 257.1137. The enantiomeric excess of **2-9** was determined by HPLC analysis; DAICEL Chiralpak OJ-H, hexane/*i*PrOH = 99/1, flow rate = 1.0 mL/min, $\lambda = 220$ nm, retention time: 19.4 min (major) and 30.4 min (minor), 63% ee.

2.4.5. Large-Scale Preparation of **2-7aa**

In an oven dried 100 mL Schlenk flask were placed **[Ru]-2-2** (63.0 mg, 0.050 mmol) and NH_4BF_4 (11.0 mg, 0.10 mmol) under N_2 . Anhydrous $\text{ClCH}_2\text{CCH}_2\text{Cl}$ (20 mL) was added, and then the mixture was magnetically stirred at room temperature for 60 min. Then, 1,1,1-trifluoro-2-phenylbut-3-yn-2-ol (**2-3a**) (200 mg, 1.0 mmol), diethyl 4-benzyl-2,6-dimethyl-1,4-dihydropyridine-3,5-dicarboxylate (**2-4a**) (412.1 mg, 1.2 mmol), *fac*- $[\text{Ir}(\text{ppy})_3]$ (6.4 mg, 0.01 mmol) were added under N_2 at room temperature. The reaction flask was placed in an As One LTB-125 constant low temperature water bath set at 25 °C, and was illuminated from the bottom of the bath with an Aitech System TMN100×120–22WD 12 W white LED lamp (400 nm to 750 nm) at a distance of approximately 2 cm from the light source for 48 h. The volatiles were removed *in vacuo*, and the residue was purified by column chromatography (SiO_2) with *n*-hexane as an eluent to afford (*R*)-(2-(trifluoromethyl)but-3-yn-1,2-diyl)dibenzene (**2-7aa**) as a colorless oil (205.5 mg, 0.75 mmol, 75% yield based on the amount of **2-3a**), with 93% ee.

2.4.6. Synthesis of (*S*)-(4-bromo-2-(trifluoromethyl)but-3-yn-1,2-diyl)dibenzene (**2-10**)

Scheme 2-10.

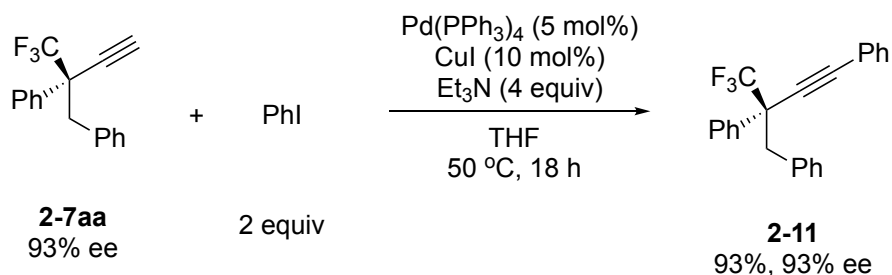


In a 20 mL Schlenk flask were placed (*R*)-**2-7aa** (27.4 mg, 0.10 mmol, 93% ee), *N*-bromosuccinimide (NBS) (21.4 mg, 0.12 mmol) and AgNO_3 (1.7 mg, 0.010 mmol) under N_2 , where acetone (5.0 mL) was added at room temperature. And the mixture was stirred at room temperature for 2 h. The volatiles were then removed *in vacuo*, and the residue was purified by column chromatography (SiO_2) with *n*-hexane as an eluent to afford (*S*)-(4-bromo-2-(trifluoromethyl)but-3-yn-1,2-diyl)dibenzene (**2-10**) as a colorless oil. (33.6 mg, 0.95 mmol, 95% yield based on the amount of **2-7aa**). $[\alpha]_{\text{D}}^{20} = -41.3$ ($c = 0.5$ in CHCl_3). ^1H NMR (CDCl_3 , 400 MHz) δ 7.60–7.56 (m, 2H, *o*-H of Ph), 7.38–7.33 (m, 3H, *m*-H and *p*-H of Ph), 7.16–7.11 (m, 3H, *m*-H and *p*-H of Ph), 6.97–6.94 (m, 2H, *o*-H of Ph), 3.49 (d, $J = 13.6$ Hz, 1H, CH_2), 3.42 (d, $J = 13.2$ Hz, 1H, CH_2). $^{13}\text{C}\{^1\text{H}\}$ NMR (CDCl_3 , 100 MHz): δ 134.3 (*ipso*-C of Ph), 133.5 (*ipso*-C of Ph), 130.7 (*o*-CH of Ph), 128.6 (*m*-CH of Ph), 128.4 (*m*-CH of Ph), 128.3 (*o*-CH of Ph), 127.6 (*p*-CH of Ph), 127.0 (*p*-CH of Ph), 125.5 (q, $^1J_{\text{C-F}} = 284$ Hz, CF_3), 75.5 ($\text{C}\equiv$), 54.2 (q, $^2J_{\text{C-F}} = 26.8$ Hz, $\text{CC}\equiv$), 49.6 (CH_2), 41.0 (CBr). ^{19}F NMR (CDCl_3): δ -73.2. HRMS (FAB+) Calcd. for $\text{C}_{17}\text{H}_{12}\text{BrF}_3$ $[\text{M}]^+$: 352.0074. Found: 352.0080. The enantiomeric excess of

2-10 was determined by HPLC analysis; DAICEL Chiralpak OJ-H, hexane/*i*PrOH = 100/0, flow rate = 0.5 mL/min, λ = 220 nm, retention time: 16.0 min (major) and 19.4 min (minor), 93% ee.

2.4.7. Synthesis of (*S*)-(2-(trifluoromethyl)but-3-yn-1,2,4-triyl)tribenzene (**2-11**)

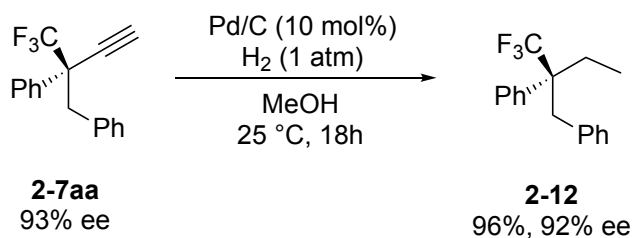
Scheme 2-11.



In a 20 mL Schlenk flask were placed (*R*)-**2-7aa** (27.4 mg, 0.10 mmol, 93% ee), iodobenzene (40.8 mg, 0.20 mmol), Pd(PPh₃)₄ (5.8 mg, 0.0050 mmol), CuI (1.9 mg, 0.010 mmol), and Et₃N (56 μ L, 0.40 mmol) under N₂, where THF (2.0 mL) was added at room temperature. And the mixture was stirred at 50 $^\circ$ C for 18 h. The volatiles were then removed *in vacuo*, and the residue was purified by column chromatography (SiO₂) with *n*-hexane as an eluent to afford (*S*)-(2-(trifluoromethyl)but-3-yn-1,2,4-triyl)tribenzene (**2-11**) as a white solid. (32.6 mg, 0.93 mmol, 93% yield based on the amount of **2-7aa**). m.p.= 57.0-58.5 $^\circ$ C. $[\alpha]_{\text{D}}^{20}$ = -53.5 (*c* = 0.5 in CHCl₃). ¹H NMR (CDCl₃, 400 MHz) δ 7.71-7.69 (m, 2H, *o*-H of Ph), 7.46-7.44 (m, 2H, *o*-H of Ph), 7.39-7.33 (m, 6H, *m*-H and *p*-H of Ph), 7.18-7.11 (m, 3H, *m*-H and *p*-H of Ph), 7.05-7.01 (m, 2H, *o*-H of Ph), 3.58 (d, *J* = 13.2 Hz, 1H, CH₂), 3.50 (d, *J* = 13.2 Hz, 1H, CH₂). ¹³C{¹H} NMR (CDCl₃, 100 MHz): δ 134.8 (*ipso*-C of Ph), 134.3 (*ipso*-C of Ph), 131.7 (*m*-CH of Ph), 130.8 (*m*-CH of Ph), 128.7 (*m*-CH of Ph), 128.6 (*p*-CH of Ph), 128.4 (*m*-CH of Ph), 128.3 (*m*-CH of Ph), 128.3 (*m*-CH of Ph), 127.5 (*p*-CH of Ph), 126.9 (*p*-CH of Ph), 125.9 (q, ¹*J*_{C-F} = 283 Hz, CF₃), 122.2 (*ipso*-C of Ph), 89.6 (C \equiv), 84.5 (HC \equiv), 53.6 (q, ²*J*_{C-F} = 25.9 Hz, CC \equiv), 41.2 (CH₂). ¹⁹F NMR (CDCl₃): δ -73.2. HRMS (FAB+) Calcd. for C₂₃H₁₇F₃ [M]⁺: 350.1282. Found: 350.1289. The enantiomeric excess of **2-11** was determined by HPLC analysis; DAICEL Chiralpak OJ-H, hexane/*i*PrOH = 99/1, flow rate = 0.5 mL/min, λ = 220 nm, retention time: 8.0 min (major) and 9.5 min (minor), 93% ee.

2.4.8. Synthesis of (*S*)-(2-(trifluoromethyl)butane-1,2-diyl)dibenzene (**2-12**).

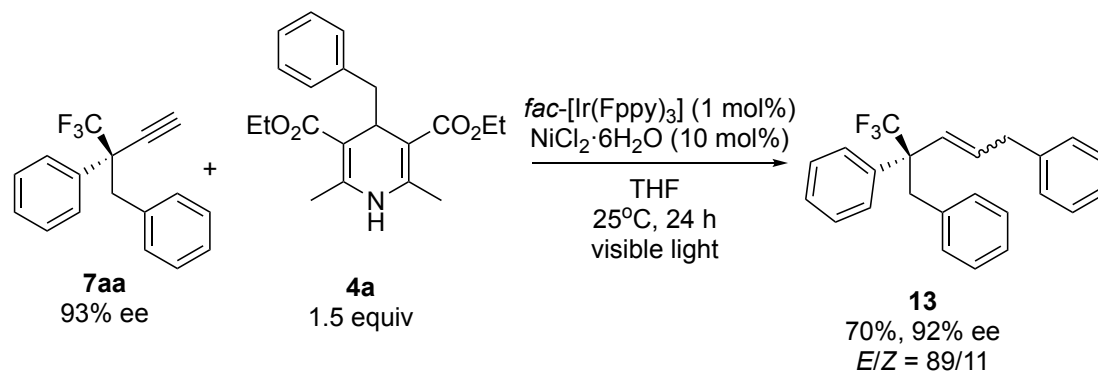
Scheme 2-12.



In a 20 mL Schlenk flask were placed (*R*)-**2-7aa** (27.4 mg, 0.10 mmol, 93% ee), and Pd/C (10.6 mg, 0.01 mmol, Palladium 10% on Carbon) under N₂, where MeOH (4.0 mL) was added at room temperature. After substitution of N₂ atmosphere to H₂ atmosphere by a hydrogen balloon, the mixture was stirred at room temperature for 18 h. The volatiles were then removed *in vacuo*, and the residue was purified by column chromatography (SiO₂) with *n*-hexane as an eluent to afford (*S*)-(2-(trifluoromethyl)butane-1,2-diyl)dibenzene (**2-12**) as a colorless oil. (26.7 mg, 0.96 mmol, 96% yield based on the amount of **2-7aa**). [α]_D²⁰ = -50.3 (c = 0.5 in CHCl₃). ¹H NMR (CDCl₃, 400 MHz) δ 7.39-7.29 (m, 5H, H of Ph), 7.20-7.12 (m, 3H, *m*-H and *p*-H of Ph), 6.82-6.79 (m, 2H, *o*-H of Ph), 3.22 (s, 2H, CH₂), 2.00 (q, *J* = 6.9 Hz, 2H, CH₂CH₃), 0.98-0.94 (m, 3H, CH₃). ¹³C {¹H} NMR (CDCl₃, 100 MHz): δ 137.1 (*ipso*-C of Ph), 135.7 (*ipso*-C of Ph), 130.7 (*m*-CH of Ph), 128.6 (q, ¹*J*_{C-F} = 285 Hz, CF₃), 128.2 (*m*-CH of Ph), 127.7 (*o*-CH of Ph), 127.4 (*p*-CH of Ph), 126.6 (*o*-CH and *p*-CH of Ph), 52.6 (q, ²*J*_{C-F} = 21.1 Hz, CC \equiv), 42.0 (CH₂), 25.0 (CH₂CH₃), 8.9 (CH₃). ¹⁹F NMR (CDCl₃): δ -68.4. HRMS (FAB⁺) Calcd. for C₁₇H₁₇F₃ [M]⁺: 278.1282. Found: 278.1293. The enantiomeric excess of **2-12** was determined by HPLC analysis; DAICEL Chiralpak OJ-H, hexane/*i*PrOH = 99/1, flow rate = 0.5 mL/min, λ = 220 nm, retention time: 11.5 min (minor) and 36.1 min (major), 92% ee.

2.4.9. Synthesis of (*R*)-(2-(trifluoromethyl)pent-3-ene-1,2,5-triyl)tribenzene (**2-13**)

Scheme 2-13.



In a 20 mL Schlenk flask were placed (*R*)-**2-7aa** (27.4 mg, 0.10 mmol, 93% ee), **2-4a** (51.5 mg, 0.375 mmol), *fac*-[Ir(Fppy)₃] (0.8 mg, 0.0011 mmol), and NiCl₂·6H₂O (2.4 mg, 0.020 mmol) under N₂, where THF (2.0 mL) was added at room temperature.

The reaction flask was placed in an As One LTB-125 constant low temperature water bath set at 25 °C, and was illuminated from the bottom of the bath with an Aitech System TMN100×120–22WD 12 W white LED lamp (400 nm to 750 nm) at a distance of approximately 2 cm from the light source for 24 h. *E/Z* ratio of (*R*)-(2-(trifluoromethyl)pent-3-ene-1,2,5-triyl)tribenzene in the crude mixture was determined to be 55/45 by quantitative measurement of GC-MS. The volatiles were then removed *in vacuo*, and the residue was purified by column chromatography (SiO₂) with *n*-hexane as an eluent to afford a mixture of (*R,E*)-(2-(trifluoromethyl)pent-3-ene-1,2,5-triyl)tribenzene ((*E*)-**2-13**) and (*R,Z*)-(2-(trifluoromethyl)pent-3-ene-1,2,5-triyl)tribenzene ((*Z*)-**2-13**) as a colorless oil (*E/Z* = 89/11, 25.6 mg, 0.70 mmol, 70% yield based on the amount of **2-7aa**). [α]_D²⁰ = -26.5 (c = 0.5 in CHCl₃).

¹H NMR (CDCl₃, 400 MHz)

((*E*)-**2-13**): δ 7.48-7.44 (m, 2H, *o*-H of Ph), 7.36-7.29 (m, 5H, H of Ph), 7.24-7.18 (m, 1H, *p*-H of Ph), 7.17-7.08 (m, 5H, H of Ph), 6.87-6.85 (m, 2H *o*-H of Ph), 5.97-5.89 (m, 1H, =CH), 5.67-5.62 (m, 1H, =CH), 3.50 (d, *J* = 14.4 Hz, 1H, CH₂), 3.47 (s, 2H, CH₂), 3.37 (d, *J* = 14.4 Hz, 1H, CH₂).

((*Z*)-**2-13**): δ 7.90-7.44 (m, 1H, H of Ph), 7.70-7.68 (m, 4H, H of Ph), 7.44-7.42 (m, 4H, H of Ph), 7.24-7.18 (m, 4H), 6.96-6.94 (m, 1H, H of Ph), 6.91-6.89 (m, 1H, H of Ph), 5.86-5.81 (m, 1H, =CH), 5.65 (d, *J* = 56.4 Hz, 1H, =CH), 3.50 (d, *J* = 14.4 Hz, 1H, CH₂), 3.47 (s, 2H, CH₂), 3.37 (d, *J* = 14.4 Hz, 1H, CH₂).

¹³C{¹H} NMR (CDCl₃, 100 MHz)

((*E*)-**2-13**): δ 139.6 (*ipso*-C of Ph), 137.4 (*ipso*-C of Ph), 135.6 (*ipso*-C of Ph), 133.3 (=C), 131.0 (*o*-CH of Ph), 129.2 (*o*-CH of Ph), 129.1 (*m*-CH of Ph), 128.6 (*m*-CH of Ph), 128.5 (*m*-CH of Ph), 128.0 (*o*-CH of Ph), 127.7 (*p*-CH of Ph), 127.6 (*p*-CH of Ph), 127.3 (q, ¹*J*_{C-F} = 283 Hz, CF₃), 126.5 (*p*-CH of Ph), 126.2 (=C), 55.2 (q, ²*J*_{C-F} = 23.0 Hz, CC=), 40.7 (CH₂), 39.5 (CH₂).

((*Z*)-**2-13**): δ 139.7 (*ipso*-C of Ph), 136.2 (=C), 131.3 (*o*-CH of Ph), 129.3 (*o*-CH of Ph), 128.8 (*m*-CH of Ph), 128.3 (*m*-CH of Ph), 128.1 (*p*-CH of Ph), 126.7 (*p*-CH of Ph), 126.0 (=C), 42.9 (CH₂), 35.6 (CH₂).

¹⁹F NMR (CDCl₃): δ -69.9.

HRMS (FAB+) Calcd. for C₂₄H₂₁F₃ [M]⁺: 366.1595. Found: 366.1605.

The enantiomeric excess of **2-13** was determined by HPLC analysis; DAICEL Chiralpak OJ-H, hexane/^{*i*}PrOH = 99/1, flow rate = 0.5 mL/min, λ = 220 nm, retention time: ((*E*)-**2-13**): 13.8 min (minor) and 15.8 min (major), 92% ee; ((*Z*)-**2-13**): 11.9 min (minor) and 18.3 min (major), 92% ee.

2.4.10. Stoichiometric Reaction of Complex **2-14** with **2-4a**

In an oven dried 20 mL Schlenk flask were placed **2-14** (138 mg, 0.10 mmol) and under N₂. Anhydrous ClCH₂CCH₂Cl (2.0 mL) was added and then, 1,1,1-trifluoro-2-(*p*-tolyl)but-3-yn-2-ol (**2-3b**) (21.4 mg, 0.10 mmol), diethyl 4-benzyl-2,6-dimethyl-1,4-dihydropyridine-3,5-dicarboxylate (**2-4a**) (41.2 mg, 0.12 mmol), *fac*-[Ir(ppy)₃] (0.7 mg, 0.0011 mmol) were added under N₂ at room temperature. The reaction flask was placed

in an As One LTB-125 constant low temperature water bath set at 25 °C, and was illuminated from the bottom of the bath with an Aitech System TMN100×120–22WD 12 W white LED lamp (400 nm to 750 nm) at a distance of approximately 2 cm from the light source for 48 h. The volatiles were removed *in vacuo*, and the residue was purified by column chromatography (SiO₂) with *n*-hexane as an eluent to afford (*R*)-(2-(trifluoromethyl)but-3-yn-1,2-diyl)dibenzene (**2-7aa**) as a colorless oil (18.1 mg, 0.066 mmol, 66% yield based on the amount of **2-3a**) with 88% ee ([Scheme 2-5a](#)).

2.4.11. Catalytic Reaction of **2-3a** with **2-4a** by Using **2-14** as a Catalyst

In an oven dried 20 mL Schlenk flask were placed **2-14** (6.9 mg, 0.0050 mmol) and under N₂. Anhydrous ClCH₂CCH₂Cl (2.0 mL) was added, and then, 1,1,1-trifluoro-2-phenylbut-3-yn-2-ol (**2-3a**) (20.0 mg, 0.10 mmol), diethyl 4-benzyl-2,6-dimethyl-1,4-dihydropyridine-3,5-dicarboxylate (**2-4a**) (41.2 mg, 0.12 mmol), *fac*-[Ir(ppy)₃] (0.7 mg, 0.0011 mmol) were added under N₂ at room temperature. The reaction flask was placed in an As One LTB-125 constant low temperature water bath set at 25 °C, and was illuminated from the bottom of the bath with an Aitech System TMN100×120–22WD 12 W white LED lamp (400 nm to 750 nm) at a distance of approximately 2 cm from the light source for 48 h. The volatiles were removed *in vacuo*, and the residue was purified by column chromatography (SiO₂) with *n*-hexane as an eluent to afford (*R*)-(2-(trifluoromethyl)but-3-yn-1,2-diyl)dibenzene (**2-7aa**) as a colorless oil (23.3 mg, 0.085 mmol, 85% yield based on the amount of **2-3a**) with 85% ee ([Scheme 2-5b](#)).

2.4.12. Reactions in the Presence of TEMPO

In an oven dried 20 mL Schlenk flask were placed [**Ru**]-**2-2** (6.3 mg, 0.0050 mmol) and NH₄BF₄ (1.1 mg, 0.010 mmol) under N₂. Anhydrous ClCH₂CCH₂Cl (2.0 mL) was added, and then the mixture was magnetically stirred at room temperature for 30 min. Then, 1,1,1-trifluoro-2-phenylbut-3-yn-2-ol (**2-3a**) (20.0 mg, 0.10 mmol), diethyl 4-benzyl-2,6-dimethyl-1,4-dihydropyridine-3,5-dicarboxylate (**2-4a**) (41.2 mg, 0.12 mmol), *fac*-[Ir(ppy)₃] (0.7 mg, 0.0011 mmol) were added under N₂ at room temperature. The reaction flask was placed in an As One LTB-125 constant low temperature water bath set at 25 °C, and was illuminated from the bottom of the bath with an Aitech System TMN100×120–22WD 12 W white LED lamp (400 nm to 750 nm) at a distance of approximately 2 cm from the light source for 48 h. The volatiles were removed *in vacuo*, and the crude yield of 1-(benzyloxy)-2,2,6,6-tetramethylpiperidine (**2-15**)²⁸ (34% NMR yield) was determined by ¹H NMR in CDCl₃, where 1,1,2,2-tetrachloroethane (16.8 mg, 0.100 mmol) was added as an internal standard ([Figure 2-1a](#)).

2.4.13. Deuterium Labeled Reaction

In an oven dried 20 mL Schlenk flask were placed **[Ru]-2-2** (6.3 mg, 0.0050 mmol) and NH_4BF_4 (1.1 mg, 0.010 mmol) under N_2 . Anhydrous $\text{ClCH}_2\text{CCH}_2\text{Cl}$ (2.0 mL) was added, and then the mixture was magnetically stirred at room temperature for 30 min. Then, 1,1,1-trifluoro-2-phenylbut-3-yn-2-ol (**2-3a**) (20.0 mg, 0.10 mmol), diethyl 4-benzyl-2,6-dimethyl-1-deuterium-4-hydropyridine-3,5-dicarboxylate (**2-4a-D**) (41.2 mg, 0.12 mmol), *fac*-[Ir(ppy)₃] (0.7 mg, 0.0011 mmol) were added under N_2 at room temperature. The reaction flask was placed in an As One LTB-125 constant low temperature water bath set at 25 °C, and was illuminated from the bottom of the bath with an Aitech System TMN100×120–22WD 12 W white LED lamp (400 nm to 750 nm) at a distance of approximately 2 cm from the light source for 48 h. The volatiles were removed *in vacuo*, and the residue was purified by column chromatography (SiO_2) with *n*-hexane as an eluent to afford (*R*)-(2-(trifluoromethyl)but-3-yn-1,2-diyl)dibenzene (**2-7aa**) as a colorless oil (21.1 mg, 0.077 mmol, 77% yield based on the amount of **2-3a**) with 93% ee. The ratio of protium/deuterium is determined by ^1H NMR at δ 2.66, where the ratio is 70/30 (Figure 2-1b).

2.4.14. Stern–Volmer Analysis

Luminescence quenching experiments for the THF solution of *fac*-[Ir(ppy)₃] (2.0 $\mu\text{mol/L}$, prepared by stepwise dilutions of *fac*-[Ir(ppy)₃] (1.3 mg, 2.0 μmol) with $\text{ClCH}_2\text{CH}_2\text{Cl}$) with **2-16**, **2-3a** or **2-4a** in selected concentrations were performed on a Shimadzu RF-5300PC spectrophotometer, where the solutions containing *fac*-[Ir(ppy)₃] and **2-16**, **2-3a** or **2-4a** were excited at $\lambda_{\text{max}} = 440$ nm, and emissions were measured at $\lambda = 494$ nm.

From the slopes (32.6 for **2-16**, 100.5 for **2-3a** and 208.3 for **2-4a**) obtained by the plot and the excited-state lifetime of *fac*-[Ir(ppy)₃] ($\tau = 1.9$ μs),⁴⁷ the rate constants for the energy transfer of **2-3a** and the oxidation of **2-4a** were calculated to be at $k_{2-10} = 1.7 \times 10^7 \text{ M}^{-1} \text{ s}^{-1}$ (**2-16**), $k_{2-3a} = 5.3 \times 10^7 \text{ M}^{-1} \text{ s}^{-1}$ (**2-3a**) and $k_{2-4a} = 1.1 \times 10^8 \text{ M}^{-1} \text{ s}^{-1}$ (**2-4a**), respectively (Figure 2-1c).

2.4.15. Light on/off Experiments

In an oven dried 20 mL Schlenk flask were placed **[Ru]-2-2** (6.3 mg, 0.0050 mmol) and NH_4BF_4 (1.1 mg, 0.010 mmol) under N_2 . Anhydrous $\text{ClCH}_2\text{CCH}_2\text{Cl}$ (2.0 mL) was added, and then the mixture was magnetically stirred at room temperature for 30 min. Then, 1,1,1-trifluoro-2-phenylbut-3-yn-2-ol (**2-3a**) (20.0 mg, 0.10 mmol), diethyl 4-benzyl-2,6-dimethyl-1,4-dihydropyridine-3,5-dicarboxylate (**2-4a**) (41.2 mg, 0.12 mmol), *fac*-[Ir(ppy)₃] (0.7 mg, 0.0011 mmol) were added under N_2 at room temperature. The reaction flask was placed in an As One LTB-125 constant low temperature water bath set at 25 °C. The reaction was conducted for 32 h under

alternating periods of (1) irradiation from the bottom of the bath with an Aitech System TMN100×120–22WD 12 W white LED lamp (400 nm to 750 nm) at a distance of approximately 2 cm from the light source, and (2) darkness with the reaction vessel wrapped with aluminum foil, where yields of **2-7aa** were determined every 4 hours by quantitative measurements of gas chromatography–mass spectroscopy (GC-MS) recorded on a Shimadzu GCMS-QP2010 PLUS instrument, where *n*-octane was added as an internal standard (Figure 2-2a).

2.4.16. Determination of Quantum Yield

In an oven dried 20 mL Schlenk flask were placed [**Ru**]-**2-1** (6.3 mg, 0.0050 mmol) and NH₄BF₄ (1.1 mg, 0.010 mmol) under N₂. Anhydrous ClCH₂CCH₂Cl (2.0 mL) was added, and then the mixture was magnetically stirred at room temperature for 30 min. Then, 1,1,1-trifluoro-2-phenylbut-3-yn-2-ol (**2-3a**) (20.0 mg, 0.10 mmol), diethyl 4-benzyl-2,6-dimethyl-1,4-dihydropyridine-3,5-dicarboxylate (**2-4a**) (41.2 mg, 0.12 mmol), *fac*-[Ir(ppy)₃] (0.7 mg, 0.0011 mmol) were added under N₂ at room temperature. The reaction flask was illuminated from the side with an Ushio SX-U1251HQ ultrahigh pressure 250 W Hg lamp equipped with a 440-nm band pass filter (Kenko B440) at a distance of approximately 2 cm from the light source for 6 h. The volatiles were removed in vacuo, and the crude yield of **2-7aa** (0.00920 mmol, 9.2% NMR yield based on the amount of **2-3a**) was determined by ¹H NMR in CDCl₃, where 1,1,2,2-tetrachloroethane (16.8 mg, 0.100 mmol) was added as an internal standard. Independently, the yields of **2-7aa** were determined by terminating the reactions at 2 and 4 h, which clarified a zero-order reaction rate at $4.26 \times 10^{-8} \text{ mol s}^{-1}$. The irradiated light intensity to a 2.5 mL solution in 50-mL Schlenk was estimated to be $8.50 \times 10^{-7} \text{ E s}^{-1}$ at 440 nm by using K₃[Fe(C₂O₄)₃] as a chemical actinometer.³² Thus, the quantum yield of the photoredox- and ruthenium-catalyzed reaction of **2-3a** with **2-4a** to afford propargylic alkylated product **2-7aa** is given as $\Phi = 0.050$ (Figure 2-4).

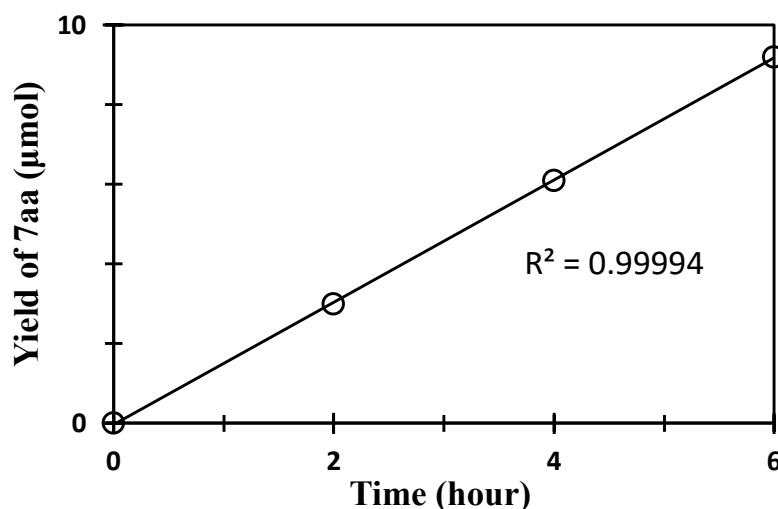


Figure 2-4. Determination of quantum yield.

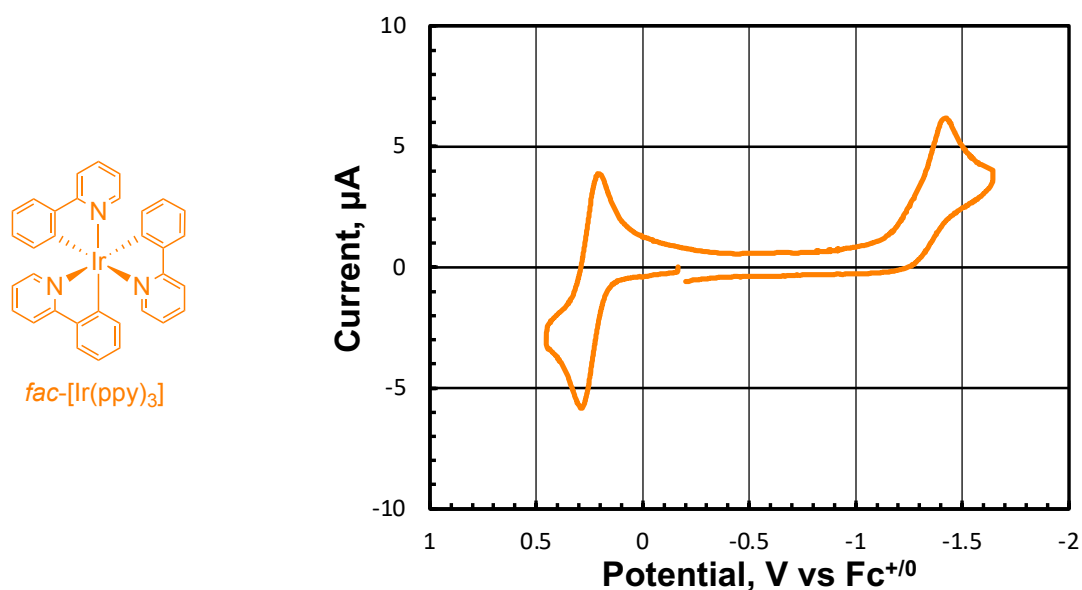
2.4.17. Time Profile Experiment

In an oven dried 20 mL Schlenk flask were placed **[Ru]-2-2** (6.3 mg, 0.0050 mmol) and NH_4BF_4 (1.1 mg, 0.010 mmol) under N_2 . Anhydrous $\text{ClCH}_2\text{CCH}_2\text{Cl}$ (2.0 mL) was added, and then the mixture was magnetically stirred at room temperature for 30 min. Then, 1,1,1-trifluoro-2-phenylbut-3-yn-2-ol (**2-3a**) (20.0 mg, 0.10 mmol), diethyl 4-benzyl-2,6-dimethyl-1,4-dihydropyridine-3,5-dicarboxylate (**2-4a**) (41.2 mg, 0.12 mmol), *fac*-[Ir(ppy)₃] (0.7 mg, 0.0011 mmol) were added under N_2 at room temperature. The reaction flask was placed in an As One LTB-125 constant low temperature water bath set at 25 °C, and was illuminated from the bottom of the bath with an Aitech System TMN100×120–22WD 12 W white LED lamp (400 nm to 750 nm) at a distance of approximately 2 cm from the light source. Yields of **2-7aa** at selected times (2, 4, 8, 12, 24 and 48 h) were determined by quantitative measurements of gas chromatography–mass spectroscopy (GC-MS) recorded on a Shimadzu GCMS-QP2010 PLUS instrument, where *n*-octane was added as an internal standard (Figure 2-2b).

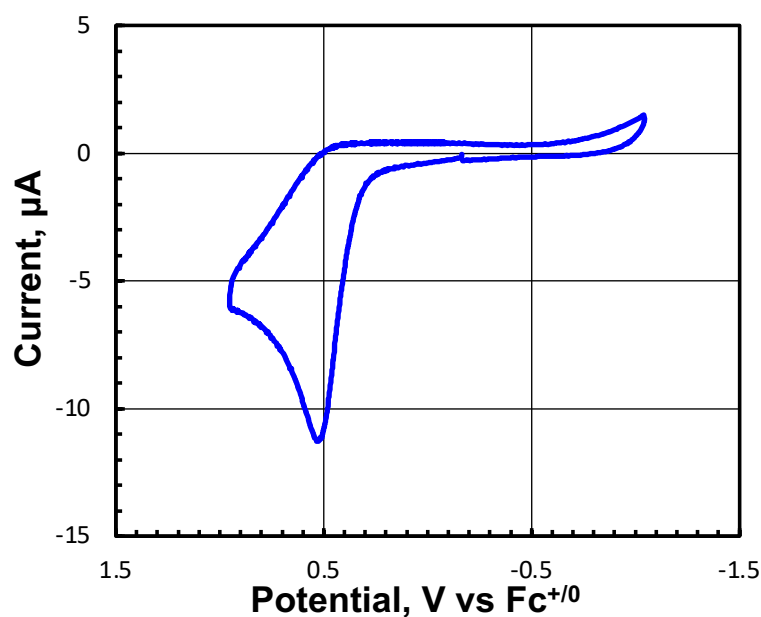
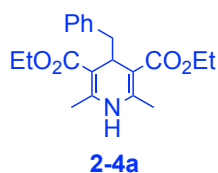
2.4.14. Cyclic Voltammetric Studies

Cyclic voltammograms were recorded on an ALS/Chi model 610C electrochemical analyzer in $\text{ClCH}_2\text{CH}_2\text{Cl}$ containing 1 mM of sample and 0.1 M of $n\text{Bu}_4\text{NPF}_6$ as a supporting electrolyte using glassy carbon working electrode and platinum wire counter electrode at a scan rate of 0.1 V/s at room temperature. All potentials were measured against Ag/AgNO₃ reference electrode (0.01 M AgNO₃, 0.1 M $n\text{Bu}_4\text{ClO}_4$, MeCN) and converted to the values vs $\text{Fc}^{+/0}$ ($\text{Cp} = \eta^5\text{-C}_5\text{H}_5$). The cyclic voltammograms of *fac*-[Ir(ppy)₃], **2-4a**, and **2-3a** in $\text{ClCH}_2\text{CH}_2\text{Cl}$ are shown in Figures 2-5.

a)



b)



c)

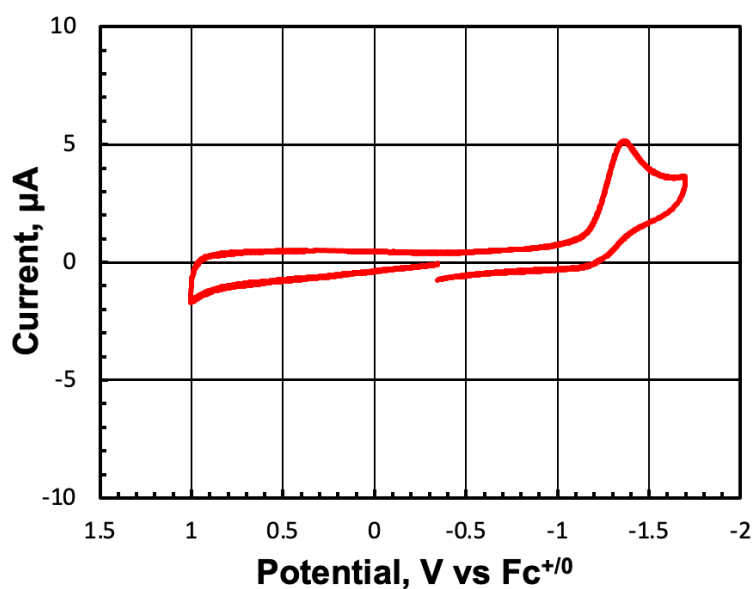
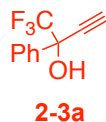


Figure 2-5. Cyclic voltammetric studies. (a) Cyclic voltammogram of *fac*-[Ir(ppy)₃] in ClCH₂CH₂Cl. $E_{1/2}(\text{Ir}/\text{Ir}^-) = -1.60$ V vs $\text{FeCp}_2^{+/0}$, $E_{\text{pa}}(\text{Ir}/\text{Ir}^+) = +0.25$ V vs $\text{FeCp}_2^{+/0}$. Therefore, $E_{\text{pc}}(\text{Ir}^*/\text{Ir}^-) = +0.90$ V vs $\text{FeCp}_2^{+/0}$, $E_{1/2}(\text{Ir}^{*+}) = -2.25$ V vs $\text{FeCp}_2^{+/0}$, based on the emission energy of *fac*-[Ir(ppy)₃] at 2.50 eV.³¹ (b) Cyclic voltammogram of **2-4a** in THF. $E_{\text{pa}}(\text{2-4a}/\text{2-4a}^+) = +0.53$ V vs $\text{FeCp}_2^{+/0}$. (c) Cyclic voltammogram of **2-3a** in ClCH₂CH₂Cl. $E_{\text{pc}}(\text{2-3a}/\text{2-3a}^-) = -1.36$ V vs $\text{FeCp}_2^{+/0}$.

2.4.15. DFT Calculations

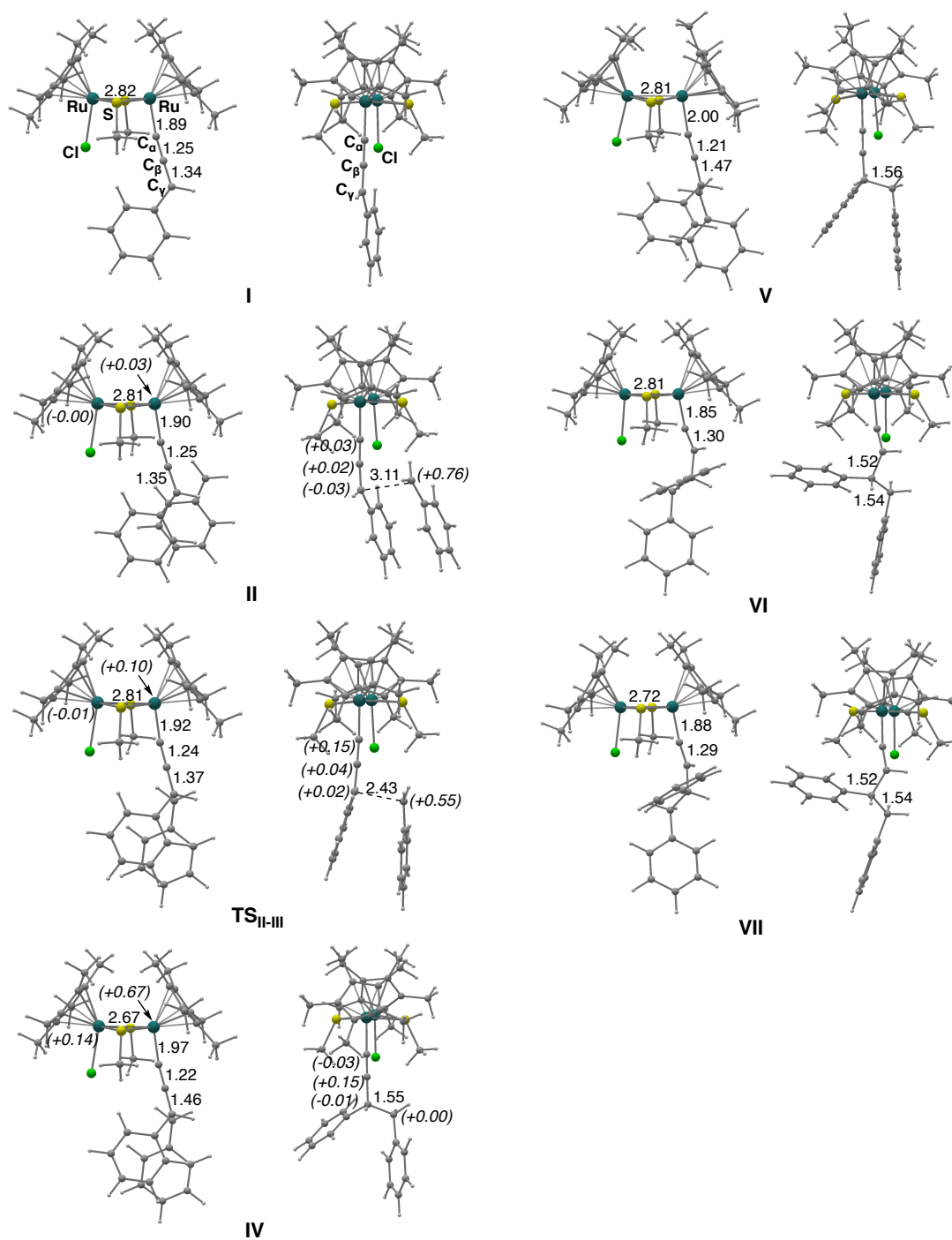


Figure 2-6. DFT calculations. Structures optimized at ω B97X-D/(SDD, 6-311G**) level of theory. Bond lengths are given in Å.

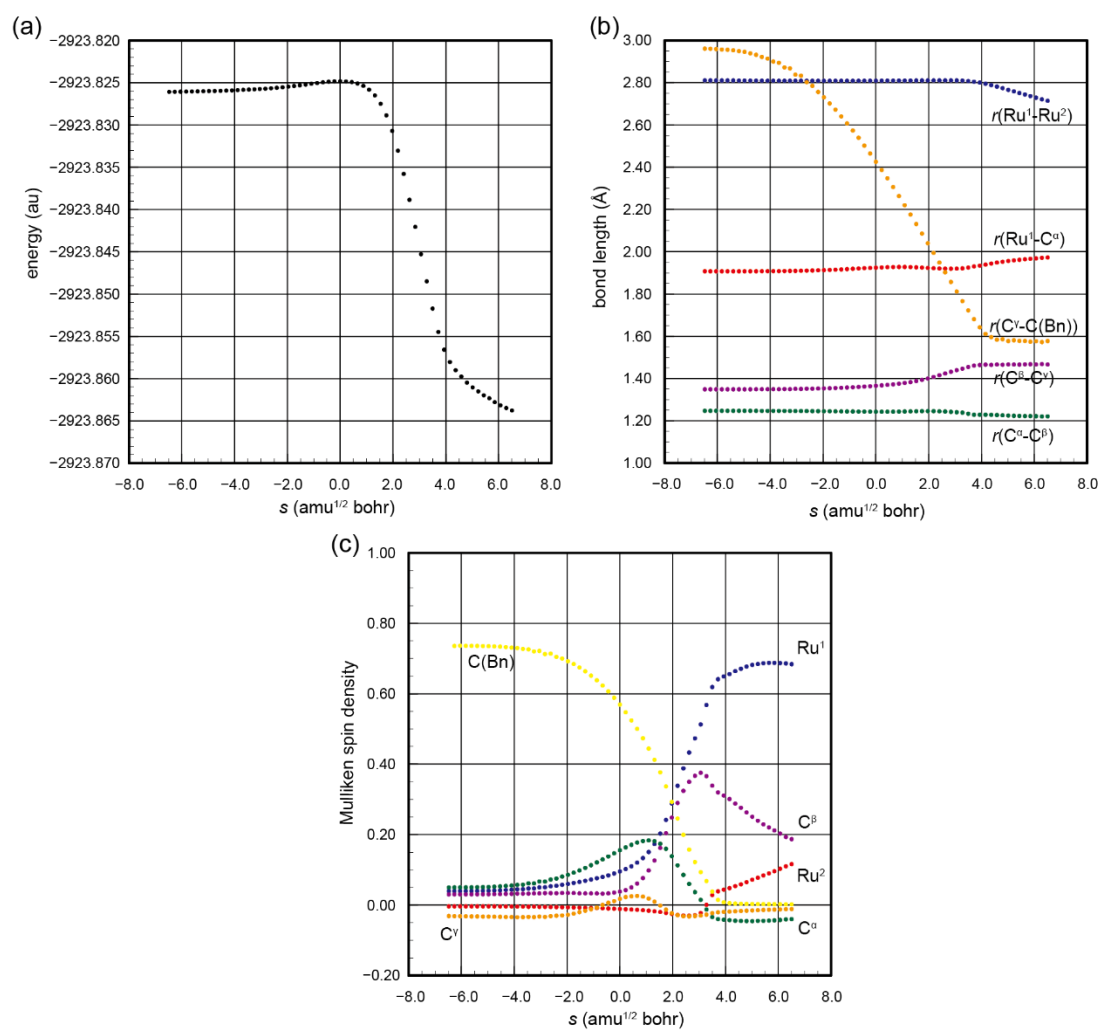


Figure 2-7. (a) Potential energy profile along IRC for TS_{II-III}. (b) Changes in bond lengths along the IRC for TS_{II-III}. (c) Changes in Mulliken spin density along the IRC for TS_{II-III}.

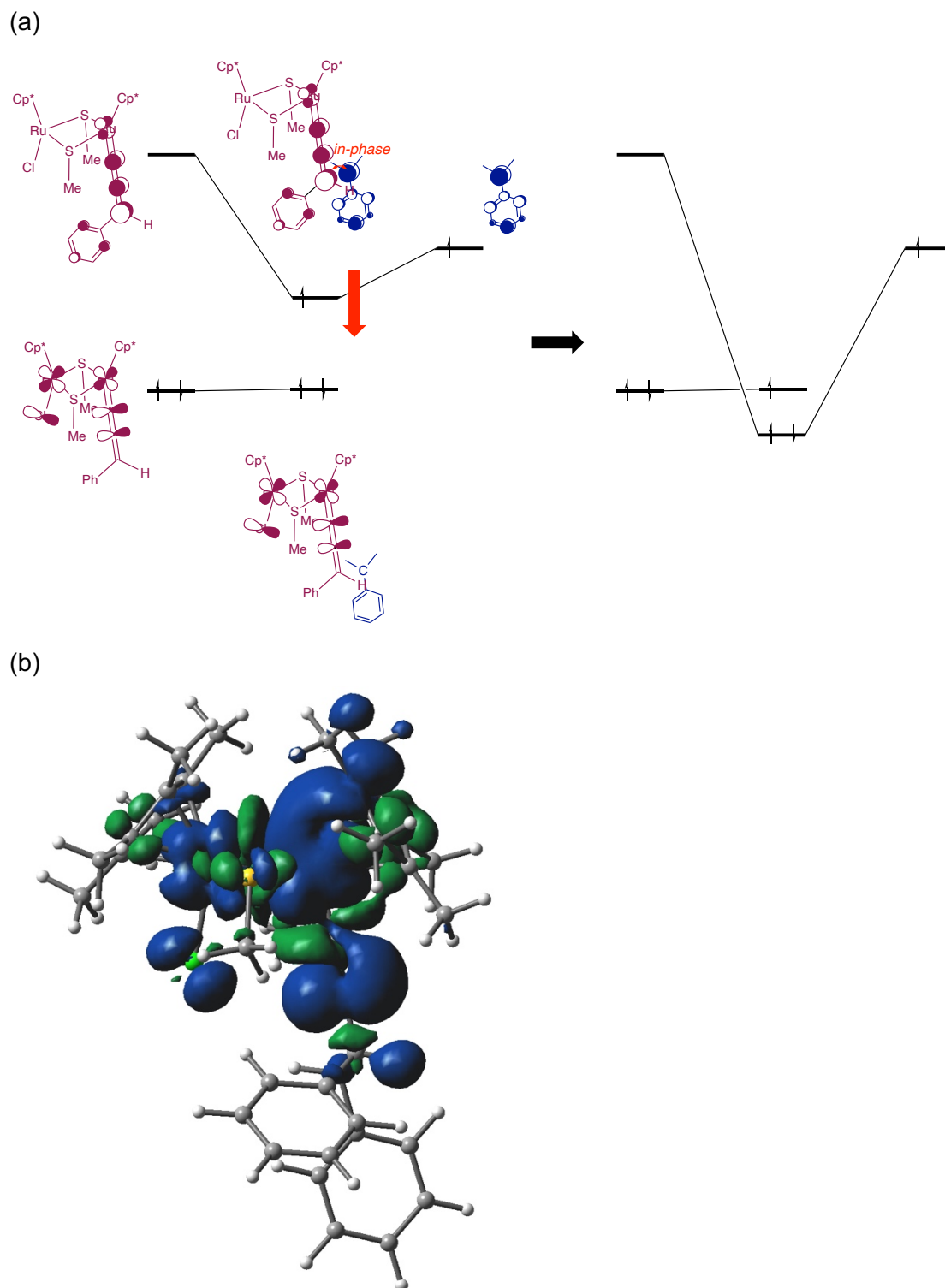


Figure 2-8. (a) Change in SOMO along the reaction. (b) Spin density in **III**.

Computational Details

DFT calculations were carried out with the Gaussian16 (Revision A.03) program package.⁵⁶ Geometry optimization and analytical vibrational frequency analysis were performed by ω B97XD Kohn-Sham DFT⁵⁷ (restricted KS method for singlet state and unrestricted KS method for doublet and triplet states). In the numerical integration, a

larger grid (*superfinegrid*) was used.⁵⁶ Pople's 6-311G** basis set⁵⁸ for C, H, S, and Cl atoms and the SDD basis set with the effective core potential (ECP60NWB)⁵⁹ for Ru atom were used for the Gaussian basis functions (5d-type). The solvent effects of dichloroethane were estimated by the IEF-PCM method⁶⁰ for the gas phase optimized structures. For the IEF-PCM calculations, the ω B97XD functional was used with the larger basis set (Pople's 6-311++G** basis set⁵⁸ for C, H, N, O, S, and Cl atoms (5d-type) and the SDD basis set for Ru atom; ω B97XD(IEFPCM)/(SDD, 6-311++G**)// ω B97XD(IEFPCM)/(SDD, 6-311G**)). The Gibbs free energy at 298K was estimated by the IEF-PCM energy and the gas-phase thermal correction term.

2.4.16. X-ray Crystallographic Study of (*R*)-1-(2-(3-bromophenyl)-1,1,1-trifluorobut-3-yn-2-yl)naphthalene (**2-7lr**)

Diffraction data for a crystal of **2-7lr** were collected for the 2θ range of 4.5° to 62.2° at -180°C on a Rigaku XtaLAB Synergy-S diffractometer equipped with a HyPix-6000HE Hybrid Photon Counting (HPC) detector and VariMax optics using multi-layer mirror monochromated Mo-K α ($\lambda = 0.71073\text{ \AA}$) radiation, and VariMax optics. Intensity data were corrected for Lorentz and polarization effect and for empirical absorptions (CrysAlisPro),⁶¹ while structure solutions and refinements were carried out by using CrystalStructure package.⁶² Positions of non-hydrogen atoms were determined by direct methods (SHELXT Version 2014/5),⁶³ and subsequent Fourier syntheses (SHELXL Version 2016/6),⁶⁴ and were refined on F_o^2 with all the unique reflections by full-matrix least squares with anisotropic thermal parameters. All the hydrogen atoms were placed at the calculated positions with fixed isotropic parameters. Anomalous dispersion effects were included in F_c ,⁶⁵ and mass attenuation coefficients, values for $\Delta f'$ and $\Delta f''$, and neutral atom scattering factors were taken from references.⁶⁶⁻⁶⁸ The absolute configuration of **2-7lr** with a chiral center at the C(1) atom was determined to be (*R*), with the Flack parameter refined to be $-0.005(5)$. Details of the crystal and data collection parameters of (*R*)-**2-7lr** are summarized in Table 2-2. An ORTEP drawing of (*R*)-**2-7lr** is shown in Figure 2-9.

Table 2-2. Crystallographic Data for (R)-2-7Ir.

compound	(R)-2-7Ir
chemical formula	C ₂₁ H ₁₄ BrF ₃
CCDC number	2172478
formula weight	403.24
crystal size, mm ³	0.131 × 0.066 × 0.037
crystal color, habit	colorless, needle
temperature, °C	−180
crystal system	monoclinic
space group	<i>P</i> 2 ₁ (no. 4)
<i>a</i> , Å	9.1554(4)
<i>b</i> , Å	7.1034(3)
<i>c</i> , Å	13.5438(6)
α, deg	90
β, deg	103.113(4)
γ, deg	90
<i>V</i> , Å ³	857.85(7)
<i>Z</i>	2
<i>d</i> _{calcd} , g, cm ^{−3}	1.561
<i>F</i> (000)	404
μ, cm ^{−1}	24.327
transmission factors range	0.847 – 0.914
number of measured reflections	13715
number of unique reflections	4344
number of refined parameters	226
<i>R</i> _{int}	0.0457
<i>R</i> 1 (<i>I</i> > 2 σ(<i>I</i>)) ^a	0.0297
<i>wR</i> 2 (all data) ^b	0.0564
GOF ^c	1.000
maximum residual peak / hole, e Å ^{−3}	+0.30 / −0.33
Flack parameter	−0.005(5)

^a $R1 = \sum ||F_o| - |F_c|| / \sum |F_o|$. ^b $wR2 = [\sum \{w(F_o^2 - F_c^2)^2\} / \sum w(F_o^2)^2]^{1/2}$, $w = 1/[\sigma^2(F_o^2) + rP]$, $P = (\text{Max}(F_o^2, 0) + 2 F_c^2)/3$ [$r = 3.65$]. ^c $\text{GOF} = [\sum w(F_o^2 - F_c^2)^2 / (N_o - N_{\text{params}})]^{1/2}$.

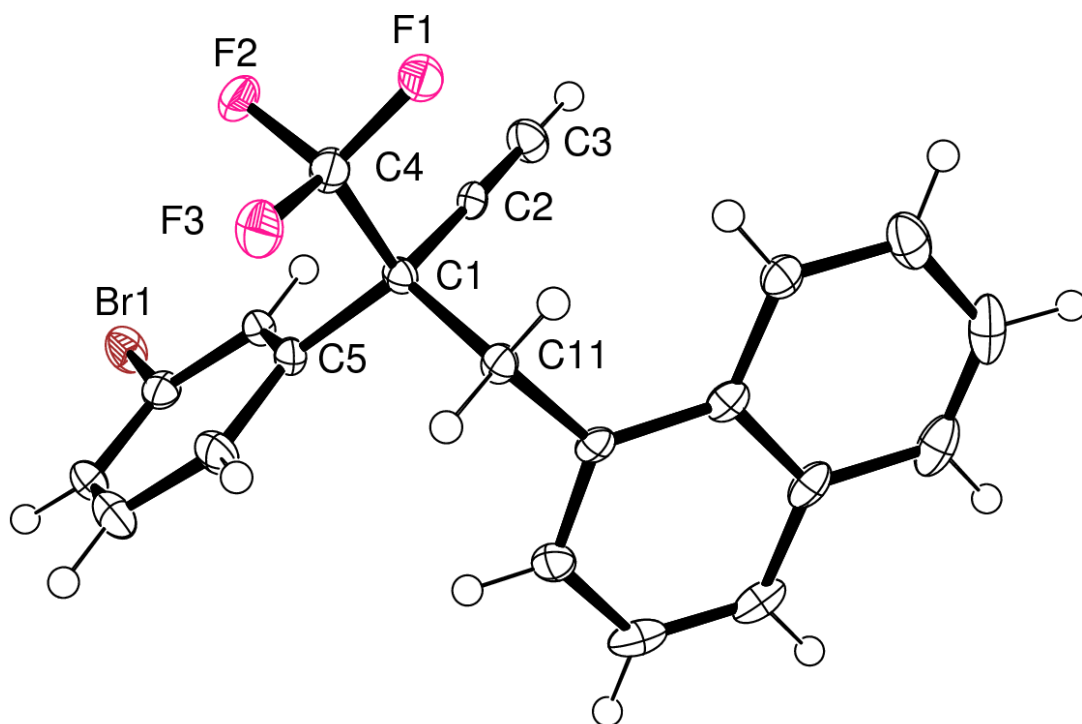


Figure 2-9. ORTEP drawing of (*R*)-**2-7Ir**. Thermal ellipsoids are drawn at the 50% probability level. Selected bond lengths (Å) and angles (°): C(1)–C(2): 1.468(4), C(1)–C(4): 1.535(4), C(1)–C(5): 1.548(4), C(1)–C(11): 1.556(4), C(2)–C(3): 1.188(5); C(2)–C(1)–C(4): 106.6(2), C(2)–C(1)–C(5): 111.3(2), C(4)–C(1)–C(5): 106.9(2), C(2)–C(1)–C(11): 110.4(3), C(4)–C(1)–C(11): 108.1(2), C(5)–C(1)–C(11): 113.2(2), C(3)–C(2)–C(1): 178.4(3).

2.5. References

- (1) Trost, B. M.; van Vranken, D. L. *Chem. Rev.* **1996**, *96*, 395–422. (b) Trost, B. M.; Crawley, M. L. *Chem. Rev.* **2003**, *103*, 2921–2944. (c) Hartwig, J. F. *Organotransition Metal Chemistry*; University Science Books: 2010; Chapter 20.
- (2) (a) Nakamura, K.; Ohno, A.; Oka, S. *Tetrahedron Lett.* **1983**, *24*, 3335–3336. (b) Hayashi, T.; Iwamura, H.; Naito, M.; Matsumoto, Y.; Uozumi, Y.; Miki, M.; Yanagi, K. *J. Am. Chem. Soc.* **1994**, *116*, 775–776.
- (3) (a) Nishibayashi, Y.; Wakiji, I.; Hidai, M. *J. Am. Chem. Soc.* **2000**, *122*, 11019–11020. (b) Miyake, Y.; Uemura, S.; Nishibayashi, Y. *ChemCatChem* **2009**, *1*, 342–356.
- (4) Inada, Y.; Nishibayashi, Y.; Uemura, S. *Angew. Chem., Int. Ed.* **2005**, *44*, 7715–7717.
- (5) For review: (a) Miyake, Y.; Uemura, S.; Nishibayashi, Y. *ChemCatChem* **2009**, *1*, 342–356. (b) Ding, C.-H.; Hou, X.-L. *Chem. Rev.* **2011**, *111*, 1914–1937. (c) Nishibayashi, Y. *Synthesis* **2012**, *44*, 489–503. (d) Zhang, D.-Y.; Hu, X.-P. *Tetrahedron Lett.* **2015**, *56*, 283–295. (e) Sakata, K.; Nishibayashi, Y. *Catal. Sci. Technol.* **2018**, *8*, 12–25. (f) Roh, S. W.; Choi, K.; Lee, C. *Chem. Rev.* **2019**, *119*, 4293 – 4356. (g) Tsuji, H.; Kawatsura, M. *Asian J. Org. Chem.* **2020**, *9*, 1924 – 1941. (h) Nishibayashi, Y. *Chem. Lett.* **2021**, *50*, 1282–1288.
- (6) For ruthenium: (a) Matsuzawa, H.; Miyake, Y.; Nishibayashi, Y. *Angew. Chem., Int. Ed.* **2007**, *46*, 6488–6491. (b) Matsuzawa, H.; Kanao, K.; Miyake, Y.; Nishibayashi, Y. *Org. Lett.* **2007**, *9*, 5561–5564. (c) Fukamizu, K.; Miyake, Y.; Nishibayashi, Y. *J. Am. Chem. Soc.* **2008**, *130*, 10498–10499. (d) Kanao, K.; Miyake, Y.; Nishibayashi, Y. *Organometallics* **2009**, *28*, 2920–2926. (e) Kanao, K.; Miyake, Y.; Nishibayashi, Y. *Organometallics* **2010**, *29*, 2126–2131. (f) Liu, S.; Tanabe, Y.; Kuriyama, S.; Sakata, K.; Nishibayashi, Y. *Angew. Chem. Int. Ed.* **2021**, *60*, 11231–11236.
- (7) For copper: (a) Hattori, G.; Matsuzawa, H.; Miyake, Y.; Nishibayashi, Y. *Angew. Chem. Int. Ed.* **2008**, *47*, 3781–3783. (b) Detz, R. J.; Delville, M. M. E.; Hiemstra, H.; van Maarseveen, J. H. *Angew. Chem. Int. Ed.* **2008**, *47*, 3777–3780. (c) Fang, P.; Hou, X.-L. *Org. Lett.* **2009**, *11*, 4612–4615. (d) Wang, B.; Liu, C.; Guo, H. *RSC Adv.* **2014**, *4*, 53216–53219. (e) Zhu, F.-L.; Zou, Y.; Zhang, D.-Y.; Wang, Y.-H.; Hu, X.-H.; Chen, S.; Xu, J.; Hu, X.-P. *Angew. Chem. Int. Ed.* **2014**, *53*, 1410–1414. (f) Zhu, F.-L.; Wang, Y.-H.; Zhang, D.-Y.; Hu, X.-H.; Chen, S.; Hou, C.-J.; Xu, J.; Hu, X.-P. *Adv. Synth. Catal.* **2014**, *356*, 3231–3236. (g) Zhang, D.-Y.; Zhu, F.-L.; Wang, Y.-H.; Hu, X.-H.; Chen, S.; Hou, C.-J.; Hu, X.-P. *Chem. Commun.* **2014**, *50*, 14459–14462. (h) Han, F.-Z.; Zhu, F.-L.; Wang, Y.-H.; Zou, Y.; Hu, X.-H.; Chen, S.; Hu, X.-P. *Org. Lett.* **2014**, *16*, 588–591. (i) Zhang, C.; Hui, Y.-Z.; Zhang, D.-Y.; Hu, X.-P. *RSC Adv.* **2016**, *6*, 14763–14767. (j) Xia, J.-T.; Hu, X.-P. *Org. Lett.* **2020**, *22*, 1102–1107. (k) Zhao, L.; Huang, G.; Guo, B.; Xu, L.; Chen, J.; Cao, W.; Zhao, G.; Wu, X. *Org. Lett.* **2014**, *16*, 5584–5587. (l) Huang, G.; Cheng, C.; Ge, L.; Guo, B.; Zhao, L.; Wu, X. *Org. Lett.* **2015**, *17*, 4894–4897. (m) Zhang, K.; Lu, L.-Q.; Yao, S.; Chen, J.-R.; Shi, D.-Q.; Xiao, W.-J. *J. Am. Chem. Soc.* **2017**, *139*, 12847–12854. (n) Shao, W.; Li, H.; Liu, C.; Liu, C.-J.; You, S.-L. *Angew. Chem. Int. Ed.* **2015**, *54*, 7684 – 7687. (o) Gao, X.; Cheng, R.; Xiao, Y.-L.; Wan, X.-L.; Zhang, X. *Chem* **2019**, *5*, 2987–2999. (p) Detz, R. J.; Abiri, Z.; le Griel, R.; Hiemstra,

H.; van Maarseveen, J. H. *Chem.–Eur. J.* **2011**, *17*, 5921–5930. (q) Tsuchida, K.; Senda, Y.; Nakajima, K.; Nishibayashi, Y. *Angew. Chem. Int. Ed.* **2016**, *55*, 9728–9732. (r) Yang, L.; Pu, X.; Niu, D.; Fu, Z.; Zhang, X. *Org. Lett.* **2019**, *21*, 8553–8557. (s) Shao, L.; Hu, X.-P. *Org. Biomol. Chem.* **2017**, *15*, 9837–9844. (t) Liu, S.; Tanabe, Y. Kuriyama, S.; Sakata, K.; Nishibayashi, Y. *Chem. Eur. J.* **2021**, *27*, 15650–15659.

(8) For nickel: (a) Watanabe, K.; Miyazaki, Y.; Okubo, M.; Zhou, B.; Tsuji, H.; Kawatsura, M. *Org. Lett.* **2018**, *20*, 5448–5451. (b) Miyazaki, Y.; Zhou, B.; H. Tsuji, H.; Kawatsura, M. *Org. Lett.* **2020**, *22*, 2049–2053. (c) Peng, L.; He, Z.; Xu, X.; Guo, C. *Angew. Chem. Int. Ed.* **2020**, *59*, 14270–14274. (d) Chang, X.; Zhang, J.; Peng, L.; Guo, C. *Nat. Commun.* **2021**, *12*, 299. (e) Xu, X.; Peng, L.; Chang, X.; Guo, C. *J. Am. Chem. Soc.* **2021**, *143*, 21048–21055. (f) Hu, Q.; He, Z.; Peng, L.; Guo, C. *Nat. Synth.* **2022**, *1*, 322–331.

(9) (a) Smith, S. W.; Fu, G. C. *J. Am. Chem. Soc.* **2008**, *130*, 12645–12647. (b) Schley, N. D.; Fu, G. C. *J. Am. Chem. Soc.* **2014**, *136*, 16588–16593. (c) Oelke, A. J.; Sun, J.; Fu, G. C. *J. Am. Chem. Soc.* **2012**, *134*, 2966–2969. (d) Huo, H.; Gorsline, B. J.; Fu, G. C. *Science* **2020**, *367*, 559–564.

(10) (a) Lu, F.-D.; Liu, D.; Zhu, L.; Lu, L.-Q.; Yang, Q.; Zhou, Q.-Q.; Wei, Y.; Lan, Y.; Xiao, W.-J. *J. Am. Chem. Soc.* **2019**, *141*, 6167–6172. (b) Lu, R.; Yang, T.; Chen, X.; Fan, W.; Chen, P.; Lin, Z.; Liu, G. *J. Am. Chem. Soc.* **2021**, *143*, 14451–14457. (c) Wang, F.; Chen, P.; Liu, G. *Nat. Synth.* **2022**, *1*, 107–116.

(11) Recent reviews on Hantzsch ester in photoredox catalysis: (a) Huang, W.; Cheng, X. *Synlett* **2017**, *28*, 148–158. (b) Wang, P.-Z.; Chen, J.-R.; Xiao, W.-J. *Org. Biomol. Chem.* **2019**, *17*, 6936–6951.

(12) Shen, G.-B.; Xie, L.; Yu, H.-Y.; Liu, J.; Fu, Y.-H.; Yan, M. *RSC Adv.* **2020**, *10*, 31425–31434.

(13) Nakajima, K.; Nojima, S.; Sakata, K.; Nishibayashi, Y. *ChemCatChem* **2016**, *8*, 1028–1032.

(14) (a) Chen, W.; Liu, Z.; Tian, J.; Li, M.; Ma, J.; Cheng, X.; Li, G. *J. Am. Chem. Soc.* **2016**, *138*, 12312–12315. (b) Gu, F.; Huang, W.; Liu, X.; Chen, W.; Cheng, X. *Adv. Synth. Catal.* **2018**, *360*, 925–931.

(15) (a) de Assis, F. F.; Huang, X.; Akiyama, M.; Pilli, R. A.; Meggers, E. *J. Org. Chem.* **2018**, *83*, 10922–10932. (b) Song, Z.-Y.; Zhang, C.-L.; Ye, S. *Org. Biomol. Chem.* **2019**, *17*, 181–185. (c) Du, J.; Sun, H.-W.; Gao, Q.-S.; Wang, J.-Y.; Wang, H.; Xu, Z.; Zhou, M.-D. *Org. Lett.* **2020**, *22*, 1542–1546. (d) Angnes, R. A.; Potnis, C.; Liang, S.; Correia, C. R. D.; Hammond, G. B. *J. Org. Chem.* **2020**, *85*, 4153–4164. (e) Guo, Q.; Peng, Q.; Chai, H.; Huo, Y.; Wang, S.; Xu, Z. *Nat. Commun.* **2020**, *11*, 1463. (f) He, X.-K.; Lu, J.; Zhang, A.-J.; Zhang, Q.-Q.; Xu, G.-Y.; Xuan, J. *Org. Lett.* **2020**, *22*, 5984–5989. (g) Kim, I.; Park, S.; Hong, S. *Org. Lett.* **2020**, *22*, 8730–8734.

(16) (a) Wang, X.; Li, H.; Qiu, G.; Wu, J. *Chem. Commun.* **2019**, *55*, 2062–2065. (b) Wang, X.; Yang, M.; Xie, W.; Fan, X.; Wu, X. *J. Chem. Commun.* **2019**, *55*, 6010–6013. (c) Gong, X.; Yang, M.; Liu, J.-B.; He, F.-S.; Fan, X.; Wu, J. *Green Chem.* **2020**, *22*, 1906–1910.

(17) Nakajima, K.; Nojima, S.; Nishibayashi, Y. *Angew. Chem. Int. Ed.* **2016**, *55*, 14106–14110.

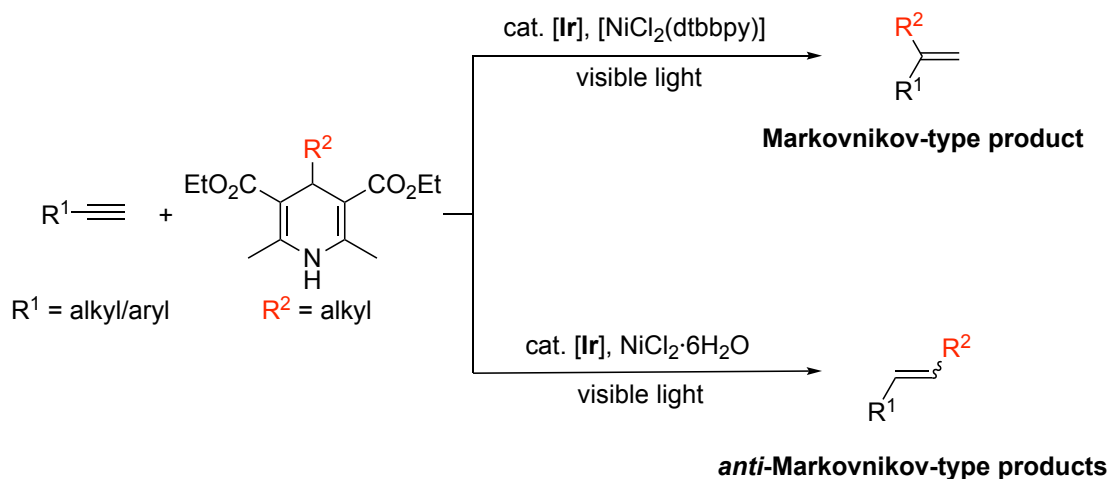
- (18) Nakajima, K.; Guo, X.; Nishibayashi, Y. *Chem. Asian J.* **2018**, *13*, 3653–3657.
- (19) Zhang, Y.; Tanabe, Y.; Kuriyama, S.; Nishibayashi, Y. *J. Org. Chem.* **2021**, *86*, 12577–12590.
- (20) Buzzetti, L.; Prieto, A.; Roy, S. R.; Melchiorre, P. *Angew. Chem. Int. Ed.* **2017**, *56*, 15039–15043.
- (21) (a) Zhang, H.-H.; Yu, S. *J. Org. Chem.* **2017**, *82*, 9995–10006. (b) van Leeuwen, T.; Buzzetti, L.; Perego, L. A.; Melchiorre, P. *Angew. Chem. Int. Ed.* **2019**, *58*, 4953–4957. (c) Schwarz, J. L.; Huang, H.-M.; Paulisch, T. O.; Glorius, F. *ACS Catal.* **2020**, *10*, 1621–1627. (d) Zhou, Z.-Z.; Jiao, R.-Q.; Yang, K.; Chen, X.-M.; Liang, Y.-M. *Chem. Commun.* **2020**, *56*, 12957–12960. (e) Huang, H.-M.; Bellotti, P.; Daniliuc, C. G.; Glorius, F. *Angew. Chem. Int. Ed.* **2021**, *60*, 2464–2471. (f) Yang, T.; Wei, Y.; Kooh, M. *J. ACS Catal.* **2021**, *11*, 6519–6525. (g) Liang, Z.; Lv, K.; Zhou, S.; Bao, X. *Org. Chem. Front.* **2021**, *8*, 6499–6507. (h) Zhou, Z.-Z.; Song, X.-R.; Du, S.; Xia, K.-J.; Tian, W.-F.; Xiao, Q.; Liang, Y.-M. *Chem. Commun.* **2021**, *57*, 9390–9393.
- (22) Qu, Q.-Y.; Min, Q.-Q.; Ao, G.-Z.; Liu, F. *Org. Biomol. Chem.* **2018**, *16*, 6391–6394.
- (23) Phelan, J. P.; Lang, S. B.; Sim, J.; Berritt, S.; Peat, A. J.; Billings, K.; Fan, L.; Molander, G. A. *J. Am. Chem. Soc.* **2019**, *141*, 3723–3732.
- (24) (a) Gutiérrez-Bonet, Á.; Tellis, J. C.; Matsui, J. K.; Vara, B. A.; Molander, G. A. *ACS Catal.* **2016**, *6*, 8004–8008. (b) Milligan, J. A.; Phelan, J. P.; Polites, V. C.; Kelly, C. B.; Molander, G. A. *Org. Lett.* **2018**, *20*, 6840–6844. (c) McDonald, B. R.; Scheidt, K. A. *Org. Lett.* **2018**, *20*, 6877–6881. (d) Chen, H.; Anand, D.; Zhou, L. *Asian J. Org. Chem.* **2019**, *8*, 661–664. (e) Wang, Z.-J.; Zheng, S.; Romero, E.; Matsui, J. K.; Molander, G. A. *Org. Lett.* **2019**, *21*, 6543–6547. (f) Liang, S.; Angnes, R. A.; Potnis, C.; Hammond, G. B. *Tetrahedron Lett.* **2019**, *60*, 151230. (g) Chen, X.; Ye, F.; Luo, X.; Liu, X.; Zhao, J.; Wang, S.; Zhou, Q.; Chen, G.; Wang, P. *J. Am. Chem. Soc.* **2019**, *141*, 18230–18237. (h) Xue, S.; Limburg, B.; Ghorai, D.; Benet-Buchholz, J.; Kleij, A. W. *Org. Lett.* **2021**, *23*, 4447–4451. (i) Ren, S.-C.; Lv, W.-X.; Yang, X.; Yan, J.-L.; Xu, J.; Wang, F.-X.; Hao, L.; Chai, H.; Jin, Z.; Chi, Y. R.; *ACS Catal.* **2021**, *11*, 2925–2934.
- (25) (a) Gandolfo, E.; Tang, X.; Raha Roy, S.; Melchiorre, P. *Angew. Chem. Int. Ed.* **2019**, *58*, 16854–16858. (b) Zhang, H.-H.; Zhao, J.-J.; Yu, S. *J. Am. Chem. Soc.* **2018**, *140*, 16914–16919.
- (26) Zhang, Y.; Tanabe, Y.; Kuriyama, S.; Nishibayashi, Y. *Chem. Eur. J.* **2022**, *28*, e202200727.
- (27) (a) Ammal, S. C.; Yoshikai, N.; Inada, Y.; Nishibayashi, Y.; Nakamura, E. *J. Am. Chem. Soc.* **2005**, *127*, 9428–9438.
- (28) Miroshnichenko, E. A.; Kon'kova, T. S.; Matyushin, Yu. N.; Orlov, Yu. D.; Pashchenko, L. L.; Vorob'ev, A. B.; Inozemtsev, A. V. *Russ. J. Phys. Chem. B* **2019**, *13*, 225–230.
- (29) Sakata, K.; Uehara, Y.; Kohara, S.; Yoshikawa, T.; Nishibayashi, Y. Submitted.
- (30) (a) Bradsher, L. *Preparative Acetylene Chemistry*. 2nd ed. Elsevier, 1985; (b) Stang, P. J.; Diederich, F. *Modern Acetylene Chemistry*. VCH, 2008; (c) Aitken, R. A.; Aitken, K. *Sci. Synth.* **2008**, *43*, 555–630.
- (31) Jiang, H.; Zhu, C.; Wu, W. Preparation of haloalkynes. in *Haloalkyne Chemistry*

- (eds. Jiang, H, Zhu C. & Wu, W.) 5–7. Springer, 2016.
- (32) Sonogashira, K. *Handb. Organopalladium Chem. Org. Synth.* **2002**, *1*, 493–529.
- (33) King, A. O.; Shinkai, I. *e-EROS Encycl. Reagents Org. Synth.* **2001**, 1–5.
- (34) Yasu, Y.; Koike, T.; Akita, M. *Adv. Synth. Catal.* **2012**, *354*, 3414–3420.
- (35) (a) Liao, J.; Basch, C. H.; Hoerner, M. E.; Talley, M. R.; Boscoe, B. P.; Tucker, J. W.; Garnsey, M. R.; Watson, M. P. *Org. Lett.* **2019**, *21*, 2941–2946. (b) Wang, J.; Pang, Y.-B.; Tao, N.; Zeng, R.-S.; Zhao, Y. *J. Org. Chem.* **2019**, *84*, 15315–15322. (c) Zhang, D.; Tang, Z.-L.; Ouyang, X.-H.; Song, R.-J.; Li, J.-H. *Chem. Commun.* **2020**, *56*, 14055–14508.
- (36) Pitre, S. P.; McTiernan, C. D.; Scaiano, J. C. *Acc. Chem. Res.* **2016**, *49*, 1320–1330.
- (37) Dixon, I. M.; Collin, J.-P.; Sauvage, J.-P.; Flamigni, L.; Encinas, S.; Barigelletti, F. *Chem. Soc. Rev.* **2000**, *29*, 385–191.
- (38) Flamigni, L.; Barbieri, A.; Sabatini, C.; Ventura, B.; Barigelletti, F. *Top. Curr. Chem.* **2007**, *281*, 143–203.
- (39) (a) Miyake, Y.; Endo, S.; Nomaguchi, Y.; Yuki, M.; Nishibayashi, Y. *Organometallics* **2008**, *27*, 4017–4020. (b) Miyake, Y.; Endo, S.; Yuki, M.; Tanabe, Y.; Nishibayashi, Y. *Organometallics* **2008**, *27*, 6039–6042.
- (40) Hatchard, C. G.; Parker, C. A. *Proc. R. Soc. London Ser. A* **1956**, *235*, 518–526.
- (41) (a) Cismesia, M.; Yoon, T. P. *Chem. Sci.* **2015**, *6*, 5426–5436. (b) Kärkäs, M. D.; Matsuura, B. S.; Stephenson, C. R. J. *Science* **2015**, *349*, 1285–1286.
- (42) (a) Miyake, Y.; Nakajima, K.; Nishibayashi, Y. *J. Am. Chem. Soc.* **2012**, *134*, 3338–3341. (b) Miyake, Y.; Ashida, Y.; Nakajima, K.; Nishibayashi, Y. *Chem. Commun.* **2012**, *48*, 6966–6968. (c) Miyake, Y.; Nakajima, K.; Nishibayashi, Y. *Chem. Commun.* **2013**, *49*, 7854–7856. (d) Nakajima, K.; Kitagawa, M.; Ashida, Y.; Miyake, Y. *Chem. Commun.* **2014**, *50*, 8900–8903. (e) Nakajima, K.; Miyake, Y.; Nishibayashi, Y. *Acc. Chem. Res.* **2016**, *49*, 1946–1956.
- (43) Ong, K. C.; Douglas, B.; Robinson, R. A. *J. Chem. Eng. Data* **1966**, *11*, 574–576.
- (44) Rigaut, S.; Maury, O.; Touchard, D.; Dixneuf, P. H. *Chem. Commun.* **2001**, *37*, 373–374.
- (45) Rigaut, S.; Monnier, F.; Mousset, F.; Touchard, D.; Dixneuf, P. H. *Organometallics* **2002**, *21*, 2654–266. (b) Rigaut, S.; Costuas, K.; Touchard, D.; Saillard, J.; Golhen, S.; Dixneuf, P. H. *J. Am. Chem. Soc.* **2004**, *126*, 4072–4073.
- (46) Onodera, G.; Nishibayashi, Y.; Uemura, S. *Organometallics* **2006**, *25*, 35–37.
- (47) Sathyamoorthy, B.; Axelrod, A.; Farwell, V.; Bennett, S. M.; Calitree, B. D.; Benedict, J. B.; Sukumaran, D. K.; Detty, M. R. *Organometallics* **2010**, *29*, 3431–3441.
- (48) Xu, C.-F.; Xu, M.; Yang, L.-Q.; Li, C.-Y. *J. Org. Chem.* **2012**, *77*, 3010–3016.
- (49) McAdam, C. A.; McLaughlin, M. G.; Johnston, A. J. S.; Chen, J.; Walter, M. W.; Cook, M. J. *Org. Biomol. Chem.* **2013**, *11*, 4488–4502.
- (50) Kawai, H.; Tachi, K.; Tokunaga, E.; Shiro, M.; Shibata, N. *Org. Lett.* **2010**, *12*, 5104–5107.
- (51) Kourist, R.; Bartsch, S.; Bornscheuer, U. T. *Adv. Synth. Catal.* **2007**, *349*, 1393–1398.
- (52) Holmes, M.; Nguyen, K. D.; Schwartz, L. A.; Luong, T.; Krische, M. J. *J. Am. Chem. Soc.* **2017**, *139*, 8114–8117.

- (53) Li, G.; Chen, R.; Wu, L.; Fu, Q.; Zhang, X.; Tang, Z. *Angew. Chem. Int. Ed.* **2013**, *52*, 8432–8436.
- (54) Bai, Z.; Zhang, H.; Wang, H.; Yu, H.; Chen, G.; He, G. *J. Am. Chem. Soc.* **2021**, *143*, 1195–1202.
- (55) Kidwai, M.; Saxena, S.; Mohan, R.; Venkataramanan, R. *J. Chem. Soc., Perkin Trans. 1* **2022**, 1845–1846.
- (56) J. M. Frisch et al. Gaussian 16, Revision A.03, Gaussian, Inc., Wallingford CT, **2016**.
- (57) Chai, J.-D.; Head-Gordon, M. *Phys. Chem. Chem. Phys.* **2008**, *10*, 6615–6620.
- (58) Hehre, W. J.; Radom, L.; Schleyer, P. v. R.; Pople, J. A. *Ab Initio Molecular Orbital Theory*, Wiley, New York, **1986**.
- (59) Dolg, M.; Wedig, U.; Preuss, H. *J. Chem. Phys.* **1987**, *86*, 866–872.
- (60) (a) Miertuš, S.; Scrocco, E.; Tomasi, J. *Chem. Phys.* **1981**, *55*, 117–129; (b) Scalmani, G.; Frisch, M. *J. Chem. Phys.* **2010**, *132*, 114110.
- (61) CrysAlisPro, version 1.171.41.99a, Data Collection and Processing Software, Rigaku Corporation, Tokyo, Japan, **2021**.
- (62) CrystalStructure, version 4.3, Crystal Structure Analysis Package, Rigaku Corporation, Tokyo, Japan, **2019**.
- (63) Sheldrick, G. M. *Acta Crystallogr.* **2014**, *A70*, C1437.
- (64) Sheldrick, G. M. *Acta Crystallogr.* **2015**, *C71*, 3–8.
- (65) Ibers, J. A.; Hamilton, W. C. *Acta Crystallogr.* **1964**, *17*, 781–782.
- (66) Creagh, D. C.; Hubbell, J. H. in *International Tables for Crystallography*, Vol. C (Ed: Wilson, A. J. C.), Kluwer Academic Publishers, Dordrecht, The Netherlands, **1992**; Table 4.2.3.3., pp. 200–206.
- (67) Creagh, D. C.; McAuley, W. J. in *International Tables for Crystallography*, Vol. C (Ed: Wilson, A. J. C.), Kluwer Academic Publishers, Dordrecht, The Netherlands, **1992**; Table 4.2.6.8., pp. 219–222.
- (68) Maslen, E. N.; Fox, A. G.; O’Keefe, M. A. in *International Tables for Crystallography*, Vol. C (Ed: Wilson, A. J. C.), Kluwer Academic Publishers, Dordrecht, The Netherlands, **1992**; Table 6.1.1.4., pp. 500–503.

Chapter 3

Photoredox- and Nickel-Catalyzed Hydroalkylation of Alkynes with 4-Alkyl-1,4-dihydropyridines: Ligand-Controlled Regioselectivity



In Chapter 3, the author has developed the dual photoredox- and nickel-catalyzed hydroalkylation of terminal alkynes with 4-alkyl-1,4-dihydropyridines under visible light irradiation to afford Markovnikov- or *anti*-Markovnikov-type alkylated alkenes in good to high yields, where regioselectivity of the products has been effectively controlled by coordination ligands for nickel species. Use of $[\text{NiCl}_2(\text{dtbbpy})]$ as a catalyst has led to the formation of Markovnikov-type products, whereas that of $\text{NiCl}_2\cdot 6\text{H}_2\text{O}$ has led to the formation of *anti*-Markovnikov-type products.

3.1. Introduction

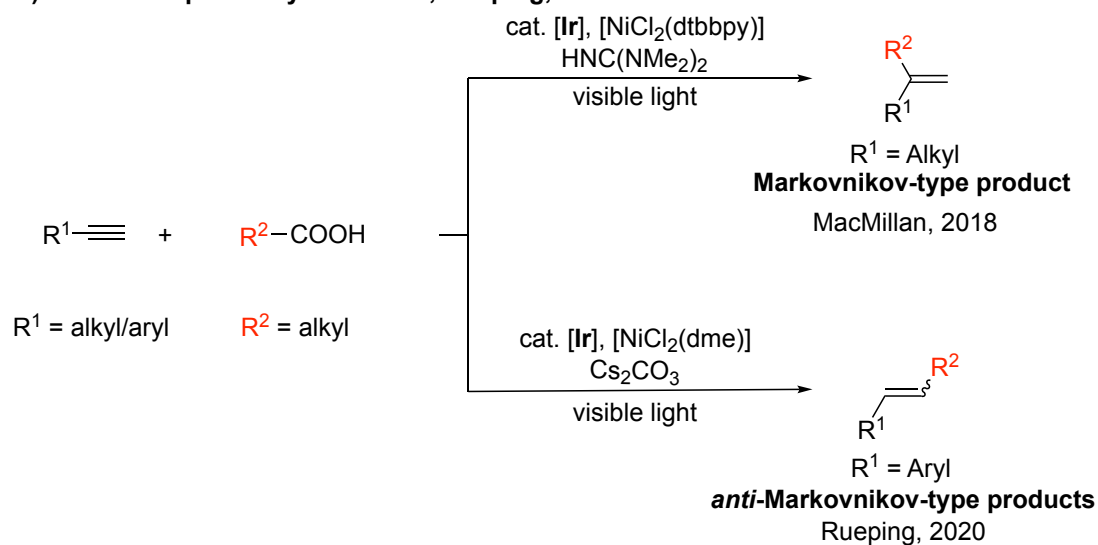
Functionalized alkenes are versatile synthetic intermediates found in various useful molecules and materials.¹ Among the vast range of methods to prepare functionalized alkenes,^{2,3} hydroalkylation of alkynes^{4–7} has been gaining attention as convenient synthetic method to prepare functionalized alkenes with Markovnikov^{8–11} or *anti*-Markovnikov^{12–17} selectivity. In addition, functionalization of alkynes has been recently expanded by the introduction of visible light-triggered generation of carbon-centered radicals via a single electron transfer (SET) processes mediated by photoredox catalysts,¹⁸ which have been also applied to the hydroalkylation of alkynes to form functionalized alkenes.^{6,7,9–11,13–17,19} Indeed, both Markovnikov-type^{9–11} and *anti*-Markovnikov-type^{15,16} hydroalkylation of terminal alkynes mediated by dual photoredox and nickel catalysts has been reported,^{20,21} where alkyl carboxylic acids,^{9,16} benzyl chlorides,¹⁰ cycloalkanols,¹¹ or dialkyl acyl peroxides¹⁵ are used as alkylation reagents. For example, MacMillan's or Rueping's group has demonstrated visible light-mediated Markovnikov-type or *anti*-Markovnikov-type decarboxylative hydroalkylation of terminal alkynes with alkyl carboxylic acids in the presence of an iridium-based photoredox catalyst by using [NiCl₂(dtbbpy)] (dtbbpy = 4,4'-di-*tert*-butyl-2,2'-bipyridine) or [NiCl₂(dme)] (dme = 1,2-dimethoxyethane) as a co-catalyst, respectively, where addition of a base such as HNC(NMe₂)₂ or Cs₂CO₃ is also required (Scheme 3-1a).^{9,16} Here, regioselectivity of the products is likely controlled by coordination ligands of nickel catalysts²² as has been reported for regioselective alkyne functionalization such as silaboration,²³ hydroacylation,²⁴ hydrothiolation,²⁵ hydrosilylation,²⁶ hydroborylation,²⁷ and hydroallylation,²⁸ although substrate scope of terminal alkynes available for photoredox- and nickel-catalyzed regioselective hydroalkylation reactions is rather limited (alkylacetylenes or arylacetylenes).^{9,16} Thus, ligand-controlled regioselective hydroalkylation of alkynes has been still left unexplored.

On the other hand, 4-alkyl-1,4-dihydropyridines have been recently shown to work as powerful alkylation reagents to give a variety of alkylative reactions in photoredox-catalyzed molecular transformations, declaring that 4-alkyl-1,4-dihydropyridines can act as mild alkylation reagents alternative to classical but highly reactive, organometallic alkylation reagents.^{29–39} In this reaction systems, SET processes from the visible light-excited photoredox catalysts to 4-alkyl-1,4-dihydropyridines give rise to the formation of alkyl radicals,^{18,29,30} which enables simple alkylation^{31–34} as well as alkylative reactions^{35–42} along with other transformations such as cross-coupling reactions in the presence of supplementary catalysts. Relatedly, the author's group has already reported the photoredox-catalyzed aromatic substitution reactions of cyanoarenes,³¹ and dual photoredox- and nickel-catalyzed cross-coupling reactions of aryl,³⁵ alkenyl,³⁶ and alkynyl halides³⁷ with 4-alkyl-1,4-dihydropyridines acting as alkylation reagents. As our extensive work of the use of 4-alkyl-1,4-dihydropyridines, the author has now envisaged the combination of photoredox-catalyzed reactions of alkylacetylenes or arylacetylenes with 4-alkyl-1,4-dihydropyridines, which have not been used as alkylation reagents to afford

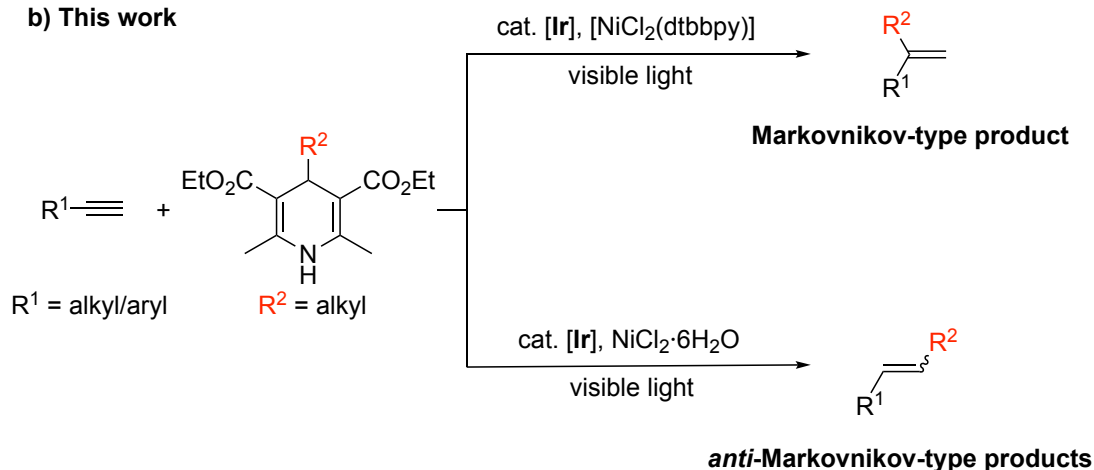
Markovnikov or *anti*-Markovnikov type alkylated alkenes.⁴³ After the detailed investigation, the author has found that the regioselectivity can be controlled by the difference in coordination ligands for nickel catalysts without the requirement of addition of bases (Scheme 3-1b). Herein, the author wishes to report the photoredox- and nickel-catalyzed regioselective hydroalkylation of terminal alkynes simply controlled by the choice of coordination ligands, providing a new strategy in the preparation of functionalized alkenes from alkynes.

Scheme 3-1. Photoredox- and Nickel-catalyzed Regioselective Hydroalkylation Reactions

a) Previous reported by MacMillan, Rueping, *et al.*



b) This work

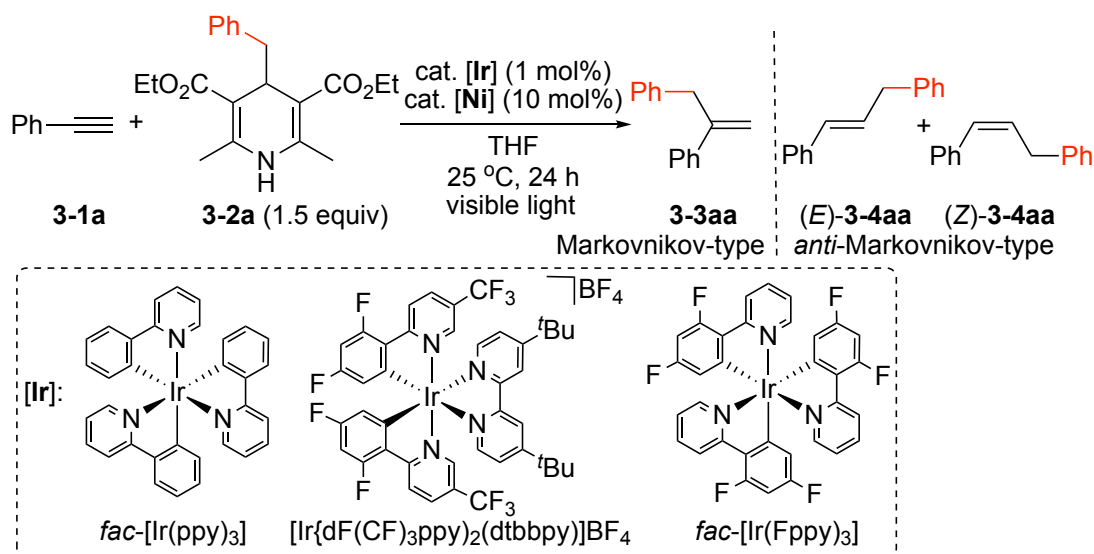


3.2. Results and Discussions

As beginning of this investigation, the author selected the ethynylbenzene (**3-1a**) and 4-benzyl-3,5-bis(ethoxycarbonyl)-2,6-dimethyl-1,4-dihydropyridine (**3-2a**) as typical substrates for the hydroalkylation reaction to afford prop-2-ene-1,2-diylidibenzene (**3-3aa**) as the Markovnikov-type product or (*E*)- and (*Z*)-prop-1-ene-1,3-diylidibenzene ((*E*)-**3-4aa** and (*Z*)-**3-4aa**) as the *anti*-Markovnikov-type products, selectively (Table 3-1).

When the reaction of **3-1a** with 1.5 equiv of **3-2a** in THF was carried out in the presence of 1 mol% of *fac*-[Ir(ppy)₃] (ppy = 2-(2-pyridyl)phenyl) and 10 mol% of anhydrous NiCl₂ as a photoredox catalyst and a cross-coupling catalyst, respectively, at 25 °C for 24 h under visible light illumination with a 12 W white LED, both Markovnikov-type **3-3aa** and *anti*-Markovnikov-type **3-4aa** were obtained, where the former was obtained in 10% yield as a minor product and the latter was isolated in 44% yield as the major product but as a mixture of *E*- and *Z*-isomers with an *E/Z* ratio of 65/35 (Table 3-1, entry 1). Nickel phosphine complexes instead of anhydrous NiCl₂ as catalysts did not work (Table 3-1, entries 2 and 3). In contrast, Markovnikov-type **3-3aa** became the major product isolated in 72% yield when [NiCl₂(dtbbpy)] was used as a catalyst (Table 3-1, entry 4) similar to the decarboxylative hydroalkylation reported by MacMillan and co-workers.⁹ Yields of both **3-3aa** and **3-4aa** decreased when DMF, MeCN, toluene, or CH₂Cl₂ was used as a solvent instead of THF (Table 3-1, entries 5–8), thus THF was selected as the appropriate solvent to carry out the hydroalkylation reactions. Use of [Ir{dF(CF₃)ppy}₂(dtbbpy)]BF₄ (dF(CF₃)ppy = 3,5-difluoro-2-(5-trifluoromethyl-2-pyridyl)phenyl) instead of *fac*-[Ir(ppy)₃] as a photoredox catalyst was not effective (Table 3-1, entry 9), while **3-3aa** was obtained almost solely (98% isolated yield) without the formation of **3-4aa**, when *fac*-[Ir(Fppy)₃] (Fppy = 3,5-difluoro-2-(2-pyridyl)phenyl) was used as a photoredox catalyst (Table 3-1, entry 10). On the other hand, yields of **3-3aa** and **3-4aa** became almost the same when [Ni(acac)₂] (acac = acetylacetonate) was used as a catalyst (Table 3-1, entry 11), whereas **3-4aa** became the major product with drastic decrease in the yields of **3-3aa** when nickel dihalide complexes with more labile coordination ligands such as NiBr₂·diglyme (diglyme = 1-methoxy-2-(2-methoxyethoxy)ethane) and [NiCl₂(dme)] were used as catalysts (Table 3-1, entries 12 and 13) similar to the decarboxylative hydroalkylation reported by Rueping and co-workers.¹⁶ Surprisingly, use of NiCl₂·6H₂O as a catalyst drastically increased the yield of **3-4aa** up to 83%, where (*E*)- and (*Z*)-**3-4aa** were obtained as a mixture with an *E/Z* ratio of 55/45 (Table 3-1, entry 14). The change in reactivity between anhydrous NiCl₂ and NiCl₂·6H₂O may be due to their solubility in THF; anhydrous NiCl₂ is almost insoluble in THF, while NiCl₂·6H₂O is sparingly but enough soluble in THF (0.016 mol/L) to give NiCl₂·1.5C₄H₈O.⁴⁴ Yields of **3-4aa** hardly increased with longer time of visible light irradiation (84% for 48 h or 72 h), but *E/Z* ratio gradually changed down from 55/45 (24 h) via 32/68 (48 h) to 18/82 (72 h) (Table 3-1, entries 14–16), indicating that photoinduced *E* to *Z* isomerization catalyzed by iridium-based photoredox catalyst further occurred after the formation of (*E*)-**4aa**, as also previously observed for aryl-substituted alkenes by our group.^{36,45}

Table 3-1. Photoredox- and Nickel-Catalyzed Hydroalkylation of **3-1a** with **3-2a**^a



entry	cat. [Ir]	cat. [Ni]	solvent	3aa (%) ^b	4aa (%) ^b (<i>E/Z</i>) ^c
1	<i>fac</i> -[Ir(ppy) ₃]	anhydrous NiCl ₂	THF	10	44 (65/35)
2	<i>fac</i> -[Ir(ppy) ₃]	[NiCl ₂ (PPh ₃) ₂]	THF	n.d. ^d	n.d.
3	<i>fac</i> -[Ir(ppy) ₃]	[NiCl ₂ (dppe)]	THF	n.d.	trace ^e
4	<i>fac</i> -[Ir(ppy) ₃]	[NiCl ₂ (dtbbpy)]	THF	72	8 (59/41)
5	<i>fac</i> -[Ir(ppy) ₃]	[NiCl ₂ (dtbbpy)]	DMF	66	3 (78/28)
6	<i>fac</i> -[Ir(ppy) ₃]	[NiCl ₂ (dtbbpy)]	MeCN	53	3 (62/38)
7	<i>fac</i> -[Ir(ppy) ₃]	[NiCl ₂ (dtbbpy)]	toluene	33	2 (42/58)
8	<i>fac</i> -[Ir(ppy) ₃]	[NiCl ₂ (dtbbpy)]	CH ₂ Cl ₂	trace	trace
9	[Ir{dF(CF ₃) ₃ ppy} ₂ (dtbbpy)]BF ₄	[NiCl ₂ (dtbbpy)]	THF	52	3 (59/41)
10	<i>fac</i> -[Ir(Fppy) ₃]	[NiCl ₂ (dtbbpy)]	THF	98	n.d.
11	<i>fac</i> -[Ir(Fppy) ₃]	[Ni(acac) ₂]	THF	32	32 (58/42)
12	<i>fac</i> -[Ir(Fppy) ₃]	NiBr ₂ ·diglyme	THF	trace	23 (45/55)
13	<i>fac</i> -[Ir(Fppy) ₃]	[NiCl ₂ (dme)]	THF	trace	57 (58/42)
14	<i>fac</i> -[Ir(Fppy) ₃]	NiCl ₂ ·6H ₂ O	THF	trace	83 (55/45)
15 ^f	<i>fac</i> -[Ir(Fppy) ₃]	NiCl ₂ ·6H ₂ O	THF	trace	84 (32/68)
16 ^g	<i>fac</i> -[Ir(Fppy) ₃]	NiCl ₂ ·6H ₂ O	THF	trace	84 (18/82)
17	<i>fac</i> -[Ir(Fppy) ₃]	None	THF	n.d.	n.d.
18	none	[NiCl ₂ (dtbbpy)]	THF	n.d.	n.d.
19	none	NiCl ₂ ·6H ₂ O	THF	n.d.	n.d.
20 ^h	<i>fac</i> -[Ir(Fppy) ₃]	[NiCl ₂ (dtbbpy)]	THF	n.d.	n.d.
21 ^h	<i>fac</i> -[Ir(Fppy) ₃]	NiCl ₂ ·6H ₂ O	THF	n.d.	n.d.
22 ⁱ	<i>fac</i> -[Ir(Fppy) ₃]	[NiCl ₂ (dtbbpy)]	THF	97	n.d.
23 ^j	<i>fac</i> -[Ir(Fppy) ₃]	[NiCl ₂ (dtbbpy)]	THF	n.d.	n.d.

^aReactions of **3-1a** (0.25 mmol) with **3-2a** (0.375 mmol) were carried out in the presence of catalytic amounts of [Ir] (0.0025 mmol) and [Ni] (0.025 mmol) in THF (2.5 mL) with 12 W white LED illumination at 25 °C for 24 h. ^bIsolated yield. ^c*E/Z* ratio determined by quantitative

measurement of GC-MS for crude mixture. ^dNot detected by GC-MS. ^eDetected by GC-MS for crude mixture but not isolable. ^f48 h instead of 24 h. ^g72 h instead of 24 h. ^hIn dark. ⁱ $\lambda > 500$ nm. ^j $\lambda > 580$ nm.

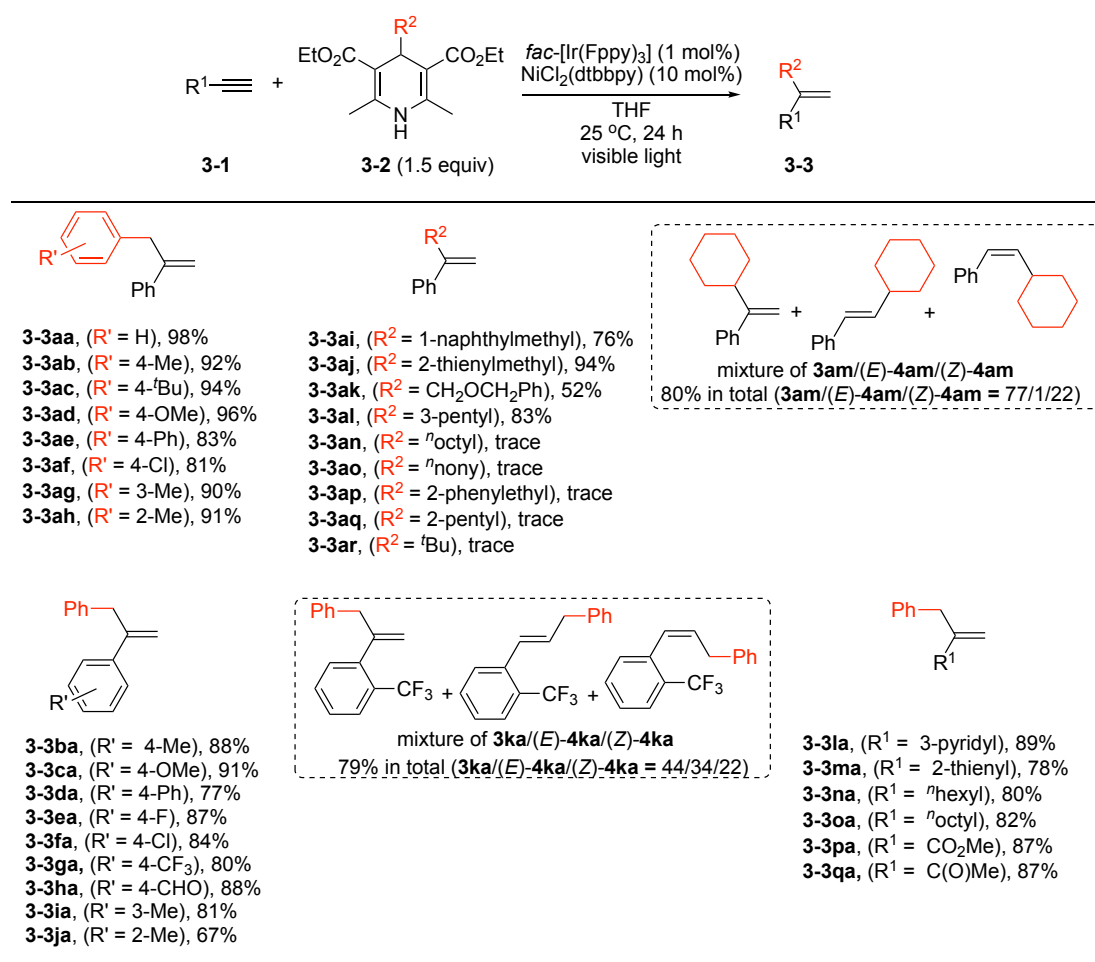
When reactions were carried out in the absence of a nickel catalyst, a photoredox catalyst, or visible light irradiation, hydroalkylation did not take place (Table 3-1, entries 17–21), revealing that both nickel and photoredox catalysts as well as visible light irradiation are all essential to promote the catalytic reaction. As *fac*-[Ir(Fppy)₃] is known to possess the maximum absorption and emission peaks at 378 nm and 476 nm, respectively, range of wavelengths effective against catalyses was examined by using glass filters cutting lower wavelengths.⁴⁶ Yield of Markovnikov-type **3-3aa** with cutting visible light below 500 nm was almost the same with that without filters (Table 3-1, entry 22), but hydroalkylation did not take place with cutting visible light below 580 nm (Table 3-1, entry 23), demonstrating that reactions are promoted by blue to green visible light, where singlet-to-triplet absorption of *fac*-[Ir(Fppy)₃] can also contribute to this photoredox catalytic system.⁴⁷

With the optimized reaction conditions in hand, reactions of **3-1a** with various 4-alkyl-1,4-dihydropyridines to afford Markovnikov-type products were next investigated (Scheme 3-2). All the 4-benzyl-1,4-dihydropyridine derivatives with either electron-donating or electron-withdrawing substituents introduced at the 4-position of the benzene moiety (**3-2b**: Me, **3-2c**: ^tBu, **3-2d**: MeO, **3-2e**: Ph, **3-2f**: Cl) or at the 3- or 2- position (**3-2g**: 3-Me, **3-2h**: 2-Me) were successfully used as alkylation reagents to afford the corresponding Markovnikov-type alkylated alkenes (**3-3ab–3-3ah**) in high yields. Other 1,4-dihydropyridine derivatives with primary alkyl groups such as 1-naphthylmethyl (**3-2i**), 2-thienylmethyl (**3-2j**), benzyloxymethyl (**3-2k**), or even with secondary alkyl groups (**3-2l**: 3-pentyl) were also found to be applicable to afford the corresponding Markovnikov-type alkylated alkenes (**3-3ai–3-3al**) in good to high yields. In contrast, reaction of **3-1a** with 1,4-dihydropyridine derivative containing cyclopentyl group (**3-2m**) afforded a mixture of Markovnikov-type and anti-Markovnikov-type products (**3-3am** and **3-4am**). In addition, 1,4-dihydropyridine derivative with long-chain primary alkyl (**3-2n**: *n*-octyl, **3-2o**: *n*-nonyl), α -arylalkyl (**3-2p**: 1-phenylethyl), unsymmetrical secondary alkyl (**3-2q**: 2-pentyl), or tertiary alkyl group (**3-2r**: ^tBu) led to the formation of only a trace amount of the corresponding alkylated alkene (**3-3an–3-3ar**), while no desired product was obtained for the reaction of **3-1a** with a 3-pyridylmethyl substituent (**3-2s**), mostly transformed into 3-methylpyridine. Here, both steric bulkiness and stability of alkyl radicals⁴⁸ may contribute to the formation of the desired alkylated products. Next, Markovnikov-type hydroalkylation reactions of various terminal alkynes with **3-2a** were investigated. Ethynylbenzene derivatives with either electron-donating or electron-withdrawing substituents including aldehyde group introduced at the 4-position of the benzene moiety (**3-1b**: Me, **3-1c**: MeO, **3-1d**: Ph, **3-1e**: F, **3-1f**: Cl, **3-1g**: CF₃, **3-1h**: CHO) or at the 3- or 2- position (**3-1i**: 3-Me, **3-1j**: 2-Me) were successfully alkylated to afford the corresponding Markovnikov-type alkenes (**3-3ba–3-3ja**) in good to high yields, whereas a mixture of Markovnikov-type and *anti*-Markovnikov-type products (**3-3ka**

and **3-4ka**) was obtained for the introduction of CF₃ group at the 2-position. Heterocycle could be also introduced when 3-ethynylpyridine (**3-1l**) or 2-ethynylthiophene (**3-1m**) was used as a substrate to afford the corresponding alkyne (**3-3la**, **3-3ma**) in a high yield. In addition, alkylacetylenes (**3-1n**: *n*-hexyl, **3-1o**: *n*-octyl), methyl propiolate (**3-1p**), and but-3-yn-2-one (**3-1q**) were available to afford the corresponding Markovnikov-type alkylated alkenes (**3-3ma**–**3-3qa**) in high yields.

The author next examined the reactions of **3-1a** with various 4-alkyl-1,4-dihydropyridines to afford *anti*-Markovnikov-type products using NiCl₂·6H₂O as the catalyst (Scheme 3-3). 4-Benzyl-1,4-dihydropyridine derivatives with either electron-donating or electron-withdrawing substituents introduced at the 4-position of the benzene moiety (**3-2d**, **3-2f**), 4-methyl-1,4-dihydropyridine derivatives with aromatic substituents introduced at the 4-methyl group (**3-2i**, **3-2j**), or 1,4-dihydropyridine derivatives with secondary alkyl groups (**3-2l**, **3-2m**) were found to work as alkylation reagents to afford the corresponding *anti*-Markovnikov-type alkylated products (**3-4ad**, **3-4af**, **3-4ai**, **3-4aj**, **3-4al**, **3-4am**) as mixtures of *E*- and *Z*- isomers (17/83 < *E/Z* < 94/6) in good to high yields when visible light irradiation was all stopped after 24 h. Formation of the corresponding *anti*-Markovnikov-type alkylated products (**3-4ab**, **3-4ac**, **3-4ae**, **3-4ag**, **3-4ah**, **3-4ak**) was also spectroscopically confirmed for several 1,4-dihydropyridine derivatives (**3-2b**, **3-2c**, **3-2e**, **3-2g**, **3-2h**, **3-2k**) as mixture of *E*- and *Z*- isomers, although substituted 1,2-diphenylethanes (**3-5b**, **3-5c**, **3-5e**, **3-5g**, **3-5h**, **3-5k**), formed via the dimerization of substituted benzyl radicals originated from 1,4-dihydropyridine derivatives, were also obtained as the major contaminant by-products in substantial amounts, thus isolated yields of *anti*-Markovnikov-type products could not be determined. It must be noted that *anti*-Markovnikov-type arylalkenes with secondary alkyl groups have been also reported to be obtained by the photoinduced deaminative hydroalkylation of terminal arylalkynes with Katritzky alkylpyridinium salts without the addition of transition metal catalysts other than iridium-based photoredox catalyst.¹⁷ Indeed, **3-4al** and **3-4am** were obtained but in lower yields in the absence of NiCl₂·6H₂O. On the other hand, reactions of **3-1a** with 1,4-dihydropyridine derivative with long-chain primary alkyl (**3-2n**, **3-2o**), α -arylalkyl (**3-2p**), unsymmetrical secondary alkyl (**3-2q**), or tertiary alkyl group (**3-2s**) afforded only a trace amount of the corresponding alkylated alkene (**3-4an**–**3-4as**), similarly to that obtained for the Markovnikov-type hydroalkylation reaction to afford **3-3an**–**3-3as** (Scheme 3-2). In addition, *anti*-Markovnikov-type product containing alkoxyethyl or 3-pyridylmethyl group was not obtained from the reaction of **3-1a** with **3-2k** or **3-2s** (Scheme 3-3). Next, *anti*-Markovnikov-type hydroalkylation reactions of various terminal alkynes with **3-2a** were investigated (Scheme 3-3). Ethynylbenzene derivatives with either electron-donating or electron-withdrawing substituents introduced at the 4-position of the benzene moiety (**3-1b**, **3-1c**, **3-1f**, **3-1g**) or at the 2-position (**3-1k**: 2-CF₃) were found to be alkylated to afford the corresponding *anti*-Markovnikov-type products (**3-4ba**, **3-4ca**, **3-4fa**, **3-4ga**, **3-4ka**) as mixtures of *E*- and *Z*- isomers (49/51 < *E/Z* < 73/27) in good to high yields, while introduction of benzaldehyde was not successful (**3-4ha**) in contrast to that obtained for Markovnikov-type hydroalkylation (**3-3ha**) (Scheme 3-2).

Scheme 3-2. Scope of Markovnikov-type Hydroalkylation^a

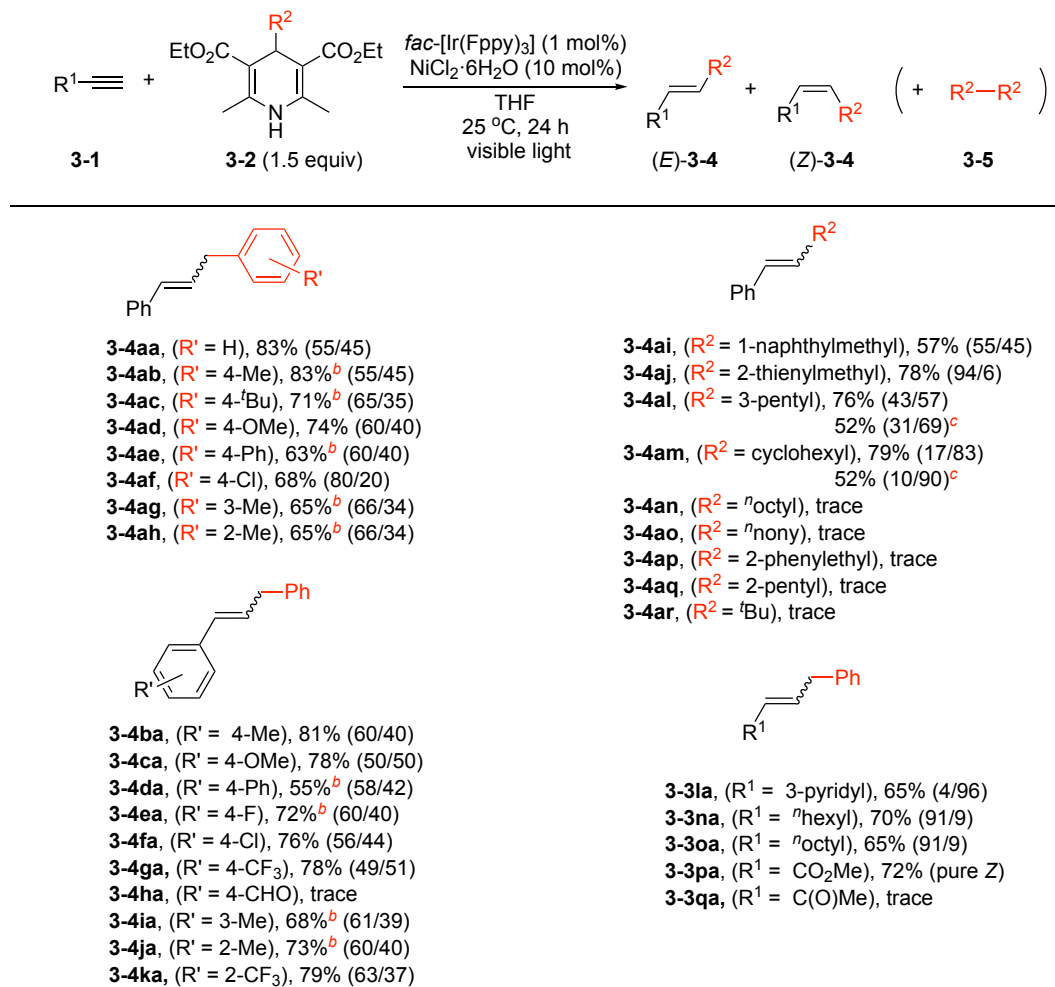


^a Isolated yield of **3-3**. No desired product for the reaction of **3-1a** with **3-2s** ($R^2 = 3\text{-pyCH}_2$).

Formation of the corresponding *anti*-Markovnikov-type alkylated products (**3-4da**, **3-4ea**, **3-4ia**, **3-4ja**) was also spectroscopically confirmed for several substituted ethynylbenzenes (**3-1d**, **3-1e**, **3-1i**, **3-1j**), although 1,2-diphenylethane (**3-5a**), formed via the dimerization of benzyl radical from **3-2a**, was also obtained as the major contaminant by-product in substantial amounts, thus isolated yields of the *anti*-Markovnikov-type products could not be determined. Pyridine could be introduced by the reaction of **3-1l** with **3-2a** afford the corresponding alkyne (**3-4la**) in 65% yield with *Z*-isomer being the major product (*E/Z* = 4/96) (Scheme 3-3), whereas thiophene could not be introduced by the reaction of **3-1m** with **3-2a**. As the author's group has previously observed, aryl-substituted alkenes are known to undergo *E* to *Z* isomerization in the presence of photoredox catalysts, thus longer irradiation time can contribute to the increase in the amounts of *Z*-isomers.^{36,45} Such *E* to *Z* isomerization does not occur for alkyl-substituted alkenes. Indeed, alkylacetylenes (**3-1n**, **3-1o**) reacted with **3-2a** to afford the corresponding alkylated products (**3-4ln**, **3-4mo**) in good yields with *E*-isomers being the major products (*E/Z* = 91/9). On the contrary to alkylacetylenes, reaction of **3-1p** with **3-2a** solely afforded methyl (*Z*)-4-phenylbut-2-enoate ((*Z*)-**3-4pa**) in 72% yield, where photochemical *E* to *Z* isomerization has been well known for α,β -unsaturated esters such as crotonate and maleate.⁴⁹ On the other

hand, only a trace amount of 5-phenylpent-3-en-2-one (**3-4qa**) was obtained from the reaction of **3-1q** with **3-2a** in contrast to the Markovnikov-type hydroalkylation to afford **3-3qa**.

Scheme 3-3. Scope of *anti*-Markovnikov-type Hydroalkylation^a

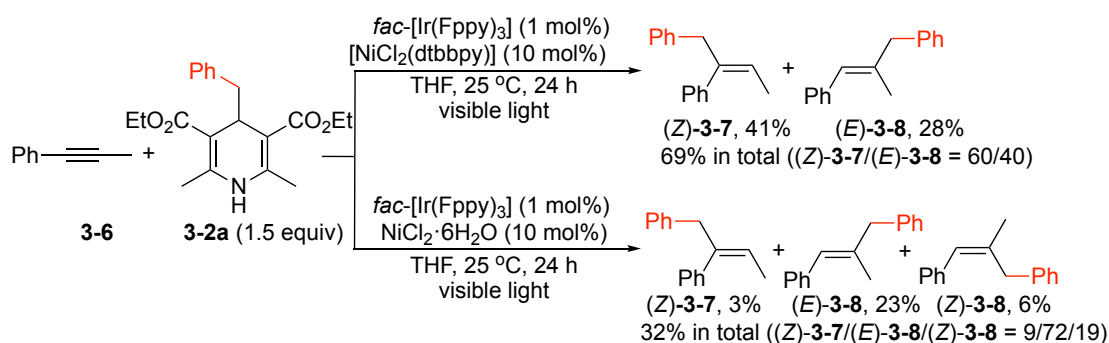


^a Isolated yield of **3-4** with *E/Z* ratio in parentheses determined by quantitative measurement of GC-MS for crude mixture. No desired product for the reaction of **3-1a** with **3-2k** ($\text{R}^2 = \text{PhCH}_2\text{OCH}_2$) or **3-2s** ($\text{R}^2 = 3\text{-pyCH}_2$), or **3-1m** with **3-2a**. ^b GC-MS yield. Isolation of the products unsuccessful because of formation of substantial amounts of the by-product **3-5**. ^c In the absence of $\text{NiCl}_2 \cdot 6\text{H}_2\text{O}$.

Hydroalkylation of internal alkyne was further examined for the reaction of prop-1-yn-1-ylbenzene (**3-6**) with **3-2a** under the optimized Markovnikov-type and *anti*-Markovnikov-type reaction conditions (Scheme 3-4). When $[\text{NiCl}_2(\text{dtbbpy})]$ was used as a catalyst, the alkylated products were obtained in 69% NMR yields as a mixture of (*Z*)-but-2-ene-1,2-diyl dibenzene ((*Z*)-**3-7**) and (*E*)-(2-methylprop-1-ene-1,3-diyl) dibenzene ((*E*)-**3-8**) in a ratio of 60:40, where alkylation took place preferentially at the carbon atom connected to phenyl group rather than that connected to methyl group. Similar hydroalkylation of **3-6** with almost the same regioselectivity (2:1) was reported by Wu and co-workers who used $[\text{Ir}\{\text{dF}(\text{CF}_3\text{ppy})_2(\text{dtbbpy})\}]\text{PF}_6$ and anhydrous NiCl_2 with dtbbpy as catalysts, although available alkylation reagents are limited to specific ethers and amides, requiring elevated temperatures.⁶ Contrariwise, (*E*)-**3-8**

became the major product when $\text{NiCl}_2 \cdot 6\text{H}_2\text{O}$ was used as a catalyst, with (Z)-**3-7** and (Z)-**3-8** obtained as minor products. Similar hydroalkylation of **3-6** to afford alkenes with the carbon attached to methyl group preferentially alkylated in the presence of nickel catalysts but without photoirradiation has been reported by several groups,⁵ where alkyl halides, carboxylates, Katritzky salts, or cycloketone oxime esters are used as alkylation reagents.

Scheme 3-4. Hydroalkylation of Internal Alkyne



In order to get further mechanistic information, the author next investigated the Markovnikov-type and *anti*-Markovnikov-type hydroalkylation reactions of **3-1a** with **3-2a** under the optimized reaction conditions but in the presence of 1.5 equiv of (2,2,6,6-tetramethylpiperidin-1-yl)oxyl (TEMPO) as a radical inhibitor. As a result, formation of Markovnikov or *anti*-Markovnikov-type desired hydroalkylation product **3-3aa** or **3-4aa** was perfectly inhibited. On the other hand, 1-(benzyloxy)-2,2,6,6-tetramethylpiperidine (**3-9a**),⁵⁰ the TEMPO-trapped benzyl adduct, was obtained in 41% or 47% yield in the Markovnikov or *anti*-Markovnikov-type optimized reaction conditions, respectively (Figure 3-1a). The experimental results demonstrate that the formation of a benzyl radical as a reactive intermediate is involved in the main catalytic reaction pathway.^{7,10,11,13,15,31,33,35,37–39,51} Subsequently, Stern–Volmer analyses for emission quenching of $\text{fac}[\text{Ir}(\text{Fppy})_3]$ by **3-1a** or **3-2a** was performed in THF, where the quenching rate constants were determined to be $k_{3-1a} = (7.8 \pm 0.4) \times 10^7 \text{ M}^{-1} \text{ s}^{-1}$ and $k_{3-2a} = (1.81 \pm 0.04) \times 10^8 \text{ M}^{-1} \text{ s}^{-1}$, respectively, based on the slope obtained by the Stern–Volmer plot⁵² and the excited-state lifetime of $\text{fac}[\text{Ir}(\text{Fppy})_3]$ at $\tau = 1.6 \mu\text{s}$,⁴⁷ indicating that the quenching of photoexcited $\text{fac}[\text{Ir}(\text{Fppy})_3]$ by **3-2a** can occur twice as fast as that by **3-1a**. Here, 1st reduction potential of $\text{fac}[\text{Ir}(\text{Fppy})_3]$ in THF was measured to be -1.54 V vs $\text{FeCp}_2^{+/0}$ ($\text{Cp} = \eta^5\text{-C}_5\text{H}_5$) (Figure 3-3c), corresponding to the estimated redox potential of $\text{fac}[\text{Ir}(\text{Fppy})_3]^*/\text{fac}[\text{Ir}(\text{Fppy})_3]^-$ at $+0.67 \text{ V}$ vs $\text{FeCp}_2^{+/0}$ by using the reported optical gap of $\text{fac}[\text{Ir}(\text{Fppy})_3]$.⁴⁶ Cyclic voltammogram of **3-2a** showed irreversible oxidation wave at $+0.63 \text{ V}$ vs $\text{FeCp}_2^{+/0}$ (Figure 3-3a), considerably lower than that measured in MeCN,^{38,53} indicating that photoexcited $\text{fac}[\text{Ir}(\text{Fppy})_3]$ can oxidize **3-2a** to afford the radical cation **3-2a**^{•+} via a SET process, followed by the cleavage of C–C bond to afford the benzyl radical and an aromatized pyridinium cation (Figure 1a). On the other hand, oxidation of **3-1a**⁵⁴ was found to be difficult in THF (Figure 3-3b), whereas oxidation of **3-1a** was observed at $+2.06 \text{ V}$ vs $\text{FeCp}_2^{+/0}$ in MeCN,⁵⁵ and emission quenching of Ir catalysts by **3-1a** itself was not observed in

DMF.⁵⁶ These results have demonstrated that oxidation of **3-1a** by *fac*-[Ir(Fppy)₃] via a SET process does not occur, but is only sensitized to the triplet state by *fac*-[Ir(Fppy)₃] to afford triplet **3-1a*** (Figure 3-1b).^{55,56}

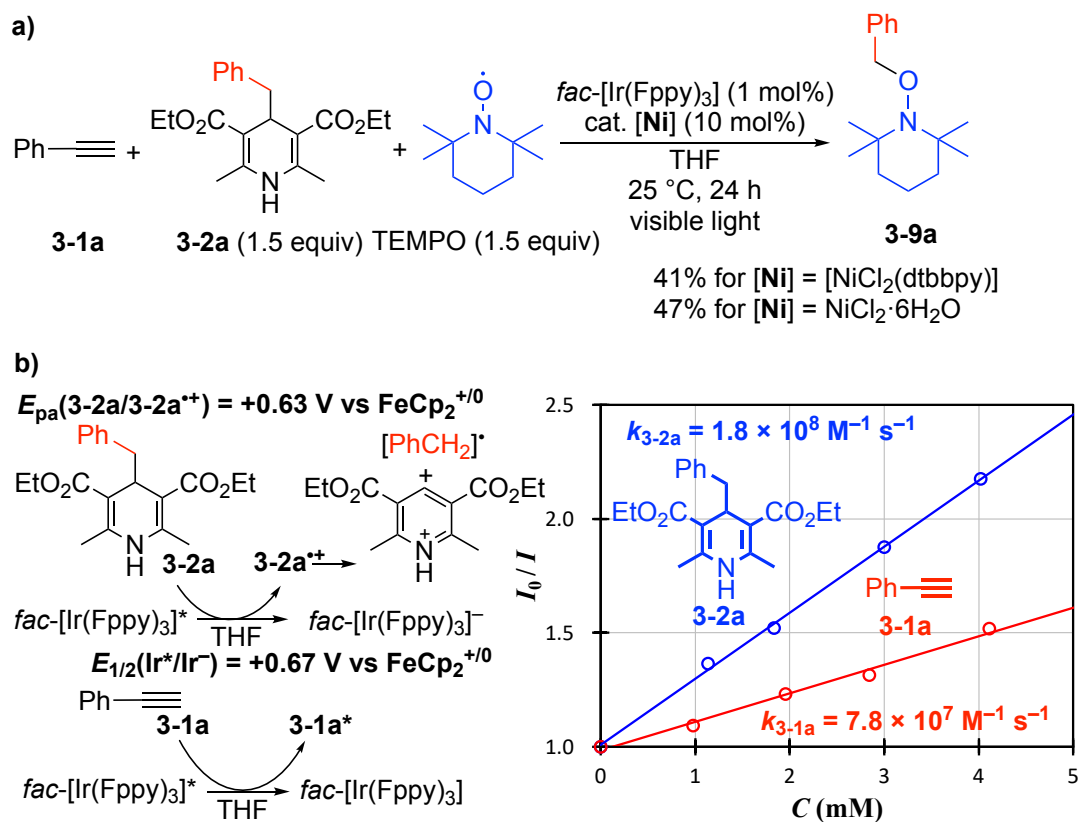


Figure 3-1. Mechanistic studies on the Markovnikov-type and *anti*-Markovnikov-type hydroalkylation of **3-1a** with **3-2a**. (a) Reactions in the presence of TEMPO. (b) Determination of quenching constants by Stern–Volmer plot.

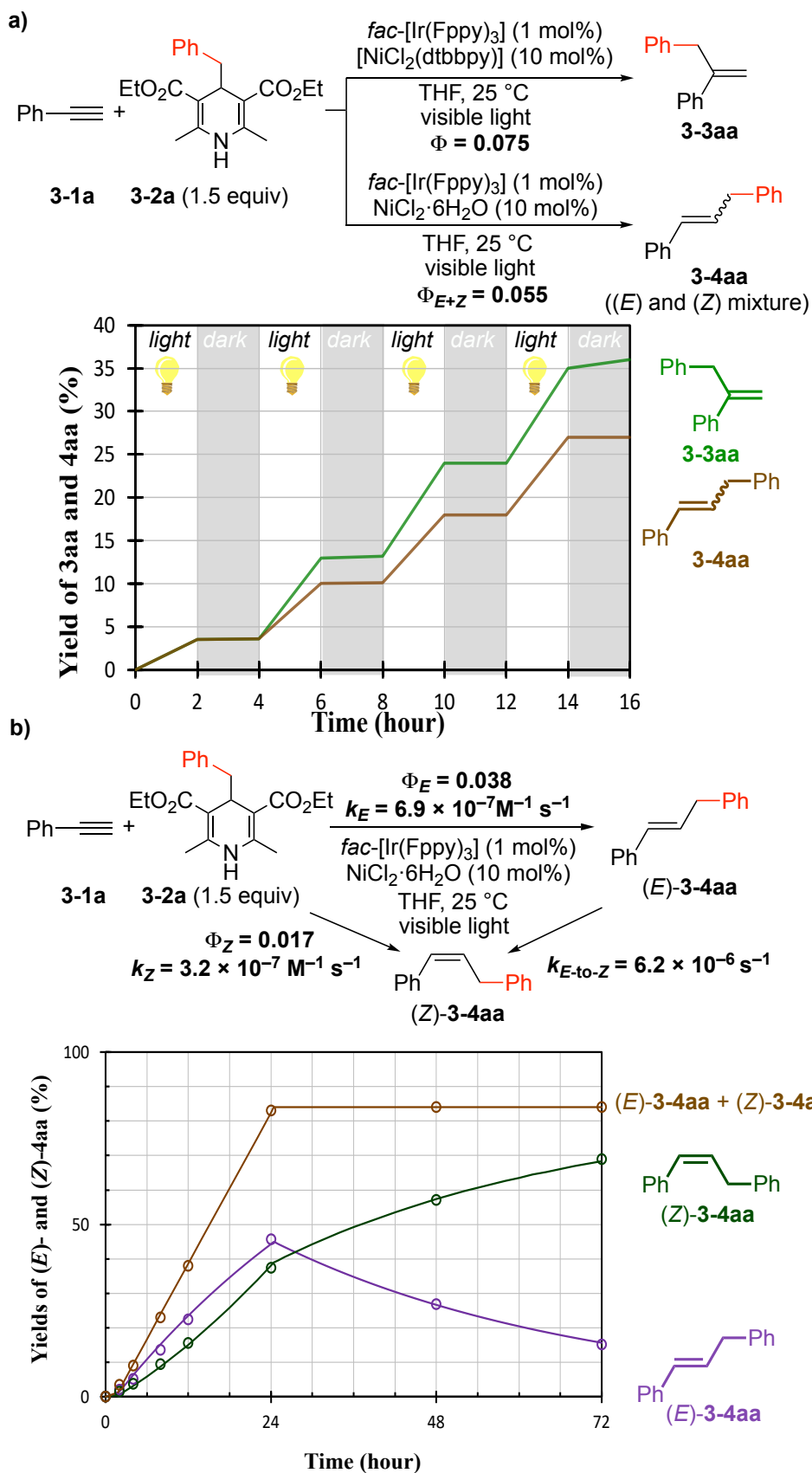


Figure 3-2. Reaction profiles for the Markovnikov-type and *anti*-Markovnikov-type hydroalkylation of **3-1a** with **3-2a**. (a) Reaction profiles during the light-on and -off sequences. (b) Reaction profile for the *anti*-Markovnikov-type hydroalkylation.

Additionally, light on/off experiments were performed for both Markovnikov-type and *anti*-Markovnikov-type hydroalkylation of **3-1a** with **3-2a** to afford **3-3aa** and a mixture of (*E*)-**3-4aa** and (*Z*)-**3-4aa**, respectively, under the typical catalytic reaction conditions. As shown in Figure 3-2a, both Markovnikov-type and *anti*-Markovnikov-type hydroalkylation reactions did not proceed in dark, confirming the necessity of continuous visible light irradiation and disconfirming the possibility of chain propagation as the main reaction pathway. Quantum yields of hydroalkylation reactions of **3-1a** with **3-2a** were further measured by using $\text{K}_3[\text{Fe}(\text{C}_2\text{O}_4)_3]$ as a chemical actinometer,⁵⁷ where the formation of **3-3aa** or mixtures of (*E*)-**3-4aa** and (*Z*)-**3-4aa** in the Markovnikov or *anti*-Markovnikov reaction conditions typical except for using Hg lamp filtered at 440 nm instead of LED light, respectively, was found to follow zeroth order kinetics with quantum yields at $\Phi = 0.075 \pm 0.002$ for the formation of **3-3aa** or $\Phi_{E+Z} = 0.055 \pm 0.002$ for the formation of mixtures of (*E*)-**3-4aa** and (*Z*)-**3-4aa** (Figure 3-2a). Both the light on/off experiment as well as the quantum yield measurement have clarified that the rate-determining step of the catalytic formation of **3-3aa** or **3-4aa** proceeds not via a radical chain process but rather via sequential redox pathways,⁵⁸ where alkyl radicals are mainly generated by the SET process between 4-alkyl-1,4-dihydropyridines and an excited-state photoredox catalyst.^{31,35–37,59,60}

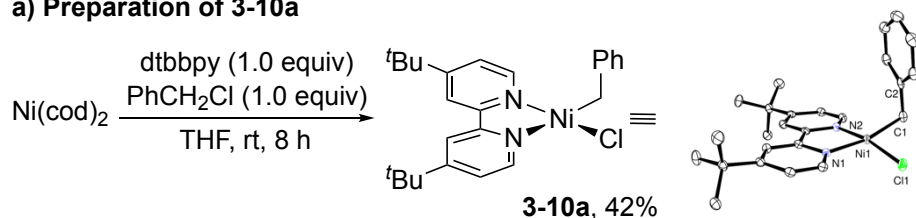
In order to get more information on the reaction pathway for the *E* to *Z* isomerization which occurs for aryl-substituted alkenes^{36,45} in the *anti*-Markovnikov-type reaction conditions, a time course study was further investigated. As shown in Figure 3-2b, formation of both (*E*)-**3-4aa** and (*Z*)-**3-4aa** follow pseudo zeroth order kinetics for the first 24 hours with *E/Z* ratio kept at $55/45 < E/Z < 59/41$. After 24 h, further hydroalkylation does not occur, because **3-2a** is perfectly consumed for the formation of mixtures of (*E*)-**3-4aa** and (*Z*)-**3-4aa** as well as the formation of 1,2-diphenylethane, a side product directly formed by the dimerization of benzyl radical.³² Instead, photoinduced isomerization of (*E*)-**3-4aa** into (*Z*)-**3-4aa** that follows typical first-order kinetics dependent on the concentration of (*E*)-**3-4aa** with the calculated reaction rate at $k_{E \rightarrow Z} = (6.2 \pm 0.3) \times 10^{-6} \text{ s}^{-1}$ is observed without change in total amounts of (*E*)-**3-4aa** into (*Z*)-**3-4aa**.^{36,45} By assuming that *E* to *Z* isomerization always occurs with the same reaction rate, zeroth order reaction rates for the formation of (*E*)-**3-4aa** and (*Z*)-**3-4aa** from the reaction of **3-1a** with **3-2a** under the typical *anti*-Markovnikov-type reaction conditions are calculated to be $k_E = (6.9 \pm 0.2) \times 10^{-7} \text{ M}^{-1} \text{ s}^{-1}$ and $k_Z = (3.2 \pm 0.1) \times 10^{-7} \text{ M}^{-1} \text{ s}^{-1}$, respectively, with an induction period of 1.4 h. Based on these two reaction rates, quantum yield for the formation of (*E*)-**3-4aa** and (*Z*)-**3-4aa** from the reaction of **3-1a** with **3-2a** at $\Phi_{E+Z} = 0.055 \pm 0.002$ can now be divided as $\Phi_E = 0.038 \pm 0.003$ and $\Phi_Z = 0.017 \pm 0.002$, respectively. These results reveal that the stereoselectivity between *E*- and *Z*-isomers is not perfectly controlled, but the formation of (*E*)-**3-4aa** from the reaction of **3-1a** with is preferred more than twice as much as the formation of (*Z*)-**3-4aa** under the typical *anti*-Markovnikov-type reaction conditions (Figure 3-2b). It must be cautioned such *E* to *Z* isomerization occurs only for aryl-substituted alkenes, whereas alkyl substituted alkenes do not isomerize under this photochemical reaction conditions.^{36,45} Independently, isomerization of (*E*)-**3-4aa** into (*Z*)-**3-4aa** was examined under several reaction conditions, which confirmed that such

E-to-*Z* isomerization required both the photoredox catalyst and visible light irradiation, and (*E*)-**3-4aa** itself was not directly excited toward isomerization by the visible light, but Ni catalyst did not mediate the *E*-to-*Z* isomerization even under visible light irradiation (Table 3-2).

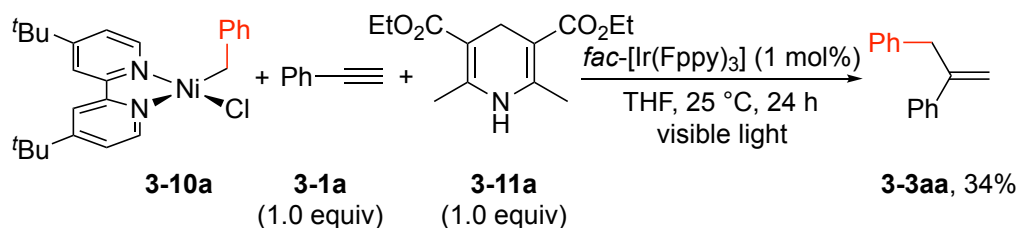
To obtain more information on the Markovnikov-type regioselectivity, the Ni(II) benzyl complex [NiCl(CH₂Ph)(dtbbpy)] (**3-10a**), a possible reaction intermediate in the Markovnikov-type catalysis, was prepared by the oxidative addition of PhCH₂Cl to [Ni(cod)₂], similarly to the method described for the preparation of [NiCl(CH₂Ph)(bpy)],⁶¹ with the molecular structure of **3-10a** characterized by a single crystal X-ray diffraction analysis as shown in Scheme 3-5a. The stoichiometric reaction of **3-10a** with **3-1a** was further examined where addition of *fac*-[Ir(Fppy)₃] and irradiation of visible light were necessary to reduce **3-10a**, and addition of nonsubstituted 1,4-dihydropyridine **3-11a** was also necessary as a proton source, to afford the Markovnikov-type product **3-3aa** in 34% yield (Scheme 3-5b). This clearly denotes that **3-10a** works as a key reactive intermediate in the Markovnikov-type hydroalkylation of **3-1a** with **3-2a** to afford **3-3aa**.

Scheme 3-5. Preparation and Stoichiometric Reaction of Ni(II) Benzyl Complex

a) Preparation of 3-10a



b) Stoichiometric reaction of 3-10a to afford 3-3aa



Based on our mechanism studies and recent reports by Rueping and other groups,¹⁶ plausible reaction pathways for the ligand-controlled regioselective cooperative photoredox- and nickel-catalyzed hydroalkylation of alkynes with 4-alkyl-1,4-dihydropyridines can be drawn as shown in Scheme 3-6, consisting of photoredox and nickel catalytic cycles. In the photoredox cycle, single electron transfer between a photoexcited iridium catalyst and 4-alkyl-dihydropyridine (**3-2**) occurs to afford the reduced iridium catalyst, an alkyl radical, and an aromatized pyridine derivative via C–C bond cleavage. In the nickel cycle, an in situ-generated Ni(I) species (**3-A**) captures the alkyl radical to generate the alkyl-Ni(II) complex (**3-10**), which is reduced by the reduced iridium catalyst to afford the Ni(I) alkyl complex (**3-B**). Then, coordination of an alkyne (**3-1**) occurs to this Ni(I) alkyl complex to afford the Ni(I) π -

alkyne alkyl complex (**3-C**). Further migratory insertion of the coordinated alkyne differs based on the size of the coordination ligand bound to the nickel catalyst. In the Markovnikov-type pathway, a bulky ligand such as dtbbpy inhibits the formation of *anti*-Markovnikov-type insertion, leading to the formation of Markovnikov-type intermediate (**3-D**). On the other hand, small ligands such as aqua and thf do not inhibit the *anti*-Markovnikov-type insertion, leading to the formation of *anti*-Markovnikov-type intermediate (**3-E**).⁶² Finally, protodemetalation occurs to liberate the Markovnikov-type (**3-3**) or the *anti*-Markovnikov-type product (**3-4**). The major product obtained for the *anti*-Markovnikov-type hydroalkylation is *E*-isomer, but *Z*-isomer is also formable. However, further *E* to *Z* isomerization occurs via energy transfer process with visible light for aryl-substituted alkenes.^{36,45}

The reaction scheme illustrates the synthesis of (E)-alkenes through a nickel-catalyzed E to Z isomerization. The process begins with the photocatalytic generation of an alkyl radical $\text{R}^1\cdot$ from a photocatalyst (3-2) using visible light. This radical then reacts with a nickel complex (3-10) to form a nickel species (3-A). The nickel species (3-A) undergoes a Markovnikov-type addition with an alkyne (3-1) to form a nickel hydride intermediate (3-C). This intermediate (3-C) can follow two pathways: a Markovnikov-type addition to form a nickel species (3-D) or an anti-Markovnikov-type addition to form a nickel species (3-E). The nickel species (3-E) then undergoes E to Z isomerization to form the (Z)-alkene (Z)-3-4. Finally, the (Z)-alkene (Z)-3-4 is irradiated with visible light to produce the (E)-alkene (E)-3-4. The photocatalytic cycle involves Ir(III) and Ir(IV) species, and the nickel cycle involves Ni(II) and Ni(I) species. The ligand L is defined as dtbbpy for the Markovnikov-type reaction and thf or H₂O for the anti-Markovnikov-type reaction.

Photoredox Catalytic Cycle:

- Photocatalyst (3-2) is excited by visible light to form $[\text{Ir}]^*$.
- $[\text{Ir}]^*$ undergoes SET (Single Electron Transfer) with the alkyl radical $\text{R}^1\cdot$ to form $[\text{Ir}]^+$ and the alkyl radical $\text{R}^1\cdot$.
- $[\text{Ir}]^+$ is reduced back to $[\text{Ir}]$ by the nickel complex (3-10) to form $[\text{Ir}]^+$ and the nickel species (3-A).

Nickel Catalytic Cycle:

- Nickel complex (3-10) reacts with the alkyl radical $\text{R}^1\cdot$ to form the nickel species (3-A).
- Nickel species (3-A) reacts with the alkyne (3-1) to form the nickel hydride intermediate (3-C).
- Nickel hydride intermediate (3-C) can follow two pathways:
 - Markovnikov-type:** Formation of nickel species (3-D) via addition of H^+ and Cl^- .
 - anti-Markovnikov-type:** Formation of nickel species (3-E) via addition of H^+ and Cl^- .
- Nickel species (3-E) undergoes E to Z isomerization to form the (Z)-alkene (Z)-3-4.
- (Z)-3-4 is irradiated with visible light to form the (E)-alkene (E)-3-4.

Legend:

- $L_n = \text{dtbbpy}$ (green text) for Markovnikov-type.
- $L = \text{thf or H}_2\text{O}$ (purple text) for anti-Markovnikov-type.

3.3. Conclusion for Chapter 3

The author has succeeded in the cooperative nickel- and photoredox-catalyzed hydroalkylation reactions of alkynes with 4-alkyl-1,4-dihydropyridines at room temperature under the irradiation of visible light, where Markovnikov or *anti*-Markovnikov regioselectivity of the products are controlled by the coordination ligands bound to nickel species. Here, wide range of alkyl groups can be introduced to alkyne to afford alkylated products, which have not been achieved in the previously reported catalytic hydroalkylation reactions.^{6,7,9–11,13–17,19} In addition to terminal alkynes, internal alkyne can also be converted into the desired product. The author believes these works described herein will expand the utility of 4-alkyl-1,4-dihydropyridine skeletons as mild formal alkylation reagents in combination of photoredox and cross-coupling catalysts to use for further organic syntheses under mild reaction conditions.

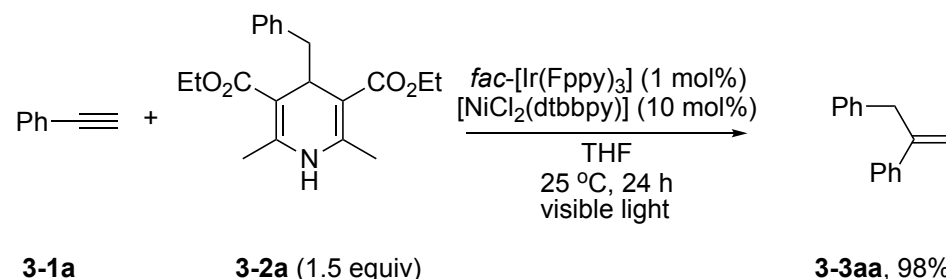
3.4. Experimental Section

3.4.1. General Methods

All reactions were carried out under dry nitrogen atmosphere by using standard Schlenk techniques unless otherwise stated. Starting materials including **3-2a**,⁶³ **3-2b**,⁶³ **3-2c**,³¹ **3-2d**,⁶³ **3-2e**,³⁵ **3-2f**,⁶³ **3-2g**,³¹ **3-2h**,³¹ **3-2i**,³⁶ **3-2j**,⁴⁰ **3-2k**,^{35,64} **3-2l**,⁶⁴ **3-2m**,⁶⁵ **3-2n**,⁶⁶ **3-2o**,⁶³ **3-2p**,⁴⁰ **3-2q**,⁶³ **3-2r**,⁴¹ and **3-2s**⁶⁷ were prepared according to the literature procedures. Other reagents such as terminal and internal alkynes (**3-1a–q** and **3-5**), *fac*-[Ir(ppy)₃], [Ir{dF(CF₃)ppy}₂(dtbbpy)]BF₄, *fac*-[Ir(Fppy)₃], anhydrous NiCl₂, [NiCl₂(PPh₃)₂], [NiCl₂(dppe)], [NiCl₂(dtbbpy)], [Ni(acac)₂], NiBr₂·diglyme, [NiCl₂(dme)], NiCl₂·6H₂O, TEMPO, starting materials for the preparation of **3-2a–s** and **3-10a**, reagents for measurements, and solvents were purchased from commercial sources. THF, dichloromethane, diethyl ether, and *n*-hexane were purified by passing through a purification system (Glass Contour) and were degassed before use. Other solvents were dried by general methods and degassed before use. Flash column chromatography was carried out on a Yamazen YFLC-AI-580 system. Gas chromatography–mass spectroscopy (GC-MS) was performed on a Shimadzu GCMS-QP2010 PLUS instrument. *E/Z* ratios in crude products were determined by quantitative measurements of GC-MS with supplementary support by ¹H NMR spectra for identification. X-ray analysis was performed by a Rigaku XtaLAB Synergy-S diffractometer. Photoluminescence spectra were measured on a Shimadzu RF-5300PC spectrophotometer. High-resolution FAB mass spectra were measured on a JEOL JMS-700 mass spectrometer. ¹H NMR (400 MHz), ¹³C{¹H} NMR (100 MHz), and ¹⁹F NMR (376 MHz, referenced to CF₃C₆H₅ in CDCl₃ at δ –64.0) spectra were measured in CDCl₃ or CD₂Cl₂ on a JEOL ECS-400 spectrometer with δ values in ¹H and ¹³C{¹H} NMR calibrated by using residual peaks of CHCl₃ (¹H: 7.26; ¹³C: 77.0) or CDHCl₂ (¹H, 5.32), respectively.

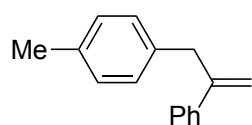
3.4.2. General Procedure for the Preparation of Markovnikov-type Products (Taking prop-2-ene-1,2-diylidibenzene (**3aa**) as an Example)

Scheme 3-7. Preparation of Markovnikov-type Products **3-3**



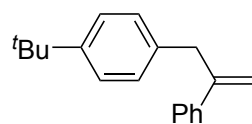
In a 20 mL Schlenk flask were placed **3-1a** (25.5 mg, 0.250 mmol), **3-2a** (128.8 mg, 0.375 mmol), *fac*-[Ir(Fppy)₃] (1.7 mg, 0.0022 mmol), and [NiCl₂(dtbbpy)] (10.0 mg, 0.025 mmol) under N₂, where THF (2.5 mL) was added at room temperature. The reaction flask was placed in an As One LTB-125 constant low temperature water bath set at 25 °C and was illuminated from the bottom of the bath with an Aitech System

TMN100×120–22WD 12 W white LED lamp (400 nm to 750 nm) at a distance of approximately 2 cm from the light source for 24 h. The volatiles were removed *in vacuo*, and the residue was purified by column chromatography (SiO₂) with *n*-hexane as an eluent to afford prop-2-ene-1,2-diylidibenzene (**3-3aa**)¹⁰ as a colorless oil (47.6 mg, 0.245 mmol, 98% isolated yield based on the amount of **3-1a**). ¹H NMR (400 MHz, CDCl₃, δ): 7.44 (d of pseudo t, *J* = 6.8, 1.6 Hz, 2H, *o*-H of Ph), 7.32–7.15 (m, 8H, aromatic H of benzyl and *m*- and *p*-H of Ph), 5.50, 5.02 (both d, *J* = 1.4 Hz, 1H each, CH₂=), 3.84 (s, 2H, CH₂). ¹³C{¹H} NMR (100 MHz, CDCl₃, δ): 146.9 (C=), 140.8 (*ipso*-C of Ph), 139.5 (*ipso*-C of benzyl), 128.9 (*o*-C of benzyl), 128.3 (*m*-C of benzyl), 128.2, (*m*-C of Ph), 127.4 (*p*-C of Ph), 126.1 (*o*-C of Ph), 126.1 (*p*-C of benzyl), 114.6 (CH₂=), 41.6 (CH₂).



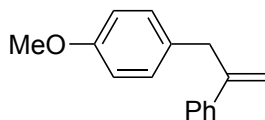
3-3ab

1-Methyl-4-(2-phenylallyl)benzene (3-3ab).⁶⁸ A colorless oil (47.9 mg, 0.230 mmol, 92% isolated yield based on the amount of **3-1a**). ¹H NMR (400 MHz, CDCl₃, δ): 7.46 (d of pseudo t, *J* = 6.8, 1.7 Hz, 2H, *o*-H of Ph), 7.33–7.27 (pseudo tt, *J* = 7.5, 1.8 Hz, 2H, *m*-H of Ph), 7.25 (t of pseudo t, *J* = 7.1, 1.9 Hz, 1H, *p*-H of Ph), 7.14, 7.09 (both d, *J* = 8.0 Hz, 2H each, *o*- and *m*-H of C₆H₄), 5.50, 5.04 (both d, *J* = 1.2 Hz, 1H each, CH₂=), 3.82 (s, 2H, CH₂), 2.32 (s, 3H, Me). ¹³C{¹H} NMR (100 MHz, CDCl₃, δ): 147.1 (C=), 140.8 (*ipso*-C of Ph), 136.4, 135.5 (*ipso*- and *p*-C of C₆H₄), 129.0, 128.8 (*o*- and *m*-C of C₆H₄), 128.2 (*m*-C of Ph), 127.4 (*p*-C of Ph), 126.1 (*o*-C of Ph), 114.4 (CH₂=), 41.1 (CH₂), 21.0 (Me).



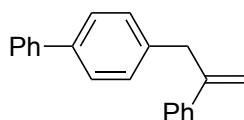
3-3ac

1-(tert-Butyl)-4-(2-phenylallyl)benzene (3-3ac).⁶⁹ A colorless oil (58.8 mg, 0.235 mmol, 94% isolated yield based on the amount of **3-1a**). ¹H NMR (400 MHz, CDCl₃, δ): 7.48 (d of pseudo t, *J* = 6.7, 1.6 Hz, 2H, *o*-H of Ph), 7.34–7.29 (m, 4H, *m*-H of C₆H₄ and *m*-H of Ph), 7.25 (t of pseudo t, *J* = 7.4, 1.8 Hz, 1H, *p*-H of Ph), 7.18 (d, *J* = 8.4 Hz, 2H, *o*-H of C₆H₄), 5.52, 5.03 (both d, *J* = 1.2 Hz, 1H each, CH₂=), 5.03 (s, 1H), 3.83 (s, 2H, CH₂), 1.31 (s, 9H, tBu). ¹³C{¹H} NMR (100 MHz, CDCl₃, δ): 148.8 (*p*-C of C₆H₄), 146.9 (C=), 140.9 (*ipso*-C of Ph), 136.4 (*ipso*-C of C₆H₄), 128.5 (*o*-C of C₆H₄), 128.2 (*m*-C of Ph), 127.4 (*p*-C of Ph), 126.1 (*o*-C of Ph), 125.2 (*m*-C of C₆H₄), 114.5 (CH₂=), 40.9 (CH₂), 34.3 (CMe₃), 31.4 (Me).



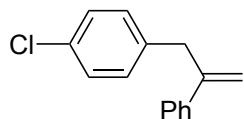
3-3ad

1-Methoxy-4-(2-phenylallyl)benzene (3-3ad).⁶⁹ A colorless oil (53.8 mg, 0.240 mmol, 96% isolated yield based on the amount of **3-1a**). ¹H NMR (400 MHz, CDCl₃, δ): 7.43 (d of pseudo t, *J* = 6.5, 1.6 Hz, 2H, *o*-H of Ph), 7.29 (pseudo tt, *J* = 7.4, 1.5 Hz, 2H, *m*-H of Ph), 7.23 (t of pseudo t, *J* = 7.1, 1.4 Hz, 1H, *p*-H of Ph), 7.14 (d, *J* = 8.6 Hz, 2H, *o*-H of C₆H₄), 6.81 (d, *J* = 8.6 Hz, 2H, *m*-H of C₆H₄), 5.47, 5.01 (both d, *J* = 1.4 Hz, 1H each, CH₂=), 3.78 (s, 5H, CH₂ and Me, overlapping). ¹³C{¹H} NMR (100 MHz, CDCl₃, δ): 157.9 (*p*-C of C₆H₄), 147.3 (C=), 140.8 (*ipso*-C of Ph), 131.5 (*ipso*-C of C₆H₄), 129.8 (*o*-C of C₆H₄), 128.2 (*m*-C of Ph), 127.4 (*p*-C of Ph), 126.1 (*o*-C of Ph), 114.3 (CH₂=), 113.7 (*m*-C of C₆H₄), 55.2 (Me), 40.7 (CH₂).



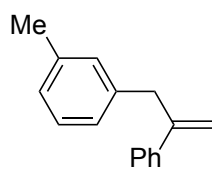
3-3ae

4-(2-Phenylallyl)-1,1'-biphenyl (3-3ae).⁶⁹ A colorless oil (56.1 mg, 0.207 mmol, 83% isolated yield based on the amount of **3-1a**). ¹H NMR (400 MHz, CDCl₃, δ): 7.58 (d, *J* = 7.8 Hz, 2H, 2',6'-H of biphenyl), 7.51 (d, *J* = 8.0 Hz, 2H, 3,5-H of biphenyl), 7.58 (d, *J* = 7.6 Hz, 2H, *o*-H of Ph), 7.43 (t, *J* = 7.8 Hz, 2H, 3',5'-H of biphenyl), 7.35–7.29 (m, 5H, 2,6- and 4'-H of biphenyl and *m*-H of Ph), 7.26 (t, *J* = 7.2 Hz, 1H, *p*-H of Ph), 5.54, 5.09 (both d, *J* = 1.6 Hz, 1H each, CH₂=), 3.90 (s, 2H, CH₂). ¹³C{¹H} NMR (100 MHz, CDCl₃, δ): 146.8 (C=), 141.0 (1'-C of biphenyl), 140.7 (*ipso*-C of Ph), 139.0, 138.6 (1- and 4-C of biphenyl), 129.3, 128.7 (2,6- and 3',5'-C of biphenyl), 128.3 (*m*-C of Ph), 127.5 (*p*-C of Ph), 127.1, 127.0 (3,5- and 2',6'-C of biphenyl), 127.0 (4'-C of biphenyl), 126.1 (*o*-C of Ph), 114.7 (CH₂=), 41.2 (CH₂).



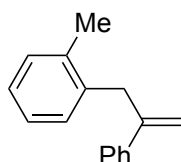
3-3af

1-Chloro-4-(2-phenylallyl)benzene (3-3af).⁶⁹ A colorless oil (46.3 mg, 0.202 mmol, 81% isolated yield based on the amount of **3-1a**). ¹H NMR (400 MHz, CDCl₃, δ): 7.41 (d of pseudo t, *J* = 6.8, 2.0 Hz, 2H, *o*-H of Ph), 7.30 (pseudo tt, *J* = 7.0, 1.6 Hz, 2H, *m*-H of Ph), 7.29–7.21 (m, 3H, *o*-H of C₆H₄ and *p*-H of Ph), 7.16 (d, *J* = 8.8 Hz, 2H, *m*-H of C₆H₄), 5.50, 5.04 (both d, *J* = 1.6 Hz, 1H each, CH₂=), 5.04 (s, 1H), 3.81 (s, 2H, CH₂). ¹³C{¹H} NMR (100 MHz, CDCl₃, δ): 146.5 (C=), 140.4 (*ipso*-C of Ph), 137.9, 131.8 (*ipso*- and *p*-C of C₆H₄), 130.2, 128.4 (*o*- and *m*-C of C₆H₄), 128.3 (*m*-C of Ph), 127.6 (*p*-C of Ph), 126.1 (*o*-C of Ph), 114.8 (CH₂=), 41.0 (CH₂).



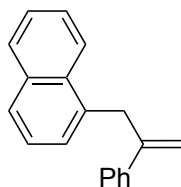
3-3ag

Methyl-3-(2-phenylallyl)benzene (3-3ag).⁶⁸ A colorless oil (46.9 mg, 0.225 mmol, 90% isolated yield based on the amount of **3-1a**). ¹H NMR (400 MHz, CDCl₃, δ): 7.49–7.45 (d of pseudo t, *J* = 6.5, 1.6 Hz, 2H, *o*-H of Ph), 7.35–7.29 (pseudo tt, *J* = 7.3, 1.8 Hz, 2H, *m*-H of Ph), 7.26 (t of pseudo t, *J* = 7.2, 1.2 Hz, 1H, *p*-H of Ph), 7.19 (t, *J* = 7.5 Hz, 1H, 5-H of C₆H₄), 7.09 (s, 1H, 2-H of C₆H₄), 7.06, 7.03 (both d, *J* = 7.5 Hz, 1 H each, 4- and 6-H of C₆H₄), 5.53, 5.05 (both d, *J* = 1.4 Hz, 1 H each, CH₂=), 3.83 (s, 2H, CH₂), 2.34 (s, 3H, Me). ¹³C{¹H} NMR (100 MHz, CDCl₃, δ): 146.9 (C=), 140.9 (*ipso*-C of Ph), 139.4, 137.8 (1- and 3-C of C₆H₄), 129.7 (2-C of C₆H₄), 128.2 (5-C of C₆H₄ and *m*-C of Ph, overlapping), 127.4 (*p*-C of Ph), 126.8, 125.9 (4- and 6-C of C₆H₄), 126.1 (*o*-C of Ph), 125.9, 114.5 (CH₂=), 41.5 (CH₂), 21.4 (Me).



3-3ah

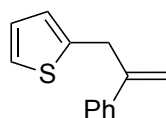
1-Methyl-2-(2-phenylallyl)benzene (3-3ah).⁷⁰ A colorless oil (47.4 mg, 0.228 mmol, 91% isolated yield based on the amount of **3-1a**). ¹H NMR (400 MHz, CDCl₃, δ): 7.50 (d of pseudo t, *J* = 7.2, 1.6 Hz, 2H, *o*-H of Ph), 7.35 (pseudo tt, *J* = 7.1, 1.3 Hz, 2H, *m*-H of Ph), 7.23 (t of pseudo t, 1H, *p*-H of Ph), 7.22–7.12 (m, 4H, C₆H₄), 5.47, 4.75 (both d, *J* = 1.2 Hz, 1H each, CH₂=), 3.79 (s, 2H, CH₂), 2.32 (s, 3H, Me). ¹³C{¹H} NMR (100 MHz, CDCl₃, δ): 146.3 (C=), 141.4 (*ipso*-C of Ph), 137.7, 136.7 (1- and 2-C of C₆H₄), 130.1, 129.9 (3- and 6-C of C₆H₄), 128.3 (*m*-C of Ph), 127.5 (*p*-C of Ph), 126.4, 125.9, (4- and 5-C of C₆H₄), 125.9 (*m*-C of Ph), 113.9 (CH₂=), 38.8 (CH₂), 19.4 (Me).



3-3ai

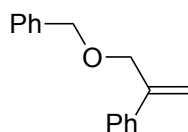
1-(2-Phenylallyl)naphthalene (3-3ai).⁷⁰ A colorless oil (46.4 mg, 0.190 mmol, 76% isolated yield based on the amount of **3-1a**). ¹H NMR (400 MHz, CDCl₃, δ): 8.03–7.99, 7.91–7.86, 7.79–7.75 (all m, 1H each, aromatic H), 7.59–7.54, 7.52–7.48 (both m, 2H each, aromatic H), 7.45–7.28 (m, 5H, aromatic H), 5.54, 4.80 (both d, *J* = 0.8 Hz, 1H each, CH₂=), 4.27 (s, 2H, CH₂). ¹³C{¹H} NMR (100 MHz, CDCl₃, δ): 146.2 (C=), 141.2 (*ipso*-C of Ph), 135.5, 133.8, 132.2 (1-, 4a-, and 8a-C of naphthyl), 128.7 (CH of

naphthyl), 128.4 (*m*-C of Ph), 127.6 (*p*-C of Ph), 127.3, 127.1 (CH of naphthyl), 125.9 (CH of naphthyl and *o*-C of Ph, overlapping), 125.6, 125.5, 124.2 (CH of naphthyl), 114.8 (CH₂=), 38.3 (CH₂).



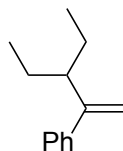
3-3aj

2-(2-Phenylallyl)thiophene (3-3aj) (new compound). A colorless oil (47.1 mg, 0.235 mmol, 94% isolated yield based on the amount of **3-1a**). HRMS–FAB (*m/z*): [*M*]⁺ calcd for C₁₃H₁₂S, 200.0660; found, 200.0664. ¹H NMR (400 MHz, CDCl₃, δ): 7.48 (d of pseudo t, *J* = 6.7, 1.7 Hz, 2H, *o*-H of Ph), 7.34 (pseudo tt, *J* = 7.3, 1.8 Hz, 2H, *m*-H of Ph), 7.28 (t of pseudo t, *J* = 7.6, 1.8 Hz, 1H, *p*-H of Ph), 7.14 (dd, *J* = 5.2, 1.1 Hz, 1H, 5-H of C₄H₃S), 6.92 (dd, *J* = 5.2, 3.5 Hz, 1H, 4-H of C₄H₃S), 6.94 (dd, *J* = 3.5, 1.1 Hz, 1H, 3-H of C₄H₃S), 5.52, 5.20 (both d, *J* = 1.2 Hz, 1H each, CH₂=), 4.05 (s, 2H, CH₂). ¹³C{¹H} NMR (100 MHz, CDCl₃, δ): 146.4 (C=), 142.5, 140.2 (2-C of C₄H₃S and *ipso*-C of Ph), 128.3 (*m*-C of Ph), 127.6 (*p*-C of Ph), 126.7 (CH of C₄H₃S), 126.1 (*o*-C of Ph), 125.4, 123.7 (CH of C₄H₃S), 114.5 (CH₂=), 35.9 (CH₂).



3-3ak

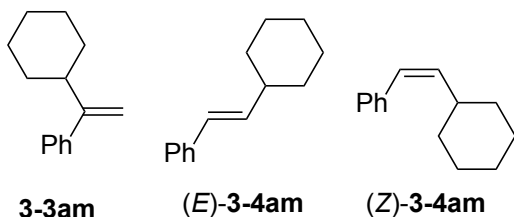
(3-(Benzyloxy)prop-1-en-2-yl)benzene (3-3ak).⁷¹ A colorless oil (29.4 mg, 0.131 mmol, 52% isolated yield based on the amount of **3-1a**). ¹H NMR (400 MHz, CDCl₃, δ): 7.49 (d of pseudo t, *J* = 6.8, 1.8 Hz, 2H, *o*-H of Ph), 7.38–7.26 (m, 8H, Ph), 5.57, 5.39 (both d, *J* = 1.2 Hz, 1H each, CH₂=), 4.58, 4.43 (both s, 2H each, CH₂). ¹³C{¹H} NMR (100 MHz, CDCl₃, δ): 144.2 (C=), 138.8, 138.2 (*ipso*-C of benzyl and Ph), 128.4, 128.3 (*m*-C of benzyl and Ph), 127.8 (*o*-C of benzyl), 127.8 (*p*-C of benzyl), 127.6 (*p*-C of Ph), 126.1 (*o*-C of Ph), 114.5 (CH₂=), 72.0, 71.9 (CH₂).



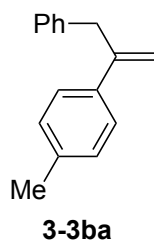
3-3al

(3-Ethylpent-1-en-2-yl)benzene (3-3al) (new compound). A colorless oil (36.1 mg, 0.207 mmol, 83% isolated yield based on the amount of **3-1a**). HRMS–FAB (*m/z*): [*M*]⁺ calcd for C₁₃H₁₈, 174.1409; found, 174.1406. ¹H NMR (400 MHz, CDCl₃, δ): 7.36–7.25 (m, 5H, Ph), 5.24, 4.00 (both d, *J* = 1.2 Hz, 1H each, CH₂=), 2.39 (quintet, *J* = 6.6 Hz, 1H, CHC=), 1.50 (pseudo quintet, *J* = 7.4 Hz, 4H, CH₂), 0.88 (t, *J* = 7.4 Hz, 6H, Me). ¹³C{¹H} NMR (100 MHz, CDCl₃, δ): 152.5 (C=), 143.7 (*ipso*-C of Ph), 128.0 (*m*-C of Ph), 126.9 (*p*-C of Ph), 126.7 (*o*-C of Ph), 112.3 (CH₂=), 47.3 (CHC=), 26.6 (CH₂),

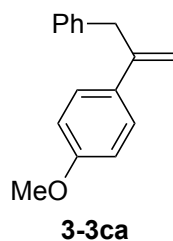
11.6 (Me).



Mixture of **(1-cyclohexylvinyl)benzene (3-3am)**.⁷² Mixture of **(E)-(2-cyclohexylvinyl)benzene ((E)-3-4am)**⁷³ and **(Z)-(2-cyclohexylvinyl)benzene ((Z)-3-4am)**.⁷⁴ A colorless oil (37.3 mg, 0.200 mmol, 80% isolated yield based on the amount of **1a**, obtained as a mixture of **3-3am**, **(E)-3-4am**, and **(Z)-3-4am** in a ratio of 77/1/22, determined by ¹H NMR). **3am**: ¹H NMR (400 MHz, CDCl₃, δ): 7.35–7.24 (m, 5H, Ph), 5.13, 5.00 (both d, *J* = 1.6 Hz, 1H each, CH₂=), 2.42 (tt, *J* = 10.6, 2.8 Hz, 1H, 1-H of Cy), 1.88–1.68 (m, 4H, CH₂ of Cy), 1.41–1.00 (m, 6H, CH₂ of Cy). For **(E)-4am** and **(Z)-4am**, see section 3.4.3.

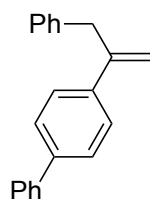


1-Methyl-4-(3-phenylprop-1-en-2-yl)benzene (3-3ba).⁶⁹ A colorless oil (45.8 mg, 0.220 mmol, 88% isolated yield based on the amount of **3-1b**). ¹H NMR (400 MHz, CDCl₃, δ): 7.36 (d, *J* = 8.4 Hz, 2H, *m*-H of C₆H₄), 7.31–7.23 (m, 4H, *o*- and *m*-H of Ph), 7.20 (t of pseudo t, *J* = 6.7, 1.8 Hz, 1H, *p*-H of Ph), 7.11 (d, *J* = 8.4 Hz, 2H, *o*-H of C₆H₄), 5.50, 5.00 (both d, *J* = 1.4 Hz, 1H each, CH₂=), 3.85 (s, 2H, CH₂), 2.34 (s, 3H, Me). ¹³C{¹H} NMR (100 MHz, CDCl₃, δ): 146.6 (C=), 139.6 (*ipso*-C of Ph), 137.8, 137.2 (*ipso*- and *p*-C of C₆H₄), 128.9 (*m*-C of C₆H₄), 128.9 (*o*-C of Ph), 128.3 (*m*-C of Ph), 126.0 (*p*-C of Ph), 126.0 (*o*-C of C₆H₄), 113.8 (CH₂=), 41.6 (CH₂=), 21.1 (Me).



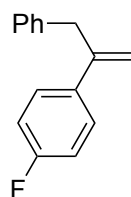
1-Methoxy-4-(3-phenylprop-1-en-2-yl)benzene (3-3ca).¹⁰ A colorless oil (51.0 mg, 0.227 mmol, 91% isolated yield based on the amount of **3-1c**). ¹H NMR (400 MHz, CDCl₃, δ): 7.35 (d, *J* = 8.6 Hz, 2H, *o*-H of C₆H₄), 7.27–7.18 (m, 4H, *o*- and *m*-H of Ph), 7.15 (t, *J* = 6.6 Hz, 1H, *p*-H of Ph), 6.79 (d, *J* = 8.6 Hz, 2H, *m*-H of C₆H₄), 5.41, 4.93 (both s, 1H each, CH₂=), 3.79 (s, 2H, CH₂), 3.76 (s, 3H, Me). ¹³C{¹H} NMR (100 MHz, CDCl₃, δ): 159.0 (*p*-C of C₆H₄), 146.0 (C=), 139.7 (*ipso*-C of Ph), 133.1 (*ipso*-C of

C₆H₄), 128.8 (*o*-C of Ph), 128.3 (*m*-C of Ph), 127.2 (*o*-C of C₆H₄), 126.0 (*p*-C of Ph), 113.6 (CH₂=), 112.9 (*m*-C of C₆H₄), 55.2 (Me), 41.7 (CH₂).



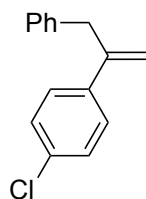
3-3da

4-(3-Phenylprop-1-en-2-yl)-1,1'-biphenyl (3-3da).⁷⁵ A colorless oil (52.0 mg, 0.192 mmol, 77% isolated yield based on the amount of **3-1d**). ¹H NMR (400 MHz, CDCl₃, δ): 7.58 (d, *J* = 7.6 Hz, 2H, 2',6'-CH of biphenyl), 7.53 (br, 4H, C₆H₄), 7.43 (t, *J* = 7.6 Hz, 2H, 3',5'-CH of biphenyl), 7.35 (t, *J* = 7.6 Hz, 1H, 4'-CH of biphenyl), 7.30–7.25 (m, 4H, *o*- and *m*-H of Ph), 7.20 (t of pseudo t, *J* = 6.4, 2.6, Hz, 1H, *p*-H of Ph), 5.58, 5.06 (both s, 1H each), 5.06 (s, 1H, CH₂=), 3.88 (s, 2H, CH₂). ¹³C{¹H} NMR (100 MHz, CDCl₃, δ): 146.3 (C=), 140.6, 140.2 (1- and 1'-C of biphenyl), 139.6, 139.5 (4-C of biphenyl and *ipso*-C of Ph), 128.9 (3',5'-C of biphenyl), 128.7 (*o*-C of Ph), 128.4 (*m*-C of Ph), 127.2 (4'-C of biphenyl), 126.9, 126.5 (2,5- and 2',5'-C of biphenyl), 126.1 (*p*-C of Ph), 114.6 (CH₂=), 41.5 (CH₂).



3-3ea

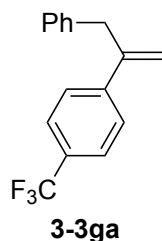
1-Fluoro-4-(3-phenylprop-1-en-2-yl)benzene (3-3ea).¹⁰ A colorless oil (46.2 mg, 0.218 mmol, 87% isolated yield based on the amount of **3-1e**). ¹H NMR (400 MHz, CDCl₃, δ): 7.42–7.37 (m, 2H, *o*-C of C₆H₄), 7.28 (t of pseudo t, *J* = 7.6, 2.2 Hz, 2H, *m*-H of Ph), 7.24–7.16 (m, 3H, *o*- and *p*-H of Ph), 7.00–6.94 (dd of pseudo t, *J* = 8.8, 7.2, 2.2 Hz, 2H, *m*-C of C₆H₄), 5.44, 5.04 (both d, *J* = 1.6 Hz, 1H each, CH₂=), 3.82 (s, 2H, CH₂). ¹³C{¹H} NMR (100 MHz, CDCl₃, δ): 162.2 (d, ¹*J*_{CF} = 34.5 Hz, *p*-C of C₆H₄), 145.8 (C=), 139.2 (*ipso*-C of Ph), 136.7 (d, ⁴*J*_{CF} = 2.9 Hz, *ipso*-C of C₆H₄), 128.8 (*o*-C of Ph), 128.4 (*m*-C of Ph), 127.7 (d, ³*J*_{CF} = 8.6 Hz, *o*-C of C₆H₄), 126.2 (*p*-C of Ph), 115.0 (d, ²*J*_{CF} = 21.9 Hz, *m*-C of C₆H₄), 114.5 (CH₂=), 41.8 (CH₂). ¹⁹F NMR (376 MHz, CDCl₃, δ): –118.3.



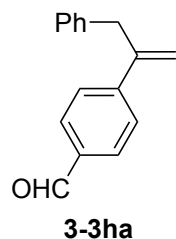
3-3fa

1-Chloro-4-(3-phenylprop-1-en-2-yl)benzene (3-3fa).¹⁰ A colorless oil (48.0 mg,

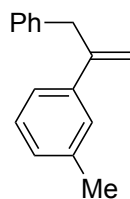
0.210 mmol, 84% isolated yield based on the amount of **3-1f**). ^1H NMR (400 MHz, CDCl_3 , δ): 7.36 (d, $J = 8.4$ Hz, 2H, *m*-H of C_6H_4), 7.31–7.15 (m, 7H, *o*-H of C_6H_4 and Ph), 5.49, 5.07 (both d, $J = 1.2$ Hz, 1H each, $\text{CH}_2=$), 3.81 (s, 2H, CH_2). $^{13}\text{C}\{^1\text{H}\}$ NMR (100 MHz, CDCl_3 , δ): 145.7 (C=), 139.1 (*ipso*-C of C_6H_4 and Ph, overlapping), 133.2 (*p*-C of C_6H_4), 128.8 (*o*-C of Ph), 128.4 (*m*-C of Ph), 128.4 (*m*-C of C_6H_4), 127.4 (*o*-C of C_6H_4), 126.2 (*p*-C of Ph), 115.1 ($\text{CH}_2=$), 41.6 (CH_2).



1-(3-Phenylprop-1-en-2-yl)-4-(trifluoromethyl)benzene (3-3ga).¹⁰ A colorless oil (52.5 mg, 0.200 mmol, 80% isolated yield based on the amount of **3-1g**). ^1H NMR (400 MHz, CDCl_3 , δ): 7.56–7.50 (m, 4H, C_6H_4), 7.28 (pseudo tt, $J = 7.4$, 2.6 Hz, 2H, *m*-H of Ph), 7.24–7.17 (m, 3H, *o*- and *p*-H of Ph), 5.57, 5.16 (both d, $J = 1.2$ Hz, 1H each, $\text{CH}_2=$), 3.86 (s, 2H, CH_2). $^{13}\text{C}\{^1\text{H}\}$ NMR (100 MHz, CDCl_3 , δ): 145.8 (C=), 144.3 (*ipso*-C of C_6H_4), 138.8 (*ipso*-C of Ph), 129.4 (q, $^2J_{\text{CF}} = 32.5$ Hz, *p*-C of C_6H_4), 128.9 (*o*-C of Ph), 128.5 (*m*-C of Ph), 126.4 (*o*-C of C_6H_4), 126.4 (*p*-C of Ph), 125.2 (q, $^3J_{\text{CF}} = 10.5$ Hz, *m*-C of C_6H_4), 124.2 (q, $^1J_{\text{CF}} = 272.2$ Hz, CF_3), 116.6 ($\text{CH}_2=$), 41.5 (CH_2). ^{19}F NMR (376 MHz, CDCl_3 , δ): –64.1.

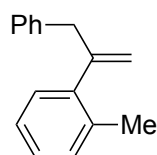


4-(3-Phenylprop-1-en-2-yl)benzaldehyde (3-3ha) (new compound). A colorless oil (48.9 mg, 0.220 mmol, 88% isolated yield based on the amount of **3-1h**). HRMS–FAB (m/z): $[\text{M}]^+$ calcd for $\text{C}_{16}\text{H}_{14}\text{O}$, 222.1045; found, 222.1045. ^1H NMR (400 MHz, CDCl_3 , δ): 9.97 (s, 1H, CHO), 7.80 (d, $J = 8.4$ Hz, 2H, *m*-H of C_6H_4), 7.58 (d, $J = 8.4$ Hz, 2H, *o*-H of C_6H_4), 7.27 (pseudo t, $J = 7.0$ Hz, 2H, *m*-H of Ph), 7.24–7.17 (m, 3H, *o*- and *p*-H of Ph), 5.62, 5.20 (both d, $J = 0.8$ Hz, 1H each, $\text{CH}_2=$), 3.87 (s, 2H, CH_2). $^{13}\text{C}\{^1\text{H}\}$ NMR (100 MHz, CDCl_3 , δ): 191.8 (CHO), 146.8 (*ipso*-C of C_6H_4), 146.0 (C=), 138.8 (*ipso*-C of Ph), 135.3 (*p*-C of C_6H_4), 129.8 (*m*-C of C_6H_4), 128.8 (*o*-C of Ph), 128.5 (*m*-C of Ph), 126.7 (*o*-C of C_6H_4), 126.3 (*p*-C of Ph), 117.3 ($\text{CH}_2=$), 41.4 (CH_2).



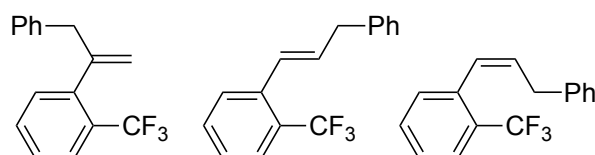
3-3ia

1-Methyl-3-(3-phenylprop-1-en-2-yl)benzene (3-3ia).¹⁰ A colorless oil (42.2 mg, 0.203 mmol, 81% isolated yield based on the amount of **1i**). ¹H NMR (400 MHz, CDCl₃, δ): 7.31–7.16 (m, 8H, Ph and 2-, 5-, and 6-H of C₆H₄), 7.07 (d, *J* = 7.6 Hz, 1H, 4-H of C₆H₄), 5.48, 4.99 (both d, *J* = 1.6 Hz, 1H each, CH₂=), 3.83 (s, 2H, CH₂), 2.34 (s, 3H, Me). ¹³C{¹H} NMR (100 MHz, CDCl₃, δ): 147.1 (C=), 140.8 (3-C of C₆H₄), 139.6 (*ipso*-C of Ph), 137.7 (1-C of C₆H₄), 128.9 (*o*-C of Ph), 128.3 (*m*-C of Ph), 128.2, 128.1 (5- and 6-C of C₆H₄), 126.8 (2-C of C₆H₄), 126.0 (*p*-C of Ph), 123.2 (4-C of C₆H₄), 114.4 (CH₂=), 41.6 (CH₂), 21.5 (Me).



3-3ja

1-Methyl-2-(3-phenylprop-1-en-2-yl)benzene (3-3ja) (new compound). A colorless oil (34.9 mg, 0.168 mmol, 67% isolated yield based on the amount of **3-1j**). HRMS–FAB (*m/z*): [*M*]⁺ calcd for C₁₆H₁₆, 208.1252; found, 208.1245. ¹H NMR (400 MHz, CDCl₃, δ): 7.29–7.24 (m, 2H, *m*-H of Ph), 7.23–7.07 (m, 6H, 3-, 4-, and 6-H of C₆H₄ and *o*- and *p*-H of Ph), 7.03–6.99 (m, 1H, 5-H of C₆H₄), 5.09, 4.94 (both s, 1H each, CH₂=), 3.62 (s, 2H, CH₂), 2.26 (s, 3H, Me). ¹³C{¹H} NMR (100 MHz, CDCl₃, δ): 149.3 (C=), 142.6 (2-C of C₆H₄), 138.9 (*ipso*-C of Ph), 134.8 (1-C of C₆H₄), 130.0 (6-C of C₆H₄), 129.3 (*o*-C of Ph), 128.4 (5-C of C₆H₄), 128.2 (*m*-C of Ph), 126.8 (4-C of C₆H₄), 126.1 (*p*-C of Ph), 125.3 (3-C of C₆H₄), 115.3 (CH₂=), 44.5 (CH₂), 19.7 (Me).



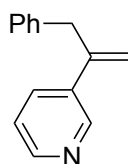
3-3ka

(E)-3-4ka

(Z)-3-4ka

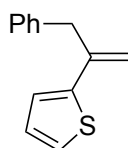
Mixture of **1-(3-phenylprop-1-en-2-yl)-2-(trifluoromethyl)benzene (3-3ka)**, of **(E)-1-(3-phenylprop-1-en-1-yl)-2-(trifluoromethyl)benzene ((E)-3-4ka)** and **(Z)-1-(3-phenylprop-1-en-1-yl)-2-(trifluoromethyl)benzene ((Z)-3-4ka) (new compounds)**. A colorless oil (51.8 mg, 0.198 mmol, 79% isolated yield based on the amount of **1k**, obtained as a mixture of **3-3ka**, **(E)-3-4ka**, and **(Z)-3-4ka** in a ratio of 44/34/22 determined by ¹H NMR). **3-3ka**: HRMS–FAB (*m/z*): [*M*]⁺ calcd for C₁₆H₁₃F₃, 262.0969; found, 262.0978. ¹H NMR (400 MHz, CDCl₃, δ): 7.68 (d, *J* = 7.6 Hz, 1H, 3-H of C₆H₄),

7.43–7.02 (m, 8H, Ph and 4-, 5-, and 6-H of C₆H₄), 5.05, 5.02 (both d, $J = 1.2$ Hz, 1H each, CH₂=), 3.65 (s, 2H, CH₂). ¹⁹F NMR (376 MHz, CDCl₃, δ): –59.4. For (*E*)-**3-4ka**, and (*Z*)-**3-4ka**, see section 3.4.3.



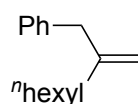
3-3la

3-(3-Phenylprop-1-en-2-yl)pyridine (3-3la) (new compound). A colorless oil (43.4 mg, 0.222 mmol, 89% isolated yield based on the amount of **3-1l**). HRMS–FAB (m/z): $[M + H]^+$ calcd for C₁₄H₁₄N, 196.1126; found, 196.1135. ¹H NMR (400 MHz, CDCl₃, δ): 8.69 (d, $J = 2.4$ Hz, 1H, 2-H of C₅H₃N), 8.46 (dd, $J = 5.0, 1.4$ Hz, 1H, 6-H of C₅H₃N), 7.66 (d of pseudo t, $J = 7.6, 1.9$ Hz, 1H, 4-H of C₅H₃N), 7.37 (pseudo t, $J = 7.6$ Hz, 2H, *m*-H of Ph), 7.23–7.16 (m, 4H, 5-H of C₅H₃N and *o*- and *p*-H of Ph), 5.53, 5.15 (both d, $J = 0.8$ Hz, 1H each, CH₂), 3.84 (s, 2H, CH₂). ¹³C{¹H} NMR (100 MHz, CDCl₃, δ): 148.5, 147.6 (2- and 6-C of C₅H₃N), 144.0 (C=), 138.5 (*ipso*-C of Ph), 136.1 (3-C of C₅H₃N), 133.3 (5-C of C₅H₃N), 128.8 (*o*-C of Ph), 128.4 (*m*-C of Ph), 126.3 (*p*-C of Ph), 123.0 (4-C of C₅H₃N), 116.2 (CH₂=), 41.4 (CH₂).



3-3ma

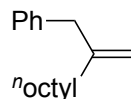
2-(3-phenylprop-1-en-2-yl)thiophene (3-3ma).¹⁰ A colorless oil (39.1 mg, 0.195 mmol, 78% isolated yield based on the amount of **3-1m**). ¹H NMR (400 MHz, CDCl₃, δ): 7.32–7.27 (4H, *o*- and *m*-H of Ph), 7.23–7.19 (t of pseudo t, $J = 7.2, 2.5$ Hz, 1H, *p*-H of Ph), 7.13 (dd, $J = 5.2, 0.8$ Hz, 1H, 5-H of C₄H₃S), 7.01 (dd, $J = 3.5, 0.8$ Hz, 1H, 4-H of C₄H₃S), 6.92 (dd, $J = 5.2, 3.5$ Hz, 1H, 3-H of C₄H₃S), 5.56, 4.90 (both s, 1H each, CH₂=), 3.81 (s, 2H, CH₂). ¹³C{¹H} NMR (100 MHz, CDCl₃, δ): 144.9 (C=), 140.4, 138.9 (2-C of C₄H₃S and *ipso*-C of Ph), 128.9 (*m*-C of Ph), 128.4 (*p*-C of Ph), 127.3 (CH of C₄H₃S), 126.3 (*o*-C of Ph), 124.2, 124.0 (CH of C₄H₃S), 113.2 (CH₂=), 41.7 (CH₂).



3-3na

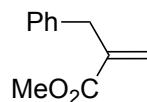
(2-Methylenooctyl)benzene (3-3na).⁷² A colorless oil (40.4 mg, 0.199 mmol, 80% isolated yield based on the amount of **3-1n**). ¹H NMR (400 MHz, CDCl₃, δ): 7.29 (pseudo t, $J = 7.6$ Hz, 2H, *m*-H of Ph), 7.23–7.17 (m, 3H, *o*- and *p*-H of Ph), 4.82, 4.73 (both s, 1H each, CH₂=), 3.34 (PhCH₂), 1.97 (t, $J = 7.6$ Hz, 2H, 1-CH₂ of *n*-hexyl), 1.43 (pseudo quintet, $J = 6.5$ Hz, 2H, 3-CH₂ of *n*-hexyl), 1.33–1.23 (m, 6H, CH₂ of *n*-hexyl),

0.88 (t, $J = 6.4$ Hz, 3H, Me). $^{13}\text{C}\{^1\text{H}\}$ NMR (100 MHz, CDCl_3 , δ): 149.3 (C=), 139.9 (*ipso*-C of Ph), 129.0 (*o*-C of Ph), 128.2 (*m*-C of Ph), 126.0 (*p*-C of Ph), 110.9 (PhCH₂), 43.0 (CH₂=), 35.4 (1-CH₂ of *n*-hexyl), 31.7 (4-CH₂ of *n*-hexyl), 29.0 (3-CH₂ of *n*-hexyl), 27.6 (2-CH₂ of *n*-hexyl), 22.6 (5-CH₂ of *n*-hexyl), 14.1 (Me).



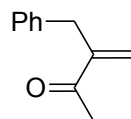
3-3oa

(2-Methylenedecyl)benzene (3-3oa) (new compound). A colorless oil (47.2 mg, 0.204 mmol, 82% isolated yield based on the amount of **3-1o**). HRMS–FAB (m/z): $[\text{M}]^+$ calcd for $\text{C}_{17}\text{H}_{26}$, 230.2035; found, 230.2032. ^1H NMR (400 MHz, CDCl_3 , δ): 7.32–7.25 (pseudo tt, $J = 7.4$, 2.0 Hz, 2H, *m*-H of Ph), 7.23–7.17 (m, 3H, *o*- and *p*-H of Ph), 4.82, 4.73 (both s, 1H each, CH₂=), 3.33 (s, 2H, PhCH₂), 1.96 (t, $J = 7.6$ Hz, 2H, 1-CH₂ of *n*-octyl), 1.43 (pseudo quintet, $J = 7.2$ Hz, 2H, 3-CH₂ of *n*-octyl), 1.33–1.23 (m, 10H, CH₂ of *n*-octyl), 0.89 (t, $J = 6.8$ Hz, 3H, Me). $^{13}\text{C}\{^1\text{H}\}$ NMR (100 MHz, CDCl_3 , δ): 149.3 (C=), 139.9 (*ipso*-C of Ph), 129.0 (*o*-C of Ph), 128.2 (*m*-C of Ph), 126.0 (*p*-C of Ph), 110.9 (PhCH₂), 43.0 (CH₂=), 35.4 (1-CH₂ of *n*-octyl), 31.9 (6-CH₂ of *n*-octyl), 29.5 (3-CH₂ of *n*-octyl), 29.3, 29.3 (4- and 5-CH₂ of *n*-octyl), 27.6 (2-CH₂ of *n*-octyl), 22.7 (7-CH₂ of *n*-octyl), 14.1 (Me).



3-3pa

Methyl 2-benzylacrylate (3-3pa).⁷⁶ A colorless oil (38.3 mg, 0.217 mmol, 87% isolated yield based on the amount of **3-1p**). ^1H NMR (400 MHz, CDCl_3 , δ): 7.30 (pseudo t, $J = 7.2$ Hz, 2H, *m*-H of Ph), 7.24–7.18 (m, 3H, *o*- and *p*-H of Ph), 6.24, 5.46 (both d, $J = 1.2$ Hz, 1H each, CH₂=), 3.74 (s, 3H, Me), 3.64 (s, 2H, CH₂). $^{13}\text{C}\{^1\text{H}\}$ NMR (100 MHz, CDCl_3 , δ): 167.4 (CO), 140.1 (*ipso*-C of Ph), 138.6 (C=), 129.0 (*o*-C of Ph), 128.4 (*m*-C of Ph), 126.3 (*p*-C of Ph), 126.3 (CH₂=), 51.9 (Me), 38.0 (CH₂).

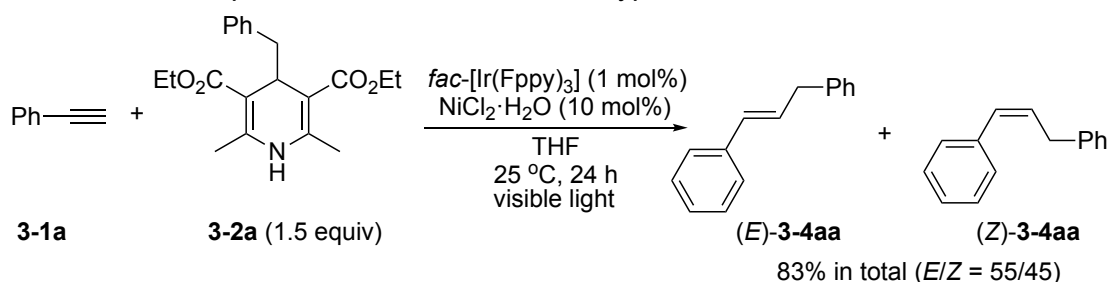


3-3qa

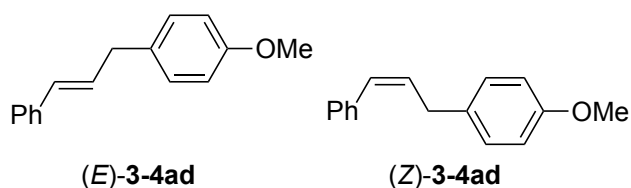
3-Benzyl-3-buten-2-one (3-3qa).⁷⁷ A colorless oil (33.2 mg, 0.207 mmol, 83% isolated yield based on the amount of **3-1q**). ^1H NMR (400 MHz, CDCl_3 , δ): 7.32–7.26 (pseudo tt, $J = 7.2$, 1.5 Hz, 2H, *m*-H of Ph), 7.23–7.15 (m, 3H, *o*- and *p*-H of Ph), 6.09, 5.65 (both d, $J = 1.2$ Hz, 1H each, CH₂=), 3.60 (s, 3H, Me), 2.35 (s, 2H, CH₂). $^{13}\text{C}\{^1\text{H}\}$ NMR (100 MHz, CDCl_3 , δ): 199.2 (CO), 148.6 (C=), 139.1 (*ipso*-C of Ph), 129.1 (*o*-C of Ph), 128.4 (*m*-C of Ph), 126.4 (CH₂=), 126.2 (*p*-C of Ph), 36.7 (CH₂), 26.0 (Me).

3.4.3. General Procedure for the Preparation of *anti*-Markovnikov-type Products (Taking prop-1-ene-1,3-diylidibenzene (**4aa**) as an Example)

Scheme 3-8. Preparation of *anti*-Markovnikov-type Products **3-4**

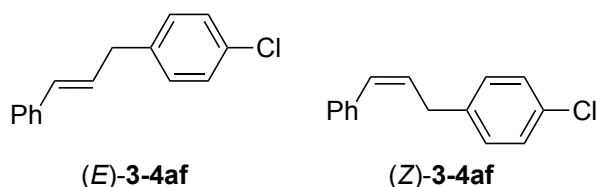


In a 20 mL Schlenk flask were placed **3-1a** (25.5 mg, 0.250 mmol), **3-2a** (128.8 mg, 0.375 mmol), *fac*-[Ir(Fppy)₃] (1.7 mg, 0.0022 mmol), and NiCl₂·6H₂O (5.8 mg, 0.024 mmol) under N₂, where THF (2.5 mL) was added at room temperature. The reaction flask was placed in an As One LTB-125 constant low temperature water bath set at 25 °C, and was illuminated from the bottom of the bath with an Aitech System TMN100×120–22WD 12 W white LED lamp (400 nm to 750 nm) at a distance of approximately 2 cm from the light source for 24 h. *E/Z* ratio of prop-1-ene-1,3-diylidibenzene (**3-4aa**) in the crude mixture was determined to be 55/45 by quantitative measurement of GC-MS. The volatiles were then removed *in vacuo*, and the residue was purified by column chromatography (SiO₂) with *n*-hexane as an eluent to afford a mixture of *(E)*-prop-1-ene-1,3-diylidibenzene (*(E)*-**3-4aa**) and *(Z)*-prop-1-ene-1,3-diylidibenzene (*(Z)*-**3-4aa**) as a colorless oil (40.3 mg, 0.207 mmol, 83% yield based on the amount of **3-1a**). Further purification by column chromatography lead to the separation of pure *(E)*-**3-4aa** from *(Z)*-**3-4aa**. *(E)*-**3-4aa**:^{36,77} ¹H NMR (400 MHz, CDCl₃, δ): 7.40–7.17 (m, 10H, Ph), 6.46 (d, *J* = 15.6 Hz, 1H, CH=CHCH₂), 6.36 (dt, *J* = 15.6, 6.7 Hz, 1H, CH=CHCH₂), 3.56 (d, *J* = 6.7 Hz, 2H, CH₂). ¹³C{¹H} NMR (100 MHz, CDCl₃, δ): 140.1 (*ipso*-C of benzyl), 137.4 (*ipso*-C of Ph), 131.0 (CH=CHCH₂), 129.2 (CH=CHCH₂), 128.7 (*m*-C of benzyl), 128.5 (*o*-C of benzyl and *m*-C of Ph, overlapping), 127.1 (*p*-C of Ph), 126.2 (*p*-C of benzyl and), 126.1 (*o*-C of Ph), 39.3 (CH₂). *(Z)*-**4aa**:^{36,78} ¹H NMR (400 MHz, CDCl₃, δ): 7.35–7.20 (m, 10H, Ph), 6.60 (d, *J* = 11.1 Hz, 1H, CH=CHCH₂), 5.86 (dt, *J* = 11.1, 7.4 Hz, 1H, CH=CHCH₂), 3.69 (d, *J* = 7.4 Hz, 2H, CH₂). ¹³C{¹H} NMR (100 MHz, CDCl₃, δ): 140.8 (*ipso*-C of benzyl), 137.2 (*ipso*-C of Ph), 130.7 (CH=CHCH₂), 130.0 (CH=CHCH₂), 128.7, 128.5, 128.3, 128.2 (*o*- and *m*-C of benzyl and Ph), 126.8 (*p*-C of Ph), 126.1 (*p*-C of benzyl), 34.6 (CH₂).

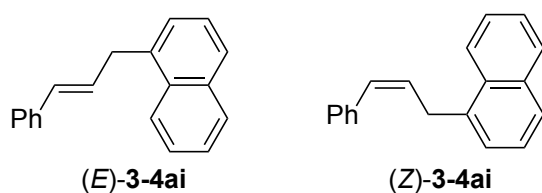


Mixture of *(E)*-1-methoxy-4-(3-phenylallyl)benzene (*(E)*-**3-4ad**)^{36,77} and *(Z)*-1-methoxy-4-(3-phenylallyl)benzene (*(Z)*-**3-4ad**).³⁶ A colorless oil (41.5 mg, 0.185 mmol, 74% isolated yield based on the amount of **3-1a**, obtained as a mixture of *E/Z* =

55/45 determined by ^1H NMR; $E/Z = 60/40$ determined by quantitative measurement of GC-MS for crude mixture). (*E*)-**3-4ad**: ^1H NMR (400 MHz, CDCl_3 , δ): 7.38–7.12 (m, 7H, Ph and *o*-H of C_6H_4), 6.88–6.83 (m, 2H, *m*-H of C_6H_4), 6.43 (d, $J = 15.8$ Hz, 1H, $\text{CH}=\text{CHCH}_2$), 6.34 (dt, $J = 15.8$ Hz, 6.6 Hz, 1H, $\text{CH}=\text{CHCH}_2$), 3.80 (s, 3H), 3.49 (d, $J = 6.6$ Hz, 2H, CH_2). $^{13}\text{C}\{^1\text{H}\}$ NMR (100 MHz, CDCl_3 , δ): 158.0 (*p*-C of C_6H_4), 137.5 (*ipso*-C of Ph), 132.2 (*ipso*-C of C_6H_4), 130.7 ($\text{CH}=\text{CHCH}_2$), 129.7 ($\text{CH}=\text{CHCH}_2$), 129.6 (*o*-C of C_6H_4), 128.5 (*m*-C of Ph), 127.0 (*p*-C of Ph), 126.1 (*o*-C of Ph), 113.9 (*m*-C of C_6H_4), 55.3 (Me), 38.4 (CH_2). (*Z*)-**3-4ad** (^1H NMR resonances due to aromatic H atoms overlapping with those of (*E*)-**3-4ad** not fully listed): ^1H NMR (400 MHz, CDCl_3 , δ): 6.57 (d, $J = 11.4$ Hz, 1H, $\text{CH}=\text{CHCH}_2$), 5.84 (dt, $J = 11.4$, 6.9 Hz, 1H, $\text{CH}=\text{CHCH}_2$), 3.80 (s, 3H, Me), 3.62 (d, $J = 6.9$ Hz, 2H, CH_2). $^{13}\text{C}\{^1\text{H}\}$ NMR (100 MHz, CDCl_3 , δ): 157.9 (*p*-C of C_6H_4), 137.3 (*ipso*-C of Ph), 132.8 (*ipso*-C of C_6H_4), 131.1 ($\text{CH}=\text{CHCH}_2$), 129.7 ($\text{CH}=\text{CHCH}_2$), 129.2 (*o*-C of C_6H_4), 128.7, 128.2 (*o*- and *m*-C of Ph), 126.8 (*p*-C of Ph), 113.8 (*m*-C of C_6H_4), 55.3 (Me), 33.7 (CH_2).

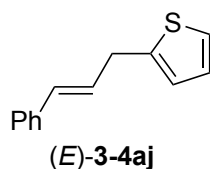


Mixture of (*E*)-1-chloro-4-(3-phenylallyl)benzene ((*E*)-**3-4af**)⁷⁹ and (*Z*)-1-chloro-4-(3-phenylallyl)benzene ((*Z*)-**3-4af**). A colorless oil (38.9 mg, 0.170 mmol, 68% isolated yield based on the amount of **3-1a**, obtained as a mixture of $E/Z = 80/20$ determined by ^1H NMR; $E/Z = 80/20$ determined by quantitative measurement of GC-MS for crude mixture). (*E*)-**3-4af**: ^1H NMR (400 MHz, CDCl_3 , δ): δ 7.38–7.13 (m, 9H, C_6H_4 and Ph), 6.45 (d, $J = 15.8$ Hz, 1H, $\text{CH}=\text{CHCH}_2$), 6.31 (dt, $J = 15.8$, 6.7 Hz, 1H, $\text{CH}=\text{CHCH}_2$), 3.52 (d, $J = 6.7$ Hz, 2H, CH_2). $^{13}\text{C}\{^1\text{H}\}$ NMR (100 MHz, CDCl_3 , δ): 138.6, 137.2 (*ipso*-C of C_6H_4 and Ph), 131.9 (*p*-C of C_6H_4), 131.5 ($\text{CH}=\text{CHCH}_2$), 130.0 ($\text{CH}=\text{CHCH}_2$), 128.6, 128.5 (*o*- and *m*-C of C_6H_4 and *m*-C of Ph with the resonance at 128.5 overlapping), 127.3 (*p*-C of Ph), 126.1 (*o*-C of Ph), 38.6 (CH_2). (*Z*)-**3-4af** (^1H and $^{13}\text{C}\{^1\text{H}\}$ NMR resonances due to unsaturated hydrocarbon atoms overlapping with those of (*E*)-**3-4af** not fully listed): ^1H NMR (400 MHz, CDCl_3 , δ): 6.61 (dt, $J = 11.3$, 1.6 Hz, 1H, $\text{CH}=\text{CHCH}_2$), 5.81 (dt, $J = 11.3$ Hz, 7.5 Hz, 1H, $\text{CH}=\text{CHCH}_2$), 3.64 (dd, $J = 7.5$, 1.6 Hz, 2H, CH_2). $^{13}\text{C}\{^1\text{H}\}$ NMR (100 MHz, CDCl_3 , δ): 130.4, 130.0, 129.8, 129.7, 128.6, 128.4, 128.3, 126.9, 33.9.

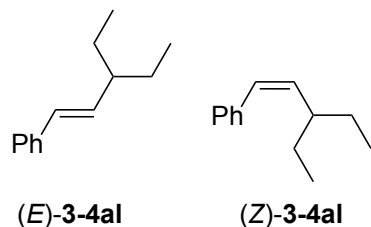


Mixture of (*E*)-1-(3-phenylallyl)naphthalene ((*E*)-**3-4ai**)^{79,80} and (*Z*)-1-(3-phenylallyl)naphthalene ((*Z*)-**3-4ai**).⁷⁸ A white solid (34.8 mg, 0.142 mmol, 57% isolated yield based on the amount of **3-1a**, obtained as a mixture of $E/Z = 49/51$

determined by ^1H NMR; $E/Z = 79/21$ determined by quantitative measurement of GC-MS for crude mixture). (*E*)-**3-4ai**: ^1H NMR (400 MHz, CDCl_3 , δ): 8.09 (d, $J = 7.6$ Hz, 1H, 5-H of naphthyl), 7.88, 7.77 (both d, $J = 8.0$ Hz, 1H each, 4- and 8-H of naphthyl), 7.54–7.16 (m, 9H, Ph and 2-, 3-, 6-, and 7-H of naphthyl), 6.55–6.44 (m, 2H, $\text{CH}=\text{CH}$), 4.01 (d, $J = 5.2$ Hz, 2H, CH_2). $^{13}\text{C}\{^1\text{H}\}$ NMR (100 MHz, CDCl_3 , δ): 137.4 (*ipso*-C of Ph), 136.2, 133.8, 132.0 (1-, 4a-, and 8a-C of naphthyl), 131.3 ($\text{CH}=\text{CHCH}_2$), 128.8, 128.5, 127.1, 126.4, 125.9, 125.6, 124.0 ($\text{CH}=\text{CHCH}_2$, CH of naphthyl, and *p*-C of Ph with the resonances at 127.1 and 125.6 overlapping), 128.7 (*m*-C of Ph), 126.1 (*o*-C of Ph), 36.4 (CH_2). (*Z*)-**3-4ai** (^1H and $^{13}\text{C}\{^1\text{H}\}$ NMR resonances due to unsaturated hydrocarbon atoms overlapping with those of (*E*)-**3-4ai** not fully listed): ^1H NMR (400 MHz, CDCl_3 , δ): 6.64 (d, $J = 10.8$ Hz, 1H), 5.94 (dt, $J = 10.8, 7.2$ Hz, 1H), 4.11 (d, $J = 7.2$ Hz, 2H, CH_2). $^{13}\text{C}\{^1\text{H}\}$ NMR (100 MHz, CDCl_3 , δ): 137.2 (*ipso*-C of Ph), 136.8, 133.8, 131.9 (1-, 4a-, and 8a-C of naphthyl), 130.5, 130.2, 128.8, 128.3, 127.3, 126.9, 126.9, 125.6, 123.9 (unsaturated CH), 32.3 (CH_2).

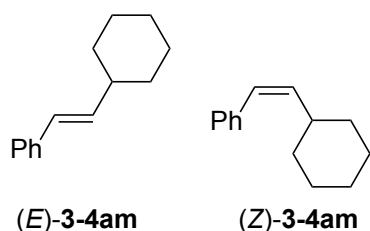


(*E*)-2-(3-Phenylallyl)thiophene ((*E*)-**3-4aj**).⁸⁰ A colorless oil (38.9 mg, 0.194 mmol, 78% isolated yield based on the amount of **3-1a**, obtained as a pure *E*-isomer; $E/Z = 94/6$ determined by quantitative measurement of GC-MS for crude mixture). ^1H NMR (400 MHz, CDCl_3 , δ): 7.38 (d, $J = 8.0$ Hz, 2H, *o*-H of Ph), 7.31 (pseudo t, $J = 7.6$ Hz, 2H, *m*-H of Ph), 7.22 (t, $J = 7.1$ Hz, 1H, *p*-H of Ph), 7.17 (dd, $J = 4.8, 0.8$ Hz, 1H, 5-H of $\text{C}_4\text{H}_3\text{S}$), 6.96 (dd, $J = 4.8, 2.8$ Hz, 1H, 4-H of $\text{C}_4\text{H}_3\text{S}$), 6.87 (dd, $J = 2.8, 0.8$ Hz, 1H, 3-H of $\text{C}_4\text{H}_3\text{S}$), 6.52 (d, $J = 15.7$ Hz, 1H, $\text{CH}=\text{CHCH}_2$), 6.37 (dt, $J = 15.7, 6.5$ Hz, 1H, $\text{CH}=\text{CHCH}_2$), 3.75 (d, $J = 6.5$ Hz, 2H, CH_2). $^{13}\text{C}\{^1\text{H}\}$ NMR (100 MHz, CDCl_3 , δ): 143.1 (2-C of $\text{C}_4\text{H}_3\text{S}$), 137.2 (*ipso*-C of Ph), 131.4 ($\text{CH}=\text{CHCH}_2$), 128.5 (*m*-C of Ph), 128.2, 126.9, 124.7, 123.7 ($\text{CH}=\text{CHCH}_2$ and 3-, 4-, and 5-C of $\text{C}_4\text{H}_3\text{S}$), 127.3 (*p*-C of Ph), 126.2 (*o*-C of Ph), 33.3 (CH_2).

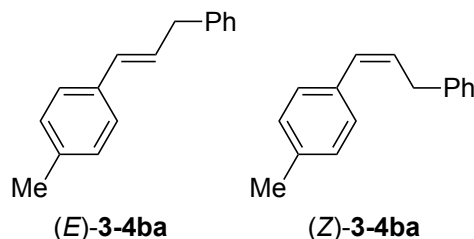


Mixture of (*E*)-(3-ethylpent-1-en-1-yl)benzene ((*E*)-**3-4al**)⁷⁴ and (*Z*)-(3-ethylpent-1-en-1-yl)benzene ((*Z*)-**3-4al**). A white oil (33.1 mg, 0.190 mmol, 76% isolated yield based on the amount of **3-1a**, obtained as a mixture of $E/Z = 41/59$ determined by ^1H NMR; $E/Z = 43/57$ determined by quantitative measurement of GC-MS for crude mixture). (*E*)-**3-4al**: ^1H NMR (400 MHz, CDCl_3 , δ): 7.38–7.27 (m, 4H, *o*- and *m*-H of Ph), 7.21 (t, $J = 6.4$ Hz, 1H, *p*-H of Ph), 6.34 (d, $J = 15.7$ Hz, 1H, $\text{CH}=\text{CHCH}$), 5.96

(dd, $J = 15.7, 9.9$ Hz, 1H, CH=CHCH), 1.96–1.89 (m, 1H, CH=CHCH), 1.58–1.42, 1.40–1.22 (both m, 2H each, CH₂CH₃), 0.86 (t, $J = 7.4$ Hz, 6H, Me). ¹³C{¹H} NMR (100 MHz, CDCl₃, δ): 138.2 (*ipso*-C of Ph), 135.3 (CH=CHCH), 129.8 (CH=CHCH), 128.6 (*m*-C of Ph), 126.7 (*p*-C of Ph), 125.9 (*o*-C of Ph), 46.8 (CH=CHCH), 27.8 (CH₂CH₃), 11.8 (Me). (*Z*)-**3-4al**: ¹H NMR (400 MHz, CDCl₃, δ): 7.38–7.27 (m, 4H, *o*- and *m*-H of Ph), 7.24–7.16 (m, 1H, *p*-H of Ph), 6.49 (d, $J = 11.2$ Hz, 1H, CH=CHCH), 5.37 (pseudo t, $J = 11.2$ Hz, 1H, CH=CHCH), 2.58–2.43 (m, 1H, CH=CHCH), 0.89 (t, $J = 7.4$ Hz, 6H, Me). ¹³C{¹H} NMR (100 MHz, CDCl₃, δ): 138.0 (*ipso*-C of Ph), 135.3 (CH=CHCH), 129.1 (CH=CHCH), 128.4, 128.0 (*o*- and *m*-C of Ph), 126.2 (*p*-C of Ph), 40.5 (CH=CHCH), 28.0 (CH₂Me), 11.7 (Me).

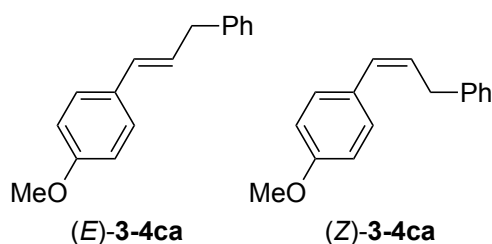


Mixture of (*E*)-(2-cyclohexylvinyl)benzene ((*E*)-**3-4am**)⁷⁴ and (*Z*)-(2-cyclohexylvinyl)benzene ((*Z*)-**3-4am**).⁷⁵ A colorless oil (36.8 mg, 0.198 mmol, 79% isolated yield based on the amount of **3-1a**, obtained as a mixture of $E/Z = 17/83$ determined by ¹H NMR; $E/Z = 17/83$ determined by quantitative measurement of GC-MS for crude mixture). (*E*)-**3-4am**: ¹H NMR (400 MHz, CDCl₃, δ): 7.34 (d, $J = 8.0$ Hz, 2H, *o*-H of Ph), 7.29 (pseudo t, $J = 7.6$ Hz, 2H, *m*-H of Ph), 7.20 (t, $J = 7.4$ Hz, 1H, *p*-H of Ph), 6.35 (d, $J = 15.8$ Hz, 1H, CH=CHCH), 6.18 (dd, $J = 15.8, 7.2$ Hz, 1H, CH=CHCH), 2.18–2.08 (m, 1H, CH=CHCH), 1.84–1.63 (m, 4H, Cy), 1.36–1.09 (m, 6H, Cy). ¹³C{¹H} NMR (100 MHz CDCl₃, δ): 138.0 (*ipso*-C of Ph), 136.8 (CH=CHCH), 128.4 (*m*-C of Ph), 127.2 (CH=CHCH), 126.7 (*p*-C of Ph), 125.9 (*o*-C of Ph), 41.1 (1-C of Cy), 32.9 (2- and 6-C of Cy), 26.2 (4-C of Cy), 25.7 (3- and 5-C of Cy). (*Z*)-**3-4am**: ¹H NMR (400 MHz, CDCl₃, δ): 7.33 (pseudo t, $J = 7.6$ Hz, 2H, *m*-H of Ph), 7.26 (d, $J = 7.2$ Hz, 2H, *o*-H of Ph), 7.22 (t, $J = 7.2$ Hz, 1H, *p*-H of Ph), 6.31 (d, $J = 11.3$ Hz, 1H, CH=CHCH), 5.49 (dd, $J = 11.3, 10.2$ Hz, 1H, CH=CHCH), 2.58 (pseudo q of t, $J = 10.6, 3.4$ Hz, 1H, CH=CHCH), 1.84–1.63 (m, 4H, Cy), 1.36–1.09 (m, 6H, Cy). ¹³C{¹H} NMR (100 MHz, CDCl₃, δ): 139.0 (CH=CHCH), 137.9 (*ipso*-C of Ph), 128.6, 128.2 (*o*- and *m*-C of Ph), 126.8 (*p*-C of Ph), 126.4 (CH=CHCH), 36.9 (1-C of Cy), 33.2 (2- and 6-C of Cy), 26.0 (4-C of Cy), 25.7 (3- and 5-C of Cy).

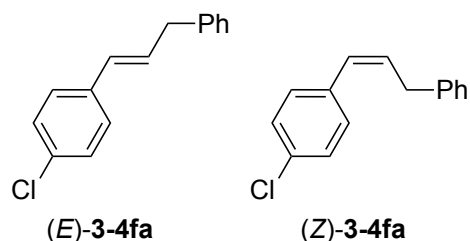


Mixture of (*E*)-1-methyl-4-(3-phenylprop-1-en-1-yl)benzene ((*E*)-**3-4ba**)⁷⁹ and (*Z*)-1-methyl-4-(3-phenylprop-1-en-1-yl)benzene ((*Z*)-**3-4ba**).⁸¹ A colorless oil (42.2 mg,

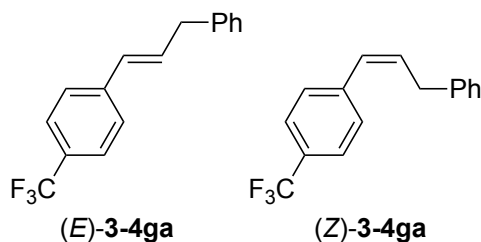
0.203 mmol, 81% isolated yield based on the amount of **3-1b**; $E/Z = 60/40$ determined by quantitative measurement of GC-MS for crude mixture). Further purification by column chromatography lead to the separation of pure (*E*)-**3-4ba** from (*Z*)-**3-4ba**. (*E*)-**3-4ba**: ^1H NMR (400 MHz, CDCl_3 , δ): 7.31 (pseudo t, $J = 8.0$ Hz, 2H, *m*-H of Ph), 7.27–7.19 (m, 5H, *o*-H of C_6H_4 and *o*- and *p*-H of Ph), 7.10 (d, $J = 6.8$ Hz, 2H, *m*-H of C_6H_4), 6.43 (d, $J = 15.8$ Hz, 1H, $\text{CH}=\text{CHCH}_2$), 6.31 (dt, $J = 15.8, 7.0$ Hz, 1H, $\text{CH}=\text{CHCH}_2$), 3.54 (d, $J = 7.0$ Hz, 2H, CH_2), 2.32 (s, 3H, Me). $^{13}\text{C}\{^1\text{H}\}$ NMR (100 MHz, CDCl_3 , δ): 140.3 (*ipso*-C of Ph), 136.8 (*p*-C of C_6H_4), 134.7 (*ipso*-C of C_6H_4), 130.9 ($\text{CH}=\text{CHCH}_2$), 129.2 (*m*-C of C_6H_4), 128.6 (*o*-C of Ph), 128.4 (*m*-C of Ph), 128.1 ($\text{CH}=\text{CHCH}_2$), 126.1 (*p*-C of Ph), 126.0 (*o*-C of C_6H_4), 39.3 (CH_2), 21.1 (Me). (*Z*)-**3-4ba**: ^1H NMR (400 MHz, CDCl_3 , δ): 7.33–7.08 (m, 9H, C_6H_4 and Ph), 6.56 (d, $J = 11.7$ Hz, 1H, $\text{CH}=\text{CHCH}_2$), 5.81 (dt, $J = 11.7$ Hz, 7.5 Hz, 1H, $\text{CH}=\text{CHCH}_2$), 3.68 (dd, $J = 7.5, 1.4$ Hz, 2H, CH_2), 2.35 (s, 3H, Me). $^{13}\text{C}\{^1\text{H}\}$ NMR (100 MHz, CDCl_3 , δ): 140.9 (*ipso*-C of Ph), 136.5 (*p*-C of C_6H_4), 134.3 (*ipso*-C of C_6H_4), 130.0 ($\text{CH}=\text{CHCH}_2$), 129.8 ($\text{CH}=\text{CHCH}_2$), 128.9, 128.6, 128.5, 128.3 (*o*- and *m*-C of C_6H_4 and Ph), 126.0 (*p*-C of Ph), 34.7 (CH_2), 21.2 (Me).



Mixture of (*E*)-1-methoxy-4-(3-phenylprop-1-en-1-yl)benzene ((*E*)-**3-4ca**)⁷⁹ and (*Z*)-1-methoxy-4-(3-phenylprop-1-en-1-yl)benzene ((*Z*)-**3-4ca**).⁷⁷ A colorless oil (43.7 mg, 0.195 mmol, 78% isolated yield based on the amount of **3-1c**, obtained as a mixture of $E/Z = 48/52$ determined by ^1H NMR; $E/Z = 50/50$ determined by quantitative measurement of GC-MS for crude mixture). (*E*)-**3-4ca**: ^1H NMR (400 MHz, CDCl_3 , δ): 7.34–7.18 (m, 7H, Ph and *o*-H of C_6H_4), 6.84 (d, $J = 8.8$ Hz, 2H, *m*-H of C_6H_4), 6.41 (d, $J = 15.6$ Hz, 1H, $\text{CH}=\text{CHCH}_2$), 6.22 (dt, $J = 15.6$ Hz, 6.8 Hz, 1H, $\text{CH}=\text{CHCH}_2$), 3.80 (s, 3H, Me), 3.53 (d, $J = 6.8$ Hz, 2H, CH_2). $^{13}\text{C}\{^1\text{H}\}$ NMR (100 MHz, CDCl_3 , δ): 158.8 (*p*-C of C_6H_4), 140.4 (*ipso*-C of Ph), 130.4 ($\text{CH}=\text{CHCH}_2$), 130.3 (*ipso*-C of C_6H_4), 128.6 (*o*-C of Ph), 128.4 (*m*-C of Ph), 127.2 (*o*-C of C_6H_4), 127.0 ($\text{CH}=\text{CHCH}_2$), 126.1 (*p*-C of Ph), 113.9 (*m*-C of C_6H_4), 55.3 (Me), 39.3 (CH_2). (*Z*)-**3-4ca**: ^1H NMR (400 MHz, CDCl_3 , δ): 7.34–7.18 (m, 7H, Ph and *o*-H of C_6H_4), 6.89 (d, $J = 8.4$ Hz, 2H, *m*-H of C_6H_4), 6.53 (d, $J = 11.6$ Hz, 1H, $\text{CH}=\text{CHCH}_2$), 5.77 (dt, $J = 11.6$ Hz, 7.3 Hz, 1H, $\text{CH}=\text{CHCH}_2$), 3.82 (s, 3H, Me), 3.68 (d, $J = 7.2$ Hz, 2H, CH_2). $^{13}\text{C}\{^1\text{H}\}$ NMR (100 MHz, CDCl_3 , δ): 158.4 (*p*-C of C_6H_4), 140.9 (*ipso*-C of Ph), 129.6 (*ipso*-C of C_6H_4), 129.4, 129.1 ($\text{CH}=\text{CH}$), 129.9, 128.5, 128.3 (*o*- and *m*-C of C_6H_4 and Ph with the resonance at 128.5 overlapping), 126.0 (*p*-C of Ph), 113.6 (*m*-C of C_6H_4), 55.3 (Me), 34.6 (CH_2).

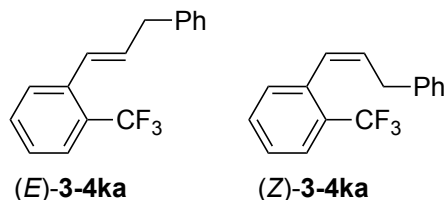


Mixture of (*E*)-1-chloro-4-(3-phenylprop-1-en-1-yl)benzene ((*E*)-3-4fa)⁸² and (*Z*)-1-chloro-4-(3-phenylprop-1-en-1-yl)benzene ((*Z*)-3-4fa). A colorless oil (43.5 mg, 0.190 mmol, 76% isolated yield based on the amount of **1f**, obtained as a mixture of *E/Z* = 56/44 determined by ¹H NMR; *E/Z* = 56/44 determined by quantitative measurement of GC-MS for crude mixture): (*E*)-3-4fa: ¹H NMR (400 MHz, CDCl₃, δ): 7.38–7.17 (m, 9H, aromatic H), 6.40 (d, *J* = 15.8 Hz, 2H, CH=CHCH₂), 6.34 (dt, *J* = 15.8, 6.3 Hz, 1H, CH=CHCH₂), 3.55 (d, *J* = 6.3 Hz, 2H, CH₂). ¹³C{¹H} NMR (100 MHz, CDCl₃, δ): 139.8 (*ipso*-C of Ph), 135.9 (*ipso*-C of C₆H₄), 132.6 (*p*-C of C₆H₄), 130.0, 129.8 (CH=CH), 128.6, 128.6 (*o*-C of C₆H₄ and Ph), 128.5 (*m*-C of Ph), 127.3 (*m*-C of C₆H₄), 126.3 (*p*-C of Ph), 39.3 (CH₂). (*Z*)-3-4fa: ¹H NMR (400 MHz, CDCl₃, δ): δ 7.38–7.17 (m, 9H), 6.54 (d, *J* = 11.4 Hz, 2H, CH=CHCH₂), 5.89 (dt, *J* = 11.4, 7.4 Hz, 1H, CH=CHCH₂), 3.64 (d, *J* = 7.4 Hz, 2H). ¹³C{¹H} NMR (100 MHz, CDCl₃, δ): 140.4 (*ipso*-C of Ph), 135.6 (*ipso*-C of C₆H₄), 132.6 (*p*-C of C₆H₄), 131.3, 128.8 (CH=CH), 130.0, 128.6, 128.4, 128.3 (*o*- and *m*- of C₆H₄ and Ph), 126.2 (*p*-C of Ph), 34.5 (CH₂).

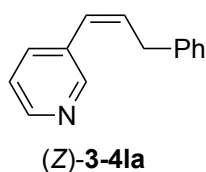


Mixture of (*E*)-1-(3-phenylprop-1-en-1-yl)-4-(trifluoromethyl)benzene ((*E*)-3-4ga) and (*Z*)-1-(3-phenylprop-1-en-1-yl)-4-(trifluoromethyl)benzene ((*Z*)-3-4ga).⁸³ A colorless oil (51.1 mg, 0.195 mmol, 79% isolated yield based on the amount of **1g**, obtained as a mixture of *E/Z* = 44/56 determined by ¹H NMR; obtained a mixture of *E/Z* = 49/51 determined by quantitative measurement of GC-MS for crude mixture). (*E*)-3-4ga: ¹H NMR (400 MHz, CDCl₃, δ): 7.54 (d, *J* = 8.4 Hz, 2H, *o*-H of C₆H₄), 7.44 (d, *J* = 8.0 Hz, 2H, *m*-H of C₆H₄), 7.36–7.29 (m, 2H, CH of Ph), 7.26–7.20 (m, 3H, CH of Ph), 6.49–6.46 (m, 2H, CH=CH), 3.58 (d, *J* = 8.0 Hz, 2H, CH₂). ¹³C{¹H} NMR (100 MHz, CDCl₃, δ): 140.9 (*ipso*-C of Ph), 139.5 (*ipso*-C of C₆H₄), 132.1 (CH=CHCH₂), 129.8 (CH=CHCH₂), 128.9 (q, ²*J*_{CF} = 30.7 Hz, *m*-C of C₆H₄), 128.7 (*o*-C of Ph), 128.6 (*m*-C of Ph), 126.3 (*o*-C of C₆H₄), 126.2 (*p*-C of Ph), 125.4 (q, *J* = 3.6 Hz, *m*-CH of C₆H₄), 124.2 (q, ¹*J*_{CF} = 272.2 Hz, CF₃), 39.3 (CH₂). ¹⁹F NMR (376 MHz, CDCl₃, δ): –65.6 (overlapping with (*Z*)-3-4ga). (*Z*)-3-4ga: ¹H NMR (400 MHz, CDCl₃, δ): 7.83–7.75 (m, 3H, CH of Ph), 7.60 (d, *J* = 8.0 Hz, *o*-H of C₆H₄, 2H), 7.32 (d, *J* = 8.0 Hz, 2H, *m*-H of C₆H₄), 7.36–7.29 (m, 2H, CH of Ph), 6.62 (d, *J* = 11.7 Hz, 1H, CH=CHCH₂), 6.00 (dt, *J* = 11.7, 7.8 Hz, 1H, CH=CHCH₂), 3.66 (dd, *J* = 7.6, 1.2 Hz, 2H, CH₂). ¹³C{¹H} NMR (100 MHz, CDCl₃, δ): 141.5 (*ipso*-C of Ph), 140.1 (*ipso*-C of C₆H₄),

132.7 (CH=CHCH₂), 128.9 (*o*-C of Ph), 128.8 (q, ²J_{CF} = 10.5 Hz, *m*-C of C₆H₄), 128.7 (CH=CHCH₂), 128.6 (*m*-C of Ph), 126.3 (*o*-C of C₆H₄), 126.2 (*p*-C of Ph), 125.2 (q, *J* = 3.8 Hz, *m*-CH of C₆H₄), 124.2 (q, ¹J_{CF} = 272.2 Hz, CF₃), 34.6 (CH₂). ¹⁹F NMR (376 MHz, CDCl₃, δ): -65.6 (overlapping with (*E*)-**3-4ga**).

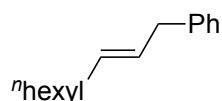


Mixture of (*E*)-1-(3-phenylprop-1-en-1-yl)-2-(trifluoromethyl)benzene ((*E*)-**3-4ka**) and (*Z*)-1-(3-phenylprop-1-en-1-yl)-2-(trifluoromethyl)benzene ((*Z*)-**3-4ka**) (new compounds). A colorless oil (51.8 mg, 0.198 mmol, 79% isolated yield based on the amount of **3-1k**; *E/Z* = 63/37 determined by quantitative measurement of GC-MS for crude mixture). Further purification by column chromatography lead to the separation of pure (*E*)-**3-4ka** and (*Z*)-**3-4ka**. (*E*)-**3-4ka**: HRMS-FAB (*m/z*): [M]⁺ calcd for C₁₆H₁₃F₃, 262.0969; found, 262.0960. ¹H NMR (400 MHz, CDCl₃, δ): 7.69 (d, *J* = 7.6 Hz, 1H, 3-H of C₆H₄), 7.50 (pseudo t, *J* = 7.6 Hz, 1H, 5-H of C₆H₄), 7.40–7.34 (m, 2H, 4- and 6-H of C₆H₄), 7.30 (pseudo tt, *J* = 7.4, 1.2 Hz, 2H, *m*-H of Ph), 7.21 (t of pseudo t, *J* = 7.2, 1.4 Hz, 1H, *p*-H of Ph), 7.18 (d, *J* = 7.2 Hz, 2H, *o*-H of Ph), 6.80 (d of pseudo q, *J* = 11.5, 1.0 Hz, 1H, CH=CHCH₂), 6.00 (dt, *J* = 11.5, 7.6 Hz, 1H, CH=CHCH₂), 3.47 (dd, *J* = 7.6, 1.0 Hz, 2H, CH₂). ¹³C{¹H} NMR (100 MHz, CDCl₃, δ): 140.2 (*ipso*-C of Ph), 135.9 (br, 1-C of C₆H₄), 132.5 (5-C of C₆H₄), 131.3 (CH=CHCH₂), 130.9 (CH=CHCH₂), 128.5 (q, ²J_{CF} = 18.3 Hz, 2-C of C₆H₄), 128.5 (*o*-C of Ph), 128.3 (*m*-C of Ph), 127.0, 126.9 (4- and 6-C of C₆H₄), 126.1 (*p*-C of Ph), 125.8 (q, ³J_{CF} = 5.4 Hz, 3-C of C₆H₄), 124.2 (q, ¹J_{CF} = 272.2 Hz, CF₃), 34.5 (CH₂). ¹⁹F NMR (376 MHz, CDCl₃, δ): -62.3. (*Z*)-**3-4ka**: ¹H NMR (400 MHz, CDCl₃, δ): 7.62, 7.60 (both d, *J* = 7.6 Hz, 1H each, 3- and 6-H of C₆H₄), 7.46 (pseudo t, *J* = 7.6 Hz, 1H, 5-H of C₆H₄), 7.35–7.28 (m, 3H, 4-H of C₆H₄ and *m*-H of Ph), 7.26–7.18 (m, 3H, *o*- and *p*-H of Ph), 6.86 (dd, *J* = 15.2, 1.2 Hz, 1H, CH=CHCH₂), 6.32 (dt, *J* = 15.2, 7.1 Hz, 1H, CH=CHCH₂), 3.59 (dd, *J* = 7.1, 1.2 Hz, 2H, CH₂). ¹³C{¹H} NMR (100 MHz, CDCl₃, δ): 139.6 (*ipso*-C of Ph), 136.6 (br, 1-C of C₆H₄), 133.5 (5-C of C₆H₄), 131.7 (CH=CHCH₂), 128.6, 128.5 (*o*- and *m*-C of Ph), 127.3 (CH=CHCH₂), 127.3 (q, ²J_{CF} = 21.4 Hz, 2-C of C₆H₄), 127.2 (4-C of C₆H₄), 126.8 (6-C of C₆H₄), 126.3 (*p*-C of Ph), 125.7 (q, ³J_{CF} = 6.4 Hz, 3-C of C₆H₄), 124.3 (q, ¹J_{CF} = 278.3 Hz, CF₃), 39.6 (CH₂). ¹⁹F NMR (376 MHz, CDCl₃, δ): -61.1.



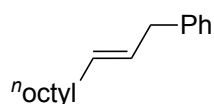
(*Z*)-3-(3-phenylprop-1-en-1-yl)pyridine ((*Z*)-**3-4la**) (new compound). A colorless oil (31.7 mg, 0.162 mmol, 65% isolated yield based on the amount of **3-1l**, obtained as a

pure *Z*-isomer; *E/Z* = 4/96 determined by quantitative measurement of GC-MS for crude mixture). HRMS–FAB (*m/z*): [*M* + *H*]⁺ calcd for C₁₄H₁₄N, 196.1126; found, 196.1127. ¹H NMR (400 MHz, CDCl₃, δ): 8.59 (d, *J* = 1.2 Hz, 1H, 2-H of C₅H₄N), 8.49 (dd, *J* = 4.0, 1.2 Hz, 1H, 6-H of C₅H₄N), 7.63 (d of pseudo t, *J* = 7.5, 1.9 Hz, 1H, 4-H of C₅H₄N), 7.31 (pseudo t, *J* = 7.6 Hz, 2H, *m*-H of Ph), 7.29 (dd, *J* = 7.5, 4.0 Hz, 1H, 5-H of C₅H₄N), 6.55 (dt, *J* = 11.7, 1.4 Hz, 1H, CH=CHCH₂), 6.02 (dt, *J* = 11.7, 7.6 Hz, 1H, CH=CHCH₂), 3.66 (dd, *J* = 7.6, 1.4 Hz, 2H, CH₂). ¹³C{¹H} NMR (100 MHz, CDCl₃, δ): 149.8 (6-C of C₅H₄N), 147.9 (2-C of C₅H₄N), 140.0 (*ipso*-C of Ph), 135.6, 133.0 (4-C of C₅H₄N and CH=CHCH₂), 132.8 (3-C of C₅H₄N), 128.6 (*o*-C of Ph), 128.2 (*m*-C of Ph), 126.3 (CH=CHCH₂), 126.2 (*p*-C of Ph), 123.1 (5-C of C₅H₄N), 34.5 (CH₂).



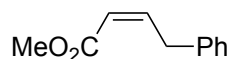
(*E*)-**3-4na**

(*E*)-non-2-en-1-ylbenzene ((*E*)-**3-4na**).³⁶ A colorless oil (35.4 mg, 0.174 mmol, 70% isolated yield based on the amount of **3-1n**, obtained as a pure *Z*-isomer; *E/Z* = 91/9 determined by quantitative measurement of GC-MS for crude mixture). ¹H NMR (400 MHz, CDCl₃, δ): 7.29 (pseudo tt, *J* = 7.2, 1.9 Hz, 2H, *m*-H of Ph), 7.21–7.15 (m, 3H, *o*- and *p*-H of Ph), 5.62–5.47 (m, 2H, CH=CH), 3.34 (d, *J* = 6.0 Hz, 2H, PhCH₂), 2.03 (q, *J* = 6.7 Hz, 2H, 1-CH₂ of *n*-hexyl), 1.44–1.23 (m, 8H, 2-, 3-, 4-, and 5-CH₂ of *n*-hexyl), 0.89 (t, *J* = 7.0 Hz, 3H, Me). ¹³C{¹H} NMR (CDCl₃, 100 MHz): δ 141.1 (*ipso*-C of Ph), 132.2 (CH=CHCH₂), 128.6 (CH=CHCH₂), 128.5 (*o*-C of Ph), 128.3 (*m*-C of Ph), 125.8 (*p*-C of Ph), 39.1 (CH₂Ph), 32.5 (1-CH₂ of *n*-hexyl), 31.7 (4-CH₂ of *n*-hexyl), 29.4 (2-CH₂ of *n*-hexyl), 28.9 (3-CH₂ of *n*-hexyl), 22.6 (5-CH₂ of *n*-hexyl), 14.1 (Me).



(*E*)-**3-4oa**

(*E*)-undec-2-en-1-ylbenzene ((*E*)-**3-4oa**) (new compound). A colorless oil (37.4 mg, 0.162 mmol, 65% isolated yield, based on the amount of **3-1o**, obtained as a pure *Z*-isomer; *E/Z* = 91/9 determined by quantitative measurement of GC-MS for crude mixture). HRMS–FAB (*m/z*): [*M*]⁺ calcd for C₁₇H₂₆, 230.2035; found, 230.2028. ¹H NMR (400 MHz, CDCl₃, δ): 7.29 (pseudo tt, *J* = 7.2, 2.0 Hz, 2H, *m*-H of Ph), 7.22–7.17 (m, 3H, *o*- and *p*-H of Ph), 5.61–5.47 (m, 2H, CH=CH), 3.34 (d, *J* = 6.0 Hz, 2H, PhCH₂), 2.03 (q, *J* = 6.8 Hz, 2H, 1-CH₂ of *n*-octyl), 1.42–1.22 (m, 12H, 2-, 3-, 4-, 5-, 6-, and 7-CH₂ of *n*-octyl), 0.89 (t, *J* = 7.0 Hz, 3H, Me). ¹³C{¹H} NMR (100 MHz, CDCl₃, δ): 141.1 (*ipso*-C of Ph), 132.2 (CH=CHCH₂), 128.6 (CH=CHCH₂), 128.5 (*o*-C of Ph), 128.3 (*m*-C of Ph), 125.8 (*p*-C of Ph), 39.1 (CH₂Ph), 32.5 (1-CH₂ of *n*-octyl), 31.9 (6-CH₂ of *n*-octyl), 29.5 (2- and 4-CH₂ of *n*-octyl, overlapping), 29.3 (3-CH₂ of *n*-octyl), 29.2 (5-CH₂ of *n*-octyl), 22.7 (7-CH₂ of *n*-octyl), 14.1 (Me).



(Z)-**3-4pa**

Methyl (Z)-4-phenylbut-2-enoate ((Z)-3-4pa**) (new compound).** A colorless oil (31.7 mg, 0.180 mmol, 72% isolated yield based on the amount of **3-1p**, obtained as a pure Z-isomer; already only Z-isomer determined by quantitative measurement of GC-MS for crude mixture). HRMS–FAB (m/z): $[M]^+$ calcd for $C_{11}H_{12}O_2$, 176.0837; found, 176.0840. 1H NMR (400 MHz, $CDCl_3$, δ): 7.31 (pseudo t, $J = 7.4$ Hz, 2H, *m*-H of Ph), 7.24 (t, $J = 7.2$ Hz, 1H, *p*-H of Ph), 7.17 (d, $J = 7.2$ Hz, 2H, *o*-H of Ph), 7.11 (dt, $J = 15.6, 6.9$ Hz, 1H, $CH=CHCH_2$), 5.82 (dt, $J = 15.6, 1.7$ Hz, 1H, $CH=CHCH_2$), 3.72 (s, 3H, Me), 3.53 (d, $J = 6.9$ Hz, 2H, CH_2). $^{13}C\{^1H\}$ NMR (100 MHz, $CDCl_3$, δ): 166.9 (CO_2), 147.6 ($CH=CHCH_2$), 137.6 (*ipso*-C of Ph), 128.8 (*o*-C of Ph), 128.7 (*m*-C of Ph), 126.7 (*p*-C of Ph), 121.9 ($CH=CHCH_2$), 51.5 (Me), 38.5 (CH_2).

3.4.4. Hydroalkylation Reactions of Internal Alkyne

In a 20 mL Schlenk flask were placed **3-6** (29.0 mg, 0.250 mmol), **3-2a** (128.8 mg, 0.375 mmol), *fac*-[Ir(Fppy)₃] (1.7 mg, 0.0022 mmol), and [NiCl₂(dtbbpy)] (10.0 mg, 0.025 mmol) or NiCl₂·6H₂O (5.8 mg, 0.024 mmol) under N₂, where THF (2.5 mL) was added at room temperature. The reaction flask was placed in an As One LTB-125 constant low temperature water bath set at 25 °C. The reaction was conducted for 24 h under irradiation from the bottom of the bath with an Aitech System TMN100×120–22WD 12 W white LED lamp (400 nm to 750 nm) at a distance of approximately 2 cm from the light source. The volatiles were then removed *in vacuo*, and the residue was purified by column chromatography (SiO₂) with *n*-hexane as an eluent to afford a mixture of ((Z)-but-2-ene-1,2-diyl)dibenzene ((Z)-**3-7**)/(E)-(2-methylprop-1-ene-1,3-diyl)dibenzene ((E)-**3-8**) (0.026 mmol (41% yield based on the amount of **6**) and 0.079 mmol (28% yield) in a ratio of 60/40, respectively, determined by 1H NMR) for [NiCl₂(dtbbpy)]-catalyzed reaction conditions, or a mixture of (Z)-**3-7**/(E)-**3-8**/(E)-**3-8** (0.010 mmol (3% yield), 0.079 mmol (23% yield), and 0.014 mmol (6% yield) in a ratio of 9/72/19, respectively, determined by 1H NMR) for NiCl₂·6H₂O-catalyzed reaction conditions, respectively (Scheme 3-4). (Z)-**3-7**:⁷⁹ 1H NMR (400 MHz, $CDCl_3$, δ): 7.36–7.17 (m, 10H, Ph), 5.56 (q, $J = 6.8$ Hz, 1H, MeCH), 3.65 (s, 2H, CH_2), 1.60 (d, $J = 6.8$ Hz, 3H, Me). (E)-**3-7**:^{84,85} 1H NMR (400 MHz, $CDCl_3$, δ): 7.36–7.17 (m, 10H, Ph), 6.38 (s, 1H, CH), 3.49 (s, 2H, CH_2), 1.81 (s, 3H, Me). (Z)-**3-8**:⁸¹ 1H NMR (400 MHz, $CDCl_3$, δ): 7.36–7.17 (m, 10H, Ph), 6.53 (s, 1H, PhCH), 3.62 (s, 2H, CH_2), 1.82 (s, 3H, Me).

3.4.5. Reactions in the Presence of TEMPO

In a 20 mL Schlenk flask were placed ethynylbenzene (**3-1a**) (25.5 mg, 0.250 mmol), diethyl 4-benzyl-2,6-dimethyl-1,4-dihydropyridine-3,5-dicarboxylate (**3-2a**) (128.8 mg, 0.375 mmol), (2,2,6,6-tetramethylpiperidin-1-yl)oxyl (TEMPO) (58.7 mg, 0.375 mmol), *fac*-[Ir(Fppy)₃] (1.7 mg, 0.0022 mmol), and [NiCl₂(dtbbpy)] (10.0 mg,

0.025 mmol) or $\text{NiCl}_2 \cdot 6\text{H}_2\text{O}$ (5.8 mg, 0.024 mmol) under N_2 , where THF (2.5 mL) was added at room temperature. The reaction flask was placed in an As One LTB-125 constant low temperature water bath set at 25 °C and was illuminated from the bottom of the bath with an Aitech System TMN100×120–22WD 12 W white LED lamp (400 nm to 750 nm) at a distance of approximately 2 cm from the light source for 24 h. The volatiles were removed in vacuo, and the crude yield of 1-(benzyloxy)-2,2,6,6-tetramethylpiperidine (**3-9a**)⁵⁰ (41% NMR yield in the presence of $[\text{NiCl}_2(\text{dtbbpy})]$ or 47% NMR yield in the presence of $\text{NiCl}_2 \cdot 6\text{H}_2\text{O}$ based on the amount of **3-1a**) was determined by ^1H NMR in CDCl_3 , where 1,1,2,2-tetrachloroethane (42.1 mg, 0.251 mmol) was added as an internal standard (Figure 3-1a).

3.4.6. Stern–Volmer Analysis

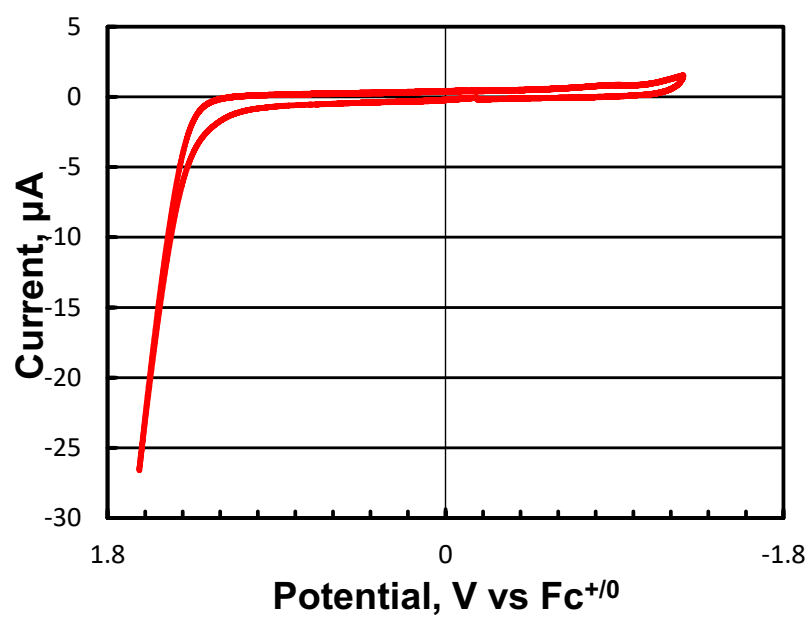
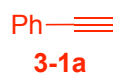
Luminescence quenching experiments for the THF solution of *fac*- $[\text{Ir}(\text{Fppy})_3]$ (2.0 $\mu\text{mol/L}$, prepared by stepwise dilutions of *fac*- $[\text{Ir}(\text{Fppy})_3]$ (1.5 mg, 2.0 μmol) with THF) with **3-1a** or **3-2a** in selected concentrations were performed on a Shimadzu RF-5300PC spectrophotometer, where the solutions containing *fac*- $[\text{Ir}(\text{Fppy})_3]$ and **3-1a** or **3-2a** were excited at $\lambda_{\text{max}} = 440$ nm, and emissions were measured at $\lambda = 570$ nm.

From the slopes (125.3 ± 6.9 for **3-1a** and 290.0 ± 6.2 for **3-2a**) obtained by the plot and the excited-state lifetime of *fac*- $[\text{Ir}(\text{Fppy})_3]$ ($\tau = 1.6$ μs),⁴⁷ the rate constants for the energy transfer of **3-1a** and the oxidation of **3-2a** were calculated to be at $k_{3-1a} = (7.8 \pm 0.4) \times 10^7 \text{ M}^{-1} \text{ s}^{-1}$ (**3-1a**) and $k_{3-2a} = (1.81 \pm 0.04) \times 10^8 \text{ M}^{-1} \text{ s}^{-1}$ (**3-2a**), respectively (Figure 3-1b).

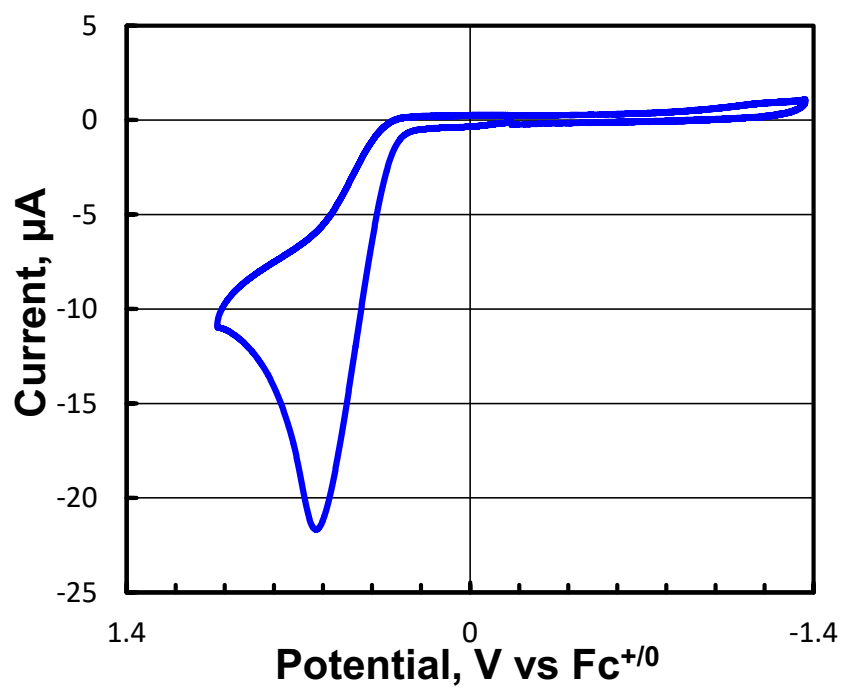
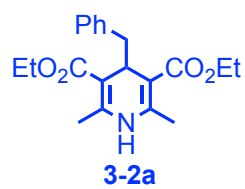
3.4.7. Cyclic Voltammetric Studies

Cyclic voltammograms were recorded on an ALS/Chi model 610C electrochemical analyzer in THF containing 1 mM of sample and 0.1 M of $n\text{Bu}_4\text{NPF}_6$ as a supporting electrolyte using glassy carbon working electrode and platinum wire counter electrode at a scan rate of 0.1 V/s at room temperature. All potentials were measured against Ag/AgNO_3 reference electrode (0.01 M AgNO_3 , 0.1 M $n\text{NBu}_4\text{ClO}_4$, MeCN) and converted to the values vs $\text{FeCp}_2^{+/0}$ ($\text{Cp} = \eta^5\text{-C}_5\text{H}_5$). The cyclic voltammograms of **3-1a**, **3-2a**, and *fac*- $[\text{Ir}(\text{Fppy})_3]$ in THF are shown in Figures 3-3.

a)



b)



c)

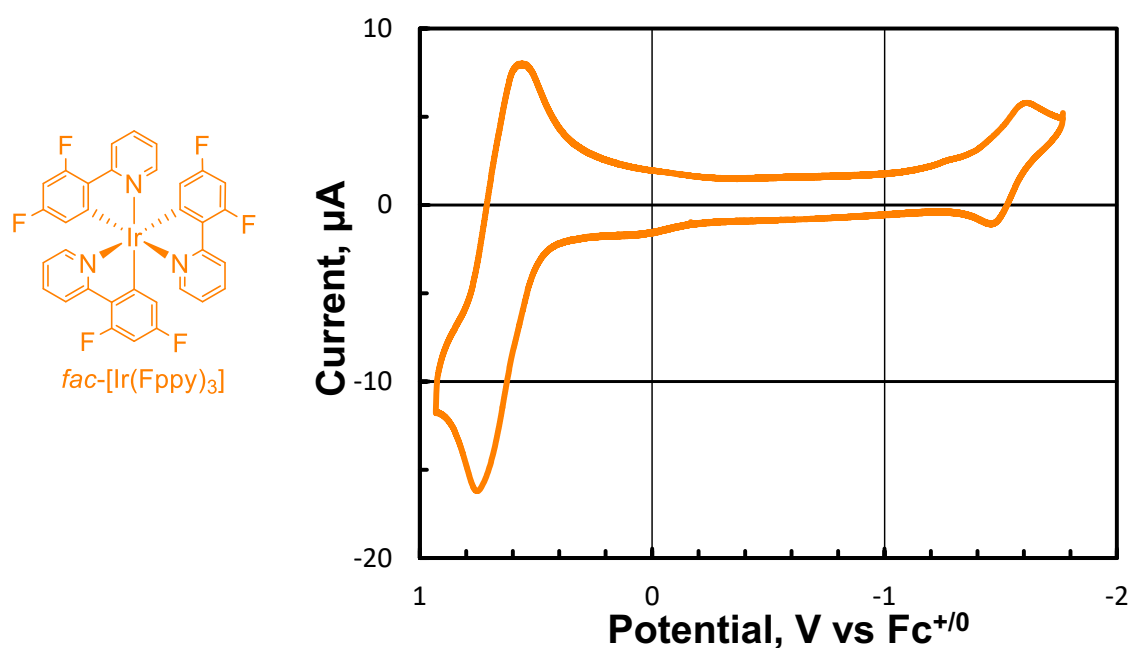


Figure 3-3. Cyclic Voltammetric Studies. (a) Cyclic voltammogram of **3-1a** in THF. No oxidation waves observed in THF at least less than +1.2 V vs $\text{FcCp}_2^{+/0}$. (b) Cyclic voltammogram of **3-2a** in THF. $E_{\text{pa}}(\mathbf{3-2a}/\mathbf{3-2a}^{+}) = +0.63$ V vs $\text{FcCp}_2^{+/0}$. (c) Cyclic voltammogram of *fac*-[Ir(Fppy)₃] in THF. $E_{1/2}(\text{Ir}/\text{Ir}^{-}) = -1.54$ V vs $\text{FcCp}_2^{+/0}$, $E_{1/2}(\text{Ir}/\text{Ir}^{+}) = +0.66$ V vs $\text{FcCp}_2^{+/0}$. Therefore, $E_{1/2}(\text{Ir}^{*}/\text{Ir}^{-}) = +0.67$ V vs $\text{FcCp}_2^{+/0}$, $E_{1/2}(\text{Ir}^{*}/\text{Ir}^{+}) = -1.55$ V vs $\text{FcCp}_2^{+/0}$, based on the emission energy of *fac*-[Ir(Fppy)₃] at 2.21 eV.⁴⁶

3.4.8. Light On/Off Experiments

In a 20 mL Schlenk flask were placed ethynylbenzene (**3-1a**) (25.5 mg, 0.250 mmol), diethyl 4-benzyl-2,6-dimethyl-1,4-dihydropyridine-3,5-dicarboxylate (**3-2a**) (128.8 mg, 0.375 mmol), *fac*-[Ir(Fppy)₃] (1.7 mg, 0.0022 mmol), and [NiCl₂(dtbbpy)] (10.0 mg, 0.025 mmol) or NiCl₂·6H₂O (5.8 mg, 0.024 mmol) under N₂, where THF (2.5 mL) was added at room temperature. The reaction flask was placed in an As One LTB-125 constant low temperature water bath set at 25 °C. The reaction was conducted for 16 h under alternating periods of (1) irradiation from the bottom of the bath with an Aitech System TMN100×120–22WD 12 W white LED lamp (400 nm to 750 nm) at a distance of approximately 2 cm from the light source, and (2) darkness with the reaction vessel wrapped with aluminum foil, where yields of **3-3aa** and **3-4aa** were determined every 2 hours by quantitative measurements of GC-MS recorded on a Shimadzu GCMS-QP2010 PLUS instrument, where *n*-octane was added as an internal standard (Figure 3-2a).

3.4.9. Determination of Quantum Yields

In a 20 mL Schlenk flask were **3-1a** (25.5 mg, 0.250 mmol), **3-2a** (128.8 mg, 0.375 mmol), *fac*-[Ir(Fppy)₃] (1.7 mg, 0.0022 mmol), and [NiCl₂(dtbbpy)] (10.0 mg, 0.025 mmol) under N₂, where THF (2.5 mL) was added at room temperature. The reaction flask was illuminated from the side with an Ushio SX-U1251HQ ultrahigh pressure 250 W Hg lamp equipped with a 440-nm band pass filter (Kenko B440) at a distance of approximately 0 cm from the light source for 9.0 h. The volatiles were removed in vacuo, and the crude yield of **3-3aa** (0.0850 mmol, 34% NMR yield based on the amount of **3-1a**) was determined by ¹H NMR in CDCl₃, where 1,1,2,2-tetrachloroethane (42.0 mg, 0.250 mmol) was added as an internal standard. Independently, the yields of **3-3aa** were determined by terminating the reactions at 4.0 and 6.5 h, which clarified a zero-order reaction rate at $(2.62 \pm 0.07) \times 10^{-9} \text{ mol s}^{-1}$. The irradiated light intensity to a 2.5 mL solution in 50-mL Schlenk was estimated to be $3.50 \times 10^{-8} \text{ E s}^{-1}$ at 440 nm by using K₃[Fe(C₂O₄)₃] as a chemical actinometer.⁵⁷ Thus, the quantum yield of the photoredox- and nickel-catalyzed reaction of **3-1a** with **3-2a** to afford Markovnikov-type product **3-3aa** is given as $\Phi = 0.075 \pm 0.002$.

Similarly, reaction rate and quantum yield of the reaction to afford **3-4aa** in the presence of NiCl₂·6H₂O in place of [NiCl₂(dtbbpy)] are given as $k = (1.92 \pm 0.08) \times 10^{-9} \text{ mol s}^{-1}$ and $\Phi_{E+Z} = 0.055 \pm 0.002$, respectively.

By using the reaction rates ($k_E = (6.9 \pm 0.2) \times 10^{-7} \text{ M}^{-1} \text{ s}^{-1}$ and $k_Z = (3.2 \pm 0.1) \times 10^{-7} \text{ M}^{-1} \text{ s}^{-1}$ under white LED light irradiation), quantum yields for the formation of (*E*)-**3-4aa** and (*Z*)-**3-4aa** can be given as $\Phi_E = 0.038 \pm 0.003$ and $\Phi_Z = 0.017 \pm 0.002$, respectively (Figure 3-2b).

3.4.10. Time Profile Experiments for *anti*-Markovnikov-type Reaction

In a 20 mL Schlenk flask were placed **3-1a** (25.5 mg, 0.250 mmol), **3-2a** (128.8

mg, 0.375mmol), *fac*-[Ir(Fppy)₃] (1.7 mg, 0.0022 mmol), NiCl₂·6H₂O (5.8 mg, 0.024 mmol), and methyl 4-methoxybenzoate (41.5 mg, 0.250 mmol, added as an internal standard) under N₂, where THF (2.5 mL) was added at room temperature. The reaction flask was placed in an As One LTB-125 constant low temperature water bath set at 25 °C and was illuminated from the bottom of the bath with an Aitech System TMN100×120–22WD 12 W white LED lamp (400 nm to 750 nm) at a distance of approximately 2 cm from the light source for 72 h. Yields of (*E*)-**3-4aa** and (*Z*)-**3-4aa** at selected times were determined by quantitative measurements of GC-MS.

Suppose that the formation of both (*E*)-**3-4aa** and (*Z*)-**3-4aa** from the reaction of **3-1a** with **3-2a** follows zeroth order kinetics (reaction rates: k_E and k_Z in M⁻¹ s⁻¹) and that *E* to *Z* isomerization from (*E*)-**3-4aa** to (*Z*)-**3-4aa** follows first order kinetics (reaction rates k_{E-to-Z} in s⁻¹) dependent on the concentration of (*E*)-**3-4aa**, concentration of (*E*)-**3-4aa** (C_E in M) and (*Z*)-**3-4aa** (C_Z in M) during the period for the reaction of **3-1a** with **3-2a** (time: $t_0 < t < t_1$ in s, where t_0 is the end of an induction period and t_1 is the turning point in time when **2a** is completely consumed) can be given as follows:

$$C_E = \frac{k_E}{k_{E-to-Z}} [1 - \exp\{-k_{E-to-Z}(t - t_0)\}]$$

$$C_Z = (k_E + k_Z)(t - t_0) - \frac{k_E}{k_{E-to-Z}} [1 - \exp\{-k_{E-to-Z}(t - t_0)\}]$$

After **3-2a** is consumed ($t > t_1$), only *E* to *Z* isomerization that follows first order kinetics occurs. Reaction rates can be calculated by using least square methods as follows:

$$k_E = (6.9 \pm 0.2) \times 10^{-7} \text{ M}^{-1} \text{ s}^{-1}$$

$$k_Z = (3.2 \pm 0.1) \times 10^{-7} \text{ M}^{-1} \text{ s}^{-1}$$

$$k_{E-to-Z} = (6.2 \pm 0.3) \times 10^{-6} \text{ s}^{-1}$$

with an induction period of $t_0 = 5139.9$ s (1.4 h) and a turning point of $t_1 = 87959.4$ s (24.4 h) (Figure 3-2b).

3.4.11. *E*-to-*Z* Isomerizaion Reaction

In a 20 mL Schlenk flask were placed isolated (*E*)-**3-4aa** (48.6 mg, 0.250 mmol), *fac*-[Ir(Fppy)₃] (1.7 mg, 0.0022 mmol), NiCl₂·6H₂O (5.8 mg, 0.024 mmol), and methyl 4-methoxybenzoate (41.5 mg, 0.250 mmol, added as an internal standard) under N₂, where THF (2.5 mL) was added at room temperature. The reaction flask was placed in an As One LTB-125 constant low temperature water bath set at 25 °C and was illuminated from the bottom of the bath with an Aitech System TMN100×120–22WD 12 W white LED lamp (400 nm to 750 nm) at a distance of approximately 2 cm from the light source for 24 h. Yield of (*Z*)-**3-4aa** was determined by quantitative measurements of GC-MS.

Table 3-2. Reaction Conditions for *E*-to-*Z* Isomerization^a

$(E)\text{-4aa} \xrightarrow[\text{THF, 25 } ^\circ\text{C, 24 h, visible light}]{\text{fac-[Ir(Fppy)}_3\text{] (1 mol\%), NiCl}_2\cdot 6\text{H}_2\text{O (10 mol\%)}} (Z)\text{-4aa}$

entry	reaction conditions	yield of (Z)-4aa (%) ^b
1	Without NiCl ₂ ·6H ₂ O	81%
2	Without <i>fac</i> -[Ir(Fppy) ₃]	n.d. ^c
3	Without NiCl ₂ ·6H ₂ O and <i>fac</i> -[Ir(Fppy) ₃]	n.d.
4	Without NiCl ₂ ·6H ₂ O and visible light	n.d.
5	Without <i>fac</i> -[Ir(Fppy) ₃] and visible light	n.d.

^aReactions of (*E*)-4aa (0.25 mmol) was carried out in different conditions in THF (2.5 mL) at 25 °C for 24 h. ^bIsolated yield. ^cNot detected by GC-MS.

3.4.12. Preparation of [NiCl(CH₂Ph)(dtbbpy)] (benzylchlorido(4,4'-di-*tert*-butyl-2,2'-bipyridine-κ²N,N')nickel(II)) (3-10a)

In a 20 mL Schlenk flask were placed [Ni(cod)₂] (277.1 mg, 1.01 mmol) and dtbbpy (269.0 mg, 1.00 mmol), where THF (5.0 mL) was added at room temperature in an Ar glovebox. The suspension was stirred at room temperature for 8 h, then benzyl chloride (126.6 mg, 1.00 mmol) was added dropwise. After the mixture was stirred at room temperature for additional 8 h, the solvent was removed in vacuo. The residue was washed with Et₂O (5 mL × 3) and dried in vacuo. The residue was recrystallized from THF (5 mL)–*n*-hexane (15 mL) to afford dark purple crystals of **3-10a**·0.5C₆H₁₄ suitable for single crystal X-ray diffraction analysis. The obtained crystals were efflorescent and further lost *n*-hexane by dryness in vacuo to afford **3-10a** as a dark purple powder (190.5 mg, 0.42 mmol, 42% isolated yield based on the amount of benzyl chloride) (Scheme 3-5a). ¹H NMR (400 MHz, CD₂Cl₂, δ): 8.91 (d, *J* = 5.8 Hz, 2H, 3,3'-H of dtbbpy), 7.77 (d, *J* = 2.1 Hz, 2H, 6,6'-H of dtbbpy), 7.55 (d, *J* = 7.2 Hz, 2H, *o*-H of Ph), 7.45 (dd, *J* = 5.8, 2.1 Hz, 2H, 5,5'-H of dtbbpy), 7.06 (t, *J* = 7.2 Hz, 1H, *p*-H of Ph), 7.00 (pseudo t, *J* = 7.4 Hz, 2H, *m*-H of Ph), 2.49 (s, 2H, CH₂), 1.38 (s, 18H, ^{*t*}Bu). Anal. Calcd for C₂₅H₃₁ClN₂Ni: C, 66.19; H, 6.89; N, 6.17. Found: C, 65.91; H, 6.72; N, 6.23. ESI-TOFMS: (*m/z*): [M – Cl]⁺ calcd for C₂₅H₃₁N₂Ni, 417.23. found, 417.26.

3.4.13. Stoichiometric Reaction of [NiCl(CH₂Ph)(dtbbpy)] to Afford Markovnikov-type Product

In a 20 mL Schlenk flask were placed **3-10a** (45.1 mg, 0.100 mmol), **3-1a** (10.1 mg, 0.099 mmol), ethyl 2,6-dimethyl-1,4-dihydropyridine-3,5-dicarboxylate (25.2 mg, 0.100 mmol) and *fac*-[Ir(Fppy)₃] (1.0 mg, 0.0013 mmol), where THF (2.0 mL) was added at room temperature in an Ar glove box. The reaction flask was taken outside the glove box, placed in an As One LTB-125 constant low temperature water bath set at 25 °C, and was illuminated from the bottom of the bath with an Aitech System TMN100×120–22WD 12 W white LED lamp (400 nm to 750 nm) at a distance of

approximately 2 cm from the light source for 24 h. The volatiles were removed *in vacuo*, and the residue was purified by column chromatography (SiO₂) with *n*-hexane as an eluent to afford **3-3aa** as a colorless oil (6.6 mg, 0.034 mmol, 34% yield based on the amount of **3-1a**) (Scheme 3-5b).

3.4.14. X-ray Crystallographic Study of [NiCl(CH₂Ph)(dtbbpy)] (**3-10a**)

Diffraction data for a crystal of **10a**·0.5C₆H₁₄ were collected for the 2 θ range of 3.6° to 62.2° at –180 °C on a Rigaku XtaLAB Synergy-S diffractometer equipped with a HyPix-6000HE Hybrid Photon Counting (HPC) detector and VariMax optics using multi-layer mirror monochromated Mo-K α (λ = 0.71073 Å) radiation, and VariMax optics. Intensity data were corrected for Lorentz and polarization effect and for empirical absorptions (CrysAlisPro),⁸⁶ while structure solutions and refinements were carried out by using CrystalStructure package.⁸⁷ Positions of non-hydrogen atoms were determined by direct methods (SHELXT Version 2014/5),⁸⁸ and subsequent Fourier syntheses (SHELXL Version 2016/6),⁸⁹ and were refined on F_o^2 with all the unique reflections by full-matrix least squares with anisotropic thermal parameters. All the hydrogen atoms were placed at the calculated positions with fixed isotropic parameters. Anomalous dispersion effects were included in F_c ,⁹⁰ and mass attenuation coefficients, values for $\Delta f'$ and $\Delta f''$, and neutral atom scattering factors were taken from references.⁹¹⁻⁹³ Details of the crystal and data collection parameters of **3-10a**·0.5C₆H₁₄ are summarized in Table 3-3. ORTEP drawing of **3-10a** is shown in Figure 3-4.

Table 3-3. Crystallographic Data for **3-10a**·0.5C₆H₁₄

compound	3-10a·0.5C ₆ H ₁₄
chemical formula	C ₂₈ H ₃₈ ClN ₂ Ni
CCDC number	2153992
formula weight	496.77
crystal size, mm ³	0.280 × 0.113 × 0.043
crystal color, habit	dark brown, block
temperature, °C	−180
crystal system	monoclinic
space group	<i>P</i> 2 ₁ / <i>c</i> (no. 14)
<i>a</i> , Å	11.6808(3)
<i>b</i> , Å	17.5338(5)
<i>c</i> , Å	12.8063(3)
α, deg	90
β, deg	105.902(3)
γ, deg	90
<i>V</i> , Å ³	2522.47(12)
<i>Z</i>	4
<i>d</i> _{calcd} , g, cm ^{−3}	1.308
<i>F</i> (000)	1068
μ, cm ^{−1}	8.932
transmission factors range	0.934 – 0.962
number of measured reflections	19448
number of unique reflections	6488
number of refined parameters	296
<i>R</i> _{int}	0.0489
<i>R</i> 1 (<i>I</i> > 2 σ(<i>I</i>)) ^a	0.0444
<i>wR</i> 2 (all data) ^b	0.0824
GOF ^c	1.000
maximum residual peak / hole, e Å ^{−3}	+0.54 / −0.32

^a $R1 = \sum ||F_o| - |F_c|| / \sum |F_o|$. ^b $wR2 = [\sum \{w(F_o^2 - F_c^2)^2\} / \sum w(F_o^2)^2]^{1/2}$, $w = 1/[\sigma^2(F_o^2) + rP]$, $P = (\text{Max}(F_o^2, 0) + 2 F_c^2)/3$ [$r = 3.53$]. ^c $\text{GOF} = [\sum w(F_o^2 - F_c^2)^2 / (N_o - N_{\text{params}})]^{1/2}$.

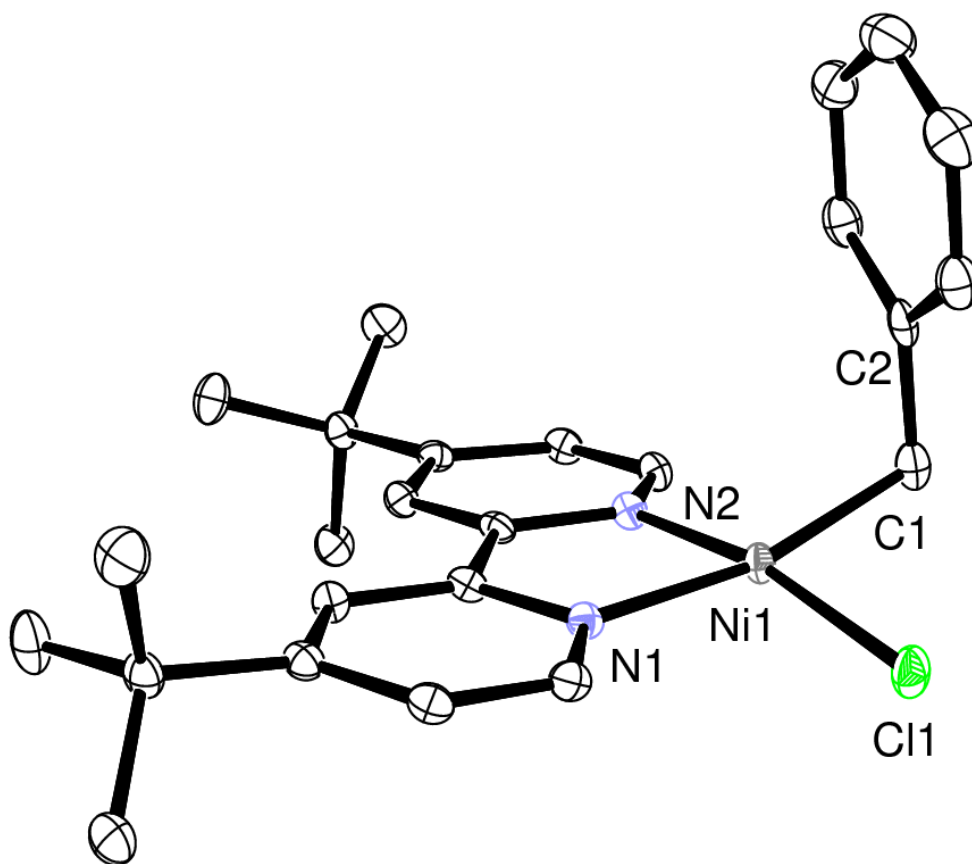


Figure 3-4. ORTEP drawing of **3-10a**. Thermal ellipsoids are drawn at the 50% probability level. Hydrogen atoms as well as *n*-hexane molecules are omitted for clarity. Selected bond lengths (Å) and angles (°): Ni(1)–Cl(1): 2.1976(6), Ni(1)–N(1): 1.9913(16), Ni(1)–N(2): 1.9249(17), Ni(1)–C(1): 1.9638(19), C(1)–C(2): 1.483(3); N(1)–Ni(1)–Cl(1): 94.46(5), N(2)–Ni(1)–C(1): 168.80(5), C(1)–Ni(1)–Cl(1): 89.74(6), N(2)–Ni(1)–N(1): 82.21(7), C(1)–Ni(1)–N(1): 166.15(8), N(2)–Ni(1)–C(1): 96.00 (8), C(2)–C(1)–Ni(1): 103.40(13). Geometry index:⁹⁴ $\tau_4 = 0.18$ (square planar).

3.5. References

- (1) Lappin, G. R.; Nemec, L. H.; Sauer, J. D.; Wagner, J. D. in *Kirk-Othmer Encyclopedia of Chemical Technology*, 5th ed., Vol. 17 (Ed.: Kirk-Othmer), John Wiley & Sons, Hoboken, **2005**, pp. 709–728.
- (2) (a) *Alkenes (Sci. Synth. 47b)* (Ed.: de Meijere, A.), Georg Thieme, Stuttgart, **2010**. (b) *Stereoselective Alkene Synthesis (Top. Curr. Chem. 327)* (Ed.: Wang, J.), Springer, Heidelberg, **2012**.
- (3) Recent reviews containing the preparation of alkenes from alkynes by addition reactions: (a) Negishi, E.; Wang, G. *Sci. Synth.* **2010**, 47b, 909–970. (b) Negishi, E.; Wang, G. *Sci. Synth.* **2010**, 47b, 971–1016. (c) Wille, U. *Chem. Rev.* **2013**, 113, 813–853. (d) Boyarskiy, V. P.; Ryabukhim, D. S.; Bokach, N. A.; Vasilyev, A. V. *Chem. Rev.* **2016**, 116, 5894–5986. (e) Fernández, D. F.; Mascareñas, J. L.; López, F. *Chem. Soc. Rev.* **2020**, 49, 7378–7405.
- (4) (a) Miller, J. A.; Negishi, E. *Tetrahedron Lett.* **1984**, 25, 5863–5866. (b) Wakamatsu, T.; Nagao, K.; Ohmiya, H.; Sawamura, M. *Beilstein J. Org. Chem.* **2015**, 11, 2444–2450. (c) Liu, H.; Fu, Z.; Gao, S.; Huang, Y.; Lin, A.; Yao, H. *Adv. Synth. Catal.* **2018**, 360, 3171–3175.
- (5) (a) Lu, X.-Y.; Hong, M.-L.; Zhou, H.-P.; Wang, Y.; Wang, J.-Y.; Ge, X.-T. *Chem. Commun.* **2018**, 54, 4417–4420. (b) Lu, X.-Y.; Li, J.-S.; Hong, M.-L.; Wang, J.-Y.; Ma, W.-J. *Tetrahedron* **2018**, 74, 6979. (c) Zhu, Z.-F.; Tu, J.-L.; Liu, F. *Chem. Commun.* **2019**, 55, 11478–11481. (d) Lu, X.-Y.; Liu, C.-C.; Jiang, R.-C.; Yan, L.-Y.; Liu, Q.-L.; Wang, Q.-Q.; Li, J.-M. *Chem. Commun.* **2020**, 56, 14191–14194.
- (6) Ding, H.-P.; Fan, X.-Z.; Chen, Z.-H.; Xu, Q.-H.; Wu, J. *J. Am. Chem. Soc.* **2017**, 139, 13579–13584.
- (7) (a) Go, S. Y.; Lee, G. S.; Hong, S. H. *Org. Lett.* **2018**, 20, 4691–4694. (b) Adak, T.; Hoffmann, M.; Witzel, S.; Rudolph, M.; Dreuw, A.; Hashmi, A. S. K. *Chem. Eur. J.* **2020**, 26, 15573–15580.
- (8) (a) Sabarre, A.; Love, J. *Org. Lett.* **2008**, 10, 3941–3944. (b) DeBergh, J. R.; Spivey, K. M.; Ready, J. M. *J. Am. Chem. Soc.* **2008**, 130, 7828–7829. (c) Lu, X.-Y.; Liu, J.-H.; Lu, X.; Zhang, Z.-Q.; Gong, T.-J.; Xiao, B.; Fu, Y. *Chem. Commun.* **2016**, 52, 5324–5327. (d) Yu, L.; Lv, L.; Qiu, Z.; Chen, Z.; Tan, Z.; Liang, Y.-F.; Li, C.-J. *Angew. Chem. Int. Ed.* **2020**, 59, 14009–14013.
- (9) Till, N. A.; Smith, R. T.; MacMillan, D. W. C. *J. Am. Chem. Soc.* **2018**, 140, 5701–5705.
- (10) Zhao, X.; Zhu, S.; Qing, F.; Chu, L. *Chem. Commun.* **2021**, 57, 9414–9417.
- (11) Zhao, T.-T.; Yu, W.-L.; Feng, Z.-T.; Qin, H.-N.; Zheng, H.; Xu, P.-F. *Chem. Commun.* **2022**, 58, 1171–1174.
- (12) (a) Huang, L.; Cheng, K.; Yao, B.; Zhao, J.; Zhang, Y. *Synthesis* **2009**, 3504–3510. (b) Chen, L.; Yang, J.; Li, L.; Weng, Z.; Kang, Q. *Tetrahedron Lett.* **2014**, 55, 6096–6100. (c) Uehling, M. R.; Suess, A. M.; Lalic, G. *J. Am. Chem. Soc.* **2015**, 137, 1424–1427. (d) Cheung, C. W.; Zhurkin, F. E.; Hu, X. *J. Am. Chem. Soc.* **2015**, 137, 4932–4935. (e) Suess, A. M.; Uehling, M. R.; Kaminsky, W.; Lalic, G. *J. Am. Chem. Soc.* **2015**, 137, 7747–7753. (f) Suess, A. M.; Lalic, G. *Synlett* **2016**, 27, 1165–1174. (g)

Mailing, M.; Hazra, A.; Armstrong, M. K.; Lalic, G. *J. Am. Chem. Soc.* **2017**, *139*, 6969–6977. (h) Nakamura, K.; Nishikata, T. *ACS Catal.* **2017**, *7*, 1049–1052. (i) Hazra, A.; Chen, J.; Lalic, G. *J. Am. Chem. Soc.* **2019**, *141*, 12464–12469. (j) Lee, M. T.; Goodstein, M. B.; Lalic, G. *J. Am. Chem. Soc.* **2019**, *141*, 17086–17091. (k) Hu, L.; Gao, H.; Hu, Y.; Lv, X.; Wu, Y.-B.; Lu, G. *Chem. Commun.* **2021**, *57*, 6412–6415. (l) Hazra, A.; Kephart, J. A.; Velian, A.; Lalic, G. *J. Am. Chem. Soc.* **2021**, *143*, 7903–7908. (m) Lee, M. T.; Lalic, G. *J. Am. Chem. Soc.* **2021**, *143*, 16663–16672.

(13)(a) Li, J.; Zhang, J.; Tan, H.; Wang, D. Z. *Org. Lett.* **2015**, *17*, 2522–2525. (b) Mastandrea, M. M.; Cañellas, S.; Caldentey, X.; Pericàs, M. A. *ACS Catal.* **2020**, *10*, 6402–6408.

(14) Dai, G.-L.; Lai, S.-Z.; Luo, Z.; Tang, Z.-Y. *Org. Lett.* **2019**, *21*, 2269–2272.

(15) Li, Y.; Ge, L.; Qian, B.; Babu, K. R.; Bao, H. *Tetrahedron Lett.* **2016**, *57*, 5677–5680.

(16) Yue, H.; Zhu, C.; Kancherla, R.; Liu, F.; Rueping, M. *Angew. Chem. Int. Ed.* **2020**, *59*, 5738–5746.

(17) Lai, S.-Z.; Yang, Y.-M.; Xu, H.; Tang, Z.-Y.; Luo, Z. *J. Org. Chem.* **2020**, *85*, 15638–15644.

(18) Recent reviews on photoredox catalysis: (a) Koike, A.; Akita, M. *Inorg. Chem. Front.* **2014**, *1*, 562–576. (b) Shaw, M. H.; Twilton, J.; MacMillan, D. W. C. *J. Org. Chem.* **2016**, *81*, 6898–6926. (c) Glaser, F.; Kerzig, C.; Wegner, O. S. *Angew. Chem. Int. Ed.* **2020**, *59*, 10266–10284. (d) Bell, J. D.; Murphy, J. A. *Chem. Soc. Rev.* **2021**, *50*, 9540–9685.

(19) Recent review on photocatalytic functionalization of alkynes: Chalotra, N.; Kumar, J.; Naqvi, T.; Shah, B. A. *Chem. Commun.* **2021**, *57*, 11285–11300.

(20) Recent reviews on dual photoredox catalysis: (a) Prier, C. K.; Rankic, F. A.; MacMillan, D. W. C. *Chem. Rev.* **2013**, *113*, 5322–5363. (b) Angnes, R. A.; Li, Z.; Correia, C. R. D.; Hammond, G. B. *Org. Biomol. Chem.* **2015**, *13*, 9152–9167. (c) Glaser, F.; Kerzig, C.; Wenger, O. S. *Angew. Chem. Int. Ed.* **2020**, *59*, 10266–10284. (d) Mastandrea, M. M.; Pericàs, M. A. *Eur. J. Inorg. Chem.* **2021**, 3421–3431.

(21) Recent reviews on cooperative photoredox and nickel catalysis: (a) Zuo, Z.; Ahneman, D. T.; Chu, L.; Terrett, J. A.; Doyle, A. G.; MacMillan, D. W. C. *Science* **2014**, *345*, 437–440. (b) Vila, C. *ChemCatChem* **2015**, *7*, 1790–1793. (c) Gui, Y.-Y.; Sun, L.; Lu, Z.-P.; Yu, D.-G. *Org. Chem. Front.* **2016**, *3*, 522–526. (d) Cavalcanti, L. N.; Molander, G. A. *Top. Curr. Chem.* **2016**, *374*, 39. (e) Luo, J.; Zhang, J. *ACS Catal.* **2016**, *6*, 873–877. (f) Börjesson, M.; Tortajada, A.; Martin, R. *Chem.* **2019**, *5*, 254–262. (g) Milligan, J. A.; Phelan, J. P.; Badir, S. O.; Molander, G. A. *Angew. Chem., Int. Ed.* **2019**, *58*, 6152–6163. (h) Zhu, C.; Yue, H.; Chu, L.; Rueping, M. *Chem. Sci.* **2020**, *11*, 4051–4064. (i) Badir, S. O.; Molander, G. A. *Chem.* **2020**, *6*, 1327–1339. (j) Zhu, C.; Yue, H.; Jia, J.; Rueping, M. *Angew. Chem. Int. Ed.* **2021**, *60*, 17810–17831. (k) Mantry, L.; Maayuri, R.; Kumar, V.; Gandeepan, P. *Beilstein J. Org. Chem.* **2021**, *17*, 2209–2259.

(22) Recent reviews on ligand-controlled selectivity: (a) Yamaguchi, M.; Manabe, K. *Top. Curr. Chem.* **2016**, *372*, 1–25. (b) Peng, J.-B.; Wu, X.-F. *Angew. Chem. Int. Ed.* **2018**, *57*, 1152–1160. (c) Gu, Y.; Lu, C.; Gu, Y.; Shen, Q.; *Chin. J. Chem.* **2018**, *36*, 55–

58. (d) Durand, D. J.; Fey, N. *Chem. Rev.* **2019**, *119*, 6561–6594. (e) Cao, M.; Xie, H. *Chim. Chem. Lett.* **2021**, *32*, 319–327.
- (23)(a) Ohmura, T.; Oshima, K.; Taniguchi, H.; Sugimoto, M. *J. Am. Chem. Soc.* **2010**, *132*, 12194–12196. (b) Zhao, M.; Shan, C.-C.; Wang, Z.-L.; Yang, C.; Fu, Y.; Xu, Y.-H. *Org. Lett.* **2019**, *21*, 6016–6029.
- (24) González-Rodríguez, C.; Pawley, R. J.; Chaplin, A. B.; Thompson, A. L.; Weller, A. S.; Willis, M. C. *Angew. Chem. Int. Ed.* **2011**, *50*, 5134–5138.
- (25) Di Giuseppe, A.; Castarlenas, R.; Pérez-Torrente, J. J.; Crucianelli, M.; Polo, V.; Sancho, R.; Lahoz, F. J.; Oro, L. A. *J. Am. Chem. Soc.* **2012**, *134*, 8171–8183.
- (26)(a) Ding, S.; Song, L.-J.; Chung, L. W.; Zhang, X.; Sun, J.; Wu, Y.-D. *J. Am. Chem. Soc.* **2013**, *135*, 13835–13842. (b) Hu, M.-Y.; He, P.; Qiao, T.-Z.; Sun, W.; Li, W.-T.; Lian, J.; Li, J.-H.; Zhu, S.-F. *J. Am. Chem. Soc.* **2020**, *142*, 16894–16902.
- (27)(a) Ojha, D. P.; Prabhu, K. R. *Org. Lett.* **2016**, *18*, 432–435. (b) González, M. J.; Bauer, F.; Breit, B. *Org. Lett.* **2021**, *23*, 8199–8203.
- (28) Xu, G.; Zhao, H.; Fu, B.; Cang, A.; Zhang, G.; Zhang, Q.; Xiong, T.; Zhang, Q. *Angew. Chem. Int. Ed.* **2017**, *56*, 13130–13134.
- (29) Recent reviews on Hantzsch ester in photoredox catalysis: (a) Huang, W.; Cheng, X. *Synlett* **2017**, *28*, 148–158. (b) Wang, P.-Z.; Chen, J.-R.; Xiao, W.-J. *Org. Biomol. Chem.* **2019**, *17*, 6936–6951.
- (30) Shen, G.-B.; Xie, L.; Yu, H.-Y.; Liu, J.; Fu, Y.-H.; Yan, M. *RSC Adv.* **2020**, *10*, 31425–31434.
- (31) Nakajima, K.; Nojima, S.; Sakata, K.; Nishibayashi, Y. *ChemCatChem* **2016**, *8*, 1028–1032.
- (32)(a) Chen, W.; Liu, Z.; Tian, J.; Li, M.; Ma, J.; Cheng, X.; Li, G. *J. Am. Chem. Soc.* **2016**, *138*, 12312–12315. (b) Gu, F.; Huang, W.; Liu, X.; Chen, W.; Cheng, X. *Adv. Synth. Catal.* **2018**, *360*, 925–931.
- (33)(a) de Assis, F. F.; Huang, X.; Akiyama, M.; Pilli, R. A.; Meggers, E. *J. Org. Chem.* **2018**, *83*, 10922–10932. (b) Song, Z.-Y.; Zhang, C.-L.; Ye, S. *Org. Biomol. Chem.* **2019**, *17*, 181–185. (c) Du, J.; Sun, H.-W.; Gao, Q.-S.; Wang, J.-Y.; Wang, H.; Xu, Z.; Zhou, M.-D. *Org. Lett.* **2020**, *22*, 1542–1546. (d) Angnes, R. A.; Potnis, C.; Liang, S.; Correia, C. R. D.; Hammond, G. B. *J. Org. Chem.* **2020**, *85*, 4153–4164. (e) Guo, Q.; Peng, Q.; Chai, H.; Huo, Y.; Wang, S.; Xu, Z. *Nat. Commun.* **2020**, *11*, 1463. (f) He, X.-K.; Lu, J.; Zhang, A.-J.; Zhang, Q.-Q.; Xu, G.-Y.; Xuan, J. *Org. Lett.* **2020**, *22*, 5984–5989. (g) Kim, I.; Park, S.; Hong, S. *Org. Lett.* **2020**, *22*, 8730–8734.
- (34)(a) Wang, X.; Li, H.; Qiu, G.; Wu, J. *Chem. Commun.* **2019**, *55*, 2062–2065. (b) Wang, X.; Yang, M.; Xie, W.; Fan, X.; Wu, X. *J. Chem. Commun.* **2019**, *55*, 6010–6013. (c) Gong, X.; Yang, M.; Liu, J.-B.; He, F.-S.; Fan, X.; Wu, J. *Green Chem.* **2020**, *22*, 1906–1910.
- (35) Nakajima, K.; Nojima, S.; Nishibayashi, Y. *Angew. Chem. Int. Ed.* **2016**, *55*, 14106–14110.
- (36) Nakajima, K.; Guo, X.; Nishibayashi, Y. *Chem. Asian J.* **2018**, *13*, 3653–3657.
- (37) Zhang, Y.; Tanabe, Y.; Kuriyama, S.; Nishibayashi, Y. *J. Org. Chem.* **2021**, *86*, 12577–12590.
- (38) Buzzetti, L.; Prieto, A.; Roy, S. R.; Melchiorre, P. *Angew. Chem. Int. Ed.* **2017**, *56*,

15039–15043.

(39) (a) Zhang, H.-H.; Yu, S. *J. Org. Chem.* **2017**, *82*, 9995–10006. (b) van Leeuwen, T.; Buzzetti, L.; Perego, L. A.; Melchiorre, P. *Angew. Chem. Int. Ed.* **2019**, *58*, 4953–4957. (c) Schwarz, J. L.; Huang, H.-M.; Paulisch, T. O.; Glorius, F. *ACS Catal.* **2020**, *10*, 1621–1627. (d) Zhou, Z.-Z.; Jiao, R.-Q.; Yang, K.; Chen, X.-M.; Liang, Y.-M. *Chem. Commun.* **2020**, *56*, 12957–12960. (e) Huang, H.-M.; Bellotti, P.; Daniliuc, C. G.; Glorius, F. *Angew. Chem. Int. Ed.* **2021**, *60*, 2464–2471. (f) Yang, T.; Wei, Y.; Kooh, M. J. *ACS Catal.* **2021**, *11*, 6519–6525. (g) Liang, Z.; Lv, K.; Zhou, S.; Bao, X. *Org. Chem. Front.* **2021**, *8*, 6499–6507.

(40) Qu, Q.-Y.; Min, Q.-Q.; Ao, G.-Z.; Liu, F. *Org. Biomol. Chem.* **2018**, *16*, 6391–6394.

(41) Phelan, J. P.; Lang, S. B.; Sim, J.; Berritt, S.; Peat, A. J.; Billings, K.; Fan, L.; Molander, G. A. *J. Am. Chem. Soc.* **2019**, *141*, 3723–3732.

(42) (a) Gutiérrez-Bonet, Á.; Tellis, J. C.; Matsui, J. K.; Vara, B. A.; Molander, G. A. *ACS Catal.* **2016**, *6*, 8004–8008. (b) Zhang, H.-H.; Zhao, J.-J.; Yu, S. *J. Am. Chem. Soc.* **2018**, *140*, 16914–16919. (c) Milligan, J. A.; Phelan, J. P.; Polites, V. C.; Kelly, C. B.; Molander, G. A. *Org. Lett.* **2018**, *20*, 6840–6844. (d) McDonald, B. R.; Scheidt, K. A. *Org. Lett.* **2018**, *20*, 6877–6881. (e) Chen, H.; Anand, D.; Zhou, L. *Asian J. Org. Chem.* **2019**, *8*, 661–664. (f) Wang, Z.-J.; Zheng, S.; Romero, E.; Matsui, J. K.; Molander, G. A. *Org. Lett.* **2019**, *21*, 6543–6547. (g) Gandolfo, E.; Tang, X.; Raha Roy, S.; Melchiorre, P. *Angew. Chem. Int. Ed.* **2019**, *58*, 16854–16858. (h) Liang, S.; Angnes, R. A.; Potnis, C.; Hammond, G. B. *Tetrahedron Lett.* **2019**, *60*, 151230. (i) Chen, X.; Ye, F.; Luo, X.; Liu, X.; Zhao, J.; Wang, S.; Zhou, Q.; Chen, G.; Wang, P. *J. Am. Chem. Soc.* **2019**, *141*, 18230–18237. (j) Xue, S.; Limburg, B.; Ghorai, D.; Benet-Buchholz, J.; Kleij, A. W. *Org. Lett.* **2021**, *23*, 4447–4451. (k) Ren, S.-C.; Lv, W.-X.; Yang, X.; Yan, J.-L.; Xu, J.; Wang, F.-X.; Hao, L.; Chai, H.; Jin, Z.; Chi, Y. R.; *ACS Catal.* **2021**, *11*, 2925–2934.

(43) Hantzsch ester without alkyl substituents has been used as a photoredox mediator for hydroalkylation of alkynes: (a) Barthelemy, A.-L.; Dagousset, G.; Magnier, E. *Eur. J. Org. Chem.* **2020**, 1429–1432. (b) Li, Y.-L.; Zhang, S.-Q.; Chen, J.; Xia, J.-B. *J. Am. Chem. Soc.* **2021**, *143*, 7306–7313.

(44) (a) Kren, R. J. *J. Inorg. Nucl. Chem.* **1962**, *24*, 1105–1109. (b) Glubokov, Y. M.; Rodríguez Reinoso, J.; Hernández Martínez, B. N. *CENTRO Ser. Quim. Tecnol. Quim.* **1973**, *1*, 53–62; *Chem. Abstr.* **1973**, *87*, 142096. (c) Eckert, N. A.; Bones, E. M.; Lachicotte, R. J.; Holland, P. L. *Inorg. Chem.* **2003**, *42*, 1720–1725.

(45) Recent review on *E* to *Z* isomerization of alkenes using small molecule photocatalysts: Nevesely, T.; Wienhold, M.; Molloy, J. J.; Gilmour, R. *Chem. Rev.* **2022**, *122*, 2650–2694.

(46) Teegardin, K.; Day, J. I.; Chan, J.; Weaver, J. *Org. Process Res. Dev.* **2016**, *20*, 1156–1163.

(47) Tamayo, A. B.; Alleyne, B. D.; Djurovich, P. I.; Lamansky, S.; Tsyba, I.; Ho, N. N.; Bau, R.; Thompson, M. E. *J. Am. Chem. Soc.* **2003**, *125*, 7377–7387.

(48) Miroshnichenko, E. A.; Kon'kova, T. S.; Matyushin, Yu. N.; Orlov, Yu. D.; Pashchenko, L. L.; Vorob'ev, A. B.; Inozemtsev, A. V. *Russ. J. Phys. Chem. B* **2019**, *13*, 225–230, *Khim. Fiz.* **2019**, *38*, 3–8.

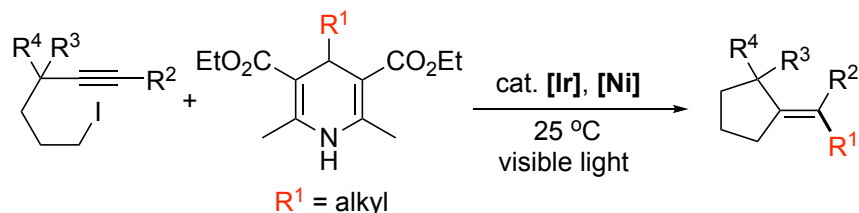
- (49)(a) Lewis, F. D.; Oxman, J. D. *J. Am. Chem. Soc.* **1981**, *103*, 7345–7347. (b) Castro, A. J. Ellenberger, S. R.; Sluka, J. P. *J. Chem. Educ.* **1983**, *60*, 521.
- (50) Yasu, Y.; Koike, T.; Akita, M. *Adv. Synth. Catal.* **2012**, *354*, 3414–3420.
- (51)(a) Liao, J.; Basch, C. H.; Hoerner, M. E.; Talley, M. R.; Boscoe, B. P.; Tucker, J. W.; Garnsey, M. R.; Watson, M. P. *Org. Lett.* **2019**, *21*, 2941–2946. (b) Wang, J.; Pang, Y.-B.; Tao, N.; Zeng, R.-S.; Zhao, Y. *J. Org. Chem.* **2019**, *84*, 15315–15322. (c) Zhang, D.; Tang, Z.-L.; Ouyang, X.-H.; Song, R.-J.; Li, J.-H. *Chem. Commun.* **2020**, *56*, 14055–14508.
- (52) Pitre, S. P.; McTiernan, C. D.; Scaiano, J. C. *Acc. Chem. Res.* **2016**, *49*, 1320–1330.
- (53) Pavlishchuk, V. V.; Addison, A. W. *Inorg. Chim. Acta* **2000**, *298*, 97–102.
- (54) Mattes, S. K.; Farid, S. *J. Chem. Soc. Chem. Commun.* **1980**, *16*, 126–128.
- (55) Wearing, E. R.; Blackmun, D. E.; Becker, M. R.; Schindler, C. S. *J. Am. Chem. Soc.* **2021**, *143*, 16235–26242.
- (56) Zhu, C.; Yue, H.; Maity, B.; Atodiresei, I.; Cavallo, L.; Rueping, M. *Nat. Catal.* **2019**, *2*, 678–687.
- (57) Hatchard, C. G.; Parker, C. A. *Proc. R. Soc. London Ser. A* **1956**, *235*, 518–526.
- (58)(a) Cismesia, M.; Yoon, T. P. *Chem. Sci.* **2015**, *6*, 5426–5436. (b) Kärkäs, M. D.; Matsuura, B. S.; Stephenson, C. R. J. *Science* **2015**, *349*, 1285–1286.
- (59) Nakajima, K.; Miyake, Y.; Nishibayashi, Y. *Acc. Chem. Res.* **2016**, *49*, 1946–1956.
- (60)(a) Miyake, Y.; Nakajima, K.; Nishibayashi, Y. *J. Am. Chem. Soc.* **2012**, *134*, 3338–3341. (b) Miyake, Y.; Ashida, Y.; Nakajima, K.; Nishibayashi, Y. *Chem. Commun.* **2012**, *48*, 6966–6968. (c) Miyake, Y.; Nakajima, K.; Nishibayashi, Y. *Chem. Commun.* **2013**, *49*, 7854–7856. (d) Nakajima, K.; Kitagawa, M.; Ashida, Y.; Miyake, Y. *Chem. Commun.* **2014**, *50*, 8900–8903.
- (61) Jacob, K.; Niebuhr, R. *Z. Chem.* **1975**, *15*, 32.
- (62) Recent reviews on the photoredox catalysts-mediated *anti*-Markovnikov-type hydrofunctionalization of alkenes: (a) Angnes, R. A.; Li, Z.; Correia, C. R. D.; Hammond, G. B. *Org. Biomol. Chem.* **2015**, *13*, 9152–9167. (b) Margrey, K. A.; Nicewicz, D. A. *Acc. Chem. Res.* **2016**, *49*, 1997–2006.
- (63) Li, G.; Chen, R.; Wu, L.; Fu, Q.; Zhang, X.; Tang, Z. *Angew. Chem. Int. Ed.* **2013**, *52*, 8432–8436.
- (64) Gutiérrez-Bonet, Á.; Remeur, C.; Matsui, J. K.; Molander, G. A. *J. Am. Chem. Soc.* **2017**, *139*, 12251–12258.
- (65) Chen, B.; Kuai, C.-S.; Xu, J.-X.; Wu, X.-F. *Adv. Synth. Catal.* **2022**, *364*, 487–492.
- (66) Nakajima, K.; Zhang, Y.; Nishibayashi, Y. *Org. Lett.* **2019**, *21*, 4642–4645.
- (67) Patel, S. S.; Kumar, D.; Tripathi, C. B. *Chem. Commun.* **2021**, *57*, 5151–5154.
- (68) Hou, Z.-L.; Yang, F.; Zhou, Z.; Ao, Y.-F.; Yao, B. *Tetrahedron Lett.* **2018**, *59*, 4557–4561.
- (69) Zhou, Z.; Hou, Z.-L.; Yang, F.; Yao, B. *Tetrahedron* **2018**, *74*, 7228–7236.
- (70) Wu, Q.; Wang, L.; Jin, R.; Kang, C.; Bian, Z.; Du, Z.; Ma, X.; Guo, H.; Gao, L. *Eur. J. Org. Chem.* **2016**, 5415–5422.
- (71) Barluenga, J.; Fañanás, F. J.; Sanz, R.; Marcos, C.; Ignacio, J. M. *Chem. Commun.* **2005**, *41*, 933–935.
- (72) Matsubara, R.; Gutierrez, A. C.; Jamison, T. F. *J. Am. Chem. Soc.* **2011**, *133*,

19020–19023.

- (73) Zou, Y.; Zhou, J. S. *Chem. Commun.* **2014**, 50, 3725–3728.
- (74) Kusy, R.; Grela, K. *Green Chem.* **2021**, 23, 5494–5502.
- (75) Zhang, S.; Bedi, D.; Cheng, L.; Unruh, D. K.; Li, G.; Findlater, M. *J. Am. Chem. Soc.* **2020**, 142, 8910–8917.
- (76) Guttroff, C.; Baykal, A.; Wang, H.; Popella, P.; Krais, F.; Biber, N.; Krauss, S.; Götz, F.; Plietker, B. *Angew. Chem. Int. Ed.* **2017**, 56, 15852–15856.
- (77) Luo, J.; Hu, B.; Wu, W.; Hu, M.; Liu, T. L. *Angew. Chem. Int. Ed.* **2021**, 61, 6107–6116.
- (78) Horino, Y.; Ishibashi, M.; Nakasai, K.; Korenaga, T. *Tetrahedron* **2020**, 76, 131493.
- (79) Mino, T.; Kogure, T.; Abe, T.; Koizumi, T.; Fujita, T.; Sakamoto, M. *Eur. J. Org. Chem.* **2013**, 1501–1505.
- (80) Riveiros, R.; Tato, R.; Pérez Sestelo, J.; Sarandeses, L. A. *Eur. J. Org. Chem.* **2012**, 3018–3023.
- (81) Chin, C. S.; Kim, M.; Won, G.; Jung, H.; Lee, H. *Dalton Trans.* **2003**, 32, 2325–2328.
- (82) Adam, W.; Baeza, J.; Liu, J.-C. *J. Am. Chem. Soc.* **1972**, 94, 2000–2006.
- (83) Wang, H.; Yang, M.; Wang, Y.; Man, X.; Lu, X.; Mon, Z.; Luo, Y.; Liang, H. *Org. Lett.* **2021**, 23, 8183–8388.
- (84) Zhou, B.; Sato, H.; Ilies, L.; Nakamura, E. *ACS Catal.* **2018**, 8, 8–11.
- (85) Li, X.; Li, Y.; Zhang, Z.; Shi, X.; Liu, R.; Wang, Z.; Li, X.; Shi, D. *Org. Lett.* **2021**, 23, 6612–6616.
- (86) CrysAlisPro, version 1.171.41.99a, Data Collection and Processing Software, Rigaku Corporation, Tokyo, Japan, **2021**.
- (87) CrystalStructure, version 4.3, Crystal Structure Analysis Package, Rigaku Corporation, Tokyo, Japan, **2019**.
- (88) Sheldrick, G. M. *Acta Crystallogr.* **2014**, A70, C1437.
- (89) Sheldrick, G. M. *Acta Crystallogr.* **2015**, C71, 3–8.
- (90) Ibers, J. A.; Hamilton, W. C. *Acta Crystallogr.* **1964**, 17, 781–782.
- (91) Creagh, D. C.; Hubbell, J. H. in *International Tables for Crystallography*, Vol. C (Ed: Wilson, A. J. C.), Kluwer Academic Publishers, Dordrecht, The Netherlands, **1992**; Table 4.2.3.3., pp. 200–206.
- (92) Creagh, D. C.; McAuley, W. J. in *International Tables for Crystallography*, Vol. C (Ed: Wilson, A. J. C.), Kluwer Academic Publishers, Dordrecht, The Netherlands, **1992**; Table 4.2.6.8., pp. 219–222.
- (93) Maslen, E. N.; Fox, A. G.; O’Keefe, M. A. in *International Tables for Crystallography*, Vol. C (Ed: Wilson, A. J. C.), Kluwer Academic Publishers, Dordrecht, The Netherlands, **1992**; Table 6.1.1.4., pp. 500–503.
- (94) Yang, L.; Powell, D. R.; Houser, R. P. *Dalton Trans.* **2007**, 36, 955–964.

Chapter 4

Cooperative Photoredox- and Nickel-Catalyzed Alkylative Cyclization Reactions of Alkynes with 4-Alkyl-1,4-dihydropyridines



In Chapter 4, the author has developed the cooperative photoredox- and nickel-catalyzed alkylative cyclization reactions of iodoalkynes with 4-alkyl-1,4-dihydropyridines as alkylation reagents under visible light irradiation to afford the corresponding alkylated cyclopentylidenes in good to high yields. Introduction of substituents at the propargylic position of iodoalkynes has led to the stereoselective formation of *E*-isomers. The present reaction system provides a novel synthetic method for alkylative cyclization reactions of both terminal and internal alkynes with cooperative photoredox and nickel catalysis.

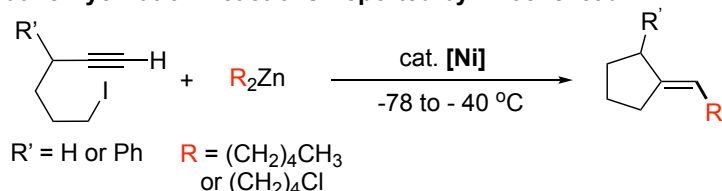
4.1. Introduction

Recently, the author's group and others have demonstrated that 4-alkyl-1,4-dihydropyridines can be used as powerful alkylation reagents to offer a variety of alkylative reactions in photoredox-catalyzed molecular transformations,¹⁻¹³ providing an alternative to using classical, but highly reactive, organometallic alkylation reagents. The use of visible light excitement of a photoredox catalyst, followed by single-electron-transfer (SET) processes, leads to the generation of alkyl radicals from 4-alkyl-1,4-dihydropyridines,^{1,2,14} enabling not only simple alkylation³⁻⁵ but also alkylative reactions accompanied by other transformations such as cross-coupling reactions in the presence of additional catalysts.^{6-13,15} In fact, the author's group has recently succeeded in photoredox-catalyzed aromatic substitution reactions of cyanoarenes with 4-alkyl-1,4-dihydropyridines³ and cooperative nickel- and photoredox-catalyzed cross-coupling reactions of aryl and alkenyl halides with 4-alkyl-1,4-dihydropyridines.^{8,9}

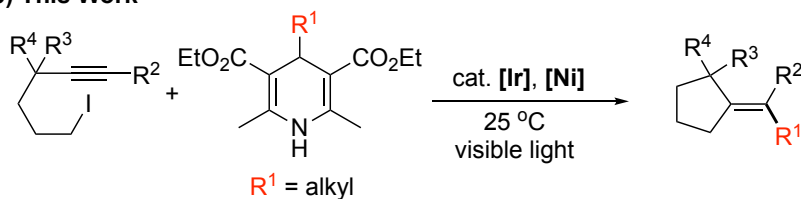
In the course of the study to expand the utility of 4-alkyl-1,4-dihydropyridines toward alkylative reactions, the author next planned to apply 4-alkyl-1,4-dihydropyridines to the alkylative cyclization reactions of haloalkynes.^{16,17} Indeed, transition metal-catalyzed alkylative cyclization reactions have been explored intensively to prepare the corresponding cyclic compounds valuable for both biological and pharmaceutical utilities.¹⁸⁻²⁰ As a selected example, Knochel and co-workers reported nickel-catalyzed alkylative cyclization reactions of 6-iodohex-1-yne with alkyl zinc reagents to afford the corresponding alkylated cyclopentylidenes, where a lower temperature was required to suppress side reactions (Scheme 4-1a).¹⁶ Thus, the author has applied 4-alkyl-1,4-dihydropyridines to the alkylative cyclization reactions of 6-iodohex-1-yne in the presence of photoredox and nickel dual catalysts.²¹ Here, the author wishes to report the cooperative photoredox- and nickel-catalyzed alkylative cyclization reactions of 6-iodohex-1-yne with 4-alkyl-1,4-dihydropyridines employed as alkylation reagents at 25 °C under the irradiation of visible light to afford the corresponding alkylated cyclopentylidenes. In addition, introduction of substituents at the propargylic position of 6-iodohex-1-yne has led to the stereoselective formation of *E*-isomers (Scheme 4-1b).

Scheme 4-1. Nickel-Catalyzed Alkylative Cyclization Reactions of Iodoalkynes with Alkylation Reagents

a) Alkylative Cyclization Reactions Reported by Knochel *et al.*



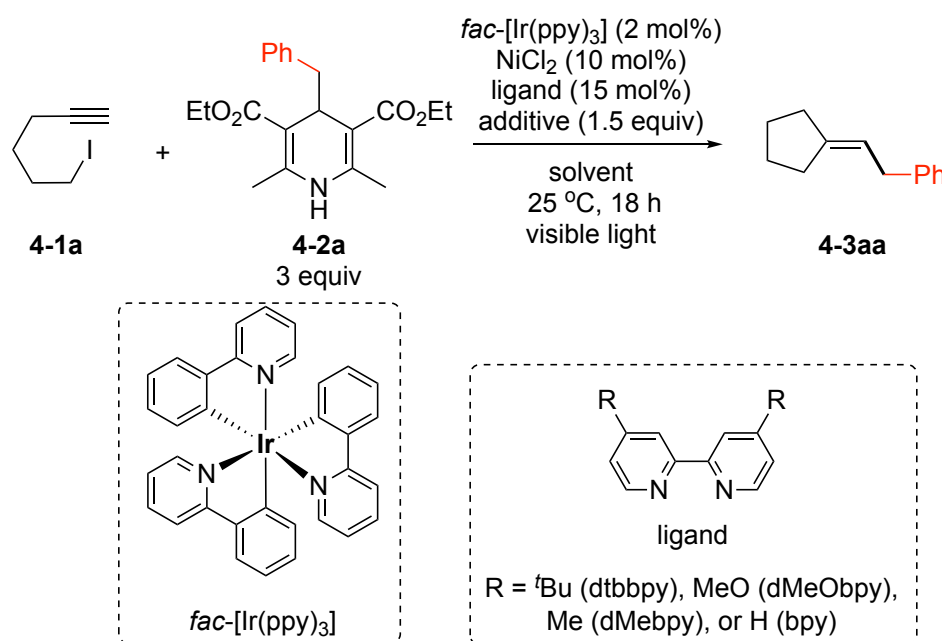
b) This Work



4.2. Results and Discussions

The author initially investigated the reaction of 6-iodohex-1-yne (**4-1a**) with 4-benzyl-3,5-bis(ethoxycarbonyl)-2,6-dimethyl-1,4-dihydro-2-pyridine (**4-2a**) as typical substrates for the photoredox- and nickel-catalyzed alkylative cyclization reaction to afford (2-cyclopentylideneethyl)benzene (**4-3aa**) as the major product (Table 4-1). When the reaction of **4-1a** with 3 equiv of **4-2a** in THF was carried out in the presence of 2 mol % of *fac*-[Ir(ppy)₃] (ppy = 2-(2-pyridyl)phenyl), 10 mol % of anhydrous NiCl₂, 15 mol % of 4,4'-di-*tert*-butyl-2,2'-bipyridine (dtbbpy), and 1.5 equiv of Cs₂CO₃ as a photoredox catalyst, a cross-coupling catalyst, a coordination ligand for the nickel catalyst, and an additive, respectively, at 25 °C for 18 h under visible light illumination with a 12 W white light-emitting diode (LED), **4-3aa** was isolated in 50% yield (Table 4-1, entry 1). Here, addition of a base like Cs₂CO₃, well-known as an excellent and mild base to trap HI to promote cross-coupling reactions,²² was necessary to produce **4-3aa** (Table 4-1, entry 2), whereas other bases like K₂CO₃ and NaOAc were found to be less effective to obtain **4-3aa** than Cs₂CO₃ (Table 4-1, entries 3 and 4). Solvent selection in catalysis was also examined to find out that use of 1,4-dioxane as a solvent instead of THF increased the yield of **4-3aa** up to 69% yield (Table 4-1, entry 5), while the use of other solvents such as acetonitrile, 1,2-dimethoxyethane (DME), and diethyl ether gave lower yields of **4-3aa**, respectively (Table 4-1, entries 6–8). Addition of a catalytic amount of a 2,2'-bipyridine derivative as a coordination ligand for nickel species was also found to be necessary for the formation of **4-3aa**, which was not obtained in the absence of dtbbpy (Table 4-1, entry 9). Further investigation on ligand selection for 2,2'-bipyridine derivatives revealed that use of 4,4'-dimethoxyl-2,2'-bipyridine (dMeObpy), where more electron-donating substituents were introduced onto the 4,4'-positions of the 2,2'-bipyridine skeleton, improved the yield of **4-3aa** up to 75% (Table 4-1, entry 10) compared to those found for using dtbbpy (Table 4-1, entry 5), 4,4'-dimethyl-2,2'-bipyridine (dMebpy) (Table 4-1, entry 11), or 2,2'-bipyridine (bpy) (Table 4-1, entry 12). When reactions were carried out in the absence of *fac*-[Ir(ppy)₃], anhydrous NiCl₂, or visible light irradiation, **4-3aa** was not obtained at all (Table 4-1, entries 13–15), demonstrating that both nickel and photoredox catalysts as well as visible light irradiation are all essential to promote the catalytic reaction. In addition, a longer reaction time (24 h) slightly improved the yield of **4-3aa** in up to 83% yield (Table 4-1, entry 16).

Table 4-1. Photoredox- and Nickel-Catalyzed Alkylative Cyclization of **4-1a** with **4-2a**^a



entry	ligand	additive	solvent	yield (%) ^b
1	dtbbpy	Cs ₂ CO ₃	THF	50
2	dtbbpy	none	THF	n.d. ^c
3	dtbbpy	K ₂ CO ₃	THF	40
4	dtbbpy	NaOAc	THF	32
5	dtbbpy	Cs ₂ CO ₃	1,4-dioxane	69
6	dtbbpy	Cs ₂ CO ₃	MeCN	42
7	dtbbpy	Cs ₂ CO ₃	DME	35
8	dtbbpy	Cs ₂ CO ₃	Et ₂ O	27
9	none	Cs ₂ CO ₃	1,4-dioxane	n.d.
10	dMeObpy	Cs ₂ CO ₃	1,4-dioxane	75
11	dMebpy	Cs ₂ CO ₃	1,4-dioxane	69
12	bpy	Cs ₂ CO ₃	1,4-dioxane	56
13 ^d	dMeObpy	Cs ₂ CO ₃	1,4-dioxane	n.d.
14 ^e	dMeObpy	Cs ₂ CO ₃	1,4-dioxane	n.d.
15 ^f	dMeObpy	Cs ₂ CO ₃	1,4-dioxane	n.d.
16 ^g	dMeObpy	Cs ₂ CO ₃	1,4-dioxane	83

^aReactions of **4-1a** (0.25 mmol) with **4-2a** (0.75 mmol) were carried out in the presence of *fac*-[Ir(ppy)₃] (0.005 mmol), anhydrous NiCl₂ (0.025 mmol), a ligand (0.0375 mmol), and an additive (0.375 mmol) in solvent (2.5 mL) with 12 W white LED illumination at 25 °C for 18 h. ^bIsolated yield. ^cNot detected by GC-MS. ^dIn the absence of *fac*-[Ir(ppy)₃]. ^eIn the absence of anhydrous NiCl₂. ^fIn the absence of visible light. ^g24 h instead of 18 h.

With the optimized reaction conditions in hand, reactions of **4-1a** with various 4-alkyl-1,4-dihydropyridines were next investigated (Scheme 4-2a). All the 4-benzyl-1,4-dihydropyridine derivatives, where either electron-donating or electron-withdrawing substituents (MeO: **4-2b**, Me: **4-2c**, Ph: **4-2d**, Cl: **4-2e**) were introduced at the 4-position of the benzene moiety, were successfully used as alkylation reagents to afford the corresponding alkylated cyclopentylidenes (**4-3aa–4-3ae**) in good to high yields, whereas only a trace amount of the corresponding desired product was obtained for the introduction of a cyano substituent at the same position (CN: **4-2f**) with most of **4-2f** transformed into *p*-tolunitrile as the major product. Introduction of a methyl group at the 3- or 2- position of the benzene moiety (3-Me: **4-2g**, 2-Me: **4-2h**) was also applicable to give the corresponding products (**4-3ag** and **4-3ah**) in good to high yields. Other 1,4-dihydropyridine derivatives with primary alkyl groups (1-naphthylmethyl: **4-2i**, *n*-nonyl: **4-2j**) or even with secondary alkyl groups (2-pentyl: **4-2ak**, cyclohexyl: **4-2l**) were also found to afford the corresponding alkylated cyclopentylidenes (**4-3ai–4-3al**) in good to high yields. The best yield (97%) was obtained for the isolation of (2-methylpentylidene)cyclopentane (**4-3ak**). On the other hand, the use of a bulkier secondary alkyl group such as CH(Me)Ph (**4-2m**) gave only a trace amount of the corresponding desired product. Alkylated cyclopentylidenes with ether or amine groups (**4-3an** and **4-3ao**) were also obtained in high yields from the corresponding 1,4-dihydropyridine derivatives (benzyloxymethyl: **4-2n**, *N,N*-dibenzylaminomethyl: **4-2o**), although introduction of an ester group was not successful (CH(Me)CO₂Et: **4-2p**). It must be noteworthy that the formation of the compounds with cyclopentylidene and heterocyclic units was achieved by using 4-methyl-1,4-dihydropyridine derivatives with heterocycle substituents (2-furyl: **4-2q**, 2-thienyl: **4-2r**) introduced to the methyl group to give the corresponding products (**4-3q** and **4-3r**) in high yields, whereas no desired product for the reaction of **4-1a** with a 3-pyridyl substituent (**4-2s**), mostly transformed into 3-methylpyridine.

In addition to **4-1a** containing a terminal alkyne moiety, conversion of internal iodoalkynes with methyl or phenyl groups introduced at the alkynyl group of 6-iodohex-1-yne (Me: **4-1b**, Ph: **4-1c**) was further investigated to react with **4-2a** to afford the corresponding alkylative cyclization products (**4-3ba**, **4-3ca**) in good yields (Scheme 4-2a). Thus, the present catalytic system is applicable to the internal alkynes, which was not achieved in the previous alkylative cyclization reactions using alkyl zinc reagents in the presence of nickel catalysts.¹⁶

Catalytic alkylative cyclization reactions of 6-iodohex-1-yne containing one or two aryl or alkyl substituents introduced at the propargylic position with **4-2a** were further investigated (Scheme 4-2a). Indeed, treatment of (6-iodohex-1-yn-3-yl)-benzene (**4-1d**) with **4-2a** under the optimized reaction conditions afforded 2-(2-phenylcyclopentylidene)ethyl)benzene (**4-3da**) in 62% isolated yield as a mixture of *E*- and *Z*-isomers with the former as the major product (*E/Z* = 92/8). Introduction of one alkyl group such as ethyl (**4-1e**), *n*-butyl (**4-1f**), *n*-heptyl (**4-1g**), and cyclohexyl groups (**4-1h**) at the propargylic position in the starting iodoalkynes also gave the corresponding desired products (**4-3ea–4-3ha**) in good yields with an excellent stereoselectivity (*E/Z* up to 93/7). Furthermore, the use of 6-iodo-3,3-dimethylhex-1-

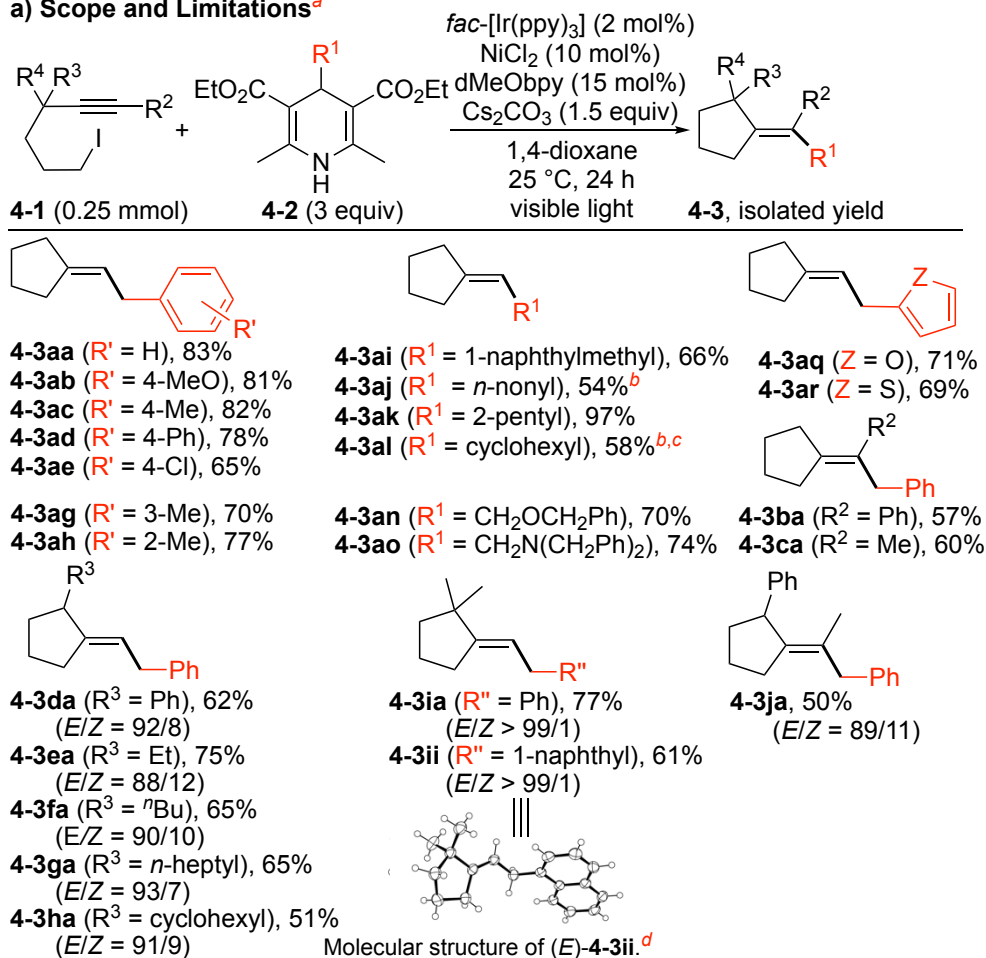
yne (**4-1i**), a terminal alkyne with two methyl groups introduced at the propargylic position, led to the formation of (2-(2,2-dimethylcyclopentylidene)ethyl)-benzene (**4-3ia**) in 77% yield almost selectively as an (*E*)-isomer ($E/Z > 99/1$). Similarly, reaction of **4-1i** with **4-2i** afforded 1-(2-(2,2-dimethylcyclopentylidene)ethyl)naphthalene (**4-3ii**) almost solely as an (*E*)-isomer ($E/Z > 99/1$), whose structure was determined by a single-crystal X-ray diffraction study (Scheme 4-2a). The alkylative cyclization reaction of (7-iodohept-2-yn-4-yl)benzene (**4-1j**), an internal alkyne with one phenyl group introduced at the propargylic position, also proceeded to afford (2-(2-phenylcyclopentylidene)propyl)-benzene (**4-3ja**) as a mixture of two isomers with an *E*-stereoselectivity ($E/Z = 89/11$).

It must be noted that **4-3aa** was not obtained in a similar manner from the reaction of 6-bromohex-1-yne (**4-1a-Br**) or 6-chlorohex-1-yne (**4-1a-Cl**) instead of **4-1a** with **4-2a** under the typical reaction conditions, where **4-3aa** was obtained only in 4% yield (Scheme 4-2b). This result suggests that the existence of an iodide substituent as a leaving group is necessary for the dual catalytic system to proceed efficiently.²³

Besides the alkylative cyclization reactions of 6-iodohex-1-ynes, the reaction of 7-iodohept-1-yne (**4-4a**) with **4-2a** was examined. Under the similar reaction conditions, the corresponding six-membered alkylative cyclization product (2-cyclohexylideneethyl)benzene (**4-5aa**) was obtained only in 5% yield (Scheme 4-2c). Expecting the Thorpe–Ingold effect,²⁴ introduction of substituents at the homopropargylic (**4-4b**) or propargylic position (**4-4c**) was also examined, but was in vain. Thus, the present catalytic alkylative cyclization reaction system is only effective for constructing a five-membered ring.

Scheme 4-2. Photoredox- and Nickel-Catalyzed Alkylative Cyclization of **4-1** with **4-2**

a) Scope and Limitations^a



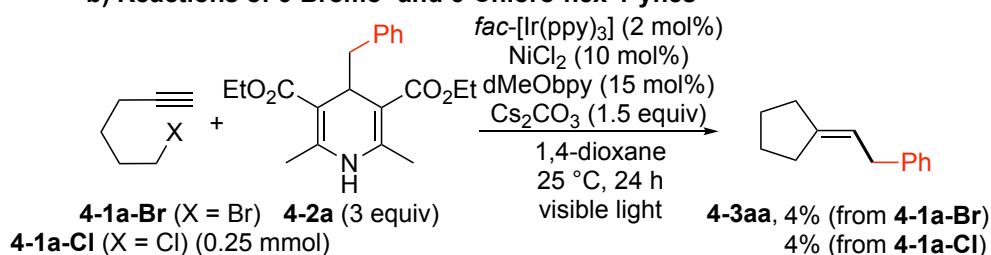
^a Trace amount of desired product from the reaction of **4-1a** with **4-2f** (R' = 4-CN), **4-2m** (R' = CH(Me)Ph), or **4-2p** (R' = CH(Me)CO₂Et); no desired product for **4-1a** with **4-2s** (R' = 3-pyCH₂).

^b 72 h instead of 24 h.

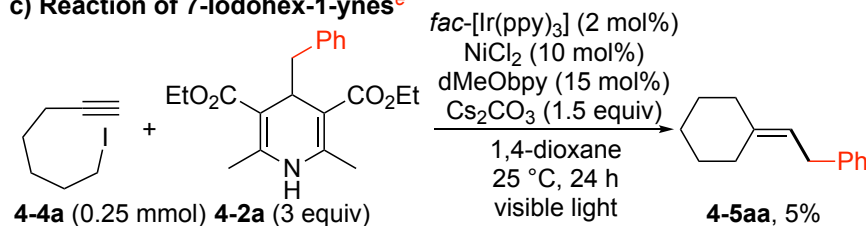
^c *fac*-[Ir(Fppy)₃] (Fppy = 3,5-difluoro-2-(2-pyridyl)phenyl) instead of *fac*-[Ir(ppy)₃].

^d Thermal ellipsoids of carbon atoms are drawn at the 50% probability level.

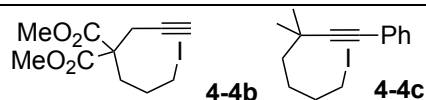
b) Reactions of 6-Bromo- and 6-Chloro-hex-1-ynes



c) Reaction of 7-Iodohept-1-ynes^e



^e Trace amount of desired product from the reaction of **4-4b** or **4-4c** with **4-2a**:



In order to obtain further mechanistic information, the author next examined the reaction of **4-1a** with **4-2a** under the optimized reaction conditions but in the presence of 3 equiv of (2,2,6,6-tetramethylpiperidin-1-yl)oxyl (TEMPO) as a radical inhibitor. In fact, formation of the desired alkylative cyclization product **4-3aa** was perfectly inhibited. Instead, 1-(benzyloxy)-2,2,6,6-tetramethylpiperidine (**4-6a**),²⁵ the TEMPO-trapped benzyl adduct, was obtained in 69% yield. This experimental result demonstrates that the formation of a benzyl radical as a reactive intermediate is involved in the main catalytic reaction pathway (Figure 4-1a).^{3,4,8,10,11,19,26}

Subsequently, Stern–Volmer analyses for emission quenching of *fac*-[Ir(ppy)₃] with **4-1** and **4-2a** were performed in 1,4-dioxane (Figure 4-1b). From the slopes obtained by the plot and the excited-state lifetime of *fac*-[Ir(ppy)₃] ($\tau = 1.90 \mu\text{s}$),²⁷ the rate constants for the reduction of **4-1a** or **4-1d** and the oxidation of **4-2a** were determined to be at $k = (1.5 \pm 0.2) \times 10^7 \text{ M}^{-1} \text{ s}^{-1}$ (**4-1a**), $k = (1.4 \pm 0.2) \times 10^7 \text{ M}^{-1} \text{ s}^{-1}$ (**4-1d**), and $k = (7.3 \pm 0.7) \times 10^7 \text{ M}^{-1} \text{ s}^{-1}$ (**4-2a**), respectively. This result indicates that reduction of **4-1** or oxidation of **4-2a** can occur via the SET process, where the oxidation of **4-2a** is 5 times as fast as the reduction of **4-1**. Additionally, the quantum yield of the typical reaction of **4-1a** with **4-2a** was measured to be $\Phi = 0.063 \pm 0.001$, suggesting that the rate-determining step of the catalytic formation of **4-3aa** proceeds not via a radical chain process²⁸ but rather via sequential redox pathways, where alkyl radicals are mainly generated by the SET process between 4-alkyl-1,4-dihydropyridines and an excited-state photoredox catalyst (Figure 4-1b).^{3,8,9,29,30} A light on/off experiment was further conducted for the reaction of **4-1a** with **4-2a** to afford **4-3aa** under the typical catalytic reaction conditions to present that the alkylative cyclization reaction perfectly ceased in the dark, which indicates that a chain propagation is not the main reaction pathway and that continuous irradiation of visible light is necessary for the reaction (Figure 4-1c).

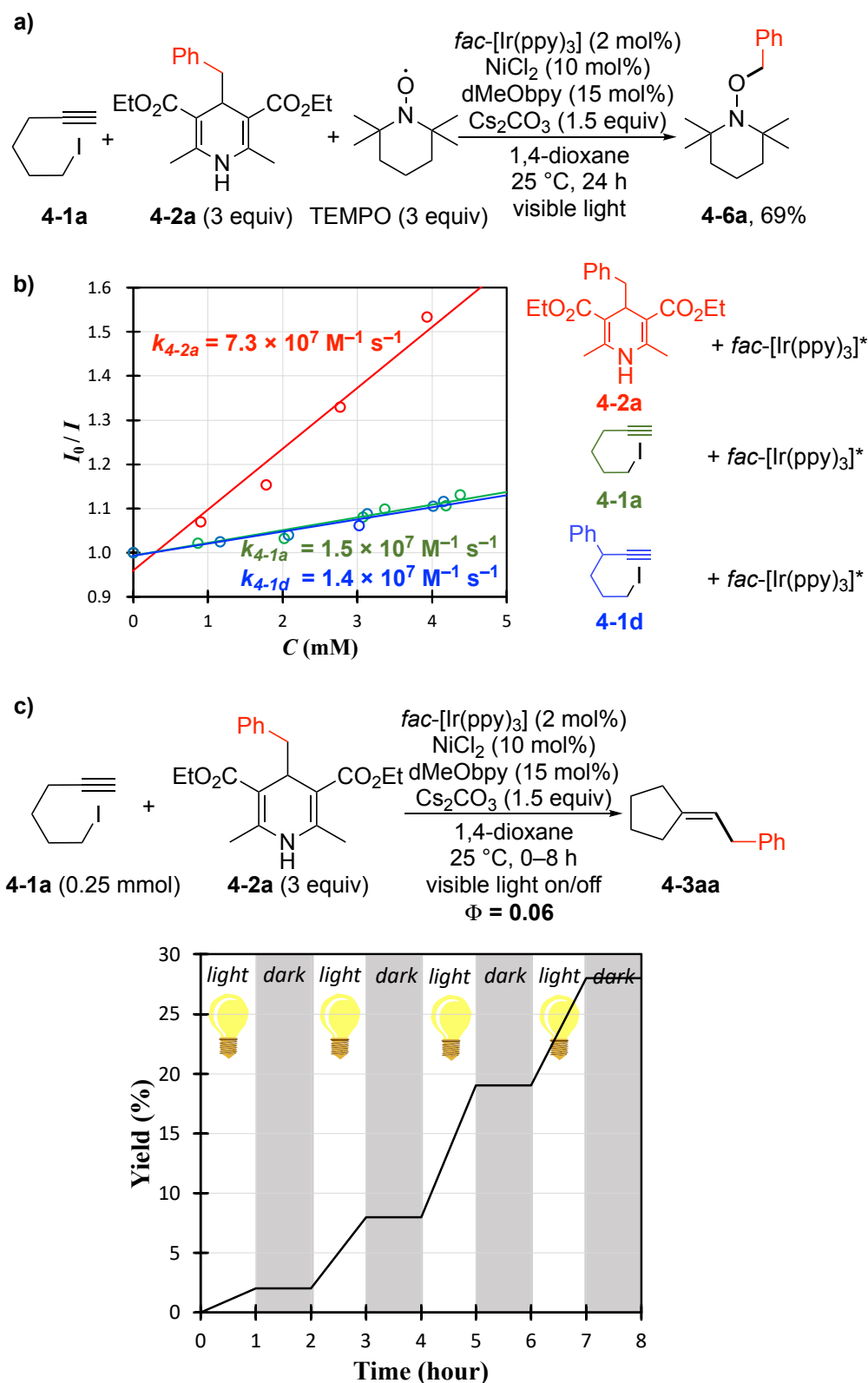


Figure 4-1. Mechanistic studies on the reactions of **4-1a** with **4-2a**. (a) Reaction in the presence of TEMPO. (b) Determination of quenching constants by Stern–Volmer plot for *fac*-[Ir(ppy)₃] with **4-1a**, **4-1d**, and **4-2a** in 1,4-dioxane. (c) Time profile of the reaction with and without visible light irradiation.

On the other hand, formation of (2-(iodomethylene)-cyclopentyl)benzene (**4-7d**), a cyclic vinyl iodide, was observed spectroscopically as a reactive intermediate during the reaction of **4-1d** with **4-2a** to afford **4-3da** under the typical catalytic reaction conditions (Figure 4-2a). Indeed, **4-7d** was isolated as the major product in 57% yield with an *E/Z* ratio of 83/17 for the reaction of **4-1d** under the typical catalytic reaction conditions but in the absence of **4-2a** (Figure 4-2b) with the quantum yield found at $\Phi = 0.072 \pm 0.002$. The control experiments exhibited that the conversion of **4-1d** into **4-7d** did not take place in the absence of any of *fac*-[Ir(ppy)₃], anhydrous NiCl₂, dMeObpy, Cs₂CO₃, or visible light irradiation, revealing that all these elements are required for the cyclization reaction to afford **4-7d**, when **4-2a** is not present. However, **4-7d** was also isolated as the major product in 59% yield with *E/Z* ratio of 83/17 without the formation of **4-3da** for the reaction of **4-1d** under the typical reaction conditions in the absence of anhydrous NiCl₂ and dMeObpy but in the presence of a catalytic amount of **4-2a** (0.1 equiv) (Figure 4-2c), clearly indicating that the cyclization reaction of **4-1d** into **4-7d** actually does not require nickel catalyst, when **4-2a** is present. It must be noted that Melchiorre and co-workers have recently demonstrated that 4-alkyl-1,4-dihydropyridines including **4-2a** have an ability to absorb visible light less than 420 nm in wavelength,^{10,13} while almost no reaction occurred for the control experiment of Figure 4-2c in the absence of *fac*-[Ir(ppy)₃], confirming that **4-2a** does not work as an efficient photosensitizer and that the presence of *fac*-[Ir(ppy)₃] is necessary for visible-light-induced cyclization reactions. Cyclization reaction of 6-iodohex-1-yne to afford cyclopentylidenes has been already known to be promoted by radical initiators,³¹ and similar visible- or UV-light-induced cyclization reactions of 6-iodohex-1-yne to afford cyclopentylidenes have been more recently reported by the groups of Martin³² and Zhang,³³ where cyclization has been proposed to occur via the formation of a weak charge-transfer complex between an amine and alkyl iodide capable of forming an exciplex state under irradiation of blue light (Scheme 4-3),³² or via chain propagation pathways triggered by the abstraction of an iodine atom from alkyl iodide.^{32,33} However, **4-2a** itself does not work to form an exciplex state,³⁴ and there is no possible partners to form a charge-transfer complex at least under the present reaction conditions. Therefore, a propagation pathway is more plausible for the formation of **4-7d**, although the observed quantum yield for the conversion of **4-1d** into **4-7d** in the presence of catalytic amount of **4-2a** is not high ($\Phi = 0.067 \pm 0.003$), deciphering the potential existence of inhibitors for propagation (Figure 4-2c). On the other hand, *E/Z* selectivity (83/17) for the formation of **4-7d** is almost the same between the reaction in the presence of a catalytic amount of Ni catalyst or **4-2a** (Figures 4-2b and 4-2c), revealing that *E/Z* selectivity is likely controlled mainly by the steric hindrance of the substituent introduced to 6-iodohex-1-yne.

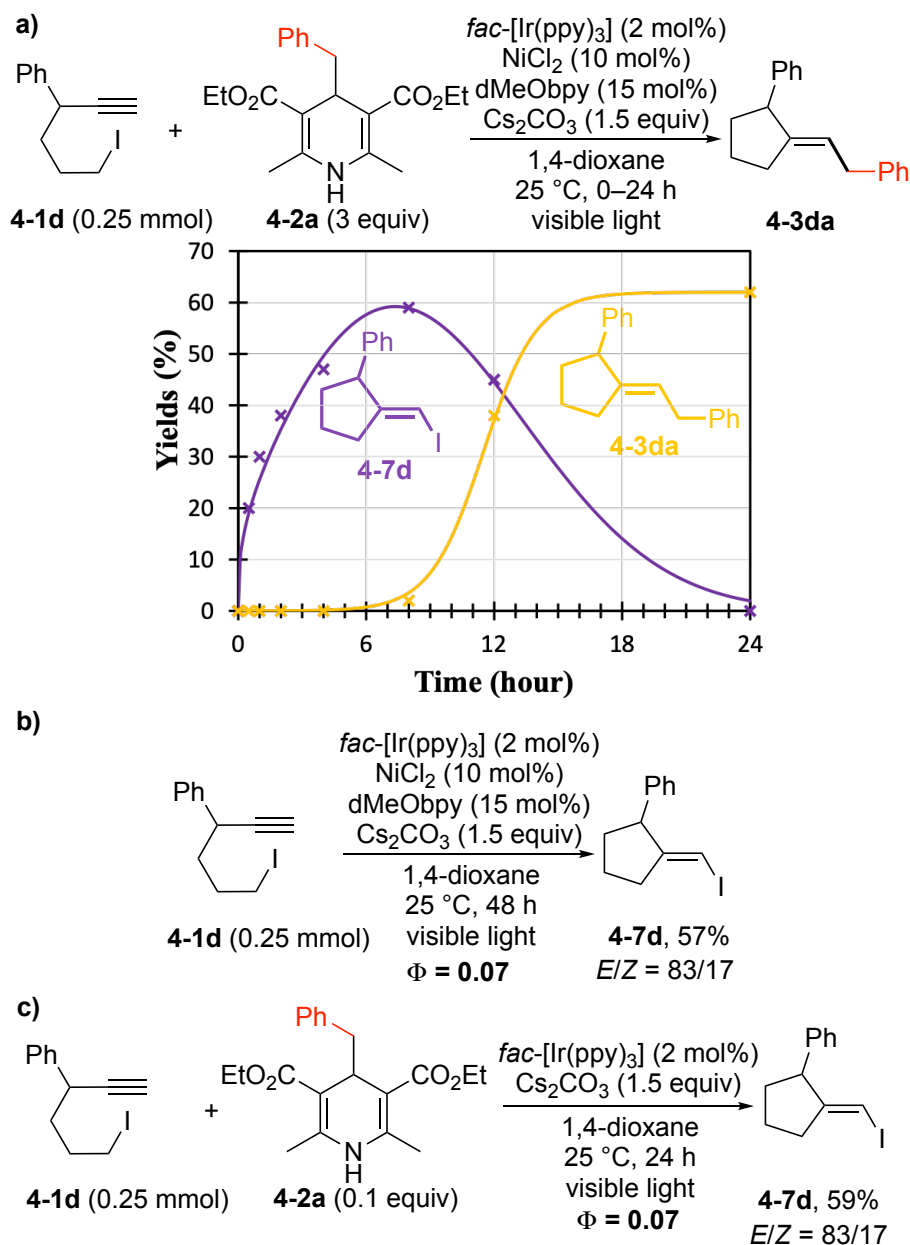
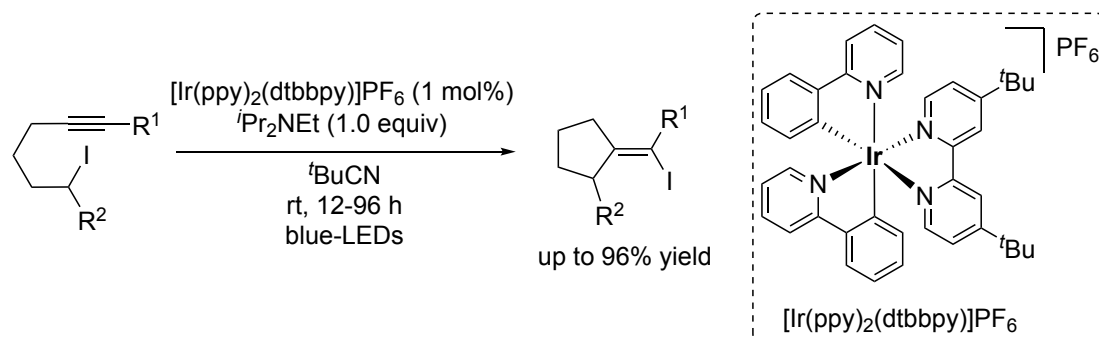


Figure 4-2. Formation of cyclopentylidene iodide as a reactive intermediate for the reactions of **4-1d** with **4-2a**. (a) Time profile of the reaction. (b) Reaction in the absence of **4-2a**. (c) Reaction in the presence of a catalytic amount of **4-2a** but in the absence of Ni catalysts.

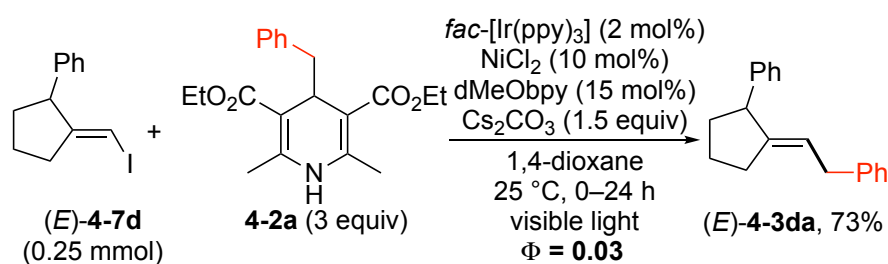
Scheme 4-3. Visible-Light-Promoted Atom Transfer Radical Cyclization of Unactivated Alkyl Iodides reported by Martin *et al.*



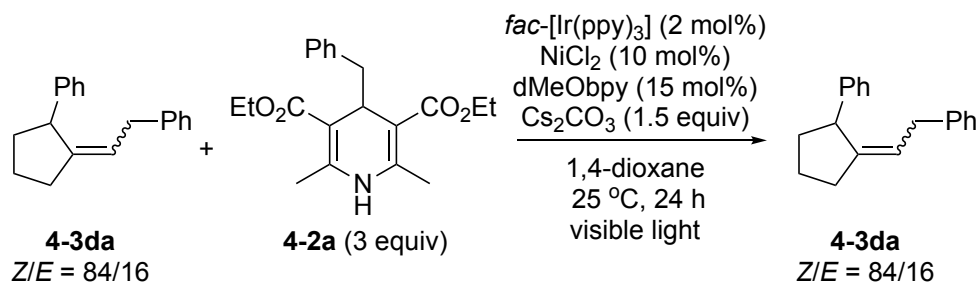
In order to confirm that vinyl iodide species like **4-7d** are the reactive intermediate of the present alkylative cyclization reactions, the reaction of isolated (*E*)-**4-7d** with **4-2a** under the similar catalytic conditions was further examined to elucidate that (*E*)-**4-3da** was obtained in 73% isolated yield as the sole stereoisomer (Scheme 4-4a) with the low quantum yield observed at $\Phi = 0.028 \pm 0.001$. This result demonstrates that **4-7d** may be formed as a reactive intermediate. The photoredox- and nickel-catalyzed cross-coupling reaction of (*E*)-**4-7d** with **4-2a** proceeds to afford (*E*)-**4-3da** without *E/Z* isomerization, which matches our previous report.⁹ In addition, irradiation of a mixture of (*E*)-**4-3da** and (*Z*)-**4-3da** (*E/Z* = 16/84) in general reaction conditions afforded a mixture of (*E*)-**4-7d** and (*Z*)-**4-7d** (*E/Z* = 16/84) with the retention of *E/Z* ratio (Scheme 4-4b), demonstrating that both *Z* to *E* and *E* to *Z* did not occur.

Scheme 4-4. Reaction of **4-7d** with **4-2a** and Reaction of **4-3da**

a) Reaction of (*E*)-4-7d with 4-2a to afford (*E*)-4-3da



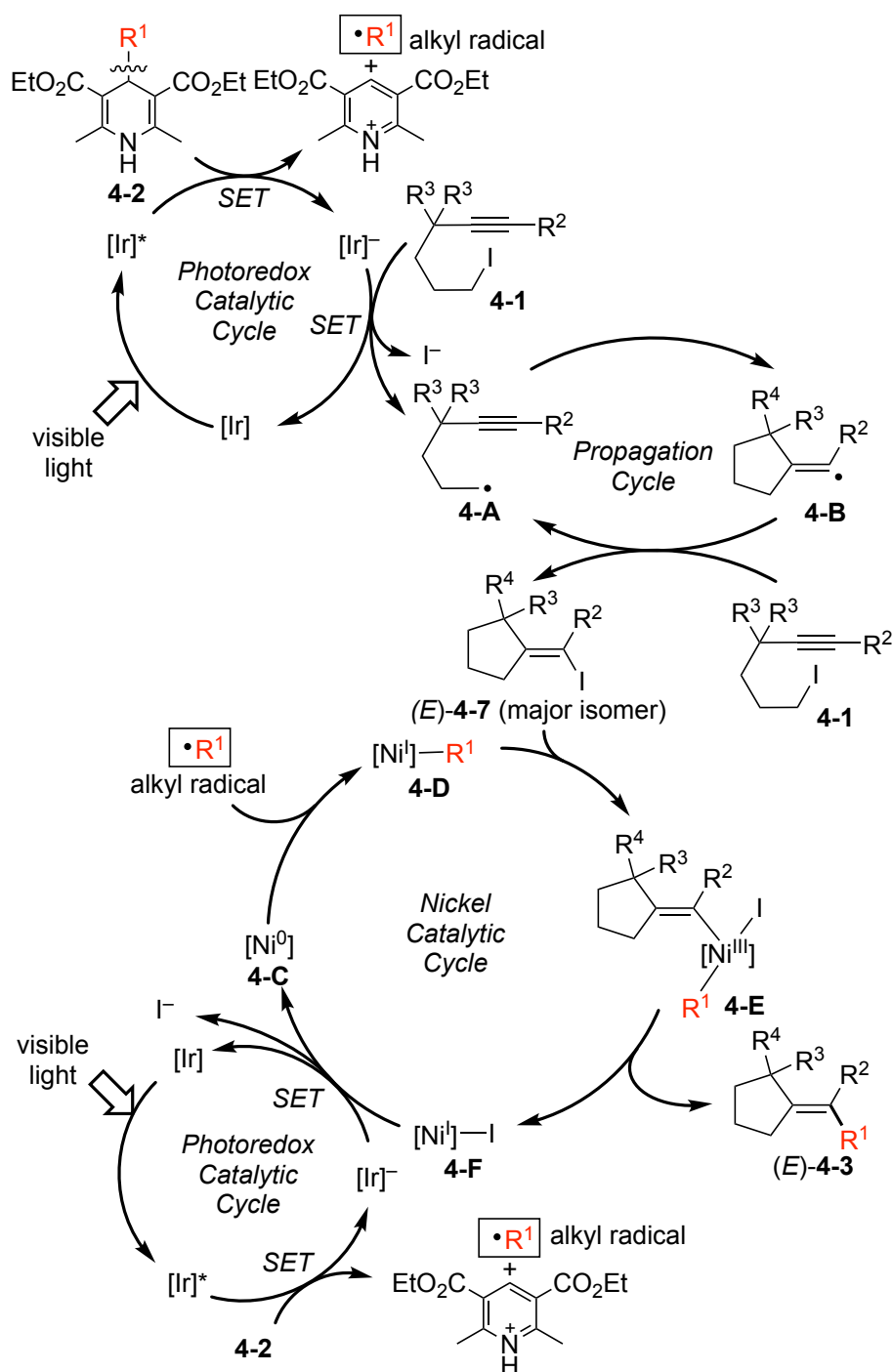
b) Reaction of a mixture of (*E*)-4-3da and (*Z*)-4-3da



A plausible reaction pathway for the cooperative photoredox- and nickel-catalyzed alkylative cyclization reactions can be drawn as shown in [Scheme 4-5](#), consisting of two sequential reactions, *i.e.*, (1) cyclization reaction of **4-1** into **4-7** and (2) alkylation of **4-7** into **4-3**, both of which require the Ir photoredox catalyst. In the initial iridium photoredox cycle, excitation of the Ir(III) catalyst *fac*-[Ir(ppy)₃] ([Ir]) by the absorption of visible light occurs to give the excited state ([Ir]*). The subsequent SET processes between [Ir]* and other substrates including **4-1** or nickel species are possible, but the fastest SET process can occur between [Ir]* and **4-2** as suggested by the Stern–Volmer analysis ([Figure 4-2b](#)) to afford the reduced Ir(II) species ([Ir][−]) and a radical cationic 1,4-dihydropyridine, which is further converted to an alkyl radical ($\cdot R^1$) and an aromatized pyridine derivative via C–C bond cleavage.^{3,29} Here, [Ir][−] is capable of abstracting iodide (I[−]) from **4-1** to generate [Ir] and the hex-5-yn-1-yl radical (**4-A**), which is further cyclized into the cyclopentylidene radical (**4-B**).^{32,33} **4-B** can be engaged in the iodine atom transfer with **4-1** to afford the radical **4-A** and the cyclopentylidene iodide **4-7**, where the (*E*)-isomer is rather preferentially formed. On the other hand, rather low quantum yields observed for the formation of **4-7** suggest that such propagation is inhibited by alkyl and other radicals formed in situ.

Subsequently to the formation of **4-7**, alkylation of **4-7** with the alkyl radical $\cdot R^1$ into **4-3** occurs by the cooperation of photoredox and nickel catalyst. In the nickel cycle, capture of the alkyl radical $\cdot R^1$ by an in situ-generated Ni(0) species (**4-C**) occurs to afford a Ni(I)–alkyl complex (**4-D**), where the oxidative addition of (*E*)-**4-7** occurs to give a Ni(III) (alkenyl)(alkyl) iodide complex (**4-E**), followed by the reductive elimination of the desired coupling product (*E*)-**4-3** along with the formation of a Ni(I) iodide complex (**4-F**). Finally, the nickel catalytic cycles are completed by a SET process between the reduced Ir(II) catalyst [Ir][−] and the Ni(I) iodide complex **4-F**. (*Z*)-**4-7** can also participate in the nickel-catalyzed transformation to afford (*Z*)-**4-3**, although (*E*)-**4-7** more preferentially adds the nickel catalyst to afford (*E*)-**4-3**, resulting in a slight increase in the ratio of (*E*)-**4-3** compared to that of (*E*)-**4-7** (83/17 to 92/8 in the case of **4-7d** and **4-3da**, respectively). The combination of two sequential reactions, *i.e.*, (1) cyclization reaction of **4-1** into **4-7** and (2) alkylation of **4-7** into **4-3**, can cause a long induction period for the conversion of **4-7d** into **4-3da** as it appears in [Figure 4-2a](#), where the generated alkyl radical $\cdot R^1$ can be quenched in several ways.

Scheme 4-5. Plausible Reaction Pathway



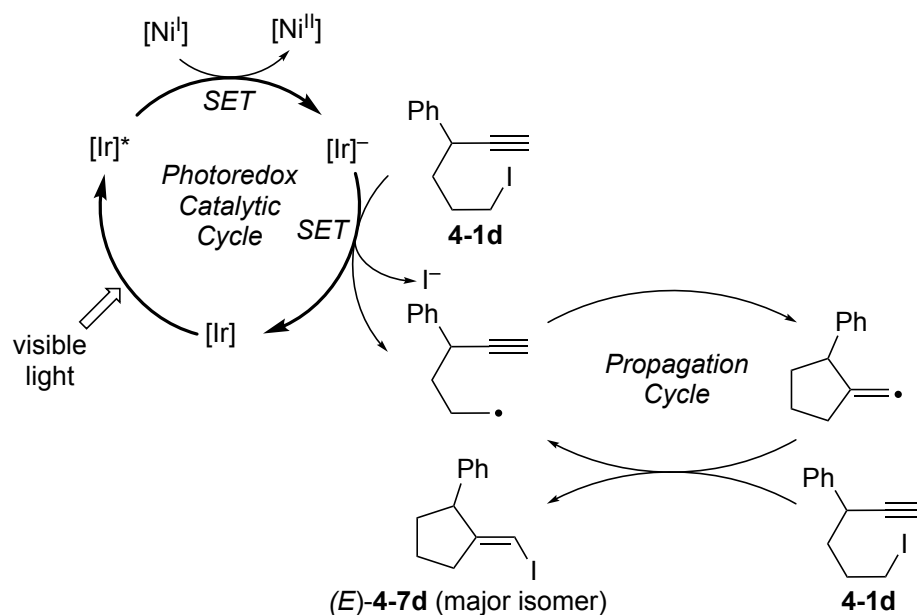
Concerning the initial cyclization of **4-1** into **4-7**, cyclization of alkyl iodide has been known to proceed by several radical initiators^{31b} or photoredox catalysts.^{32,33} The reaction pathway for the initial cyclization reaction depicted here follows the one reported by Martin and co-workers.³² However in contrast to their proposals, possibility of the formation of exciplex complex with **4-1d** is rather excluded, because *fac*-[Ir(ppy)₃] is the only photosensitizer that can absorb visible light in this reaction. At the same time, quenching of propagation cycle should frequently occur by the termination with the photoredox catalyst or with alkyl radicals based on the observation of a low

quantum yield.

On the other hand, the initial conversion of **4-1** into **4-7** was shown to occur without the addition of **4-2** (Scheme 4-4b). Thus, other reaction pathways where $[\text{Ir}]^-$ species is formed via the SET process with Ni catalyst, not with **4-2**, cannot be excluded (Schemes 4-6 and 4-7). Here, two possible reaction pathways can be drawn where Ni catalyst directly participates in the formation of **4-7** (Scheme 4-7) or not (Scheme 4-6).

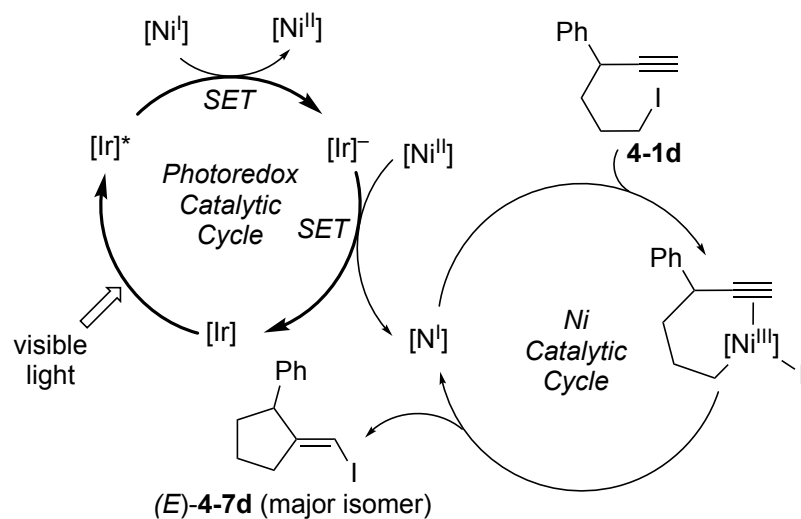
The other possible reaction pathway I: This reaction pathway is drawn where Ni participates in photoredox catalytic cycle, while cyclopentylidene iodide is formed via propagation cycle which is initiated by the photoredox catalyst (Scheme 4-6). Same with Scheme 4-5, this cycle also depicted based on the proposals by Martin and co-workers,³² where possibility of the formation of exciplex complex with **4-2a** or benzyl radical-initiated propagation cycle are excluded, because **2a** did not work as a photosensitizer, nor formation of benzyl iodide was observed for the crude mixtures. At the same time, quenching of chain propagation should frequently occur by the termination with the photoredox catalyst or alkyl radicals based on the observation of a low quantum yield.

Scheme 4-6. The other possible reaction pathway I



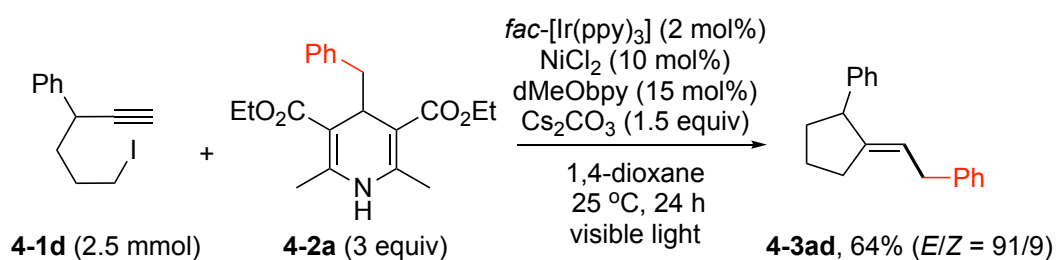
The other possible reaction pathway II: This reaction pathway is drawn where both Ni and photoredox catalysts participate in both photoredox and cyclization catalytic cycles (Scheme 4-7). Here the oxidative addition of **4-1d** and reductive elimination of **4-7d** are shown at the Ni(I)/Ni(III) cycle based on the recent work by Nocera and co-workers for the iridium photoredox and $\text{NiCl}_2(\text{dtbbpy})$ catalytic systems,³⁵ whereas Ni(0)/Ni(II) cycle can be also possible.

Scheme 4-7. The other possible reaction pathway II



Finally, a larger scale reaction of **4-1d** (2.5 mmol) with **4-2a** (7.5 mmol) was performed under the optimized reaction conditions to afford the alkylative cyclization product **4-3da** in 64% isolated yield as a mixture of *E*- and *Z*-isomers with an *E/Z* ratio of 91/9 ([Scheme 4-8](#)).

Scheme 4-8. Large-Scale Preparation of **4-3da**



4.3. Conclusion for Chapter 4

The author has achieved the cooperative photoredox- and nickel-catalyzed alkylative cyclization reactions of 6-iodohex-1-ynes with 4-alkyl-1,4-dihydropyridines employed as alkylation reagents at 25 °C under the irradiation of visible light to afford the corresponding alkylated cyclopentylidenes in good to high yields. In addition to terminal alkynes, internal alkynes can also be converted into the desired products, which were not achieved in the previously reported catalytic alkylative cyclization reactions with alkyl zinc reagents as alkylation reagents.¹⁶ Introduction of substituents at the propargylic position of 6-iodohex-1-ynes has led to the stereoselective formation of *E*-isomers. The author considers that the method described herein expands the usage of 4-alkyl-1,4-dihydropyridines as mild formal alkylation reagents in the combination of photoredox and transition metal catalysts to provide novel transformations of organic compounds under mild reaction conditions.

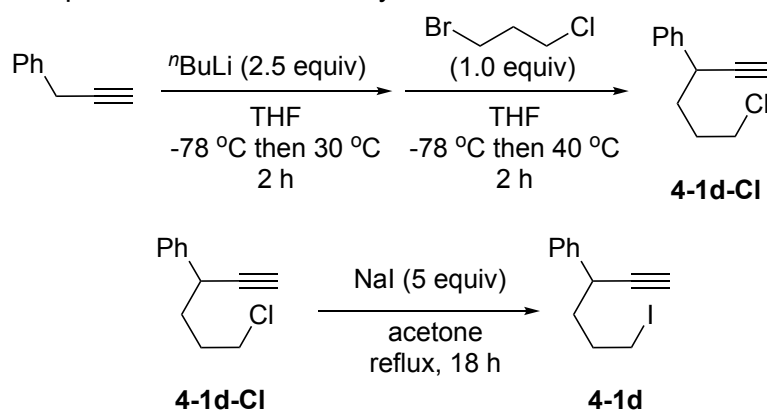
4.4. Experimental Section

4.4.1. General Methods

All reactions were carried out under a dry nitrogen atmosphere by using standard Schlenk techniques. **4-1a**,³⁶ **4-1a-Br**,³⁷ **4-1b**,³⁸ **4-1c**,³⁹ **4-1i**,⁴⁰ **4-2a**,⁴¹ **4-2b**,⁴¹ **4-2c**,⁴¹ **4-2d**,⁸ **4-2e**,⁴¹ **4-2g**,³ **4-2h**,³ **4-2i**,⁹ **4-2j**,⁴² **4-2k**,⁴¹ **4-2l**,⁴¹ **4-2m**,⁴¹ **4-2n**,⁸ **4-2o**,³ **4-2p**,⁴² **4-2r**,⁶ **4-2s**,⁴³ **4-4a**,⁴⁴ **4-4c**,⁴⁵ and **4-5aa**⁴⁶ were prepared according to the literature procedures. Other reagents including starting materials for the preparation of **4-1a-j**, **4-2a-s**, **4-4a-c**, **4-1a-Cl**, *fac*-[Ir(ppy)₃], *fac*-[Ir(Fppy)₃], anhydrous NiCl₂, ligands (bpy, dtbbpy, dMebpy, dMeObpy), bases, TEMPO, and solvents were obtained from commercial sources. Acetonitrile, diethyl ether, *n*-hexane, and THF were purified by passing through a purification system (Glass Contour) and were degassed before use. Other solvents were dried by general methods and degassed before use. Flash column chromatography was carried out on a Yamazen YFLC-AI-580 system. Gas chromatography–mass spectroscopy (GC–MS) was performed on a Shimadzu GCMS-QP2010 PLUS instrument. *E/Z* ratios were determined by quantitative measurements of GC–MS. X-ray analysis was performed by a Rigaku XtaLAB Synergy-S diffractometer. Photoluminescence spectra were measured on a Shimadzu RF-5300PC spectrophotometer. Melting points were measured by using a Stanford Research Systems OptiMelt MPA100. High-resolution FAB mass spectra were measured on a JEOL JMS-700 mass spectrometer. ¹H NMR (400 MHz) and ¹³C{¹H} NMR (100 MHz) spectra were measured in CDCl₃ on a JEOL ECS-400 spectrometer with δ values calibrated by using residual peaks of CHCl₃ (¹H: 7.26) and CDCl₃ (¹³C: 77.0), respectively.

4.4.2. General Procedure for the Preparation of 6-Iodohept-1-yne Derivatives (**4-1**) (Taking (6-Iodohept-1-yn-3-yl)benzene (**4-1d**) as an Example)

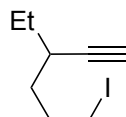
Scheme 4-9. Preparation of 6-Iodohept-1-yne derivatives **4-1d**



In a 100 mL Schlenk flask were placed prop-2-yn-1-ylbenzene (2.32 g, 20.0 mmol) and THF (25 mL) at -78 °C by using a dry ice-methanol bath under N₂, where a hexane solution of ⁿBuLi (32 mL, 1.57 M, *ca.* 50 mmol) was added dropwise. The reaction mixture was gradually warmed to 30 °C by using an oil bath and was further stirred for 2 h. Then the reaction mixture was cooled back to -78 °C by using a dry ice-methanol

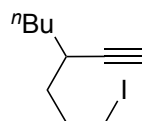
bath, and 1-bromo-3-chloropropane (3.15 g, 20.0 mmol) was added dropwise. The reaction mixture was gradually warmed to 40 °C by using an oil bath and was further stirred for 2 h. The resultant mixture was quenched with a saturated aqueous solution of NH₄Cl (40 mL), and the aqueous phase was extracted with Et₂O (50 mL × 3). The combined organic layers were washed with brine (50 mL), dried over anhydrous MgSO₄, and filtered. The filtrate was collected, and the solvent was removed under reduced pressure. The residue was further purified by column chromatography (SiO₂) with *n*-hexane as an eluent to afford (6-chlorohex-1-yn-3-yl)benzene (**4-1d-Cl**) as a colorless oil (2.72 g, 14.1 mmol, 71% yield based on the amount of prop-2-yn-1-ylbenzene), which was directly used in the subsequent transformation to obtain (6-iodohex-1-yn-3-yl)benzene (**4-1d**) without further purification.

In a 100 mL Schlenk flask were placed **4-1d-Cl** (2.60 g, 13.5 mmol), NaI (10.1 g, 67.5 mmol), and acetone (40 mL) under N₂, and the reaction mixture was stirred and refluxed for 18 h by using an oil bath. Then, acetone was removed in vacuo, and the resultant mixture was diluted with 100 mL of *n*-hexane and was filtered. Solvent was removed from the collected filtrate under reduced pressure, and the residue was purified by column chromatography (SiO₂) with *n*-hexane as an eluent to afford (6-iodohex-1-yn-3-yl)benzene (**4-1d**) as a colorless oil (3.64 g, 12.8 mmol, 95% yield based on the amount of **4-1d-Cl**, 64% yield based on the amount of prop-2-yn-1-ylbenzene). HRMS (FAB) *m/z* [M]⁺ Calcd for C₁₂H₁₃I 284.0062; Found: 284.0059. ¹H NMR (400 MHz, CDCl₃, δ): 7.36–7.16 (m, 5H, CH of Ph), 3.62 (td, *J* = 6.0, 2.3 Hz, 1H, CHC≡), 3.12 (t, *J* = 6.8 Hz, 2H, CH₂I), 2.24 (d, *J* = 2.3 Hz, 1H, HC≡), 2.01–1.73 (m, 4H, CH₂). ¹³C{¹H} NMR (100 MHz, CDCl₃, δ): 140.7 (*ipso*-C of Ph), 128.5, 127.2 (*o*- and *m*-CH of Ph), 126.9 (*p*-CH of Ph), 85.0 (C≡), 71.6 (HC≡), 38.7, 36.4, 30.8 (CH(CH₂)₂), 6.2 (CH₂I).



4-1e

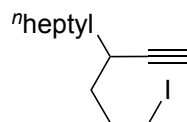
3-Ethyl-6-iodohex-1-yne (4-1e). A colorless oil (283 mg, 1.20 mmol, 12% yield based on the amount of pent-1-yne (680 mg, 9.98 mmol)). HRMS (FAB) *m/z* [M]⁺ Calcd for C₈H₁₃I 236.0062; Found: 236.0054. ¹H NMR (400 MHz, CDCl₃, δ): 3.19 (t of pseudo d, *J* = 4.8, 2.1 Hz, 2H, CH₂I), 2.31–2.22 (m, 1H, CHC≡), 2.10–1.97 (m, 1H, CH₂CH₂I), 2.05 (d, *J* = 2.4 Hz, 1H, HC≡), 1.96–1.84 (m, 1H, CH₂CH₂I), 1.62–1.39 (m, 4H, CH₂CHCH₂), 0.99 (t, *J* = 7.6 Hz, 3H, CH₃). ¹³C{¹H} NMR (100 MHz, CDCl₃, δ): 86.8 (C≡), 69.8 (HC≡), 35.1, 32.2, 31.0, 27.9 (CH₂CH(CH₂)₂), 11.6 (CH₃), 6.7 (CH₂I).



4-1f

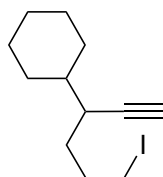
4-Ethynyl-1-iodooctane (4-1f). A colorless oil (451 mg, 1.71 mmol, 17% yield based

on the amount of hept-1-yne (962 mg, 10.0 mmol)). HRMS (FAB) m/z $[M]^+$ Calcd for $C_{10}H_{17}I$ 264.0375; Found: 264.0383. 1H NMR (400 MHz, $CDCl_3$, δ): 3.20 (t of pseudo d, $J = 6.9, 2.5$ Hz, 2H, CH_2I), 2.38–2.28 (m, 1H, $CHC\equiv$), 2.14–1.98 (m, 1H, CH_2CH_2I), 2.05 (d, $J = 2.2$ Hz, 1H, $HC\equiv$), 1.97–1.84 (m, 1H, CH_2CH_2I), 1.64–1.22 (m, 8H, $(CH_2)_3CHCH_2$), 0.90 (t, $J = 7.2$ Hz, 3H, CH_3). $^{13}C\{^1H\}$ NMR (100 MHz, $CDCl_3$, δ): 87.1 ($C\equiv$), 69.7 ($HC\equiv$), 35.5, 34.6, 31.1, 30.5, 29.3, 22.5 ($(CH_2)_3CH(CH_2)_2$), 14.0 (CH_3), 6.7 (CH_2I).



4-1g

4-Ethynyl-1-iodoundecane (4-1g). A colorless oil (334 mg, 1.09 mmol, 11% yield based on the amount of 1-bromo-3-chloropropane (1.57 g, 9.99 mmol)). HRMS (FAB) m/z $[M]^+$ Calcd for $C_{13}H_{23}I$ 306.0845; Found: 306.0840. 1H NMR (400 MHz, $CDCl_3$, δ): 3.20 (t of pseudo d, $J = 7.0, 2.4$ Hz, 2H, CH_2I), 2.37–2.28 (m, 1H, $CHC\equiv$), 2.12–1.98 (m, 1H, CH_2CH_2I), 2.04 (d, $J = 2.4$ Hz, 1H, $HC\equiv$), 1.97–1.84 (m, 1H, CH_2CH_2I), 1.63–1.20 (m, 14H, $(CH_2)_6CHCH_2$), 0.87 (t, $J = 6.8$ Hz, 3H, CH_3). $^{13}C\{^1H\}$ NMR (100 MHz, $CDCl_3$, δ): 87.1 ($C\equiv$), 69.7 ($HC\equiv$), 35.6, 34.9, 31.8, 31.1, 30.6, 29.4, 29.2, 27.2, 22.6 ($(CH_2)_6CH(CH_2)_2$), 14.1 (CH_3), 6.7 (CH_2I).

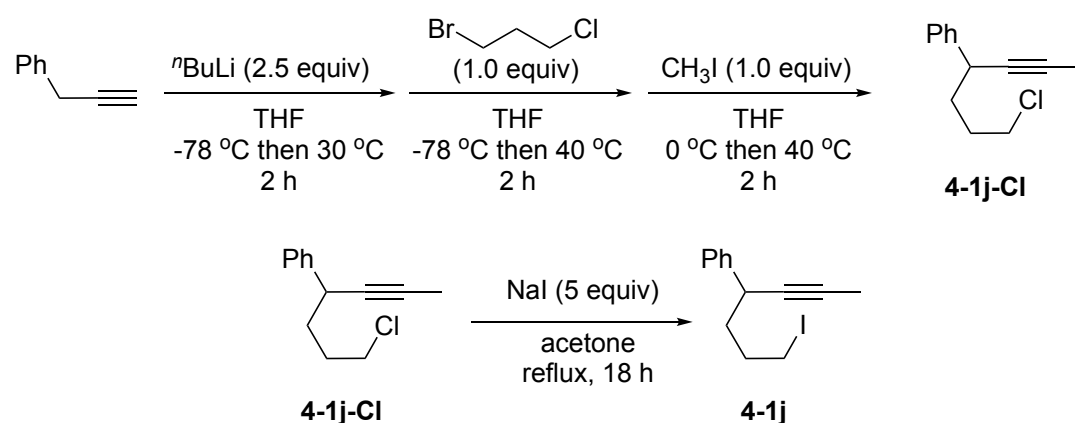


4-1h

(6-Iodohept-1-yn-3-yl)cyclohexane (4-1h). A colorless oil (627 mg, 2.16 mmol, 28% yield based on the amount of 1-bromo-3-chloropropane (1.21 g, 7.69 mmol)). HRMS (FAB) m/z $[M]^+$ Calcd for $C_{12}H_{19}I$ 290.0532; Found: 290.0528. 1H NMR (400 MHz, $CDCl_3$, δ): 3.18 (t of pseudo d, $J = 6.9, 1.5$ Hz, 2H, CH_2I), 2.22–2.16 (m, 1H, $CHC\equiv$), 2.08–1.98 (m, 1H, CH of Cy), 2.03 (d, $J = 2.4$ Hz, 1H, $HC\equiv$), 1.91–1.44, 1.36–1.04 (both m, 8H and 6H, respectively, CH_2 of $CyCH(CH_2)_2$). $^{13}C\{^1H\}$ NMR (100 MHz, $CDCl_3$, δ): 85.7 ($C\equiv$), 70.6 ($HC\equiv$), 40.9, 40.8, 36.7, 32.7, 31.3, 31.1, 29.0, 26.2, 26.1 ($CyCH(CH_2)_2$), 6.8 (CH_2I).

4.4.3. Preparation of (7-Iodohept-2-yn-4-yl)benzene (4-1j)

Scheme 4-10. Preparation of (7-Iodohept-2-yn-4-yl)benzene **4-1j**



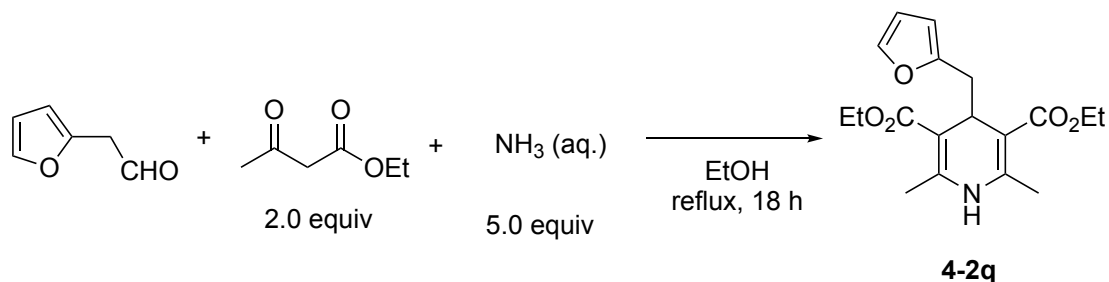
In a 100 mL Schlenk flask were placed prop-2-yn-1-ylbenzene (1.16 g, 10.0 mmol) and THF (14 mL) at $-78\text{ }^{\circ}\text{C}$ by using a dry ice-methanol bath under N_2 , where a hexane solution of $n\text{BuLi}$ (16.1 mL, 1.57 mol/L, ca. 25 mmol) was added dropwise. The reaction mixture was gradually warmed to $30\text{ }^{\circ}\text{C}$ by using an oil bath and was further stirred for 2 h. The reaction mixture was cooled back to $-78\text{ }^{\circ}\text{C}$ by using a dry ice-methanol bath, and 1-bromo-3-chloropropane (1.57 g, 10.0 mmol) was added dropwise. The reaction mixture was gradually warmed to $40\text{ }^{\circ}\text{C}$ by using an oil bath and was further stirred for 2 h. Then, the reaction mixture was cooled to $0\text{ }^{\circ}\text{C}$ by using an ice-water bath, and iodomethane (1.42 g, 10.0 mmol) was added dropwise. The reaction mixture was gradually warmed to $40\text{ }^{\circ}\text{C}$ by using an oil bath and was further stirred for 2 h. The resultant mixture was quenched with a saturated solution of NH_4Cl (40 mL), and the aqueous phase was extracted with Et_2O ($30\text{ mL} \times 3$). The combined organic layers were washed with brine ($20\text{ mL} \times 2$), dried over anhydrous MgSO_4 , and filtered. The filtrate was collected, and the solvent was removed under reduced pressure. The residue was further purified by column chromatography (SiO_2) with n-hexane as an eluent to afford (7-chlorohept-2-yn-4-yl)benzene (**4-1j-Cl**) as a colorless oil (924 mg, 0.447 mmol, 45% yield based on the amount of 1-bromo-3-chloropropane), which was directly used in the subsequent transformation to obtain (7-Iodohept-2-yn-4-yl)benzene (**4-1j**) without further purification.

In a 100 mL Schlenk flask were placed **4-1j-Cl** (621 mg, 3.02 mmol), NaI (2.25 g, 15.0 mmol), and acetone (40 mL) under N_2 , and the reaction was stirred and refluxed by using an oil bath for 18 h. Then, acetone was removed in vacuo, and the resultant mixture was diluted with 100 mL of n-hexane and was filtered. Solvent was removed from the collected filtrate under reduced pressure, and the residue was purified by column chromatography (SiO_2) with n-hexane as an eluent to afford (7-Iodohept-2-yn-4-yl)benzene (**4-1j**) as a colorless oil (608 mg, 2.04 mmol, 68% yield based on the amount of **4-1j-Cl**, 20% yield based on the amount of 1-bromo-3-chloropropane). HRMS (FAB) m/z $[\text{M}]^+$ Calcd for $\text{C}_{13}\text{H}_{15}\text{I}$ 298.0219; Found 298.0207. ^1H NMR (400 MHz, CDCl_3 , δ): 7.38–7.30 (m, 4H, *o*- and *m*-CH of Ph), 7.24 (tt, $J = 6.7, 2.1\text{ Hz}$, 1H,

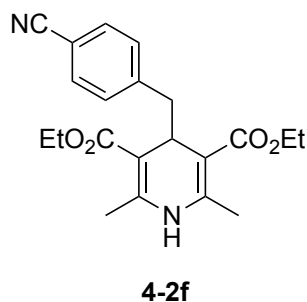
p-CH of Ph), 3.62 (t of pseudo t, $J = 8.3, 2.4$ Hz, 1H, $\text{CHC}\equiv$), 3.20 (t, 2H, $J = 6.8$, CH_2I), 2.04–1.89 (m, 2H, CH_2CH_3), 1.88 (d, $J = 2.8$ Hz, 3H, CH_3), 1.88–1.74 (m, 2H, $\text{CH}_2\text{CH}_2\text{CH}_3$). $^{13}\text{C}\{^1\text{H}\}$ NMR (100 MHz, CDCl_3 , δ): 142.0 (*ipso*-C of Ph), 128.3, 127.2 (*o*- and *m*-CH of Ph), 126.6 (*p*-CH of Ph), 80.0, 78.9 ($\text{C}\equiv\text{C}$), 39.2, 36.7, 31.1 ($\text{CH}(\text{CH}_2)_2$), 6.5, 3.6 (CH_2I and CH_3).

4.4.4. General Procedure for the Preparation of Diethyl 4-Alkyl-2,6-dimethyl-1,4-dihydropyridine-3,5-dicarboxylate Derivatives (4-2) (Taking Diethyl 4-(Furan-2-ylmethyl)-2,6-dimethyl-1,4-dihydropyridine-3,5-dicarboxylate (4-2q) as an Example)

Scheme 4-11. Preparation of Diethyl 4-Alkyl-2,6-dimethyl-1,4-dihydropyridine-3,5-dicarboxylate Derivatives **4-2**



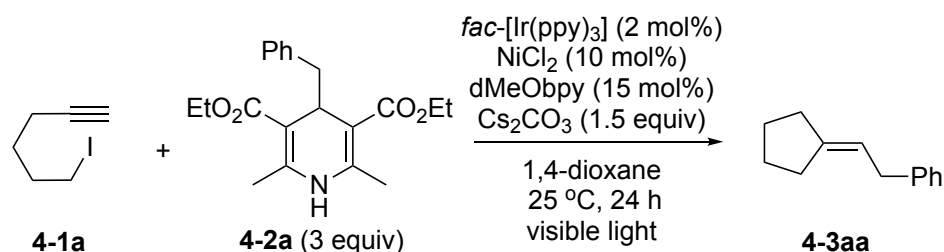
In a 50 mL Schlenk flask were placed 2-furanacetaldehyde (396 mg, 3.60 mmol), ethyl acetoacetate (938 mg, 7.20 mmol), and ethanol (20 mL) at room temperature under N_2 , where an aqueous solution of 28 wt % NH_3 (1.1 mL, *ca.* 18 mmol) was added. The reaction mixture was stirred and refluxed for 18 h by using an oil bath, then was dried in vacuo. The residue was further purified by column chromatography (SiO_2) with a mixture of *n*-hexane/ethyl acetate (7:3) as an eluent to afford diethyl 4-(furan-2-ylmethyl)-2,6-dimethyl-1,4-dihydropyridine-3,5-dicarboxylate (**4-2q**) as a white solid (600 mg, 1.80 mmol, 50% yield based on the amount of 2-furanacetaldehyde). mp 106.0–107.3 °C. HRMS (FAB) m/z $[\text{M}]^+$ Calcd for $\text{C}_{18}\text{H}_{23}\text{NO}_5$ 333.1576; Found 333.1579. ^1H NMR (400 MHz, CDCl_3 , δ): 7.24 (dd, $J = 1.8, 1.0$ Hz, 1H, 5-CH of furyl), 6.19 (dd, $J = 3.1, 1.8$ Hz, 1H, 4-CH of furyl), 5.84 (d, $J = 3.1$ Hz, 1H, 3-CH of furyl), 5.69 (br, 1H, NH), 4.18 (t, $J = 5.7$ Hz, 1H, 4-CH of 1,4-dihydropyridine), 4.15–4.03 (m, 4H, CH_3CH_2), 2.59 (d, $J = 5.7$ Hz, 2H, CH_2 of furan-2-ylmethyl), 2.22 (s, 6H, 2- CCH_3 of 1,4-dihydropyridine) 1.25 (t, $J = 7.0$ Hz, 6H, CH_3CH_2). $^{13}\text{C}\{^1\text{H}\}$ NMR (100 MHz, CDCl_3 , δ): 167.6 (CO_2), 154.0 (2-C of furyl), 145.3 (2-C of 1,4-dihydropyridine), 140.8 (5-CH of furyl), 110.1, 106.8 (3-CH and 4-CH of furyl), 101.9 (3-C of 1,4-dihydropyridine), 59.7 (CH_3CH_2), 34.2, 33.9 (4- CHCH_2 of 1,4-dihydropyridine), 19.3 (2- CCH_3 of 1,4-dihydropyridine), 14.3 (CH_3CH_2).



Diethyl 4-(4-Cyanobenzyl)-2,6-dimethyl-1,4-dihydropyridine-3,5-dicarboxylate (4-2f). A white solid (371 mg, 1.01 mmol, 25% yield based on the amount of 4-(2-oxoethyl)benzonitrile (581 mg, 4.00 mmol)). mp 156.7–158.5 °C. HRMS (FAB) m/z $[M]^+$ Calcd for $C_{21}H_{24}N_2O_4$ 368.1736; Found: 368.1741. 1H NMR (400 MHz, $CDCl_3$, δ): 7.44, 7.10 (both d, J = 8.0 Hz, 2H each, C_6H_4), 5.74 (br, 1H, NH), 4.21 (t, J = 5.4 Hz, 1H, 4-CH of 1,4-dihydropyridine), 4.12–3.98 (m, 4H, CH_3CH_2), 2.62 (d, J = 5.4 Hz, 2H, CH_2 of 4-cyanobenzyl), 2.14 (s, 6H, 2- CCH_3 of 1,4-dihydropyridine) 1.21 (t, J = 7.2 Hz, 6H, CH_3CH_2). $^{13}C\{^1H\}$ NMR (100 MHz, $CDCl_3$, δ): 167.5 (CO_2), 146.0 (*ipso*-C of C_6H_4), 145.4 (2-C of 1,4-dihydropyridine), 130.8, 130.7 (*o*- and *m*-CH of C_6H_4), 119.3 (CN), 109.2 (*p*-C of C_6H_4), 101.0 (3-C of 1,4-dihydropyridine), 59.6 (CH_3CH_2), 42.3 (4- $CHCH_2$ of 1,4-dihydropyridine), 35.4 (4- $CHCH_2$ of 1,4-dihydropyridine), 18.9 (2- CCH_3 of 1,4-dihydropyridine), 14.3 (CH_3CH_2).

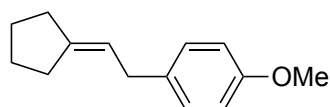
4.4.5. General Procedure for the Preparation of Alkylated Cyclopentylidenes (Taking (2-cyclopentylideneethyl)benzene (4-3aa) as an Example)

Scheme 4-12. Preparation of Alkylated Cyclopentylidenes 4-3



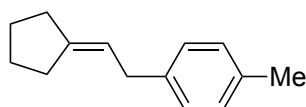
In a 20 mL Schlenk flask were placed 6-iodohex-1-yne (**4-1a**) (50.1 mg, 0.241 mmol), diethyl 4-benzyl-2,6-dimethyl-1,4-dihydropyridine-3,5-dicarboxylate (**4-2a**) (260 mg, 0.756 mmol), *fac*-[Ir(ppy)₃] (3.4 mg, 0.0052 mmol), anhydrous NiCl₂ (3.4 mg, 0.026 mmol), dMeObpy (8.0 mg, 0.037 mmol), and Cs₂CO₃ (122 mg, 0.375 mmol) under N₂, where 1,4-dioxane (2.5 mL) was added at room temperature. The reaction flask was placed in an As One LTB-125 constant low temperature water bath set at 25 °C, and was illuminated from the bottom of the bath with an Aitech System TMN100×120–22WD 12 W white LED lamp (400 nm to 750 nm) at a distance of approximately 2 cm from the light source for 24 h. The volatiles were removed *in vacuo*, and the residue was purified by column chromatography (SiO₂) with *n*-hexane as an eluent to afford (2-cyclopentylideneethyl)benzene (**4-3aa**) as a colorless oil (34.5 mg,

0.200 mmol, 83% yield based on the amount of **4-1a**). HRMS (FAB) m/z $[M]^+$ Calcd for $C_{13}H_{16}$ 172.1252; Found: 172.1247. 1H NMR (400 MHz, $CDCl_3$, δ): 7.30 (t, $J = 7.6$ Hz, 2H, *m*-CH of Ph), 7.24–7.17 (m, 3H, *o*- and *p*-CH of Ph), 5.47 (tt, $J = 7.2$, 2.3 Hz, 1H, CH=), 3.35 (d, $J = 7.2$ Hz, 2H, $CH_2CH=$), 2.31 (pseudo q, $J = 7.6$ Hz, 4H, α - CH_2 of cyclopentylidene), 1.73, 1.65 (both quint, $J = 6.9$ Hz, 2H each, β - CH_2 of cyclopentylidene). $^{13}C\{^1H\}$ NMR (100 MHz, $CDCl_3$, δ): 144.4 (*ipso*-C of cyclopentylidene), 141.8 (*ipso*-C of Ph), 128.3, 128.3 (*o*- and *m*-CH of Ph), 125.7 (*p*-CH of Ph), 118.6 (CH=), 35.9 ($CH_2CH=$), 33.6, 28.8 (α - CH_2 of cyclopentylidene), 26.4, 26.3 (β - CH_2 of cyclopentylidene).



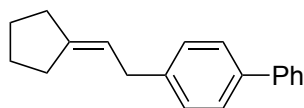
4-3ab

1-(2-Cyclopentylideneethyl)-4-methoxybenzene (4-3ab). A colorless oil (39.4 mg, 0.195 mmol, 81% yield based on the amount of **4-1a** (50.3 mg, 0.242 mmol)). HRMS (FAB) m/z $[M]^+$ Calcd for $C_{14}H_{18}O$ 202.1358; Found: 202.1357. 1H NMR (400 MHz, $CDCl_3$, δ): 7.11, 6.84 (both dt, $J = 8.8$, 2.2 Hz, 2H each, C_6H_4), 5.44 (t of quint, $J = 7.1$, 2.1 Hz, 1H, CH=), 3.79 (s, 3H, CH_3), 3.28 (d, $J = 7.1$ Hz, 2H, $CH_2CH=$), 2.33–2.25 (m, 4H, α - CH_2 of cyclopentylidene), 1.71, 1.64 (both quint, $J = 6.7$ Hz, 2H each, β - CH_2 of cyclopentylidene). $^{13}C\{^1H\}$ NMR (100 MHz, $CDCl_3$, δ): 157.7 (*p*-C of C_6H_4), 144.0 (*ipso*-C of cyclopentylidene), 133.9 (*ipso*-C of C_6H_4), 129.1 (*o*-C of C_6H_4), 119.0 (CH=), 113.7 (*m*-C of C_6H_4), 55.2 (CH_3), 35.0 ($CH_2CH=$), 33.6, 28.8 (α - CH_2 of cyclopentylidene), 26.4, 26.3 (β - CH_2 of cyclopentylidene).



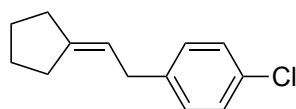
4-3ac

1-(2-Cyclopentylideneethyl)-4-methylbenzene (4-3ac). A colorless oil (36.8 mg, 0.198 mmol, 82% yield based on the amount of **4-1a** (50.1 mg, 0.241 mmol)). HRMS (FAB) m/z $[M]^+$ Calcd for $C_{14}H_{18}$ 186.1409; Found: 186.1400. 1H NMR (400 MHz, $CDCl_3$, δ): 7.17–7.06 (m, 4H, C_6H_4), 5.46 (t of quint, $J = 7.1$, 1.9 Hz, 1H, CH=), 3.31 (d, $J = 7.1$ Hz, 2H, $CH_2CH=$), 2.34 (s, 3H, CH_3), 2.34–2.26 (m, 4H, α - CH_2 of cyclopentylidene), 1.72, 1.65 (both quint, $J = 6.8$ Hz, 2H each, β - CH_2 of cyclopentylidene). $^{13}C\{^1H\}$ NMR (100 MHz, $CDCl_3$, δ): 144.1 (*ipso*-C of cyclopentylidene), 138.7, 135.1 (*ipso*- and *p*-C of C_6H_4), 129.0, 128.1 (CH of C_6H_4), 118.9 (CH=), 35.5 ($CH_2CH=$), 33.6, 28.8 (α - CH_2 of cyclopentylidene), 26.4, 26.3 (β - CH_2 of cyclopentylidene), 21.0 (CH_3).



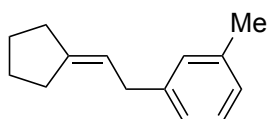
4-3ad

4-(2-Cyclopentylideneethyl)-1,1'-biphenyl (4-3ad). A colorless oil (46.6 mg, 0.188 mmol, 78% yield based on the amount of **4-1a** (50.1 mg, 0.241 mmol)). HRMS (FAB) m/z $[M]^+$ Calcd for $C_{19}H_{20}$ 248.1565; Found: 248.1561. 1H NMR (400 MHz, $CDCl_3$, δ): 7.58 (dt, $J = 7.8, 1.8$ Hz, 2H, 2'- and 6'-CH of 1,1'-biphenyl), 7.53 (dt, $J = 8.5, 1.8$ Hz, 2H, 2- and 6-CH of 1,1'-biphenyl), 7.44 (tt, $J = 7.8, 1.8$ Hz, 2H, 3'- and 5'-CH of 1,1'-biphenyl), 7.33 (tt, $J = 7.8, 1.8$ Hz, 1H, 4'-CH of 1,1'-biphenyl), 7.28 (d, $J = 8.5$ Hz, 2H, 3- and 5-CH of 1,1'-biphenyl), 5.50 (t of quint, $J = 7.2, 2.3$ Hz, 1H, CH=), 3.39 (d, $J = 7.2$ Hz, 2H, $CH_2CH=$), 2.34, 2.32 (both t, $J = 6.7$ Hz, 2H each, α - CH_2 of cyclopentylidene), 1.73, 1.66 (both quint, $J = 6.7$ Hz, 2H each, β - CH_2 of cyclopentylidene). $^{13}C\{^1H\}$ NMR (100 MHz, $CDCl_3$, δ): 144.6 (*ipso*-C of cyclopentylidene), 141.2, 140.9, 138.7 (1, 1'-, and 4-C of 1,1'-biphenyl), 128.7, 127.1, 127.0 (*o*- and *m*-CH of 1,1'-biphenyl with two resonances overlapping at δ 128.7), 126.9 (4'-CH of 1,1'-biphenyl), 118.5 (CH=), 35.6 ($CH_2CH=$), 33.7, 28.9 (α - CH_2 of cyclopentylidene), 26.5, 26.4 (β - CH_2 of cyclopentylidene).



4-3ae

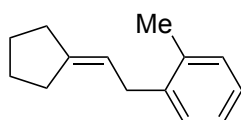
1-Chloro-4-(2-cyclopentylideneethyl)benzene (4-3ae). A colorless oil (32.6 mg, 0.158 mmol, 65% yield based on the amount of **4-1a** (50.1 mg, 0.241 mmol)). HRMS (FAB) m/z $[M]^+$ Calcd for $C_{13}H_{15}Cl$ 206.0862; Found: 206.0863. 1H NMR (400 MHz, $CDCl_3$, δ): 7.24, 7.12 (both d, $J = 7.8$ Hz, 2H each, C_6H_4), 5.41 (t of quint, $J = 7.4, 2.4$ Hz, 1H, CH=), 3.30 (d, $J = 7.4$ Hz, 2H, $CH_2CH=$), 2.28 (t, $J = 6.7$ Hz, 4H, α - CH_2 of cyclopentylidene), 1.71, 1.64 (both quint, $J = 6.7$ Hz, 2H each, β - CH_2 of cyclopentylidene). $^{13}C\{^1H\}$ NMR (100 MHz, $CDCl_3$, δ): 145.0 (*ipso*-C of cyclopentylidene), 140.2 (*ipso*-C of C_6H_4), 131.3 (*p*-C of C_6H_4), 129.6, 128.4 (CH of C_6H_4), 118.1 (CH=), 35.2 ($CH_2CH=$), 33.6, 28.8 (α - CH_2 of cyclopentylidene), 26.4, 26.3 (β - CH_2 of cyclopentylidene).



4-3ag

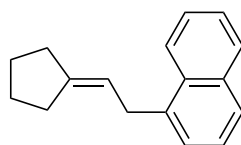
1-(2-Cyclopentylideneethyl)-3-methylbenzene (4-3ag). A colorless oil (31.7 mg, 0.170 mmol, 70% yield based on the amount of **4-1a** (50.3 mg, 0.242 mmol)). HRMS (FAB) m/z $[M]^+$ Calcd for $C_{14}H_{18}$ 186.1409; Found: 186.1411. 1H NMR (400 MHz,

CDCl₃, δ): 7.18 (t, J = 7.6, 1H, 5-CH of C₆H₄), 7.03–6.98 (m, 3H, 1-, 4-, and 6-CH of C₆H₄), 5.45 (t of quint, J = 7.4, 2.3 Hz, 1H, CH=), 3.31 (d, J = 7.4 Hz, 2H, CH₂CH=), 2.34 (s, 3H, CH₃), 2.34–2.26 (m, 4H, α -CH₂ of cyclopentylidene), 1.72, 1.64 (both quint, J = 7.0 Hz, 2H each, β -CH₂ of cyclopentylidene). ¹³C{¹H} NMR (100 MHz, CDCl₃, δ): 144.2 (*ipso*-C of cyclopentylidene), 141.7, 137.9 (1- and 3-C of C₆H₄), 129.1, 128.2, 126.4, 125.3 (CH of C₆H₄), 118.8 (CH=), 35.9 (CH₂CH=), 33.6, 28.8 (α -CH₂ of cyclopentylidene), 26.4, 26.3 (β -CH₂ of cyclopentylidene), 21.4 (CH₃).



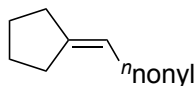
4-3ah

1-(2-Cyclopentylideneethyl)-2-methylbenzene (4-3ah). A white solid (54.1 mg, 0.186 mmol, 77% yield based on the amount of **4-1a** (52.2 mg, 0.242 mmol)). HRMS (FAB) m/z [M]⁺ Calcd for C₁₄H₁₈ 186.1409; Found 186.1413. ¹H NMR (400 MHz, CDCl₃, δ): 7.22–7.09 (m, 4H, C₆H₄), 5.40 (t of quint, J = 7.2, 2.4 Hz, 1H, CH=), 3.31 (d, J = 7.2 Hz, 2H, CH₂CH=), 2.32 (s, 3H, CH₃), 2.35–2.27 (m, 4H, α -CH₂ of cyclopentylidene), 1.73, 1.65 (both quint, J = 7.0 Hz, 2H each, β -CH₂ of cyclopentylidene). ¹³C{¹H} NMR (100 MHz, CDCl₃, δ): 144.2 (*ipso*-C of cyclopentylidene), 139.9, 136.1 (1- and 2-C of C₆H₄), 130.0, 128.6, 125.9, 125.9 (CH of C₆H₄), 117.9 (CH=), 33.7, 33.6, (CH₂CH= and α -CH₂ of cyclopentylidene), 28.8 (α -CH₂ of cyclopentylidene), 26.4, 26.4 (β -CH₂ of cyclopentylidene), 19.5 (CH₃).



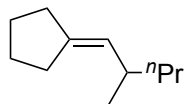
4-3ai

1-(2-Cyclopentylideneethyl)naphthalene (4-3ai). A colorless oil (35.6 mg, 0.160 mmol, 66% yield based on the amount of **4-1a** (50.3 mg, 0.242 mmol)). HRMS (FAB) m/z [M]⁺ Calcd for C₁₇H₁₈ 222.1409; Found: 222.1402. ¹H NMR (400 MHz, CDCl₃, δ): 8.05 (d, 1H, J = 8.0 Hz, 1H, 4-CH of 1-naphthyl), 7.86 (d, J = 7.6 Hz, 1H, 8-CH of 1-naphthyl), 7.73 (d, J = 7.6 Hz, 1H, 4-CH of 1-naphthyl), 7.56–7.46, 7.45–7.34 (both m, 2H each, 2-, 3-, 6-, and 7-CH of 1-naphthyl), 5.56 (t of quint, J = 6.5, 2.1 Hz, 1H, CH=), 3.78 (d, J = 6.5 Hz, 2H, CH₂CH=), 2.39, 2.30 (both br, 2H each, α -CH₂ of cyclopentylidene), 1.75, 1.65 (both quint, J = 6.7 Hz, 2H each, β -CH₂ of cyclopentylidene). ¹³C{¹H} NMR (100 MHz, CDCl₃, δ): 144.5 (*ipso*-C of cyclopentylidene), 137.8, 133.8, 132.0 (1-, 4a-, and 8a-C of 1-naphthyl), 128.6, 126.5, 125.7, 125.6, 125.5, 125.4, 124.1 (CH of 1-naphthyl), 118.3 (CH=), 33.7 (α -CH₂ of cyclopentylidene), 33.3 (CH₂CH=), 28.9 (α -CH₂ of cyclopentylidene), 26.5, 26.4 (β -CH₂ of cyclopentylidene).



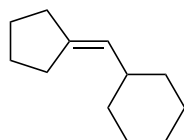
4-3aj

Decyldenecyclopentane (4-3aj). A colorless oil (27.1 mg, 0.130 mmol, 54% yield based on the amount of **4-1a** (50.2 mg, 0.241 mmol)). HRMS (FAB) m/z $[M]^+$ Calcd for $C_{15}H_{28}$ 208.2191; Found 208.2183. 1H NMR (400 MHz, $CDCl_3$, δ): 5.23 (t, $J = 6.9$ Hz, 1H, CH=), 2.21, 2.16 (both t, $J = 7.0$ Hz, 2H each, α -CH₂ of cyclopentylidene), 1.94 (q, $J = 6.9$ Hz, 2H, CH₂CH=), 1.65, 1.58 (both quint, $J = 7.0$ Hz, 2H each, β -CH₂ of cyclopentylidene), 1.35–1.21 (m, 14H, (CH₂)₇), 0.88 (t, $J = 6.6$ Hz, 3H, CH₃). $^{13}C\{^1H\}$ NMR (100 MHz, $CDCl_3$, δ): 142.9 (*ipso*-C of cyclopentylidene), 120.4 (CH=), 33.5 (α -CH₂ of cyclopentylidene), 31.9, 29.7, 29.7, 29.6, 29.4, 29.4 ((CH₂)₇ with two resonances overlapping at δ 29.6), 28.6 (α -CH₂ of cyclopentylidene), 26.5, 26.4 (β -CH₂ of cyclopentylidene), 22.7 (CH₂CH₃), 14.1 (CH₃).



4-3ak

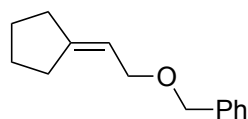
(2-Methylpentylidene)cyclopentane (4-3ak). A colorless oil (35.7 mg, 0.234 mmol, 97% yield based on the amount of **4-1a** (50.2 mg, 0.241 mmol)). HRMS (FAB) m/z $[M]^+$ Calcd for $C_{11}H_{20}$ 152.1565; Found 152.1559. 1H NMR (400 MHz, $CDCl_3$, δ): 5.00 (d of quint, $J = 9.2, 2.5$ Hz, 1H, CH=), 2.25–2.13 (m, 5H, CHCH₃ and α -CH₂ of cyclopentylidene), 1.64, 1.58 (both quint, $J = 7.0$ Hz, 2H each, β -CH₂ of cyclopentylidene), 1.33–1.14 (m, 4H, (CH₂)₂), 0.90 (d, $J = 6.8$ Hz, 3H, CH₃), 0.86 (t, $J = 7.0$ Hz, 3H, CH₃). $^{13}C\{^1H\}$ NMR (100 MHz, $CDCl_3$, δ): 141.2 (*ipso*-C of cyclopentylidene), 126.9 (CH=), 40.1 (CH₂CHCH=), 34.0 (α -CH₂ of cyclopentylidene), 33.5 (CHCH=), 28.5 (α -CH₂ of cyclopentylidene), 26.4, 26.4 (β -CH₂ of cyclopentylidene), 21.1, 20.6 (CH₃CH and CH₂CH₃), 14.3 (CH₃CH₂).



4-3al

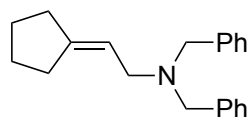
(Cyclopentylidenemethyl)cyclohexane (4-3al). A colorless oil (23.0 mg, 0.140 mmol, 58% yield based on the amount of **4-1a** (50.2 mg, 0.241 mmol)). HRMS (FAB) m/z $[M]^+$ Calcd for $C_{12}H_{20}$ 164.1565; Found 164.1564. 1H NMR (400 MHz, $CDCl_3$, δ): 5.12–5.08 (m, 1H, CH=), 2.23–2.13 (m, 4H, α -CH₂ of cyclopentylidene), 2.08–1.95 (m, 1H, CH of Cy), 1.74–1.52, 1.32–1.08, 1.07–0.94 (all m, 8H, 4H, and 2H, respectively, CH₂ of Cy and β -CH₂ of cyclopentylidene). $^{13}C\{^1H\}$ NMR (100 MHz, $CDCl_3$, δ): 141.1 (*ipso*-C of cyclopentylidene), 126.4 (CH=), 38.7 (1-CH of Cy), 33.5 (α -CH₂ of

cyclopentylidene), 33.2 (2- and 6-CH₂ of Cy), 28.4 (α -CH₂ of cyclopentylidene), 26.4, 26.3, 26.2 (4-CH₂ of Cy and β -CH₂ of cyclopentylidene), 26.2 (3- and 5-CH₂ of Cy).



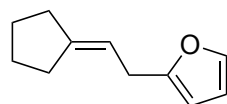
4-3an

((2-Cyclopentylideneethoxy)methyl)benzene (4-3an). A colorless oil (33.9 mg, 0.168 mmol, 70% yield based on the amount of **4-1a** (50.1 mg, 0.241 mmol)). HRMS (FAB) m/z $[M]^+$ Calcd for C₁₄H₁₈O 202.1358; Found 202.1352. ¹H NMR (400 MHz, CDCl₃, δ): 7.39–7.25 (m, 5H, CH of Ph), 5.52 (t of quint, J = 6.9, 2.3 Hz, 1H, CH=), 4.51 (s, 2H, CH₂Ph), 4.01 (d of quint, J = 6.9, 1.1 Hz, 2H, CH₂CH=), 2.30, 2.22 (both t, J = 6.8 Hz, 2H each, α -CH₂ of cyclopentylidene), 1.68, 1.62 (both quint, J = 6.8 Hz, 2H each, β -CH₂ of cyclopentylidene). ¹³C{¹H} NMR (100 MHz, CDCl₃, δ): 148.6 (*ipso*-C of cyclopentylidene), 138.6 (*ipso*-C of Ph), 128.3, 127.8 (*o*- and *m*-CH of Ph), 127.5 (*p*-CH of Ph), 116.4 (CH=), 72.0 (OCH₂Ph), 68.1 (CH₂CH=), 33.7, 28.8 (α -CH₂ of cyclopentylidene), 26.3, 26.0 (β -CH₂ of cyclopentylidene).



4-3ao

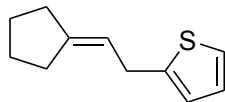
***N,N*-Dibenzyl-2-cyclopentylideneethan-1-amine (4-3ao).** A white solid (54.1 mg, 0.186 mmol, 74% yield based on the amount of **4-1a** (52.2 mg, 0.251 mmol)). mp 176.8–178.0 °C (decomp.). HRMS (FAB) m/z $[M]^+$ Calcd for C₂₁H₂₅N 291.1987; Found 291.1985. ¹H NMR (400 MHz, CDCl₃, δ): 7.70–7.66 (m, 4H, CH of Ph), 7.46–7.40 (m, 6H, CH of Ph), 5.65 (t of quint, J = 5.8, 2.2 Hz, 1H, CH=), 4.20–4.06 (m, 4H, CH₂Ph), 3.53–3.47 (m, 2H, CH₂CH=), 2.39–2.33, 1.99–1.93 (both m, 2H each, α -CH₂ of cyclopentylidene), 1.69–1.59 (m, 4H, β -CH₂ of cyclopentylidene). ¹³C{¹H} NMR (100 MHz, CDCl₃, δ): 155.7 (*ipso*-C of cyclopentylidene), 131.2, 129.3 (*o*- and *m*-CH of Ph), 129.8 (*p*-CH of Ph), 129.0 (*ipso*-C of Ph), 107.2 (CH=), 55.9 (NCH₂Ph), 50.7 (CH₂CH=), 34.3, 29.5 (α -CH₂ of cyclopentylidene), 26.0, 25.9 (β -CH₂ of cyclopentylidene).



4-3aq

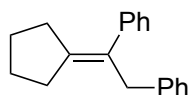
2-(2-Cyclopentylideneethyl)furan (4-3aq). A colorless oil (29.1 mg, 0.179 mmol, 71% yield based on the amount of **4-1a** (52.2 mg, 0.251 mmol)). HRMS (FAB) m/z $[M]^+$ Calcd for C₁₁H₁₄O 162.1045; Found 162.1041. ¹H NMR (400 MHz, CDCl₃, δ): 7.31 (d, J = 1.4 Hz, 1H, 5-CH of furyl), 6.28 (dd, J = 3.2, 1.4 Hz, 1H, 4-CH of furyl), 5.98 (dd, J = 3.2, 0.9 Hz, 1H, 3-CH of furyl), 5.43 (t of quint, J = 7.2, 2.5 Hz, 1H, CH=), 3.33 (dd, J = 7.2, 0.9 Hz, 2H, CH₂CH=), 2.32–2.23 (m, 4H, α -CH₂ of cyclopentylidene),

1.74–1.58 (m, 4H, β -CH₂ of cyclopentylidene). ¹³C{¹H} NMR (100 MHz, CDCl₃, δ): 155.3, 145.8 (*ipso*-C of cyclopentylidene and 2-C of furyl), 140.9 (5-CH of furyl), 114.9, 110.1, 104.5 (3- and 4-CH of furyl and CH=), 33.6, 28.7, 28.5 (CH₂CH= and α -CH₂ of cyclopentylidene), 26.4, 26.3 (β -CH₂ of cyclopentylidene).



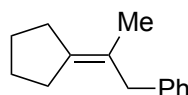
4-3ar

2-(2-Cyclopentylideneethyl)thiophene (4-3ar). A colorless oil (30.8 mg, 0.173 mmol, 69% yield based on the amount of **4-1a** (52.2 mg, 0.251 mmol)). HRMS (FAB) m/z [M]⁺ Calcd for C₁₁H₁₄S 178.0816; Found 178.0814. ¹H NMR (400 MHz, CDCl₃, δ): 7.11 (dd, J = 4.9, 1.7 Hz, 1H, 5-CH of thienyl), 6.92 (dd, J = 4.9, 3.2 Hz, 1H, 4-CH of thienyl), 6.79 (dd, J = 3.2, 1.7 Hz, 1H, 3-CH of thienyl), 5.50 (t of quint, J = 6.6, 2.2 Hz, 1H, CH=), 3.52 (d, J = 6.6 Hz, 2H, CH₂CH=), 2.32–2.26 (m, 4H, α -CH₂ of cyclopentylidene), 1.76–1.59 (m, 4H, β -CH₂ of cyclopentylidene). ¹³C{¹H} NMR (100 MHz, CDCl₃, δ): 145.2, 145.0 (*ipso*-C of cyclopentylidene and 2-C of thienyl), 126.7, 123.7, 123.0 (3-, 4- and 5-CH of thienyl), 118.0 (CH=), 33.6, 30.1, 28.7 (CH₂CH= and α -CH₂ of cyclopentylidene), 26.4, 26.3 (β -CH₂ of cyclopentylidene).



4-3ba

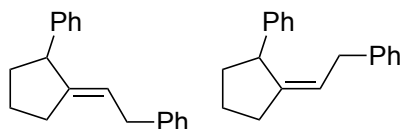
(1-Cyclopentylideneethane-1,2-diyl)dibenzene (4-3ba). A colorless oil (35.4 mg, 0.143 mmol, 57% yield based on the amount of **4-1b** (71.0 mg, 0.250 mmol)). HRMS (FAB) m/z [M]⁺ Calcd for C₁₉H₂₀ 248.1565; Found 248.1561. ¹H NMR (400 MHz, CDCl₃, δ): 7.26–7.09 (m, 10H, CH of Ph), 3.74 (s, 2H, CH₂C=), 2.47, 2.26 (both t, J = 6.9 Hz, 2H each, α -CH₂ of cyclopentylidene), 1.74, 1.62 (both quint, J = 6.9 Hz, 2H each, β -CH₂ of cyclopentylidene). ¹³C{¹H} NMR (100 MHz, CDCl₃, δ): 143.7, 142.6, 140.3 (*ipso*-C of cyclopentylidene and Ph), 129.9 (C=), 128.4, 128.3, 128.1, 127.8 (*o*- and *m*-CH of Ph), 125.8, 125.6 (*p*-CH of Ph), 41.1 (CH₂C=), 32.7, 31.2 (α -CH₂ of cyclopentylidene), 27.1, 26.4 (β -CH₂ of cyclopentylidene).



4-3ca

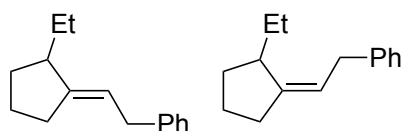
(2-Cyclopentylidenepropyl)benzene (4-3ca). A colorless oil (28.1 mg, 0.151 mmol, 60% yield based on the amount of **4-1c** (55.6 mmol, 0.250 mmol)). HRMS (FAB) m/z [M]⁺ Calcd for C₁₄H₁₈ 186.1409; Found 186.1411. ¹H NMR (400 MHz, CDCl₃, δ): 7.33–7.25 (m, 2H, *m*-CH of Ph), 7.24–7.15 (m, 3H, *o*- and *p*-CH of Ph), 3.38 (s, 2H, CH₂C=), 2.38, 2.27 (both br, 2H each, α -CH₂ of cyclopentylidene), 1.72, 1.71 (both quint, J = 7.0 Hz, 2H each, β -CH₂ of cyclopentylidene), 1.59 (s, 3H, CH₃). ¹³C{¹H}

NMR (100 MHz, CDCl₃, δ): 140.9 (*ipso*-C of cyclopentylidene), 138.2 (*ipso*-C of Ph), 128.5, 128.2 (*o*- and *m*-CH of Ph), 125.6 (*p*-CH of Ph), 123.8 (C=), 41.5 (CH₂C=), 30.8, 30.8 (α -CH₂ of cyclopentylidene), 27.1, 26.8 (β -CH₂ of cyclopentylidene), 18.9 (CH₃).



4-3da

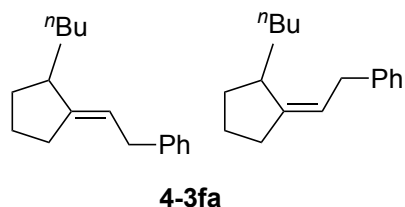
(2-(2-Phenylcyclopentylidene)ethyl)benzene (4-3da). A colorless oil (38.6 mg, 0.155 mmol, 62% yield based on the amount of **4-1d** (55.6 mmol, 0.250 mmol)) as a mixture of *E* and *Z* isomers (*E/Z* = 92/8). (*E*)-**4-3da**: HRMS (FAB) m/z [M]⁺ Calcd for C₁₉H₂₀ 248.1565; Found 248.1558. ¹H NMR (400 MHz, CDCl₃, δ): 7.33–7.12 (m, 10H, CH of Ph), 5.13 (tq, *J* = 7.8, 2.5 Hz, 1H, CH=), 3.59 (pseudo t, *J* = 8.2 Hz, 1H, 2-CH of cyclopentylidene), 3.37 (d, *J* = 7.8 Hz, 2H, CH₂CH=), 2.65–2.44 (m, 2H, 5-CH₂ of cyclopentylidene), 2.22–2.11, 2.01–1.89 (both m, 1H each, 3-CH₂ of cyclopentylidene), 1.83–1.65 (m, 2H, 4-CH₂ of cyclopentylidene). Relative nOe's observed at 2.0% for δ 3.37 and 2.55 (PhCH₂CH=CCH₂) and at 1.7% for δ 5.13 and 3.59 (PhCH₂CHC=CCHPh), respectively. ¹³C{¹H} NMR (100 MHz, CDCl₃, δ): 147.9, 145.2, 141.4 (*ipso*-C of cyclopentylidene and Ph), 128.4, 128.3, 128.2, 128.2 (*o*- and *m*-CH of Ph), 125.9, 125.7 (*p*-CH of Ph), 121.4 (C=), 51.6 (2-CH of cyclopentylidene), 36.6 (CH₂CH=), 35.8 (5-CH₂ of cyclopentylidene), 29.7 (4-CH₂ of cyclopentylidene), 24.6 (3-CH₂ of cyclopentylidene). (*Z*)-**4-3da**: HRMS (FAB) m/z [M]⁺ Calcd for C₁₉H₂₀ 248.1565; Found 248.1560. ¹H NMR (400 MHz, CDCl₃, δ): 7.33–7.09 (m, 8H, CH of Ph), 6.94 (d, *J* = 7.2 Hz, 2H, *o*-CH of Ph), 5.60 (tq, *J* = 7.2, 1.9 Hz, 1H, CH=), 3.86 (pseudo t, *J* = 7.0 Hz, 1H, 2-CH of cyclopentylidene), 3.12, 2.98 (both dd, *J* = 15.5, 7.2 Hz, 1H each, CH₂CH=), 2.62–2.40 (m, 2H, 5-CH₂ of cyclopentylidene), 2.33–2.22 (m, 1H, 3-CH₂ of cyclopentylidene), 1.84–1.54 (m, 3H, 3- and 4-CH₂ of cyclopentylidene). ¹³C{¹H} NMR (100 MHz, CDCl₃, δ): 146.6, 146.1, 141.4 (*ipso*-C of cyclopentylidene and Ph), 128.4, 128.3, 128.2, 127.6 (*o*- and *m*-CH of Ph), 125.6, 125.6 (*p*-CH of Ph), 121.9 (C=), 47.1 (2-CH of cyclopentylidene), 38.3 (CH₂CH=), 35.6 (5-CH₂ of cyclopentylidene), 35.3 (4-CH₂ of cyclopentylidene), 25.1 (3-CH₂ of cyclopentylidene).



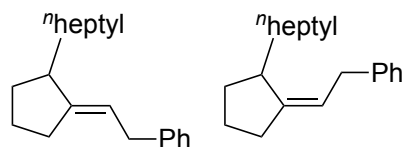
4-3ea

(2-(2-Ethylcyclopentylidene)ethyl)benzene (4-3ea). A colorless oil (37.6 mg, 0.188 mmol, 75% yield based on the amount of **4-1e** (59.1 mmol, 0.250 mmol)) as a mixture of *E* and *Z* isomers (*E/Z* = 88/12). HRMS (FAB) m/z [M]⁺ Calcd for C₁₅H₂₀ 200.1565; Found 200.1572. (*E*)-**4-3ea**: ¹H NMR (400 MHz, CDCl₃, δ): 7.32–7.28 (m, 2H, *m*-CH of Ph), 7.24–7.19 (m, 3H, *o*- and *p*-CH of Ph), 5.39 (tq, *J* = 7.2, 2.4 Hz, 1H, CH=), 3.38 (d, *J* = 7.2 Hz, 2H, CH₂CH=), 2.49–2.39 (m, 1H, 5-CH₂ of cyclopentylidene), 2.38–

2.25 (m, 2H, 2-CH and 5-CH₂ of cyclopentylidene), 1.96–1.86, 1.85–1.73 (both m, 1H each, 3-CH₂ of cyclopentylidene), 1.72–1.53 (m, 2H, 4-CH₂ of cyclopentylidene), 1.35–1.20 (m, 2H, CH₂CH₃), 0.94 (t, J = 7.4 Hz, 3H, CH₃). ¹³C{¹H} NMR (100 MHz, CDCl₃, δ): 147.9 (1-C of cyclopentylidene), 141.9 (*ipso*-C of Ph), 128.3, 128.3 (*o*- and *m*-CH of Ph), 125.6 (*p*-CH of Ph), 118.3 (CH=), 46.0 (2-CH of cyclopentylidene), 35.7 (5-CH₂ of cyclopentylidene), 32.3 (CH₂CH=), 29.5 (4-CH₂ of cyclopentylidene), 27.1 (CH₂CH₃), 24.1 (3-CH₂ of cyclopentylidene), 12.1 (CH₃). (*Z*)-**4-3ea** (overlapping peaks indistinctive from those of (*E*)-**4-3ea** not listed): ¹H NMR (400 MHz, CDCl₃, δ): 5.44 (tq, J = 8.0, 1.9 Hz, 1H, CH=), 3.44 (dd, J = 15.8, 8.0 Hz, 1H, CH₂CH=), 2.63 (br, 1H, 2-CH of cyclopentylidene), 0.95 (t, J = 7.4 Hz, 3H, CH₃). ¹³C{¹H} NMR (100 MHz, CDCl₃, δ): 148.2 (1-C of cyclopentylidene), 128.1 (*o*- or *m*-CH of Ph), 125.7 (*p*-CH of Ph), 119.1 (CH=), 41.9 (2-CH of cyclopentylidene), 35.4 (5-CH₂ of cyclopentylidene), 33.4 (CH₂CH=), 31.4 (4-CH₂ of cyclopentylidene), 27.8 (CH₂CH₃), 24.0 (3-CH₂ of cyclopentylidene), 12.3 (CH₃).

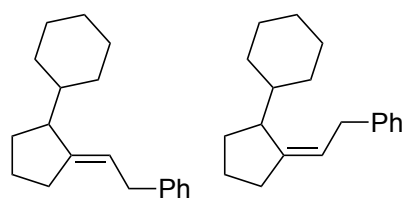


(2-(2-Butylcyclopentylidene)ethyl)benzene (4-3fa). A colorless oil (37.1 mg, 0.162 mmol, 65% yield based on the amount of **4-1f** (66.0 mg, 0.250 mmol)) as a mixture of *E* and *Z* isomers (*E/Z* = 90/10). HRMS (FAB) m/z [M]⁺ Calcd for C₁₇H₂₄ 228.1878; Found 228.1882. (*E*)-**4-3fa**: ¹H NMR (400 MHz, CDCl₃, δ): 7.34–7.27 (m, 2H, *m*-CH of Ph), 7.24–7.16 (m, 3H, *o*- and *p*-CH of Ph), 5.38 (tq, J = 7.0, 2.4 Hz, 1H, CH=), 3.37 (d, J = 7.0 Hz, 2H, CH₂CH=), 2.49–2.38 (m, 1H, 5-CH₂ of cyclopentylidene), 2.38–2.20 (m, 2H, 2-CH and 5-CH₂ of cyclopentylidene), 1.95–1.85, 1.84–1.73 (both m, 1H each, 3-CH₂ of cyclopentylidene), 1.67–1.51 (m, 2H, 4-CH₂ of cyclopentylidene), 1.42–1.16 (m, 6H, (CH₂)₃CH₃), 0.91 (t, J = 6.0 Hz, 3H, CH₃). ¹³C{¹H} NMR (100 MHz, CDCl₃, δ): 148.2 (1-C of cyclopentylidene), 141.9 (*ipso*-C of Ph), 128.3 (*o*- and *m*-CH of Ph), 125.6 (*p*-CH of Ph), 118.1 (CH=), 44.3 (2-CH of cyclopentylidene), 35.7 (5-CH₂ of cyclopentylidene), 34.2 (1-CH₂ of ^{*n*}Bu), 32.8 (CH₂CH=), 30.1 (2-CH₂ of ^{*n*}Bu), 29.4 (4-CH₂ of cyclopentylidene), 24.1 (3-CH₂ of cyclopentylidene), 23.0 (3-CH₂ of ^{*n*}Bu), 14.2 (CH₃). (*Z*)-**4-3fa** (overlapping peaks indistinctive from those of (*E*)-**4-3fa** not listed): ¹H NMR (400 MHz, CDCl₃, δ): 5.40 (tq, J = 7.6, 1.8 Hz, 1H, CH=), 3.34 (dd, J = 15.6, 7.6 Hz, 1H, CH₂CH=), 2.68 (br, 1H, 2-CH of cyclopentylidene), 0.91 (t, J = 7.4 Hz, 3H, CH₃). ¹³C{¹H} NMR (100 MHz, CDCl₃, δ): 148.4 (1-C of cyclopentylidene), 128.1 (*o*- or *m*-CH of Ph), 125.7 (*p*-CH of Ph), 118.9 (CH=), 40.2 (2-CH of cyclopentylidene), 35.4 (5-CH₂ of cyclopentylidene), 34.8 (1-CH₂ of ^{*n*}Bu), 33.3 (CH₂CH=), 31.9 (2-CH₂ of ^{*n*}Bu), 24.1 (3-CH₂ of cyclopentylidene), 22.8 (3-CH₂ of ^{*n*}Bu).



4-3ga

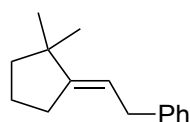
(2-(2-Heptylcyclopentylidene)ethyl)benzene (4-3ga). A colorless oil (41.9 mg, 0.155 mmol, 65% yield based on the amount of **4-1g** (73.1 mg, 0.239 mmol)) as a mixture of *E* and *Z* isomers (*E/Z* = 93/7). HRMS (FAB) m/z $[M]^+$ Calcd for $C_{20}H_{30}$ 270.2348; Found 270.2338. (*E*)-**4-3ga**: 1H NMR (400 MHz, $CDCl_3$, δ): 7.33–7.26 (m, 2H, *m*-CH of Ph), 7.24–7.16 (m, 3H, *o*- and *p*-CH of Ph), 5.38 (tq, J = 6.8, 2.0 Hz, 1H, CH=), 3.37 (d, J = 6.8 Hz, 2H, $CH_2CH=$), 2.48–2.38 (m, 1H, 5- CH_2 of cyclopentylidene), 2.38–2.26 (m, 2H, 2-CH and 5- CH_2 of cyclopentylidene), 1.95–1.86, 1.84–1.73 (both m, 1H each, 3- CH_2 of cyclopentylidene), 1.65–1.51 (m, 2H, 4- CH_2 of cyclopentylidene), 1.45–1.16 (m, 12H, $(CH_2)_6$), 0.90 (t, J = 6.6 Hz, 3H, CH_3). $^{13}C\{^1H\}$ NMR (100 MHz, $CDCl_3$, δ): 148.2 (1-C of cyclopentylidene), 141.9 (*ipso*-C of Ph), 128.3 (*o*- and *m*-CH of Ph, overlapping), 125.6 (*p*-CH of Ph), 118.1 (C=), 44.4 (2-CH of cyclopentylidene), 35.7 (5- CH_2 of cyclopentylidene), 34.5 (1- CH_2 of *n*-heptyl), 32.8 ($CH_2CH=$), 31.9 (5- CH_2 of *n*-heptyl), 29.9 (3- CH_2 of *n*-heptyl), 29.4 (4- CH_2 of *n*-heptyl and 4- CH_2 of cyclopentylidene, overlapping), 27.8 (2- CH_2 of *n*-heptyl), 24.1 (3- CH_2 of cyclopentylidene), 22.7 (6- CH_2 of *n*-heptyl), 14.1 (CH_3). (*Z*)-**4-3ga** (overlapping peaks indistinctive from those of (*E*)-**4-3ga** not listed): 1H NMR (400 MHz, $CDCl_3$, δ): 5.40 (tq, J = 7.6, 1.8 Hz, 1H, CH=), 3.34 (dd, J = 15.6, 7.6 Hz, 1H, $CH_2CH=$), 2.68 (br, 1H, 2-CH of cyclopentylidene), 0.91 (t, J = 7.4 Hz, 3H, CH_3). $^{13}C\{^1H\}$ NMR (100 MHz, $CDCl_3$, δ): 148.5 (1-C of cyclopentylidene), 128.0 (*o*- or *m*-CH of Ph), 125.5 (*p*-CH of Ph), 118.9 (CH=), 40.2 (2-CH of cyclopentylidene), 35.4 (5- CH_2 of cyclopentylidene), 35.1 (1- CH_2 of *n*-heptyl), 33.4 ($CH_2CH=$), 29.8 (3- CH_2 of *n*-heptyl).



4-3ha

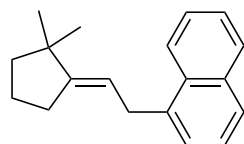
(2-(2-Cyclohexylcyclopentylidene)ethyl)benzene (4-3ha). A colorless oil (33.0 mg, 0.130 mmol, 51% yield based on the amount of **4-1h** (73.5 mg, 0.253 mmol)) as a mixture of *E* and *Z* isomers (*E/Z* = 91/9). HRMS (FAB) m/z $[M]^+$ Calcd for $C_{19}H_{26}$ 254.2035; Found 254.2035. (*E*)-**4-3ha**: 1H NMR (400 MHz, $CDCl_3$, δ): 7.33–7.27 (m, 2H, *m*-CH of Ph), 7.24–7.16 (m, 3H, *o*- and *p*-CH of Ph), 5.36 (tq, J = 7.1, 2.4 Hz, 1H, CH=), 3.39 (d, J = 7.2 Hz, 2H, $CH_2CH=$), 2.49–2.39 (m, 1H, 5- CH_2 of cyclopentylidene), 2.34–2.26 (m, 1H, 2-CH of cyclopentylidene), 2.24–2.13 (m, 1H, 5- CH_2 of cyclopentylidene), 1.82–1.63, 1.61–1.42, 1.31–1.02 (all m, 7H, 3H, and 4H, respectively, CH and CH_2 of Cy, and 3- and 4- CH_2 of cyclopentylidene), 0.93 (qd, J =

11.9, 2.8 Hz, 1H, 3-CH of cyclopentylidene). $^{13}\text{C}\{^1\text{H}\}$ NMR (100 MHz, CDCl_3 , δ): 146.2 (1-C of cyclopentylidene), 141.9 (*ipso*-C of Ph), 128.3 (*o*- and *m*-CH of Ph, overlapping), 125.6 (*p*-CH of Ph), 118.7 ($\text{CH}=\text{}$), 50.0 (2-CH of cyclopentylidene), 40.3 (1-CH of Cy), 35.8 (5- CH_2 of cyclopentylidene), 32.4 ($\text{CH}_2\text{CH}=\text{}$), 29.8 (3- CH_2 of cyclopentylidene), 28.1 (2- and 6- CH_2 of Cy, overlapping), 27.0 (4- CH_2 of Cy), 26.8, 26.7 (3- and 5- CH_2 of Cy), 24.5 (4- CH_2 of cyclopentylidene). (*Z*)-**4-3ha** (overlapping peaks indistinctive from those of (*E*)-**4-3ha** not listed): ^1H NMR (400 MHz, CDCl_3 , δ): 5.45 (tq, $J = 7.3, 1.8$ Hz, 1H, $\text{CH}=\text{}$), 3.46 (dd, $J = 16.0, 7.3$ Hz, 1H, $\text{CH}_2\text{CH}=\text{}$), 3.33 (dd, $J = 15.8, 7.3$ Hz, 1H, $\text{CH}_2\text{CH}=\text{}$), 2.69–2.55 (m, 1H, 2-CH of cyclopentylidene). $^{13}\text{C}\{^1\text{H}\}$ NMR (100 MHz, CDCl_3 , δ): 147.0 (1-C of cyclopentylidene), 128.1, 128.0 (*o*- and *m*-CH of Ph), 125.5 (*p*-CH of Ph), 119.8 ($\text{CH}=\text{}$), 45.8 (2-CH of cyclopentylidene), 41.4 (1-CH of Cy), 35.6 (5- CH_2 of cyclopentylidene), 34.4 (3- CH_2 of cyclopentylidene), 31.9 ($\text{CH}_2\text{CH}=\text{}$), 28.9, 28.0 (2- and 6- CH_2 of Cy), 26.9 (4- CH_2 of Cy), 26.7, 26.6 (3- and 5- CH_2 of Cy), 24.0 (4- CH_2 of cyclopentylidene).



(E)-4-3ia

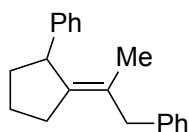
(E)-(2-(2,2-dimethylcyclopentylidene)ethyl)benzene ((E)-4-3ia). A colorless oil (39.0 mg, 0.195 mmol, 77% yield based on the amount of **4-1i** (59.9 mg, 0.254 mmol)). HRMS (FAB) m/z $[\text{M}]^+$ Calcd for $\text{C}_{15}\text{H}_{20}$ 200.1565; Found 200.1564. ^1H NMR (400 MHz, CDCl_3 , δ): 7.31–7.24 (m, 2H, *m*-CH of Ph), 7.21–7.15 (m, 3H, *o*- and *p*-CH of Ph), 5.30 (tt, $J = 7.2, 2.5$ Hz, 1H, $\text{CH}=\text{}$), 3.33 (d, $J = 7.2$ Hz, 2H, $\text{CH}_2\text{CH}=\text{}$), 2.42 (tdt, $J = 7.1, 2.5, 1.3$ Hz, 2H, 3- CH_2 of cyclopentylidene), 1.70 (quint, $J = 7.1$ Hz, 2H, 4- CH_2 of cyclopentylidene), 1.53 (t, $J = 7.1$ Hz, 2H, 5- CH_2 of cyclopentylidene), 1.06 (s, 6H, CH_3). $^{13}\text{C}\{^1\text{H}\}$ NMR (100 MHz, CDCl_3 , δ): 152.9 (1-C of cyclopentylidene), 141.9 (*ipso*-C of Ph), 128.6 (*o*- and *m*-CH of Ph), 125.6 (*p*-CH of Ph), 116.7 ($\text{CH}=\text{}$), 42.2 (3- CH_2 of cyclopentylidene), 41.9 (2-C of cyclopentylidene), 35.5 ($\text{CH}_2\text{CH}=\text{}$), 29.3 (5- CH_2 of cyclopentylidene), 28.8 (CH_3), 22.3 (4- CH_2 of cyclopentylidene).



(E)-4-3ii

(E)-1-(2-(2,2-dimethylcyclopentylidene)ethyl)naphthalene ((E)-4-3ii). A colorless oil (38.2 mg, 0.153 mmol, 61% yield based on the amount of **4-1i** (59.0 mmol, 0.250 mmol)). Colorless block crystals suitable for crystallographic study were further obtained by recrystallization from diethyl ether at -30 °C. HRMS (FAB) m/z $[\text{M}]^+$ Calcd for $\text{C}_{19}\text{H}_{22}$ 250.1722; Found 250.1724. ^1H NMR (400 MHz, CDCl_3 , δ): 8.02 (dd, $J = 8.0, 1.6$ Hz, 1H, 5-CH of 1-naphthyl), 7.86 (dd, $J = 8.0, 1.6$ Hz, 8-CH of 1-naphthyl), 7.72 (d, $J = 7.5$ Hz, 1H, 4-CH of 1-naphthyl), 7.51 (td, $J = 8.0, 1.6$ Hz, 1H, 6-CH of 1-

naphthyl), 7.48 (td, $J = 8.0, 1.6$ Hz, 7-CH of 1-naphthyl), 7.40 (t, $J = 7.5$ Hz, 1H, 3-CH of 1-naphthyl) 7.33 (d, $J = 7.5$ Hz, 1H, 2-CH of 1-naphthyl), 5.38 (tt, $J = 7.2, 2.6$ Hz, 1H, CH=), 3.75 (d, $J = 6.8$ Hz, 2H, CH₂CH=), 2.50 (tdt, $J = 7.2, 2.6, 1.3$ Hz, 2H, 3-CH₂ of cyclopentylidene), 1.74 (quint, $J = 7.2$ Hz, 2H, 4-CH₂ of cyclopentylidene), 1.55 (t, $J = 7.2$ Hz, 2H, 5-CH₂ of cyclopentylidene), 1.07 (s, 6H, CH₃). ¹³C{¹H} NMR (100 MHz, CDCl₃, δ): 153.0 (1-C of cyclopentylidene), 137.8, 133.8, 132.1 (1-, 4a-, and 8a-C of 1-naphthyl), 128.6, 126.5, 125.6, 125.4, 125.3, 124.1 (CH of 1-naphthyl with two resonances overlapping at δ 125.6), 116.6 (CH=), 42.2 (3-CH₂ of cyclopentylidene), 42.1 (2-C of cyclopentylidene), 32.9 (CH₂CH=), 29.4 (5-CH₂ of cyclopentylidene), 28.8 (CH₃), 22.4 (4-CH₂ of cyclopentylidene).

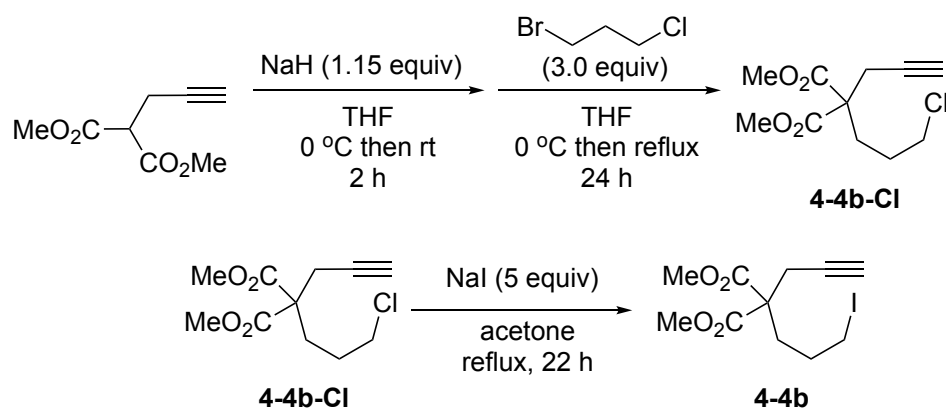


4-3ja

(2-(2-Phenylcyclopentylidene)propyl)benzene (4-3ja). A colorless oil (32.8 mg, 0.125 mmol, 50% yield based on the amount of **4-1j** (75.0 mg, 0.251 mmol)) as a mixture of *E* and *Z* isomers (*E/Z* = 89/11). HRMS (FAB) m/z [M]⁺ Calcd for C₂₀H₂₂ 262.1722; Found 262.1723. (*E*)-**4-3ja**: ¹H NMR (400 MHz, CDCl₃, δ): 7.32–7.23 (m, 4H, *m*-CH of Ph), 7.23–7.11 (m, 6H, *o*- and *p*-CH of Ph), 3.87 (dd, $J = 7.6, 2.4$ Hz, 1H, 2-CH of cyclopentylidene), 3.44 (s, 2H, CH₂CH=), 2.58 (t, $J = 6.4$ Hz, 2H, 5-CH₂ of cyclopentylidene), 2.24–2.14, 1.80–1.64 (both m, 1H and 3H, respectively, 3- and 4-CH₂ of cyclopentylidene), 1.33 (s, 3H, CH₃). ¹³C{¹H} NMR (100 MHz, CDCl₃, δ): 146.8, 140.7, 140.3 (*ipso*-C of cyclopentylidene and Ph), 128.5, 128.3, 128.2, 127.5 (*o*- and *m*-CH of Ph), 127.4 (C=), 125.7, 125.3 (*p*-CH of Ph), 48.3 (2-CH of cyclopentylidene), 41.8 (CH₂CH=), 37.9 (5-CH₂ of cyclopentylidene), 32.0 (4-CH₂ of cyclopentylidene), 24.6 (3-CH₂ of cyclopentylidene), 19.2 (CH₃). (*Z*)-**4-3ja** (overlapping peaks indistinctive from those of (*E*)-**4-3ga** not listed): ¹³C{¹H} NMR (100 MHz, CDCl₃, δ): 128.4 (*o*- or *m*-CH of Ph), 125.5 (*p*-CH of Ph), 36.7 (5-CH₂ of cyclopentylidene), 31.6 (4-CH₂ of cyclopentylidene), 22.6 (3-CH₂ of cyclopentylidene), 14.1 (CH₃).

4.4.6. Preparation of Dimethyl 2-(3-Iodopropyl)-2-(prop-2-yn-1-yl)malonate (**4-4b**)

Scheme 4-13. Preparation of Dimethyl 2-(3-Iodopropyl)-2-(prop-2-yn-1-yl)malonate **4-4b**



In a 50 mL Schlenk flask were placed a suspension of NaH, prepared from 461 mg of NaH (60% dispersion in mineral oil, 11.5 mmol) and 11 mL of THF at 0 °C by using an ice–water bath under N₂, where a THF solution (10 mL) of dimethyl propargylmalonate (1.70 g, 10.0 mmol) was added dropwise. The reaction mixture was gradually warmed to room temperature and was further stirred for 2 h. Then the reaction mixture was cooled back to 0 °C by using an ice–water bath, and 1-bromo-3-chloropropane (4.72 g, 30.0 mmol) was added dropwise. The reaction mixture was gradually warmed to room temperature, then was further refluxed for 24 h by using an oil bath. The resultant mixture was quenched with saturated aqueous solution of NH₄Cl (20 mL), and the aqueous phase was extracted with ethyl acetate (20 mL × 3). The combined organic layers were washed with brine (30 mL), dried over anhydrous MgSO₄, and filtered. The filtrate was collected, and the solvent was removed under reduced pressure. The residue was further purified by column chromatography (SiO₂) with a mixture of *n*-hexane/ethyl acetate (7:3) as an eluent to afford dimethyl 2-(3-chloropropyl)-2-(prop-2-yn-1-yl)malonate (**4-4b-Cl**) as a colorless oil (1.61 g, 6.54 mmol, 65% yield based on the amount of dimethyl propargylmalonate), which was directly used in the subsequent transformation to obtain 2-(3-iodopropyl)-2-(prop-2-yn-1-yl)malonate (**4-4b**) without further purification.

In a 50 mL Schlenk flask were placed **4-4b-Cl** (1.61 g, 6.54 mmol), NaI (4.88 g, 32.6 mmol), and acetone (20 mL) under N₂, and the reaction mixture was stirred and refluxed for 22 h by using an oil bath. Then, acetone was removed *in vacuo*, and the resultant mixture was diluted with 20 mL of ethyl acetate and was filtered. Solvent was removed from the collected filtrate under reduced pressure, and the residue was purified by column chromatography (SiO₂) with a mixture of *n*-hexane/ethyl acetate (7:3) as an eluent to afford dimethyl 2-(3-iodopropyl)-2-(prop-2-yn-1-yl)malonate (**4-4b**) as a white waxy oil (1.72 g, 5.09 mmol, 78% yield based on the amount of **4-4b-Cl**, 65% yield based on the amount of dimethyl propargylmalonate). mp 266.5–268.1 °C (decomp.). HRMS (FAB) *m/z* [M]⁺ Calcd for C₁₁H₁₅IO₄ 338.0015; Found: 338.0019. ¹H NMR (400 MHz, CDCl₃, δ): 3.76 (CO₂Me), 3.17 (t, *J* = 7.0 Hz, 2H, CH₂I), 2.83 (d, *J* = 2.5 Hz, 2H, CH₂C≡), 2.19–2.13 (m, 2H, CH₂CH₂CH₂I), 2.03 (t, *J* = 2.5 Hz,

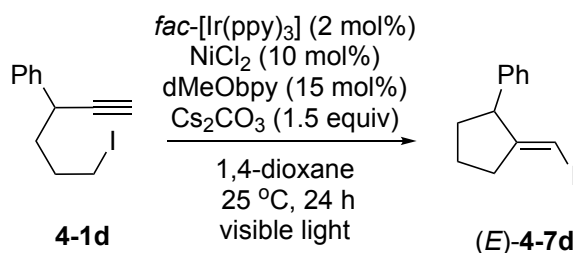
¹H, HC≡), 1.81–1.71 (m, 2H, CH₂CH₂I). ¹³C{¹H} NMR (100 MHz, CDCl₃, δ): 170.3 (CO₂), 78.4 (C≡), 71.7 (HC≡), 56.3 (C(CH₂)₃I), 52.9 (CH₃), 33.2 (CH₂(CH₂)₂I), 28.3 (CH₂CH₂I), 23.2 (CH₂C≡), 5.2 (CH₂I).

4.4.7. Preparation of (*E*)-(2-(iodomethylene)cyclopentyl)benzene ((*E*)-4-7d)

Method 1 (in the absence of 4-2a)

Scheme 4-14. Preparation of (*E*)-(2-(iodomethylene)cyclopentyl)benzene (*E*-4-7d)

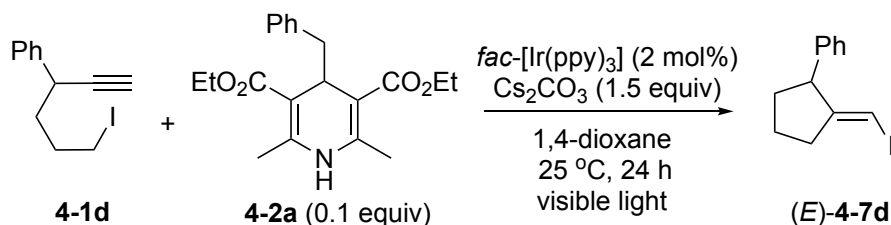
Method 1 (in the absence of 4-2a)



In a 20 mL Schlenk flask were placed **4-1d** (71.2 mg, 0.251 mmol), *fac*-[Ir(ppy)₃] (3.4 mg, 0.0052 mmol), anhydrous NiCl₂ (3.4 mg, 0.026 mmol), dMeObpy (8.2 mg, 0.038 mmol), and Cs₂CO₃ (122 mg, 0.374 mmol) under N₂, where 1,4-dioxane (2.5 mL) was added at room temperature. The reaction flask was placed in an As One LTB-125 constant low temperature water bath set at 25 °C, and was illuminated from the bottom of the bath with an Aitech System TMN100×120–22WD 12 W white LED lamp (400 nm to 750 nm) at a distance of approximately 2 cm from the light source for 48 h. The volatiles were removed *in vacuo*, and the residue was purified by column chromatography (SiO₂) with *n*-hexane as an eluent to afford ((2-(iodomethylene)cyclopentyl)benzene (**4-7d**) as a colorless oil (40.6 mg, 0.143 mmol, 57% yield based on the amount of **4-1d**) as a mixture of *E* and *Z* isomers (*E/Z* = 83/17). Further purification by column chromatography (SiO₂) with *n*-hexane as an eluent gave (*E*)-((2-(iodomethylene)cyclopentyl)benzene) ((*E*)-**4-7d**) in a pure form (35.5 mg, 0.125 mmol, 50 % yield based on the amount of **4-1d**).

Method 2 (in the presence of a catalytic amount of 4-2a but in the absence of NiCl₂/dMeObpy)

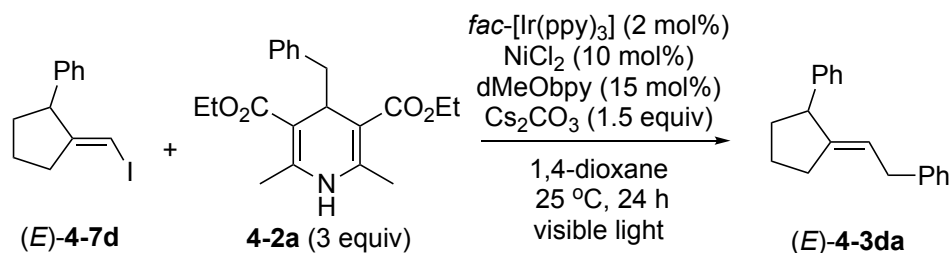
Scheme 4-15. Preparation of (*E*)-(2-(iodomethylene)cyclopentyl)benzene (*E*)-**4-7d**
 Method 2 (in the presence of a catalytic amount of **4-2a** but in the absence of NiCl₂/dMeObpy)



In a 20 mL Schlenk flask were placed **4-1d** (71.1 mg, 0.250 mmol), **4-2a** (8.7 mg, 0.025 mmol), *fac*-[Ir(ppy)₃] (3.4 mg, 0.0052 mmol), and Cs₂CO₃ (122 mg, 0.374 mmol) under N₂, where 1,4-dioxane (2.5 mL) was added at room temperature. The reaction flask was placed in an As One LTB-125 constant low temperature water bath set at 25 °C, and was illuminated from the bottom of the bath with an Aitech System TMN100×120–22WD 12 W white LED lamp (400 nm to 750 nm) at a distance of approximately 2 cm from the light source for 24 h. The volatiles were removed *in vacuo*, and the residue was purified by column chromatography (SiO₂) with *n*-hexane as an eluent to afford ((2-(iodomethylene)cyclopentyl)benzene (**4-7d**) as a colorless oil (42.0 mg, 0.148 mmol, 59% yield based on the amount of **4-1d**) as a mixture of *E* and *Z* isomers (*E/Z* = 83/17). Further purification by column chromatography (SiO₂) with *n*-hexane as an eluent gave (*E*)-((2-(iodomethylene)cyclopentyl)benzene) (*E*)-**4-7d** in a pure form (33.4 mg, 0.118 mmol, 47 % yield based on the amount of **4-1d**). HRMS (FAB) *m/z* [M]⁺ Calcd for C₁₂H₁₃I 284.0062; Found: 284.0063. ¹H NMR (400 MHz, CDCl₃, δ): 7.35–7.28 (m, 2H, *m*-CH of Ph), 7.27–7.16 (m, 3H, *o*- and *p*-CH of Ph), 5.57 (pseudo quint, *J* = 2.4 Hz, 1H, CH=), 3.57 (t, *J* = 7.6 Hz, 1H, 2-CH of cyclopentylidene), 2.59–2.49, 2.48–2.36, 2.36–2.27, 2.00–1.84, 1.82–1.68 (all m, 1H, 1H, 1H, 2H, and 1H respectively, 3-, 4-, and 5-CH of cyclopentylidene). ¹³C{¹H} NMR (100 MHz, CDCl₃, δ): 159.4 (1-C of cyclopentylidene), 142.8 (*ipso*-C of Ph), 128.5, 128.2 (*o*- and *m*-CH of Ph), 126.5 (*p*-CH of Ph), 72.9 (CH=), 53.6 (2-CH of cyclopentylidene), 37.8, 37.6 (4- and 5-CH₂ of cyclopentylidene), 23.8 (3-CH₂ of cyclopentylidene).

4.4.8. Preparation of (*E*)-4-3da by the reaction of (*E*)-4-7d with 4-2a

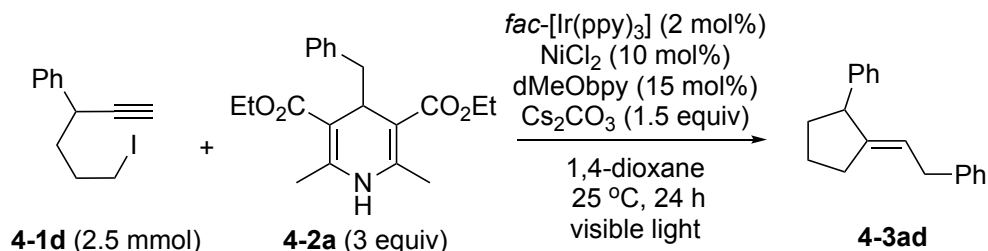
Scheme 4-16. Preparation of (*E*)-4-3da by the reaction of (*E*)-4-7d with 4-2a



In a 20 mL Schlenk flask were placed (*E*)-4-7d (71.0 mg, 0.251 mmol), 4-2a, (257 mg, 0.751 mmol), *fac*-[Ir(ppy)₃] (3.4 mg, 0.0052 mmol), anhydrous NiCl₂ (3.5 mg, 0.027 mmol), dMeObpy (8.0 mg, 0.037 mmol), and Cs₂CO₃ (123 mg, 0.378 mmol) under N₂, where 1,4-dioxane (2.5 mL) was added at room temperature. The reaction flask was placed in an As One LTB-125 constant low temperature water bath set at 25 °C, and was illuminated from the bottom of the bath with an Aitech System TMN100×120–22WD 12 W white LED lamp (400 nm to 750 nm) at a distance of approximately 2 cm from the light source for 24 h. The volatiles were removed *in vacuo*, and the residue was purified by column chromatography (SiO₂) with *n*-hexane as an eluent to afford (*E*)-4-3da as a colorless oil (45.3 mg, 0.182 mmol, 73% yield based on the amount of (*E*)-4-7d).

4.4.9. Large-Scale Preparation of 4-3da

Scheme 4-17. Large-Scale Preparation of 4-3da



In a 100 mL Schlenk flask were placed 4-1d (710 mg, 2.50 mmol), 4-2a (2.57 g, 7.49 mmol), *fac*-[Ir(ppy)₃] (32.0 mg, 0.0489 mmol), anhydrous NiCl₂ (34.2 mg, 0.264 mmol), dMeObpy (81.0 mg, 0.375 mmol), and Cs₂CO₃ (1.22 g, 3.74 mmol) under N₂, where 1,4-dioxane (25.1 mL) was added at room temperature. The reaction flask was placed in an As One LTB-125 constant low temperature water bath set at 25 °C, and was illuminated from the bottom of the bath with an Aitech System TMN100×120–22WD 12 W white LED lamp (400 nm to 750 nm) at a distance of approximately 2 cm from the light source for 24 h. The volatiles were removed *in vacuo*, and the resultant mixture was extracted with dichloromethane via filtration. Solvent was removed from the collected filtrate under reduced pressure, and the residue was purified by column chromatography (SiO₂) with *n*-hexane as an eluent to afford 4-3da as a colorless oil (397 mg, 1.60 mmol, 64% yield based on the amount of 4-1d) as a mixture of *E* and *Z* isomers (*E/Z* = 91/9).

4.4.10. X-ray diffraction studies of (E)-4-3ii

Diffraction data for a crystal of (E)-1-(2-(2,2-dimethylcyclopentylidene)ethyl)naphthalene ((E)-4-3ii) were collected for the 2θ range of 5.2° to 62.6° at -180°C on a Rigaku XtaLAB Synergy-S diffractometer equipped with a HyPix-6000HE Hybrid Photon Counting (HPC) detector and VariMax optics using multi-layer mirror monochromated Mo-K α ($\lambda = 0.71073\text{ \AA}$) radiation, and VariMax optics. Intensity data were corrected for Lorentz and polarization effect and for empirical absorptions (CrysAlisPro),⁴⁷ while structure solutions and refinements were carried out by using CrystalStructure package.⁴⁸ Positions of non-hydrogen atoms were determined by direct methods (SHELXS Version 2013/1),⁴⁹ and subsequent Fourier syntheses (SHELXL Version 2016/6),⁵⁰ and were refined on F_o^2 with all the unique reflections by full-matrix least squares with anisotropic thermal parameters. All the hydrogen atoms were placed at the calculated positions with fixed isotropic parameters. Anomalous dispersion effects were included in F_c ,⁵¹ and mass attenuation coefficients, values for $\Delta f'$ and $\Delta f''$, and neutral atom scattering factors were taken from references.⁵²

Table 4-2. Crystallographic Data for (E)-4-3ii

compound	(E)-4-3ii
chemical formula	C ₁₉ H ₂₂
CCDC number	2061338
formula weight	250.38
crystal size, mm ³	0.123 × 0.056 × 0.040
crystal color, habit	colorless, block
temperature, °C	−180
crystal system	monoclinic
space group	<i>P</i> 2 ₁ / <i>c</i> (no. 14)
<i>a</i> , Å	6.9419(4)
<i>b</i> , Å	15.5787(8)
<i>c</i> , Å	13.4022(8)
α , deg	90
β , deg	91.814(6)
γ , deg	90
<i>V</i> , Å ³	1448.66(14)
<i>Z</i>	4
<i>d</i> _{calcd} , g, cm ^{−3}	1.148
<i>F</i> (000)	544
μ , cm ^{−1}	6.41
transmission factors range	0.163 – 0.997
number of measured reflections	13165
number of unique reflections	3920
number of refined parameters	174
<i>R</i> _{int}	0.01192
<i>R</i> 1 (<i>I</i> > 2 σ (<i>I</i>)) ^a	0.0636
<i>wR</i> 2 (all data) ^b	0.1183
GOF ^c	1.000
maximum residual peak / hole, e Å ^{−3}	+0.18 / −0.19

^a $R1 = \sum ||F_o| - |F_c|| / \sum |F_o|$. ^b $wR2 = [\sum \{w(F_o^2 - F_c^2)^2\} / \sum w(F_o^2)^2]^{1/2}$, $w = 1/[\sigma^2(F_o^2) + rP]$, $P = (\text{Max}(F_o^2, 0) + 2 F_c^2) / 3$ [$r = 0.143$]. ^c $\text{GOF} = [\sum w(F_o^2 - F_c^2)^2 / (N_o - N_{\text{params}})]^{1/2}$.

Details of the crystal and data collection parameters of (*E*)-**4-3ii** are summarized in Table 4-2. ORTEP drawing of (*E*)-**4-3ii** is shown in Figure 4-3.

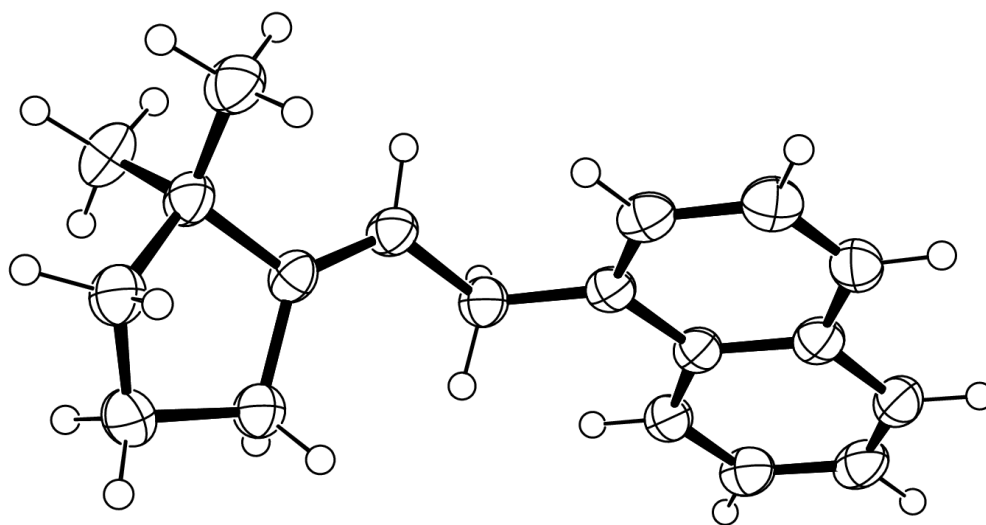


Figure 4-3. ORTEP drawing of (*E*)-**4-3ii**. Thermal ellipsoids of carbon atoms are drawn at the 50% probability level.

4.4.11. Reaction of 1a with 2a in the presence of TEMPO

In a 20 mL Schlenk flask were placed 6-iodohex-1-yne (**4-1a**) (50.3 mg, 0.242 mmol), diethyl 4-benzyl-2,6-dimethyl-1,4-dihydropyridine-3,5-dicarboxylate (**4-2a**) (257 mg, 0.749 mmol), (2,2,6,6-tetramethylpiperidin-1-yl)oxyl (TEMPO) (117 mg, 0.748 mmol), *fac*-[Ir(ppy)₃] (ppy = 2-(2-pyridyl)phenyl) (3.4 mg, 0.0052 mmol), anhydrous NiCl₂ (3.4 mg, 0.026 mmol), dMeObpy (dMeObpy = 4,4'-dimethoxyl-2,2'-bipyridine) (8.2 mg, 0.038 mmol) and Cs₂CO₃ (122 mg, 0.374 mmol) under N₂, where 1,4-dioxane (2.5 mL) was added at room temperature. The reaction flask was placed in an As One LTB-125 constant low temperature water bath set at 25 °C, and was illuminated from the bottom of the bath with an Aitech System TMN100×120–22WD 12 W white LED lamp (400 nm to 750 nm) at a distance of approximately 2 cm from the light source for 24 h. The volatiles were removed *in vacuo*, and the crude yield of 1-(benzyloxy)-2,2,6,6-tetramethylpiperidine (**4-6a**) (0.167 mmol, 69% NMR yield based on the amount of **4-1a**) was determined by ¹H NMR in CDCl₃, where 1,1,2,2-tetrachloroethane (42.1 mg, 0.251 mmol) was added as an internal standard (Figure 4-1a).

4.4.12. Determination of quantum yields

In a 20 mL Schlenk flask were placed 6-iodohex-1-yne (**4-1a**) (50.1 mg, 0.241 mmol), diethyl 4-benzyl-2,6-dimethyl-1,4-dihydropyridine-3,5-dicarboxylate (**4-2a**) (257 mg, 0.749 mmol), *fac*-[Ir(ppy)₃] (ppy = 2-(2-pyridyl)phenyl) (3.4 mg, 0.0052

mmol), anhydrous NiCl_2 (3.4 mg, 0.026 mmol), dMeObpy (dMeObpy = 4,4'-dimethoxyl-2,2'-bipyridine) (8.1 mg, 0.037 mmol) and Cs_2CO_3 (120 mg, 0.370 mmol) under N_2 , where 1,4-dioxane (2.5 mL) was added at room temperature. The reaction flask was illuminated from the side with an Ushio SX-U1251HQ ultrahigh pressure 250 W Hg lamp equipped with a 440-nm band pass filter (Kenko B440) at a distance of approximately 2 cm from the light source for 1.5 h. The volatiles were removed *in vacuo*, and the crude yield of (2-cyclopentylideneethyl)benzene (**4-3aa**) (0.0475 mmol, 20% NMR yield based on the amount of **4-1a**) was determined by ^1H NMR in CDCl_3 , where 1,1,2,2-tetrachloroethane (42.0 mg, 0.250 mmol) was added as an internal standard. Independently, the yields of **4-3aa** were determined by terminating the reactions at 0.5 and 1.0 h, which clarified a zero-order reaction rate at $(8.89 \pm 0.20) \times 10^{-9} \text{ mol s}^{-1}$. The irradiated light intensity to a 2.5 mL solution in 50-mL Schlenk was estimated to be $1.41 \times 10^{-7} \text{ E s}^{-1}$ at 440 nm by using $\text{K}_3[\text{Fe}(\text{C}_2\text{O}_4)_3]$ as a chemical actinometer.⁵³ Thus, the quantum yield of the photoredox- and nickel-catalyzed reaction of **4-1a** with **4-2a** to afford **4-3aa** is given as $\Phi = 0.0630 \pm 0.0014$ (Figure 4-1c).

Similarly, quantum yields of other reactions shown in Figure 4-2 were determined by quantitative measurements of gas chromatography–mass spectroscopy (GC-MS) recorded on a Shimadzu GCMS-QP2010 PLUS instrument, where 1,1,2,2-tetrachloroethane was added as an internal standard.

4.4.13. Stern–Volmer analysis

Luminescence quenching experiments for the 1,4-dioxane solution of *fac*-[Ir(ppy)₃] (2.0 $\mu\text{mol/L}$, prepared by stepwise dilutions of *fac*-[Ir(ppy)₃] (1.3 mg, 2.0 μmol) with 1,4-dioxane) with **4-1a**, (iodohex-1-yl)benzene (**4-1d**), or **4-2a** in selected concentrations were performed on a Shimadzu RF-5300PC spectrophotometer, where the solutions containing *fac*-[Ir(ppy)₃] and **4-1a**, **4-1d**, or **4-2a** were excited at $\lambda_{\text{max}} = 440 \text{ nm}$, and emissions were measured at $\lambda = 494 \text{ nm}$.

From the slopes (28.9 ± 2.9 for **4-1a**, 27.5 ± 2.9 for **4-1d**, and 138 ± 14 for **4-2a**) obtained by the plot and the excited-state lifetime of *fac*-[Ir(ppy)₃] ($\tau = 1.90 \mu\text{s}$),²⁸ the rate constants for the reduction of **4-1a** or **4-1d**, and the oxidation of **4-2a** were calculated to be at $k = (1.5 \pm 0.2) \times 10^7 \text{ M}^{-1} \text{ s}^{-1}$ (**1a**), $k = (1.4 \pm 0.2) \times 10^7 \text{ M}^{-1} \text{ s}^{-1}$ (**4-1d**), and $k = (7.3 \pm 0.7) \times 10^7 \text{ M}^{-1} \text{ s}^{-1}$ (**4-2a**), respectively (Figure 4-1b).

4.4.14. Light on/off experiment

In a 20 mL Schlenk flask were placed 6-iodohex-1-yne (**4-1a**) (52.0 mg, 0.250 mmol), diethyl 4-benzyl-2,6-dimethyl-1,4-dihydropyridine-3,5-dicarboxylate (**4-2a**) (257 mg, 0.749 mmol), *fac*-[Ir(ppy)₃] (ppy = 2-(2-pyridyl)phenyl) (3.4 mg, 0.0052 mmol), anhydrous NiCl_2 (3.4 mg, 0.026 mmol), dMeObpy (dMeObpy = 4,4'-dimethoxyl-2,2'-bipyridine) (8.2 mg, 0.038 mmol), Cs_2CO_3 (123 mg, 0.378 mmol), and octane (28.5 mg, 0.249 mmol, added as an internal standard) under N_2 , where 1,4-

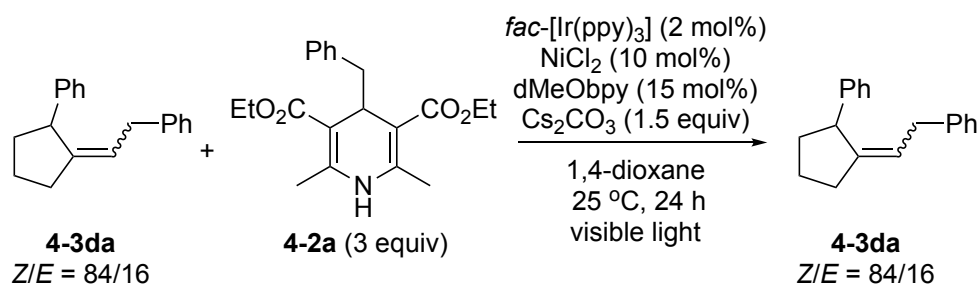
dioxane (2.5 mL) was added at room temperature. The reaction flask was placed in an As One LTB-125 constant low temperature water bath set at 25 °C. The reaction was conducted for 8 h under alternating periods of (1) irradiation from the bottom of the bath with an Aitech System TMN100×120–22WD 12 W white LED lamp (400 nm to 750 nm) at a distance of approximately 2 cm from the light source, and (2) darkness with the reaction vessel wrapped with aluminum foil, where yields of **4-3aa** were determined every hour by quantitative measurements of gas chromatography–mass spectroscopy (GC-MS) recorded on a Shimadzu GCMS-QP2010 PLUS instrument (Figure 4-1c).

4.4.15. Time profile experiment

In a 20 mL Schlenk flask were placed (6-iodohex-1-yl)benzene (**4-1d**) (71.1 mg, 0.250 mmol), **4-2a** (256 mg, 0.746 mmol), *fac*-[Ir(ppy)₃] (3.4 mg, 0.00532 mmol), anhydrous NiCl₂ (3.3 mg, 0.025 mmol), dMeObpy (8.3 mg, 0.038 mmol), Cs₂CO₃ (122 mg, 0.375 mmol), and methyl 4-methoxybenzoate (41.5 mg, 0.250 mmol, added as an internal standard), under N₂, where 1,4-dioxane (2.5 mL) was added at room temperature. The reaction flask was placed in an As One LTB-125 constant low temperature water bath set at 25 °C, and was illuminated from the bottom of the bath with an Aitech System TMN100×120–22WD 12 W white LED lamp (400 nm to 750 nm) at a distance of approximately 2 cm from the light source. Yields of (2-(2-phenylcyclopentylidene)ethyl)benzene (**4-3da**) as well as ((2-(iodomethylene)cyclopentyl)benzene) (**4-7d**) at selected times (0.5, 1, 2, 4, 8, 12, and 24 h) were determined by quantitative measurements of GC-MS (Figure 4-2a).

4.4.16. Transformation reaction of a mixture of (*E*)- and (*Z*)-isomers

Scheme 4-18. Transformation reaction of a mixture of (*E*)- and (*Z*)-isomers



In a 20 mL Schlenk flask were placed **4-3da** (Z/E = 84/16, 24.8 mg, 0.100 mmol), **4-2a** (103 mg, 0.299 mmol), *fac*-Ir(ppy)₃ (1.4 mg, 0.0021 mmol), anhydrous NiCl₂ (1.4 mg, 0.011 mmol), dMeObpy (3.3 mg, 0.015 mmol), and Cs₂CO₃ (49.1 mg, 0.151 mmol) under N₂, where 1,4-dioxane (1.0 mL) was added at room temperature. The reaction flask was placed in an As One LTB-125 constant low temperature water bath set at 25 °C, and was illuminated from the bottom of the bath with an Aitech System TMN100×120–22WD 12 W white LED lamp (400 nm to 750 nm) at a distance of approximately 2 cm from the light source for 24 h. After the reaction, the Z/E ratio of **4-4a** was determined to be 84/16 by quantitative measurements of GC-MS, by adding

methyl 4-methoxybenzoate (41.5 mg, 0.250 mmol) to the reaction mixture as an internal standard.

4.5. References

- (1) Recent reviews on Hantzsch esters in photoredox catalysis: (a) Huang, W.; Cheng, X. *Synlett* **2017**, 28, 148–158. (b) Zhao, Y.; Xia, W. *Org. Biomol. Chem.* **2019**, 17, 4951–4963. (c) Wang, P.-Z.; Chen, J.-R.; Xiao, W.-J. *Org. Biomol. Chem.* **2019**, 17, 6936–6951.
- (2) Shen, G.-B.; Xie, L.; Yu, H.-Y.; Liu, J.; Fu, Y.-H.; Yan, M. *RSC Adv.* **2020**, 10, 31425–31434.
- (3) Nakajima, K.; Nojima, S.; Sakata, K.; Nishibayashi, Y. *ChemCatChem* **2016**, 8, 1028–1032.
- (4) (a) Chen, W.; Liu, Z.; Tian, J.; Li, M.; Ma, J.; Cheng, X.; Li, G. *J. Am. Chem. Soc.* **2016**, 138, 12312–12315. (b) Gu, F.; Huang, W.; Liu, X.; Chen, W.; Cheng, X. *Adv. Synth. Catal.* **2018**, 360, 925–931. (c) de Assis, F. F.; Huang, X.; Akiyama, M.; Pilli, R. A.; Meggers, E. *J. Org. Chem.* **2018**, 83, 10922–10932. (d) Song, Z.-Y.; Zhang, C.-L.; Ye, S. *Org. Biomol. Chem.* **2019**, 17, 181–185. (e) Du, H.-W.; Sun, J.; Gao, Q.-S.; Wang, J.-Y.; Wang, H.; Xu, Z.; Zhou, M.-D. *Org. Lett.* **2020**, 22, 1542–1546. (f) Angnes, R. A.; Potnis, C.; Liang, S.; Correia, C. R. D.; Hammond, G. B. *J. Org. Chem.* **2020**, 85, 4153–4164. (g) Guo, Q.; Peng, Q.; Chai, H.; Huo, Y.; Wang, S.; Xu, Z. *Nat. Commun.* **2020**, 11, 1463. (h) He, X.-K.; Lu, J.; Zhang, A.-J.; Zhang, Q.-Q.; Xu, G.-Y.; Xuan, J. *Org. Lett.* **2020**, 22, 5984–5989. (i) Kim, I.; Park, S.; Hong, S. *Org. Lett.* **2020**, 22, 8730–8734.
- (5) (a) Wang, X.; Li, H.; Qiu, G.; Wu, J. *Chem. Commun.* **2019**, 55, 2062–2065. (b) Wang, X.; Yang, M.; Xie, W.; Fan, X.; Wu, J. *Chem. Commun.* **2019**, 55, 6010–6013. (c) Gong, X.; Yang, M.; Liu, J.-B.; He, F.-S.; Fan, X.; Wu, J. *Green Chem.* **2020**, 22, 1906–1910.
- (6) Qu, Q.-Y.; Min, Q.-Q.; Ao, G.-Z.; Liu, F. *Org. Biomol. Chem.* **2018**, 16, 6391–6394.
- (7) (a) Milligan, J. A.; Phelan, J. P.; Polites, V. C.; Kelly, C. B.; Molander, G. A. *Org. Lett.* **2018**, 20, 6840–6844. (b) Chen, H.; Anand, D.; Zhou, L. *Asian J. Org. Chem.* **2019**, 8, 661–664. (c) Liang, S.; Angnes, R. A.; Potnis, C.; Hammond, G. B. *Tetrahedron Lett.* **2019**, 60, 151230. (d) Chen, X.; Ye, F.; Luo, X.; Liu, X.; Zhao, J.; Wang, S.; Zhou, Q.; Chen, G.; Wang, P. *J. Am. Chem. Soc.* **2019**, 141, 18230–18237.
- (8) Nakajima, K.; Nojima, S.; Nishibayashi, Y. *Angew. Chem., Int. Ed.* **2016**, 55, 14106–14110.
- (9) Nakajima, K.; Guo, X.; Nishibayashi, Y. *Chem. Asian J.* **2018**, 13, 3653–3657.
- (10) (a) Buzzetti, L.; Prieto, A.; Roy, S. R.; Melchiorre, P. *Angew. Chem., Int. Ed.* **2017**, 56, 15039–15043. (b) van Leeuwen, T.; Buzzetti, L.; Perego, L. A.; Melchiorre, P. *Angew. Chem., Int. Ed.* **2019**, 58, 4953–4957.
- (11) (a) Zhang, H.-H.; Yu, S.; *J. Org. Chem.* **2017**, 82, 9995–10006. (b) Schwarz, J. L.; Huang, H.-M.; Paulisch, T. O.; Glorius, F. *ACS Catal.* **2020**, 10, 1621–1627. (c) Zhou, Z.-Z.; Jiao, R.-Q.; Yang, K.; Chen, X.-M.; Liang, Y.-M. *Chem. Commun.* **2020**, 56, 12957–12960. (d) Huang, H.-M.; Bellotti, P.; Daniliuc, C. G.; Glorius, F. *Angew. Chem., Int. Ed.* **2021**, 60, 2464–2471.
- (12) (a) Gutiérrez-Bonet, Á.; Tellis, J. C.; Matsui, J. K.; Vara, B. A.; Molander, G. A. *ACS Catal.* **2016**, 6, 8004–8008. (b) Zhang, H.-H.; Zhao, J.-J.; Yu, S. *J. Am. Chem. Soc.*

- 2018**, *140*, 16914–16919. (c) McDonald, B. R.; Scheidt, K. A. *Org. Lett.* **2018**, *20*, 6877–6881. (d) Phelan, J. P.; Lang, S. B.; Sim, J.; Berritt, S.; Peat, A. J.; Billings, K.; Fan, L.; Molander, G. A. *J. Am. Chem. Soc.* **2019**, *141*, 3723–3732. (e) Wang, Z.-J.; Zheng, S.; Romero, E.; Matsui, J. K.; Molander, G. A. *Org. Lett.* **2019**, *21*, 6543–6547.
- (13) Gandolfo, E.; Tang, X.; Raha Roy, S.; Melchiorre, P. *Angew. Chem., Int. Ed.* **2019**, *58*, 16854–16858.
- (14) Recent reviews on photoredox catalysis: (a) Koike, T.; Akita, M. *Inorg. Chem. Front.* **2014**, *1*, 562–576. (b) Shaw, M. H.; Twilton, J.; MacMillan, D. W. C. *J. Org. Chem.* **2016**, *81*, 6898–6926. (c) Glase, F. Kerzig, C.; Wenger, O. S. *Angew. Chem., Int. Ed.* **2020**, *59*, 10266–10284.
- (15) Recent reviews on dual photoredox catalysis: (a) Prier, C. K.; Rankic, D. A.; MacMillan, D. W. C. *Chem. Rev.* **2013**, *113*, 5322–5363. (b) Angnes, R. A.; Li, Z.; Correia, C. R.; Hammond, G. B. *Org. Biomol. Chem.* **2015**, *13*, 9152–9167. (c) Skubi, K. L.; Blum, T. R.; Yoon, T. P. *Chem. Rev.* **2016**, *116*, 10035–10074. (d) Levin, M. D.; Kim, S.; Toste, F. D. *ACS Cent. Sci.* **2016**, *2*, 293–301. (e) Twilton, J.; Le, C. (C.); Zhang, P.; Shaw, M. H.; Evans, R. W.; MacMillan, D. W. C. *Nat. Rev. Chem.* **2017**, *1*, 0052.
- (16) (a) Stüdemann, T.; Knochel, P. *Angew. Chem., Int. Ed. Engl.* **1997**, *36*, 93–95. (b) Stüdemann, T.; Ibrahim-Ouali, M.; Knochel, P. *Tetrahedron* **1998**, *54*, 1299–1316.
- (17) (a) Crandall, J. K.; Battioni, P.; Wehlacz, J. T.; Bindra, R. *J. Am. Chem. Soc.* **1975**, *97*, 7171–7172. (b) Negishi, E.; Nguyen, T.; Boardman, L. D.; Sawada, H.; Morrison, J. A. *Heteroat. Chem.* **1992**, *3*, 293–302. (c) Harada, T.; Imaoka, D.; Kitano, C.; Kusukawa, T. *Chem. Eur. J.* **2010**, *16*, 9164–9174.
- (18) Reviews containing discussions on alkylative cyclization: (a) Naito, T. *Pure Appl. Chem.* **2008**, *80*, 717–726. (b) Ghorai, M. K.; Halder, S.; Samanta, S. Carboamination and alkylative cyclization with C–N bond formation in stereoselective syntheses. In *Stereoselective Synthesis of Drugs and Natural Products*; Andrushko, V., Andrushko, N., Eds.; John Wiley & Sons: Hoboken, 2013; Vol. 2, pp 1211–1250. (c) Ila, H.; Acharya, A.; Peruncheralathan, S. Domino Reactions Initiated by Nucleophilic Substitution. In *Domino Reactions: Concepts for Efficient Organic Synthesis*; Tietze, L. F., Ed.; Wiley-VCH: Weinheim, 2014; pp. 105–140. (d) Trost, B. M.; Kalnmals, C. A. *Chem. Eur. J.* **2020**, *26*, 1906–1921.
- (19) Phapale, V. B.; Buñuel, E.; García-Iglesias, M.; Cárdenas, D. J. *Angew. Chem., Int. Ed.* **2007**, *46*, 8790–8795.
- (20) Selected examples of catalytic alkylative cyclization of unsaturated halogenated compounds: (a) Seashore-Ludlow, B.; Somfai, P. *Org. Lett.* **2012**, *14*, 3858–3861. (b) Ye, J.; Shi, Z.; Sperger, T.; Yasukawa, Y.; Kingston, C.; Schoenebeck, F.; Lautens, M. *Nat. Chem.* **2017**, *9*, 361–368. (c) Kuang, Y.; Wang, X.; Anthony, D.; Diao, T. *Chem. Commun.* **2018**, *54*, 2558–2561. (e) Jin, Y.; Wang, C. *Angew. Chem., Int. Ed.* **2019**, *58*, 6722–6726.
- (21) Recent reviews on cooperative nickel- and photoredox catalysis: (a) Zuo, Z.; Ahneman, D. T.; Chu, L.; Terrett, J. A.; Doyle, A. G.; MacMillan, D. W. C. *Science* **2014**, *345*, 437–440. (b) Villa, C. *Merging ChemCatChem* **2015**, *7*, 1790–1793. (c) Gui, Y.-Y.; Sun, L.; Lu, Z.-P.; Yu, D.-G. *Org. Chem. Front.* **2016**, *3*, 522–526. (d) Cavalcanti,

L. V.; Molander, G. A. *Top. Curr. Chem.* **2016**, *374*, 39. (e) Luo, J.; Zhang, J. *ACS Catal.* **2016**, *6*, 873–877. (f) Börjesson, M.; Tortajada, A.; Martin, R. *Chem* **2019**, *5*, 254–262. (g) Milligan, J. A.; Phelan, J. P.; Badir, S. O.; Molander, G. A. *Angew. Chem., Int. Ed.* **2019**, *58*, 6152–6163. (h) Zhu, C.; Yue, H.; Chu, L.; Rueping, M. *Chem. Sci.* **2020**, *11*, 4051–4064. (i) Badir, S. O.; Molander, G. A. *Chem* **2020**, *6*, 1327–1339.

(22) (a) Varala, R. Rao, K. S. *Curr. Org. Chem.* **2015**, *19*, 1242–1274. (b) Rabie, R.; Hammouda, M. M.; Elattar, K. M. *Res. Chem. Intermed.* **2017**, *43*, 1979–2015.

(23) Recent reviews on halide effect in photoredox chemistry: (a) Troian-Gautier, L.; Swords, W. B.; Meyer, G. J. *Acc. Chem. Res.* **2019**, *52*, 170–179. (b) Troian-Gautier, L.; Turlington, M. D.; Wehlin, S. A. A.; Maurer, A. B.; Brady, M. D.; Swords, W. B.; Meyer, G. J. *Chem. Rev.* **2019**, *119*, 4628–4683. (c) Ye, S.; Xiang, T.; Li, X.; Wu, J. *Org. Chem. Front.* **2019**, *6*, 2183–2199.

(24) Jung, M. E.; Piizzi, G. *Chem. Rev.* **2005**, *105*, 1735–1766.

(25) Yaku, Y.; Koike, T.; Akita, M. *Adv. Synth. Catal.* **2012**, *354*, 3414–3420.

(26) (a) Liao, J.; Basch, C. H.; Hoerrner, M. E.; Talley, M. R.; Boscoe, B. P.; Tucker, J. W.; Garnsey, M. R.; Watson, M. P. *Org. Lett.* **2019**, *21*, 2941–2946. (b) Wang, J.; Pang, Y.-B.; Tao, N.; Zeng, R.-S.; Zhao, Y. *J. Org. Chem.* **2019**, *84*, 15315–15322. (c) Zhang, D.; Tang, Z.-L.; Ouyang, X.-H.; Song, R.-J.; Li, J.-H. *Chem. Commun.* **2020**, *56*, 14055–14058.

(27) Dixon, I. M.; Collin, J.-P.; Sauvage, J.-P.; Flamigni, L.; Encinas, S.; Barigelletti, F. *Chem. Soc. Rev.* **2000**, *29*, 385–191.

(28) (a) Cismesia, M.; Yoon, T. P. *Chem. Sci.* **2015**, *6*, 5426–5436. (b) Kärkäs, M. D.; Matsuura, B. S.; Stephenson, C. R. J. *Science* **2015**, *349*, 1285–1286.

(29) Nakajima, K.; Miyake, Y.; Nishibayashi, Y. *Acc. Chem. Res.* **2016**, *49*, 1946–1956.

(30) (a) Miyake, Y.; Nakajima, K.; Nishibayashi, Y. *J. Am. Chem. Soc.* **2012**, *134*, 3338–3341. (b) Miyake, Y.; Ashida, Y.; Nakajima, K.; Nishibayashi, Y. *Chem. Commun.* **2012**, *48*, 6966–6968. (c) Miyake, Y.; Nakajima, K.; Nishibayashi, Y. *Chem. Commun.* **2013**, *49*, 7854–7856. (d) Nakajima, K.; Kitagawa, M.; Ashida, Y.; Miyake, Y.; Nishibayashi, Y. *Chem. Commun.* **2014**, *50*, 8900–8903.

(31) (a) Curran, D. P.; Chen, M.-H.; Kim, D. *J. Am. Chem. Soc.* **1986**, *108*, 2489–2490. (b) Curran, D. P.; Chen, M.-H.; Kim, D. *J. Am. Chem. Soc.* **1989**, *111*, 6265–6276.

(32) Shen, Y.; Cornella, J.; Juliá-Hernández, F.; Martin, R. *ACS Catal.* **2017**, *7*, 409–412.

(33) Weng, W.-Z.; Liang, H.; Liu, R.-Z.; Ji, Y.-X.; Zhang, B. *Org. Lett.* **2019**, *21*, 5586–5590.

(34) Jimenez, A. J.; Fagnoni, M.; Mella, M.; Albin, A. *J. Org. Chem.* **2009**, *74*, 6615–6622.

(35) Qin, Y.; Sun, R.; Gianoulis, N. P.; Nocera, D. G. *J. Am. Chem. Soc.* **2021**, *143*, 2005–2015.

(36) Trost, B. M.; Breder, A.; Kai, B. *Org. Lett.* **2012**, *14*, 1708–1711.

(37) Coombs, J. R.; Zhang, L.; Morken, J. P. *J. Am. Chem. Soc.* **2014**, *136*, 16140–16143.

(38) Zhong, Z.; Wang, Z.-Y.; Ni, S.-F.; Dang, L.; Lee, H. K.; Peng, X.-S.; Wong, H. N. *C. Org. Lett.* **2019**, *21*, 700–704.

- (39) Meng, Z.; Fürstner, A. *J. Am. Chem. Soc.* **2020**, *142*, 11703–11708.
- (40) Simmons, E. M.; Sarpong, R. *Org. Lett.* **2006**, *8*, 2883–2886.
- (41) Li, G.; Chen, R.; Wu, L.; Fu, Q.; Zhang, X.; Tang, Z. *Angew. Chem., Int. Ed.* **2013**, *52*, 8432–8436.
- (42) Nakajima, K.; Zhang, Y.; Nishibayashi, Y. *Org. Lett.* **2019**, *21*, 4642–4645.
- (43) Patel, S. S.; Kumar, D.; Tripathi, C. B. *Chem. Commun.* **2021**, *57*, 5151–5154.
- (44) Krasinski, A.; Radic, Z.; Manetsch, R.; Raushel, J.; Taylor, P.; Sharpless, K. B.; Kolb, H. C. *J. Am. Chem. Soc.* **2005**, *127*, 6686–6692.
- (45) Bailey, W. F.; Ovaska, T. V. *J. Am. Chem. Soc.* **1993**, *115*, 3080–3090.
- (46) Pérez-Aguilar, M. C.; Valdés, C. *Angew. Chem., Int. Ed.* **2012**, *51*, 5953–5957.
- (47) *CrysAlisPro*, Data Collection and Processing Software; Rigaku Corporation: Tokyo, Japan, 2015.
- (48) *CrystalStructure*, version 4.3; Crystal Structure Analysis Package; Rigaku Corporation: Tokyo, Japan, 2015.
- (49) Sheldrick, G. M. A short history of *SHELX*. *Acta Crystallogr., Sect. A: Found. Crystallogr.* **2008**, *A64*, 112–122.
- (50) Sheldrick, G. M. Crystal structure refinement with *SHELXL*. *Acta Crystallogr., Sect. C: Struct. Chem.* **2015**, *C71*, 3–8.
- (51) Ibers, J. A.; Hamilton, W. C. *Acta Crystallogr.* **1964**, *17*, 781–782.
- (52) (a) Creagh D. C.; Hubbell, J. H. Table 4.2.4.3. Mass attenuation coefficients (cm² g⁻¹). In *International Tables for Crystallography*, Wilson, A. J. C., Ed.; Kluwer Academic Publishers: Dordrecht, The Netherlands, 1992; vol. C, pp. 200–206. (b) Creagh, D. C.; McAuley, W. J. Table 4.2.6.8. Dispersion corrections for forward scattering. In *International Tables for Crystallography*, Wilson, A. J. C., Ed.; Kluwer Academic Publishers: Dordrecht, The Netherlands, 1992; vol. C, pp. 219–222. (c) Maslen, E. N.; Fox, A. G.; O’Keefe, M. A. Table 6.1.1.4. Coefficients for analytical approximation to the scattering factors of Tables 6.1.1.1 and 6.1.1.3. In *International Tables for Crystallography*, Wilson, A. J. C., Ed.; Kluwer Academic Publishers: Dordrecht, The Netherlands, 1992; vol. C, pp. 500–503.
- (53) Hatchard, C. G.; Parker, C. A. *Proc. R. Soc. London, Ser. A* **1956**, *235*, 518–536.

Chapter 5

Summary and Perspective

In this doctoral thesis, the author has succeeded in the development of a series of dual photoredox- and transition metal-catalyzed alkylation of alkynes with 4-alkyl-1,4-dihydropyridines. In these works, the author has clarified that the alkyl radicals generated from 4-alkyl-1,4-dihydropyridines act as alkylation reagents that can be treated with various alkyne substrates under rather milder reaction conditions, compared to those using organometallic alkylation reagents, to afford several alkylated products, containing completely new ones (Figure 5-1).

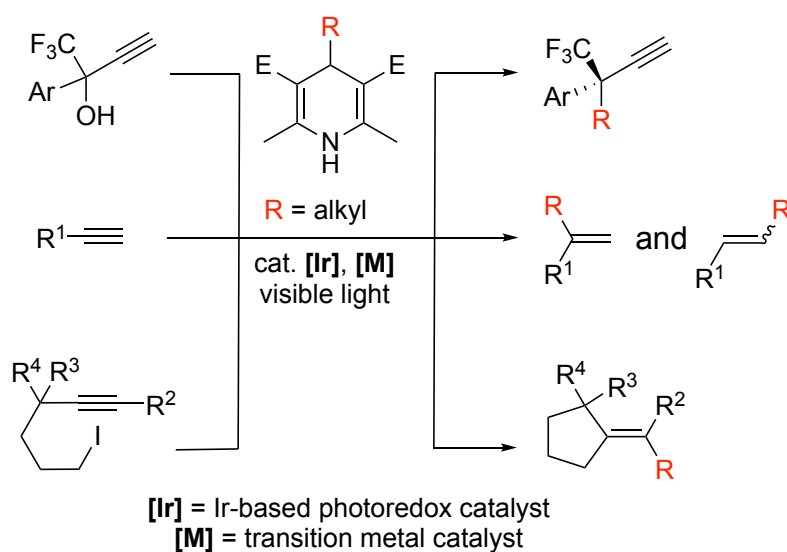


Figure 5-1. Alkylation of alkynes with 4-alkyl-1,4-dihydropyridines.

In Chapter 2, the author has described enantioselective photoredox- and ruthenium-catalyzed propargylic alkylation reactions of propargylic alcohols with 4-alkyl-1,4-dihydropyridines. Propargylic alcohols bearing a trifluoromethyl group at the propargylic position were revealed to be critical to achieve a high enantioselectivity. A broad range of substrates were applicable to this reaction system to afford a variety of propargylic alkylated products with a chiral tetrasubstituted stereogenic carbon center in high yields with a high enantioselectivity. This is the first successful example of photoredox- and ruthenium-catalyzed enantioselective propargylic substitution reactions, where alkyl radicals as alkylation reagents are generated from 4-alkyl-1,4-dihydropyridines under photoredox reaction conditions, providing a new strategy to the chemistry of enantioselective propargylic substitution reactions.

In Chapter 3, the author has described photoredox- and nickel-catalyzed hydroalkylation of alkynes with 4-alkyl-1,4-dihydropyridines with ligand-controlled regioselectivity. In this work, The author has examined the use of 4-alkyl-1,4-dihydrpyridines that have not been used for the formation of regioselective alkylated

alkenes. And have developed cooperative photoredox- and nickel-catalyzed hydroalkylation of alkylacetylenes or arylacetylenes with 4-alkyl-1,4-dihydropyridines to afford Markovnikov- or *anti*-Markovnikov-type alkylated alkenes without the addition of bases, where the regioselectivity is controlled by the difference in coordination ligands for nickel catalysts. This work provides a new strategy in the preparation of regioselective functionalized alkenes from alkynes.

In Chapter 4, the author has described photoredox- and nickel-catalyzed alkylative cyclization reactions of alkynes with 4-alkyl-1,4-dihydropyridines. A broad range of substrates were applicable to afford various alkylated cyclopentylidenes products. Mechanistic studies have revealed that the photoredox-catalyzed cyclization of 6-iodohex-1-yne to afford cyclopentylidene iodides first occurs, followed by the photoredox- and nickel-catalyzed substitution reactions of the cyclopentylidene iodides with alkyl radicals to yield the alkylated cyclopentylidenes. The present reaction system provides a novel synthetic method for alkylative cyclization reactions of both terminal and internal alkynes with cooperative photoredox and nickel catalysis.

Overall, the author has investigated dual photoredox- and transition metal-catalyzed alkylation of alkynes with 4-alkyl-1,4-dihydropyridines under rather mild reaction conditions to generate new chemical products. Especially, the author has succeeded in the construction of stereogenic quaternary carbon center at the propargylic position. Further expansion of the range of substrate application can be expected, providing a powerful synthetic method for synthesizing high-value-added pharmaceuticals and chemical products such as Efavirenz and Dynemicin A, both of which contain asymmetric carbon centers at the propargylic positions (Figure 5-2).

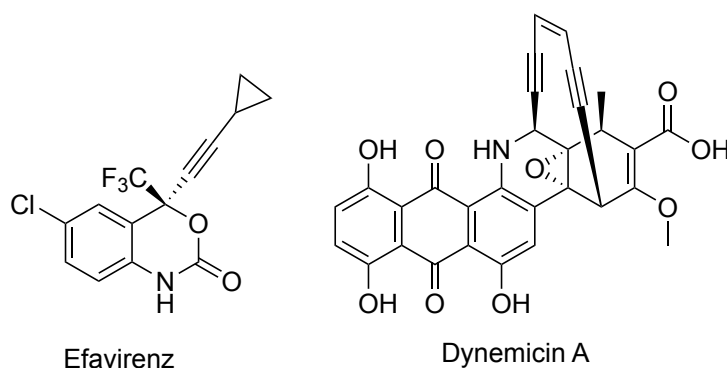


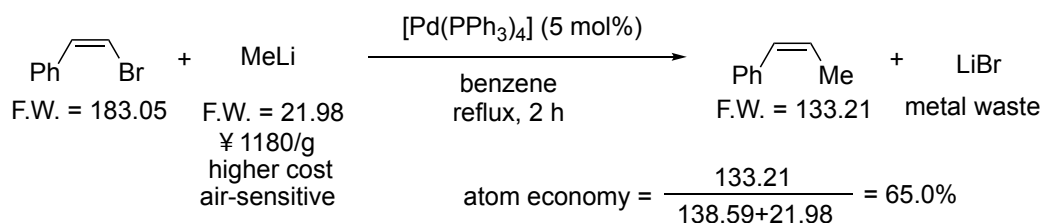
Figure 5-2. Structures of Efavirenz and Dynemicin A, containing asymmetric carbon centers at the propargylic positions.

Form the viewpoint of safety and improving reaction efficiencies, the author has succeeded in the development of the utilization of 4-alkyl-1,4-dihydropyridines as alkylation reagents alternative to organometallic alkylation reagents, which has been playing important roles in a variety of direct alkylation reactions. In order to evaluate the importance of the author's system, merits and demerits of Murahashi coupling, as a representative of the previous reaction system using organometallic alkylation reagents, will be compared with those of the author's new system (Scheme 5-1a). In the viewpoint of atom economy (65% in the previous system vs 44% in the author's

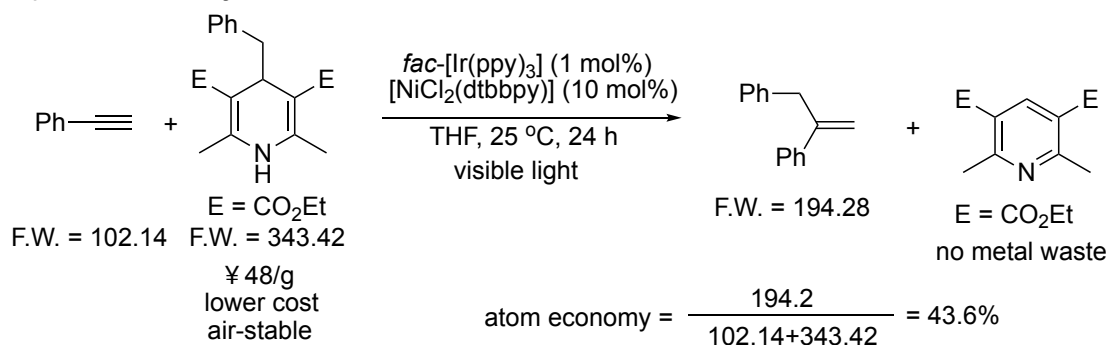
system), the use of dihydropyridines is not an advantage over the previous reaction system using organometallic alkylation reagents. However except for this, the author's system in this PhD thesis has many advantages over the previous system. First of all, the previous reaction system emits stoichiometric amounts of metal wastes (LiBr in this case), but the author's system does not. Secondly, the cost of the dihydropyridines (48 yen/g) is much lower than the organometallic reagent (1180 yen/g). Finally, the organometallic reagent (MeLi) used in the previous reaction system is very air-sensitive and reactive thus to be treated carefully, but in the author's system, dihydropyridine is stable under air ([Scheme 5-1b](#)).

Scheme 5-1. Comparison of Previous System and the Author's System

a) Previous system (Murahashi coupling)



b) The author's system



Although use of dihydropyridines gains many advantages, there are still some problems with them. For instance, there have been limited examples reported so far to prepare dihydropyridines containing tertiary alkyl groups or complicated alkyl groups. To overcome these problems, besides the dihydropyridines, there are several candidates for photoredox-initiated nonmetal organic alkylation reagents such as Katritzky salts and *N*-(acyloxy)phthalimides, which are more suitable for the introduction of tertiary alkyl or complicated alkyl groups. For the next generation, the author has now proposed to develop other organic alkylation reagents such as Katritzky salts and *N*-(acyloxy)phthalimides to apply for the dual photoredox- and transition metal-catalyzed reactions systems to expand the scope of alkyl radicals generated *in situ* in photoredox reaction conditions to mediate new C–C bond formation reactions ([Figure 5-3](#)).

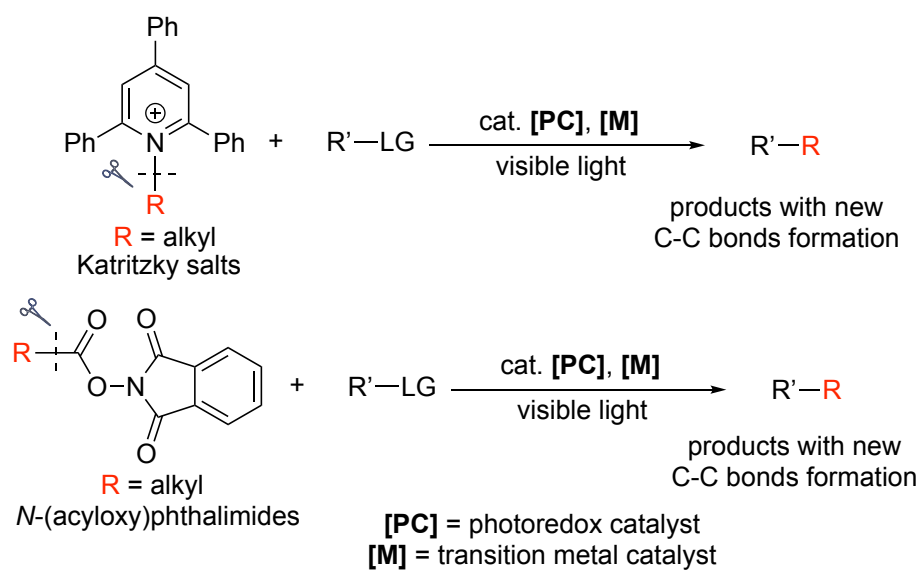


Figure 5-3. Katritzky salts and *N*-(acyloxy)phthalimides as alkylation reagents.

List of Publications

- (1) Cooperative Photoredox- and Nickel-Catalyzed Alkylative Cyclization Reactions of Alkynes with 4-Alkyl-1,4-dihydropyridines
Yulin Zhang, Yoshiaki Tanabe, Shogo Kuriyama, Yoshiaki Nishibayashi
J. Org. Chem. **2021**, 86, 12577-12590.
- (2) Photoredox- and Nickel-Catalyzed Hydroalkylation of Alkynes with 4-Alkyl-1,4-dihydropyridines: Ligand-Controlled Regioselectivity
Yulin Zhang, Yoshiaki Tanabe, Shogo Kuriyama, Yoshiaki Nishibayashi
Chem. Eur. J. **2022**, 28, e202200727.
- (3) Enantioselective Photoredox- and Ruthenium-Catalyzed Propargylic Alkylation of Propargylic Alcohols with 4-Alkyl-1,4-dihydropyridines
Yulin Zhang, Yoshiaki Tanabe, Shogo Kuriyama, Ken Sakata, Yoshiaki Nishibayashi
To be submitted.

The following paper is not included in this thesis

- (4) Alkylation Reactions of Azodicarboxylate Esters with 4-Alkyl-1,4-dihydropyridines under Catalyst-Free Conditions
Kazunari Nakajima, Yulin Zhang, Yoshiaki Nishibayashi
Org. Lett. **2019**, 21, 4642-4645.

Acknowledgement

The author is deeply grateful to Professor Yoshiaki Nishibayashi for his helpful discussions, experimental guidance, hearty advice, contribution to revising author's manuscripts, and encouragement throughout the course of the studies. The author is deeply grateful to Project Lecturer Yoshiaki Tanabe, Associate Professor Kazunari Nakajima, and Assistant Professor Shogo Kuriyama for helpful discussions, experimental guidance, contribution to revising the author's manuscripts and continuous encouragement throughout the course of the studies.

The author appreciates to the members of his committee (Professor Daisuke Kitazawa, Associate Professor Gjergj Dodbiba, Professor Ken Sakata, and Associate Professor Yoshihiro Miyake) for their instructive and helpful discussions.

The author is appreciative to the member of the Nishibayashi group. The author thanks to Dr. Kazuya Arashiba, Dr. Masahiro Yuki, Dr. Yasuomi Yamazaki, Dr. Shun Suginome, Dr. Aya Eizawa, Dr. Wenbin Liang, Dr. Yuya Ashida, Dr. Shiyao Liu, Dr. Hiroki Otsuka, Dr. Hiroki Toda, Dr. Takayuki Itabashi, Mr. Fanqiang Meng, Mr. Haowei Ding, Mr. Takeru Kato, Mr. Xifeng Guo, Mr. Ryosuke Kawakami, Mr. Takuro Mizushima, Ms. Shenglan Wei, Mr. Taichi Mitsumoto, Mr. Koyo Uema, Mr. Kosuke Somemori, Mr. Kaito Kuroki, Mr. Kazuki Kamiyama, Ms. Aiwei Zhao, Mr. Yuto Onozuka, Mr. Koshiro Kido, Mr. Yuto Suga, Mr. Hayato Takase, Mr. Takahiro Kubo, Ms. Kurumi Morota, Ms. Zuyi Xue, Ms. Yuye Zhang, Mr. Hiroki, Takekuma, Mr. Masaru Ogasawara, Mr. Yoshikatsu Kameda, Mr. Keita Sugiyama, Mr. Ryo Takabatake and Mr. Kaito Nakaya for their continuous encouragement and kind assistance.

The author thanks JSPS Research Fellowship for Young Scientists for financial support.

Finally, the author expresses his deep gratitude to his family, Mr. Wei Zhang, Ms. Hongjuan Zhao, and Ms. Xiuxiu Cheng for their financial support or continuous and heartwarming encouragement through his studies.